

# **NON-LINEAR ANALYSIS AND BEHAVIOUR OF REINFORCED SOIL STRUCTURES**

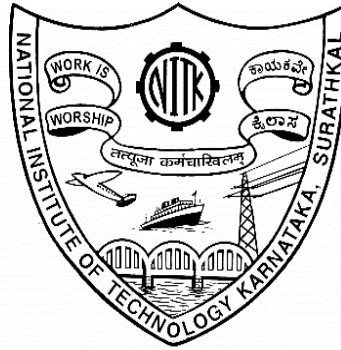
**Thesis**

**Submitted in partial fulfillment of the requirements for the degree of**

**DOCTOR OF PHILOSOPHY**

*by*

**Smt. NAYANA N. PATIL**



**DEPARTMENT OF CIVIL ENGINEERING**

**NATIONAL INSTITUTE OF TECHNOLOGY KARNATAKA  
SURATHKAL, MANGALORE-575 025**

**Karnataka**

**April, 2018**

## DECLARATION

I hereby declare that the Research Thesis entitled “**NONLINEAR ANALYSIS AND BEHAVIOUR OF REINFORCED SOIL STRUCTURES** “ which is being submitted to the **National Institute of Technology Karnataka, Surathkal** in partial fulfillment of the requirements for the award of the degree of **Doctor of Philosophy in Civil Engineering** is *a bonafide report of the research work carried out by me*. The material contained in this Research Thesis has not been submitted to any University or Institution for the award of any degree.

**NAYANA N. PATIL**

Register Number: **081030CV08P01**

Department of Civil Engineering

Place: NITK, Surathkal

Date :6<sup>th</sup> April 2018

## CERTIFICATE

This is to certify that the Research Thesis entitled “**Nonlinear Analysis and Behaviour of Reinforced soil Structures** “ submitted by **Smt. Nayana N.Patil** (Register number 081030CV08P01) as the record of the research work carried out by her is *accepted as the Research Thesis Submission* in partial fulfillment of the requirements for the award of degree of **Doctor of Philosophy**.

**Prof. R. Shivashankar,**  
**Department of Civil Engineering,**  
**(Research Supervisor)**

**Prof. Varghese George,**  
**Department of Civil Engineering,**  
**Chairman-DRPC**



**Dedicated to  
H.M. and Patil  
Families**



## ACKNOWLEDGEMENTS

While a completed dissertation bears the single name of the researcher, the process that leads to its completion is always accomplished in combination with the dedicated work of other people. The completion of this doctoral thesis was possible with the support of a number of people. I wish to express my sincere gratitude to all of them.

Firstly, I am extremely grateful to my research advisor, **Prof. R.Shivashankar**, for his excellent guidance, scholarly inputs and advice at every stage, and constant encouragement and support throughout.

Besides my advisor, I am thankful to **Prof. Subba Rao** and **Prof. A. Kandasamy**, members of my Research Progress Assessment Committee for their valuable comments and advice. I profusely thank my Examiners **Prof. K.Premalatha**, HOD, Dept. of Civil Engineering, Guindy Engineering College, Anna University and **Prof. Panich Voottipruex**, King Mangkut University of Technology, Thailand for reviewing my thesis with patience and giving valuable suggestions and corrections. I am thankful to the members of my Doctoral Thesis Research Committee, **Prof. Varghese George**, **Prof. R. Shivashankar**, **Prof B.R.Jayalekshmi**, **Prof. Lakshman Nandagiri** and **Prof. K.Premalatha** for evaluating the Thesis and conducting the Viva-Voce Seminar and also for providing valuable inputs and suggestions .

With deep sense of regards, I would like to thank all the previous HODs and present HOD, **Prof. Varghese George** for their constant encouragement. My sincere thanks also goes to the **Department of Civil Engg., NIT-K, Surathkal** who gave access to the laboratory and research facilities. Without their precious support it would not be possible to conduct this research.

I would like to thank the Management and Director of Sahyadri College of Engg. and Management **Dr.D.L.Prabhakara** for their academic and logistic support in my Doctoral programme. A special thanks to **Dr. M.R.Jayaram**, Chancellor, Ramaiah

University of Applied Sciences, Bangalore and the Vice Chancellor **Dr. S.R.Shankapal** for their constant encouragement and support in my research activities.

I am extremely thankful to Mr. **Rajakumar Manisana**, my M.Tech student for helping me in the Experimental studies on Reinforced soil foundation. I would extend my thanks to **Ms. Veena K.V, Gouri S. Patil** and **Chandrakala R.** for providing me invaluable help in editing the thesis.

I am very much indebted to my family, my mother **Mrs Vimala N.Patil**, my father late **Dr. N.A.Patil** who were constantly behind me to complete my Doctoral programme. I owe a lot of gratitude to my father-in-law **Mr. H.M.Vrushabendraswamy**, my mother in-law late **Mrs K.R.Thungamma** who have supported me whole heartedly in all my academic ventures.

My heartfelt thanks to my beautiful children **H.M.Karthik** and my sweet **H.M.SiriGouri** who have patiently co-operated and borne all the inconvenience caused during my research. My husband, mentor, guide and friend **Prof. H.M.Rajashekharswamy** was a constant source of inspiration for my research. I thank him immensely for supporting me endlessly to see the completion of this work. It would be incomplete if I do not mention my sister-in-law **Dr.H.M.Shobha, Dr. L.B.Swami** and their family for supporting me in accomplishing this degree and beyond it. I would also like to thank my ever encouraging sister **Dr. Jaya N.Patil**, brothers **Mr. Mrutyunjaya N. Patil** and **Mr. Shivayogi N.Patil** for morally supporting me for the completion of this doctoral thesis and beyond it.

*My deepest and sincere gratitude for inspiring and guiding this humble being are due to Almighty GOD.*

*Nayana N.Patil*

**Place: NIT-K**

**Date: 6<sup>th</sup> April 2018**

## ABSTRACT

Soil is a complicated material that behaves non-linearly and often shows anisotropic and time dependent behaviour when subjected to stresses. It exhibits non-linear behaviour well below failure condition with stress dependent stiffness. To describe behavior of a material suitably, it is necessary to establish constitutive models (constitutive relations or equations) representing mathematical descriptions of their behavior under external load. Reinforced soil is a composite material formed by the association of frictional soil and tension resistant elements in various forms such as sheets, strips, nets or mats of metal, synthetic fabrics, arranged in the soil mass to reduce or suppress the tensile strain which might develop under gravity and boundary forces.

The past few decades have shown tremendous improvements in the reinforced soil systems from using stiff to the more flexible reinforcing elements and geosynthetic reinforcements. In most of the investigations, the effect of reinforcement on the behaviour of soil mass was studied by pull out tests, direct shear tests, equivalent homogeneous method. Existing methods have been found to over predict the stress in the reinforcement, because of which, designs based on these methods are very uneconomical.

In this research, an effort has been made to improve our understanding of the internal stress-strain distribution in reinforced soil structures by carrying out linear and nonlinear analyses. Reinforced soil systems like Retaining wall, MSE Embankment, Reinforced soil foundation have been studied by developing programs in Fortran 77. The programs developed are RWPT-LIN, RWSW-LIN and RWSW-INT to study the unreinforced and reinforced soil retaining wall. Programs MSE-PRO and RSF-PRO have been developed to conduct studies on MSE wall and reinforced soil foundation. Linear and Nonlinear SSI of unreinforced soil have been carried out by developing programs SSI-LIN and SSI-NLIN. Linear and Nonlinear SSI of reinforced soil has been carried out by developing programs RSSI-LIN and RSSI-NLIN. The nonlinear analysis is being carried out using Drucker-

Prager constitutive relation. Goodman's interface element has been used in the linear analysis of Retaining wall. The results obtained from the developed programs are validated either with experimental studies or by comparing with previously published work.

Pilot studies have been carried out on unreinforced soil retaining wall and reinforced soil retaining wall subjected to point loads and self-weight separately. Studies have also been carried out on a mechanically stabilized MSE wall (AIT wall available in literature) to validate the developed program for linear and nonlinear analysis respectively.

For the reinforced soil foundation, the bearing capacity ratio, effect of top layer spacing on bearing capacity, variation of modulus of subgrade reaction of reinforced soil under square and circular footings resting on a reinforced granular bed overlying weak soil have been studied. Parametric studies have been carried out to study the effects of type, number and length of reinforcement layers on foundation soil both numerically and experimentally. The developed programs are working well for the retaining wall, the MSE wall, the foundation soil and the soil structure interaction for unreinforced and reinforced cases. It has also been validated with the experimental studies on reinforced foundation soil. All the studies carried out have proved that the results of nonlinear analysis are closer to experimental and field studies. Interface element is found to enhance the performance of the reinforced soil and increases the compressive stresses.

Soil structure Interaction (SSI) refers to the effect of soil and the foundation on its structure. It is the difference between the actual response of the structure and the response of the structure when fixed base is considered. In this connection, Soil structure interaction analysis for fixed base structure, unreinforced and reinforced soil foundation have been carried out both linearly and nonlinearly by adopting the macro element concept. Encouraging results have been obtained for the chosen structure and foundation soil. Fixed base structure shows very less moments, shear and axial forces as it is very

stiff. The structure resting on unreinforced soil shows the maximum displacements, moments, shear and axial forces. The structure resting on reinforced soil shows a reduction in displacements, moments, shear and axial forces which may promote more economical design of structures.

**Keywords: Finite Element method, Retaining wall, MSE Embankment, Reinforced soil foundation, macro element, Reinforced soil structure interaction (RSSI)**

## CONTENTS

<b>DECLARATION</b>	
<b>CERTIFICATE</b>	
<b>ACKNOWLEDGEMENTS</b>	
<b>ABSTRACT</b>	
<b>TABLE OF CONTENTS</b>	<b>i</b>
<b>LIST OF FIGURES</b>	<b>ix</b>
<b>LIST OF TABLES</b>	<b>xx</b>
<b>NOMENCLATURE</b>	<b>xxiii</b>
<b>CHAPTER 1 INTRODUCTION</b>	<b>1</b>
1.1 GENERAL	1
1.2 SCOPE AND PURPOSE OF THIS STUDY	2
1.3 RESEARCH OBJECTIVES	3
1.3.1 Research Objectives on Retaining Wall	4
1.3.2 Research Objectives on Reinforced Soil Foundation	4
1.3.3 Research Objectives on Mechanically Stabilised Earth Wall (AIT Wall)	5
1.3.4 Research Objectives on Soil-Structure Interaction Analysis of a 3d Frame with Isolated Footings Resting on Reinforced Soil	5
1.4 ORGANIZATION OF THE THESIS	6
1.5 SUMMARY	7
<b>CHAPTER 2 INTRODUCTION TO REINFORCED SOIL STRUCTURES</b>	<b>8</b>
2.1 GENERAL	8
2.2 INTRODUCTION TO REINFORCED SOIL	8
2.2.1 Theory of Reinforced Soil	8
2.2.2 Reinforced Soil Technology	9
2.2.2.1 York Method	9
2.2.2.2 Geosynthetic Reinforced Soil Retaining Wall (GRS-RW System)	9
2.2.2.3 Miscellaneous	10
2.2.3 Soil Reinforcing Materials	10
2.2.3.1 Extensible Reinforcements (Geosynthetic and related products)	11
2.2.3.2 Inextensible Reinforcements (Steel Bars / Fiber Glass)	11
2.2.3.3 Miscellaneous	11
2.2.4 Geosynthetics and their Applications	12
2.2.4.1 Identification of Geosynthetics	12
2.2.4.2 Types of Geosynthetics	13
2.2.4.3 Functions of Geosynthetics	14

2.2.5 Concepts of Reinforced Soil	16
2.2.5.1 Anisotropic Cohesion Concept	16
2.2.5.2 Enhanced Cohesion Concept	16
2.2.6 Reinforcing Mechanisms	17
2.2.7 Interaction of Geosynthetics with the Surrounding Soil	17
2.2.8 Facings in Reinforced Soil Structures	17
2.2.9 Applications of Reinforced Soil	18
2.2.9.1 Embankments/ Retaining Walls	18
2.2.9.2 Subsoil Reinforcement beneath Foundations	19
2.2.9.3 In-Situ Reinforcement (Soil Nailing/ Slope Stability/ Excavation)	19
<b>2.3 REINFORCED SOIL STRUCTURES STUDIED</b>	<b>20</b>
2.3.1.1 Behaviour of Reinforced Soil Structures	20
2.3.1.2 Failure Modes	20
2.3.2.3 Stability of GRS Retaining Structures	21
2.3.2.4 Design Considerations of GRS-RW	22
2.3.3 Mechanically Stabilised Earth Walls (MSE Walls)	23
2.3.3.1 Components of MSE Wall	23
2.3.3.2 Advantages of Mechanically Stabilized Earth (MSE) Walls	24
2.3.4 Reinforced Soil Foundation	25
2.3.4.1 General	25
2.3.4.2 Mechanism of Reinforcement in Reinforced Soil Foundation	26
2.3.4.3 Analytical Modelling of Reinforced Soil Foundation	27
2.3.5 Soil Structure Interaction/Reinforced Soil Structure Interaction	27
2.3.5.1 Derivation Approaches	28
2.3.5.2 Numerical Modelling of SSI analysis	29
<b>2.4 SUMMARY</b>	<b>30</b>
<b>2.5 FIGURES RELATED TO REINFORCED SOIL STRUCTURES</b>	<b>31</b>
<b>CHAPTER 3 LITERATURE REVIEW</b>	<b>39</b>
3.1 GENERAL	39
3.2 REVIEW OF STUDIES ON REINFORCED SOIL RETAINING WALL	40
3.2.1 Numerical / Analytical Studies on Retaining Wall	40
3.2.2 Experimental Investigations on Retaining Wall	46
3.3 REVIEW OF STUDIES ON REINFORCED SOIL FOUNDATION (RSF)	52
3.3.1 General	52
3.3.2 Experimental Investigations Reinforced Soil Foundation	53
3.3.2.1 Footings resting on reinforced sandy soil with geogrids as reinforcing material	53
3.3.2.2 Other reinforcing materials	57
3.3.2.3 Footings resting on reinforced c- $\phi$ soil using geogrid as the reinforcing material	61
3.3.2.4 Footings resting on reinforced c- $\phi$ soil using other reinforcing materials	64

3.3.3 Studies on Modulus of Subgrade Reaction of Soil	64
3.4 REVIEW OF STUDIES ON MECHANICALLY STABILISED EARTH WALLS	66
3.4.1 General	66
3.4.2 Experimental Investigations	67
3.4.2.1 Triaxial Tests	67
3.4.2.2 Direct Shear Tests	68
3.4.3 Role of Facing Elements in the Mechanically Stabilized Earth (MSE) Wall	68
3.4.4 Various Reinforced Soil Systems	69
3.4.4.1 Failure surface and line of maximum tension line with extensible reinforcements	69
3.4.4.2 Lateral pressure coefficients with extensible reinforcements	70
3.4.4.3 Failure surfaces and line of maximum tensions with extensible Reinforcements	70
3.4.4.4 Pullout resistance of grid reinforcements	70
3.4.4.5 Frictional and bearing resistances	71
3.4.4.6 Recent Studies in MSE Walls	71
3.5 REVIEW OF STUDIES ON STATIC SSI	73
3.5.1 General	73
3.5.2 Analytical Methods	73
3.6 SUMMARY OF LITERATURE REVIEW ON REINFORCED SOIL RETAINING WALLS AND MSE WALLS	76
3.6.1 Conclusions on Literature Review of Reinforced Soil Retaining Walls and MSE Walls	77
3.7 SUMMARY OF LITERATURE REVIEW ON REINFORCED SOIL FOUNDATION SOILS	77
3.7.1 Conclusions on Literature Review of Reinforced Soil Foundation	78
3.8 SUMMARY OF LITERATURE REVIEW ON REINFORCED SOIL FOUNDATION SSI / RSSI	78
3.8.1 Conclusions on Literature Review on SSI / RSSI	78
3.9 FUTURE DIRECTIONS FOR RESEARCH	79
3.10 VARIOUS FIGURES RELATED TO LITERATURE REVIEW	80
<b>CHAPTER 4 FINITE ELEMENT MODELLING OF REINFORCED SOIL SYSTEMS</b>	<b>84</b>
4.1 GENERAL	84
4.2 CONSIDERATIONS IN MODEL DEVELOPMENT	85
4.2.1 Elastic Models in Geotechnical Engineering	85
4.2.1.1 Linear elastic models	85
4.2.1.2 Cauchy elastic models	85
4.3 NON LINEAR ANALYSIS OF SOIL MEDIA	86
4.3.1 Incremental method	86
4.3.2 Iterative method	86



4.3.3 Causes of Nonlinear Behaviour	87
4.3.3.1 Geometric Nonlinearities	87
4.3.3.2 Material Nonlinearities	87
4.4 CONSTITUTIVE LAWS	87
4.4.1 Hypoelasticity	88
4.4.1.1 Hypoelastic Model	88
4.4.2 Mohr-Coulomb Model	91
4.4.3 Modified Cam-Clay (MCC) Model	91
4.4.4 Duncan-Chang (Hyperbolic) Model	92
4.4.5 Drucker Prager Model	92
4.5 PREVIOUS APPROACHES USED TO MODEL INTERFACES IN GEOLOGIC MATERIALS	93
4.5.1 Goodman et. al.'s Element (1968)	94
4.5.1.1 Interface Element Proposed by Goodman et al. (1968)	95
4.5.1.2 Interface "stresses"	97
4.5.1.3 Modes of interface Deformation	97
4.5.1.4 Analysis of a single Interface Element	98
4.5.2 Element Proposed By Ghaboussi et al. and Wilson (1973)	99
4.5.3 Element Proposed By Herrmann (1978)	99
4.6 MODELLING OF COMPONENTS	100
4.6.1 Modelling of Soil	100
4.6.2 Soil reinforcement	100
4.7 VARIOUS FIGURES RELATED TO FEM	105

## **CHAPTER 5 LINEAR ANALYSIS OF REINFORCED SOIL STRUCTURES**

	<b>109</b>
5.1 GENERAL	109
5.1.1 Linear Isotropic Elasticity	112
5.1.2 Two-Dimensional Specialisations of Elasticity	113
5.1.2.1 Plane Strain	113
5.1.2.2 Plane Stress	113
5.2 FORMULATION OF THE PROBLEM AND PROGRAMMING	114
5.2.1 Flow of Program / Algorithm	115
5.2.1.1 Subroutine BSSTIF	116
5.2.1.2 Subroutine ELESTRESS	117
5.3 FEM ANALYSIS & RESULTS OF RETAINING WALL UNDER POINT LOADS	117
5.3.1 Definition of Problem	117
5.3.2 Details of Soil studied	117
5.3.3 FEM Model and results of retaining wall for linear analysis under point loads obtained using developed software RWPT-LIN	118
5.3.3.1 Displacements in unreinforced and reinforced soil retaining wall under point loads	118
5.3.3.2 Stresses in unreinforced and reinforced soil retaining wall for Linear under point loads	119
5.3.3.3 Strains in unreinforced and reinforced soil retaining wall for	

Linear analysis under point loads	120
5.3.4 Fem Analysis & Results of Retaining Wall under Point Loads obtained using RWPT-LIN	122
5.4 FEM analysis and results of retaining wall under dead loads obtained using developed software RWSW-LIN and RWSW-INT	141
5.4.1 Horizontal stresses in soil for different cases under dead loads	141
5.4.2 Vertical Stresses in Soil for Different Cases under dead loads	142
5.4.3 Shear Stresses in Soil for Different Cases under dead loads	142
5.4.4 Strains in soil for Different Young's modulus of soil	143
5.4.5 Maximum Shear Stresses for Different Cases	143
5.4.6 Major Principal Stresses in Soil for Different Cases	143
5.4.7 Settlements and Displacements in Soil for Different Cases	144
5.4.8 Fem Analysis & Results of Retaining Wall Under Dead Loads (Self Weight)	146
5.4.8.1 Horizontal Stresses in Soil for Different Cases	146
5.4.8.2 Vertical Stresses in Soil for Different Cases	148
5.4.8.3 Shear Stresses in Soil for Different Cases	151
5.4.8.4 Maximum Shear Stresses in Soil for Different Cases	153
5.4.8.5 Major Principal Stresses in Soil For Different Cases	156
5.5 VARIOUS TABLES RELATED TO STUDIES ON RETAINING WALL	160
5.6 SUMMARY OF STUDIES ON LINEAR ANALYSIS OF REINFORCED SOIL RETAINING WALL UNDER POINT LOADS	168
5.7 SUMMARY OF STUDIES ON LINEAR ANALYSIS OF REINFORCED SOIL RETAINING WALL UNDER DEAD LOADS	170
<b>CHAPTER 6 STUDIES ON MECHANICALLY STABILIZED EARTH WALL (MSE WALL)</b>	<b>172</b>
6.1 GENERAL	172
6.2 DETAILS OF THE EXPERIMENTAL PROGRAMME CHOSEN FOR NUMERICAL STUDY	173
6.2.1 Case Study	173
6.3 CONSTRUCTION OF MSE WALL AND ANALYSIS (Using Program REA)	174
6.4 FEM ANALYSIS AND RESULTS	176
6.4.1 FEM Model	176
6.4.2 Results and Discussions	177
6.4.3 Figures Plotted from MSE (AIT) wall studies	179
6.4.4 GRAPHS PLOTTED FROM MSE (AIT) WALL STUDIES	182
6.4.5 TABLES USED IN AND OBTAINED FROM MSE (AIT) WALL STUDIES	193
6.4.6 Summary of Results on MSE (AIT) Wall	199
6.4.7 CONCLUSIONS OF STUDIES ON MSE WALL	200
<b>CHAPTER 7 STUDIES ON REINFORCED FOUNDATION SOIL</b>	<b>202</b>
7.1 GENERAL	202
7.2 EXPERIMENTAL STUDY	203

7.2.1 Experimental Programme	203
7.2.2 Properties of materials used	203
7.2.3 Test Procedure	204
7.2.4 Test Details	205
7.2.5 Results of Experimental Studies	206
7.2.5.1 Improvement in Bearing Capacity	206
7.2.5.2 Effect of Reinforcement on u/B ratio and BCR values	208
7.2.6 Figures Plotted In Reinforced Soil Foundation	209
7.2.7 Graphs Plotted In Reinforced Soil Foundation	212
<b>7.3 STUDIES ON EFFECT OF REINFORCED SOIL FOUNDATION ON MODULUS OF SUBGRADE REACTION</b>	<b>218</b>
7.3.1 General	218
7.3.2. Determination of modulus of subgrade reaction of soil “ks”	219
7.3.3 Results and Discussions	220
7.3.3.1 Determination of ultimate bearing capacity using model plate Load test results	220
7.3.3.2 Determination of subgrade reaction “k <sub>s</sub> ” using experimental Results	220
7.3.4 Graphs Plotted in Reinforced Soil Foundation	222
<b>7.4 COMPARITIVE STUDIES ON LOAD SETTLEMENT CHARACTERISTICS OF SQUARE FOOTING RESTING ON GEOSYNTHETIC REINFORCED LOOSE SAND</b>	<b>226</b>
7.4.1 Details of Various Studies Carried out on Foundation Soil	226
7.4.2 Numerical Studies (By Developing Software RSF-PRO)	226
7.4.3 FEM Model	227
7.4.4 Geosynthetic Reinforcement Modelling	227
7.4.5 Soil Modelling	227
7.4.6 Modelling of Square Footing	227
7.4.7 Results of Numerical and Experimental Studies for varying number of reinforcement layers	228
7.4.8 Conclusions drawn from the study	229
7.4.9 Graphs Plotted In Numerical Studies Reinforced Soil Foundation	230
7.4.10 Tables Used In Reinforced Soil Foundation	233
 <b>CHAPTER 8 REINFORCEDSOIL-STRUCTURE-INTERACTION ANALYSIS OF THREE DIMENSIONAL FRAMES</b>	 <b>240</b>
8.1 Introduction to SSI and RSSI	240
8.2 Linear SSI analysis of space frame-Footing -soil system	244
8.2.1 Problem Definition:	244
8.2.2 Discretisation	244
8.2.3 Validity of the proposed physical model	245
8.3 Linear RSSI analysis of space frame-footing -soil system	245
8.4 Results of Linear SSI and RSSI analyses and discussions	248
8.4.1 Displacements in linear analyses	248

8.4.1.1 Displacements in Linear SSI analysis	248
8.4.1.2 Displacements in Linear RSSI analysis	248
8.4.2 Stresses in soil	249
8.4.2.1 Stresses in soil in Linear SSI analysis	249
8.4.2.2 Stresses in soil in Linear RSSI analysis	250
8.4.3 Stress resultants in members of 3-Dimensional frame	250
8.4.3.1 Axial and shear forces in beams.	251
8.4.3.2 Axial and Shear forces in Columns	253
8.4.3.3 Bending moments along beams	254
8.4.3.4 Bending moments in columns	255
8.4.4 Discussions on linear SSI and RSSI analyses	256
8.4.4.1 Discussion on displacements in soil	256
8.4.4.2 Discussion on stresses in soil	256
8.4.5 Figures and Graphs plotted in Linear SSI and RSSI Analysis	258
8.4.6 Tables Related To Linear Analysis in SSI and RSSI	276
8.5 NON-LINEAR SSI AND RSSI ANALYSES OF SPACE FRAME-FOOTING –	
SOIL SYSTEM	284
8.5.1 Results of Nonlinear SSI and RSSI analyses and discussions	285
8.5.1.1 Deformation and settlements in nonlinear SSI analysis	285
8.5.1.2 Deformation and settlements in Nonlinear RSSI analysis	286
8.5.1.3 Discussion on Displacements in Non-Linear Analyses	286
8.5.2 Stresses in soil	286
8.5.2.1 Stresses in soil in Nonlinear SSI analysis	286
8.5.2.2 Stresses in soil in Non-Linear RSSI analysis	287
8.5.2.3 Discussion on stresses in Non-Linear Analyses	287
8.5.3 Stress resultants in members of 3-Dimensional frame	288
8.5.3.1 Axial and shear forces in beams	288
8.5.3.2 Axial and Shear forces in Columns	290
8.5.3.3 Bending moments in beams	291
8.5.3.4 Bending moments in columns	292
8.5.4 Graphs plotted in Non-Linear SSI and RSSI Analyses	294
8.5.5 Tables related to nonlinear analysis of SSI and RSSI	302
8.6 Summary	311
<b>CHAPTER 9 CONCLUSIONS</b>	<b>314</b>
9.1 GENERAL	314
9.2 CONCLUSIONS ON STUDIES ON RETAINING WALLS	314
9.2.1 Linear Analysis of Reinforced Soil Retaining Wall under Point Loads	314
9.2.2 Linear Analysis of Reinforced Soil Retaining Wall under Dead Loads	315
9.3 CONCLUSIONS ON STUDIES CARRIED OUT ON MSE WALL	317
9.4 CONCLUSIONS ON STUDIES CARRIED OUT ON REINFORCED FOUNDATION SOIL	318
9.4.1 Results of Experimental Studies on Reinforced soil Foundation	318
9.4.2 Effect of Reinforcement on u/b ratio and BCR values	318

9.4.3 Conclusions on Determination of modulus of subgrade reaction of Reinforced soil foundation “ks”	318
9.4.4 Conclusions on Numerical and Experimental studies carried out on reinforced soil foundation	319
9.5 CONCLUSIONS ON STUDIES CARRIED OUT ON SSI and RSSI	320
9.5.1 Linear Interactive Analysis of Space Frame-Footing -Soil System	320
9.5.2 Non-Linear Interactive Analysis of Space Frame-Footing -Soil System	321
9.6 GENERAL CONCLUSIONS	322
9.7 SCOPE FOR FUTURE WORK	325
<b>APPENDIX</b>	326
<b>REFERENCES</b>	346
<b>JOURNAL/CONFERENCE PUBLICATIONS</b>	357
<b>CURRICULUM VITAE</b>	359

## LIST OF FIGURES

<b>Figure No.</b>	<b>Title</b>	<b>Page .No</b>
2.1	Typical Reinforced Earth system (Schlosser and Delage, 1987)	31
2.2	Schematic diagram of typical reinforced soil systems Geosynthetic reinforced soil-rigid wall (GRS-RW) system (Tatsuoka, 1992)	31
2.3	Typical in-situ soil- Reinforcing Techniques	31
2.4	Stress-strain characteristics of typical reinforcing material	32
2.5	Typical geogrids used as soil reinforcements (John 1987, Gu-Jie,2011)	32
2.6	Geogrids	32
2.7	Geomembranes	33
2.8	Geotextiles	33
2.9	Geosynthetics as separators	33
2.10	Geosynthetics as Reinforcement	33
2.11	Geosynthetics as Drains	33
2.12	Reinforced and unreinforced Samples in triaxial tests	34
2.13	Anisotropic Cohesion and Enhanced Cohesion Concepts	34
2.14	Reinforcement mechanisms (Chen, 2007)	34
2.15	Currently used typical facings in reinforced soil structures	35

2.16	Embankment reinforcing modes (Ingold, T.S.,1982)	36
2.17	Critical zones beneath reinforced foundations (Fukuda et al., 1982)	36
2.18	Typical in-situ soil-reinforcing techniques	36
2.19	Illustrations of multilayer geosynthetic slope reinforcement	37
2.20	Components of a Reinforced Earth wall	37
2.21	Reinforced retaining wall systems using Geosynthetics	38
2.22	Common shapes for potential failure surfaces for Limit Equilibrium Analysis techniques	38
2.23	Primary MSE wall Components (Alzamora, 2009)	38
3.1	Influence of reinforcements on potential failure lines (Basset and Last, 1978)	80
3.2	Observed tensile force distributions along reinforcement corresponding to different facing rigidities.	80
3.3	Components of Reinforced Soil Retaining Wall	81
3.4	Geosynthetic reinforced soil foundation (Farsakh et. al, 2013)	81
3.5	Typical MSE Wall Details ( <a href="http://www.fhwa.dot.gov">www.fhwa.dot.gov</a> )	82
3.6	Soil Structure Interaction ( <a href="http://www.nptel.ac.in">www.nptel.ac.in</a> )	82
4.1	Incremental Method ( Jayashree, 2008)	105
4.2	A fishing rod demonstrates geometric nonlinearity ( <a href="http://www.ansys.stuba.sk">www.ansys.stuba.sk</a> )	105
4.3	Hypoelastic Behaviour ( Kok Sien Ti, 2009)	105
4.4	Mohr-Coulomb Yield surface in Principal Stress space( Kok Sien Ti, 2009)	106
4.5	Drucker Prager Yield surface in Principal Stress space	106
4.6	Interface Element after Goodman et al. (1968)	106
4.7	Simple Constitutive Model of an Interface (Jianchao, 1993)	107
4.8	Single Goodman et al.'s (1968) Interface Element Example	107
4.9	Deformations for Goodman et al.'s (1968) Interface Element for special load case	107

4.10	Unidimensional Elements (Desai, 2012)	107
4.11	(a) Element in physical coordinates. (b) Element in natural coordinates. ( <a href="http://www.what-when-how.com">www.what-when-how.com</a> )	108
4.12	Different noded elements	108
5.1a	Details of Retaining wall being studied subjected to Point Loads	122
5.1b	Details of Retaining wall being studied subjected to Dead Loads	122
5.2	Lateral Movements predicted in unreinforced and reinforced soil retaining wall at $x=9.00\text{m}$ for Linear Analysis under point loads obtained using RWPT-LIN	123
5.3	Lateral Displacements predicted in unreinforced and reinforced soil retaining wall at $x=9.00\text{m}$ for Linear analysis under point loads obtained using RWPT-LIN	123
5.4	Lateral Movements predicted in unreinforced and reinforced soil retaining wall at $x=12.00\text{ m}$ for Linear analysis under point loads obtained using RWPT-LIN	124
5.5	Vertical Settlements predicted in unreinforced and reinforced soil retaining wall at $x=27.00\text{m}$ for Linear analysis under point loads obtained using RWPT-LIN	124
5.6	Vertical settlements predicted in unreinforced and reinforced soil retaining wall at $y =8.70\text{m}$ for Linear analysis under point loads obtained using RWPT-LIN	125
5.7	Vertical settlements predicted in unreinforced and reinforced soil retaining wall at $y =8.10\text{m}$ for Linear analysis under point loads obtained using RWPT-LIN	125
5.8	Vertical Settlements predicted in unreinforced and reinforced soil retaining wall at $y =7.80\text{m}$ for Linear analysis under point loads obtained using RWPT-LIN	126
5.9	Vertical Settlements predicted in unreinforced and reinforced soil retaining wall at $y =6.90\text{m}$ for Linear analysis under point loads obtained using RWPT-LIN	126
5.10	Vertical Settlements predicted in unreinforced and reinforced soil retaining wall at $y =0.6\text{m}$ for Linear analysis under point loads obtained using RWPT-LIN	127
5.11	Settlements (m) at different levels predicted in unreinforced soil retaining wall for Linear analysis under point loads obtained using RWPT-LIN	127
5.12	Settlements (m) predicted at different levels in reinforced soil retaining wall for Linear analysis under point loads obtained using RWPT-LIN	128
5.13	Horizontal Stresses (kPa) predicted in unreinforced soil retaining wall for Linear analysis under point loads obtained using RWPT-LIN	128
5.14	Horizontal Stresses (kPa) predicted in reinforced soil retaining wall for Linear analysis under point loads obtained using RWPT-LIN	129



5.15	Horizontal Stresses (MPa) in unreinforced soil retaining wall in STAAD Pro for Linear analysis under point loads	129
5.16	Vertical Stresses (kPa) predicted in unreinforced soil retaining wall for Linear analysis under point loads using RWPT-LIN	130
5.17	Vertical Stresses (kPa) in reinforced soil retaining wall for Linear analysis under point loads using RWPT-LIN	130
5.18	Vertical Stresses (MPa) for unreinforced soil retaining wall, $E_s=12\text{MPa}$ in STAAD Pro for Linear analysis under point loads	131
5.19	Shear Stresses (kPa) predicted in unreinforced soil retaining wall for Linear analysis under point Loads using RWPT-LIN	131
5.20	Shear Stresses (kPa) predicted in reinforced soil retaining wall for Linear analysis under point loads using RWPT-LIN	132
5.21	Shear stresses (MPa) in reinforced soil retaining wall for Linear analysis under point loads in STAAD Pro	132
5.22	Maximum Shear Stresses (kPa) in reinforced soil retaining wall for Linear analysis under point loads	133
5.23	Horizontal Strains predicted at $Y=9.00\text{m}$ in a retaining wall for Linear analysis under point loads obtained using RWPT-LIN	133
5.24	Horizontal Strains predicted at $Y=6.00\text{m}$ in a retaining wall for Linear analysis under point loads obtained using RWPT-LIN	134
5.25	Vertical Strains predicted at $Y=9.00\text{m}$ in a retaining wall for Linear analysis under point loads obtained using RWPT-LIN	134
5.26	Vertical Strains predicted at $Y=7.5\text{m}$ in a retaining wall for Linear analysis under point loads obtained using RWPT-LIN	134
5.27	Vertical Strains predicted at $Y=6.00\text{m}$ in a retaining wall for Linear analysis under point loads obtained using RWPT-LIN	135
5.28	Shear Strains predicted at $Y=9.00\text{m}$ in a retaining wall for Linear analysis under point loads obtained using RWPT-LIN	135
5.29	Shear Strains predicted at $Y=6.00\text{m}$ in a retaining wall for Linear analysis under point loads obtained using RWPT-LIN	136
5.30	Shear Strains predicted at $Y=0.3\text{m}$ in a retaining wall for Linear analysis under point loads obtained using RWPT-LIN	136
5.31	Horizontal strains predicted at all depths in a reinforced soil retaining wall for Linear analysis under point loads obtained using RWPT-LIN	137
5.32	Horizontal strains predicted in an unreinforced soil retaining wall for Linear analysis under point loads obtained using RWPT-LIN	137
5.33	Vertical Strains predicted in an unreinforced soil retaining wall at all depths for Linear analysis under point loads obtained using RWPT-LIN	138
5.34	Vertical Strains predicted in a reinforced soil retaining wall for Linear analysis under point loads obtained using RWPT-LIN	138
5.35	Shear strains predicted in an unreinforced soil retaining wall for Linear analysis under point loads obtained using RWPT-LIN	139

5.36	Shear Strains predicted in a reinforced soil retaining wall for Linear analysis under point loads obtained using RWPT-LIN	139
5.37	Major Principal Stresses (kPa) predicted in unreinforced soil retaining wall for Linear analysis under point loads using RWPT-LIN	140
5.38	Major Principal Stresses (MPa) in unreinforced soil retaining wall in STAAD Pro under point loads for Linear analysis	140
5.39	Horizontal Stresses (kPa) predicted in unreinforced soil retaining wall for Linear analysis under self-weight, $E_s = 21\text{MPa}$ obtained using RWSW-LIN	146
5.40	Horizontal Stresses (kPa) predicted in reinforced soil retaining wall for Linear analysis under self-weight for $E_s/E_r = 0.001$ , 100% Coupling obtained using RWSW-LIN	146
5.41	Horizontal Stresses (kPa) predicted in reinforced soil retaining wall for Linear analysis under self weight, for $E_s/E_r = 0.001$ , $k_s/E_s = 10+E02$ obtained using RWSW-INT	147
5.42	Horizontal Stresses (kPa) predicted in reinforced soil retaining wall for Linear analysis under self weight for $E_s/E_r = 0.001$ , $k_s/E_s = 10+E03$ obtained using RWSW-INT	147
5.43	Horizontal Stresses (kPa) predicted in reinforced soil retaining wall for Linear analysis under self weight for $E_s/E_r = 0.001$ , $k_s/E_s = 10+E04$ obtained using RWSW-INT	148
5.44	Vertical stresses (kPa) predicted in unreinforced soil retaining wall for Linear analysis under self weight for $E_s = 21\text{MPa}$ using RWSW-INT	148
5.45	Vertical stresses (kPa) predicted in reinforced soil retaining wall under self weight for Linear analysis for $E_s/E_r = 0.001$ , 100% Coupling obtained using RWSW-LIN	149
5.46	Vertical stresses (kPa) predicted in reinforced soil retaining wall under self weight for Linear analysis under self weight for $E_s/E_r = 0.001$ , $k_s/E_s = 10+E02$ obtained using RWSW-INT	149
5.47	Vertical stresses (kPa) predicted in reinforced soil retaining wall under self weight for Linear analysis for $E_s/E_r = 0.001$ , $k_s/E_s = 10+E03$ obtained using RWSW-INT	150
5.48	Vertical stresses (kPa) predicted in reinforced soil retaining wall under self weight for Linear analysis for $E_s/E_r = 0.001$ , $k_s/E_s = 10+E04$ obtained using RWSW-INT	150
5.49	Shear stresses (kPa) predicted in unreinforced soil retaining wall under self weight for Linear analysis for $E_s = 21\text{ MPa}$ obtained using RWSW-LIN	151
5.50	Shear stresses (kPa) predicted in reinforced soil retaining wall for Linear analysis under self weight for $E_s/E_r = 0.001$ , 100% coupling using RWSW-LIN	151
5.51	Shear stresses (kPa) predicted in reinforced soil retaining wall for Linear analysis under self weight for $E_s/E_r = 0.001$ and interface $K_s/E_s = 10+E02$ obtained using RWSW-INT	152
5.52	Shear stresses (kPa) predicted in reinforced soil retaining wall for Linear analysis under self weight for $E_s/E_r = 0.001$ , $k_s/E_s = 10+E03$ obtained using RWSW-INT	152

5.53	Shear stresses (kPa) predicted in reinforced soil retaining wall under self weight for Linear analysis for $E_s/E_r=0.001$ , $k_s/E_s=10+E04$ obtained using RWSW-INT	153
5.54	Maximum Shear stresses (kPa) predicted in unreinforced soil retaining wall for Linear analysis under self weight for $E_s=21\text{MPa}$ obtained using RWSW-LIN	153
5.55	Maximum Shear stresses (kPa) predicted in reinforced soil retaining wall for Linear analysis under self weight for $E_s/E_r=0.001$ and 100% Coupling obtained using RWSW-LIN	154
5.56	Maximum Shear stresses (kPa) predicted in reinforced soil retaining wall for Linear analysis under self weight for $E_s/E_r=0.001$ , $k_s/E_s=10+E02$ obtained using RWSW-INT	154
5.57	Maximum Shear stresses (kPa) predicted in reinforced soil retaining wall for Linear analysis under self weight for $E_s/E_r=0.001$ , $k_s/E_s=10+E03$ obtained using RWSW-INT	155
5.58	Maximum Shear stresses predicted in reinforced soil retaining wall for Linear analysis under self weight for $E_s/E_r=0.001$ , $k_s/E_s=10+E04$ obtained using RWSW-INT	155
5.59	Major Principal Stresses (kPa) predicted in unreinforced soil retaining wall for Linear analysis, $E_s=21\text{MPa}$ obtained using RWSW-LIN	156
5.60	Major Principal Stresses (kPa) predicted in reinforced soil retaining wall for Linear analysis under self weight for, $E_s/E_r=0.001$ , 100% Coupling obtained using RWSW-LIN	156
5.61	Major Principal Stresses (kPa) predicted in reinforced soil retaining wall for Linear analysis under self weight, $E_s/E_r=0.001$ , $k_s/E_s=10+E02$ obtained using RWSW-INT	157
5.62	Major Principal Stresses (kPa) predicted in reinforced soil retaining wall for Linear analysis under self weight, $E_s/E_r=0.001$ , $k_s/E_s=10+E03$ obtained using RWSW-INT	157
5.63	Major Principal Stresses (kPa) predicted in reinforced soil retaining wall for Linear analysis under self weight, $E_s/E_r=0.001$ , $k_s/E_s=10+E04$ obtained using RWSW-INT	158
5.64	Horizontal Displacements predicted in reinforced soil retaining wall for Linear analysis under self weight, $E_s/E_r=0.001$ obtained using RWSW-LIN and RWSW-INT	158
5.65	Vertical settlements of unreinforced and reinforced soil retaining wall for Linear analysis under self weight, $E_s/E_r=0.001$ obtained using RWSW-LIN and RWSW-INT	159
6.1	MSE (AIT) Wall with steel wire facing, Shivashankar (1991) used in Experimental and Numerical studies(MSE-PRO)	179
6.2	MSE (AIT) Wall without steel wire facing, Shivashankar (1991) used in Numerical studies (MSE-PRO)	179
6.3	MSE (AIT) Wall, Shivashankar (1991) used in Experimental studies	180
6.4	FEA Model of MSE (AIT) Wall representing mesh co-ordinates,	180

	Shivashankar (1991) used in Numerical studies (MSE-PRO)	
6.5	Plan of MSE (AIT) Wall showing three sections of soil along with strain gauges fitted, Shivashankar (1991)	181
6.6	Settlements at 0.45m below Ground Surface obtained from different studies with strain gauges between 15.0m to 20.10m	182
6.7	Settlements at 3.00m below Ground Surface obtained from different studies with strain gauges between 15.0m to 20.10m	182
6.8	Settlements at 6.00m below Ground Surface obtained using different studies (15.0m to 20.10m) with and without facing	183
6.9	Settlements at 3.00m and 6.00m from Ground Surface obtained from MSE-PRO by adopting non-linear analysis with and without facing	183
6.10	Settlements at 0.45m, 3.00m and 6.00m depths from Ground Surface plotted using REA software and Experimental studies depths, Shivashankar (1991)	184
6.11	Settlements (m) predicted using developed software using MSE-PRO at different levels for the MSE wall without facing	185
6.12	Settlements (m) predicted using developed software using MSE-PRO at different levels for the MSE (AIT) wall with RC facing	186
6.13	Reference X-Y axes for the AIT wall	186
6.14	Lateral displacements predicted using MSE-PRO by adopting non-linear analysis at x= 0m (foundation soil)	187
6.15	Lateral displacements predicted using MSE-PRO by adopting non-linear analysis at x=15.0m and x=16.20m	187
6.16	Lateral displacements predicted using MSE-PRO adopting linear and non-linear analysis at x=18.20m and x=21.00m	188
6.17	Lateral displacements predicted using MSE-PRO adopting non-linear analysis with and without wire facing at x=18.30m, x=18.60m and x=19.20m	188
6.18	Lateral Displacements observed and predicted using MSE-PRO by adopting non-linear analysis at x=0.0m and x=35.1m	189
6.19	Lateral Displacements predicted at x=21.00m using MSE-PRO by adopting non-linear analysis	189
6.20	Lateral Displacements predicted using MSE-PRO by adopting linear analysis at x=0.0m, x=5.1m, x=9.0m, x=10.2m	190
6.21	Lateral Displacements predicted using MSE-PRO by adopting non-linear analysis at x=0.0m, x=5.1m, x=9.0m, x=10.2m	190
6.22	Shear Stresses (kPa) predicted in MSE Wall at all levels without facing obtained using MSE-PRO by adopting non-linear analysis	191
6.23	Shear Stresses (kPa) predicted in MSE Wall at all levels with RC facing obtained using MSE-PRO by adopting non-linear analysis	191
6.24	Shear Stresses (kPa) predicted in MSE Wall at all levels with wire facing obtained using MSE-PRO by adopting non-linear analysis	192

6.25	Vertical Stresses (kPa) predicted in MSE Wall at all levels with wire facing obtained using MSE-PRO by adopting non-linear analysis	192
7.1	Sectional Elevation of geogrids placed on granular bed	209
7.2	Sectional Elevation of geogrids placed on weak foundation bed	209
7.3	Geometric parameters for reinforced soil foundation (Gu-Jie, 2011)	210
7.4	Photographs of the Test Setup	210
7.5	Plan of two sizes of Geosynthetics (0.80m x 0.80m, 8B x 8B) and (0.40m x 0.40m, 4B x 4B)	211
7.6	Plan of two sizes of Geosynthetics (0.80m x 0.80m, 8B x 8B) and (0.40m x 0.40m, 4B x 4B)	211
7.7	Settlement/width ratio of footing vs. stresses for unreinforced and reinforced granular bed overlain by weak silty soil under circular footing (Geogrid of size 0.40m x 0.40m, 4B x 4B)	212
7.8	Settlement/width ratio of footing vs. stresses for unreinforced and reinforced granular bed overlain by weak silty soil under square footing (Size of Geogrid 0.4m x 0.4m, 4B x 4B)	212
7.9	Settlement/width of footing ratio vs. stresses for unreinforced and reinforced granular bed overlain by weak silty soil under circular footing (Geotextile 0.4m x 0.4m, 4B x 4B))	213
7.10	Settlement/width ratio of footing vs. stresses for unreinforced and reinforced granular bed overlain by weak silty soil under circular footing (Geotextiles of size 0.8m x 0.8m, 8B x 8B)	213
7.11	Settlement/width ratio of footing vs. stresses for unreinforced and reinforced granular bed overlain by weak silty soil under square footing (Geotextiles of size 0.8m x 0.8m, 8B x 8B)	214
7.12	Settlement/width ratio of footing vs. stresses for Loose and Dense Sand for Geogrids (0.4m x 0.4m, 4B x 4B) under square footing	214
7.13	Settlement/width ratio of footing vs. stresses for unreinforced and reinforced granular bed overlain by weak silty soil under square footing ( Size of Geotextile 0.8m x 0.8m, 8B x 8B)	215
7.14	Settlement/width ratio of footing vs. stresses for Loose and Dense Sand for Geogrids (0.4m x 0.4m, 4B x 4B) under square footing	215
7.15	Settlement/width of footing ratio vs. stresses for unreinforced and reinforced granular bed overlain by weak silty soil under square and circular footings (Geotextiles 4B x 4B and 8B x 8B)	216
7.16	Settlement/width of footing ratio vs. stresses for unreinforced and reinforced granular bed overlain by weak silty soil under square and circular footing (Geogrids 4B x 4B and 8B x 8B)	216
7.17	Bearing Capacity Ratio for different u/B ratios for reinforced granular bed overlain by weak silty soil under square and circular footings (Geogrids and Geotextiles 4B x 4B and 8B x 8B)	217

7.18	BCR vs Number of Reinforcement Layers for reinforced granular bed overlain by weak silty soil under square and circular footings(Geogrid and Geotextiles 4B x 4B and 8B x 8B)	217
7.19	Semi-log graph of Settlement vs. stresses for unreinforced and reinforced granular bed overlain by weak silty soil under circular footings (Geotextile 0.40 x 0.40, 4B x 4B) (To find ks)	222
7.20	Semi-log graph of Settlement vs. stresses for unreinforced and reinforced granular bed overlain by weak silty soil under square footing (Geogrid 0.40 x 0.40m, 4B x 4B) (To find ks)	222
7.21	Semi-log graph of Settlement vs. stresses for unreinforced and reinforced granular bed overlain by weak silty soil under square footing (Geotextile 0.40mx0.40m, 4B x 4B) (To find ks)	223
7.22	Semi-log graph of Settlement vs. stresses for unreinforced and reinforced granular bed overlain by weak silty soil under square footing (Geogrid 0.8m x0.8m, 8B x 8B) (To find ks)	223
7.23	Semi-log graph of Settlement vs. stress for unreinforced and reinforced granular bed overlain by weak silty soil under square footing (Geogrid 0.80 x 0.80m, 8B x 8B) (To find ks)	224
7.24	Variation of ks for unreinforced and reinforced granular bed overlain by weak silty soil under circular footing (Geogrid / Geotextile 4B x 4B and 8B x 8B)	224
7.25	Variation of ks for unreinforced and reinforced granular bed overlain by weak silty soil under square and circular footing (Geotextile 4B x 4B and 8B x 8B)	225
7.26	Variation of ks for unreinforced and reinforced granular bed overlain by weak silty soil Geogrid/Geotextile under circular and square footing for a size of (0.80m x 0.80m, 8B x 8B)	225
7.27	Typical mesh of the model Plate Load test	229
7.28	Settlement/width of footing vs. Stress Graphs for reinforced granular bed underlain by loose sand (1 layer of Geotextile 4B x 4B)	229
7.29	Settlement/width of footing vs. Stress Graphs for reinforced granular bed underlain by loose sandy soil (2 layers of Geotextiles 4B x 4B)	230
7.30	Settlement /width ratio vs. Stress Graphs for reinforced granular bed underlain by loose sand (3 layers of Geotextiles, 4B x 4B)	230
7.31	Settlement /width vs. stresses for reinforced granular bed underlain by loose sand (4 layers of Geotextiles, 4B x 4B)	231
8.1	Structure-footing-soil system (Swamy et al., 2011)	258
8.2	Details of quarter frame (Swamy et. al. (2011))	259
8.3	(a) Frame-isolated footing-soil system. (b) Structure foundation system. (c) Reference axis and arrangement of isolated footings	260

8.4	Details of element types (a) Euler-Bernoulli beam element used for beams and columns (b) Brick element for soil (c) Plate element used for footing	261
8.5	Comparative settlements in mm at the centre in the present work and the referred work (Swamy et. al.(2011))	262
8.6	Frame-footing-reinforcement module	262
8.7	Arrangement of geogrid (a) Modelling of column-foundation- Geogrid (b) soil-geogrid arrangement represented as macroelement in RSSI analysis	263
8.8	Details of Geogrid and Macro element (a) Geogrid of size 1m x 1m with apertures (b) Geometrical details of geogrid (c) Geogrid represented as macro element of size 1m x 1m	264
8.9	(a) Footing and geogrid arrangements (b) FEM modelling of geogrid	265
8.10	Evaluation of first column elements of stiffness matrix of macro-element	265
8.11	Vertical displacements in mm in Linear SSI analysis (a) Vertical displacements at foundation level (b) Contours of vertical displacements at footing level (c) Vertical displacements along longitudinal section	266
8.12	Horizontal displacements in mm in linear SSI analysis: (a) and (b) longitudinal displacements at foundation level (c) and (d) Transverse displacements at foundation level	267
8.13	Vertical displacements in mm in Linear RSSI analysis (a) Vertical displacements at foundation level (b) Contours of vertical displacements at footing level. (c) Vertical displacements along longitudinal section at centre.	268
8.14	Horizontal displacements in mm in linear RSSI analysis (a) and (b) longitudinal displacements at foundation level (c) and (d) transverse displacements at foundation level	269
8.15	Vertical stresses in $N/mm^2$ linear SSI analysis (a) Contours of vertical stresses at footing level (b) Vertical stresses along longitudinal section at centre (c) Vertical stresses at foundation level along longitudinal sections for different values of Z/L	270
8.16	Horizontal stresses in $N/mm^2$ in linear SSI analysis (a) and (b) longitudinal stresses at foundation level (c) and (d) Transverse stresses at foundation level	271
8.17	Vertical stresses in $N/mm^2$ in linear RSSI analysis (a) Contours of vertical stresses footing level (b) Vertical stresses along longitudinal section at centre (c) Vertical stresses at foundation level along longitudinal sections for different values of Z/L	272
8.18	Horizontal stresses in linear RSSI analysis (a) and (b) longitudinal stresses at foundation level (c) and (d) transverse stresses at foundation level	273

8.19	Horizontal displacements in mm in linear RSSI analysis longitudinal displacements at foundation level (b) transverse displacements at foundation level	(a) 274
8.20	Vertical displacements in mm in linear SSI and RSSI analyses at foundation level along longitudinal line at $Z/L=0.0$	275
8.21	Vertical displacements in mm in non-linear SSI analysis (a) Vertical displacements at foundation level (b) Contours of vertical displacements at footing level (c) Vertical displacements along longitudinal section at centre.	294
8.22	Horizontal displacements in mm in non-linear SSI analysis (a) and (b) Longitudinal displacements at foundation level (c) and (d) Transverse displacements at foundation level	295
8.23	Vertical displacements in mm in Non-Linear RSSI analysis (a) Vertical displacements at foundation level along longitudinal directions. (b) Contours of vertical displacements at footing level. (c) Vertical displacements along longitudinal section at centre.	296
8.24	Horizontal displacements in mm in Non-linear RSSI analysis (a) and (b) longitudinal displacements at foundation level (c) and (d) transverse displacements at foundation level	297
8.25	Vertical stresses in Non-linear SSI analysis (a) Contours of vertical stresses at footing level (b) Vertical stresses along longitudinal section at centre (c) Vertical stresses at foundation level along longitudinal sections for different values of $Z/L$	298
8.26	Horizontal stresses $N/mm^2$ in Non-linear SSI analysis (a) and (b) longitudinal stresses at foundation level (c) and (d) Transverse stresses at foundation	299
8.27	Vertical stresses in Non-linear RSSI analysis (a) Contours of vertical stresses at footing level (b) Vertical stresses along longitudinal section at centre (c) Vertical stresses at foundation level along longitudinal sections for different values of $Z/L$	300
8.28	Horizontal stresses in Non-linear RSSI analysis (a) and (b) longitudinal stresses at foundation level (c) and (d) Transverse stresses at foundation le	301



## LIST OF TABLES

<b>Table No.</b>	<b>Title</b>	<b>Page .No</b>
1.3	Cases of study carried out on reinforced soil retaining wall	4
3.1	Details of various studies carried out by different researchers in SSI (Prakash et. al.,2016)	83
5.1	Input for the programs RWPT-LIN, RWSW-LIN and RWSW-INT	160
5.2	Predicted Lateral Displacements(m) and Settlements (m) under Point loads for unreinforced and einforced soil vertical cut at x=12.00m at all levels of y using RWPT-LIN	161
5.3	Predicted Horizontal, Vertical and Shear Strains for Unreinforced and reinforced soil under Point Loads at y=9.00m using RWPT-LIN	162
5.4	Comparison of Predicted Horizontal Stresses (kPa)between Unreinforced, Reinforced(100% coupling) soil, reinforced also considering Different interfaces using RWSW-LIN	163
5.5	Comparison of Predicted vertical Stresses (kPa)between Unreinforced, Reinforced(100% coupling) soil, reinforced also considering Different interfaces using RWSW-LIN	164
5.6	Predicted shear Stresses (kPa)between Unreinforced, Reinforced(100% coupling) soil, reinforced also considering Different interfaces using RWSW-LIN	165
5.7	Horizontal, Vertical and Shear Strains Predicted in Unreinforced and Reinforced soil Retaining wall under self weight for different Young's modulus of Soil using RWSW-LIN	166
5.8	Predicted Horizontal displacements (m) and Vertical Settlements (m) for Unreinforced and Reinforced soil Retaining wall under self weight for different Young's modulus of Soil	166
5.9	Predicted lateral and vertical displacements for unreinforced and reinforced soil under dead load using RWSW-LIN	167
6.1	Soil Parameters obtained from experimental studies (Shivashankar,1991) used in the FEM Analysis (Numerical Analysis)	193
6.2	Properties of Geostrips used for studies on MSE Wall	193
6.3	Maximum and minimum Settlements obtained from Experimental observations and predicted using developed software for MSE Wall	194
6.4	Settlements obtained from Experimental observations and predicted using developed software MSE-PRO at depths of 0.45m, 3.00m and 6.00m for MSE Wall	194

6.5	Displacements for different facings and no facing(m)	195
6.6	Horizontal Stresses (kPa) predicted for MSE wall for Linear and Non-linear Analysis	196
6.7	Vertical Stresses (kPa) for MSE Wall for Linear and Non-Linear analysis with and without facing obtained using developed software MSE-PRO	197
6.8	Shear Stresses (kPa)for Linear and Nonlinear Analysis for MSE Wall with and without facing obtained using developed software MSE-PRO	198
7.1	Details of test programme for plate load test	233
7.2	Properties of soil used	233
7.3	Properties of Geogrid used	234
7.4	Properties of Geotextile used	234
7.5	BCR for cases geogrid and geotextile under square circular footings for different u/B ratio in dense sand	235
7.6	BCR for cases geogrid and geotextile under square circular footings for varying number of reinforcement	235
7.7	Settlements under square and circular footing for unreinforced and reinforced granular bed underlain by 0.80 x 0.80m (8B x 8B) and unreinforced soil	236
7.8	Different formulae used to calculate modulus of subgrade reaction	237
7.9	Modulus of subgrade reaction for reinforced soil under two model footings obtained using plate load test for granular bed underlain by silty soil	237
7.10	Details of mesh used in developed programme RSF-PRO	238
7.11	Material properties used in code RSF-PRO	238
7.12	Settlements corresponding to varying number of reinforcement layers at failure for different studies carried out	239
8.1	Details of the Validation of SSI Problem (Swamy et al., 2011)	276
8.2	Details of the SSI analysis Problem in the present work	276
8.3	Axial and Shear forces (kN) in beams (X-direction) of external frames in Linear SSI and RSSI analysis	277
8.4	Axial and Shear forces(kN) in beams(X-direction) of Internal frames in SSI and RSSI analysis	278
8.5	Axial and Shear forces(kN) in beams (Z-direction) of Internal frames in Linear SSI and RSSI analysis	279

8.6	Axial and Shear forces (kN) in columns (forces) of external frames in Linear SSI and RSSI analysis	280
8.7	Axial and Shear forces (kN) in columns of internal frames in Linear SSI and RSSI analysis	281
8.8	Bending moment (kNm) about z-axis in X-beams in linear SSI and RSSI analysis	282
8.9	Bending moment in Z-beams (kNm) in linear SSI and RSSI analysis	283
8.10	Properties of soil used in Non-linear SSI and RSSI analysis (After Krishnamoorthy and Rao, 1995)	302
8.11	Hypoelastic model Parameters used in Non-linear SSI and RSSI analysis (After Krishnamoorthy and Rao, 1995)	302
8.12	Stress resultants, Axial forces (kN) in X-Beams of external frames in non-linear SSI and RSSI analysis	303
8.13	Stress resultants (Axial forces in kN) in X-Beams of internal frames in Non-linear SSI and RSSI analysis	304
8.14	Stress resultants (Axial forces in kN) in beams in Z-direction in Non-linear SSI and RSSI analysis (discussion in section 8.5.3.1)	305
8.15	Stress resultants (Axial and shear forces in kN) in columns of external frames in Nonlinear SSI and RSSI analysis (discussion in section 8.3.2.2)	306
8.16	Stress resultants (Axial and shear forces in kN) in columns of internal frames in nonlinear SSI and RSSI analysis (discussion in section 8.3.2.2)	307
8.17	Stress resultants (bending moment about z-axis) in X-beams in Non-linear SSI and RSSI analysis	308
8.18	Stress resultants (bending moment about z-axis) in Z-beams in Non-linear SSI and RSSI analysis	309
8.19	Stress resultants (bending moment about x and z-axes) in columns in Non-linear SSI and RSSI analysis (8.5.3.4)	310

## NOMENCLATURE

$\sigma_{ij}$	Current state of stress
$\varepsilon_{ij}$	Current state of deformation
$F_{ij}$	Elastic response function of the material
$G$	Shear modulus
$K$	Bulk modulus
$J$	Coupling modulus
$P'$	Effective mean stress
$q$	Deviator stress
$\varepsilon_v$	Volumetric strain
$\varepsilon_z$	Shear strain
$q$	Deviator stress
$\tau_f$	Shear stress on the failure plane
$c$	Apparent cohesion
$\sigma_f$	Normal stress on the failure plane
$\phi$	Angle of internal friction
$\sigma_m^{\text{eff}}$	Effective mean stress
$e$	Void ratio
$\kappa$	Slope of swelling line
$\lambda$	Slope of Normal Consolidation Line
$k_s$	Tangential stiffness
$k_n$	Normal stiffness
$\{u\}$	Nodal displacement vector
$\{w\}$	Relative displacement vector

$u$	Displacements along $x'$ -axis
$v$	Displacements along $y'$ -axis
$N_1$ & $N_2$	Linear Interpolation Functions
$\tau_s$	Tangential Stress
$\sigma_n$	Normal Stress
$[K]^e$	Element stiffness matrix
$[B]$	Strain-displacement Matrix
$\{f\}$	Nodal force vector in the local coordinate system ( $x', y'$ )
$k_{rs}$	Tangential residual stiffness
$d$	Displacement
$A$	Cross-sectional area of an element
$E$	Young's modulus
$[J]$	Jacobian matrix
$\mu$	Poisson's Ratio
$K$	Stiffness of the element for unit displacement
$E_s$	Young's Modulus of Soil
$k_s$	Tangential stiffness of interface

## **CHAPTER 1**

### **INTRODUCTION**

#### **1.1 GENERAL**

Soil is one of the oldest and the most common construction material used by mankind. It is well established that when confined, granular soils possess sufficient compressive and shear strengths but have poor tensile resistance. Soils can be enhanced by reinforcing the soil along the direction of tensile strains similar to reinforced concrete.

Reinforced soil is obtained by combining the frictional soil and tension resistant elements such as synthetic fabrics or fiber reinforced plastics, metal strips, sheets, nets or mats. They are placed such that they reduce the tensile strains likely to expand under gravity and boundary forces.

The strength of the natural fill / soil in earth structures is enhanced by various techniques, e.g., chemical, mechanical or by reinforcing the soil mass using a strong material (sand compaction piles, bamboo strip, straw, etc.) and the most interesting one is natural plant roots. Besides these natural and traditional techniques, the crucial evolution of reinforced soil as an innovative construction material was brought in by French architect, Henry Vidal (Vidal, 1969). He is considered to be the pioneer of Reinforced soil. This procedure has since been adopted in various civil engineering projects such as slopes and embankments, retaining walls, soil foundations, dams, etc. The three main categories of soil reinforcing techniques are mechanically stabilized earth (for slopes, walls, and abutments), Soil nailing and reinforcement of weak or soft embankment problems.

Soil is a complex material that exhibits non-linear, anisotropic and time dependent behavior when subjected to stresses. It behaves non-linearly below failure condition with stress dependent stiffness. It is established that soils are non-linearly elastic and

plastic for all ranges of loading. Actually the performance of soils is complex and varies greatly when subjected to different loading conditions.

It is essential to develop constitutive models (constitutive relations or equations) representing mathematical descriptions of soil behavior under external load. These models are formed by establishing relationship between the stress and strain tensor to represent, more or less rough description of the real behavior. Ideally-elastic and ideally-plastic models were the most frequently used basic models. Further, plastic properties of materials were used in constitutive models. In zero-thickness interface elements, the element model suggested by Goodman et al. (1968), is the most rudimentary model which has been widely adopted. Many approaches have been developed based on this model.

## **1.2 SCOPE AND PURPOSE OF THIS STUDY**

The past five decades have shown great advancements in research related to the reinforced soil system by stiff metal to flexible/extensible geosynthetic materials. Many reinforced soil structures have been performing well and are considered safe and convenient for construction. Parallel to the advancements in the construction technology, a lot of efforts have been made to find a suitable method for the analysis and design (e.g. Vidal (1969); Schlosser and Long (1972); Haussmann (1976); Yang (1972)) in reinforced soil structures. Many assumptions have been postulated and many solutions have been proposed about the mechanism of different components comprising these systems.

Many researches have been carried out to find a suitable method of analysis and design of reinforced soil structures. In many geotechnical problems, especially reinforced soil structures, stability and deformation of structures are considered both critical and independent and they are dealt with separately. Commonly adopted internal stability analyses of Geosynthetic Reinforced Soil (GRS) retaining structures (such as the Tie-back wedge technique and other methods) are founded on limit equilibrium approach and are identified as conservative. Designs based on the

methods which over predict stresses in the reinforcement, are uneconomical. Further, the design methods founded on limit equilibrium approach do not reveal sufficient data with respect to wall face deformations.

In the present research, an attempt has been made to ameliorate the understanding of the internal stress-strain distribution in reinforced soil structures, by developing software and using a nonlinear constitutive relation, Drucker Prager. Linear analysis of retaining wall has been carried out with and without the Goodman's zero thickness interface element. A two dimensional (plane strain) numerical analysis has been carried out adopting Finite Element Method and by developing programs in Fortran 77.

Pilot studies have been carried out on a retaining wall and Mechanically Stabilized Earth (MSE) wall subjected to point loads and dead loads to validate the program for linear and non-linear analysis respectively. Software has also been developed to carry out linear and nonlinear Soil Structure Interaction (SSI) Analysis for reinforced and unreinforced soil by incorporating Hypo elastic model for soil.

### **1.3 RESEARCH OBJECTIVES**

The objectives of this research are:

- To conduct an exhaustive literature survey on Reinforced soil structures, identify gaps and ascertain the need for the study.
- To develop software to analyze the behaviour of reinforced soil structures under different loading conditions for linear and non-linear analysis of soil by incorporating a suitable interface element.
- To conduct pilot studies on reinforced soil retaining wall and Mechanically Stabilized Earth (MSE) wall to validate the results obtained from the developed software.
- To conduct experimental and numerical investigations to study the effect of reinforcement in reinforced soil foundation on Bearing Capacity, Bearing



Capacity Ratio (BCR) and carry out parametric studies directed towards the effects of types and lengths of geosynthetics under square and circular footings.

- To conduct experimental studies on reinforced soil foundation and evaluate the subgrade reaction of soil under square and circular footings.
- To develop software and carry out the soil structure interaction analysis for unreinforced and reinforced soil foundation both linearly and nonlinearly.

### 1.3.1 Research Objectives on Retaining Wall

In this part of the research, the behaviour of reinforced soil retaining wall is being studied for linear case. The approach is to develop Code (program) RWPT-LIN (for point loads only), RWSW-LIN (for self-weight only) and RWSW-INT (for self-weight and by adopting Goodman's interface element) and validate it with software or previously published work.

The cases studied are summarized in Table 1.3.

**Table 1.3 Cases of study carried out on reinforced soil retaining wall**

<b>LINEAR ANALYSIS for unreinforced and reinforced Soils</b>
1) For different load combinations (Dead load, Point load.)
2) Without interface elements
3) With interface elements
4) Homogenous soils

### 1.3.2 Research Objectives on Reinforced Soil Foundation

The effect on settlement behavior of square and circular footings together with the enhancement in load carrying capacity of a reinforced granular bed overlying weak soil have also been proposed to be studied along with the following parameters:

- 1) Type of footing
- 2) Type of geosynthetic material
- 3) Number of reinforcement layers

- 4) Length of reinforcement
- 5) Effect of varying the depth of top geosynthetic layer

It is proposed to conduct laboratory model tests and FEM analysis by developing a code. It is also proposed to study the effect of reinforcement on the modulus of subgrade reaction of soil by using the results obtained in the laboratory model tests.

### **1.3.3 Research Objectives on Mechanically Stabilised Earth Wall (AIT Wall)**

This part of research deals with the analysis of mechanically stabilized embankments using the Finite Element Method considering the presence and absence of facing element. Currently, nonlinear analysis of mechanically stabilized embankment is conducted by developing a software (MSE-PRO) and by adopting Drucker-Prager constitutive model. The results of the the software developed in this program, MSE-PRO have been validated with the numerical analysis and experimental studies of Asian Institute of Technology (AIT) wall (Shivashankar,1991) with poor backfills resting on soft clay deposits.

### **1.3.4 Research Objectives on Soil-Structure Interaction Analysis of a 3d Frame with Isolated Footings Resting on Reinforced Soil**

The present research deals with the development of software to study of the response of a structure on a fixed base. Then the behaviour of the same structure on soil instead of fixed base i.e. considering soil structure interaction effects is studied using the developed software SSI-LIN and SSI-NLIN. Later the soil is reinforced with geosynthetics and the response is studied. Responses such as displacements and member end actions in structural members are compared between the fixed base structure, structure resting on soil with and without reinforcement. The analysis is done for both the linear and nonlinear cases on reinforced soil developing programmes RSSI-LIN and RSSI-NLIN. Nonlinear analysis is carried out by adopting Hypoelastic model for soil.

## **1.4 ORGANIZATION OF THE THESIS**

The thesis is presented in nine chapters. A brief overview of the chapters is given below,

Chapter 1: An introduction to concepts of Reinforced soil technology is presented. The need for undertaking the study is also brought out. The scope and objectives of the study are described.

Chapter 2: An introduction to Reinforced soil structures like Reinforced soil retaining wall, Reinforced soil foundation, Mechanically Stabilised Earth Wall, SSI and Reinforced Soil structure Interaction (RSSI) is presented.

Chapter 3: A brief review of literature of previous research on all the Reinforced soil structures is listed. Previous studies on SSI have also been presented. It also contains the summary of the literature review and future direction for research.

Chapter 4: A brief introduction of the Finite Element modelling and Analysis is presented.

Chapter 5: Linear Analysis of Unreinforced and Reinforced soil Retaining Wall under point loads and self-weight is presented with and without interface.

Chapter 6: The details of studies carried out on MSE (AIT) wall available in literature and the numerical analysis of the same using developed software have been presented.

Chapter 7: The details of Experimental studies carried out on Reinforced soil foundation and the computation of modulus of subgrade reaction of reinforced soil have been presented. The results of the developed software and experimental studies have been compared.

Chapter 8: The soil structure interaction analysis for unreinforced and reinforced soil foundation carried out both linearly and nonlinearly have been presented here.

Chapter 9: Presents the summary of the present work with the conclusions drawn

## **1.5 SUMMARY**

This chapter deals with the introduction to concepts of Reinforced soil technology. The need for undertaking the study is also brought out. The scope and objectives of the study are described. The research objectives on all the Reinforced soil structures have been presented. The organization of the thesis has also been presented.

## **CHAPTER 2**

### **INTRODUCTION TO REINFORCED SOIL STRUCTURES**

#### **2.1 GENERAL**

Soil is one of the most commonly available and commonly used construction material. Of late, limited availability of good sites and the pace of man's economic growth, has forced civil engineers to build structures where ever they are required, irrespective of the soil conditions. We can deal with such circumstances in two ways either by choosing an alternate site or by improving the soil at site.

As reinforced soil systems result in extensive cost savings, when compared with the traditional retaining walls, these systems have become extremely popular. Initial work carried out in France by Vidal (1969) involved inextensible reinforcements, finally paving way to a system of ribbed steel strips and the granular backfill soil. Vidal's earlier concepts emphasized the confinement of lateral deformation in the reinforced granular fill while the current design methods are based on limit state analyses.

#### **2.2 INTRODUCTION TO REINFORCED SOIL**

##### **2.2.1 Theory of Reinforced Soil**

Reinforced soil is obtained by combining frictional soil and tension resisting elements such as sheets, fiber reinforced plastics, strips or mats of metal or synthetic fabrics. They are arranged such that they reduce the tensile strains that develop under gravity and boundary forces. Reinforced soil has many special characteristics that make it suitable for the construction of soil structures. Reinforced soil retaining walls use precast units and reinforcing strips, sheet and nets which can be stored, managed and formed effortlessly. The modern hauling and compaction equipment are used to place the backfill soil. The past six decades have shown great advancements in research

related to the reinforced soil system by stiff metal to flexible/extensible geosynthetic materials. Many reinforced soil structures have been performing well and are considered safe and convenient for construction. Parallel to the advancements in the construction technology, a lot of efforts have been made to find a suitable method for the analysis and design (e.g. Vidal, (1969); Schlosser and Long (1972); Haussman (1976)). Many assumptions have been postulated and many solutions have been proposed about the mechanism of different components comprising these systems.

### **2.2.2 Reinforced Soil Technology**

The invention of reinforced soil and much of its current development can be credited to H. Vidal (Vidal, 1969). Behaviour of reinforced soil depends upon the development of friction between the soil and reinforcement Schlosser and Delage, (1987).

#### **2.2.2.1 York Method**

York method is analogous to the reinforced soil technique but for two minor differences, which include the facing units and sliding mechanism of reinforcements. Here, reinforcing strips are permitted to slide relative to the wall face along the vertical poles. The maiden reinforced soil wall was entirely built using plastic material, by adopting the York method (Schlosser and Delage, 1987). The differential settlements can be accommodated easily here. Refer Fig. 2.1.

#### **2.2.2.2 Geosynthetic Reinforced Soil Retaining Wall (GRS-RW System)**

GRS-RW system, was developed in Japan and is a hybrid wall system of mechanically reinforced soil wall with a cast-in place full height rigid facing. A schematic diagram of GRS-RW is shown in Fig. 2.2. Because of short reinforcements of GRS-RW, excavation may not be required. This system can be used in sites e.g. bridge abutment or laterally loaded walls.

### **2.2.2.3 Miscellaneous**

There are several other reinforcing systems developed by many manufacturers used for particular purpose and suitable for typical site conditions, namely, Tervoile-Websol system, Cellular Confining system, Genesis Highway Wall System consisting of Tensor structural geogrids, Con-wall system, etc. (Refer Fig. 2.3)

### **2.2.3 Soil Reinforcing Materials**

Considering the stress-strain response of the soil mass, there are two types of reinforcements, extensible and inextensible. The stress-strain characteristics of typical inextensible and extensible reinforcing elements are illustrated in Fig. 2.4. The concept of inextensible and extensible reinforcements was initially elucidated by McGown et al. (1978). The definitions were further extended by Bonaparte and Schmertmann (1987) and they are as follows:

- a) An inextensible reinforcement is the reinforcement in which the tensile strain is considerably less than the horizontal extension. This strain is not sufficient to unfold into an active plastic state in the soil. An "absolutely" inextensible reinforcement is so stiff that equilibrium is achieved at virtually zero horizontal extension ( $k_0$  conditions prevail).
- b) An extensible reinforcement is the reinforcement in which the tensile strain is equal to or greater than the horizontal extension necessary for arriving at an active plastic state in the soil. The modulus of an "absolutely" extensible reinforcement is so low that virtually no tensile forces are introduced into the soil mass at the strain required to develop an active plastic state ( $k_0$  conditions theoretically prevail).
- c) The maximum tensile force line is approximately linear and passes through the toe of the wall. It coincides with the Coulomb or Rankine active failure plane. An inextensible metallic reinforcement makes a structure brittle and the extensible geosynthetic enhances the ductility of the reinforced soil structure

### **2.2.3.1 Extensible Reinforcements (Geosynthetic and related products)**

Major geosynthetic materials currently used as reinforcements in soil structures are woven and non-woven geotextile sheet, geogrid sheet, rigid plastic strips, coated fiber strips, composites and three-dimensional honeycomb type products. Geosynthetic materials have large ranges of deformation modulus and tensile strengths compared to metals (Figure.2.5). Geosynthetic materials also exhibit creep behavior. Bonaparte and Schmertmann (1987) have grouped geosynthetic reinforcements as extensible reinforcements.

### **2.2.3.2 Inextensible Reinforcements (Steel Bars / Fiber Glass)**

The reinforcing material varies from the extensible polyester resins to the inextensible reinforcement like steel, fiberglass etc. The corrosion mechanism of Galvanized steel and its rate of corrosion have been known since long. Similarly, polyester coated fiberglass, stainless steel and aluminum are also used. The rate of corrosion of these metals is more than the galvanized steel.

Despite these limitations, the steel and fiberglass reinforcing materials have gained popularity especially when the construction requires less post construction deformation as in the case of bridge abutments, railway embankments, etc. The advantage of steel and fiberglass is their unique combination of elasticity, ductility/stiffness and favorable economics. Bonaparte and Schmertmann (1987) states that the tensile stiffness of steel reinforcements is stiff enough to keep the state of soil stress close to the at-rest ( $k_0$ ) condition.

### **2.2.3.3 Miscellaneous**

There are several other types of reinforcing materials used as soil reinforcement. They may be either in the form of small insertions (fibers, small plates) or continuous strands (e.g. Texsol). Often natural materials (e.g. bamboo, jute) are also used as



reinforcing material. In UK and USA, redundant car tyres are used as soil reinforcement.

#### **2.2.4 Geosynthetics and their Applications**

“Geosynthetics” are a family of all fabricated synthetic (usually polymeric) materials applied in drainage, reinforcement, erosion control, and lightweight fill. There are many applications of geosynthetics in various highway projects. Geosynthetics are basically synthetic polymers like polyethylene, polyamide, polypropylene, polyester, polyvinylchloride (PVC) etc. They resist degradation, chemical and biological attacks. The natural fibers like jute, cotton, bamboo, etc. could also be used as reinforcement, especially for applications temporary in nature, but they have not been researched or promoted as extensively as geosynthetics.

During the manufacture of the geotextiles, yarns or fibers are blended into planar structures. The fibers are thin, long strands of a staple fiber or short polymeric filaments having lengths approximately ranging between 20mm and 100mm. They may also be obtained by extruding plastic sheet or plastic film to develop thin flat tapes. The extrusion in both the filaments and slit films elongates the polymers and increases the fiber strength. Majority of geotextiles are either woven or nonwoven.

Synthetic polymeric filaments or fibers are laid onto a moving belt or spun, blown or continuously extruded. The fibers or filaments are either heat bonded or needle punched, and the filaments are entangled mechanically by various small needles. The fibers may also be welded together by heating or applying pressure at points of contact in the non-woven mass.

##### **2.2.4.1 Identification of Geosynthetics**

The identification of Geosynthetics is governed by the following factors (a) the type of polymer; (b) fiber or yarn (c) type of geosynthetic (d) mass per unit area or thickness and (e) physical properties.

A few examples of Geosynthetics are:

- Nonwoven, needle punched Polypropylene staple fiber 350 g/m<sup>2</sup>
- Polyethylene net, 440 g/m<sup>2</sup> with 8 mm openings
- Polypropylene biaxial geogrid with 25 mm x 25 mm openings and
- High-density polyethylene geomembrane 1.5 mm thick

#### **2.2.4.2 Types of Geosynthetics**

**1. Geogrids** principally serve as reinforcement. They consist of a series of apertures of necessary size and they interlock with the surrounding fill material. Extrusion and orientation of the sheets of polyolefins, result in the manufacture of stiff geogrids with integral junctions. Flexible geogrids are made of polyester yarns which are joined by knitting or weaving, at the crossover points, and then coated with a polymer. (Refer Fig. 2.6)

**2. Geomembranes** are a group of extremely low permeable geosynthetics which serve as fluid barriers. (Refer Fig. 2.7)

#### **3. Geotextiles**

**Geotextiles** are permeable fabrics which, when used in association with soil, have the ability to separate, filter, reinforce, protect, or drain. Typically made from polypropylene or polyester, geotextile fabrics come in three basic forms namely, woven, needle punched or heat bonded. (Refer Fig. 2.7)

#### **4. Geocomposites**

Geotextiles such as geonets and geogrids can be combined with geomembranes to serve better. These are called geocomposites, may be composites of three dimensional polymeric cell structures, geotextile-geonets, geomembrane-geonets geotextile-polymeric cores, geotextile-geogrids, geotextile-geomembranes. An

amazing range of geocomposites are available. Geosynthetics is the generic term representing all these materials.

### **2.2.4.3 Functions of Geosynthetics**

Geosynthetics form a family of polymers that are fabricated to be applied in transportation and hydraulic engineering, environmental and geotechnical applications. The various functions of geosynthetics are erosion control, drainage, reinforcement, fluid/gas containment, separation and filtration. Most of the times the geo-synthetics serve dual functions.

#### **1. Geosynthetics as Filter**

Geosynthetics act as a sand filter and allow only the water to percolate through the soil while retaining all the soil particles on the upstream. Geotextiles avert the movement of soils into drainage pipes, parallelly maintaining the flow through the system. Soil erosion can be prevented or minimized by placing the geotextiles below the rip rap and other materials, analogous to river bank protection systems.

#### **2. Geosynthetics as Separators**

Geosynthetics are used to decouple the layers of soil according to particle size distributions. Geotextiles prevent the intermixing of road base materials and the soft underlying subgrade soils. Thus, the Geosynthetics are capable of maintaining the integrity of the roadway and influence the thickness. Separators prevent intermixing of fine-grained subgrade soils and permeable granular road bases. (Refer Fig. 2.9)

#### **4. Geosynthetics as Drains**

Geosynthetics can also serve as filters or drains. They can carry the fluid through less permeable soils and also dissipate the pore water pressures at the base of roadway embankments. Geocomposite drains can be developed for higher flows. These materials serve as drains for abutments, retaining walls, pavement edge, and slope interception.

Geosynthetics can also accelerate the consolidation of soft cohesive foundation soils below the embankments with preload fills and prefabricated vertical drains (PVDs). (Refer Fig. 2.10)

## **2. Geosynthetics as Reinforcement**

In comparison with the unreinforced soil the soil reinforced with geosynthetics produce a composite material that possesses better deformation and strength properties. Addition of geotextiles and geogrids enhance the tensile strength of the soil mass. By reinforcing the embankments, it is possible to construct them on soft foundation soils and construct steeper side slopes when compared to the ones built using unreinforced soil. (Refer Fig. 2.11). Geosynthetics have often been employed to reduce the voids that may develop below the load bearing granular layers (roads and railways) or in landfill applications below the cover systems.

## **5. Geosynthetics as Fluid/Gas (Barriers) /Containment**

Geosynthetics serve as impervious barriers to liquids or gases. Some of the geosynthetic materials which are applied as barriers for fluid flow are: geomembranes, thin geotextile composites, geosynthetic clay liners (GCLs) and field-coated geotextiles. This particular function of Geotextiles is also applied for controlling the swelling property of soils, waste containment and in asphalt pavement overlays.

## **6. Geosynthetics in Reinforced Steep Slopes Concept**

The basic application of geosynthetics is the reinstatement of failed slopes and the stabilization of steep slopes. The resulting debris could be used to fix the slope (together with geosynthetic reinforcement) which results in cost savings. A steeper slope than that of a stable slope may be required in unreinforced compacted embankment soils from cost considerations. In order to reinforce the soil and enhance the stability of slopes or for the reconstruction, geotextiles or geogrids may be placed in multiple layers in a slope fill during construction. Most of the projects involving steep slopes include, fixing of failed slopes, construction of new

embankments and widening of existing embankments. Lateral confinement at the sloped face can be increased by placing narrow geosynthetic strips 1 to 2 m wide at the edge of the slopes. Thus, achieving an increase in the compacted density. Reinforced compacted slopes have been found to resist sloughing and reduce the erosion of slope.

### **2.2.5 Concepts of Reinforced Soil**

Several experimental studies and numerical analyses have been accomplished since the inception of Reinforced soil wall to understand the basic concepts of reinforced soil structures and study the interaction among its basic components, generally facing, reinforcing elements and backfill soil.

#### **2.2.5.1 Anisotropic Cohesion Concept**

Schlosser and Long (1972) have described that the addition of reinforcement in soil imparts higher shear strength to the soil when compared to its unreinforced counterpart. Haussmann (1976) on the other hand, has hypothesized a more consolidated anisotropic cohesion theory. Research findings reveal that two failure modes can develop in reinforced sand samples: (a) failure by slippage of the reinforcement at low confining pressure leading to a curved yield line passing through the origin and (b) failure by reinforcement breakage at higher confining pressure leading to a straight failure line. This in turn demonstrates (a) cohesive behavior of reinforced sand despite having the same frictional angle as the virgin sand and (b) an anisotropic pseudo-cohesive behavior due to reinforcement. This pseudo-cohesion is very rapidly mobilized at low axial deformations. (Refer Figs. 2.12 and 2.13)

#### **2.2.5.2 Enhanced Cohesion Concept**

Yang (1972) has come out with enhanced confining pressure concept on the mechanism of reinforced soil. As the shear stresses develop between the soil and reinforcements, the horizontal and vertical planes are no longer principal stress

planes. Mohr's circle of stress is shifted due to soil reinforcement while the failure envelope remains the same for both the unreinforced and reinforced soil samples. Such an effect is called the enhanced confining pressure effect.

### **2.2.6 Reinforcing Mechanisms**

The steel and geosynthetic reinforcements vary in their stiffnesses and the type of interactions that occur at the interfaces of reinforcement and soil. Steel reinforcement is usually in the form of strips or mats, while geosynthetic reinforcement usually takes the form of grids or planar sheets.

Because of the planar structure and flexibility of geosynthetics, the shear forces occurring inside the soil mass are transferred to geosynthetic reinforcement more uniformly and without interruptions; therefore, geosynthetic materials have a better ability to contain both local and global yielding of the soil mass than steel reinforcement. (Refer Fig. 2.14)

The limit equilibrium analysis assumes that the reinforcement does not reinforce the soil until global failure occurs in the soil mass. Although this analysis provides satisfactory results for steel reinforced retaining structures, it over-predicts the internal stress distribution of GRS retaining structures.

### **2.2.7 Interaction of Geosynthetics with the Surrounding Soil**

While the steel reinforcements usually possess smooth surfaces, most of the geosynthetics have grid structures (geogrids) or fabric-like surfaces (geotextiles). These produce better bond between the soil and reinforcement. Slippage occurs at the soil reinforcement interface in the steel reinforced wall. But in systems reinforced with geosynthetics, the slippage surfaces occurs in the soil close to the reinforcement. This observation is very important while using the discrete system approach to analyze the performance of the GRS retaining walls.

### **2.2.8 Facings in Reinforced Soil Structures**

Currently, the wall facing material ranges from rigid full-faced concrete facing to flexible

wrapped around geosynthetics facing as shown in Fig. 2.15. Most of the soil reinforcement techniques assume that the facing does not play any significant structural role; but are used for aesthetics only. However, the rigidity of the wall facing affects the earth pressure development within the reinforced zone as well as the reinforcement force and the lateral movement of the wall face. Based on their degree of rigidity, there are various types of facings. The facing rigidity increases the stability of wall in the following three ways:

1. Rigid facings (types d and e) support the earth pressure and tensile force in reinforcement.
2. Weight of the backfill is partially transmitted to the facing through the frictional force on the back face.
3. Due to the high confining pressure behind the rigid facing, the location of the overall reaction force becomes closer to the facing.

## **2.2.9 Applications of Reinforced Soil**

Reinforced soil structures can be grouped into three classes (Ingold, 1982) as

- (a) Embankment and retaining walls,
- (b) Foundations /sub-soil reinforcements and
- (c) In-situ reinforcement (soil nailing) for existing slopes and excavations.

### **2.2.9.1 Embankments/ Retaining Walls**

Different types of facings and reinforcing materials have been used to construct many reinforced embankments and retaining walls and a few of them are very large. The principal role of reinforcement in an embankment/ retaining wall is to support the outward earth pressure (lateral thrust) in the fill. The reinforcement provided at the embankment base prevents the lateral displacements of the foundations soils and embankment.

The stability and bearing capacity of the soft soil and of embankments are significantly increased by soil reinforcement. The role of reinforcement is to perform

as (i) edge stiffening and slope reinforcement (ii) body reinforcement; (iii) reinforcement at the base of the retaining walls. The major application in reinforced soil embankment or retaining wall structures is the reinforcement in the main body.

### **2.2.9.2 Subsoil Reinforcement beneath Foundations**

Below the reinforcement in the reinforced foundation soil two distinct zones are formed as shown in Fig. 2.16. In the top zone, the wedge of soil directly beneath the structure is forced vertically downwards (punching failure) whilst beyond the footing, there are symmetrical zones in the soil which have both upward and lateral movements. Critical zones beneath reinforced foundations (Fukuda and Chou, 1982) are shown in Fig. 2.17

### **2.2.9.3 In-Situ Reinforcement (Soil Nailing/ Slope Stability/ Excavation)**

Soil nailing is a soil reinforcement technique, which is in practice since the last two decades. By controlling the deformations, this technique limits the decompression and the opening of pre-existing discontinuities. Steel rods 20-30 mm in diameter are driven or grouted into the soil in a predrilled borehole (See Fig. 2.18). Soil nailed slopes behave like a reinforced soil wall with a few major differences between these two as stated below.

- a) Method of Construction: Soil nailed walls have top-down construction method while reinforced soil walls are constructed using the bottom up technique.
- b) Shear and bending stresses may develop in soil nailed walls depending upon the stiffness of the nails relative to soil, while this is generally not observed in reinforced soil structures.
- c) Soil nailing is applied to the existing soil slopes and may involve more cohesive soils than the selected fills used in reinforced soil walls.
- d) Usually soil reinforcement sheets or strips are laid horizontal, while the soil nails are usually driven at an inclination.
- e) Schlosser et al. (1983) observed that the active failure zone for soil nailed slopes was similar to, but larger than that of a reinforced soil wall.



In both the cases, the active failure zone is smaller than the standard Coulomb active wedge assumed with the other retaining structures. He suggested that this difference in behavior is attributed to the inclination of the soils nails.

## **2.3 REINFORCED SOIL STRUCTURES STUDIED**

The reinforced soil structures studied in this research are reinforced soil retaining wall, Mechanically Stabilized wall and reinforced soil foundation. Linear and Non-linear RSSI has been carried out on unreinforced and reinforced soil.

### **2.3.1.1 Behavior of Reinforced Soil Structures**

In the analysis and design of reinforced soil structures, stability and deformation are considered both critical and independent concerns for a soil structure and they are always dealt separately. Past research reveals that major work was concentrated on the stability analysis compared to the deformation problems. In the deformation analysis, serviceability with respect to excessive differential settlement and horizontal deformation of the sloped face are considered important. Rowe and Ho (1993) suggested that the overall behavior of a reinforced soil structure may be considered known if one understands:

- i. Stress within the reinforced soil mass.
- ii. Strain in both the soil and the reinforcement.
- iii. Axial force distribution in the reinforcement.
- iv. Horizontal soil pressure acting behind the reinforced soil mass and the vertical soil pressure at the base.
- v. Vertical soil stress on each reinforcement layer.
- vi. Horizontal soil pressure acting at the face.
- vii. Horizontal and vertical forces transferred to the wall face.
- viii. Horizontal deformation of the reinforced soil mass

### **2.3.1.2 Failure Modes**

Several possible failure modes are checked for in reinforced soil systems, based on

the type of the structure as well as the subsisting field conditions. These failure modes are grouped into two (external and internal) stability criteria. Typical failure modes that are verified/checked in the reinforced soil structures are as mentioned below:

### **1. External Stability**

- a) Vertical and horizontal deformations resulting into unacceptable differential settlement.
- b) Lateral sliding of reinforced soil.
- c) Overturning failure due to rotation about the toe of the reinforced soil wall.
- d) Bearing capacity failure (punching failure) of the foundation soil.
- e) Overall collapse of the reinforced wall or embankment or nailed slope.

### **2. Internal Stability**

- a. Rupture failure of reinforcement
- b. Pull-out failure of reinforcement

### **2.3.2.3 Stability of GRS Retaining Structures**

#### **1. External Stability**

All reinforced soil retaining walls, whether reinforced by steel or geosynthetics, have the same external stability concerns as conventional retaining structures. External stability design of retaining structures basically includes analyses of:

- 1. Friction between retaining structures and foundation soil -- possibility of base sliding failure
- 2. Bearing capacity and creep of foundation soil possibility of overturning, and excessive settlement
- 3. Overall slope stability

#### **2. Internal Stability**

Different from the conventional system in which backfill soil properties are the major concerns of internal stability, the reinforced soil system has a much more complicated

internal stability analysis. The design of the reinforced soil retaining structure involves consideration of:

1. The strength properties of backfill and reinforcement material,
2. The reinforcement arrangement,
3. Interaction between soil and reinforcement,
4. Interaction between facing element and soil,
5. Durability of the reinforcement, and
6. Connection between facing units and reinforcement (especially for systems with segmental facing structures)

#### **2.3.2.4 Design Considerations of GRS-RW**

Despite considerable differences of reinforcing mechanisms, interaction with soil and geosynthetics, and property changes due to in-soil confinement and low strain rate conditions, stability analysis of GRS retaining walls is still performed in a similar manner to that of steel reinforced retaining walls. Internal design methods adopted from steel reinforced walls are based on limiting equilibrium concepts. To compute the tensile stresses that must be withstood by the reinforcement, the presupposition of lateral earth pressure distribution against the face of the reinforced section becomes necessary.

Studies on full-scale and model GRS walls indicate that these assumptions lead to an overestimation of the internal stress distribution within the structure (Rowe and Ho, 1993). These observations suggest that the assumptions of conventional lateral earth pressure theory used in steel reinforced wall design is not appropriate for estimating the lateral earth pressure distribution of GRS walls. Development of a fitting internal stability design for GRS walls calls for an alternate approach to capture the internal distribution of lateral earth pressure behind the wall face. Common shapes for potential failure surfaces for Limit Equilibrium Analysis techniques are shown in Fig. 2.22.

### **2.3.3 Mechanically Stabilised Earth Walls (MSE Walls)**

Mechanically Stabilized Earth (MSE) walls have been the focus of research since their introduction into standard engineering practice. World's first MSE wall was constructed in Japan in 1972 (Hirai et al, 2003). Presently, there are more than 30,000 of these structures in Japan alone.

Basically, MSE walls are earth retaining structures that consist of a facing element behind which, compacted soil and alternate layers of reinforcement are placed. This type of construction forms a composite material which in turn resists lateral forces. They are moderately flexible and can tolerate horizontal and vertical deformations. The height of MSE walls ranges between 12 and 30 meters.

#### **2.3.3.1 Components of MSE Wall**

The components of a typical MSE wall have been discussed further. The wall is primarily constructed with reinforced fill/soil. Owing to its strength, drainage and durability properties, well-graded granular soil is the preferred fill. Reinforcement elements are responsible for imparting tensile strength and holding the soil together. They are essentially made up of either steel or geosynthetic materials and are available in the form of strips, bar mats, geogrids, or fabrics having a wide range of tensile strength and stiffness. Facing elements on the other hand, not only offer protection from erosion of the fill but also offer confinement of the fill for placement and compaction. The increasing demand for MSE walls can be mainly owed to their low cost, ease of construction, and structural tolerance to foundation settlement. Studies have shown that MSE walls perform on par with or even better than most of the rigid wall systems under seismic loading conditions. Also, MSE walls are technically and economically feasible to heights in excess of other wall types.

However, the behaviour of MSE walls is complicated mainly due to the complex interactions between the soil and the reinforcing elements, the soil and the facing panels and the incremental construction technique. Hence, performing an accurate

simulation of these walls using numerical modelling techniques (e.g., finite element and finite difference methods) is a real challenge.

Mechanically Stabilized Earth Walls (MSE walls) and Reinforced Soil Slopes (RSS) are cost effective soil-retaining structures that can tolerate much larger settlements than reinforced concrete walls. By placing tensile reinforcing elements (inclusions) in the soil, the strength of the soil can be improved significantly. Use of a facing system to prevent soil ravelling between the reinforcing elements allows very steep slopes and vertical walls to be constructed safely.

### **2.3.3.2 Advantages of Mechanically Stabilized Earth (MSE) Walls**

MSE walls have many advantages compared with conventional reinforced concrete and concrete gravity retaining walls. MSE walls:

- Use of simple and rapid construction procedures and do not require as large of construction equipment.
- Do not require special skills for construction.
- Require less site preparation than other alternatives.
- Need less space in front of the structure for construction operations.
- Reduces right-of way acquisition.
- Do not need rigid, unyielding foundation support because MSE structures are tolerant to deformations.
- Are cost effective.
- Are technically feasible to heights in excess of 30 m.
- Flexibility and capability to tolerate deformations due to poor subsoil foundation conditions
- Higher resistance to seismic loading than rigid concrete wall structures
- Precast concrete facing elements for MSE walls can be made with various shapes and textures (with little extra cost) for aesthetic considerations. Masonry units, timber, and gabions also can be used to blend in the environment.

## **2.3.4 Reinforced Soil Foundation**

### **2.3.4.1 General**

The construction of structures such as dams, retaining walls is costly and problematic when very soft soils occur at the site. Low shear strength and excessive consolidation settlements are the problems occurring in these weak soils which requires special precautions, care and special construction practices resulting in high construction costs.

The various methods of treatment available to minimize the problems involved with weak soils are:

- Complete replacement of weak soil.
- Staged construction - placing fill at controlled rates to allow for consolidation and strength gains.
- Installation of drains to facilitate consolidation.
- Pre-consolidation at the site to reduce settlements of the structure and provide higher strength.
- Application and usage of admixtures (e.g. soil, cement, lime)
- Soil Reinforcement using suitable reinforcements.

The use of geosynthetics to enhance the bearing capacity and improve the settlement performance of shallow foundation has attracted lot of attention in the field of geotechnical engineering. During the last few decades, several laboratory and experimental studies have been conducted, related to the improvement in the bearing capacity of soils in pavements, shallow foundations and slopes using geosynthetics.

Many of these researchers investigated the parameters related to the bearing capacity ratio (BCR). BCR is the ratio of the bearing capacity of the Reinforced Soil Foundation (RSF) to that of the unreinforced soil. The various parameters studied by the researchers include:

- (1) Number of reinforcement layers
- (2) Vertical spacing between the layers reinforcement

- (3) Top layer spacing ( $u$ )
- (4) Shape of footing
- (5) Soil type
- (6) Embedment depth of footing ( $D_f$ )
- (7) Reinforcement length ( $l$ )
- (8) Stiffness and reinforcement type

The results of the experimental studies available show great improvements in BCR.

#### **2.3.4.2 Mechanism of Reinforcement in Reinforced Soil Foundation**

The mechanisms of reinforcements used in reinforced soil analytically can be discussed as below:

(1) Rigid boundary mechanism: According to this mechanism, when the depth of the first reinforcement layer ( $u$ ) is greater than a certain value, the reinforcement acts as a rigid boundary.

The failure of soil foundation occurs above the top layer of reinforcement. This failure mechanism was first proposed by Binquet and Lee (1975b). Later on several researchers (Akinmusuru and Akinbolade, 1981 and Mandal and Sah, 1992) confirmed this finding through experiments.

(2) Membrane effect: According to this mechanism, under the applied load, the soil beneath the footing including the footing move downward. The reinforcement is deformed and tensioned. The load is supported by the upward force developed in the curved reinforcement. The reinforcement should be sufficiently long and stiff to prevent its failure by tension and pull out. At the first instance, Binquet and Lee (1975b) applied this mechanism and developed a design method for a strip footing resting on reinforced sand. Certain tensioned membrane effect is mobilised by settlement. This method was extended to a rectangular footing resting on reinforced sand by Kumar and Saran (2003).

(3) Confinement effect: The relative displacement between the soil and reinforcement induces frictional force at the interface between soil and

reinforcement. The interaction between the soil and geogrid develops the interlocking effect. Hence, the lateral deformation of the reinforced soil is controlled. Also, the vertical deformation of the reinforced soil is controlled. By improving the lateral confinement, the modulus/compressive strength of soil can be improved which in turn improves the bearing capacity of reinforced soil.

Michalowski (2004) derived formulae for computing the ultimate bearing capacity of strip footings on reinforced soils by using this reinforcing mechanism as per the limit analysis of reinforced soil foundation.

#### **2.3.4.3 Analytical Modelling of Reinforced Soil Foundation**

Four possible failure modes are identified for reinforced soil foundations and are as discussed below:

- a) Failure of the soil above the top layer of reinforcement (Binquet and Lee, 1975a,b)
- b) Failure between the reinforcement layers (Wayne et al., 1998)
- c) Failure similar to footings on a two-layered soil system (strong soil layer over weak soil layer) (Wayne et al., 1998).
- d) Bearing failure within reinforced zone

By maintaining the top layer spacing ( $u$ ) and the vertical spacing between reinforcement layers ( $h$ ) close enough, the first two failure modes mentioned above can be prevented. Chen (2007) conducted experiments and his investigations reveal that the top layer spacing ( $u$ ) and the vertical spacing ( $h$ ) need to be less than 0.5 times  $B$  to prevent the aforementioned failures from happening. Based on his experimental results, the researcher found that horizontal direction is the best orientation of geogrid in reinforced clayey and sandy soil at the ultimate load.

#### **2.3.5 Soil Structure Interaction/Reinforced Soil Structure Interaction**

Structural engineering and Geotechnical engineering are closely related subjects in the analysis of civil engineering structures. Often, analysis in either of the two subjects can be performed independently with accurate results. In order to capture the



real behaviour of the superstructure, the underlying soil needs to be modelled sufficiently well. On the other hand, an accurate model of the superstructure is needed to capture the actual response in the underlying soil. To capture the right behaviours of both superstructure and subgrade in one model, it must include a good soil-structure interaction (SSI).

However, merging today's most advanced commercial design software for the two aforementioned disciplines, would result in demand for unrealistic large computation time. The user would in such a model also need great knowledge in both of the subjects. Therefore, there is a need for simplified methods in practice to model SSI. In engineering practice there are different opinions how to model SSI. In design of the superstructure, some consider that it's enough with structural element model of the subgrade. Others claim that the soil should be modelled more physically correct with a continuum model, to achieve a good enough SSI-analysis.

#### **2.3.5.1 Derivation Approaches**

Basically there are two types of derivation approaches used for models of SSI problems; structural and continuum approach.

- **Structural Approach**

The structural approach has a rigid base from which subgrade and superstructure are built up with structural elements, such as flexural elements, springs, etc.

- **Continuum Approach**

The other alternative, continuum approach is based on three partially-differential equations (compatibility, constitutive and equilibrium) which are governing the behaviour for the subgrade as a continuum (Teodoru, 2009). When combining the two derivation approaches, the method is called a hybrid derivation approach. In continuum mechanics, continuum is defined by a continuously distributed matter

through the space. The simplest elastic continuum is described with the constitutive relation with linear elastic isotropic behaviour given by Hooke's law.

### **2.3.5.2 Numerical Modelling of SSI Analysis**

Numerical modelling of SSI analysis involves two methods and they have been discussed in the following sections.

#### **1. Direct Method**

In direct method, the soil and the structure are examined as a sole structure. In sub-structure method, each components of a model are produced distinctly and later collected together to get results. In the present study, direct method is adopted.

Various studies are carried out on the effect of soil– structure interaction under static loading. These studies has included the effect in a very simple way and verified that the force quantities are reviewed because of such contacts. A few studies were conducted on soil–structure interaction effect considering three dimensional space frames. The studies evidently directed that a two-dimensional plane frame analysis might substantially overestimate or underestimate the actual interaction effect in a space frame. From these studies, it turns out to be noticeable that the deliberation of the interaction effect significantly modifies the design force quantities. These studies, may be quantitatively approximate, but clearly emphasize the need for studying the soil–structure interaction to estimate the realistic force quantities in the structural members, accounting for their three dimensional behavior.

In direct approach the soil and structure are modelled together in one step accounting in cooperation with inertial and kinematic interaction. Inertial interaction develops in structure in line for its own vibrations producing rise to base shear and base moment, which in turn causes displacements of the foundation relative to free field. While kinematic interaction develops due to presence of stiff foundation elements on or in soil causing foundation motion to deviate from free field motions.

## **2. Substructure Method**

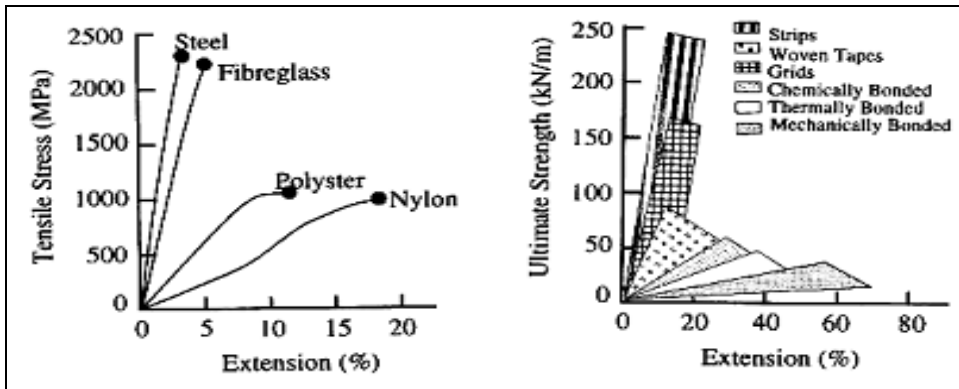
Substructure method is one in which the analysis is split into many steps that is the principal of superposition is used to isolate the two primary causes of soil structure interaction that is inability of foundation to match the free field deformation and the effect of dynamic response of structure foundation system on the movement of supporting soil. In the analysis and design of engineered structures in the past, it was presumed that the groundwork of structure was fixed to a rigid underlying medium. In the last few decades, however, it has been recognized that Soil Structure Interaction (SSI) altered the response characteristics of a structural system because of massive and stiff nature of structure and, often, soil softness. Various studies have appeared in the literature to study the effect of SSI on dynamic response of structures such as nuclear power plants, high- rise structures and elevated highways.

### **2.4 SUMMARY**

An introduction to Reinforced soil structures like Reinforced soil retaining wall, Reinforced soil foundation, Mechanically Stabilised Earth Wall and Reinforced Soil structure Interaction (RSSI) is presented in this chapter. The chapter also deals with Reinforced soil, types of reinforcements, mechanism of reinforcement. Section 2.5 presents various figures in reinforced soil structures

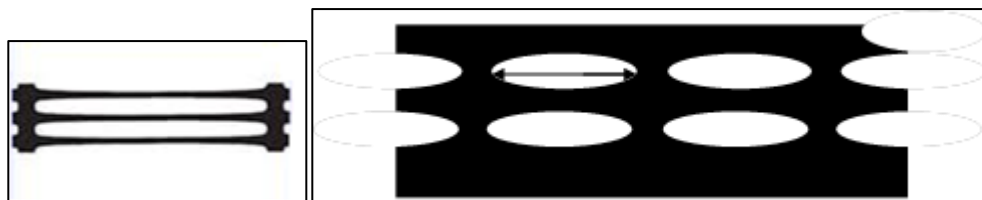
Section 2.4 presents the various figures related to reinforced soil structures available in literature.





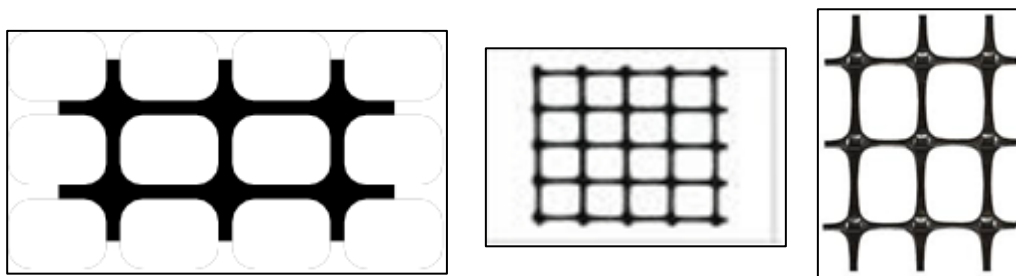
(a) Different material fibers (Schlosser and Delage, 1987)      (b) Geosynthetic products (John, 1987)

Fig. 2.4 Stress-strain characteristics of typical reinforcing material



(a) Uniaxial geogrid

Fig. 2.5 Typical geogrids used as soil reinforcements (John, 1987)



b) Biaxial geogrid (John, 1987)

c) Triaxial geogrid

Fig. 2.6 Geogrids



**Fig. 2.7 Geomembranes**



**Fig. 2.8 Geotextiles**

<https://en.wikipedia.org/wiki/Geosynthetics>

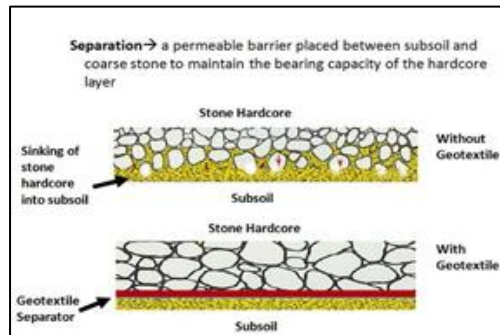


**Fig. 2.9 Geosynthetics as separators**

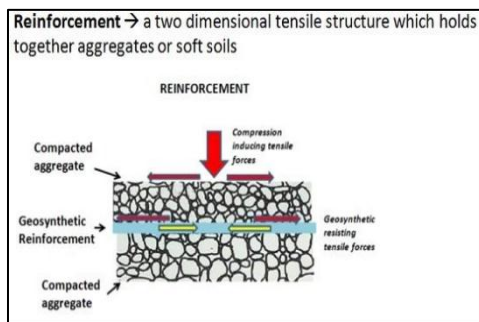


**Fig. 2.10 Geosynthetics as Reinforcement**

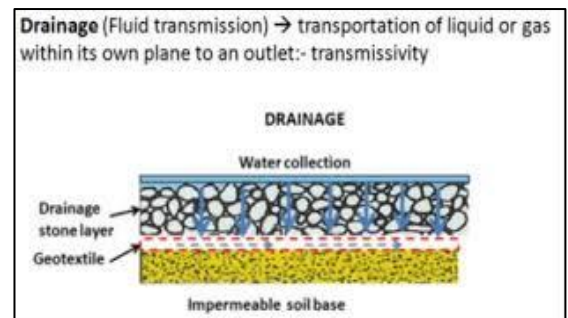


**Fig. 2.11 Geosynthetics as Drains**

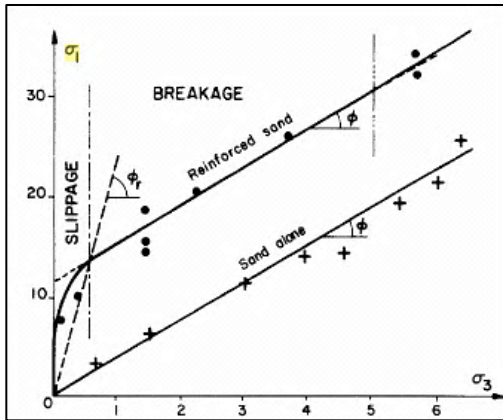


**Fig. 2.12 Reinforced and unreinforced Samples in triaxial tests**  
(Schlosser et al., 1972)

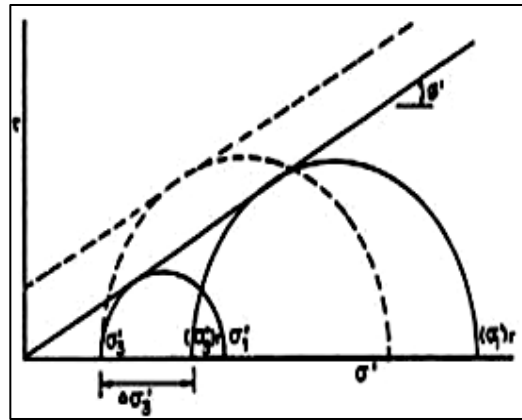


**Fig. 2.13 Anisotropic Cohesion and Enhanced Cohesion Concepts**  
(Ingold, 1984)

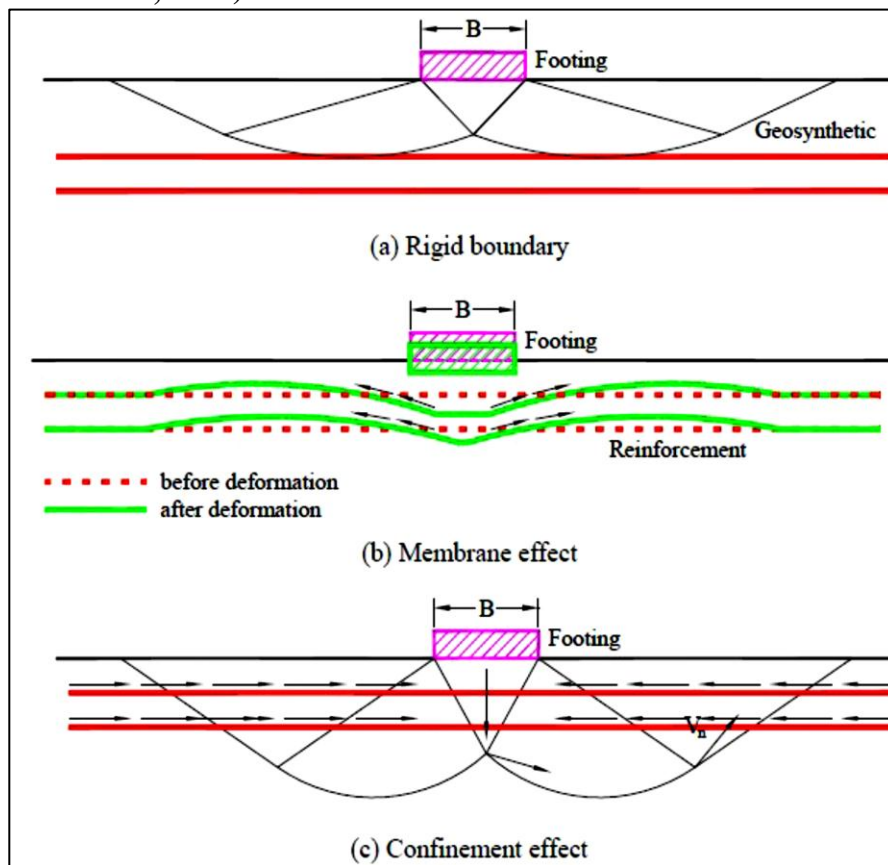
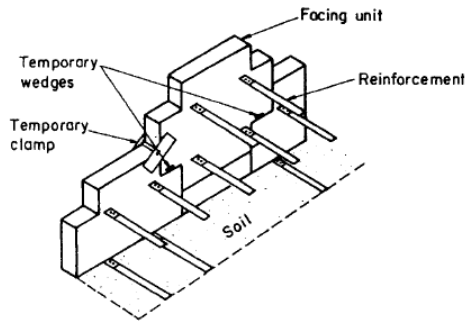
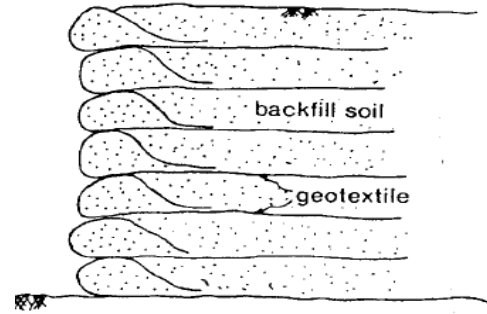


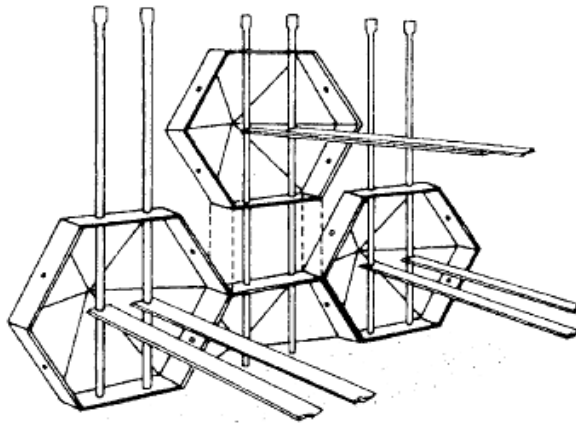
**Fig. 2.14 Reinforcement mechanisms** (Chen, 2007)



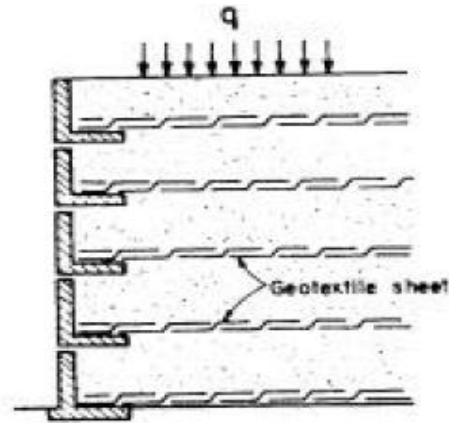
(a) Concrete Panel facing (Reinforced Earth® system)



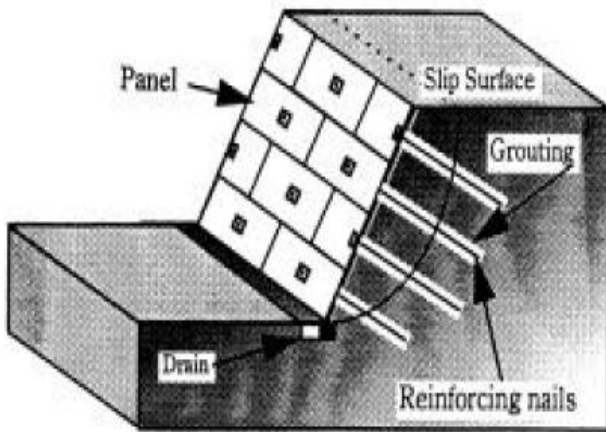
(b) Wrapped around facing



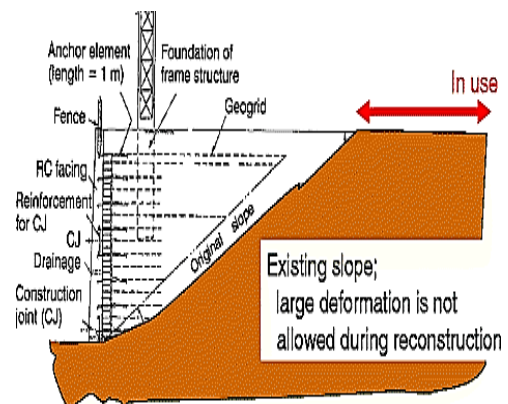
(c) York wall facing (Jones, 1992)



(d) L-shaped concrete facing (Broms, 1988)



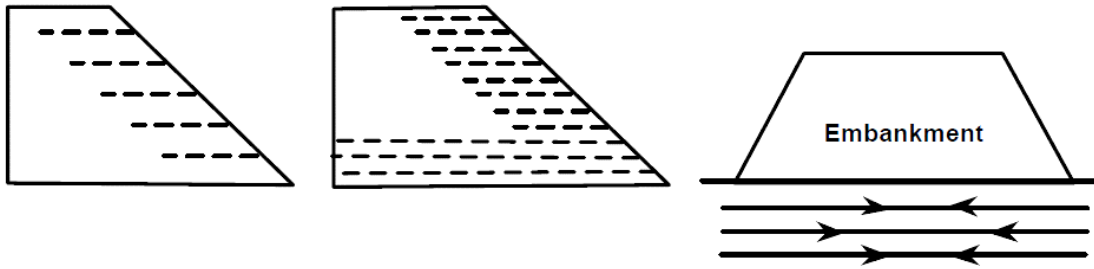
(e) Reinforced Concrete Panel (Japanese System)



(f) Full Height Rigid Reinforced Concrete Facing (GRS-RW System)

Fig. 2.15 Currently used typical facings in reinforced soil structures





(a) Superficial reinforcement (b) Body reinforcement (c) Foundation Reinforcement

Fig. 2.16 Embankment reinforcing modes ( Ingold, T.S.,1982)

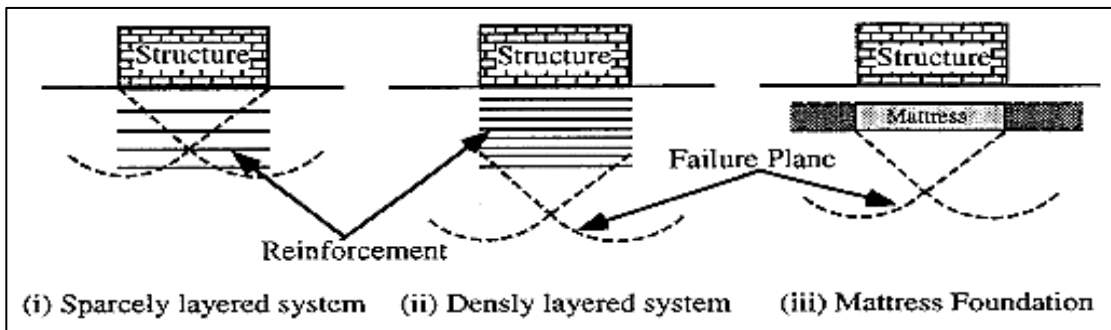
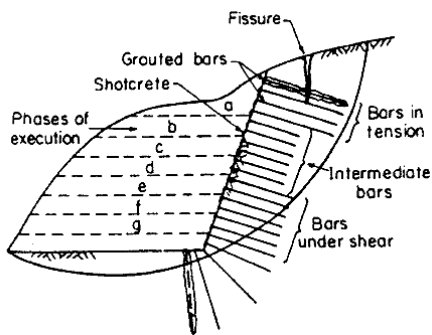
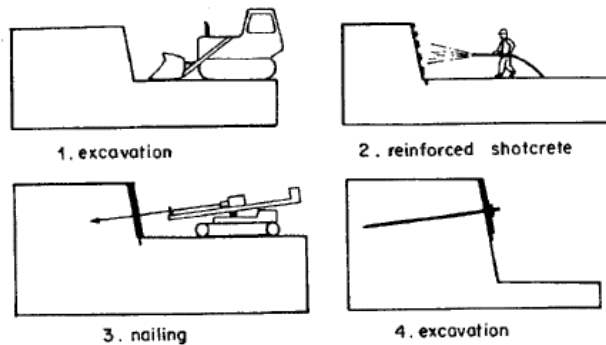


Fig. 2.17 Critical zones beneath reinforced foundations (Fukuda et al., 1987)



(a) Typical soil nailed structure.  
(Schlosser and Juran, 1979)



(b) Construction steps  
(Schlosser and Delage, 1987)

Fig. 2.18 Typical in-situ soil-reinforcing techniques

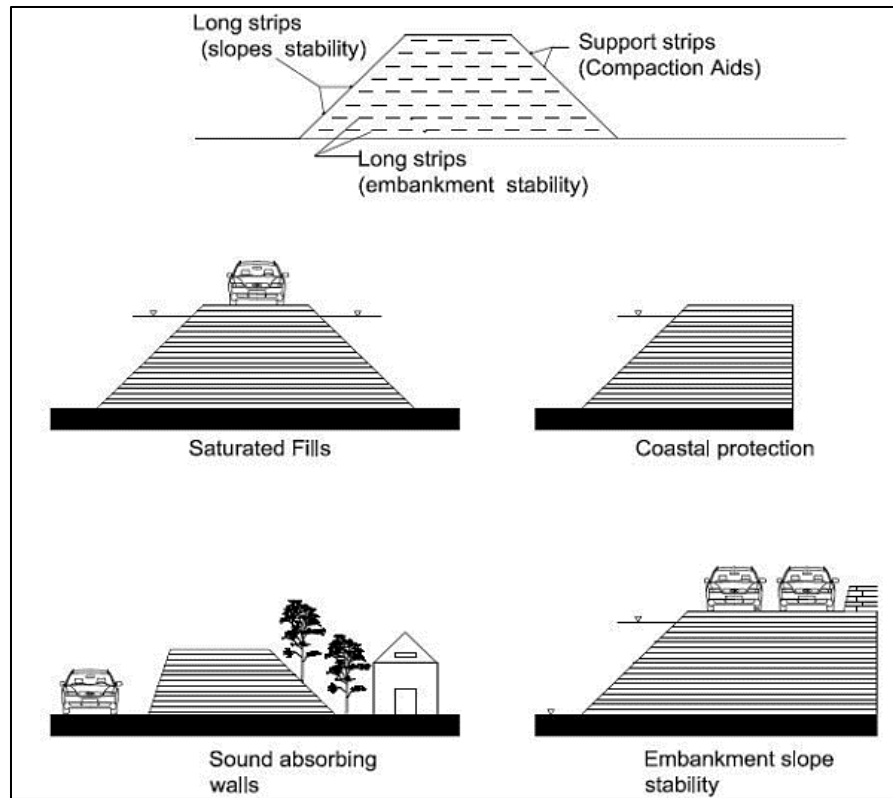


**Fig. 2.19 Illustrations of multilayer geosynthetic slope reinforcement(Christopher B.R. and Holtz R.D., 1985)**

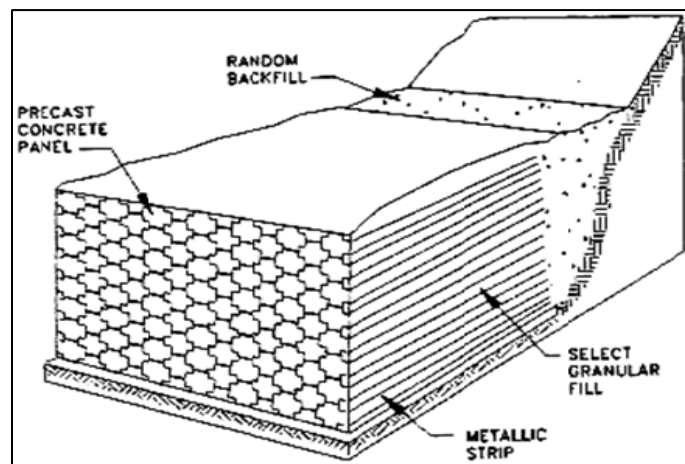
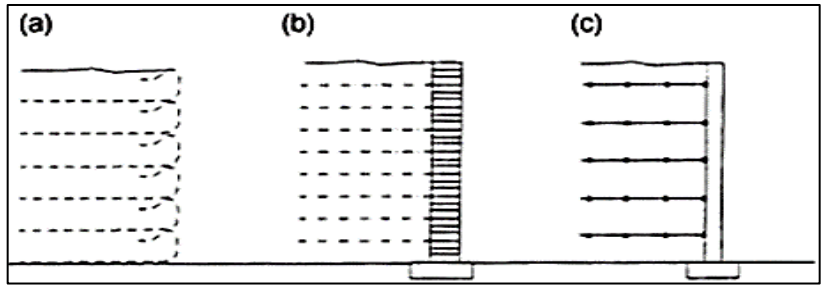
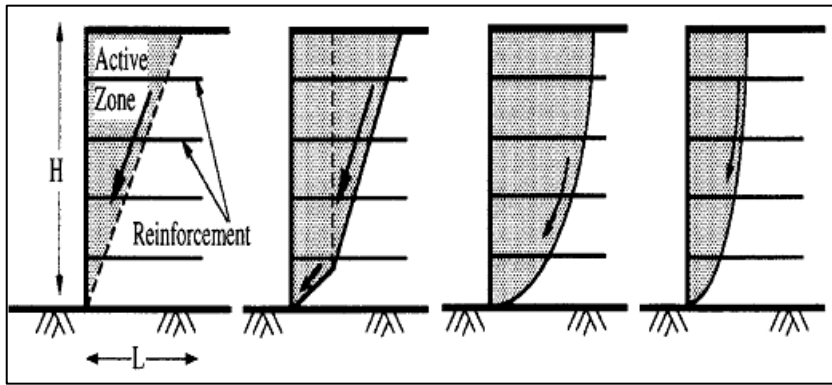


**Fig. 2.20 Components of a Reinforced Earth wall**



(a) GRW with Wrap-around facing (b) GRW with Segmental or modular concrete block, and (c) GRW with Full- height precast panels

Figure 2.21 Reinforced retaining wall systems using Geosynthetics:



(a) Straight wedge (b) Two-part wedge (c) Circular arc (d) Logarithmic spiral  
 Fig. 2.22 Common shapes for potential failure surfaces for Limit Equilibrium Analysis techniques

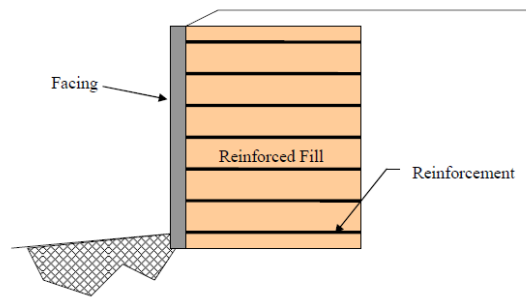


Fig. 2.23 Primary MSE wall Components (Alzamora, 2009)

## CHAPTER 3

### LITERATURE REVIEW

#### 3.1 GENERAL

In this chapter, a brief history of reinforced soil has been reviewed. The mechanism of reinforced earth and different concepts relevant to the research are being discussed. Different fields of application are presented such as foundations, dams, embankments, and reinforced earth walls. A review of current design methods and comments on them as well as conclusions are given.

Parkin et al. (1966) established a method for reinforcing the downstream slope of the composite earth and rock fill dam in California. The method involved reinforcing the rock fill in the downstream slope with horizontal metal railway lines and the facing units consisting of rails in diamond shaped configuration with horizontal reinforcing rails linked to the points of intersection of the grid. During the 17th & 18th centuries, the early French settlers in Canada built many miles of low dikes made of mud and sticks to protect farmland.

In the 1960s, French engineer, Henri Vidal came out with a modern form of reinforced earth wall. Vidal's concept of reinforced earth "Terre Armee" is more exhaustive than soil reinforcement methods proposed earlier. The Vidal system enables retaining walls to be constructed in which the soil mass behind the vertical wall face is reinforced by the addition of regularly spaced flat horizontal strips of metal. This system differs from an anchored wall system, as it is the frictional interaction between the fill and the reinforced element which maintains the equilibrium of the structure rather than the tie back force.

The beneficial effect of plant roots in stabilizing soil has been recognized for a long time. Osman (1990) mentioned that the earliest application was made by villagers in

Ancient Egypt who used straw mixed with clay to improve the quality of building material in the construction of dwellings, and such procedures have recently involved analytical as well as experimental study. Temporary roads through swampy areas are often constructed on a foundation of small trunks and branches.

## **3.2 REVIEW OF STUDIES ON REINFORCED SOIL RETAINING WALL**

### **3.2.1 Numerical / Analytical Studies on Retaining Wall**

Shen et al. (1976) performed analytical studies by using a complex prototype constructed in the field at Southern California. This wall was instrumented. The strengths and weaknesses of the analytical model and the overall behaviour of the structure were illustrated by comparing the field performance data with these analytical results. Additionally, various recommendations were made for reinforced soil structural design. Also, the significance of the study in relation to the existing design procedures were presented. The analysis of the finite element results and field performance indicated that reinforced earth is a relatively rigid supporting unit in which, under normal conditions, the stress state within the wall is approximately  $k_0$  condition and the backfill just behind the wall approaches  $k_0$  condition.

Basset and Last (1978) considered that the mechanism of tensile reinforcement involves anisotropic restraint of the soil deformations in the directions of the reinforcements. Using Roscoe's failure criteria for sands based on zero extension concepts; they demonstrated that the presence of the reinforcement leads to the rotation of the principal directions of the deformation tensors. Reinforcements should be aligned with the zero extension lines, thus, exhibiting a vertical failure surface. Thus, the stress and the strain patterns are greatly modified due to the soil reinforcement interaction (Refer Fig. 3.1).

Naylor and Richard (1978) applied the unit cell concept and devised a slipping strip analytical model for soil retaining walls by selecting a special element. The soil was modelled by six noded rectangular elements and was assumed to be linearly elastic.

An additional degree of freedom was given for modelling the displacement of a point on the strip relative to the soil matrix in a direction parallel to the strip. The effect of fixity was investigated at the face, strip slip. A parametric study was conducted using stiffness of the foundation, relative longitudinal stiffness of strips and soil.

Ogisako et al. (1988) analysed polymer grid reinforced soil retaining walls and performed finite element analysis on the same. The wall was modelled by using the beam element while the soil was modelled using quadrilateral elements. Truss elements were used to model the polymer grid. The soil reinforcement interface and the soil wall interface were modelled using joint elements. Parametric studies were performed for lengths of the polymer grid, different spacing and different heights of the wall. The wall deformation, the earth pressure acting on the wall and the effect of these parameters were reported in detail.

Bauer and Halim (1989) studied reinforced soil walls with cohesive backfill soils by using finite element method. The Hyperbolic stress function was used to model the soil by assuming the base to be rigid. Their studies showed a decrease in the wall inclination which resulted in a corresponding decrease in the lateral movement of the wall face. Maximum settlement occurred at the upper part of the wall face. The footing location influences the maximum stress in the reinforcing strip. The lateral movement and settlement were found to be largely affected by the inclination and the direction of the load. The presence of a cohesive backfill was found to reduce the lateral displacements by 25% and the settlement by 50%.

Tatsuoka et al. (1989) studied the effect of facing rigidity in a set of GRS-RWs model tests having facing Types A-D. Types A and B are very flexible geosynthetic wrapped face, gabion face, or skin facings. Type C is articulated concrete panels and Type D full height concrete panels. The test results prove that the location of failure surface moved from an intermediate elevation to the bottom of the facing depending on the wall facing rigidity. The ratio of earth pressure  $p_f$  behind the facing wall to  $q_u$  remained almost constant with the facing rigidity. Similarly, the tensile force just behind the facing is greatly influenced by the facing rigidity (Fig. 3.2). Location of

$T_{\max}$  approaches back of the facing with increasing facing rigidity. Several other researchers have also reported about the contribution of the facing rigidity on the stability of the reinforced soil structure.

Chew and Schmertmann (1990) studied the deformation behaviour of reinforced soil walls. They adopted an antecedent finite element code which was validated, for their studies. The traditional design procedures for reinforced soil walls were taken into consideration. Parameters like rupture, the overall stability and pull-out capacities of the reinforcement were analysed. But the wall deformations under working stress conditions are neglected. The authors have studied the reinforcement layout and have tried to narrow this gap. They have presented the summary of numerical studies on the effect of reinforcement length and external loadings on the wall deformation. The modelling, the construction sequence and the compaction operations were carried out by using the FEM code. Their code also considered the pressure from the unreinforced soil which is behind the reinforced soil.

Karpurapu and Bathurst (1992) modelled the controlled yielding concept and conducted two sets of numerical simulations. The simulations were done using the finite element method along with the hyperbolic model. A system of flexible springs and frictionless rollers were used to construct 1m high walls. The facing wall was constructed using a pile of 20 articulated platens. Their movement in horizontal direction was restricted. Both the panels and the soil were modelled using eight-noded quadrilateral elements. The springs were modelled using two-noded bar elements. The interface between the panels and soil, was modelled using six-noded isoparametric elements. These elements are assumed to possess negligible shear stiffness. The nodes at the bottom surface of the mesh below the soil, were fully constrained. The incremental construction sequence involved in the physical tests was simulated. The hyperbolic constitutive model was used to model the material behaviour of the soil. Preliminary design charts were generated by simulating the selection of stiffness and thickness of compressible layers placed against rigid walls. These walls were simulated for well graded sand backfills compacted to different range of densities.

Jianchao and Kaliakin (1993) studied various interface elements. Zero thickness interface elements are widely used in the finite element analysis of geological structures. However some of these elements possess evident deficiencies. By examining the behavior of Goodman et al.'s interface element, Hermann's interface element and the quadratic six noded interface element with zero thickness, their advantages and deficiencies are illustrated in their studies. They developed a new four noded zero thickness interface element which simulates the different deformation modes of the interface. Though the simplest constitutive relation has been used in deriving the element stiffness matrix, more realistic constitutive laws can be applied to model the interface behavior with reasonably good accuracy. A similar derivation as that associated with the new four node element has been applied to a six node element and the result is an improved zero thickness interface element. They have found that through analyses and comparisons with the existing interface elements, the elements have shown quite satisfactory tangential and normal behaviour.

Brocklehurst (1993) formulated interface element model and incorporated them into a large strain finite element code along with a new axisymmetric membrane. This study was undertaken to understand and analyse the mechanism of a geosynthetic membrane. It was found to influence the performance of a two-layered axisymmetric plane strain soil element. The reinforcement is placed in the soil fill or at the interface of fill overlying the subgrade of clay. For the interface the Mohr-Coulomb yield function which is an elastic-perfectly plastic model, is implemented and for the membrane, a linear elastic model is used. These new formulations consider both the displacement effects and the large global rotation. They are checked for closed form large and small strain problems. The Lagrangian description of deformation govern the finite element equations.

Rowe and Ho (1996) discussed the effects of panel continuity, reinforcing layers, shear at soil-reinforcement interface, effect of panel location connections, the foundation soil stiffness and the backfill soil on the performance of retaining wall. The authors concluded the following about the stiffness of backfill soil (a) the



modulus of elasticity does not significantly affect the forces required for either external rigid body equilibrium except for very low values of modulus nor the internal equilibrium of the reinforced soil wall system and (b) the horizontal deformations in the reinforced soil mass and the corresponding deformations of the wall face are influenced by the change in the modulus of backfill soil.

Matsuzwa and Hazarika (1996) performed numerical investigations to study the static active earth pressure based on the effect of wall movement modes. They developed new interface elements. These interface elements possessed bilinear displacement-stress relations. The frictional behaviour between the backfill soil and the wall were simulated. Conventional linkage elements were idealized suitably to prevent the separation of the wall and the backfill soil. The active state of the soil was defined on the basis of formation of the progressive failure of backfill soil. For calculating the active earth pressure coefficient empirical equations were derived. The governing parameter was the wall movement in these equations.

In their study, Ling et al. (2000), have presented the results of the finite element analysis of a concrete-block, geosynthetic reinforced soil retaining wall constructed at Japan at the Public Works Research Institute (PWR Institute). Interface elements were used to model the block-block and soil-block interactions while the soil was simulated using a hyperbolic model. A hyperbolic model for geosynthetics was incorporated into a computer program to simulate the soil-structure interaction. The results proved that the finite element model can simulate reasonably well the behavior of concrete-block geosynthetic-reinforced soil structures.

Gurung (2000) used a nonlinear theoretical elastic hyperbolic model and studied the pull-out response of anchor strip reinforcement. The study dealt with the soil reinforcement interface which was based on shear stress displacement relationship. In their study, additional terms which incorporate the anchor section for the soil reinforcement interaction, were also introduced. The interface pull-out mechanisms have been streamlined by devising boundary conditions for the anchor section. To explain the pull-out behavior, the relative stiffness and the displacement parameters,

an anchorage factor that is anchor-to-strip reinforcement capacities were defined. Parametric studies have been carried out for different anchorage factors, relative stiffness values and interface shear stresses. The pull-out force, variation of displacements with the distance along the reinforcement for different anchorage factors and the normalized load-displacement relationships have been presented. Using a zero anchorage factor, experimental results for the pull-out test for planar reinforcements have also been investigated with the model. This model helps in evaluating the pull-out displacements, stresses and strains all along the strip anchor reinforcement.

Bennis and Debuhan (2003) proposed a two-phase continuum description of reinforced soil structures wherein the soil mass and the reinforcement network are considered as mutually interacting superposed media. They developed governing equations for the aforementioned model in relation to elastoplasticity, with a special emphasis put on the soil/reinforcement interaction constitutive law. The general two-phase model developed for soils strengthened by continuous linear reinforcements, whose main features have been outlined in this paper, proves to be an interesting computational time-saving alternative to traditional calculation methods of reinforced soil structures, where reinforcements and soil are analysed by considering them as distinct elements.

Syed and Basudhar (2008) studied the reinforced soil walls by applying the Finite Element method (FEM). In their study, 4-nodd linear isoparametric rectangular elements have been adopted to model the backfill soil and the wall facing, while the geosynthetic reinforcement is modelled as a one dimensional bar element. The interaction of soil and reinforcement is simulated by considering Goodman's 'zero thickness' joint element. For a benchmark problem various studies carried out are regarding the wall movement, settlement of backfill and reinforcement strains. The results obtained using their current analysis have been found to follow those of experimentally observed values. However the present predictions when compared with the other FEM results reported in their literature show a wide variation especially the material behaviour. The total load comprises the self-weight of the

backfill and any kind of external load acting on the reinforced soil structure. The self-weight of the facing and geosynthetics being negligible are neglected.

### **3.2.2 Experimental Investigations on Retaining Wall**

Karpurapu and Bathurst (1994) monitored and studied two carefully built large-scale reinforced soil retaining walls. Dense sand fills reinforced by extensible reinforcement (geosynthetic) connected to two different facings were used to construct these walls. The model walls were studied till collapse. The sand fill surface was subjected to a series of uniform loads. This study demonstrates that accurate predictions of the wall performance can be obtained by proper modelling of the dilatant behaviour of the sandy soil. The granular soil is modelled using a modified hyperbolic constitutive model along with a dilation. The polymeric reinforcement were subjected to a few laboratory tests. The laboratory tests conducted included the constant load tests and isochronous load-strain-time data was developed. Various properties of the components of the large-scale physical models are established. The analyses show that the various models adopted in this study and their implementation can accurately predict the wall performance.

Bergado et al. (1995) studied the performance of a reinforced embankment resting on soft Bangkok clay by applying the plane strain finite element method. The analysis was carried out for the actual soil / reinforcement properties. The relative displacement pattern of upper and lower interface elements were also considered. Using this method, a full scale test involving reinforced embankment with a vertical face wall on Bangkok clay was conducted and analysed. The results of both numerical and field investigations were compared. They concluded that the interaction between the reinforced soil mass and the soft ground and the interaction between the backfill soil and the grid reinforcement principally control the response of a reinforced embankment resting on soft ground. The finite element analysis also included the variation in the permeability of the soft ground in the studies.

Rajagopal and Hari (1996) carried out experimental investigations and numerical

analysis using finite element method and predicted the anchor capacities in anchored retaining walls and proposed simple design methods for these walls. They have conducted plane strain investigations and reported the influence of the relative size and resolution of the finite element (FE) mesh. A detailed analysis is presented for unreinforced and reinforced plane strain, axisymmetric two layered soil. The authors have discussed the strains, soil displacements, principal stress directions, stresses, the stresses on the underside of the footing and mobilized fill friction angles. A few studies with axisymmetric parameters involving plane strain conditions for the various material properties have been conducted, to determine the influence and significance of those variables on the performance of the two-layered soil system under monotonic loading. Their study takes into consideration the different reinforcement lengths, fill depths, stiffness, strengths, and different clay strengths.

Careful examination of the displacements and stresses at the interfaces with the surrounding soil, load displacement response of the footing, the reinforcement tension help us to identify the mechanisms of reinforcement. A comparison between the results of the FEM model and the plane strain and axisymmetric limit equilibrium design method has been carried out.

Filz and Duncan (1997) presented the results of finite element calculations by reviewing the case history data and model test results. They constructed massive concrete walls resting on rock foundations designed for earth pressure at rest. The authors designed a simple procedure. The authors have shown that the design of retaining walls can be made economical by considering the vertical shear forces.

Mofiz et al., (2004) conducted tests using a modified direct shear apparatus to study the stress-strain characteristics of unreinforced and reinforced granite residual soil. In this study, tests were conducted for computer controlled shear box apparatus. The study was carried out for stress levels ranging between 50 to 400 kPa. The various parameters studied were shear strength and deformation properties of reinforced and unreinforced soil. Further, the results of the tests were analysed for the orientation

and volume changes on the shear strength of soil composites and the effects of reinforcement. It was observed that the degree of reinforcement orientation influences the shear strength and volume change behavior. It was also observed that the applied stress levels influence the dilation or contraction properties of the soil composites. The study of cohesive soils was carried out by incorporating a non-linear elasto-plastic model with plastic hardening. This model was later adopted to predict the behaviour of reinforced and unreinforced soil.

Desai and El-Hoseiny (2005) investigated a geosynthetic reinforced soil retaining wall constructed at Tanque Verde Road site, Ariz. This retaining wall was built with a concrete wall facing panel. The finite element code DSC-SST-2D was used to simulate this wall. The program allows for plane stress, plane strain, and axisymmetric idealizations which also includes the construction sequences. Triaxial tests were conducted for backfill soils. Cyclic multi-degree freedom shear tests were conducted for interfaces and these test results were used as material parameters for carrying out the numerical analysis. The various concepts used to model the soils and interfaces were the hierarchical single surface plasticity model and disturbed state concept.

Simulation of geogrid reinforcement was carried out by adopting a linear elastic model. The interfaces between the reinforcement layers and soil was modelled by using a thin layer element. A reasonably good agreement was observed between the measured field behavior of the wall and the results of the finite element analysis. The lateral and vertical stresses transferred to the reinforcements and wall face were compared.

Ding and Hargrove (2006) conducted static studies by taking into account the nonlinear stress-strain relationship of soil reinforced with flexible geofibers. The investigation includes homogenization technique to determine average stress and strain tensor. An elastic incremental stress-strain relation has been brought in to explain the deviatoric shear stress-strain relationship of equivalent homogeneous geofiber reinforced soil. Elastic energy method facilitates the assessment of various

parameters such as the relation of number of geofibers, contents, mechanical behaviour, distribution, and geometrical features in relation to shear modulus of geofiber reinforced soil and hence it has been adopted. Calibration of the deviatoric shear stress and axial strain curves of geofiber reinforced soil were accomplished by using the laboratory test data of geofiber reinforced soil samples. Comparison of the computational (theoretical) curves of geofiber reinforced soil and those obtained by testing data of geofiber reinforced soil is made. The experimental results and the model predictions show a good agreement.

In their work, Yoshihisa and Bathurst (2007) extended the K-stiffness method to the  $c-\phi$  soils using data obtained from nine recent case studies – three from the USA and six from Japan. In all these constructions one common feature was that all the walls were built with a vertical face using backfill soils with different range of fines content. The walls varied widely with respect to the type of wall facing. This data set is now used to isolate the influence of soil cohesion on reinforcement loads within the framework of the original K-stiffness method together with previously published data for vertical walls. The new data set which includes a cohesion influence factor is now used to calibrate a modified K-stiffness method equation. When compared to the American Association of State Highway and Transportation Officials simplified method, the modified K-stiffness method is found to improve the magnitude and distribution of reinforcement loads. The internal stability design of vertical-faced geosynthetic reinforced soil walls with  $c-\phi$  soil backfills is based on this load distribution.

Jayasree (2008) developed a code based on the finite element analysis for a two dimensional, nonlinear plane strain analysis of gabion faced retaining walls which can predict their stress-strain behaviour for both the reinforced soil type and gravity type. 20 four noded quadrilateral isoparametric elements were incorporated for modelling the backfill soil, foundation soil, in-situ foundation soil and gabion facing. 20 number of two noded linear truss elements were used to model the mesh reinforcement. 20 four noded zero thickness elements and line interface elements proposed by Desai

(1974) were used to model the mesh reinforcement soil interface as well as for the backfill wall and the facing.

Nonlinear hyperbolic formulation was used to model the tangential shear stiffness. The nonlinearity of the soil matrix was modelled using the Duncan and Chang (1970) model. The Mohr-Coulomb failure criteria was applied to soil matrix, gabion facing and interfaces. The authors also conducted experimental investigations on model walls both for field and laboratory tests. Different gabion fill materials were studied. The quarry dust and coarse aggregates were mixed together in required proportions or were placed in layers one above the other. The wall deformation was measured. Also, the behaviour of walls for different fill materials was analysed. They found that the deformation behaviour of walls would not be affected by replacing the gabion fill material by a soft material. The replacement of soft material can be up to 50% provided the deformations can be allowed to some extent.

The developed code was compared with the published and experimental results. The authors then conducted systematic and extensive parametric studies to understand the behaviour of the retaining walls. Finally, they studied the gabion faced retaining wall design. The design considered both the stability and deformation criteria. They developed handy design charts to provide a good design tool to the designers. They conducted studies and proved that the gabion faced retaining walls are economical in comparison with the RCC gravity walls. The cost breakdown and prediction ratios were also proposed.

Shouling and Jiang (2009) studied the composite soil stabilized with lime and reinforced with fiber and used neural network and considered nonlinear elastic behavior. Parameters like confining pressure, lime powder, short fiber contents, shear strain and sample-aging period were assumed to influence the shear modulus of the reinforced soil nonlinearly. To represent the nonlinear relation between shear stress and strain, a multilayer neural network was developed. Numerous triaxial tests have been conducted to validate the neural network model for 34 soil samples. The parametric sensitivities based on the neural network have been analyzed. The results

of sensitivity analysis reveal that the improvement in the mechanical properties of soil can be mainly owed to the lime content and curing time rather than the fiber content. This is the earliest attempt to model the elastic behavior of composite soils by the application of the neural network. They have found that quality data or information about the performance of reinforced soil can be obtained by modelling it using a multilayer neural network. These results help in taking better decisions and help in the improvement of construction material designs.

In their work, Ling and Liu (2009), conducted finite element analyses and validated test results of a full-scale test wall using simplistic and sophisticated methods. The nature of analysis regarding its simplicity and complexity has always been an issue. In their work, different types of material models were incorporated in the finite element analysis based on the simplicity or complexity. The results of stress-deformation analyses are compared and presented. Simple, non-linear elastic and complex elasto-plastic analyses applied to the wall construction that involve static loads, produce close and acceptable results. Finite element analyses were carried out to simulate the behaviour of reinforced soil retaining wall built with modular wall facing. Comparisons were made between the wall deformation and strains. The vertical and lateral stresses developed in the geogrid layers were also compared.

Mofiz and Rahman (2010) carried a comprehensive testing program to study the volume change and stress-strain behavior of unreinforced and reinforced residual soil. The instrument used for the study was a computer controlled GDS triaxial apparatus. A series of drained triaxial tests were carried out for unreinforced and reinforced soil. When compared to the unreinforced soils, the reinforced soils reveal higher volume contraction and failure strains. When compared to the woven geotextile reinforced residual soil, soils reinforced with non-woven geotextiles yield higher strength, failure strains and coefficient of interface friction. They proposed a simplified approach for numerical calculations to predict the shear strength of unreinforced and reinforced soils. Charts were also prepared to obtain the coefficient of interface friction from triaxial tests. These charts also helped to estimate the strength of reinforced soil. The laboratory observations show good agreement with the predictions of failure stress using



simplified approach.

Mirmoradi and Ehrlich (2017) studied the behaviour of reinforced soil walls by conducting a numerical analysis applying the finite element method (FEM). The results obtained from the numerical study were validated with those obtained for a full-scale, wrapped-faced reinforced soil retaining wall. Various studies were conducted by considering different types of facing, compaction efforts, stiffness in the reinforcement, shear resistance of the backfill. For the wrapped faced wall, the maximum values of tension occurred close to the bottom of the wall while the maximum tension in the reinforcement occurred near the mid-height for the block facing wall. By increasing the reinforcement stiffness greater values of tension developed in the reinforcement for both wrapped and block faced walls. It was also observed that lower values of reinforcement tensions occurred with the increase of backfill soil shear resistance.

### **3.3 REVIEW OF STUDIES ON REINFORCED SOIL FOUNDATION (RSF)**

#### **3.3.1 General**

Several studies both numerical and experimental have been carried out to analyse the reinforced soil foundation. These studies have time and again proved that the reinforced soil shows significant reduction in the settlement of foundation soil and improvement in the bearing capacity. Previous research has shown that the reinforced soil foundation is an economical solution to many geotechnical problems. When compared with the conventional methods, like increasing footing dimensions or by replacing natural soils reinforced soil foundation offers a better solution.

Many of the researchers investigated the parameters related to the bearing capacity ratio (BCR). BCR is the ratio of the bearing capacity of the Reinforced Soil Foundation (RSF) to that of the unreinforced soil. The various parameters studied by the researchers include:

- Number of reinforcement layers
- Vertical spacing between reinforcement layers,
- Top layer spacing (u),
- Shape of footing
- Soil type
- Embedment depth of footing ( $D_f$ )
- Reinforcement length (l)
- Stiffness and reinforcement type

The results of the experimental studies available show great improvements in BCR are obtained.

### **3.3.2 Experimental Investigations on Reinforced Soil Foundation (RSF)**

Ever since Binquet and Lee (1975a) computed the bearing capacity of sandy soil reinforced with metal strips experimentally, various studies both experimental and numerical have been carried out and the list is as follows

#### **3.3.2.1 Footings resting on reinforced sandy soil with geogrids as reinforcing material**

Omar et al. (1993) studied the influence of width (B) to length (L), (B/L) ratio of the footings on the BCR value by reinforcing using the geogrid. They tested four model strip footings of dimensions 0.0762 m × 0.0762 m, 0.0762 m × 0.1524 m, 0.0762 m × 0.2286 m, and 0.0762 m × 0.3048 m corresponding to B/L ratios of 1, 0.5, 0.333, and 0. A box of dimensions 0.91m x 0.91m x 0.91m deep was used for rectangular footings, while a box of dimensions 0.3048 x 1.10 x 0.914 m deep was used to test model strip footings. The foundation soil used in the study was uniform fine rounded sand which possessed the following properties particle size of 0.34 mm ( $D_{10}$ ), uniformity coefficient of 1.53 ( $C_u$ ), and coefficient of curvature of 1.10 ( $C_c$ ), an average dry unit weight of 17.14 kN/m<sup>3</sup>, ( $D_r = 70\%$ ) and the friction angle was about 41°. The influence depth is defined as the total depth of reinforcement

beyond which the increase in BCR is negligible. With the increase in the B/L ratio for the footing, the influence depth decreases. It was found that the influence depth was 2 times B for strip footing and 1.2 times B for square footing.

Khing et al. (1993) studied strip footings placed on geogrid reinforced sand in a steel box measuring 0.3048 m x 1.10 m x 0.914 m. The model footing made of hardwood was of size 0.3048 m x 0.1016 m x 0.0254 m and the foundation soil used was a uniform fine rounded sand with  $D_{10}$  of 0.34 mm,  $C_u$  of 1.53 and  $C_c$  as 1.10, a dry unit weight of  $17.14 \text{ kN/m}^3$ , relative density  $D_r = 70$  and friction angle of about  $40.3^\circ$ . The settlement to width ratio (s/B) was about 16 to 23% for RSF at the ultimate load and 6 to 8% for unreinforced soil foundation.

The authors reported that the best performance of reinforced soil foundation can be achieved for a length ratio (L/B) of 6. The BCR obtained for (s/B) ratio of 0.25, 0.5 and 0.75 was about 67 to 70% of their peak value. Their experimental results showed that the maximum BCR of 4.0 could be achieved for 6 layers of reinforcement.

Das et al.,(1994) investigated the influence of footing size on the BCR of footings resting on sand bed reinforced with geogrid. For conducting the tests, different sizes of model strip footings of varying widths 0.0508 m, 0.0762 m 0.1016 m, 0.127 m, and 0.1524 m, to 0.1778 m were used and the length of all the footings was maintained as 0.3048 m. A box of dimensions 1.96 m  $\times$  0.305m  $\times$  0.914 m was used to conduct the model tests. Sand with  $D_{10}$  0.34 mm,  $C_u$  of 1.53 and  $C_c$  of 1.10 and relative densities of 55%, 65%, and 75% was used as foundation soil.

Their results showed that by reducing the relative density, the bearing capacity ratio (BCR) could be increased from 2.5 - 4.1 to 3 - 5.4. By increasing the footing width, the BCR decreased from 4.1 -5.4 to 2.5-3.0. For the width of footing equal to or greater than 0.13m - 0.14m, BCR remained constant (at 2.5, 2.9, and 3.0 for reinforced sand at relative densities of 75%, 65%, and 85% respectively).

Yetimoglu et al. (1994) conducted studies on the bearing capacity of geogrid reinforced foundation sand. Both the numerical and the model laboratory tests were conducted by placing rectangular footings on geogrid reinforced foundation soil. Model tests were conducted in a steel box with a square section measuring 0.70 m x 0.70 m x 1.00 m using model steel rectangular footing of dimension 0.127 m x 0.1015m x 0.0125m. The foundation soil used possessed a particle size of 0.15 mm ( $D_{10}$ ),  $C_u$  of 2.33 and  $C_c$  of 0.76. The average dry unit weight was 17.16 kN/m<sup>3</sup>,  $D_r$  of 70-73% and the friction angle was 40°.

Their test results showed that the BCR varied between 1.8 and 3.9 and the settlement ratio ( $s/B$ ) varied between 0.03 - 0.05 for all the unreinforced and reinforced sand. They concluded that geogrid reinforcement does not significantly influence the settlement of the footing at failure. This particular observation is different from that of Das et al.,'s (1994) observation.

They concluded the following

- (1) The effective top layer spacing to the width ratio ( $u/B$ ) was about 0.25 and 0.3 in reinforced sand
- (2) Depending upon the number of reinforcement layers ( $h/B$ ) ratio was found to vary from 0.2 to 0.4
- (3) Influence depth was around 1.5 times  $B$  and the reinforcement to the effective width ratio ( $b/B$ ) was about 4.5

As per the test results of Yetimoglu et al. (1994), the ratio of grid aperture size ( $d_{min}$ ) to average particle size ( $D_{50}$ ) influences the geogrid soil interaction. The bearing capacity of reinforced foundation soil was affected by the number of reinforcement layers and their arrangement.

Adams and Collin (1997) conducted large scale field tests in a concrete box of 6.9 m × 5.4 m × 6 m deep with square footings of sizes varying from 0.3 × 0.3 m, 0.46 × 0.46 m, 0.61 × 0.61 m, and 0.91 × 0.91 m. The soil used was poorly graded fine mortar sand with a mean particle size of 0.25 mm ( $D_{50}$ ), and  $C_u$  of 1.7. The various parameters studied were the top layer spacing, number, area, spacing of reinforcement layers and the density of soil.

The soil reinforced with three layers of geogrid performed well, the bearing capacity increased enormously and the BCR could be increased by 2.6. But the magnitude of settlement was 20 mm ( $s/B = 5\%$ ) and it may be unacceptable for a few foundation types. For low settlement ratio ( $s/B$ ) and for ' $u$ ' less than 0.25 times  $B$  the reinforcement performed very well. They pointed out that for the top layer spacing less than  $0.4B$ , general shear failure was less likely to occur.

Gabr et al. (1998) studied the distribution of stresses in case of geogrid-reinforced sand. They conducted the plate load tests using a model square footing (0.33m wide) in a steel box 1.52 m x 1.52 m x 1.37 m. Ohio river sand with a unit weight ranging from  $17.3 \text{ kN/m}^3$  to  $17.9 \text{ kN/m}^3$  and a friction angle of about  $38.6^\circ$  was used. The foundation soil had  $C_u$  of 8 and  $C_c$  of 1. The stress distribution improved by including the reinforcement. The stress distribution angle ( $\alpha$ ) estimated using the measured stress beneath the center of the footing indicates higher values of the angle ( $\alpha$ ) for reinforced sand as compared to unreinforced sand.

Shin et al. (2002) studied the BCR for geogrid reinforced sand. The model tests were conducted in a steel box measuring 0.174 m x 1.00 m x 0.60 m with a wooden model strip footing of 0.172 m x 0.067 m x 0.077 m. A poorly graded sand having  $D_{10}$  of 0.15 mm, specific gravity 2.65,  $C_u$  of 1.51 and  $C_c$  of 1.1 respectively and relative density ( $D_r$ ) as 74% with the friction angle about  $38^\circ$  was used as foundation soil. For all the tests,  $u/B$ ,  $h/B$ , and  $l/B$  of the reinforcement were maintained constant as 0.4, 0.4, and 6. They found that the influence depth was  $2B$  for the reinforcement. The BCR increased with the increase in the embedment depth of the footing. For an increase in the number of reinforcement layers from 1 to 6, the BCR varied from 1.13 to 2.0, 1.25 to 2.5, and 1.38 to 2.65.

Chen (2007) studied the behavior of reinforced soil foundation by conducting more than a hundred tests. He found that the development of strain along the reinforcement and the settlement are directly related. The geogrids possessing higher tensile modulus performed better than those with lesser modulus. The author showed

that the redistribution of stresses over a wider area can be achieved by inclusion of reinforcement. The redistribution of stresses reduced the settlement due to consolidation of the underlying weak soil below the reinforced zone. The strain measured in the geogrid shows that the geogrid past the effective length of 4.0-6.0 B provides negligible reinforcement effect was proved by the authors. Using FEA program ABAQUS, the scale effect of the model footings were studied. Qiming's results indicate that the reinforced ratio ( $R_r$ ) and the scale effect of reinforced soil are related.

Kumar et al. (2008) studied the settlement of square footings resting on a layer of sand, underlain by weak soil layer by applying the non-linear constitutive laws of soil. The computation of ultimate bearing capacity is very important which can be obtained from an empirical method proposed for the same. The settlement for any given pressure intensity can be obtained from the pressure-settlement curves. Thus the rectangular footing resting on two layered reinforced sand can be proportioned in accordance with the shear and settlement requirements.

### **3.3.2.2 Other reinforcing materials**

Binquet and Lee (1975a) simulated three different foundation conditions and conducted various small-scale model tests such as:

- (1) A deep homogeneous sand foundation
- (2) Sand above a deep soft layer of clay or peat (2.25 in. thick layer of Pack Lite foam rubber)
- (3) Sand above a soft pocket of material such as clay (2 in. thick of finite soft pocket Sears foam rubber).

Model tests were conducted in a box measuring 1,500 mm x 510 mm x 330 mm. A 76mm model footing was used as a strip footing. Ottawa No. 90 sand having a  $C_u$  value of 1.5,  $C_c$  of 0.75 and a dry density of  $1500 \text{ kg/m}^3$  was used as the foundation soil. For plane and triaxial conditions, the corresponding friction angles were  $35^\circ$  and  $42^\circ$ , respectively. The household aluminium foil in the form of 13 mm wide

strips was used as the reinforcement and was placed along the length of the box, at a linear density of 42.5%, with a tensile strength of 0.57 kN/m, and a vertical spacing of 25 mm. The peak and residual soil-tie friction angles were 18° and 10° respectively as obtained from the pull out test.

Binquet and Lee (1975a) reported that by reinforcing the soil foundation, the bearing capacity could be improved by a factor of 2 to 4. They showed that a minimum critical number of reinforcement layers would be required, and that increasing the number of layers would definitely result in better improvements. Based on their results, the authors reported that the influence depth was about 2B and the reinforcement placed below this depth did not increase the bearing capacity significantly. They observed that the broken locations of reinforcements were below the edges or towards the center of the footing rather than near the classical slip surface.

Akinmusuru and Akinbolade (1981) studied the influence of number of reinforcement layers, the effect of vertical, horizontal, top layer spacing, on the bearing capacity of reinforced soil. A square wooden box measuring 1.0 m × 0.7 m high and a model footing 13 mm thick square steel plate with sides 100 mm each were used to conduct their model tests. The foundation soil consisted of sand with  $D_{50}$  of 0.43 mm, and an effective size ( $D_{10}$ ) of 0.14 mm, a dry density of 1700 kg/m<sup>3</sup> at a friction angle of 38°. The rope fiber locally referred to as “iko” served as the reinforcement. 10 mm wide and 0.03 mm thick rope strips, with a breaking strength of 80 N/mm<sup>2</sup> with a soil-tie friction angle as 12° were used as reinforcement. They reported that by reducing the horizontal spacing of the reinforcement bearing capacity of reinforced soil foundation increased. The ultimate bearing capacity of reinforced soil could be improved by a factor up to 3 times that of unreinforced soil. The performance of the reinforced soil was influenced similarly by the vertical and horizontal spacing. The optimum top layer spacing was found to be 0.5 times B. When the number of reinforcement layers was increased more than 3 layers corresponding to an influence depth of 1.75 times B it was observed that the improvement in bearing capacity was negligible.

Fragaszy and Lawton (1984) studied the effect of the soil density and reinforcement length on the soil performance by reinforcing the soil foundations. A rectangular fiberboard box measuring  $0.56 \text{ m} \times 1.22 \text{ m} \times 0.36 \text{ m}$  was used to conduct the tests. A rectangular steel plate of dimension  $7.6 \text{ cm} \times 15.2 \text{ cm}$  served as the model footing while the sand having  $D_{50}$  of  $0.4 \text{ mm}$ ,  $C_u$  of  $1.5$  and  $C_c$  of  $0.75$  was used as foundation soil. The soil used possessed the densities of  $1470$ ,  $1540$ , and  $1590 \text{ kg/m}^3$ , relative densities of  $31\%$ ,  $70\%$ , and  $90\%$  and friction angles of  $36.5^\circ$ ,  $38^\circ$ , and  $39^\circ$ , respectively. The household aluminium foil was used as reinforcement. It was used as strips  $2.54 \text{ cm}$  wide and  $0.0254 \text{ mm}$  thick possessing a tensile strength of  $1.34 \text{ kN/m}$  and was placed at a linear density of  $47\%$ . The top layer spacing was maintained at  $2.54 \text{ cm}$  and all the model tests were conducted with three layers of reinforcement. The vertical spacing of  $2.54 \text{ cm}$  ( $h/B \approx 0.33$ ) and ( $u/B \approx 0.33$ ) was maintained. Their test results indicated that the design criteria influenced the amount of improvement in the bearing capacity.

Irrespective of the soil density, at a settlement ratio of  $0.10$ , the BCR value remained constant ( $1.6 \sim 1.7$ ). They also showed that the BCR increased from  $1.25$  to  $1.7$  with increase in the length of reinforcement from  $3$  to  $7$  times  $B$ , after which the improvement was negligible. They also showed that the design method developed by Binquet and Lee (1975b) is effected by the magnitude of the interface friction coefficient of soil-reinforcement.

Huang and Tatsuoka (1990) studied the bearing capacity of reinforced sand by conducting five groups of tests in the study. A sand box measuring  $0.40 \text{ m} \times 0.183 \text{ m} \times 0.74 \text{ m}$  was used for their model tests using a model footing  $0.10 \text{ m}$  wide strip footing. Toyoura sand with  $D_{50}$  of  $0.16 \text{ mm}$ , a  $C_u$  of  $1.46$  was used as the foundation soil. In the first group of tests, short reinforcement of length  $L$  equal to width of the footing  $B$  was used and varying number of reinforcement layers were used. The second group of tests dealt with the effects of length of reinforcement. The third group of tests dealt with the effects of the number of reinforcement layers. The fourth group of tests involved the study of the cover ratio of reinforcement. The fifth



group of tests consisted of four types of reinforcement having different rupture strength and rigidity. Of the four types of reinforcement, three were of Phosphor bronze, the remaining was of aluminium foil.

Their test results showed that the bearing capacity could be enhanced with short reinforcement too having length  $L$  equal to width  $B$  of the footing. But when the model footings placed on reinforced sand were embedded to a depth  $d$  less than  $0.9B$  for a covering ratio ( $Cr$ ) of 18%, the bearing capacity was similar to that of unreinforced sand for an embedment depth  $D$  equal to  $d$ . For the reinforced sand with a short reinforcement the failure occurred below the reinforced zone.

Karim and Saiful (2009) studied the improvement in the bearing capacity of strip footing by using metal strip reinforcement resting upon sand deposit. The sand bed consists of horizontally placed metal strip reinforcement in one, two and three layers. Model tests were conducted at two different speeds of loadings to study the bearing capacity and settlement of strip footings.

Experiments were conducted in a tank on layers of sand having average densities varying from  $14.67 \text{ kN/m}^3$  to  $15.78 \text{ kN/m}^3$ . The sand bed thickness was maintained 3.9 times the least dimension of the footing. The influence of number of reinforced layers and the speed of loading on bearing capacity were studied. The result is discussed and compared among different layers of reinforcement and two rates of speeds. From the experimental results for the case of reinforced sand bed, it is observed that the bearing capacity of the reinforced soil improves significantly in comparison with the unreinforced bed. In most of the tests, it is observed that with the increase in number of the layers of reinforcement, bearing capacity has been improved. Due to change in speed of loading the bearing capacity and settlement have been affected. The results also indicate that for slow speed, bearing capacity was of higher value than that of higher speed of loading. On the other hand, settlement due to slow speed of loading is lower than that of higher speed of loading.

Kalpana et al.,(2011) conducted a series of model tests to check the feasibility of

using polypropylene fibers as a reinforcing material below footing with the idea of upgrading the engineering behaviour of clayey soil as a subsoil for the foundation. Nine model footing tests were performed on fiber reinforced soil with three different fiber contents (0.25%, 0.50%, 1.00%) and three depths of placement of fiber reinforced soil ( $b/4$ ,  $b/2$ ,  $b$ ) where  $b$  is the width of footing. The actual full scale load tests with the optimum fiber content (0.50%) and optimum depth of placement of fiber reinforced soil ( $b/4$ ) were conducted to verify small scale laboratory results. The bearing capacity of unreinforced soil was found to be  $64 \text{ kN/m}^2$ , which increased to  $250 \text{ kN/m}^2$  with the inclusion of polypropylene fibers. Also modeling of footing resting on fiber reinforced soil was done using the finite element software Plaxis 2D.

### **3.3.2.3 Footings resting on reinforced c- $\phi$ soil using geogrid as the reinforcing material**

Ramaswamy and Purushothaman (1992) conducted experimental studies on model circular footing 40 mm in diameter placed on the clayey soil foundation reinforced with geogrid. Clay (CL) with 100% passing 0.075 mm opening sieve, specific gravity of 2.66, liquid and plastic limits equal to 31 and 18, respectively was used as foundation soil.

The soil had a maximum dry density of  $1800 \text{ kg/m}^3$  with an optimum moisture content of 18%. Three moisture contents of 14%, 18%, and 20% with dry densities of  $1725 \text{ kg/m}^3$ ,  $1810 \text{ kg/m}^3$  and  $1765 \text{ kg/m}^3$  were used in the tests. Their results showed that the effective length ratio ( $l/D$ ) of the reinforcement was around 4 and the optimum top layer spacing ratio was 0.5.

When the number of the reinforcement layers was increased from 1 to 3, BCR increased from 1.15 to 1.70. Higher the moisture content, lower is the bearing capacity of both unreinforced and reinforced clay. When two layers of geogrids were used, the BCR of reinforced clay at optimum moisture content (1.47) was higher than those at wet and dry sides (1.11 and 1.26 respectively).

Mandal and Sah (1992) carried out experimental studies on model footings resting on geogrid reinforced clay in a cuboid steel box measuring 460 mm. The model footing was of size 100 mm x 100 mm x 48 mm made of hardwood. Clay (CL) having liquid and plastic limits as 72 and 41 were used as the foundation soil with moisture content of 28% and undrained shear strength of about 27 kN/m<sup>2</sup>. A maximum BCR was obtained at  $u/B = 0.175$ , while the minimum settlement reduction factor (SRF) at the ultimate bearing pressure of unreinforced clay was obtained at  $u/B=0.25$ . The ratio of the immediate settlement of the footing on a reinforced clay to that on an unreinforced clay at a particular pressure is known as the settlement reduction factor (SRF). By reinforcing using the geogrid, the settlement could be reduced up to 45% of that obtained for unreinforced soil.

Shin et al. (1993) studied experimentally the behavior of strip footings placed on the geogrid reinforced clay. Their model tests were conducted in a steel box measuring 0.304m x 1.09m x 0.91m. A strip footing of .0762 m width was used for the study. The foundation soil was made of clay with a specific gravity of 2.74, 98% passing the 0.075mm opening sieve, and liquid and plastic limits equal to 44 and 24, respectively. The soil was tested for two moisture contents, 42.5% and 37.7%. The optimum top layer spacing ratio was found to be about 0.4 and the effective length ratio ( $l/B$ ) was computed as 4.5 to 5. With the increase in the number of layers from 1 to 5, the BCR increased from 1.06 ~ 1.1 to 1.4 ~ 1.45 and remained constant thereafter. The influence depth ratio ( $d/B$ ) of the reinforcement was about 1.8 times B. They observed that BCR increased with the reduction of the undrained shear strength.

Gu (2011) studied and evaluated the benefits of reinforcing soil using geogrids for two types of structures reinforced soil foundations (RSF) and flexible pavements. The researcher used ABAQUS, developed and applied different FEM models. The bearing capacity and the settlement of RSF was evaluated using the first model. The researchers also carried out parametric studies on various design parameters affecting the performance of RSF. The effectiveness of geogrid reinforced bases in

flexible pavement was studied using the second model in terms of surface rutting. The author also performed parametric studies on the reinforced pavements.

Multiple regression models were developed on the basis of results of finite element analyses to find the advantages of reinforced geometrical structures under various design parameters. The finite element analysis of RSF showed that reinforcing the soil enhances the bearing capacity of soil and reduces the settlement of the reinforced soil. The benefit of reinforcing the soil increases proportionally with the tensile modulus and depends upon the number of reinforcement layers.

Jayamohan and Shivashankar (2012) conducted numerous laboratory tests on a model square footing placed on a geonet reinforced granular bed (RGB) underlain by weak silty soil. These small scale bearing capacity tests were conducted by prestressing the reinforcement on a model square footing. They studied the enhancement in bearing capacity and corresponding reduction in settlement. For their study, the authors considered weak soil, the thickness of granular bed and the magnitude and direction of prestressing force. The settlements at the interface were also measured.

Prestressing the reinforcement significantly enhances the load carrying capacity and settlement response of the prestressed geonet RGB. Biaxial prestressing enhances the performance of the soil rather than the uniaxial prestressing. Experimental results were also used to validate a proposed numerical model. The BCR (bearing capacity ratio) values prophecied from this model were found to match with the experimentally obtained BCR values. PLAXIS program has been adopted to study the effect of prestressing.

Kolay et al., (2013) analysed the enhancement in the bearing capacity of sand layer overlying silty clayey soil and by reinforcing using geogrids. Model tests were conducted by placing a rectangular footing on top of the reinforced soil. For both unreinforced and reinforced soil, load settlement curves were plotted. The study focused on the bearing capacity of sand underlain by silty clay for both

unreinforced and reinforced soils. For  $u/B$  and  $h/B$  ratios equal to 0.33 and for two, three and four number of geogrid layers, the enhancement in bearing capacity of sand underlain by silty clay were 44.44%, 61.11%, 72.22%, respectively. These research findings may be useful in pavement design for similar type of soil available elsewhere.

#### **3.3.2.4. Footings resting on reinforced c- $\phi$ soil using other reinforcing materials**

Kamalzare et al., (2011) conducted experimental studies on bearing capacity of soft clayey soils in places of military, economic or geological importance. Geosynthetics were used to reinforce and enhance the properties of soil, in particular, the bearing capacity. For instance, the roadways, where geosynthetics are emplaced at the interface of the soft-soil sub-grade and the granular materials. In this study, the authors have focused on the behavior of two layered soils (granular base and clayey subgrade) reinforced with geosynthetics. Large-scale direct shear tests were carried out on unreinforced and samples reinforced with different geosynthetics. The authors reported that the shear strength parameters of the interface of two-layered soils may increase or decrease depending on the characteristics of the geosynthetics. The geosynthetic reinforced soils in the sub base layer of roads are extremely sensitive to the characteristics of geosynthetics and can perform better than non-reinforced soils. As a consequence, the load-carrying capacity of the basement will improve provided, the appropriate geosynthetics are used. However, geogrid performs better under higher vertical stresses. Increasing the relative density of the clayey sub- grade would also cause the geogrid to be more effective.

#### **3.3.3 Studies on Modulus of Subgrade Reaction of Soil**

Various researchers attempted to make the Winkler model more practical and realistic by assuming some forms of interaction among the spring elements that represent the soil continuum. Terzaghi (1955) and Bowles (1998) have investigated the factors that affect the determination of  $k_s$ .

Biot (1937) solved the problem for an infinite beam with a concentrated load resting on a 3D elastic soil continuum. He found a correlation of the continuum elastic theory and Winkler mode. Terzaghi (1955) made some recommendations about  $k_s$  for a 1x1 square foot rigid slab placed on a soil medium. However, the procedure to compute a value of  $k_s$  to be used for a larger slab was not specified. Vesic (1961) matched the maximum displacement of the beam in both the models and tried to develop a value for  $k_s$  with matching bending moments. He obtained the equation for  $k_s$  to apply in the Winkler model. Ping Sien et al. (1998) conducted numerous plate-load tests to obtain the load settlement characteristics of a gravelly cobble deposit. The authors then computed the modulus of subgrade reaction “ $k_s$ ” as follows:

$$k_s = \frac{q_a}{\delta_a} \quad (3.1)$$

where:

$k_s$  = modulus of subgrade reaction,  $\text{kN/m}^3$ ;

$q_a$  = allowable bearing capacity,  $\text{kN/m}^2$ ;

$\delta_a$  = allowable settlement against  $q = q_a$ , meter

$$q_a = \frac{q_u}{f.s.} \quad (3.2)$$

where:

$q_u$  = Ultimate bearing capacity,  $\text{kN/m}^2$

$f.s.$  = Factor of safety = 3

Egyptian Code (2001) made a series of plate-load tests to investigate the load settlement characteristics and estimates the value of modulus of subgrade reaction “ $k_s$ ” as follows:

$$k_s = \frac{q}{\delta} \quad (3.3)$$

where:

$k_s$  = Modulus of subgrade reaction, ( $\text{kN/m}^3$ );

$q$  = Stress at settlement = 1.3 mm after ten times loaded, ( $\text{kN/m}^2$ )

$\delta$  = Settlement against  $q$  (meter)

Iancu and Ionut (2009) performed FEM analysis and presented a numerical simulation of plate load test to underline the effect of the size on settlements. The

numerical results obtained revealed that the subgrade reaction coefficient was strictly dependent on the size of the loaded area and the loading magnitude.

Elsamny et al. (2010) presented the field determination of the Young's modulus 'E' of footings on cohesionless soil by using plate load test. They concluded that the subgrade reaction  $k_s$  of cohesionless soil increases with increasing footing depth and size. The subgrade reaction  $k_s$  of cohesionless soil under rectangular footing was found to be higher than that under square and circular one (at same equivalent area). Their results indicated that the subgrade reaction  $k_s$  of cohesionless soil increases with increasing angle of internal friction.

Wael (2013) conducted an experimental analysis using plate load test to determine the effect of foundation depth, size as well as the shape on the modulus of subgrade reaction ( $k_s$ ) of cohesionless soils using nine rigid steel plates of different sizes and shapes (circular, square and rectangular). The tests were carried out on cohesionless soil with different relative densities under different applied pressures. He concluded that the subgrade reaction  $k_s$  of cohesionless soil increases with increasing foundation depth as well as foundation size. His results showed a fair agreement with that of Biot (1937).

### **3.4 REVIEW OF STUDIES ON MECHANICALLY STABILISED EARTH WALLS**

#### **3.4.1 General**

MSE is applicable to slopes, walls, and abutments. It may or may not have some form of facing. It includes all reinforcement systems. It is constructed by using the embankment construction techniques in the fill, i.e., constructed from the bottom up. Reinforcement of weak or soft Embankment Foundations. Sheet reinforcement in the form of geotextiles or polymer grids are usually provided to run continuously at the base, for the full width of the embankment and beyond, on soft ground conditions. These reinforcements provide additional stability to the embankments on soft

foundations. These techniques are generally being used to control the initial stability of the embankments during and immediately after construction, without controlling the settlements. If it is required to control the settlements as well, then the reinforcements are to be used as a part of the foundation stabilization system.

### **3.4.2 Experimental Investigations**

Soil reinforcement techniques have come a long way since the idea of “Reinforced Earth” was conceived. There has been a tremendous and rigorous contribution to its development by employing various forms of reinforcements of different material for varied applications. There were a series of experimental investigations using the laboratory triaxial and direct shear tests on reinforced sands to study the improved performance of the composite material in the reinforced earth structures as discussed in the following sections.

#### **3.4.2.1 Triaxial Tests**

Schlosser & Long (1972) at laboratoire central des ponts et Chaussees (LCPC), France, put forward the apparent anisotropic cohesion concept from laboratory triaxial tests of reinforced sands. A similar theory was also postulated by Hausmann (1976) at NSWIT, Australia, quite independently of the LCPC work. The apparent anisotropic cohesion concept was complimented by the enhanced confining pressure concept by Yang (1972). According to the apparent anisotropic cohesion concept, under low confining stresses a given reinforcement system would fail by slippage or pullout of the reinforcements, whereas, under high confining stresses this same system would fail by breakage of reinforcements as indicated in Fig 3.2. The strength increase was attributed to an apparent cohesion generated by the reinforcement at high confining pressures. In the enhanced confining pressure concept, however, the increased shear strength of the reinforced soil was attributed to an anisotropic restraint to the soil deformation in the direction of reinforcements provided by the reinforcements



### **3.4.2.2 Direct Shear Tests**

Direct shear or the shear box tests have been more commonly used along with the pullout tests for testing reinforced soils to study the soil-reinforcement bond. Pullout resistances of the steel grid reinforcements embedded in soils were first studied by Chang et al. (1977). It was concluded that the grid reinforcement were very efficient in resisting pullout forces. Chang et.al. (1977) performed field pullout tests of strip reinforcement in decomposed granite. Longer strips were found to give higher peak pullout resistances. The rate of increase in the peak pull load caused by an increase in the strip length was much greater than that caused by an increase in the over burden.

### **3.4.3 Role of Facing Elements in the Mechanically Stabilized Earth (MSE) Wall**

According to Schlosser (1982) , if the reinforcements are long enough and are spaced closer in a Vidalean type of reinforced earth retaining wall, the traction forces on the reinforcements at the facing end would be very small, approaching zero. In such cases the facing elements are of no consequence and therefore, can be dispensed with. The main function of the facing would then be to merely prevent the erosion of the retained backfill soil and for aesthetic purposes.

When short reinforcements are used the role of the facing elements would depend on the rigidity of the facing elements. When flexible facing units are used these facing structures also get compressed along with the compression of the backfill during construction and subsequent loading. For structures like abutments with a vertical face and a concentrated load, it is suggested to use rigid facing to retain the earth with short geotextile reinforcements. Increasing the rigidity of the facing was found to increase the stability of the wall remarkably. In the case of differential settlements between the facing structure and the backfill soil, it is suggested to use gabions to smoothen the relative movements (Tatsuoka et al. 1989). Geotextiles are used as sheet reinforcements in MSE construction. The facing elements in this case are commonly constructed by wrapping the sheet reinforcements themselves around the exposed soil

at the face, and covering the exposed fabric with gunite, asphalt emulsion or concrete, other types of structural facings are also used with geotextiles including gabions.

#### **3.4.4 Various Reinforced Soil Systems**

Chang et al. (1977) proved that grid reinforcements are more efficient than the strip reinforcements. The pullout resistances of the mesh or grid reinforcements were found to be as much as about 5 to 6 times greater than that of the strip reinforcements. Several earth reinforcement systems have been developed and used in a number of applications like dams, ground slabs, abutments and foundations, embankments for flood control dikes and for reclamations.

Duncan and Seed (1986) have presented a comprehensive compilation and observation on the currently available data concerning the compaction induced stresses and deformations. Foremost of these observations is the idea that compaction of the soil can result in significant increase in the lateral earth pressures which may be several times greater than the theoretical at rest values and may even approach the passive earth pressure magnitude. The depth to which compaction increases the lateral earth pressures is a function of the dimension and the vertical thrust of the roller, and can reach as much as 15 m for heavy compaction equipment.

##### **3.4.4.1 Failure surface and line of maximum tension line with extensible reinforcements**

Bassett & Last (1978) have theoretically demonstrated that the failure surface of a soil reinforced with inextensible inclusion is vertical in the upper part of the wall and does not correspond to the Mohr- Coulomb failure surface. It was observed that in the case of a reinforced earth wall, the reinforcement (Strips) strains increased as much as by about 25% after about 6 weeks after the construction of the wall. This increase was attributed to the redistribution of reinforcement stresses due to the ground movements. The line of maximum tensions was found to correspond very closely to the coherent gravity failure surface.

#### **3.4.4.2 Lateral pressure coefficients with extensible reinforcements**

With the extensible type of reinforcement included in layers in the backfill soil, the lateral pressure coefficients were found to reduce below the active condition (McGown et al. 1988). This is due to the fact that the extensible (Polymer) reinforcement are able to undergo considerable elongation and thereby allow considerable lateral displacement of the wall face.

#### **3.4.4.3 Failure surfaces and line of maximum tensions with extensible reinforcements**

In the case of the extensible reinforcements, Bathurst et al. (1988) observed failure surfaces of a distinct log-spiral geometry and very close to the maximum tension line. The line of maximum tensions was found to agree very closely with the Rankine failure plane behind the wall. The researcher also observed the line of maximum tensions closer to the Rankine failure plane behind the wall. Increase in the surcharge moved the peak grid stress back into the reinforced soil mass.

Christopher et.al. (1990) studied the performance of a 12.6m. high geotextile reinforced wall, also with a vertical face, with an extensive instrumentation program. The underlying foundation soils consisted of a 6m thick upper layer of granular material underlain by a slightly over consolidating and 15m thick layer of soft lacustrine silty clays and clayey silts. The backfill used was gravelly sand. The vertical spacing of the reinforcements was kept uniform at 0.38m. Maximum strains in the reinforcements after about 6 months (a surcharge of 5m height was placed immediately after construction) were in the order of about 1%. The maximum tension line generally corresponded to the Rankine's failure plane behind the wall face, except for a small height at the top, where it corresponded to the coherent gravity failure surface.

#### **3.4.4.4 Pullout resistance of grid reinforcements**

In the case of strip reinforcement, the resistance to pullout is provided wholly by friction or adhesion and friction between the reinforcement and the soil. In the case of

grid reinforcements, the resistance to pullout is provided mainly by the passive resistance in front of the transverse bars, and the frictional resistances over the longitudinal bars contribute to about 15% of the total pullout resistances.

#### **3.4.4.5 Frictional and bearing resistances**

Large scale laboratory pullout tests by Chang et al. (1977) indicated a cone shaped soil failure with welded wire mats. Reinforcements consisting of only the longitudinal wires were found to fail by slippage of the individual longitudinal wires, independent of the other wires. The author concluded that the formation of the wedge suggested that the reinforcement and the soil failed as a single whole unit. He observed that the peak pullout load decreased with the increase in the mesh sizes or decrease in the number of transverse wires. Mesh reinforcements were found to generate about 5 to 6 times more pullout resistance than the longitudinal wires only of an equivalent area. The pullout resistances of steel grid reinforcement embedded in dense silty soil was found to be greater than in less dense gravelly sand soil. Pullout resistances were concluded to be a function of the cumulative embedded area of the grids normal to the direction of the pullout and not the embedded plan area of the reinforcement.

#### **3.4.4.6 Recent Studies in MSE Walls**

Kishan et.al., (2010) carried out analysis and design of 44 meter, 4 tiered M.S.E. wall (Mechanically Stabilized Earth) by using the software Plaxis 8.2. The MSE wall considered for the study consists of 4 tiered walls each 11m high, with effective length of reinforcing layer at 1st tiered wall from the bottom is of 20m, 2nd tier having 15m, 3rd tier having 12m and top 4th tier having 10m respectively. The authors conducted the parametric studies and it was observed that the top 1st tiered wall shows the deflection of about 130mm, the total displacement of wall is about 132mm, extreme stresses on to the wall are about 29.69%, and total extreme stresses are about 973.06 kN/m<sup>2</sup> to the downward direction from the top of the wall.

The finite element analysis performed in this study has indicated that geotextile reinforcement may be an effective method of improving the performance of embankments constructed over ghat road. The stabilizing effect of the geotextile was seen to increase as the geotextile modulus increased. The effect of geotextile reinforcement was compared with alternative construction techniques which involved the use of light weight fill or berms alone and in conjunction with geotextile reinforcement. In particular, it was found that the combined use of geotextile reinforcement and light weight fill may be a very effective means of improving the performance of embankments over hilly terrain.

Jiang (2015) investigated the secondary reinforcement effects on Mechanically Stabilized Earth Walls. The AASHTO design currently specifies only primary reinforcements with relatively large spacing. But these require higher connection strength between reinforcements and wall facing. Large spacing between reinforcements has a few disadvantages. It may increase the chances of bulging of wall facing and construction-related problems. To reduce such problems, the author has proposed the use of secondary reinforcements placed between primary reinforcements. The author has studied the performance of MSE wall with secondary reinforcement for the following cases.

Three MSE wall sections reinforced with geogrids were constructed and monitored in the field: (1) an MSE wall section with uniaxial geogrids as primary and secondary reinforcements, (2) an MSE wall section with uniaxial geogrids as primary reinforcements and with biaxial geogrids as secondary reinforcements, and (3) an MSE wall section with uniaxial geogrids as primary reinforcements only (i.e., the control section). The measured results (i.e., the wall facing deflections, the vertical and horizontal earth pressures, and the strains of geogrids) were compared with those calculated using AASHTO (2007). The author concluded that the secondary reinforcements reduced the wall facing deflections as compared with those in the control section. It was also observed that the measured vertical earth pressures were close to the computed trapezoidal stresses and increased with the construction of the wall. The distribution of lateral earth pressures in the sections with secondary

reinforcements were approximately uniform with depth while they were nonuniform in case of control section without secondary reinforcement. It was found that secondary reinforcements reduced the maximum tensile strains in the primary geogrids.

### **3.5 REVIEW OF STUDIES ON STATIC SSI**

#### **3.5.1 General**

A limited number of studies have been conducted on soil–structure interaction effect considering three dimensional space frames. King and Chandrashekharan (1974a), King (1977), King and Yao (1983), Roy and Dutta (2001) were the few researchers who made use of the finite element method to consider super structure – raft / combined footing soil as a single compatible unit.

SSI studies that take into account the yielding of structures and soil non –linearity are scarce, especially investigating the effects of non-linearity of SSI system on overall behaviour in terms of displacements and stresses. Though the structural field and geotechnical field have advanced computational tools offering sophisticated non-linear modelling in their respective fields, they fail together, to model an SSI problem to the same degree of sophistication. It is therefore a real challenge to achieve the same amount of sophistication in modeling both the soil and the structure in a single soil-structure interaction analysis. In this respect, existing advanced discipline-oriented computational tools are inadequate, on their own, for modeling a soil-structure interaction problem that involves considerable nonlinearity in both the structure and the soil; rather such a problem demands an integrated interdisciplinary computational model combining the features of both structural and geotechnical modelling.

#### **3.5.2 Analytical Methods**

Analytical methods to predict lateral deflections, rotations and stresses can be grouped under the following four headings 1) Winkler Approach 2) P-Y Method 3)

Elastic Continuum Approach 4) Finite Element Method. Viladkar et al. (1994) presented a new approach for the physical and material modelling of a space frame-raft-soil system. The soil-structure interaction effect in framed structures with proper physical modeling of the structure foundation and the soil mass is evaluated by Noorzaei et al. (1995). The effects of horizontal stresses and horizontal displacements in loaded raft foundation are studied by Swamy et al. (2011a).

The effect of the differential settlement on design force quantities for frame members of building frames with isolated footings is studied by Roy and Dutta (2001). The formulation was based on the updated Lagrangian or approximate Eulerian approach with appropriate provision for constitutive laws. Hora presented the computational methodology adopted for nonlinear soil-structure interaction analysis of infilled frame-foundation-soil system. Similarly study done by researchers in SSI under dynamic loading. Brown and Yu examined the effect of progressive loading during the construction of the frame on the frame-foundation-soil interaction.

Kutani and Elmas (2001) presented an idealized 2-dimensional plane strain seismic soil-structure interaction analysis based on a substructure method. Lu et al. carried out three dimensional finite element analysis in time domain on dynamic soil-pile-structure interaction of a tall building.

Swamy et al. (2011b) investigated the effect of soil flexibility on the performance of a building frame. Soil dimensions are fixed after ensuring that stresses are negligible at the boundaries. Structure of G+3 storey is taken. Footing of size  $2.0 \times 2.0 \times 0.4\text{m}$  is used. Soil is modelled using 8-noded brick element having 3 degrees of freedom per node, foundation was modelled using plate elements having 5 degrees of freedom per node and columns and beams in structure are modelled using one-dimensional beam element with six degrees of freedom. The research findings say that the response of the structure changes significantly in SSI analysis compared to non-interactive analysis. Inclusion of interface elements between footing and the soil have much effect on the member end actions of the structure and do not affect much on

differential settlement. It was also observed that stresses increase in case of SSI analysis.

Swamy et.al., (2012) carried out the SSI analysis as explained in the above paragraph with raft foundation. Raft size of  $25.0 \times 15.0 \times 0.4\text{m}$  is used which was modelled using plate elements having 5 degrees of freedom per node and columns and beams in structure are modeled using one dimensional beam element with six degrees of freedom. The research findings say that the response of the structure changes significantly in SSI analysis compared to non-interactive analysis. Inclusion of interface elements between foundation elements and the soil do no effect the member end actions of the structure in case of raft foundation. Interface elements are found to have much effect on differential settlement. It was also observed that stresses increase in case of coupled analysis. It was concluded that interface element play a vital role in non-linear analysis.

Section 3.6 presents the various figures related to literature review. Parametric study on Effect of soil – structure interaction by various researchers is presented in Table 3.1



### **3.6 SUMMARY OF LITERATURE REVIEW ON REINFORCED SOIL RETAINING WALLS AND MSE WALLS**

Based on the Literature Review, it is observed that the following studies have been carried out on Reinforced Soil Retaining Walls

- 1) Pull out Behaviour of Reinforcement
- 2) Tensions in Reinforcement
- 3) Displacement pattern
- 4) Interaction between Backfill soil and Geogrid
- 5) Comparison of performance of Instrumented wall with analytical results
- 6) Development of design charts for the retaining walls
- 7) External Wall Performance
- 8) The influence of the reinforcement on the rotation of the principal directions of the deformation tensors
- 9) Parametric studies for different lengths of the polymer grid, different spacing and different heights of the wall.
- 10) Effect of reinforcement on lateral displacements and the settlement
- 11) The location of failure surface both in Retaining Walls and MSE Walls
- 12) Parameters like rupture, overall stability and pullout capacities of the reinforcement
- 13) Various interface elements and development of new interface elements
- 14) Modulus of backfill soil
- 15) For calculating the active earth pressure coefficient empirical equations were derived.
- 16) Consideration of vertical shear forces in the design of retaining walls
- 17) Numerical techniques to analyze and hence study the performance of GRS retaining structures by developing code
- 18) The parametric studies on the design factors like wall facing stiffnesses, spacing of layers, strength properties of geosynthetic reinforcement
- 19) Nonlinear stress-strain relationship of soil reinforced with flexible geofibers
- 20) Rate-dependent behavior of soil retaining wall reinforced with geosynthetics

- 21) Strains, soil displacements, principal stress directions, stresses, the stresses on the underside of the footing and mobilized fill friction angles.
- 22) Drained triaxial tests were carried out for both unreinforced and reinforced residual soil, for various stress paths using a computer controlled triaxial test setup.
- 23) Degree of reinforcement orientation influencing the shear strength and volume change behavior.
- 24) Studies on the gabion faced retaining wall design and development of handy design charts to provide a good design tool to the designers.
- 25) Role of Facing elements in both retaining walls and MSE Walls
- 26) Frictional and Bearing Resistances in MSE Walls
- 27) Study on Pull-out resistance in MSE walls

### **3.6.1 Conclusions on Literature Review of Reinforced Soil Retaining Walls and MSE Walls**

Based on the above literature review it is observed that though numerous studies have been carried out on Reinforced soil Retaining Walls, very few studies have been carried out on stress, strain and deformation studies. Most of the studies have been done by using standard available software or by conducting Experiments.

### **3.7 SUMMARY OF LITERATURE REVIEW ON REINFORCED SOIL FOUNDATION SOILS**

Based on the above literature review on Reinforced Soil Foundation, it is clearly observed that the following studies have been carried out

- 1) Improvement of Bearing Capacity
- 2) Reduction in settlement of the soil
- 3) Optimum top layer spacing ( $u/B$ )
- 4) optimum vertical spacing ratio ( $h/B$ )
- 5) effective length of reinforcement ( $L/B$ )
- 6) Influence depth ratio ( $d/B$ )
- 7) Effect of Prestressing force on the bearing capacity of soil

- 8) Studies on cohesionless soils, cohesive soils and cohesive soils mixed blended with industrial wastes like Fly-ash, GGBS etc.
- 9) Different types of reinforcing materials

### **3.7.1 Conclusions on Literature Review of Reinforced Soil Foundation**

Based on the above literature review, it is observed that most of the studies have focused on the improvement in bearing capacity and reduction in settlement by adopting different parameters. Few studies have been carried out on computing the modulus of subgrade reaction of unreinforced soil foundation using model plate load tests. Studies on computing the modulus of subgrade reaction of reinforced soil foundation using model plate load tests have not been reported.

## **3.8 SUMMARY OF LITERATURE REVIEW ON REINFORCED SOIL FOUNDATION SSI / RSSI**

Based on the above literature review, it is observed that a limited number of studies have been conducted on soil–structure interaction effect considering three dimensional space frames. It is also observed that SSI studies that take into account the yielding of structures and soil non –linearity are scarce, especially investigating the effects of non-linearity of SSI system on overall behaviour in terms of displacements and stresses. Few studies have been carried out on dynamic soil structure interaction considering nonlinear analysis.

### **3.8.1 Conclusions on Literature Review on SSI / RSSI**

Based on the above literature review, it is observed that static SSI has been carried out exhaustively. It has been carried out for different materials of structures, for different space frames, for different types of structures with different types of footings. All the studies have focused on unreinforced soil which is homogenous, isotropic and behaving in linear and nonlinear manner in the interaction analysis. But there are no

studies reported on RSSI or the soil structure interaction for the reinforced soil. To start with following Research gaps are observed:

- Though experimental and numerical Studies have been conducted on reinforced soil, they were on single footings and not mutilscale structures.
- Parametric study on settlement of foundations resting on reinforced soil using numerical methods.
- Study of stress resultants in members of the frame resting on reinforced soil.
- Study of stresses in the reinforced soil.
- Comparative study of unreinforced soil structure interaction analysis and reinforced soil structure interaction analysis.
- Study of interaction effects on RC frame resting on Reinforced soil

### **3.9 FUTURE DIRECTIONS FOR RESEARCH**

Great strides and advancements have been made in the research of Reinforced soil structures. A lot of parametric studies have been carried out and new designs have been devised on Reinforced soil structures individually. In this research attempts have been made to study all the Reinforced soil structures by developing software (programs). Model plate load tests have also been conducted to study BCR, optimum u/B ratio and for the computation of modulus of subgrade reaction of Reinforced soil foundation. The Soil structure interaction for the Reinforced soil and unreinforced soil has also been studied both linearly and non-linearly.

### 3.10 VARIOUS FIGURES RELATED TO LITERATURE REVIEW

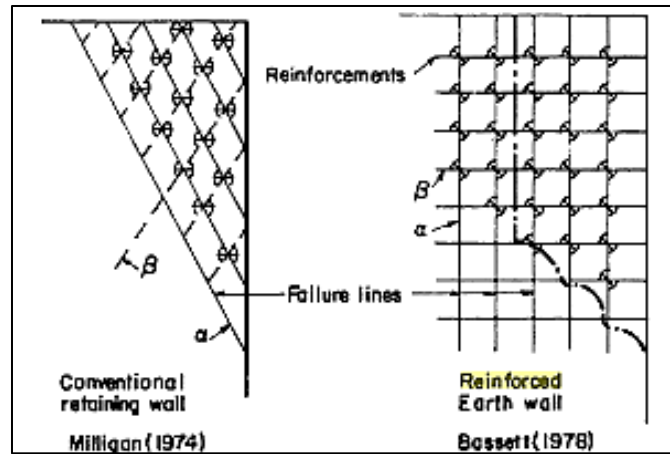


Fig. 3.1 Influence of reinforcements on potential failure lines (Basset and Last, 1978)

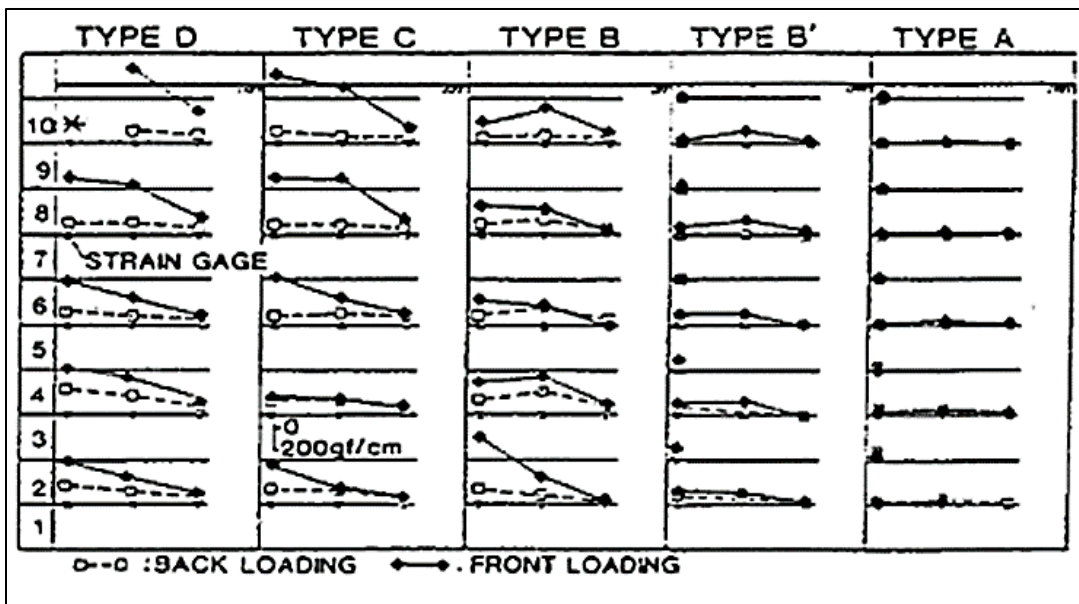
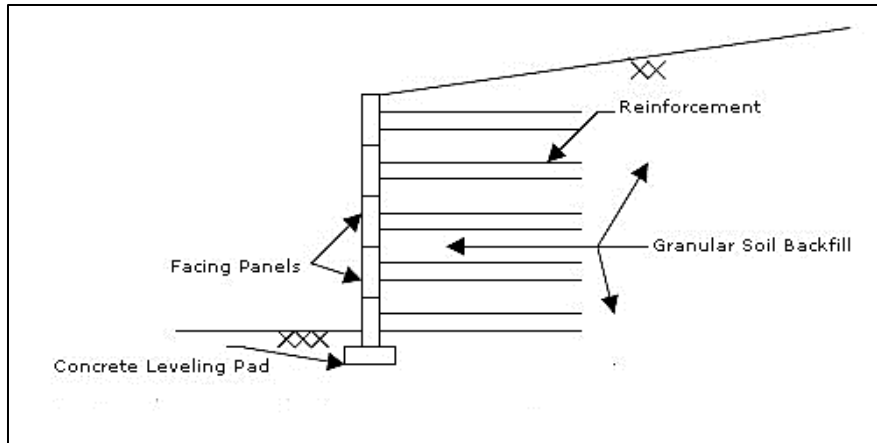
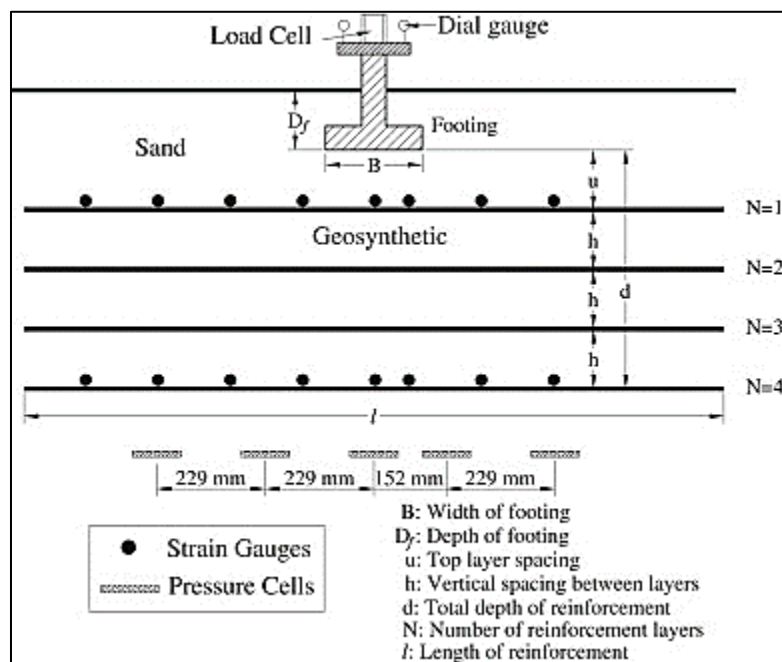


Figure 3.2 Observed tensile force distributions along reinforcement corresponding to different facing rigidities. (Tatsuoka et al., 1989)



**Figure 3.3 Components of Reinforced Soil Retaining Wall**



**Figure 3.4 Geosynthetic reinforced soil foundation (Abu-Farsakh et. al, 2013)**

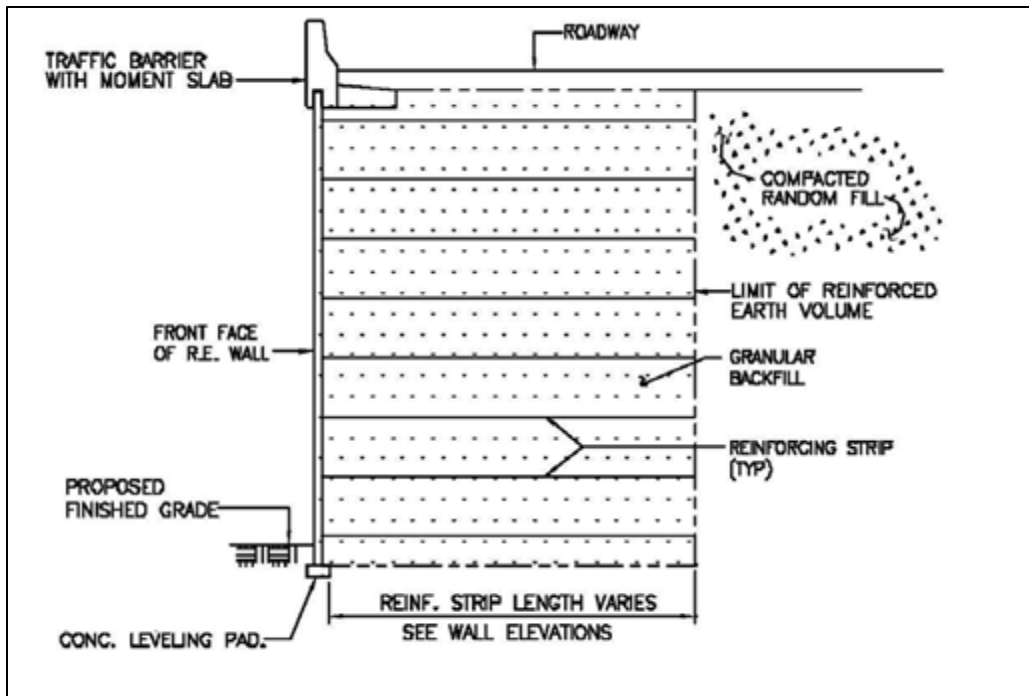


Figure 3.5 Typical MSE Wall Details ([www.fhwa.dot.gov](http://www.fhwa.dot.gov))

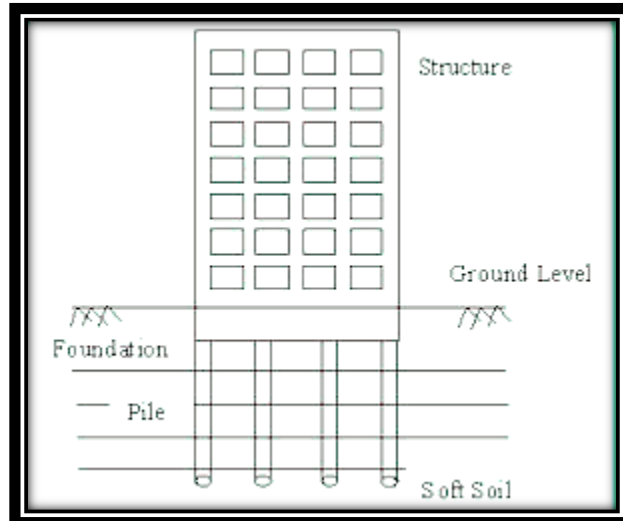


Figure 3.6 Soil Structure Interaction ([www.nptel.ac.in](http://www.nptel.ac.in))

Table 3.1 Details of various studies carried out by different researchers in SSI(Prakash et al., 2016)			
Sl.No.	Parameter	Particulars	Studies by various researchers
1	Forms of Structure	Plane Frame	Duncan and Chang (1970), Hora (2006), Kutanis and Elmas (2001), Agrawal and Hora (2012)
		Space Frame	Noorzaei (1996) , Viladkar et al. (1994), Noorzaei et al.(1994), Swamy Rajashekhar et al. (2011) ,Roy and Dutta (2001) ,Desai et al. (1982)
2	Types of foundation	Pile	Cai et al.(2000) , Hokmabadi A.S (2013), Medina et al (2013)
		Isolated	Roy and Dutta (2001), Bhattacharya et al. (2006), Agrawal and Hora (2012)
		Raft	Rajasankar et al. (2007),Noorzaei (1996),Viladkar et al. (1993), Wang et al.(2001)
3	Domain	Time Domain	Cai et al. (2000) , Viladkar et al.(1993),Kutanis and Elmas (2001)
		Frequency domain	Suleyman and Mengi (2000)
4	Other	Stochastic Processes	Dan and Roger (2002), Veletsos and Prasad (1989)



## CHAPTER 4

### FINITE ELEMENT MODELLING OF REINFORCED SOIL SYSTEMS

#### 4.1 GENERAL

Finite element method (FEM) is a well-known technique of numerically finding boundary value problems which can accommodate highly non-linear stress-strain relations of materials including creep. It can also be applied to any geometrical configuration with complex boundaries, construction sequence, etc. FEM has been used as the standard for the analysis (e.g. prediction of safety factor and settlement analysis) of many structures. Similarly it is becoming an analysis tool for the reinforced soil structures. The features of FEM can be achieved only when material parameters, constitutive equations and boundaries are appropriately defined or modelled. The fundamental concept of FEM is discretization. FEM consists of both discretization and assembling.

FEM has been applied to a wide variety of geotechnical engineering problems where stresses, movements, pore pressures, and groundwater flow are of interest. The types of problems analysed include: Anchored walls used to stabilize landslides, buildings, foundations, cellular cofferdams, embankments, dams, bracing systems, long-span flexible culverts, offshore structures, plastic concrete seepage cut-off walls, Reinforced slopes, retaining walls, seepage through earth masses, slurry trench seepage barriers, tunnels.

In the FEM analysis, the tiny components or structural elements can be used to examine the large response of any system. These elements may be one, two or three dimensional. The complexities of soil and rock behaviour can be modelled using incremental and iterative analyses. Complex geometries can be handled by using a suitable constitutive model for soil. The finite element analysis comprises of the geometric modelling of the structure and the mechanical modelling of internal forces.

## **4.2 CONSIDERATIONS IN MODEL DEVELOPMENT**

In general, the criterion for the soil model evaluation should always be a balance between the requirements from the continuum mechanics aspect, the requirements of realistic representation of soil behaviour from the laboratory testing aspect (also the convenience of parameters derivation), and the simplicity in computational application materials.

### **4.2.1 Elastic Models in Geotechnical Engineering**

Elastic material models based on the theory of continuum mechanics can be generally classified as linear elastic (generalized Hooke's law) and Cauchy elastic. These models are described briefly below.

#### **4.2.1.1 Linear elastic models**

The linear elastic model is the oldest and simplest model which gives a unique and linear relation between the state of stress and strain, and it can be classified further as isotropic, transversely isotropic, orthotropic or anisotropic depending on the materials assumed in the analysis. Linear relationship has a very limited range of applicability to materials. In the present study, Linear elastic models have been adopted to accomplish linear analysis as reported in Chapter 5.

#### **4.2.1.2 Cauchy elastic models**

For Cauchy elastic materials, the current state of stress,  $\sigma_{ij}$ , depends only on the current state of deformation,  $\epsilon_{ij}$ , stress is a function of strain (or vice versa). The constitutive relation of this material has the general form as in equation 4.1

$$\sigma_{ij} = F_{ij} (\epsilon_k) \quad (4.1)$$

Where  $F_{ij}$  is the elastic response function of the material. The elastic response function  $F_{ij}$  for an isotropic material, for example, can be expressed in a polynomial form of the strain tensor  $\epsilon_{ij}$ .

### **4.3 NON LINEAR ANALYSIS OF SOIL MEDIA**

In FEM, the non-linearity of soils is solved using three techniques, namely the incremental or piecewise linear method, the iterative method and the mixed method.

#### **4.3.1 Incremental method**

The incremental method involves the increase in weight in a succession of steps. The piecewise form of the non-linear behaviour involves linear laws being adopted for each loading phase. The incremental process provides a complete explanation of the load deformation behaviour. The tangent modulus is depicted in terms of stress only and it can be used to analyse problems involving initial stress conditions. However, the simulation of a stress-strain relationship in which the stress drops beyond the peak is not practicable, as it is not possible to acquire the negative value of the modulus.

The stage wise method (Fig. 4.1) involves the portion of the load to be split into small equal or unequal fractional loads. The equations are assumed to be linear during each load. This procedure is recurring until the entire load has been applied. The non-linear problems are evaluated as a sequence of linear problems, that is incremental procedure approximates the non-Linearity as piecewise linear effect (Desai and Abel, 1987). Modified Runge - Kutta method is used to calculate the modulus value and higher accuracy is obtained by applying small load increments.

#### **4.3.2 Iterative method**

The iterative method involves the maximum load being applied and iterations being performed to satisfy stress and strain equilibrium to provide results pertaining to that load. In the mixed procedure of FEM analysis, both the incremental and iterative procedures are combined to produce more accurate solutions.

### **4.3.3 Causes of Nonlinear Behaviour**

Nonlinear structural behaviour arises from a number of causes, which can be grouped into geometric and material nonlinearity. They are discussed in the following sections.

#### **4.3.3.1 Geometric Nonlinearities**

The changing geometric configuration of a structure experiencing large deformations can cause the structure to respond nonlinearly. Geometric nonlinearity is characterized by "large" displacements and/or rotations. An example would be the fishing rod shown in Fig. 4.2. Change in geometry as the structure deforms is taken into account in setting up the strain displacement and equilibrium equations. The various applications include: slender structures in aerospace, applications in civil and mechanical engineering, tensile structures such as cables and inflatable membranes, metal and plastic forming.

#### **4.3.3.2 Material Nonlinearities**

Nonlinear structural behaviour can be attributed to nonlinear stress-strain relationships. Some of the factors that influence a material's stress-strain properties, are environmental conditions like temperature, load history as in elasto-plastic response, and the amount of time that a load is applied (as in creep response). The material behaviour depends on past history and current state of the deformation state. Other constitutive variables (prestress, temperature, time, moisture, electromagnetic fields, etc.) may be involved. The applications are structures undergoing nonlinear elasticity, plasticity, viscoelasticity, creep, or inelastic rate effects.

### **4.4 CONSTITUTIVE LAWS**

The finite element method enables us to analyse stresses and deformations using constitutive relations that can be used to model real soil. Constitutive relations are characterized by the relationships between stresses, strain and time. Factors governing

constitutive relations with respect to soil include density, water content, drainage conditions, strain or creep conditions, duration of loading, stress histories, confining pressure etc. Various constitutive models existing for delineating the soil behaviour are linear elastic, non-linear elastic, hyperelastic, bilinear, hyperbolic, Rarnberg Osgood model, Drucker-Prager model, Cap model, Cam clay model, modified Cam clay model, soft soil creep model, strain hardening model, hysteritic model etc. In the present study, hypoelastic model has been adopted.

#### **4.4.1 Hypoelasticity**

The concept, called Hypoelasticity, establishes a generalized incremental law where actions can be simulated in percentage increase than a whole load or stress at a time. In hypoelasticity, the rise of stress is expressed as a function of stress and increment of strain. It was primarily introduced by Truesdell (1955) who anticipated a rate theory based on Cauchy formulations for such materials. From Truesdell's theory, incremental stress-strain laws can be developed. Some of the formulations of piecewise linear elastic idealization have been suggested as hybrid hyperelastic models. Literally, “hypo” means “to a lower degree” and imply that a material is elastic to a lower or incremental sense.

A hypoelastic material can:

1. Be interpreted to be capable of allowing for inelastic or plastic behaviour.
2. Offer simulation of constitutive actions in even way for hardening or softening materials.
3. Represent a material which is path dependent.

##### **4.4.1.1 Hypoelastic Model**

The model proposed by Yin (2000) is extended, enhanced and used in this work. Of the two generalised models proposed, one model which links incremental strains to incremental stress is chosen and adopted. It is this constitutive model considered for implementation. The data used is obtained from isotropic consolidation and

conventional undrained triaxial compression (CTC) tests on saturated soil. The stress is a nonlinear function of strain, even when the strains are small, as shown in Fig. 4.3

The model consists of three stress dependent modulus functions, which are as follows,

o Bulk modulus K

o Shear modulus G

o The coupling modulus J that relates effective mean stress  $p'$  to shear strain  $s$  as well as shear stress  $q$  to volumetric strain.

The model is in incremental form. The change in volumetric strain  $d\varepsilon_v$  and shear strain  $d\varepsilon_s$  corresponding to the change in effective mean stress  $dp'$  as well as shear stress  $dq$  as proposed by Yin et al.(2000) are expressed by the relationships given by equations 4.2 and 4.3.

$$d\varepsilon_v = \frac{1}{k} dp' + \frac{1}{j} dq \quad (4.2)$$

$$d\varepsilon_s = \frac{1}{j} dp' + \frac{1}{3G} dq \quad (4.3)$$

Where, in triaxial stress condition,

$$\varepsilon_v \text{ is the Volumetric strain as given by equation 4.4, } \varepsilon_v = \varepsilon_1 + 2\varepsilon_3 \quad (4.4)$$

$$P' \text{ is effective mean stress given by equation 4.5, } P' = 1/3 (\sigma'_1 + 2\sigma'_3) \quad (4.5)$$

$$q \text{ (equation 4.6) is the deviator stress, } q = \sigma_1 - \sigma_3. \quad (4.6)$$

Positive dilation, that is, expansion during shearing is associated with  $J < 0$ . The compression during shearing is associated to  $J > 0$ . If there is no dilation or no induced anisotropy. The coupling modulus  $J = \alpha$

The above equation can be inverted as given by equation 4.7

$$dp' = \bar{K} d\varepsilon_v - \bar{J} d\varepsilon_s \quad (4.7)$$

$$dp = -\bar{J}d\varepsilon_v + 3\bar{G}d\varepsilon_s \quad (4.8)$$

Which are related to  $\bar{K}, \bar{G}, \bar{J}$  as follows given in equations 4.9 to 4.11

$$\bar{K} = k \frac{J^1}{J^2 3kG} \quad (4.9)$$

$$\bar{G} = G \frac{J^2}{J^2 - 3KG} \quad (4.10)$$

$$\bar{J} = \frac{3KGJ}{J^2 - 3KG} \quad (4.11)$$

Special forms of Hypoelastic relation (Coon & Evans 1971 and Chen & Mizuno 1990) are as given in equations 4.12 and 4.13

$$d\varepsilon_{if} = C_{ijkl}(\sigma_{mn})d\sigma_{kl} = C d\sigma_{kl} \quad (4.12)$$

$$d\sigma_{if} = D_{ijkl}(\sigma_{mn})d\varepsilon_{kl} = D d\varepsilon_{kl} \quad (4.13)$$

Which after simplification result in equation 4.14

$$\begin{bmatrix} d\sigma_{11} \\ d\sigma_{22} \\ d\sigma_{22} \\ d\sigma_{12} \\ d\sigma_{23} \\ d\sigma_{13} \end{bmatrix} = \begin{bmatrix} (\beta_1 + 2\beta_2) & (\beta_2 + \beta_3 + \beta_4) & (\beta_2 + \beta_3 + \beta_4) & \frac{-J\sigma_{12}}{q} & \frac{-J\sigma_{23}}{q} & \frac{-J\sigma_{31}}{q} \\ (\beta_2 + \beta_3 + \beta_4) & \beta_1 + 2\beta_4 & (\beta_2 + \beta_4 + \beta_5) & \frac{-J\sigma_{12}}{q} & \frac{-J\sigma_{23}}{q} & \frac{-J\sigma_{31}}{q} \\ [\beta_1 + \beta_2 + \beta_3] & [\beta_1 + \beta_2 + \beta_3] & \beta_1 + 2\beta_4 & \frac{-J\sigma_{12}}{q} & \frac{-J\sigma_{23}}{q} & \frac{-J\sigma_{31}}{q} \\ \frac{-J\sigma_{12}}{q} & \frac{-J\sigma_{12}}{q} & \frac{-J\sigma_{12}}{q} & \bar{G} & 0 & 0 \\ \frac{-J\sigma_{23}}{q} & \frac{-J\sigma_{23}}{q} & \frac{-J\sigma_{23}}{q} & 0 & \bar{G} & 0 \\ \frac{-J\sigma_{31}}{q} & \frac{-J\sigma_{31}}{q} & \frac{-J\sigma_{31}}{q} & 0 & 0 & \bar{G} \end{bmatrix} \begin{bmatrix} d\varepsilon_{11} \\ d\varepsilon_{22} \\ d\varepsilon_{22} \\ d\gamma_{12} \\ d\gamma_{23} \\ d\gamma_{13} \end{bmatrix} \quad (4.14)$$

Where

$$\beta_1 - K + \frac{4}{3}\bar{G}, \beta_2 - K - \frac{2}{3}\bar{G}, \beta_3 - \frac{\bar{J}}{3q}(\sigma_{22} + \sigma_{33} - 2\sigma_{11}) \quad (4.15)$$

$$\beta_2 - \frac{\bar{J}}{3q}(\sigma_{211} + \sigma_{33} - 2\sigma_{22}), \beta_3 - \frac{\bar{J}}{3q}(\sigma_{22} + \sigma_{11} - 2\sigma_{33}) \quad (4.16)$$

$$\begin{bmatrix} d\varepsilon_{11} \\ d\varepsilon_{22} \\ d\varepsilon_{22} \\ d\gamma_{12} \\ d\gamma_{12} \\ d\gamma_{13} \end{bmatrix} = \begin{bmatrix} (\alpha_1 + 2\alpha_2) & (\alpha_2 + \alpha_3 + \alpha_4) & (\alpha_2 + \alpha_3 + \alpha_4) & \frac{\sigma_{12}}{qJ} & \frac{\sigma_{23}}{qJ} & \frac{\sigma_{31}}{qJ} \\ (\alpha_2 + \alpha_3 + \alpha_4) & \alpha_1 + 2\alpha_4 & (\alpha_2 + \alpha_4 + \alpha_5) & \frac{\sigma_{12}}{qJ} & \frac{\sigma_{23}}{qJ} & \frac{\sigma_{31}}{qJ} \\ [\alpha_1 + \alpha_2 + \alpha_3] & [\alpha_1 + \alpha_2 + \alpha_3] & \alpha_1 + 2\alpha_4 & \frac{\sigma_{12}}{qJ} & \frac{\sigma_{23}}{qJ} & \frac{\sigma_{31}}{qJ} \\ \frac{\sigma_{12}}{qJ} & \frac{\sigma_{12}}{qJ} & \frac{\sigma_{12}}{qJ} & \frac{1}{G} & 0 & 0 \\ \frac{\sigma_{23}}{qJ} & \frac{\sigma_{23}}{qJ} & \frac{\sigma_{23}}{qJ} & 0 & \frac{1}{G} & 0 \\ \frac{\sigma_{31}}{qJ} & \frac{\sigma_{31}}{qJ} & \frac{\sigma_{31}}{qJ} & 0 & 0 & \frac{1}{G} \end{bmatrix} \begin{bmatrix} d\sigma_{11} \\ d\sigma_{22} \\ d\sigma_{22} \\ d\sigma_{12} \\ d\sigma_{23} \\ d\sigma_{13} \end{bmatrix} \quad (4.17)$$

Where

$$d\gamma_{12} - 2 \varepsilon_{12}, d\gamma_{23} - 2 \varepsilon_{23}, d\gamma_{31} - 2 \varepsilon_{31} \quad (4.18)$$

$$\alpha_1 - \frac{1}{9K} + \frac{1}{3G}, \alpha_2 - \frac{1}{9K} - \frac{1}{6G}, \alpha_3 - \frac{2\sigma_{11} - \sigma_{22} - \sigma_{33}}{6qJ}, \alpha_4 - \frac{2\sigma_{22} - \sigma_{11} - \sigma_{33}}{6qJ}, \alpha_5 - \frac{2\sigma_{33} - \sigma_{11} - \sigma_{22}}{6qJ} \text{ and } \frac{\sigma_{31}}{qJ} \quad (4.19)$$

#### 4.4.2 Mohr-Coulomb Model

Mohr-Coulomb model is an elastic-perfectly plastic model often used to model soil behaviour. In the general stress state, the model's stress-strain behaves linearly in the elastic range, with two defining parameters from Hooke's law (Young's modulus,  $E$  and Poisson's ratio,  $\nu$ ). There are two parameters which define the failure criteria (the friction angle,  $\phi$  and cohesion,  $c$ ) and also a parameter to describe the flow rule (dilatancy angle,  $\psi$  which comes from the use of non-associated flow rule used to model a realistic irreversible change in volume due to shearing). Mohr-Coulomb model is a two-parameter model with criterion of shear failure and can also be a three parameter model with criterion of shear failure with a small tension cut-off. Numerous models are available to represent the stress-strain behaviour and failure of soils. The Mohr-Coulomb failure criterion can be written as the equation for the line that represents the failure envelope. Researchers have indicated by means of true-triaxial tests that stress combinations causing failure in real soil samples agree quite well with the hexagonal shape of the failure contour (Goldscheider, 1984). (Refer Fig 4.4) Mohr-Coulomb model shows the hexagonal shape of the failure cone.

The general equation is as in equation (4.20)

$$\tau_f = c + \sigma_f \cdot \tan \phi \quad (4.20)$$

#### 4.4.3 Modified Cam-Clay (MCC) Model

Soil might be referred to as a strain hardening material since the onset of plastic yielding is not synonymous with the maximum stress. A few researchers have investigated the possibility of modelling soil as a strain hardening material, and this has been one of the major thrusts of the soil mechanics group at Cambridge University for the past thirty years. Long before the maximum stress has been reached, some irreversible straining has occurred as evidenced by the fact that



reloading leaves a residual strain. The Modified Cam-Clay is an elastic plastic strain hardening model where the non-linear behaviour is modelled by means of hardening plasticity. In addition to achieve better agreement between predicted and observed soil behaviour, a large number of modifications have been proposed to the standard Cam-Clay models over the last two decades. The MCC model was originally developed for triaxial loading conditions. Experimental measurements on soft clays provided the background for the development of the constitutive model expressing the variation of void ratio  $e$  (volumetric strain  $\epsilon_v$ ) as a function of the logarithm of the effective mean stress  $\sigma_m^{\text{eff}}$

#### **4.4.4 Duncan-Chang (Hyperbolic) Model**

As known, soil behaves highly non-linear and it inhibits stress-dependant stiffness. Apart from the discussed elastic-plastic models, Duncan-Chang model is an incremental nonlinear stress-dependant model which is also known as the hyperbolic model (Duncan and Chang, 1970). This model is based on stress-strain curve in drained triaxial compression test of both clay and sand which can be approximated by a hyperbolae with a high degree of accuracy. Its failure criteria is based on Mohr-Coulomb's two strength parameters. Most importantly, this model describes the three important characteristics of soil, namely non-linearity, stress-dependant and inelastic behaviour of cohesive and cohesion less soil. Duncan-Chang model is widely used as its soil parameters can be easily obtained directly from standard triaxial test. It is a simple yet obvious enhancement to the Mohr-Coulomb model. In this respect, this model is preferred over the Mohr-Coulomb model.

#### **4.4.5 Drucker Prager Model**

The stress invariant form of the Coulomb criterion consisting of  $I_1$ ,  $J_2$  and  $J_3$  (or  $\theta$ ) is rather complicated and causes some difficulties in treatment regarding the plastic flow at corners. For practical purpose, therefore, a smooth surface is often used to approximate the yield surface with singularities in elastic plastic finite element analyses under a more general stress condition. The Drucker-Prager perfectly plastic

model (Drucker and Prager, 1952), which neglects the influence of  $J_3$  on the cross-sectional shape of failure surface, can be considered as the first attempt to approximate the well-known Coulomb criterion by a simple smooth function. This criterion is expressed as a simple stress invariant function of the first invariant of stress tensor,  $I_1$ , and the second invariant of deviatoric stress tensor,  $J_2$ , together with two material constants  $\alpha$  and  $k$ . It has the simple form as given by equation 4.21

$$f = \alpha I_1 + \sqrt{J_2} = k \quad (4.21)$$

where the constants  $\alpha$  and  $k$  may be related to the Coulomb's material constants  $c$  and  $\phi$  in several ways. The Drucker-Prager surface can be looked upon as an extension of the Von Mises surface for pressure dependent materials such as soil and concrete. Thus, this criterion is also called the extended Von Mises criterion. The yield or failure surface in the principal stress space depicts clearly a right-circular cone with the symmetry about the hydrostatic axis (Fig. 4.5). The values of  $\alpha$  and  $k$  in Drucker-Prager criteria can be expressed in terms of angle of internal friction  $\phi$  and cohesion  $c$  as in equations 4.22 and 4.23

$$\alpha = \frac{2 \sin \phi}{\sqrt{3}(3 - \sin \phi)} \quad (4.22)$$

$$k = \frac{6c \cos \phi}{\sqrt{3}(3 - \sin \phi)} \quad (4.23)$$

#### **4.5 PREVIOUS APPROACHES USED TO MODEL INTERFACES IN GEOLOGIC MATERIALS**

Theoretically, the interface elements involving reinforced soil structures can be modelled as quadrilateral or triangular elements. Due to the geometry of the interfaces, the latter elements would be quite distorted and thus undesirable, the former elements would possess narrow and long shapes.

In the finite element analyses, suitable elements can be used to model the interactions along the interface. Four basic modes of deformation control the physical behaviour of geo-materials along interfaces, namely

1. Non-slip or Stick
2. Slip or Relative tangential displacement

3. Relative normal displacement leading to separation or de-bonding

4. Re-bonding or Closure of separation

Stick refers to the behaviour of interface when shear strength of the interface is greater than that of the shear stress. Hence, no relative displacements occur between dissimilar materials. However, when the shear stress exceeds the shear strength of the interface material, relative displacement occurs. The term “de-bonding” describes the separation of the two sides of the continuum in the vicinity of the interface that were in contact initially. “Rebonding,” or subsequent contact can also develop by the movement of the two sides towards each other.

#### **4.5.1 Goodman et. al.’s Element (1968)**

One of the earliest joint elements was proposed by Goodman et al.(1968) to capture the behaviour of jointed rock masses. This four noded rectangular element possessed two degrees of freedom at each node. The thickness of the interface element is assumed to be zero. While using such an element in the analysis of soil, a pair of nodes are placed at the same initial geometric location at each mesh point along interface which makes it zero thick.

The element formulation is based on the relative displacements of the continuum elements located besides the interface. One displacement is normal and the other one is tangential to the interface. The normal and tangential components of the interface stresses (force per unit length) along the interface are related to the relative displacements. The interface constitutive relations consist of tangential stiffness  $k_s$  and one normal stiffness  $k_n$  both in an uncoupled form.

Finally the element stiffness can be explicitly given in terms of  $k_n$  and  $k_s$ . It should also be noted that this result can also be obtained within the limit, when the thickness of a rectangular element goes to zero, with transversely isotropic filling material having Poisson’s ratio equal to zero. As presented in the original paper, if the normal stress at the joint is tensile in any element, both  $k_n$  and  $k_s$  are set equal to zero for the

element. This simulates the opening of the joint. Supposing, the joint shear stress exceeds the strength, which is governed by Mohr-Coulomb friction law, then  $k_s$  is set to a residual value that is less than  $k_s$ . This represents the slip mode of the element.

The elements of Goodman et al. have been rather widely used owing to their simple formulation and the straightforward manner in which relative displacements are introduced. A higher-order two-dimensional zero-thickness element has been developed on the basis of Goodman et al.'s (1968) formulation.

#### 4.5.1.1 Interface Element Proposed by Goodman et al. (1968)

The zero-thickness element proposed by Goodman et al. (1968) is the most basic model for joints /interface, and has been extensively used. Figure 4.6 shows a four noded element of length  $L$ . The thickness  $t$  is initially zero. 1-2 and 3-4 are straight lines and the nodes 1 and 4, and nodes 2 and 3 are coincident before deformation.  $\{u\}$  is the nodal displacement vector in the local coordinate system  $(x', y')$  as given in equation 4.24. Thus

$$\{u\} = \{u_1 \ v_1 \ u_2 \ v_2 \ u_3 \ v_3 \ u_4 \ v_4\}^T \quad (4.24)$$

The vector of relative displacement  $\{w\}$  is defined as in equation 4.25

$$\{w\} = \begin{Bmatrix} w_s \\ w_n \end{Bmatrix} = \begin{Bmatrix} u_t & u_b \\ v_t & v_b \end{Bmatrix} \quad (4.25)$$

Where  $w_s$  and  $w_n$  represent tangential and normal relative displacements, respectively.  $u$  and  $v$  are displacements along  $x'$  and  $y'$  axes respectively, and the subscripts  $t$  and  $b$  are used to signify "top" and "bottom" segments of the interface. Displacements  $u$  and  $v$  can be approximated by using linear interpolation functions  $N_1$  and  $N_2$  as given in equations 4.26 and 4.27; i.e.,

And 
$$\begin{Bmatrix} u_b \\ v_b \end{Bmatrix} = \begin{bmatrix} N_1 & 0 & N_2 & 0 & 0 & 0 & 0 & 0 \\ 0 & N_1 & 0 & N_2 & 0 & 0 & 0 & 0 \end{bmatrix} \{u\} \quad (4.26)$$

$$\begin{Bmatrix} u_t \\ v_t \end{Bmatrix} = \begin{bmatrix} 0 & 0 & 0 & 0 & N_2 & 0 & N_1 & 0 \\ 0 & 0 & 0 & 0 & 0 & N_2 & 0 & N_1 \end{bmatrix} \{u\} \quad (4.27)$$

Linear interpolation functions  $N_1$  and  $N_2$  are given by equation 4.28

$$\text{Where } N_1 = \frac{1}{2} - \frac{x'}{L} \text{ and } N_2 = \frac{1}{2} + \frac{x'}{L} \text{ Thus } \{w\} = [B] \{u\} \quad (4.28)$$

Where,

$$[B] = \begin{bmatrix} -N_1 & 0 & -N_2 & 0 & N_2 & 0 & N_1 & 0 \\ 0 & -N_1 & 0 & -N_2 & 0 & N_2 & 0 & N_1 \end{bmatrix} \quad (4.29)$$

The stress-displacement relationship for the interface is given by equation 4.30

$$\begin{Bmatrix} \tau_s \\ \sigma_n \end{Bmatrix} = [D]\{w\} = \begin{bmatrix} k_s & 0 \\ 0 & k_n \end{bmatrix} \begin{Bmatrix} w_s \\ w_n \end{Bmatrix} \quad (4.30)$$

Where  $k_s$  and  $k_n$  represent the tangential and normal stiffness per unit length along the interface. The tangential and normal “stresses”  $\tau_s$  and  $\sigma_n$  have units of force per unit length. Considering  $\{w\}$  as a generalized strain, we can obtain the element stiffness matrix in the standard manner equation (4.31).

$$[K]^e = \int [B]^T [D] [B] dx' \quad (4.31)$$

Each term can be exactly integrated, giving expression 4.32

$$[K]^e = \frac{L}{6} \begin{bmatrix} 2k_s & 0 & k_s & 0 & -k_s & 0 & -2k_s & 0 \\ & 2k_n & 0 & k_n & 0 & -k_n & 0 & -2k_n \\ & & 2k_s & 0 & -2k_s & 0 & -k_s & 0 \\ & & & 2k_n & 0 & -2k_n & 0 & -k_n \\ & & & & 2k_s & 0 & k_s & 0 \\ & & & & & 2k_n & 0 & k_n \\ & & & & & & 2k_s & 0 \\ & & & & & & & 2k_n \end{bmatrix} \quad (4.32)$$

*sym*

And the element stiffness equation is given as in equation 4.33

$$[k]^e \{u\} = \{f\} \quad (4.33)$$

Where  $\{f\}$  is the nodal force vector in the local coordinate system  $(x', y')$  (equation 4.34)

$$\{f\} = \{f_{1x} \ f_{1y} \ f_{2x} \ f_{2y} \ f_{3x} \ f_{3y} \ f_{4x} \ f_{4y}\}^T \quad (4.34)$$

#### 4.5.1.2 Interface “stresses”

The joint/interface shear stress  $\tau_s$  and normal stress  $\sigma_n$  can be calculated as in equation 4.30, from relative displacement  $\{w\}$ . Evaluated at the element centre as given by equations 4.35 and 4.36.

$$w_s = \frac{1}{2} (-u_1 - u_2 + u_3 + u_4) \quad (4.35)$$

$$w_n = \frac{1}{2} (-v_1 - v_2 + v_3 + v_4) \quad (4.36)$$

Thus

$$\tau_s = \frac{k_s}{2} (-u_1 - u_2 + u_3 + u_4) \quad (4.37)$$

$$\sigma_n = \frac{k_n}{2} (-v_1 - v_2 + v_3 + v_4) \quad (4.38)$$

Since the displacement varies linearly in the element, the force will vary linearly across the element. Expanding the element stiffness equation (4.33) gives

$$f_{3x} = -f_{2x} = \frac{L}{6} k_s (-u_1 - 2u_2 + 2u_3 + u_4) \quad (4.39)$$

$$f_{4x} = -f_{1x} = \frac{L}{6} k_s (-2u_1 - u_2 + u_3 + 2u_4) \quad (4.40)$$

$$f_{3y} = -f_{2y} = \frac{L}{6} k_n (-v_1 - 2v_2 + 2v_3 + v_4) \quad (4.41)$$

$$f_{4y} = -f_{1y} = \frac{L}{6} k_n (-2v_1 - v_2 + v_3 + 2v_4) \quad (4.42)$$

Then we can also evaluate the average tangential and normal stresses by equations 4.43 and 4.44

$$\tau_s = \frac{f_{3x} + f_{4x}}{L} \quad (4.43)$$

$$\sigma_n = \frac{f_{3y} + f_{4y}}{L} \quad (4.44)$$

Yielding the expressions as in equations 4.45 and 4.46

$$\tau_s = \frac{k_s}{2} (-u_1 - u_2 + u_3 + u_4) \quad (4.45)$$

$$\sigma_n = \frac{k_n}{2} (-v_1 - v_2 + v_3 + v_4) \quad (4.46)$$

#### 4.5.1.3 Modes of interface Deformation

The identification of four modes of joints/interface deformation, namely, contact, slip, de-bonding and re-bonding calls for a special logic. Since, we lack a universal model describing the deformation behaviour of joints/interface, a simple constitutive law is assumed (Fig. 4.7). In the contact mode, the initial values of  $k_s$  and  $k_n$  apply. When

the shear stress  $\tau_s$  go beyond the shear strength  $\tau_y$ , assumed to be governed by the Mohr-Coulomb law, slip occurs and  $k_s$  is set to  $k_{rs}$ , the tangential residual stiffness of the interface after slip. For simplicity, the tangential stress-displacement relationship can be assumed to be elastic-perfectly, i.e.,  $k_{rs} = 0$ . If the interface normal stress is tensile, both  $k_s$  and  $k_n$  are set equal to zero. This is the de-bonding or opening mode. When the normal stress  $\sigma_n$  becomes compressive, the interface is re-bonded and  $k_s$  and  $k_n$  are restored to the initial values.

#### 4.5.1.4 Analysis of a single Interface Element

Let us consider a single interface element as shown in Fig. 4.8. Nodes 1 and 2 are fixed. After introduction of the boundary conditions  $u_1 = v_1 = u_2 = v_2 = 0$ , the element stiffness Equation 4.32 is reduced to four equations, i.e.

$$\frac{L}{6} \begin{bmatrix} 2k_s & 0 & k_s & 0 \\ 0 & 2k_n & 0 & k_n \\ k_s & 0 & 2k_s & 0 \\ 0 & k_n & 0 & 2k_n \end{bmatrix} \begin{Bmatrix} u_3 \\ v_3 \\ u_4 \\ v_4 \end{Bmatrix} = \begin{Bmatrix} f_{3x} \\ f_{3y} \\ f_{4x} \\ f_{4y} \end{Bmatrix} \quad (4.47)$$

Solving the equations gives horizontal displacements as in equations 4.48 and 4.49.

$$U_3 = \frac{2}{Lk_s} (2f_{3x} - f_{4x}) \quad (4.48)$$

$$U_4 = \frac{2}{Lk_s} (-f_{3x} + 2f_{4x}) \quad (4.49)$$

And vertical displacements (equations 4.50 and 4.51)

$$v_3 = \frac{2}{Lk_n} (2f_{3y} - f_{4y}) \quad (4.50)$$

$$v_4 = \frac{2}{Lk_n} (-f_{3y} + 2f_{4y}) \quad (4.51)$$

For the special cases when  $f_{3x} = P$  and  $f_{4x} = 0$  (equations 4.52 and 4.53), we have

$$u_3 = \frac{4P}{Lk_s} \quad (4.52)$$

$$u_4 = -\frac{2P}{Lk_s} \quad (4.53)$$

And when  $f_{3y} = f_{4y} = -Q$ , we have

$$v_3 = v_4 = -\frac{2Q}{Lk_n} \quad (4.54)$$

The tangential and normal “stresses” are as expected. They can be calculated directly from Equation 4.45 and Equation 4.46, yielding

$$\tau_s = \frac{P}{L} \quad (4.55)$$

$$\sigma_n = -\frac{2Q}{L} \quad (4.56)$$

The deformations of the two cases are illustrated in Fig. 4.9. The tangential displacement  $u_3$  and  $u_4$  can be considered the preslip displacements. Even though they may be negligible if we choose a very large value of  $k_s$ , the relationship  $u_4 = -1/2 u_3$  holds and this phenomenon is contrary to our expectations. The feature that node 4 displaces in an opposite direction when we pull at node 3 under the simple boundary condition is not the result of numerical ill-conditioning but only determined by this feature on practical problems.

#### **4.5.2 Element Proposed By Ghaboussi et al. (1973)**

The novel aspect of this four noded continuum element was considering relative displacements as the independent degrees of freedom with a very small thickness. The displacement degrees of freedom on one side of the interface are thus transformed into the relative displacements between the two sides of the interface. If relative displacements are introduced as independent degrees of freedom, the accuracy of the solution is greatly improved. A disadvantage of using relative displacements as independent degree of freedom is the increase in size of the element arrays for the “top” continuum element at the interface

#### **4.5.3 Element Proposed By Herrmann (1978)**

Another approach for modelling interfaces was developed by Herrmann (1978). Although more difficult to implement than the element of Goodman et al. (1968), this approach possessed definite numerical advantages realized behaviour. Thus unlike the



“stiffness” approach proposed by Goodman et al.(1968), and unlike constraint approach utilizing Lagrange multipliers Herrmann’s formulation can be viewed as a “hybrid” element.Unlike the element of Goodman et al. (1968) that used a compatibility approach to model slip and required stiffness value, Herrmann’s, approach defined three distinct behavioural regimes: the separation modes, the non-slip, and the slip modes. A compatibility approach, an equilibrium approach and a combined compatibility and equilibrium approach respectively, were then used to model these modes. This is because when slippage or separation or both, are occurring, it is equilibrium information. The bond behaviour is modelled using fictitious bond springs of which one is normal, and the other is tangential to the interface at each of the two pairs of mating nodes. These unknowns include two absolute and relative displacements in the normal ( $\delta_n$ ) and tangential ( $\delta_t$ ) directions. These potential problems are attributed to the large contributions to diagonal terms in the interface element stiffness matrix.

## **4.6 MODELLING OF COMPONENTS**

### **4.6.1 Modelling of Soil**

Most researchers have adopted non-linear elastic or elasto-plastic models for soil. Linear elastic constitutive models are adopted to compute the initial deformation and limiting equilibrium methods are adopted to assess the load at failure by incorporating appropriate constitutive models e.g. Von Mises or Mohr-Coulomb, Drucker-Prager.

### **4.6.2 Soil reinforcement**

The incorporation of mechanism of soil-reinforcement-facing interaction in the FEM are greatly influenced by the construction, propping of facing during construction and its release later including the boundary conditions (loading on top, etc.). Reinforcement is generally modelled by the linear bar element capable of taking only axial tensile forces. Behaviour of extensible geosynthetic materials is generally non-linear. Sometimes metallic reinforcements are also modelled as continuous beam

element and the bending moment is calculated. The fundamental concept of FEM is discretization. FEM consists of both discretization and assembling. In the process of assembling the elements are placed back and a) TRUSS element or b) BEAM element, Uni-dimensional Elements, Separate, combined and with Boundary assembled (Fig. 4.10)

A one-dimensional element of c/s area  $A$  and young's modulus  $E$  made of linearly elastic material as shown in Fig.4.10 has two primary nodes and hence two axial degrees of freedom one at each node. The element stiffness matrix size is  $2 \times 2$ . The displacement,  $D$  is given by equation 4.57

$$D = \frac{PL}{AE} \quad (4.57)$$

The force required to produce unit displacement is called stiffness. Let  $K$  be the stiffness of the element for unit displacement given by equation 4.58. Hence

$$K = \frac{P}{D} = \frac{AE}{L} \quad (4.58)$$

The element stiffness matrix is as given by equation 4.59

$$[K] = \frac{AE}{L} \begin{bmatrix} 1 & -1 \\ -1 & 1 \end{bmatrix} \quad (4.59)$$

The soil has been modelled as a rectangular element and the basics of obtaining the stiffness matrix is as follows. Let  $N_1, N_2, N_3$  and  $N_4$  be the shape functions. The displacement functions for  $u(x, y)$  and  $v(x, y)$  are given by four coefficients as in equations 4.60 and 4.61.

$$u(x, y) = a_1 + a_2x + a_3y + a_4xy \quad (4.60)$$

$$v(x, y) = a_5 + a_6x + a_7y + a_8xy \quad (4.61)$$

The shape functions are expressed as products of one-dimensional Lagrange interpolation Functions (Equations 4.62 to 4.65)

$$N_1(x, y) = \frac{(a-x)(b-y)}{4ab} \quad (4.62)$$

$$N2(x, y) = \frac{(a+x)(b-y)}{4ab} \quad (4.63)$$

$$N3(x, y) = \frac{(a+x)(b+y)}{4ab} \quad (4.64)$$

$$N4(x, y) = \frac{(a-x)(b+y)}{4ab} \quad (4.65)$$

The [B] matrix is obtained by equation 4.66,

$$[B] = \begin{pmatrix} \frac{\partial N1}{\partial x} & 0 \\ 0 & \frac{\partial N1}{\partial y} \\ \frac{\partial N1}{\partial y} & \frac{\partial N1}{\partial x} \end{pmatrix} \quad (4.66)$$

The stiffness matrix can be written in terms of (2x2) nodal sub matrices as in equation 4.67

$$[K_{ij}]_{2 \times 2} = \int_V [B_i]^T [D]_{3 \times 3} [B_j]_{3 \times 2} dV \quad (4.67)$$

where i and j are element node numbers. As it is not possible to perform programming for integration using computers numerical integration is adopted for which isoparametric formulation is adopted.

Let us consider the mapping of four node-quadrilateral element from a natural ( $\xi, \eta$ ) co-ordinate system to a physical (x, y) co-ordinate system. In natural co-ordinates, the element is a (2x2) square and the origin is at its centre. With the shape functions in terms of ( $\xi, \eta$ ) co-ordinates system, the co-ordinates of any point can be expressed in terms of (x, y) co-ordinates as in equation 4.68

$$\mathbf{x}(\xi, \eta) = \sum_{i=1}^4 N_i(\xi, \eta) \mathbf{x}_i, \quad \mathbf{y}(\xi, \eta) = \sum_{i=1}^4 N_i(\xi, \eta) \mathbf{y}_i, \quad (4.68)$$

[N] is the shape function matrix.

After mapping (equations 4.69 to 4.72)

$$N1(\epsilon, \mu) = \frac{(1-\epsilon)(1-\mu)}{4} \quad (4.69)$$

$$N2(\epsilon, \mu) = \frac{(1+\epsilon)(1-\mu)}{4} \quad (4.70)$$

$$\mathbf{N3}(\varepsilon, \mu) = \frac{(1+\varepsilon)(1+\mu)}{4} \quad (4.71)$$

$$\mathbf{N4}(\varepsilon, \mu) = \frac{(1-\varepsilon)(1+\mu)}{4} \quad (4.72)$$

In a like manner, derivatives of the shape function for node I are related by equation 4.73

$$\begin{matrix} \frac{\partial y}{\partial x} \\ \frac{\partial y}{\partial x} \\ \frac{\partial y}{\partial x} \end{matrix} = [\mathbf{J}]^{-1} \begin{matrix} \frac{\partial y}{\partial x} \\ \frac{\partial y}{\partial x} \\ \frac{\partial y}{\partial x} \end{matrix} \quad (4.73)$$

The element stiffness matrix is obtained by equation 4.74,

$$[\mathbf{K}] = \int_{-1}^1 \int_{-1}^1 [\mathbf{B}]^T [\mathbf{D}] [\mathbf{B}] [\mathbf{J}] d\xi d\eta \quad (4.74)$$

The individual terms  $[\mathbf{B}_i]$ , in terms of  $(\xi, \eta)$ , are

Where  $J_{ij}^*$  is the  $i, j$  form  $[\mathbf{J}]^{-1}$ , Hence we write and obtain equation 4.75,

$$[\mathbf{K}_{ij}] = \int_{-1}^1 \int_{-1}^1 [\mathbf{B}_i]^T [\mathbf{D}] [\mathbf{B}_j] [\mathbf{J}] d\xi d\eta \quad (4.75)$$

Section 4.7 shows the various figures related to Finite Element Analysis.

Since the size of stiffness matrix is very large it results in shortage of memory. Hence optimizing memory requirement to store stiffness matrix values becomes essential. The line separating the top zero elements from the first non – zero element is called the Skyline. In this system of storage, if there are zero elements at the top of a column, only the elements from the first non-zero value need to be stored. This method is called Skyline storage and is used in the present work.

Contents of the global stiffness matrix before reduction is often has less than 5% number of non-zero elements and perhaps less than 1% non-zero elements if there are thousands of degrees of freedom. During reduction of stiffness a direct solver changes most zeros between the skyline and diagonal to nonzero, but leaves zeroes above the skyline intact, so the matrix remains sparse. A profile or skyline single array storage scheme is adopted to save the memory space needed in the storage of the matrices. An active column profile (skyline) solution algorithm is employed in the equation

solution module to solve the equations efficiently. The use of this method with an active column profile storage scheme leads to a very compact program where it is very easy to use vector dot product routines to effect the triangular decomposition and forward reduction. This computational advantage is very important to modern computers which are vector oriented. Therefore software exploit this sparsity by using compact storage formats, so that nonzero elements are neither stored nor processed. Section 4.7 presents the various figures related to FEM

#### 4.7 VARIOUS FIGURES RELATED TO FEM

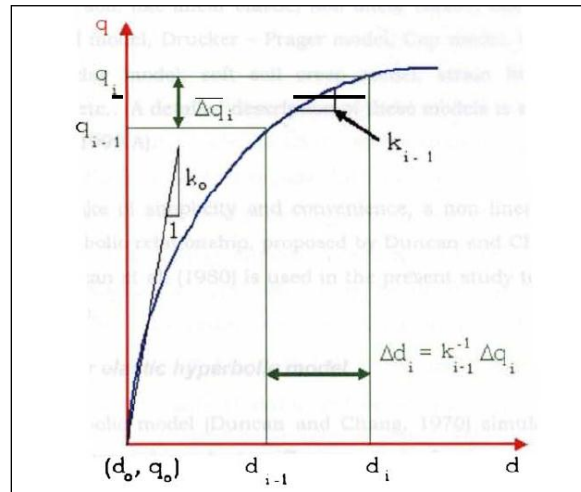


Fig. 4.1 Incremental Method (Jayashree, 2008)

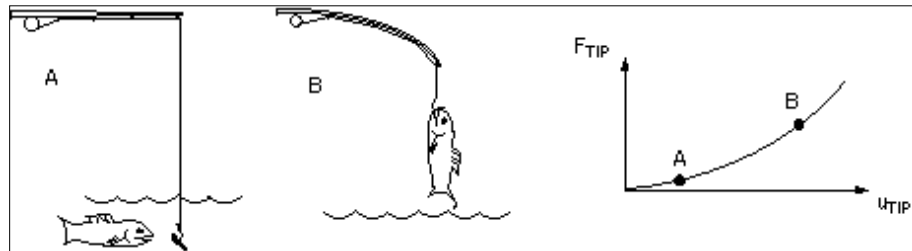


Fig. 4.2 A fishing rod demonstrates geometric nonlinearity ([www.ansys.stuba.sk](http://www.ansys.stuba.sk))

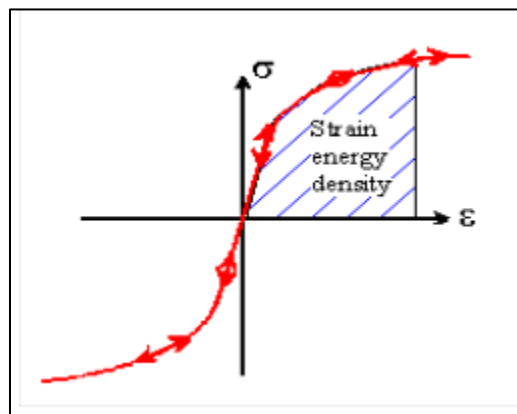


Fig. 4.3 Hypoelastic Behaviour (Kok Sien Ti, 2009)

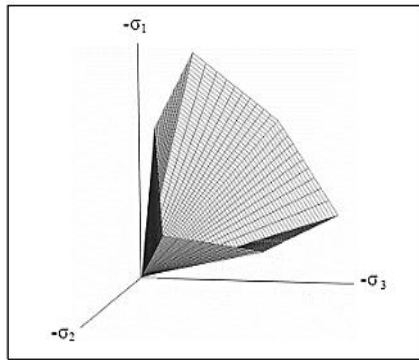


Fig. 4.4 Mohr-Coulomb Yield surface in Principal Stress space( Kok Sien Ti, 2009)

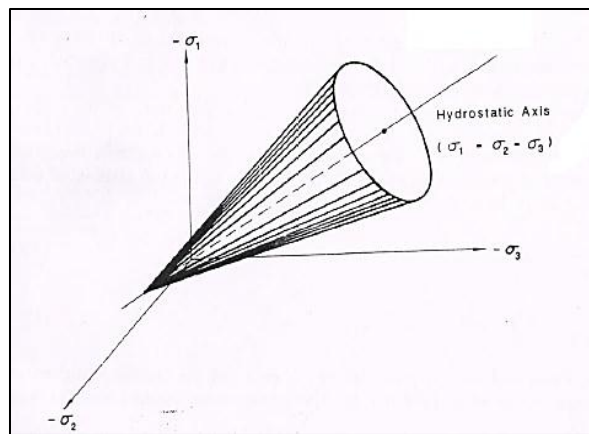


Fig. 4.5 Drucker Prager Yield surface in Principal Stress space

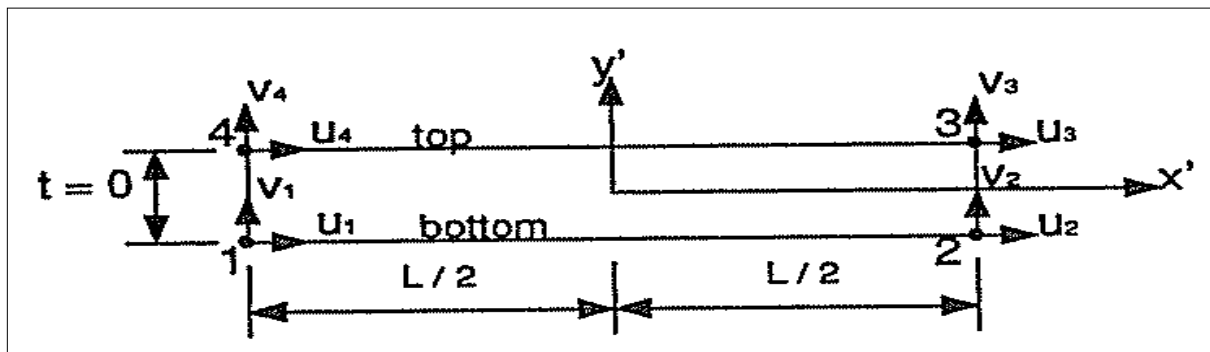


Fig. 4.6 Interface Element after Goodman et al. (1968)

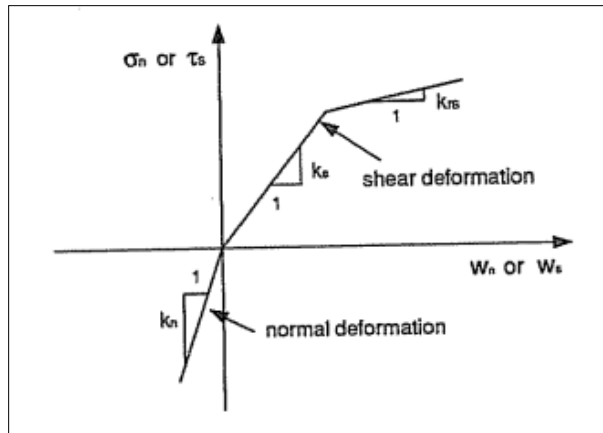


Fig. 4.7 Simple Constitutive Model of an Interface (Jianchao, 1993)

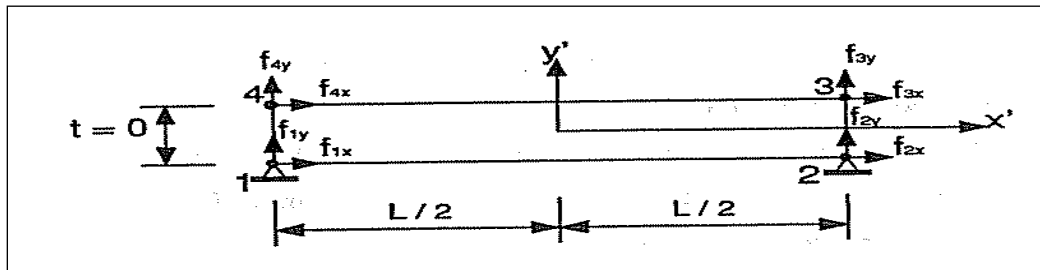


Fig. 4.8 Single Goodman et al.'s (1968) Interface Element Example (Jianchao, 1993)

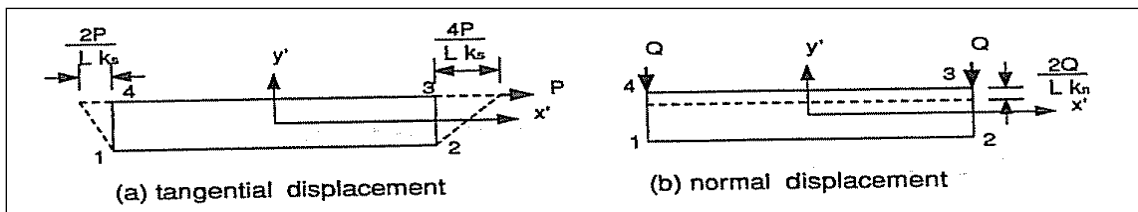


Fig. 4.9 Deformations for Goodman et al.'s Interface Element for special load case (Jianchao, 1993)

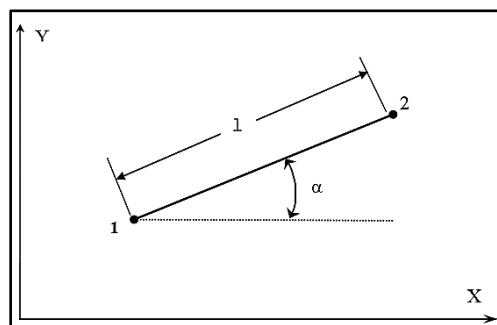
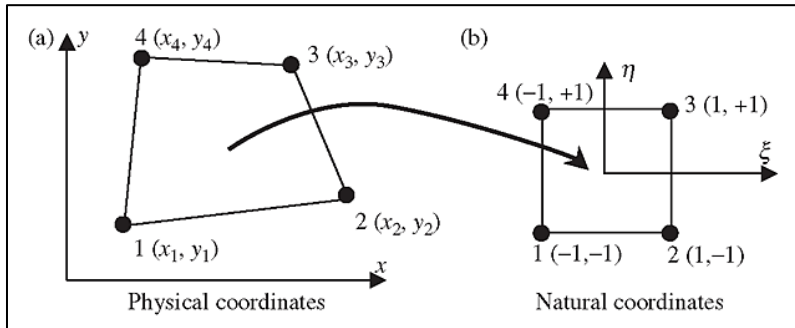


Fig. 4.10 Unidimensional Elements (Desai, 2012)





(a) (b)

**Fig. 4.11 (a) Element in physical coordinates. (b) Element in natural coordinates. (www.what-when-how.com)**

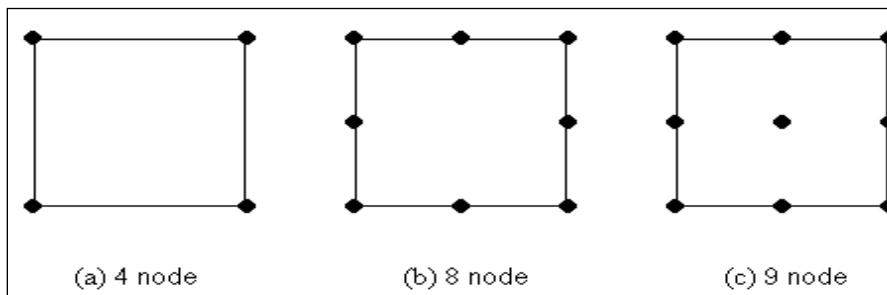


**Fig. 4.12 Different noded elements**

## CHAPTER 5

### LINEAR ANALYSIS OF REINFORCED SOIL STRUCTURES

#### 5.1 GENERAL

A structure is defined as a body or system of connected parts used to support a load and the examples are buildings, bridges, and towers. The designed structure must serve a specified function for public use and the engineer must consider its safety, aesthetics and serviceability, while also considering the economic and environmental constraints. The material properties, structural loads, geometry and support conditions are needed to perform an accurate analysis. Such an analysis typically results in support reactions, stresses and displacements which are then compared to the conditions of failure.

Advanced structural analysis deals with dynamic response, stability and non-linear behaviour. These analyses can be carried out by the Mechanics of materials approach (also known as strength of materials), the Elasticity Approach (which is actually a special case of the more general field of Continuum Mechanics) and the Finite Element Approach. The first two make use of analytical formulations which apply mostly to simple linear elastic models which can be often solved manually and can lead to closed form solutions. The Finite element approach is a numerical method for solving differential equations developed by theories of mechanics like theory of elasticity and strength of materials. This method depends heavily on the processing power of computers and is more applicable to structures of arbitrary size and which involve complexity.

For many decades, Soil Mechanics was based on Hooke's law of linear elasticity for stress and deformation analysis for a soil mass where no failure of soil mass was involved may be under a footing or behind a retaining wall. This is known as

elasticity problem in Soil Mechanics. The theory of Plasticity deals with the conditions of complete failure of soil mass.

The essential link between elasticity and plasticity in Soil Mechanics is the progressive failure condition which deals with elastic-plastic transition. Linear structural analysis is a proportional analysis based on two fundamental assumptions, namely, (a) Material linearity (b) Geometric linearity. According to Material linearity, the structures are composed of linear elastic materials. Geometric linearity implies that the structural deformations are so small that the equations of equilibrium can be expressed in the undeformed geometry of the structure. In the Linear Analysis, stresses are proportional to strains. Let us consider the mathematical equation of a straight line as expressed in equation 5.1

$$y = mx \quad (5.1)$$

If the value of slope is known,  $y$  can be found for a given value of  $x$  which can be done in a single step. Repetition is not required. If  $x$  is replaced with strain ( $\epsilon$ ),  $y$  with stress ( $\sigma$ ) and  $m$  the stiffness of material ( $E_s$ ) then the equation of the same straight line as expressed in equation 5.2

$$\sigma = E_s \epsilon \quad (5.2)$$

Hence linear analysis is simple. It will reduce the time and effort required for the analysis. Linear analysis is still popular because it considers material safety factors and specified properties. Linear analysis generally yields accurate results for most common structures. However, because of its inherent limitations, linear analysis cannot predict structural response in the large deformation and/or failure range, nor it can detect instability conditions (buckling) of structures.

A very simple definition of linear analysis would be that we design the component (column, beam etc.) or the whole structure such that even when maximum design forces are applied to the structure, the displacement of the structure does not exceed its elastic limit. So, the structure would always come back to its initial position without any damage. Hooke's law for uniaxial deformation states that strain is

proportional to stress. For three dimensional bodies, six components of stress and strain are used. Each of the six stress components may be expressed as a linear function of the six

$$\begin{Bmatrix} \sigma_x \\ \sigma_y \\ \sigma_z \\ \tau_{xy} \\ \tau_{yz} \\ \tau_{zx} \end{Bmatrix} = \begin{bmatrix} C_{11} & C_{12} & \cdots & C_{16} \\ C_{21} & C_{22} & \cdots & C_{26} \\ \vdots & & & \vdots \\ C_{61} & C_{62} & \cdots & C_{66} \end{bmatrix} \begin{Bmatrix} \epsilon_x \\ \epsilon_y \\ \epsilon_z \\ \gamma_{xy} \\ \gamma_{yz} \\ \gamma_{zx} \end{Bmatrix} \quad (5.3)$$

results for most common structures. (Refer equation 5.3). Due to its inherent limitations, linear analysis cannot predict structural response in the large deformation and/or failure range, nor can it detect instability conditions (buckling) of structures. Since Galileo's pioneering work in the 17th century, numerous methods for analysis of structures have been developed. The problem that arises with linear analysis is, that when forces become large (in case of earthquakes) the dimensions of the component or the whole building would become huge. This is not an economic solution. But here non-linear analysis can be applied.

Certain materials exhibit symmetry with respect to planes within the body, so the number of material constants will be reduced from 21 required in the anisotropic case.

The stress-strain equations for orthotropic materials may be written in terms of the Young's moduli and Poisson's ratio as follows

$$\begin{Bmatrix} \sigma_x \\ \sigma_y \\ \sigma_z \\ \tau_{xy} \\ \tau_{yz} \\ \tau_{zx} \end{Bmatrix} = \begin{bmatrix} C_{11} & C_{12} & C_{13} & 0 & 0 & 0 \\ & C_{22} & C_{23} & 0 & 0 & 0 \\ & & C_{33} & 0 & 0 & 0 \\ & & & C_{44} & 0 & 0 \\ & & & & C_{55} & 0 \\ & & & & & C_{66} \end{bmatrix} \begin{Bmatrix} \epsilon_x \\ \epsilon_y \\ \epsilon_z \\ \gamma_{xy} \\ \gamma_{yz} \\ \gamma_{zx} \end{Bmatrix} \quad (5.4)$$

There are twelve material parameters in the above equations. Only nine of these are independent.

### 5.1.1 Linear Isotropic Elasticity

The simplest specialization of the generalized Hooke's law is the case in which the material is assumed to be linear, isotropic and elastic. An isotropic material is the one that has point of symmetry. Every plane in the body is a plane of symmetry of material behaviour. Only two independent elastic constants can be used to represent the behaviour in the case of such symmetry. Hence the equation in terms of E and  $\mu$  can be expressed as in equation 5.5

$$\begin{Bmatrix} \epsilon_x \\ \epsilon_y \\ \epsilon_z \\ \gamma_{xy} \\ \gamma_{yz} \\ \gamma_{zx} \end{Bmatrix} = \begin{bmatrix} 1/E & -\nu/E & -\nu/E & 0 & 0 & 0 \\ & 1/E & -\nu/E & 0 & 0 & 0 \\ & & 1/E & 0 & 0 & 0 \\ & & & 2(1+\nu)/E & 0 & 0 \\ & & & & 2(1+\nu)/E & 0 \\ & & & & & 2(1+\nu)/E \end{bmatrix} \begin{Bmatrix} \sigma_x \\ \sigma_y \\ \sigma_z \\ \tau_{xy} \\ \tau_{yz} \\ \tau_{zx} \end{Bmatrix} \quad (5.5)$$

Hooke's law for isotropic materials is sometimes expressed in terms of Lamé's constants  $\lambda$  and  $\mu$ . (Equations 5.6 to 5.9)

$$C_{11} = C_{22} = C_{33} = \lambda + 2\mu \quad (5.6)$$

$$C_{12} = C_{13} = C_{23} = \lambda \quad (5.7)$$

$$C_{44} = C_{55} = C_{66} = \mu = G = \frac{E}{2(1+\nu)} \quad (5.8)$$

$$\text{Where } \lambda = \frac{E\nu}{(1+\nu)(1-2\nu)}, \quad (5.9)$$

Shear Modulus, G, below represents the behaviour of a material under pure shearing stresses. To characterize the behaviour of the material as a result of volumetric stresses. We use the bulk modulus, K, which is expressed in terms of E and  $\mu$  as below. (Refer equations 5.10 to 5.13)

$$\mu = G = \frac{E}{2(1+\nu)} \quad (5.10)$$

$$E = \frac{\mu(3\lambda+2\mu)}{\lambda+\mu} \quad (5.11)$$

$$\nu = \frac{\lambda}{2(\lambda + \mu)} \quad (5.12)$$

$$K = \frac{E}{3(1-2\nu)} = \frac{(3\lambda + 2\mu)}{3} \quad (5.13)$$

### 5.1.2 Two-Dimensional Specialisations of Elasticity

It is costly and time consuming to perform finite element analyses of three dimensional problems in Solid Mechanics. Practical solutions may have geometry and loading configurations that reduce these three dimensional problems in one or two dimensions.

#### 5.1.2.1 Plane Strain

Problems involving a long body whose geometry and loading do not vary significantly in the longitudinal direction are referred to as Plane Strain problems. Some examples are a loaded semi-infinite half space such as strip footing on a soil mass, a long cylinder such as a tunnel, culvert or buried pipe, a laterally loaded retaining wall and a long earthen dam. In such problems, the dependent variables can be assumed to be functions of x and y co-ordinates only, provided we consider a cross section some distance away from the ends. The strain components  $\epsilon_z$ ,  $\gamma_{yz}$  and  $\gamma_{zx}$  will vanish and the remaining non-zero components will be as expressed as equations 5.14 to 5.16

$$\epsilon_x = \frac{\sigma_x}{E_x} - \frac{\nu_{yx}}{E_y} \sigma_y - \frac{\nu_{zx}}{E_z} \sigma_z \quad (5.14)$$

$$\epsilon_y = \frac{\sigma_y}{E_y} - \frac{\nu_{xy}}{E_x} \sigma_x - \frac{\nu_{zy}}{E_z} \sigma_z \quad (5.15)$$

$$\gamma_{xy} = \frac{\tau_{xy}}{G_{xy}} \quad (5.16)$$

In the plane strain problems, we usually consider only a slice of unit thickness.

#### 5.1.2.2 Plane Stress

In contrast to the plane strain condition, in which the longitudinal dimension in the z direction is large compared to the x and y dimensions, the plane stress condition is characterised by very small dimensions in the z-direction. A thin plate loaded in its

plane is the well-known example of plane stress approximation. Let us consider the case where no loadings are applied on the surface of the plate. The stress components  $\tau_{yz}$  and  $\tau_{zx}$  vanish on the surfaces of the plates and  $\sigma_z$  is zero throughout the thickness. Since many individuals write programs for a broad range of applications, most high-level computer languages, like FORTRAN and C, have rich capabilities. Although some engineers might need to tap the full range of these capabilities, most merely require the ability to perform engineering oriented numerical calculations. Sections 5.1.1, 5.1.2, 5.1.2.1, 5.1.2.2 and Equations 5.3 to 5.17 have been taken from Desai and Abel, (1987).

## **5.2 FORMULATION OF THE PROBLEM AND PROGRAMMING**

In this part of the research, the behavior of reinforced soil retaining wall is being studied for linear case. The approach is to develop Codes (program) RWPT-LIN (for point loads only), RWSW-LIN (only for self-weight and 100% coupling) and RWSW-INT (for self-weight with interfaces only), validate it with software or previously published work.

The soil is modelled as plane strain rectangular element and the geostrip is modelled as bar element placed in a horizontal plane. For four noded two dimensional plane strain element, numerical integration is done by choosing four gauss points where as for bar element stiffness matrix is written directly. Pilot studies have been carried out on a retaining wall (Refer Fig. 5.1a) subjected to point loads [of magnitude 57kN (Vehicle load as per IRC Class A)] to validate the program for linear analysis with a standard software. In this study, two-dimensional (plane strain) numerical analysis has been conducted adopting finite element method by developing programs in FORTRAN 77. They are RWPT-LIN, RWSW-LIN and RWSW-INT. The unreinforced and reinforced soil model is analysed for the below two cases

1. Self-weight of soil
2. Point Load

The analysis has been carried out separately for point loads and dead loads only to study the effect in a better way.

### 5.2.1 Flow of Program / Algorithm

The coding is done in FORTRAN 77 and the names of the programme developed are RWPT-LIN, RWSW-LIN and RWSW-INT. The main routine reads ELTYPE (types of elements), GDOFN (global degrees of freedom for each node), nndro (number of nodes in each row), nndco (number nodes in each column), H (height of wall), ETYPE(element types, i.e. whether element is type I or type II), NEL(number of element of each type), NDE(nodes per each element),(degrees of freedom for element of each type), ym (Young's modulus), pr (Poisson's ratio), nelro (number of elements in each row) and NELCOM (number of elements in each column).

It calls subroutines COLUMH, CADNUM, PASSEM, and PASOLV (Krishnamoorthy, 1995). It also calls subroutines BSTIF, ELESTRESSThe flow of the program/ Algorithm is follows:

- 1 Read NEL-number of elements, NDE-nodes per each element, DOFN-degrees of freedom per node, pr- poisons ratio, ym- Young's modulus, NDOFE-number of degrees of freedom per element
- 2 Loop 6 generates number of global node point (element, element node wise) variable k gives maximum nodal number.NP-gives global node number.
- 3 Loop 5 reads Cartesian co-ordinates of each node local or global co-ordinates.
- 4 Loop 21 initializes values of MAT (K, DOFN) to one where K is the global node number.
- 5 Read NVFIX- the number of nodes which are suppressed, NNN-their global node number and MAT(NNN,J) is made zero for j=1,2
- 6 Loop 38 and 39 gives MAT (node wise, degree of freedom per node wise) = global degrees of freedom for each active node. The loop variable



COUNT gives max value of global degree of freedom. Loop 46 writes the same.

- 7 Loop 66 evaluates NCODE which gives global degree of freedom number for every element and local degree of freedom i.e., basically relates local degree of freedom (dof) of each element with global dof i.e., global dof (element, local dof)=MAT (global node number, dof of each node).
- 8 Loop 100 calculates element number from element type and numbers of element in each type.
- 9 Loop 251 places the amount of Live Load at nodes of vertical degrees of freedom.
- 10 Loop 252 places the amount of Self weight (Dead Load) at nodes of vertical degrees of freedom.
11. Loop 2000 will calculate the average values of Stresses, Strains at each node points.
12. Call SUBROUTINE COLUMH to calculate column heights.
13. Call SUBROUTINE CADNUM to find diagonal address of global stiffness matrix.
14. For each element  
    Call SUBROUTINE BSTIF (to calculate element stiffness matrix)
15. Call PASSEM (for each element to find the stiffness matrix).
16. Feed the nodal loads.
17. Call PASOLV to obtain nodal displacement.
18. For each element  
    Calculate nodal displacements in local co-ordinates,  
    Calculates stress for each element by calling SUBROUTINE  
    ELESTRESS.
19. GNDOF calculates global degrees of freedom.

#### **5.2.1.1 Subroutine BSTIF**

For each element  
Initialize element stiffness matrix EK and constitutive matrix C  
For each Gauss point

Calculates shape functions and their derivatives

Calculates Jacobian matrix XJAC and its inverse XJACI

Obtain strain displacement matrix B

Calculates matrix  $DB=C*B$

Get stiffness matrix  $EK=B*DB$

#### **5.2.1.2 Subroutine ELESTRESS**

For each element

Initialize element stiffness matrix EK and constitutive matrix C.

Calculates shape functions and their derivatives.

Calculates Jacobian matrix XJAC and inverse XJACI.

Obtain Strain displacement matrix B

Calculates matrix  $DB=C*B$

Get element stress matrix  $STRESS=DB*ELDISP$

### **5.3 FEM ANALYSIS & RESULTS OF RETAINING WALL UNDER POINT LOADS**

#### **5.3.1 Definition of Problem**

The wall considered in the parametric study is a 6-m high modular block-reinforced soil retaining wall built on a 3m foundation soil. To eliminate possible boundary effects, the foundation soil was extended to a distance of 12 m in the front end as shown in Fig. 5.1a.

#### **5.3.2 Details of Soil studied**

In the present study, linear constitutive relations have been chosen for soil as well as reinforcement. The soil element size is taken as 0.3m x 0.3m, throughout the retaining wall for both the reinforced and unreinforced conditions. Geostrips are placed horizontally for a length of 4.2m (i.e. 0.7 times the height of the retaining wall). The constitutive properties of both the materials (soil & bar) is taken as linear. A steel facing 0.003m (3mm) is provided to prevent erosion and the presence is

considered to be cosmetic only. The reinforcements are placed at a vertical spacing of 0.3m. Thus a total of 21 layers of reinforcements are being used. The side boundaries are rollers whereas the base is hinged. Only static stresses due to gravity have been considered in this analysis. The characteristics of the soil and reinforcement are given in Table 5.1(Section 5.5)

The developed program calculates displacements, stresses and strains at all nodes for elements. As the output is quite exhaustive it is not printed. Comparative analysis is done for the behaviour of soil with and without geostrip in the retaining wall. Numerous graphs have been plotted for the various cases to analyse the following

- Unreinforced soil with live loads only
- Unreinforced soil with Dead loads only
- Reinforced soil with Live Loads only
- Reinforced soil with Dead loads (Self weight) only

### **5.3.3 FEM Model and results of retaining wall for linear analysis under point loads obtained using developed software RWPT-LIN**

Figure 5.1a shows the typical mesh where the soil is modelled as a rectangular element with four nodes and reinforcement is modelled as bar element with two nodes. The total number of nodes, soil elements, bar elements, interface elements are 3031, 1080, 266 and 532 respectively. The various figures and graphs related to studies on unreinforced and reinforced soil retaining wall under point loads predicted using RWPT-LIN are presented in Section 5.3.4.

#### **5.3.3.1 Displacements in unreinforced and reinforced soil retaining wall under point loads**

The lateral displacements and vertical settlements for a retaining wall under two point loads (57kN) both for the unreinforced and reinforced soil are plotted and shown in Figs 5.2 to 5.10. The lateral displacements for the unreinforced soil

retaining wall are found to vary from to 0.0007m (0.7mm) to 0.00336m (3.36mm). The lateral displacements for the reinforced soil retaining wall are found to vary from 0.000167m (0.167 mm) to 0.0008m (0.8mm). The settlements for the unreinforced soil retaining wall are found to vary from 0.000295m (0.295m) to 0.0163m (16.3mm). The settlements for the reinforced soil retaining wall are found to vary from 7.09E-05m to 0.0039m (3.9mm). It is found that the lateral displacements and settlements decrease in case of a reinforced backfill when compared to displacements in unreinforced backfill by 25% and 24% respectively. Figures 5.11 and 5.12 show the settlements at all levels in unreinforced and reinforced soil retaining wall. Table 5.2 presents the lateral displacements(m) and settlements (m) predicted under point loads for unreinforced and reinforced soil retaining wall at  $x=12.00m$  at all levels of  $y$  using RWPT-LIN.

### **5.3.3.2 Stresses in unreinforced and reinforced soil retaining wall for Linear under point loads**

The horizontal, vertical and shear stresses for point loads have been shown in Figs. 5.13 to 5.22 for both the unreinforced soil and the reinforced soil retaining wall.

Figures 5.13 and 5.14 show the horizontal stresses plotted at all depths for the unreinforced and reinforced soil retaining wall with Young's modulus of soil as 12MPa predicted using developed software (RWPT-LIN). Figure 5.15 depicts the horizontal stresses in unreinforced soil retaining wall obtained by STAAD Pro software which is in a reasonably good agreement with those predicted using developed software RWPT-LIN.

Figures 5.16 and 5.17 show the vertical stresses plotted at all depths for the unreinforced and reinforced soil retaining wall with Young's modulus of soil as 12MPa using developed software. Figure 5.18 depicts the horizontal stresses in unreinforced soil retaining wall obtained by STAAD Pro software.

Figures 5.19 and 5.20 show the shear stresses plotted at all depths for the unreinforced and reinforced soil retaining wall with Young's modulus of soil as 12MPa using developed software. Figure 5.21 depicts the shear stresses in unreinforced soil retaining wall obtained from STAAD Pro software. Figure 5.22 depicts the maximum shear stresses in unreinforced soil retaining wall obtained using the developed software.

1) The horizontal stresses for the reinforced backfill vary from -52850 Pa in compression to 5687 Pa in tension whereas for the unreinforced case the horizontal stresses vary from -54030 Pa in compression to 4615 Pa in tension.

2) The vertical stresses in the reinforced soil vary from -94690Pa in compression to 2499 Pa in tension. The vertical stresses for the unreinforced soil vary from -94690 Pa in compression to 2499 Pa in tension. Though the range of stresses remain the same, it is observed that the stress contours vary in their distribution.

3) The shear stresses for the unreinforced and reinforced backfill vary from -39868Pa to 29544 Pa. Though the range of stresses remain the same, stress contours vary in their distribution.

4) The stress contours obtained using STAAD Pro for the retaining wall under point loads and the developed software are similar but there is a difference in the range of stresses between the two because of the difference in the thickness of the geostrip used. It is not possible to model the geostrip thickness less than 10mm in STAAD Pro. Hence the stresses are lesser in STAAD Pro.

### **5.3.3.3 Strains in unreinforced and reinforced soil retaining wall for Linear analysis under point loads**

Figures 5.23 to 5.30 depict the horizontal, vertical and shear strains at different levels. Figures 5.31 to 5.36 depict the horizontal, vertical and shear strains in unreinforced and reinforced soil retaining wall at all levels. Figures 5.37 and 5.38 represent the major principal stresses in reinforced and unreinforced soil retaining wall.

1) The horizontal strains for the reinforced backfill vary from 0.0003249 (compression) to 0.00044 (tension) under point loads. The strains in the horizontal directions for the unreinforced backfill vary from – 0.001354 (compression) to 0.001834 (tension) under point loads. In the vicinity of reinforcements the strains are reduced to -0.00038 in the reinforced soil whereas in the same location the strain for the unreinforced soil is of the order of 0.00086.

2) The vertical strains for the reinforced soil vary from -0.00139 (compression) to 0.0000781 (tension). The vertical strains vary from -0.00579 (compression) to 0.000325 (tension) for the unreinforced case, and the strain contours vary in their distribution.

3) The shear strains for the reinforced backfill vary from -0.00207 (compression) to 0.00153 (tension). Similarly the shear strains for the unreinforced backfill vary from 0.00864 (compression) to 0.0064 (tension).

Table 5.3 presents the predicted horizontal, vertical and shear strains for unreinforced and reinforced soil under Point Loads at  $y=9.00\text{m}$  using RWPT-LIN. Section 5.3.4 presents the FEM analysis & results of retaining wall under point loads using RWPT-LIN

### 5.3.4 Fem Analysis & Results of Retaining Wall under Point Loads obtained using RWPT-LIN

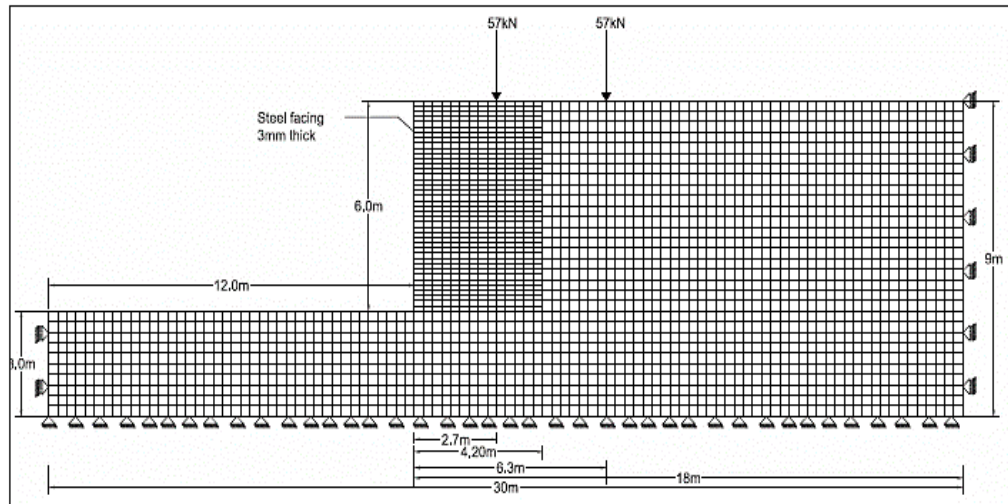


Figure 5.1a Details of Retaining wall being studied subjected to Point Loads

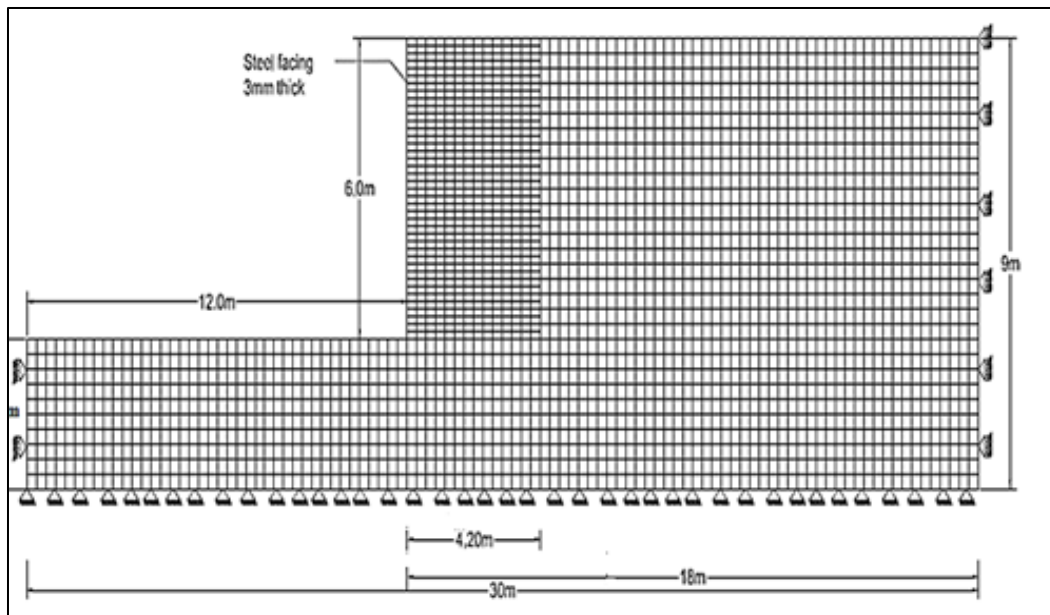
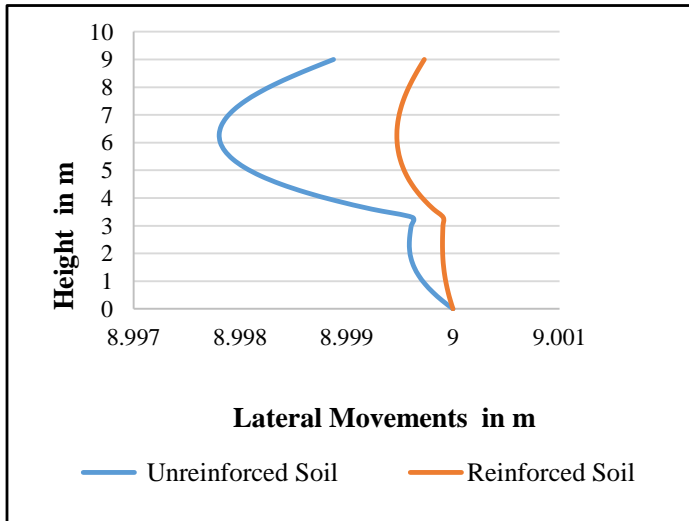
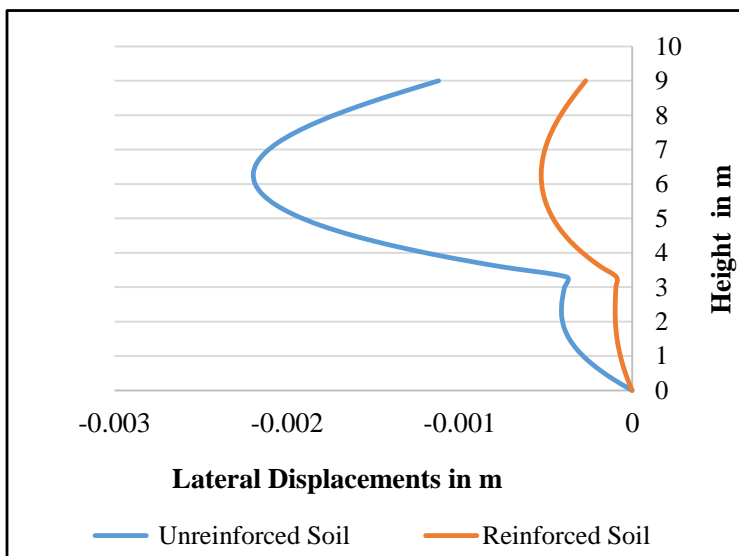


Figure 5.1b Details of Retaining wall being studied subjected to Dead Loads



**Fig. 5.2 Lateral Movements predicted in unreinforced and reinforced soil retaining wall at  $x=9.00\text{m}$  for Linear Analysis under point loads obtained using RWPT-LIN**



**Fig. 5.3 Lateral Displacements predicted in unreinforced and reinforced soil retaining wall at  $x=9.00\text{m}$  for Linear analysis under point loads obtained using RWPT-LIN**



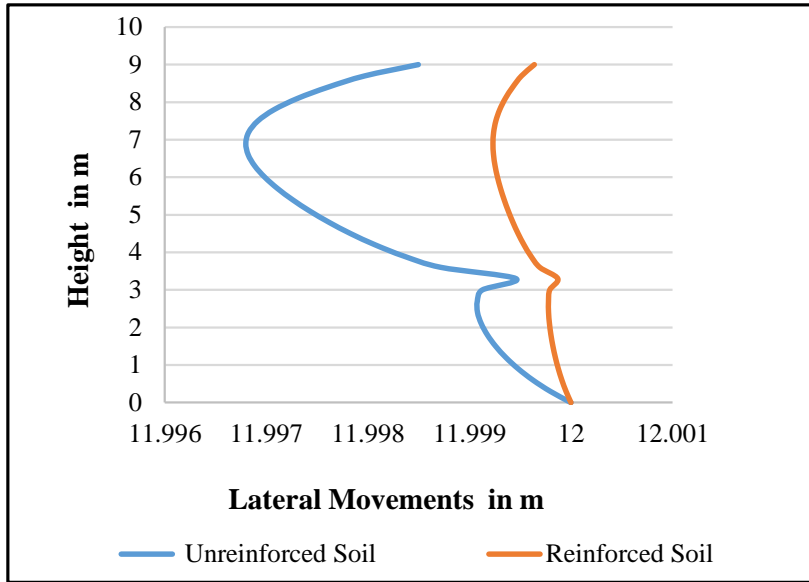


**Fig. 5.4 Lateral Movements predicted in unreinforced and reinforced soil retaining wall at x=12.00 m for Linear analysis under point loads obtained using RWPT-LIN**

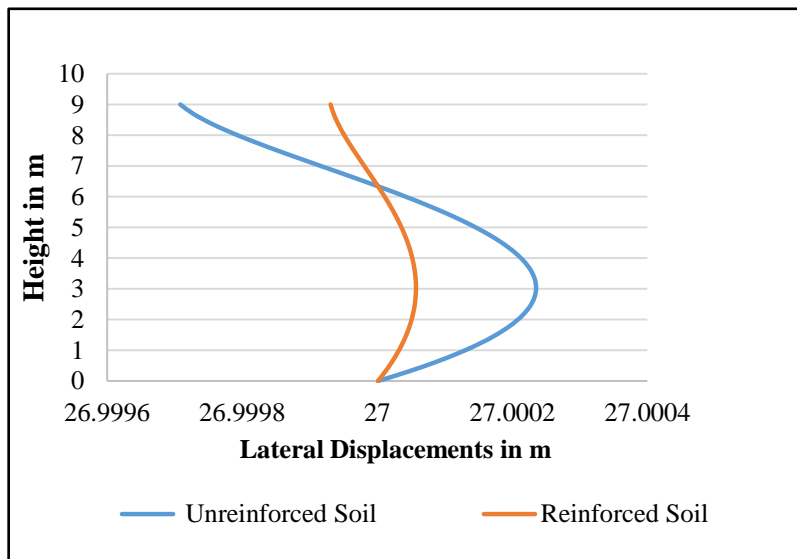


**Fig. 5.5 Lateral Displacements predicted in unreinforced and reinforced soil retaining wall at x=27.00m for Linear analysis under point loads obtained using RWPT-LIN**

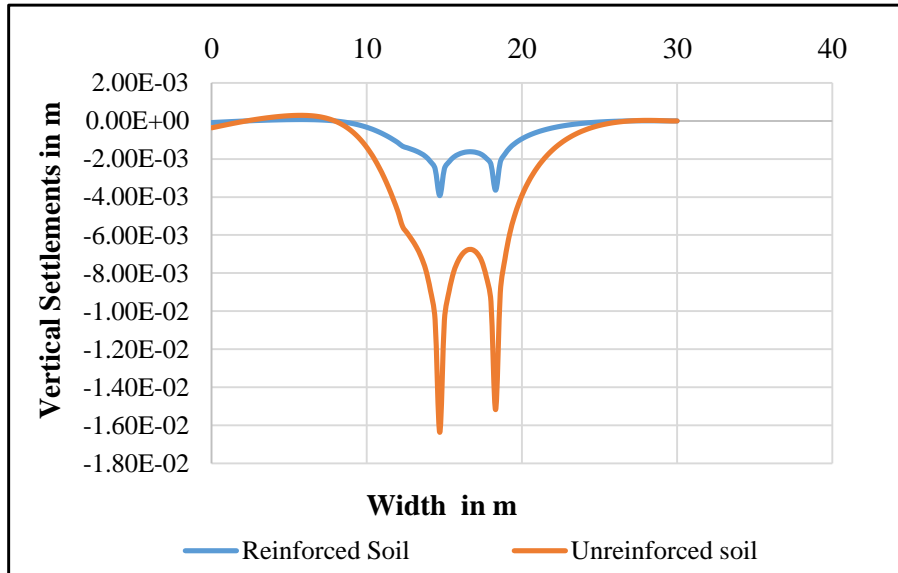


**Fig. 5.6 Vertical settlements predicted in unreinforced and reinforced soil retaining wall at  $y = 8.70\text{m}$  for Linear analysis under point loads obtained using RWPT-LIN**

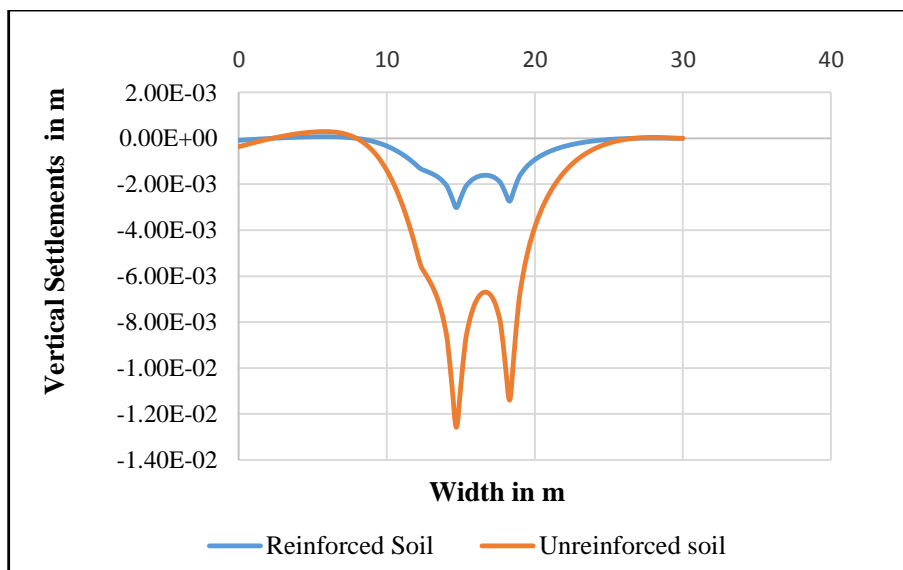


**Fig. 5.7 Vertical settlements predicted in unreinforced and reinforced soil retaining wall at  $y = 8.10\text{m}$  for Linear analysis under point loads obtained using RWPT-LIN**

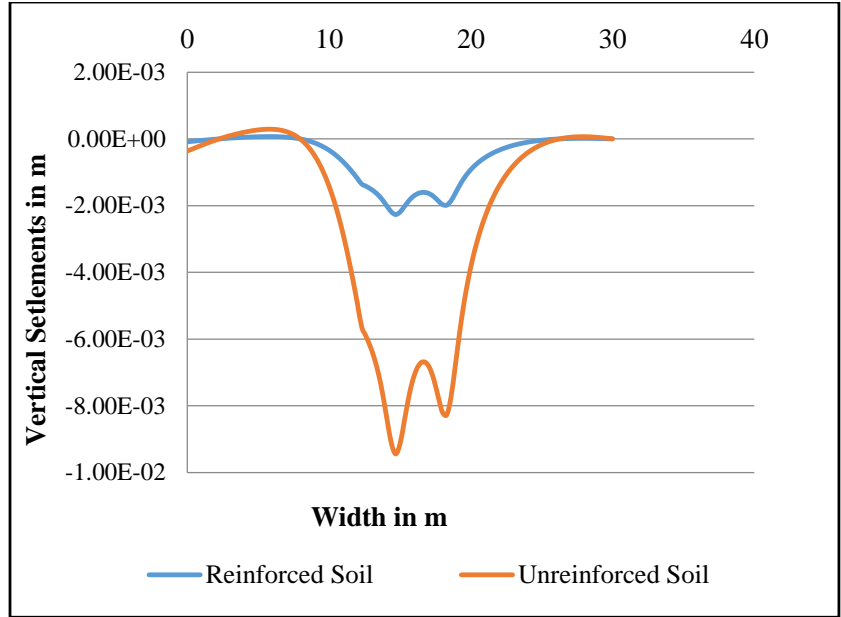


**Fig. 5.8 Vertical Settlements predicted in unreinforced and reinforced soil retaining wall at  $y = 7.80\text{m}$  for Linear analysis under point loads obtained using RWPT-LIN**

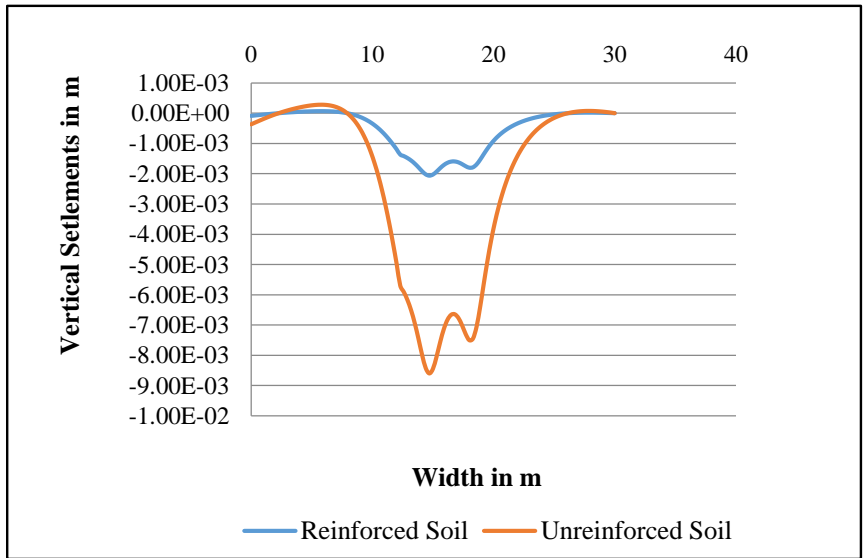


**Fig. 5.9 Vertical Settlements predicted in unreinforced and reinforced soil retaining wall at  $y = 6.90\text{m}$  for Linear analysis under point loads obtained using RWPT-LIN**

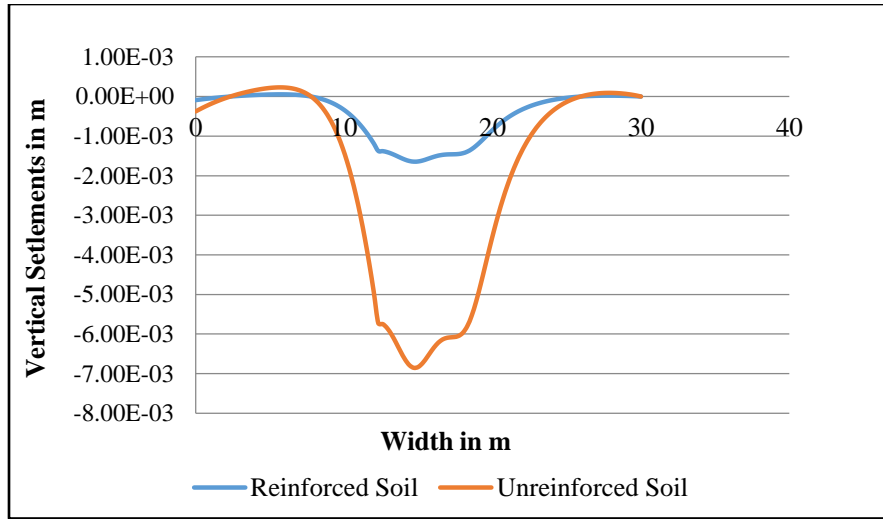


**Fig. 5.10 Vertical Settlements predicted in unreinforced and reinforced soil retaining wall at  $y=0.6m$  for Linear analysis under point loads obtained using RWPT-LIN**

Figures 5.11 and 5.12 depict the settlements at all depths for both the Unreinforced and Reinforced soil retaining wall.

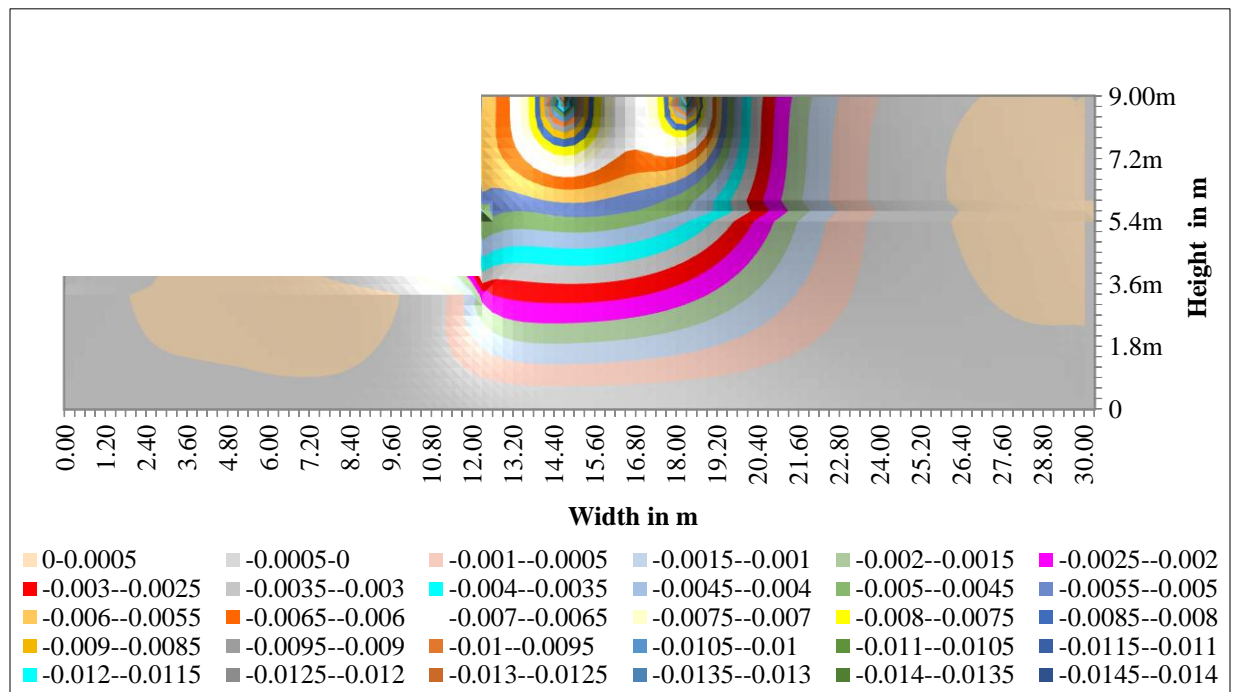


**Fig. 5.11 Settlements (m) at different levels predicted in unreinforced soil retaining wall for Linear analysis under point loads obtained using RWPT-LIN**

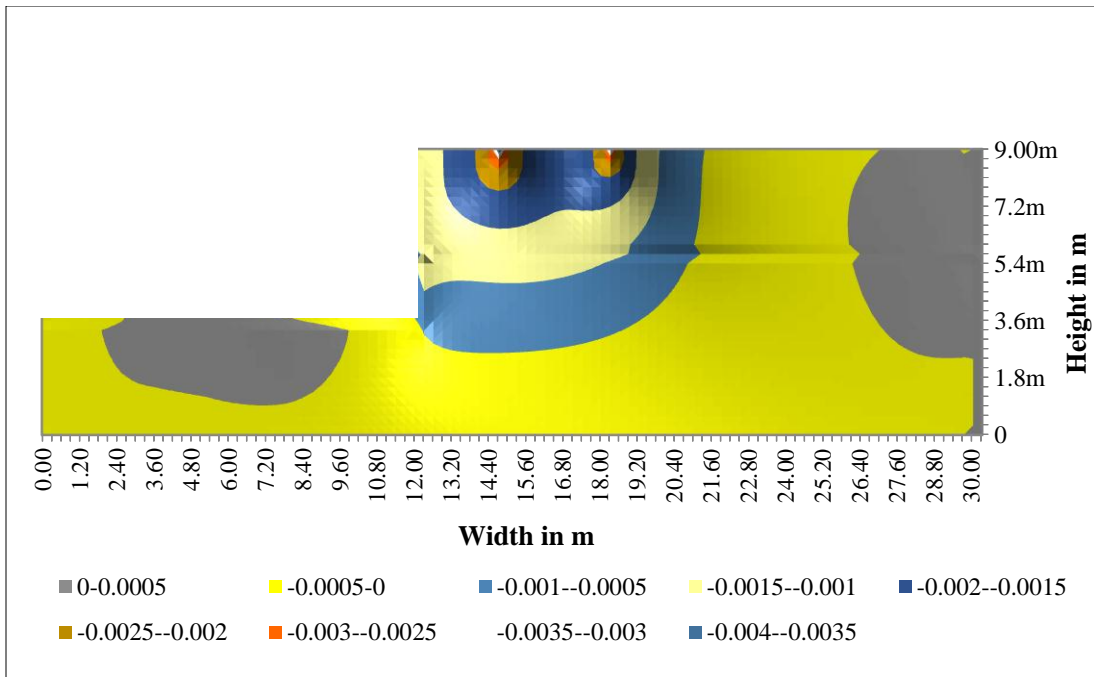


**Fig. 5.12 Settlements (m) predicted at different levels in reinforced soil retaining wall for Linear analysis under point loads obtained using RWPT-LIN**

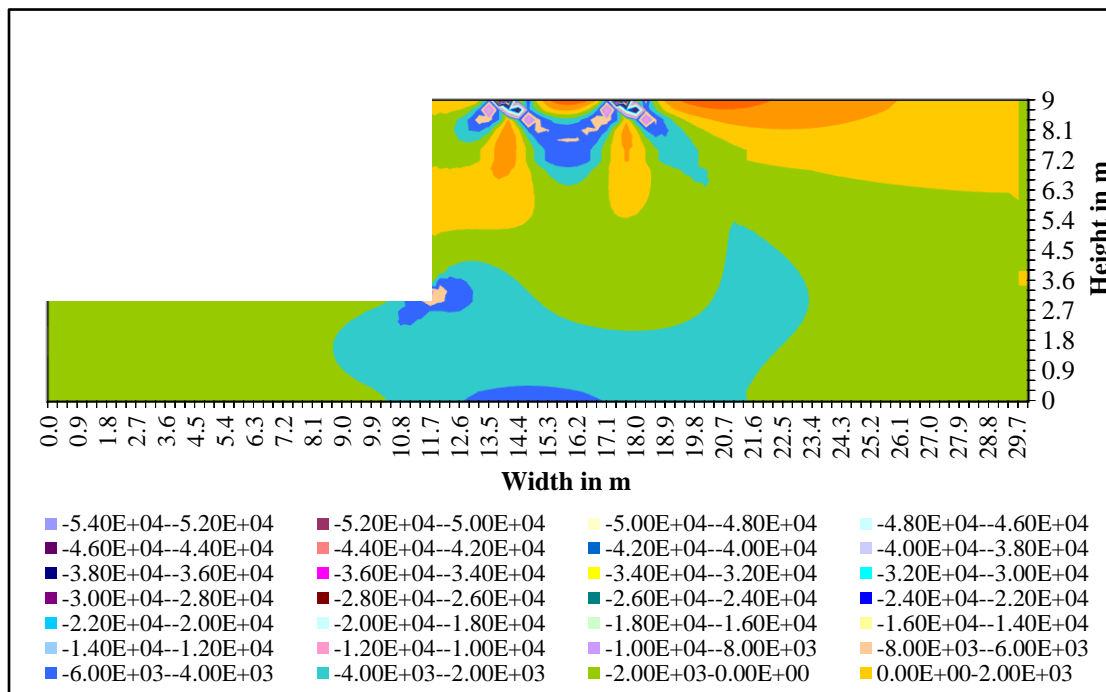


**Fig. 5.13 Horizontal Stresses (kPa) predicted in unreinforced soil retaining wall for Linear analysis under point loads obtained using RWPT-LIN**

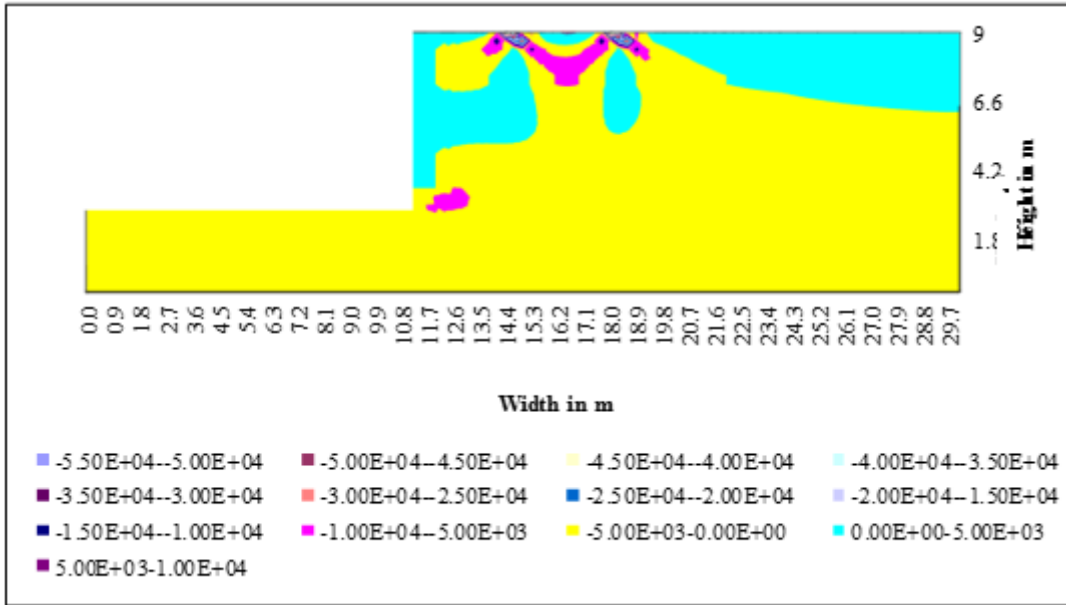


**Fig. 5.14 Horizontal Stresses (kPa) predicted in reinforced soil retaining wall for Linear analysis under point loads obtained using RWPT-LIN**

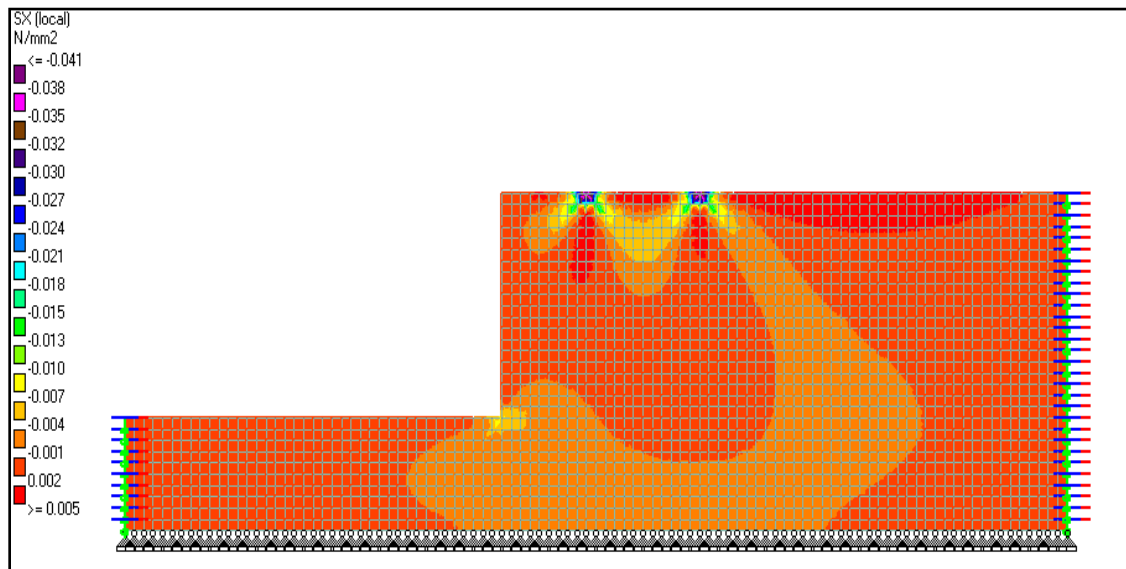


**Fig.5.15 Horizontal Stresses obtained in STAAD Pro for Linear analysis under point loads**

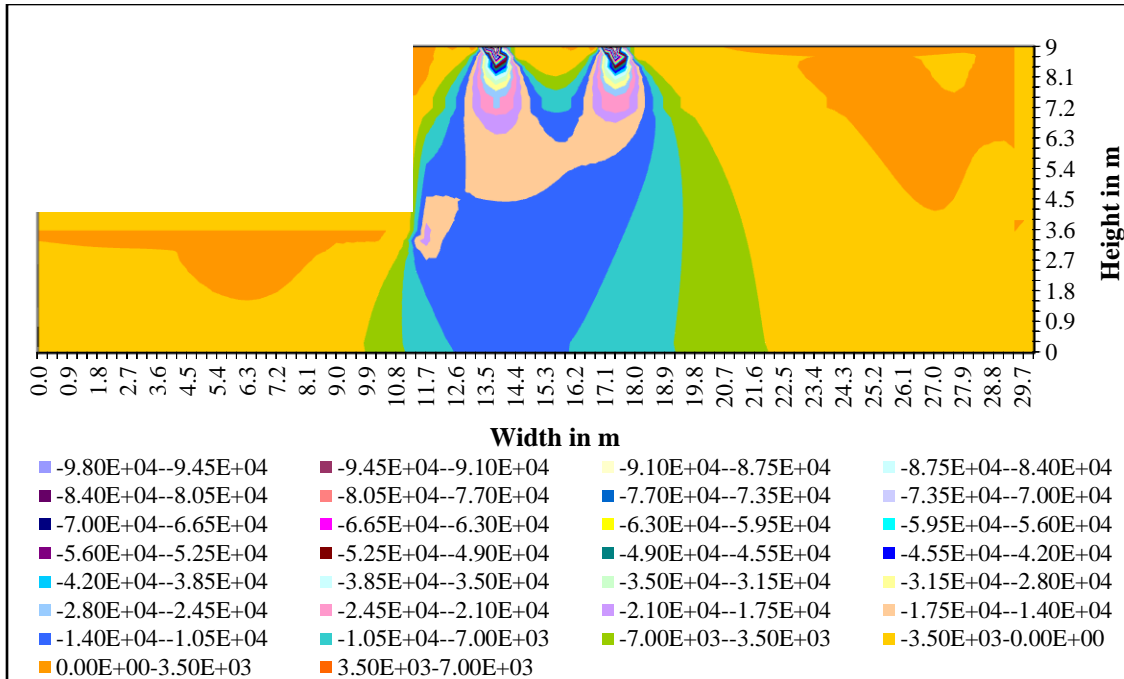


**Fig. 5.16 Vertical Stresses (kPa) predicted in unreinforced soil retaining wall for Linear analysis under point loads using RWPT-LIN**

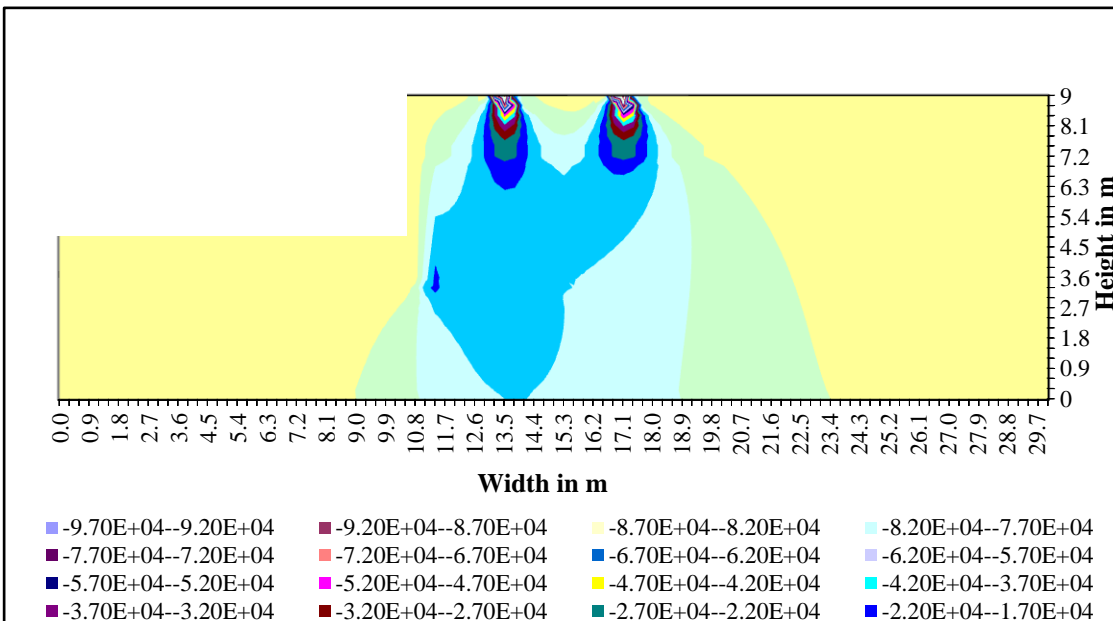


**Fig. 5.17 Vertical Stresses (kPa) in reinforced soil retaining wall for Linear analysis under point loads using RWPT-LIN**

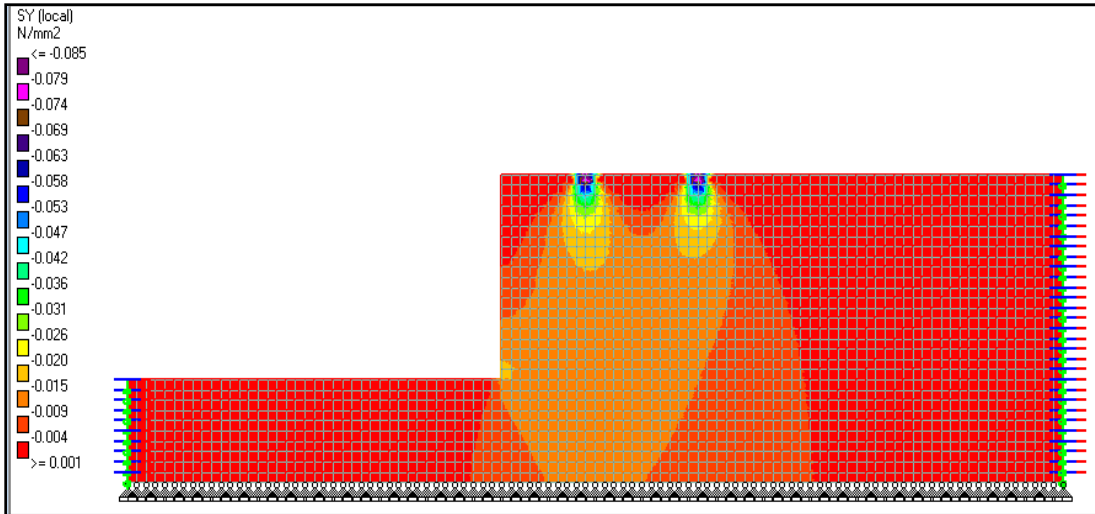


**Fig. 5.18 Vertical Stresses (MPa) for unreinforced soil retaining wall,  $E_s=12\text{MPa}$  obtained in STAAD Pro for Linear analysis under point loads**

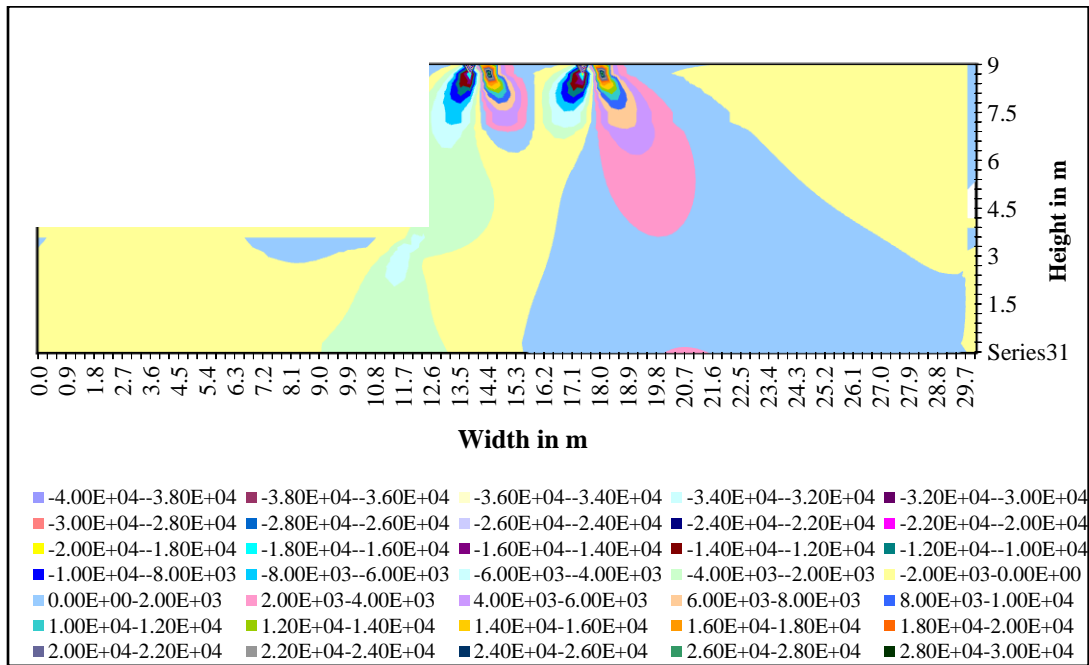


**Fig. 5.19 Shear Stresses (kPa) predicted in unreinforced soil retaining wall for Linear analysis under point Loads using RWPT-LIN**



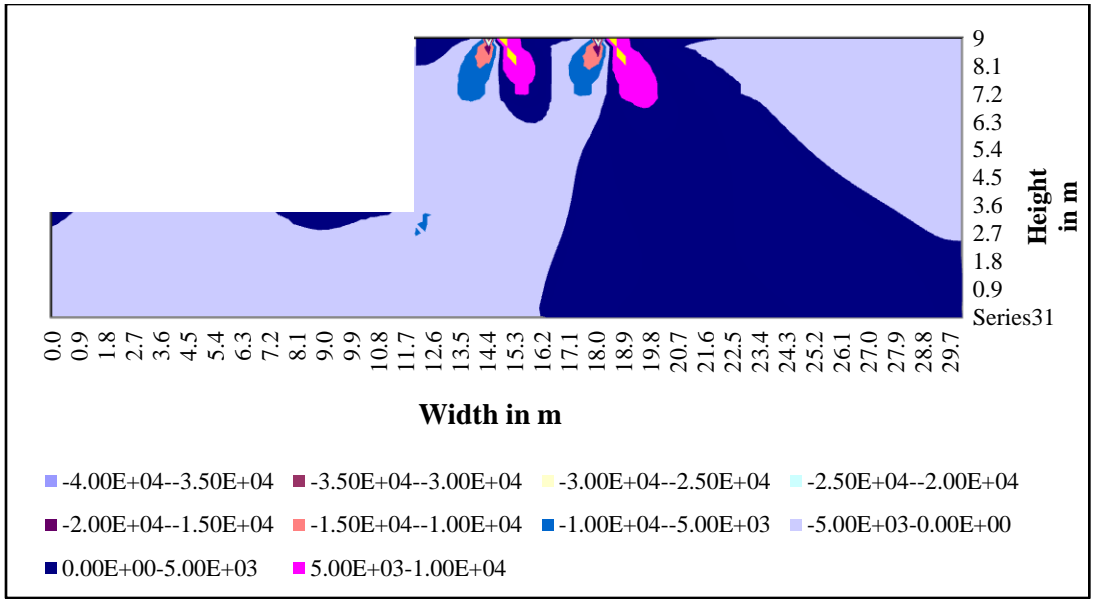


**Fig. 5.20 Shear Stresses (kPa) predicted in reinforced soil retaining wall for Linear analysis under point loads using RWPT-LIN**

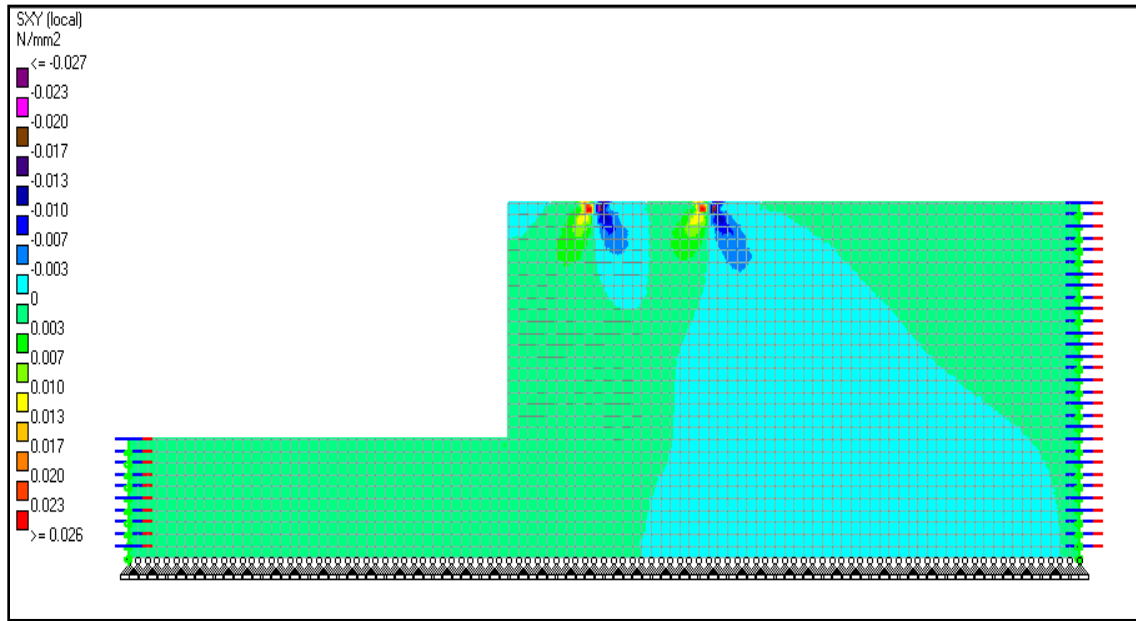


**Fig. 5.21 Shear stresses (MPa) in reinforced soil vertical cut for Linear analysis under point loads obtained in STAAD Pro**

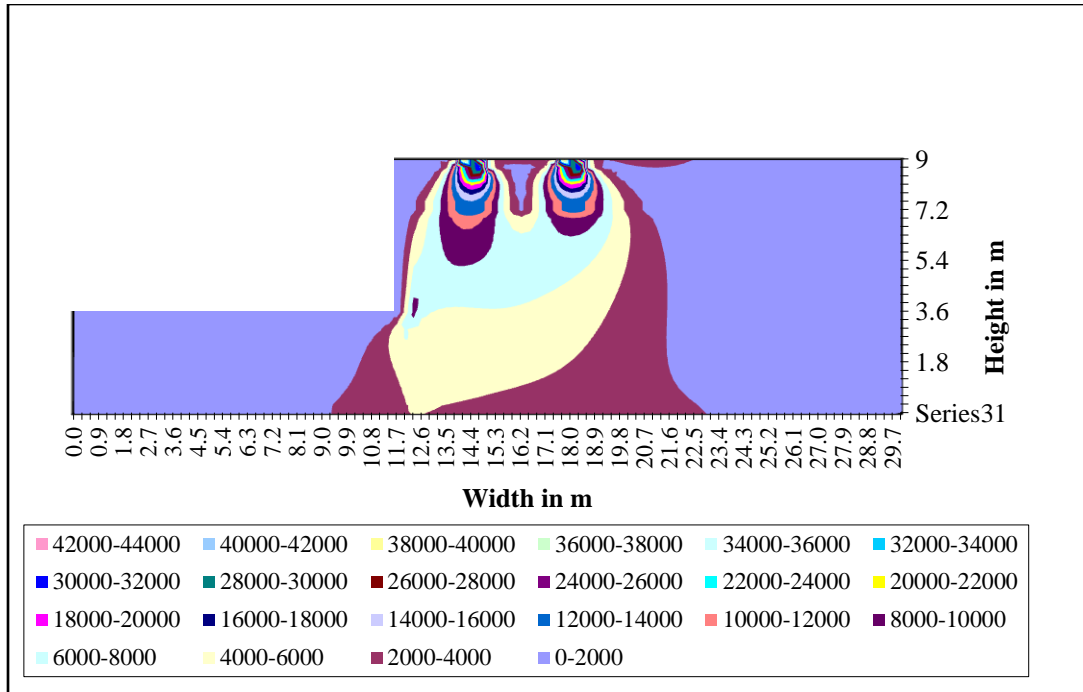


**Fig. 5.22 Maximum Shear Stresses (kPa) in reinforced soil retaining wall for Linear analysis under point loads**

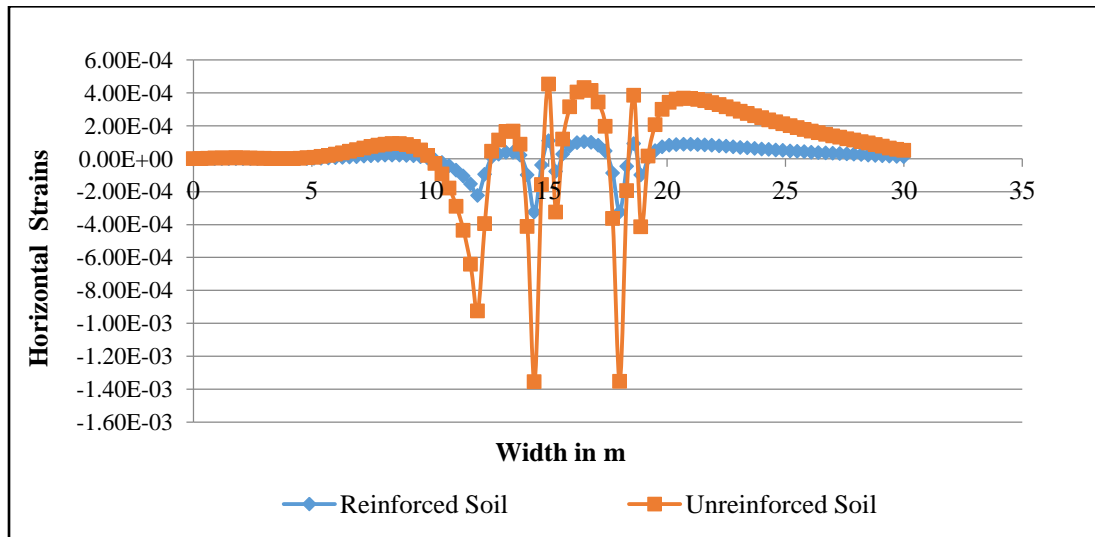


**Fig. 5.23 Horizontal Strains predicted at Y= 9.00m in a retaining wall for Linear analysis under point loads obtained using RWPT-LIN**

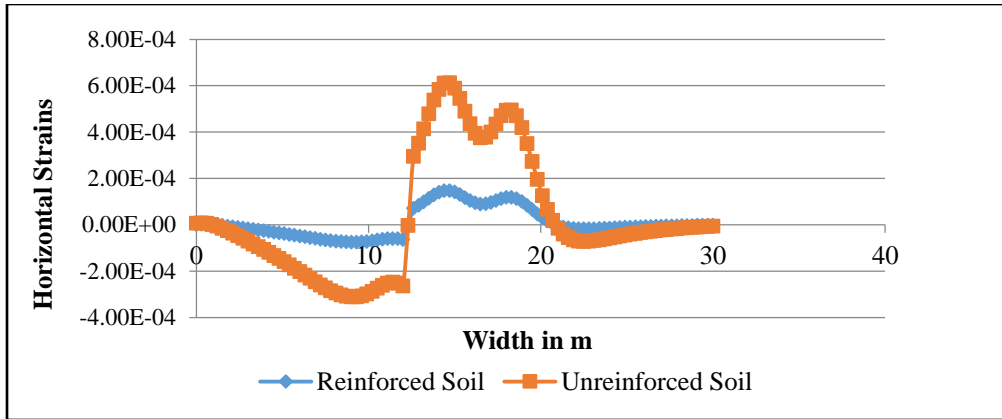


**Fig. 5.24 Horizontal Strains predicted at Y= 6.00m in a retaining wall for Linear analysis under point loads obtained using RWPT-LIN**

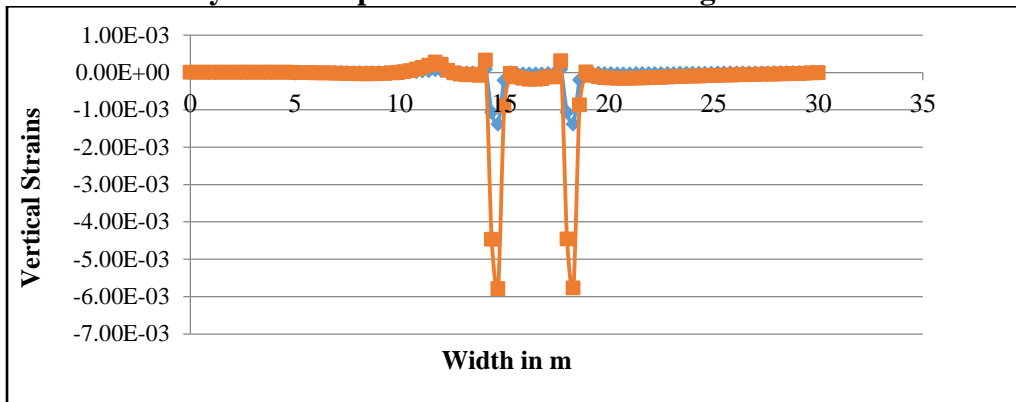


**Fig. 5.25 Vertical Strains predicted at Y=9.00m in a retaining wall for Linear analysis under point loads obtained using RWPT-LIN**

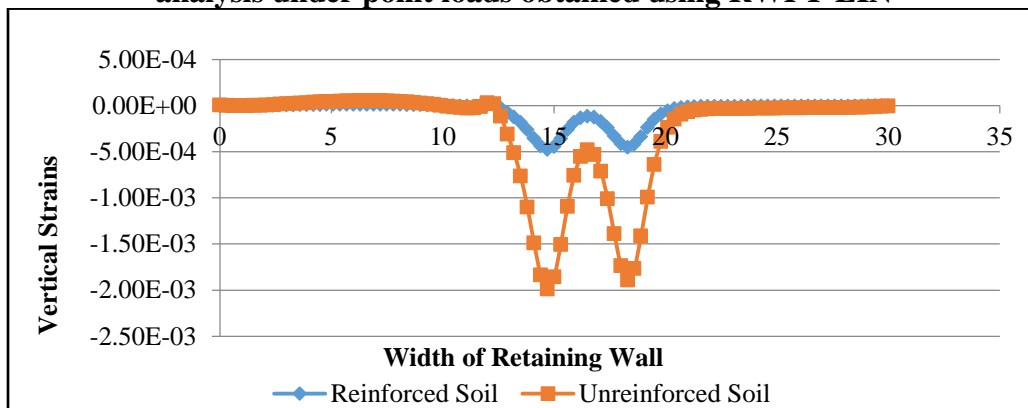


**Fig. 5.26 Vertical Strains predicted at Y=7.5m in a retaining wall for Linear analysis under point loads obtained using RWPT-LIN**

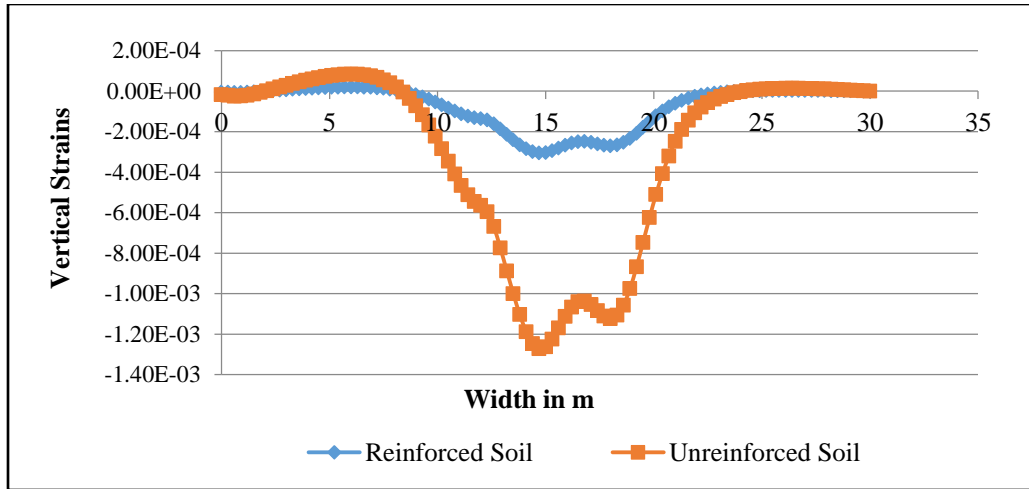


**Fig. 5.27 Vertical Strains predicted at Y=6.00m in a retaining wall for Linear analysis under point loads obtained using RWPT-LIN**

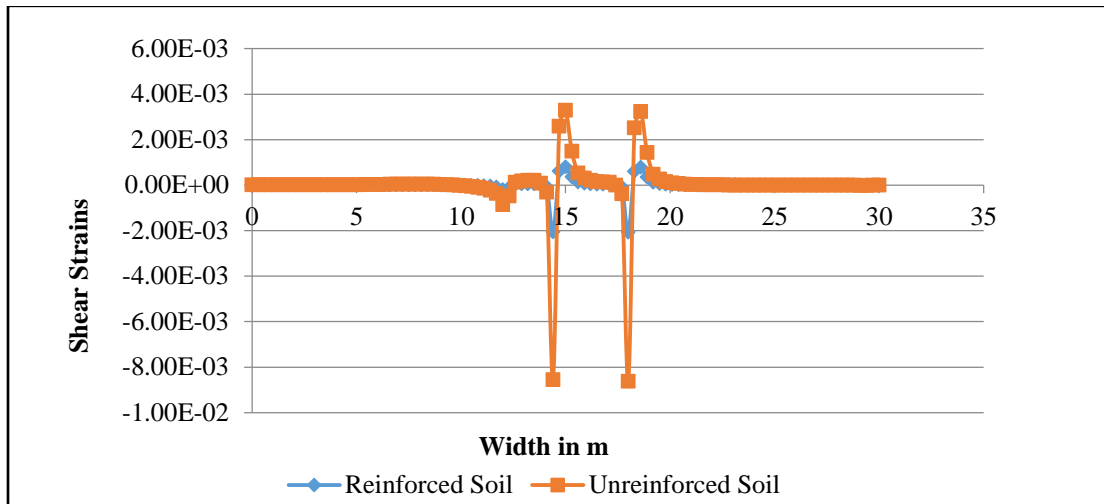


**Fig. 5.28 Shear Strains predicted at Y=9.00m in a retaining wall for Linear analysis under point loads obtained using RWPT-LIN**

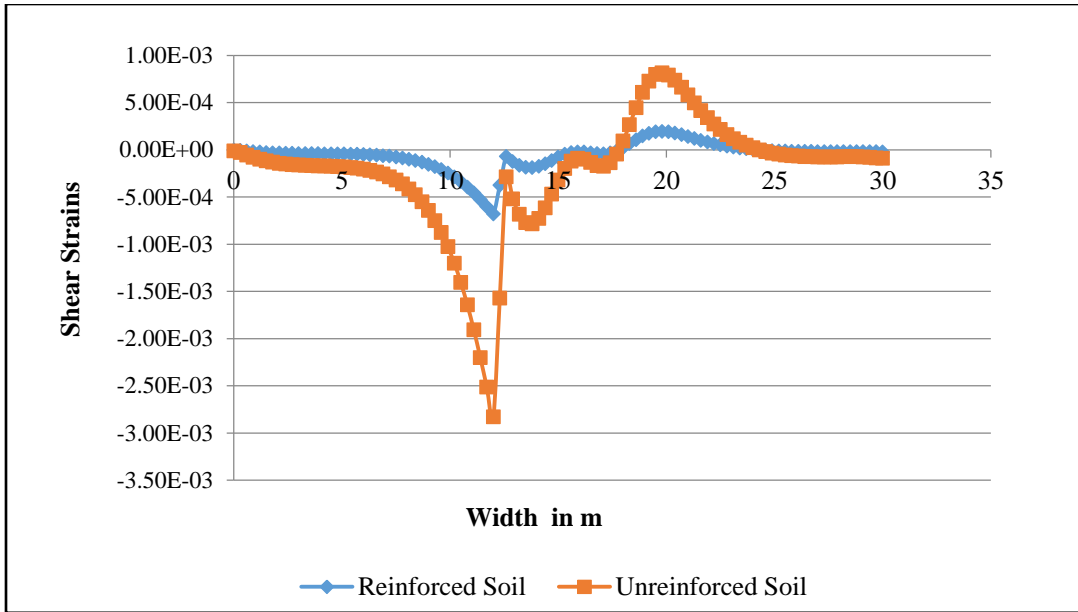


**Fig. 5.29 Shear Strains predicted at Y=6.00m in a retaining wall for Linear analysis under point loads obtained using RWPT-LIN**

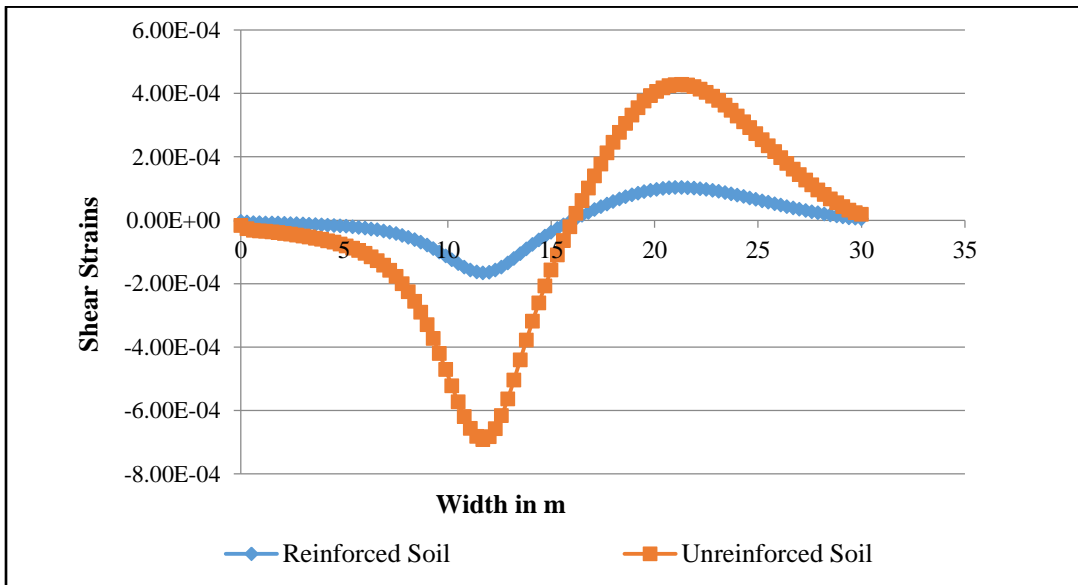


**Fig. 5.30 Shear Strains predicted at Y=0.3m in a retaining wall for Linear analysis under point loads obtained using RWPT-LIN**

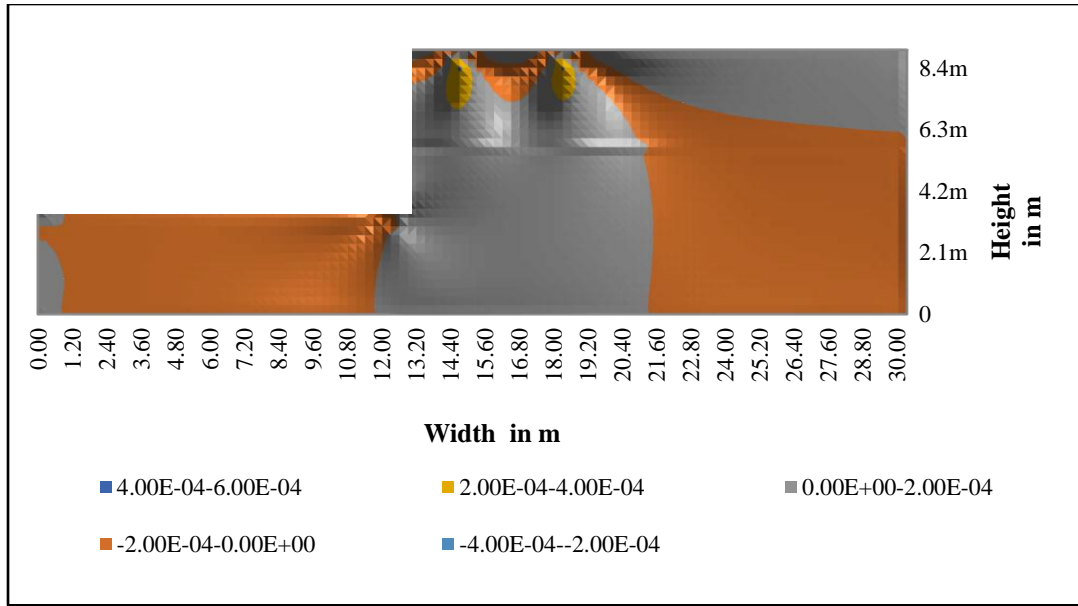


**Fig. 5.31** Horizontal strains predicted at all depths in a reinforced soil retaining wall for Linear analysis under point loads obtained using RWPT-LIN

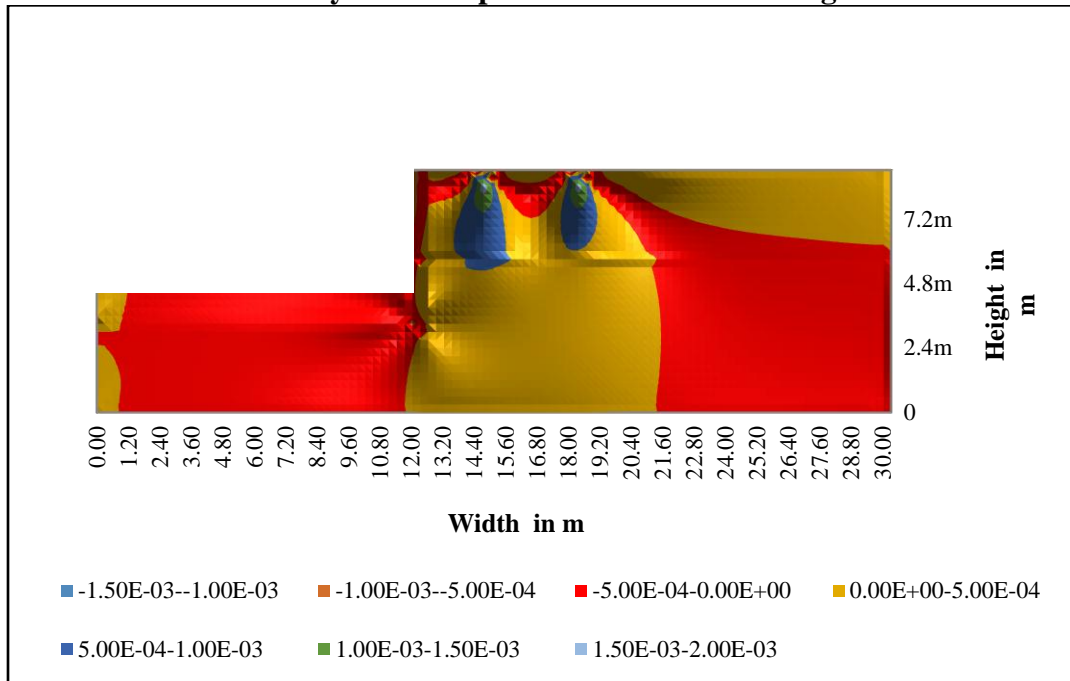


**Fig. 5.32** Horizontal strains predicted in an unreinforced soil retaining wall for Linear analysis under point loads obtained using RWPT-LIN

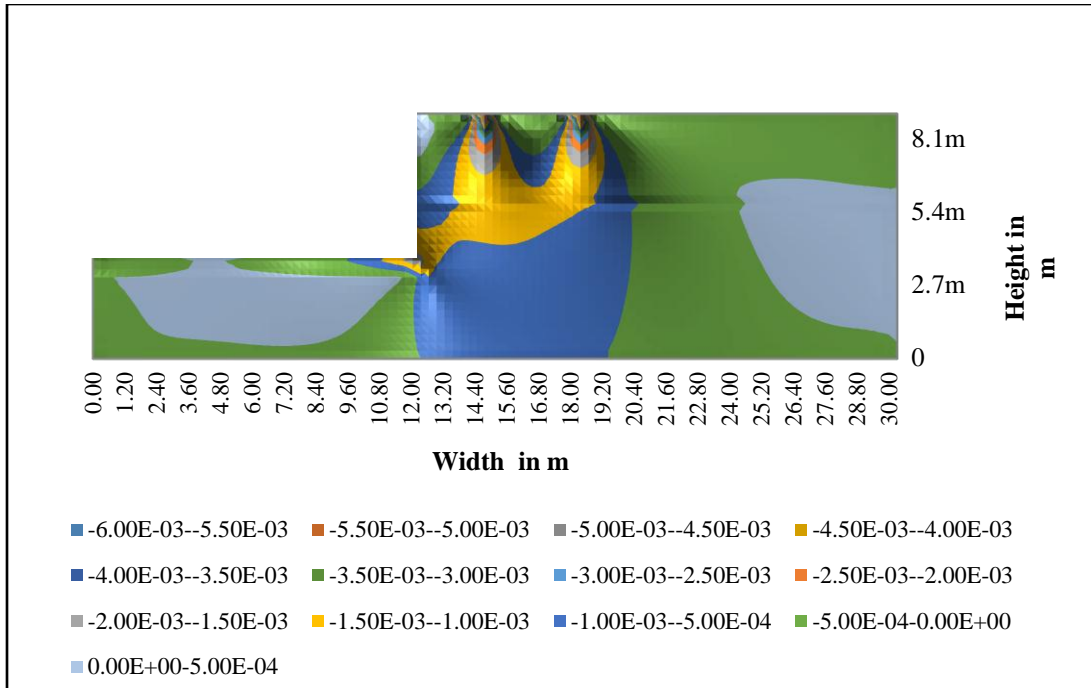


**Fig. 5.33 Vertical Strains predicted in an unreinforced soil retaining wall at all depths for Linear analysis under point loads obtained using RWPT-LIN**

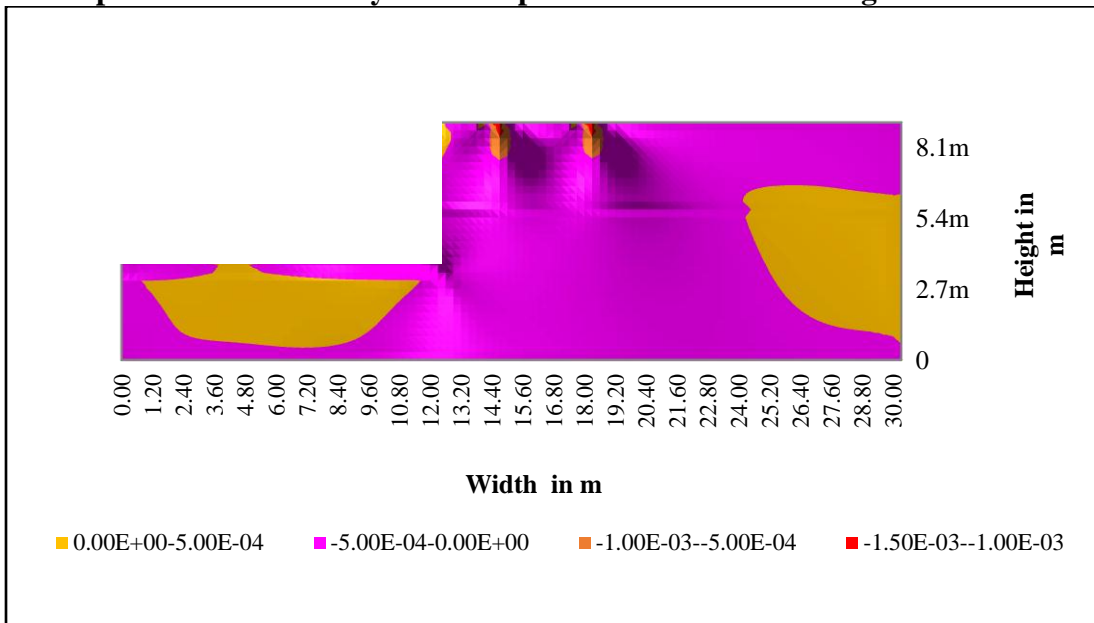


**Fig. 5.34 Vertical Strains predicted in a reinforced soil retaining wall for Linear analysis under point loads obtained using RWPT-LIN**

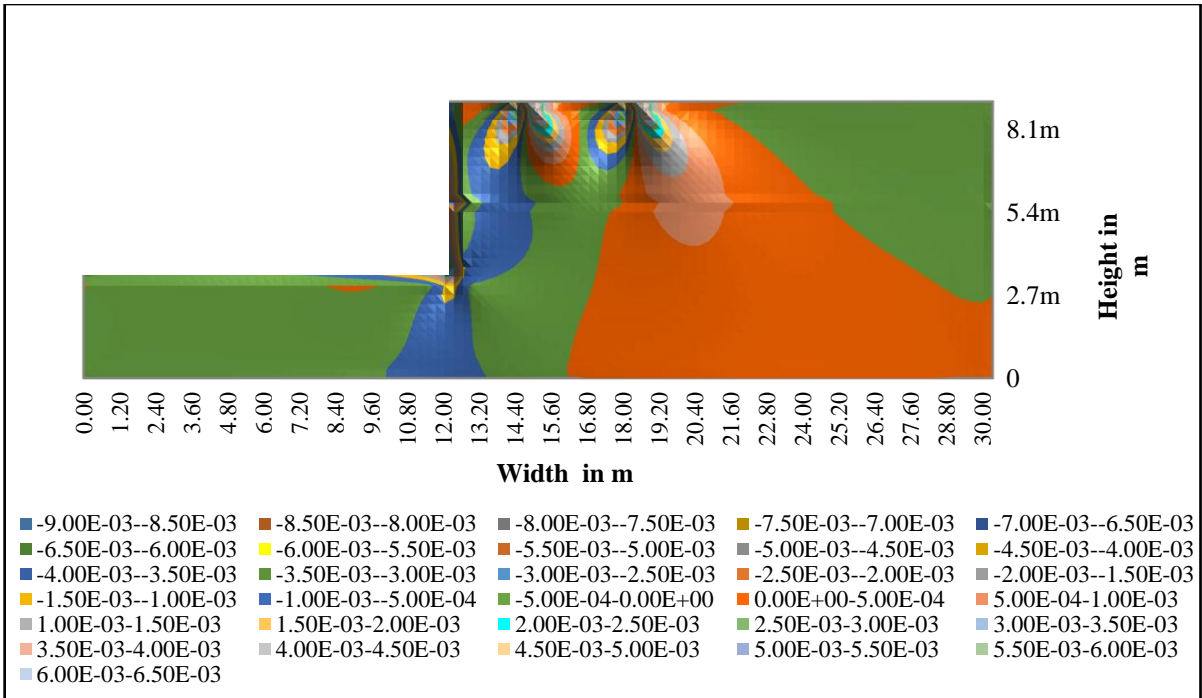


**Fig. 5.35 Shear strains predicted in an unreinforced soil retaining wall for Linear analysis under point loads obtained using RWPT-LIN**

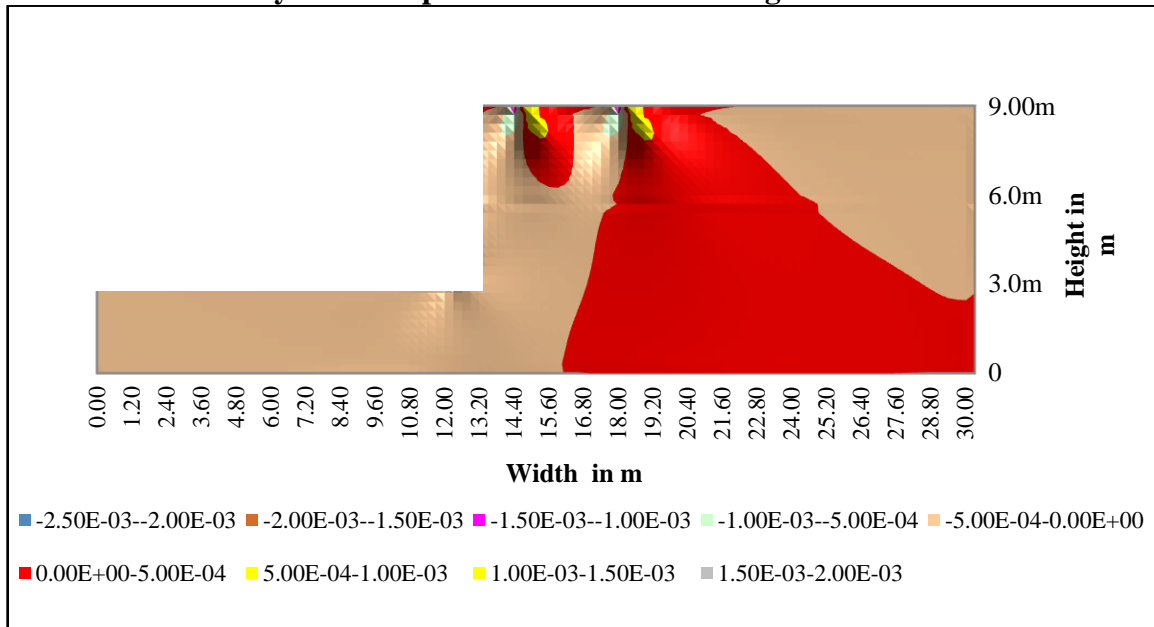


**Fig. 5.36 Shear Strains predicted in a reinforced soil retaining wall for Linear analysis under point loads obtained using RWPT-LIN**



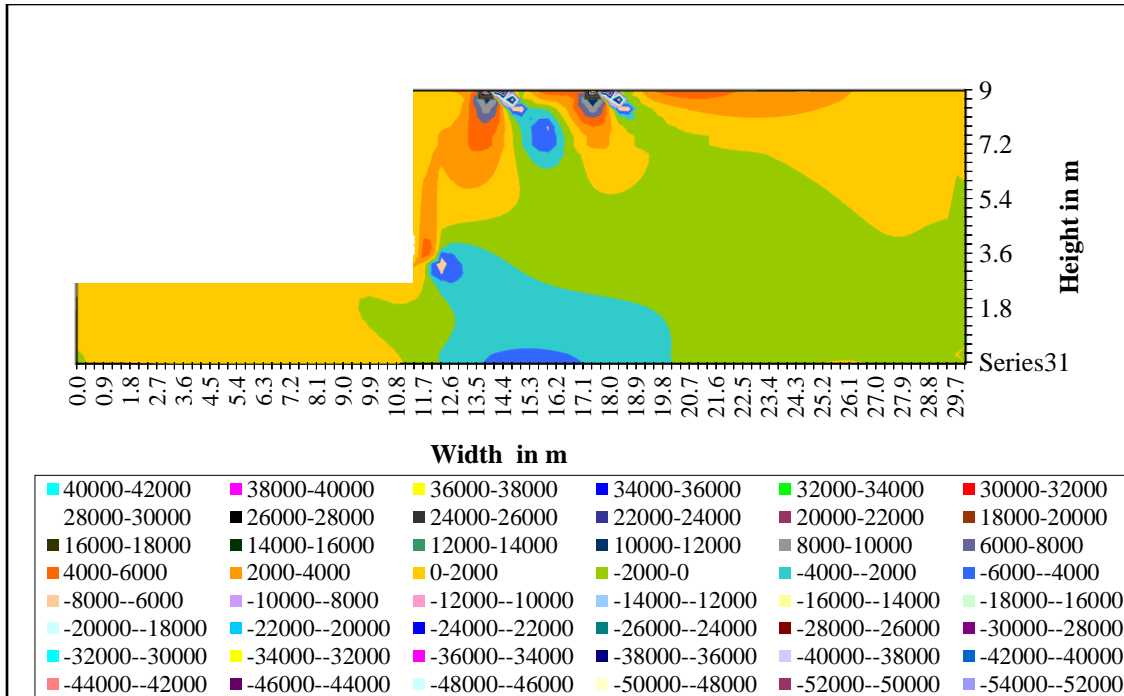


**Fig. 5.37 Major Principal Stresses (kPa) predicted in unreinforced soil retaining wall for Linear analysis under point loads using RWPT-LIN**

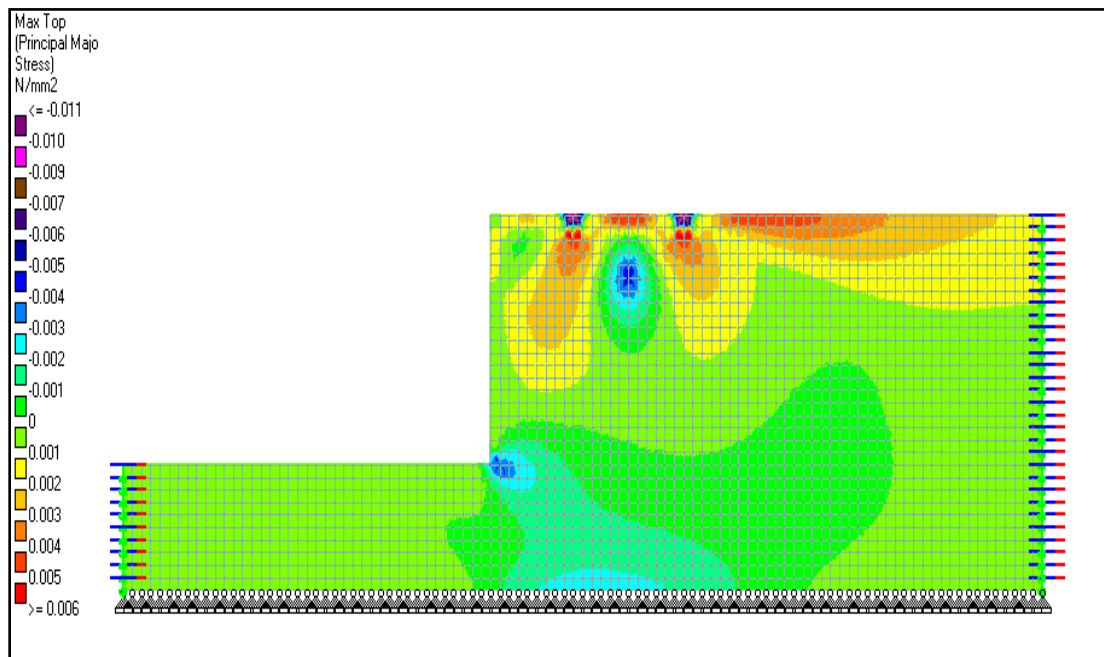


**Fig. 5.38 Major Principal Stresses (MPa) in unreinforced soil retaining wall in STAAD Pro under point loads for Linear analysis**

#### **5.4 FEM analysis and results of retaining wall under dead loads obtained using developed software RWSW-LIN and RWSW-INT**

Presently, unreinforced and reinforced soil retaining wall subjected to dead load of soil has been studied considering linear constitutive relations for both soil and reinforcement. The properties of reinforcement are adopted as mentioned in Table 5.1. presented in section 5.5 The soil was studied for varying stiffnesses of soil. The Young's modulus of soil was changed as 2.1MPa, 21MPa and 210MPa. The reinforced soil was also studied for 100% coupling and also by considering Goodman's interface element with varying tangential stiffness  $k_s$ . Different  $k_s/E_s$  values such as 100, 1000 and 10,000 were considered. The developed programme utilized for the reinforced soil retaining wall under self weight is similar to the code specified in Section 5.2. Subroutine dload is the additional subroutine used for this analysis. Refer Fig. 5.1b for the structural details of the structure used in the study. Though three lengths of reinforcement have been used for analysis, graphs plotted only for soil with Young's modulus of 21MPa and reinforcement length of 4.2m have been presented.

##### **5.4.1 Horizontal stresses in soil for different cases under dead loads**

Figures. 5.39 to 5.43 show the Horizontal stresses for unreinforced soil retaining wall, reinforced soil retaining wall (100% coupling) and reinforced soil retaining wall with Goodman's interface element for different  $k_s/E_s$  values ranging from 100,1000 and 10,000. The horizontal stresses are tensile for unreinforced and reinforced soil wall with 100% coupling. Refer Table 5.8 for the horizontal stresses. But the horizontal tensile stresses reduce in case of reinforced soil retaining wall with 100% coupling (from 73% to 900% at different locations). They tend to reverse their nature (change as compressive stresses) for reinforced soil wall with interface and are maximum for wall with  $k_s/E_s=10,000$ . The stress contours are not well oriented for unreinforced wall. They are well oriented for reinforced soil wall with and without interface. Hence reinforced soil wall shows improved performance. Table 5.4 presents the comparison of predicted horizontal stresses (kPa) between

unreinforced, reinforced (100% coupling) soil (RWSW-LIN), reinforced also considering different interfaces obtained using RWSW-INT

#### **5.4.2 Vertical Stresses in Soil for Different Cases under dead loads**

Figures. 5.44 to 5.48 show the vertical stresses for unreinforced soil retaining wall, reinforced soil retaining wall (100% coupling) and reinforced soil retaining wall with Goodman's interface element for different  $k_s/E_s$  values ranging from 100,1000 and 10,000. The vertical stresses are least for reinforced wall and slightly more for unreinforced soil retaining wall, both at different locations. Refer Table 5.9 for vertical stresses. The distribution of vertical stresses is uniform for reinforced soil retaining wall in comparison with unreinforced wall. The vertical stresses are more for reinforced soil retaining wall with interface elements and maximum for reinforced soil wall with interface and  $k_s/E_s=10,000$ . Hence reinforced soil retaining wall shows improved performance. Table 5.5 presents the comparison of predicted vertical stresses (kPa) between unreinforced, reinforced (100% coupling) soil (RWSW-LIN), and reinforced soil also considering different interfaces obtained using RWSW-INT

#### **5.4.3 Shear Stresses in Soil for Different Cases under dead loads**

Figures 5.49 to 5.53 show the variation of shear stresses for different cases of study. The shear stresses that develop on the failure surfaces are maximum for the unreinforced case. For the reinforced soil with 100% coupling (Fig. 5.55), the reduction in shear stresses when compared with the unreinforced case is 5 to 20 times. The shear stresses are maximum for unreinforced soil retaining wall. In the case of reinforced soil retaining wall with 100% coupling, they reduce in the vicinity of the reinforcement. They decrease further for the reinforced soil retaining wall with the interface elements for different values of  $k_s/E_s$ . At many locations, the predicted shear stresses are found to reverse their line of action in reinforced soil retaining wall with interface elements. They are least for reinforced soil retaining wall with interface values of  $k_s/E_s= 10+E04$ .

Table 5.6 presents the comparison of predicted shear stresses (kPa) between unreinforced, reinforced (100% coupling) soil (RWSW-LIN), reinforced also considering different interfaces obtained using RWSW-INT

#### **5.4.4 Strains in soil for Different Young's modulus of soil**

Table 5.7 presents the horizontal, vertical and shear strains predicted in unreinforced and reinforced soil retaining wall under self weight for different Young's modulus of soil using RWSW-LIN. It can be observed that the horizontal, vertical and shear strains reduce with the increase in the stiffness of the soil. More the stiffness of the soil lesser the strains.

#### **5.4.5 Maximum Shear Stresses for Different Cases**

Figures 5.54 to 5.58 show the variation of maximum shear stresses for different cases of study. For the reinforced soil with 100% coupling, the reduction in maximum shear stresses when compared with the unreinforced case is 5 to 20 times. The shear stresses that develop on the failure surfaces are maximum for the unreinforced case. The shear stresses are maximum for unreinforced soil retaining wall. In the case of reinforced soil retaining wall with 100% coupling, they reduce in the vicinity of the reinforcement. They decrease further for the reinforced soil retaining wall with the interface elements for different values of  $k_s/E_s$ . Though the range of maximum and minimum shear stresses are nearly same, the stress contours are different. They are the least for reinforced soil retaining wall with interface of  $k_s/E_s = 10+E04$ .

#### **5.4.6 Major Principal Stresses in Soil for Different Cases**

Figures 5.59 to 5.63 show the major principal stresses for unreinforced soil retaining wall, reinforced soil retaining wall (100% coupling) and reinforced soil retaining wall with Goodman's interface element for different  $k_s/E_s$  values ranging from 100,

1000 and 10,000. The major principal stresses have least values and maximum stresses for reinforced soil wall with interface ratio of  $k_s/E_s=10,000$ . The stress contours are not well oriented for unreinforced wall. They are well oriented for reinforced soil wall with interface and  $k_s/E_s=10,000$ . Hence reinforced soil wall shows improved performance.

#### **5.4.7 Settlements and Displacements in Soil for Different Cases**

Figures 5.64 and 5.65 indicate the horizontal and vertical displacements for unreinforced, reinforced soil wall with 100% coupling and reinforced soil wall for different interface stiffnesses. The horizontal displacements are maximum for unreinforced soil. The horizontal displacements are least for the reinforced soil with 100% coupling and the length of the reinforcement is 4.2m (0.7 times the height of wall  $h$ ). The displacements for soil with reinforcement provided with an interface element for  $k_s/E_s=10+E04$  and  $k_s/E_s=10+E03$  are more realistic and practical as is proved in further chapters in this thesis. The vertical displacements are maximum for the unreinforced soil. They are least for the reinforced soil.

Section 5.4.8 presents the predicted results of retaining wall under dead loads (self weight) using RWSW-LIN and RWSW-INT. Section 5.4.8.1 presents the predicted plot of horizontal stresses of retaining wall under dead loads (self weight) using RWSW-LIN and RWSW-INT. Section 5.4.8.2 presents the predicted plot of vertical stresses of retaining wall under dead loads (self weight) using RWSW-LIN and RWSW-INT. Section 5.4.8.3 presents the predicted plot of shear stresses of retaining wall under dead loads (self weight) using RWSW-LIN and RWSW-INT. Section 5.4.8.4 presents the predicted plot of major principal stresses of retaining wall under dead loads (self weight) using RWSW-LIN and RWSW-INT. Section 5.4.8.5 presents the predicted plot of horizontal stresses of retaining wall under dead loads (self weight) using RWSW-LIN and RWSW-INT.

Table 5.8 (Section 5.5) presents the predicted horizontal displacements (m) and vertical settlements (m) for unreinforced and reinforced soil retaining wall under self weight for different Young's modulus of Soil. Table 5.9 presents the predicted

horizontal displacements (m) and vertical settlements (m) for unreinforced and reinforced soil retaining wall under self weight for different Young's modulus of soil at  $y=9.00\text{m}$

The various tables used and the results obtained from the developed software have been tabulated in Section 5.5.

## 5.4.8 Fem Analysis & Results of Retaining Wall under Dead Loads (Self Weight)

### 5.4.8.1 Horizontal Stresses in Soil for Different Cases

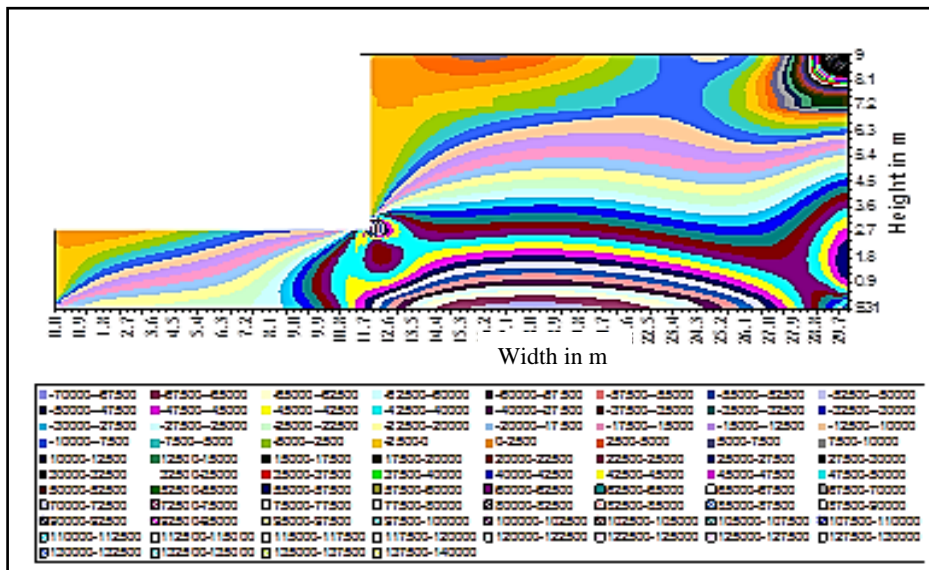


Fig. 5.39 Horizontal Stresses (kPa) predicted in unreinforced soil retaining wall for Linear analysis under self-weight,  $E_s = 21\text{MPa}$  obtained using RWSW-LIN

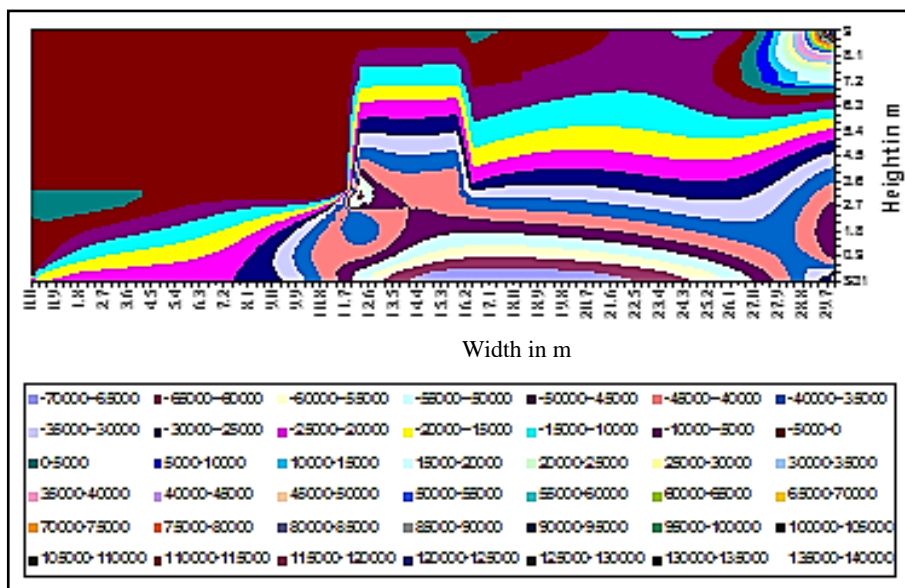
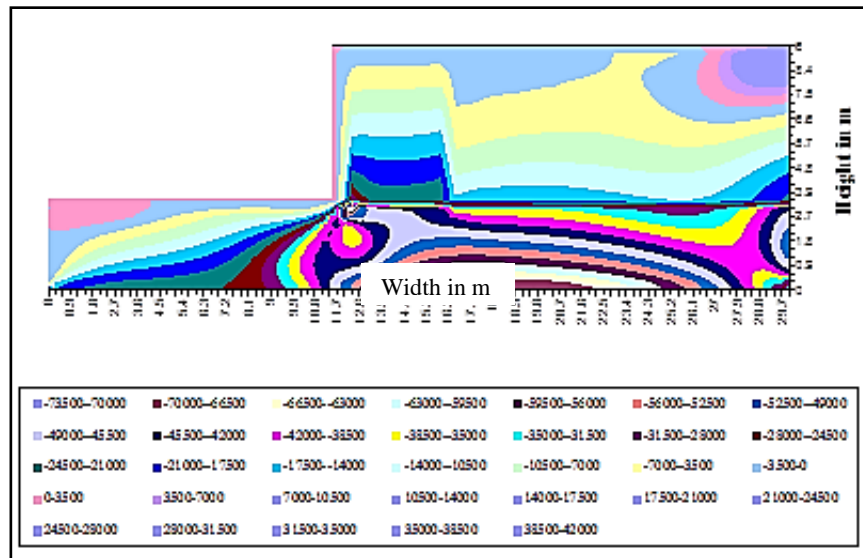
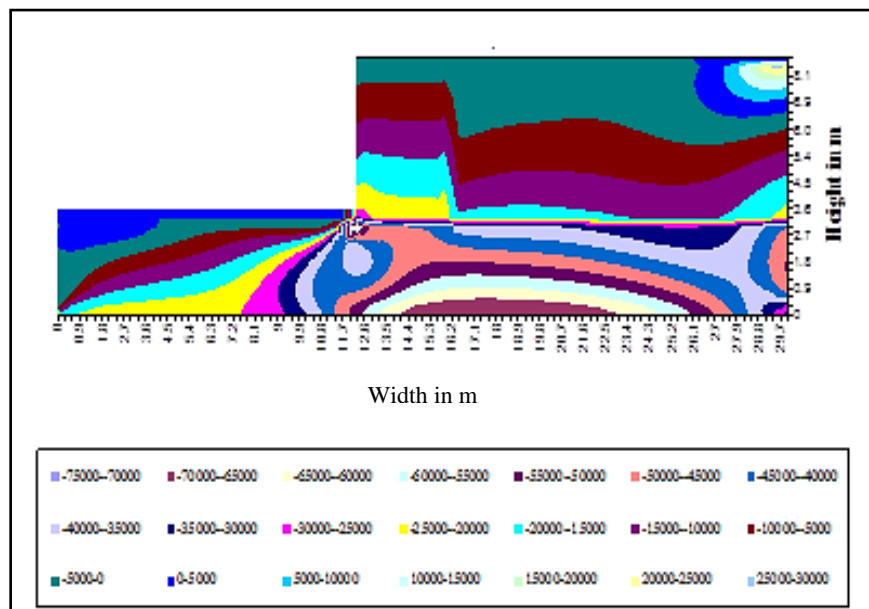


Fig. 5.40 Horizontal Stresses (kPa) predicted in reinforced soil retaining wall for Linear analysis under self-weight for  $E_s/E_r = 0.001$ , 100% Coupling obtained using RWSW-LIN



**Fig. 5.41** Horizontal Stresses (kPa) predicted in reinforced soil retaining wall for Linear analysis under self weight, for  $E_s/E_r = 0.001$ ,  $k_s/E_s = 10+E02$  obtained using RWSW-INT



**Fig. 5.42** Horizontal Stresses (kPa) predicted in reinforced soil retaining wall for Linear analysis under self weight for  $E_s/E_r = 0.001$ ,  $k_s/E_s = 10+E03$  obtained using RWSW-INT



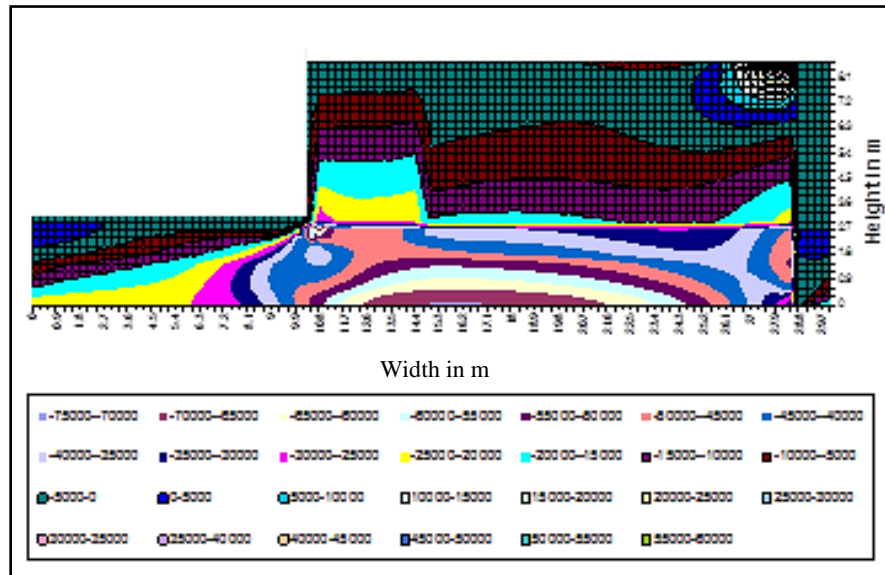


Fig. 5.43 Horizontal Stresses (kPa) predicted in reinforced soil retaining wall for Linear analysis under self weight for  $E_s/E_r= 0.001$ ,  $k_s/E_s=10+E04$  obtained using RWSW-INT

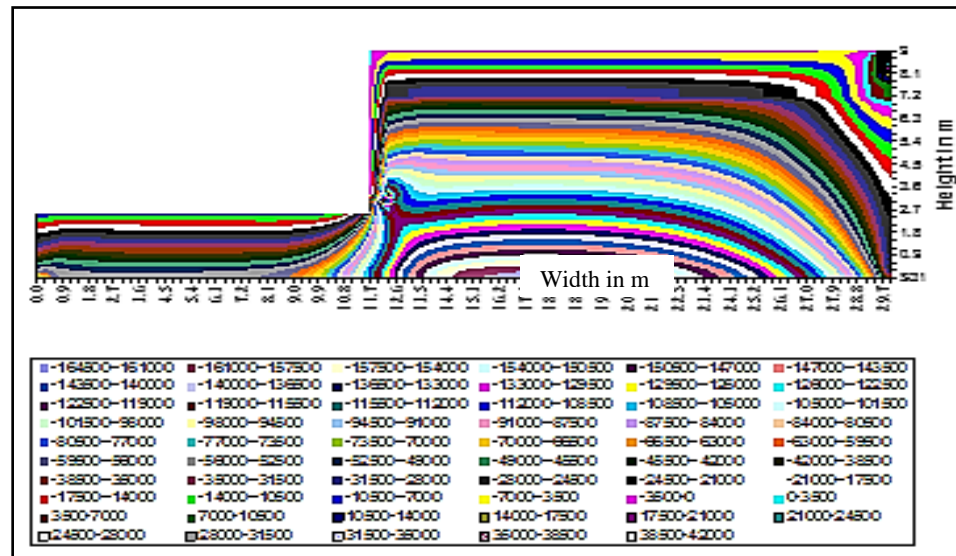


Fig. 5.44 Vertical stresses (kPa) predicted in unreinforced soil retaining wall for Linear analysis under self weight for  $E_s=21\text{MPa}$  using RWSW-LIN

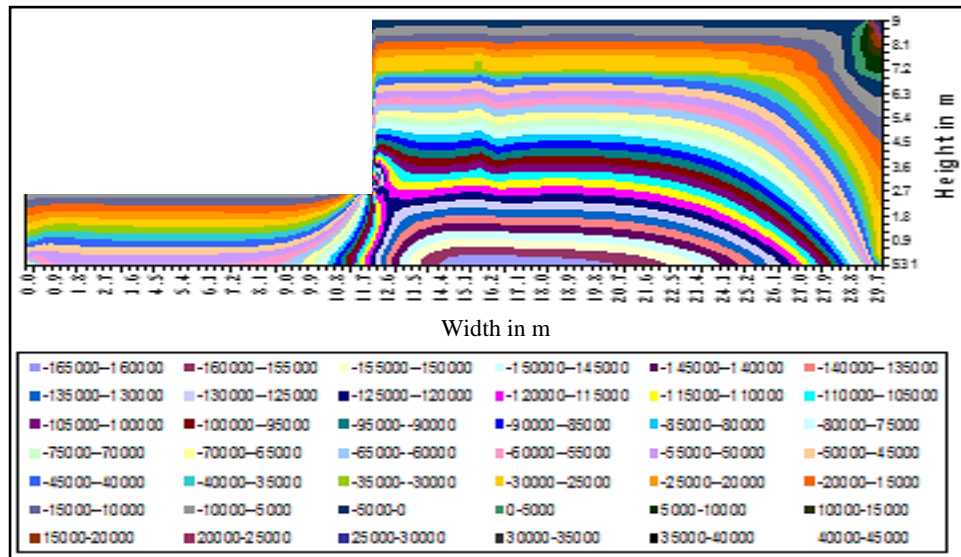


Fig. 5.45 Vertical stresses (kPa) predicted in reinforced soil retaining wall under self weight for Linear analysis for  $E_s/E_r=0.001$ , 100% Coupling obtained using RWSW-LIN

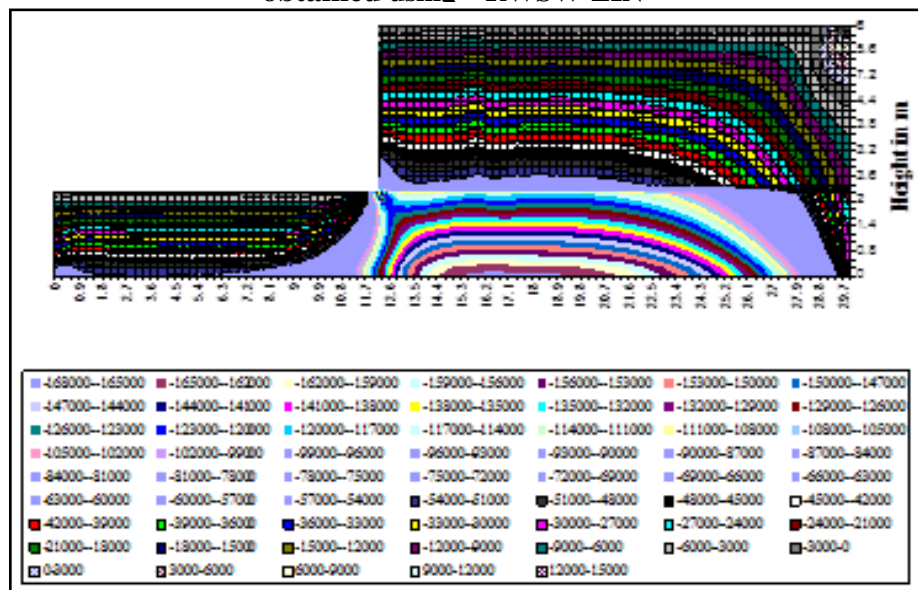


Fig. 5.46 Vertical stresses (kPa) predicted in reinforced soil retaining wall under self weight for Linear analysis under self weight for  $E_s/E_r=0.001$ ,  $k_s/E_s=10+E_2$  obtained using RWSW-INT

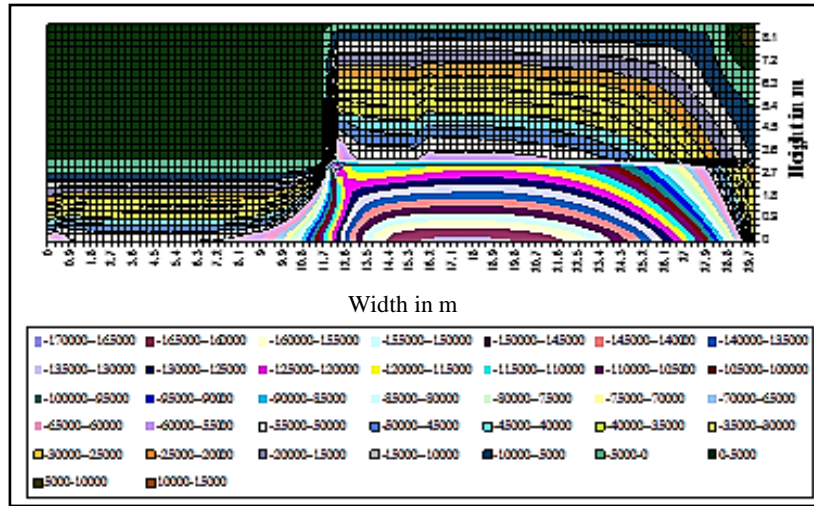


Fig.5.47 Vertical stresses (kPa) predicted in reinforced soil retaining wall under self weight for Linear analysis for  $E_s/E_r=0.001$ ,  $k_s/E_s=10+E03$  obtained using RWSW-INT

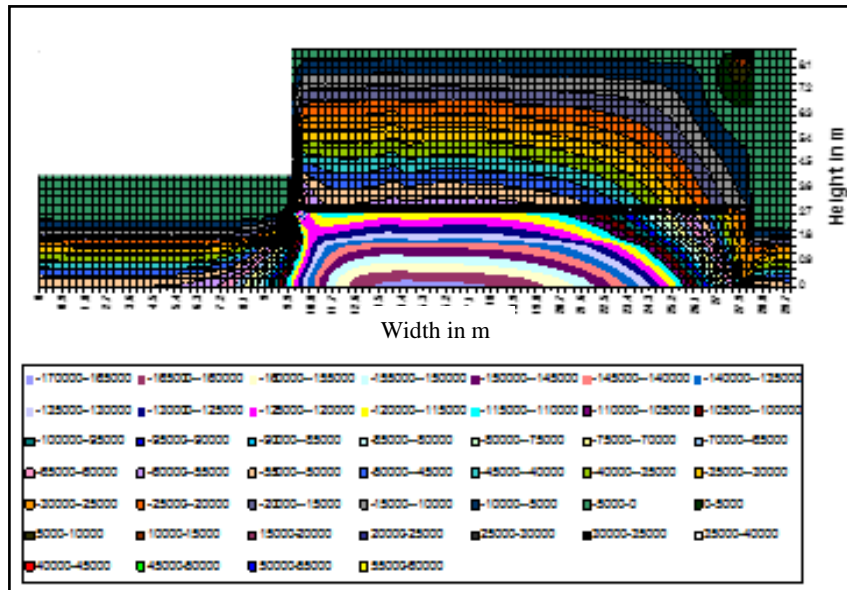
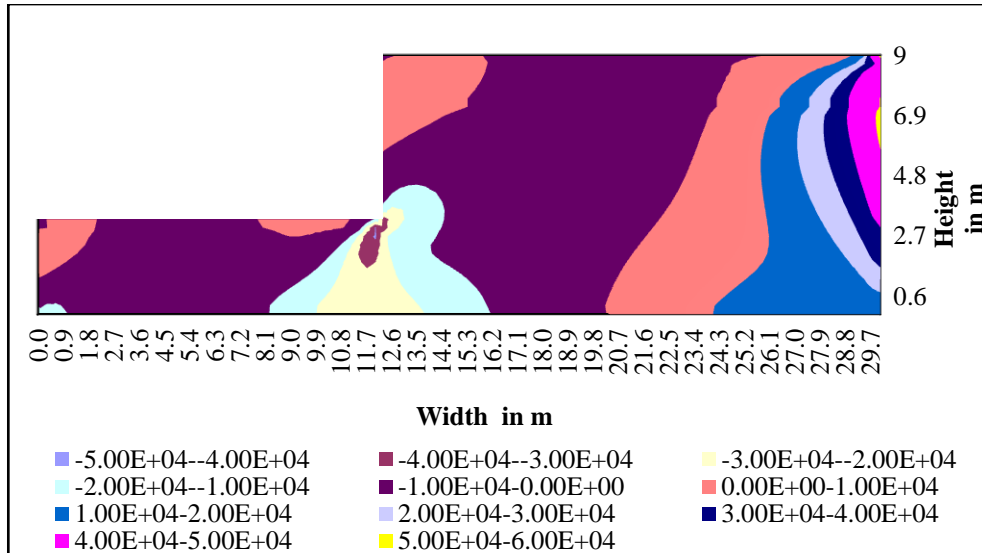
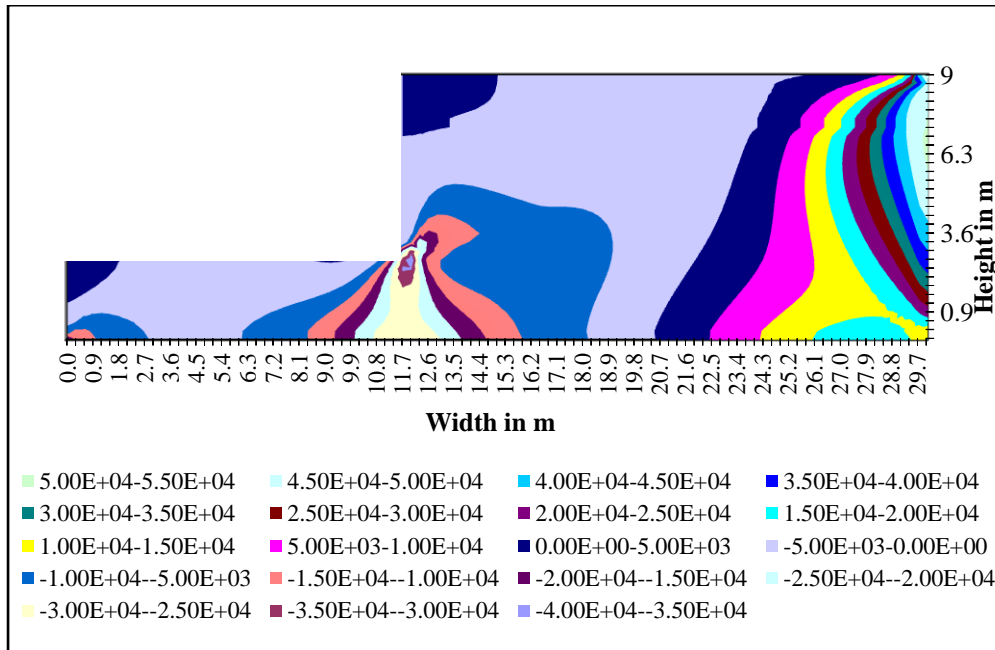


Fig. 5.48 Vertical stresses (kPa) predicted in reinforced soil retaining wall under self weight for Linear analysis for  $E_s/E_r=0.001$ ,  $k_s/E_s=10+E04$  obtained using RWSW-INT

### 5.4.8.3 Shear Stresses in Soil for Different Cases



**Fig. 5.49 Shear stresses (kPa) predicted in unreinforced soil retaining wall under self weight for Linear analysis for  $E_s=21$  MPa obtained using RWSW-LIN**



**Fig. 5.50 Shear stresses (kPa) predicted in reinforced soil retaining wall for Linear analysis under self weight for  $E_s/E_r=0.001$ , 100% coupling using RWSW-LIN**

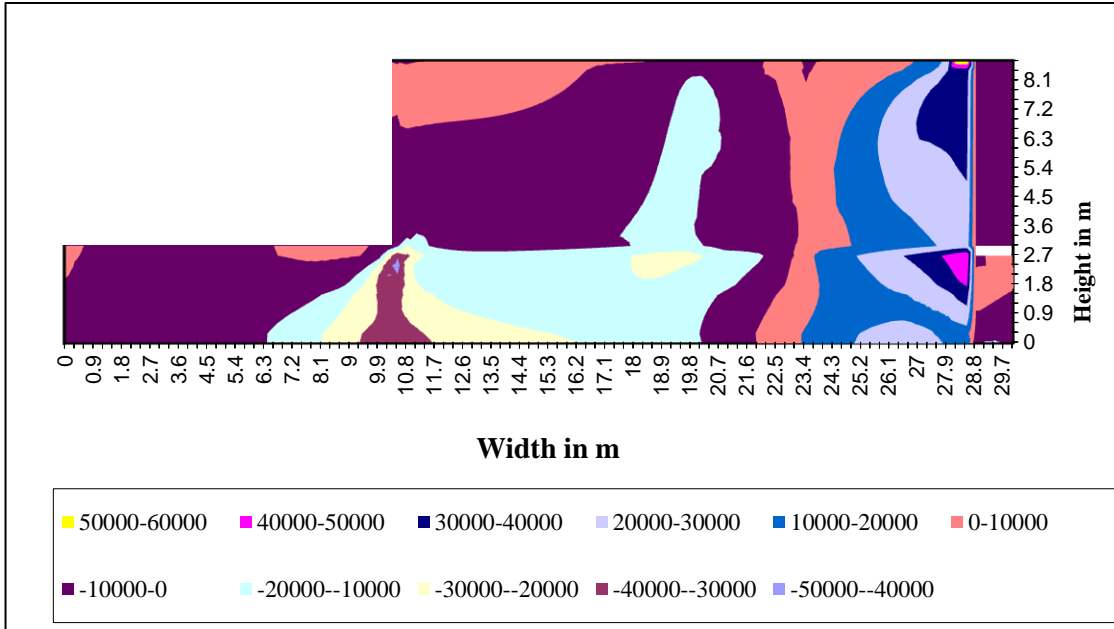


**Fig. 5.51 Shear stresses (kPa) predicted in reinforced soil retaining wall for Linear analysis under self weight for  $E_s/E_r=0.001$  and interface  $K_s/E_s=10+E02$  obtained using RSW-INT**

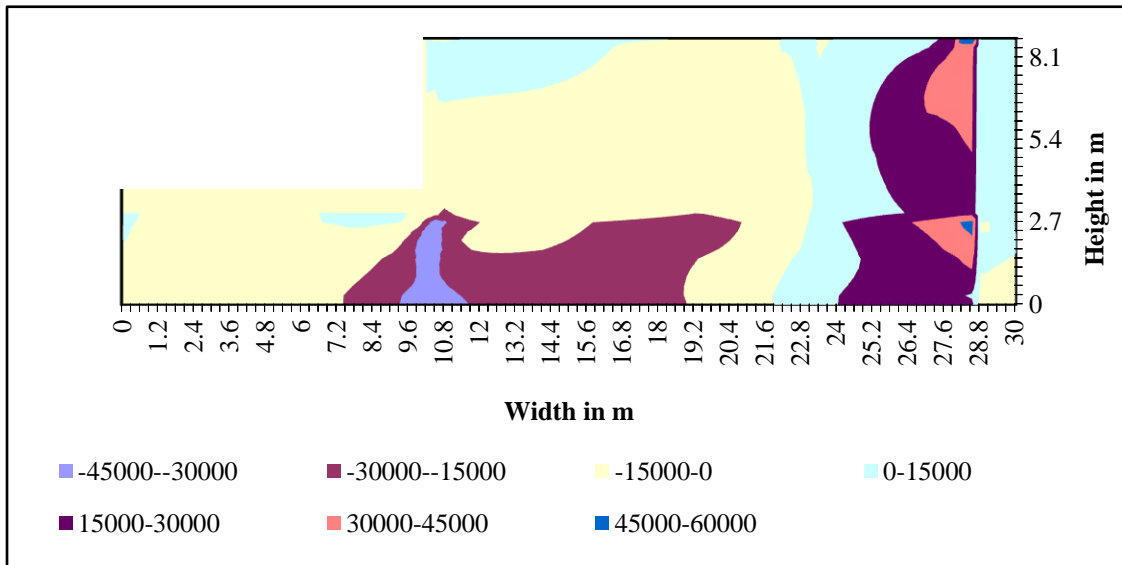


**Fig.5.52 Shear stresses (kPa) predicted in reinforced soil retaining wall for Linear analysis under self weight for  $E_s/E_r=0.001$ ,  $k_s/E_s=10+E03$  obtained using RSW-INT**

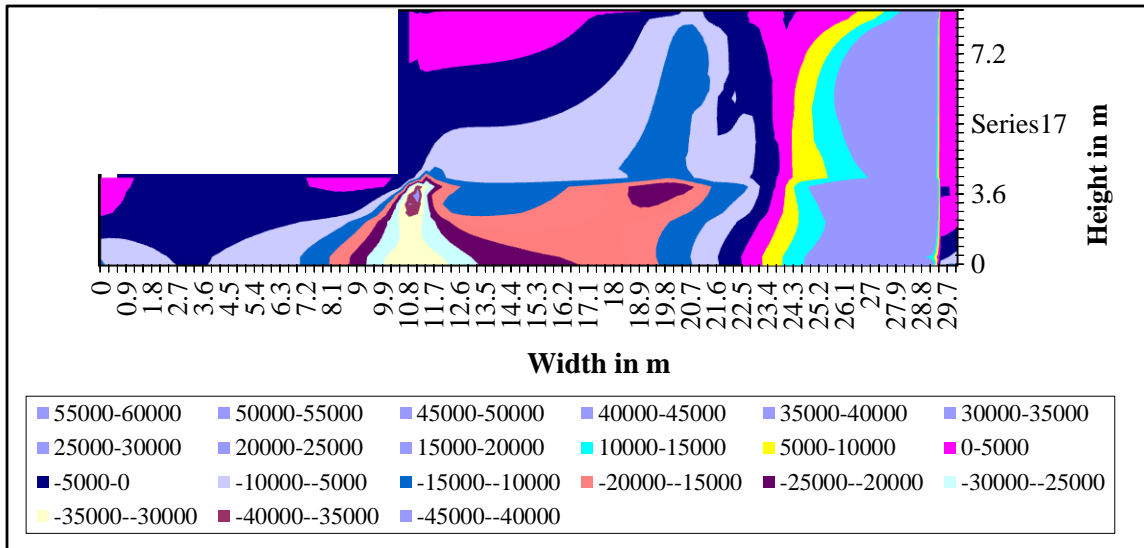


**Fig.5.53 Shear stresses (kPa) predicted in reinforced soil retaining wall under self weight for Linear analysis for  $E_s/E_r=0.001$ ,  $k_s/E_s=10+E04$  obtained using RWSW-INT**

#### 5.4.8.4 Maximum Shear Stresses in Soil for Different Cases

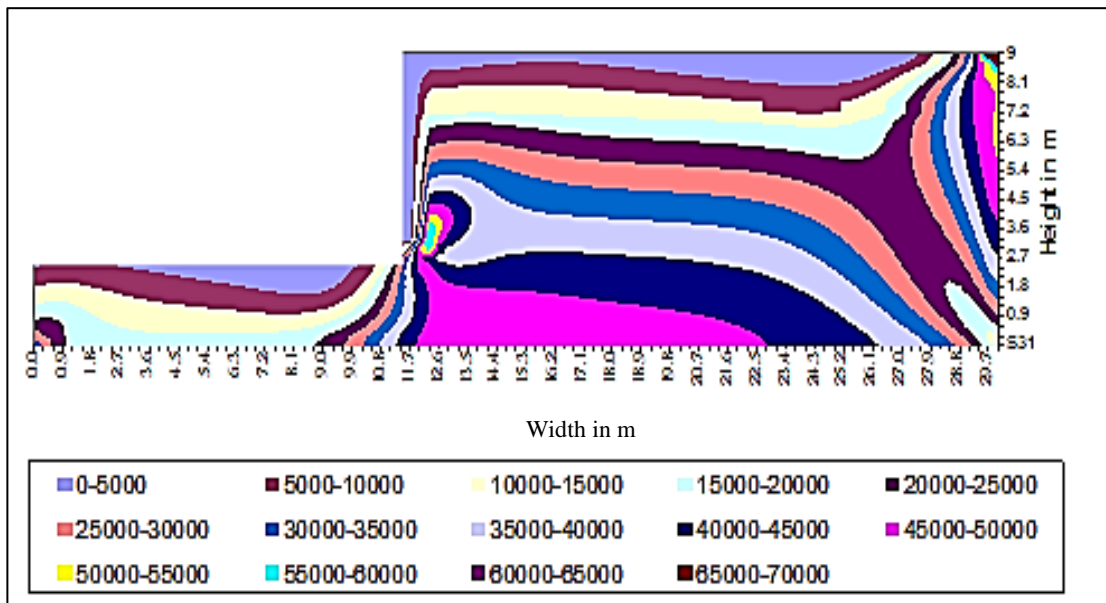


**Fig. 5.54 Maximum Shear stresses (kPa) predicted in unreinforced soil retaining wall for Linear analysis under self weight for  $E_s=21\text{MPa}$  obtained using RWSW-LIN**

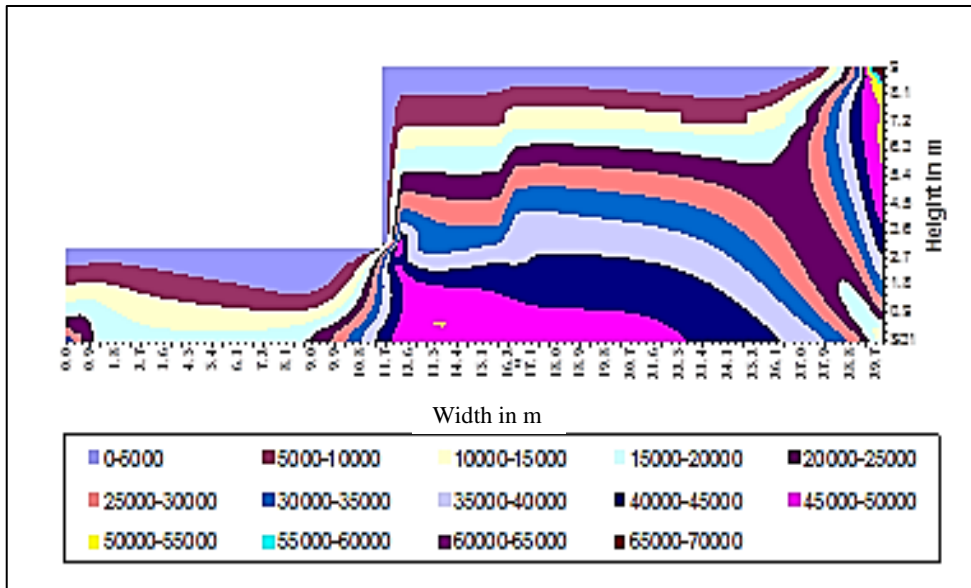


**Fig. 5.55 Maximum Shear stresses (kPa) predicted in reinforced soil retaining wall for Linear analysis under self weight for  $E_s/E_r=0.001$  and 100% Coupling obtained using RSW-LIN**

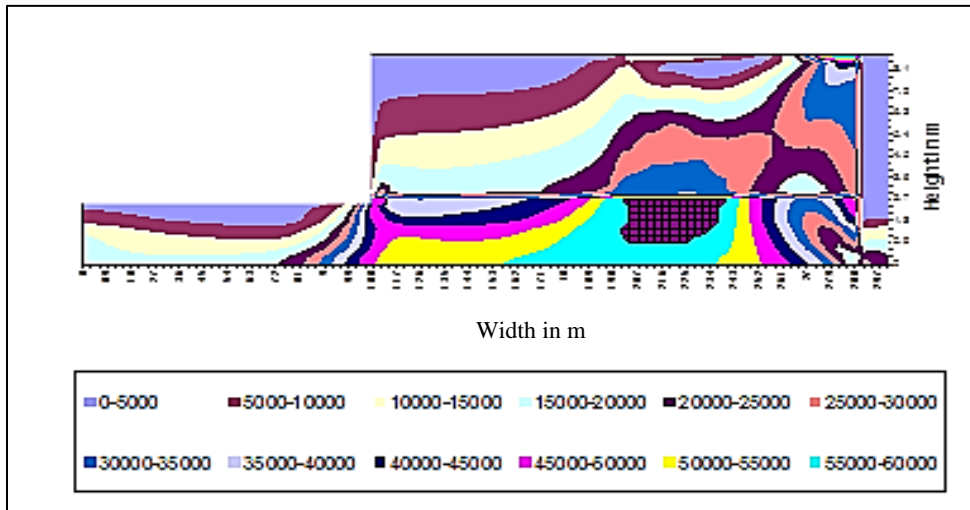


**Fig.5.56 Maximum Shear stresses (kPa) predicted in reinforced soil retaining wall for Linear analysis under self weight for  $E_s/E_r=0.001$ ,  $k_s/E_s=10+E02$  obtained using RSW-INT**



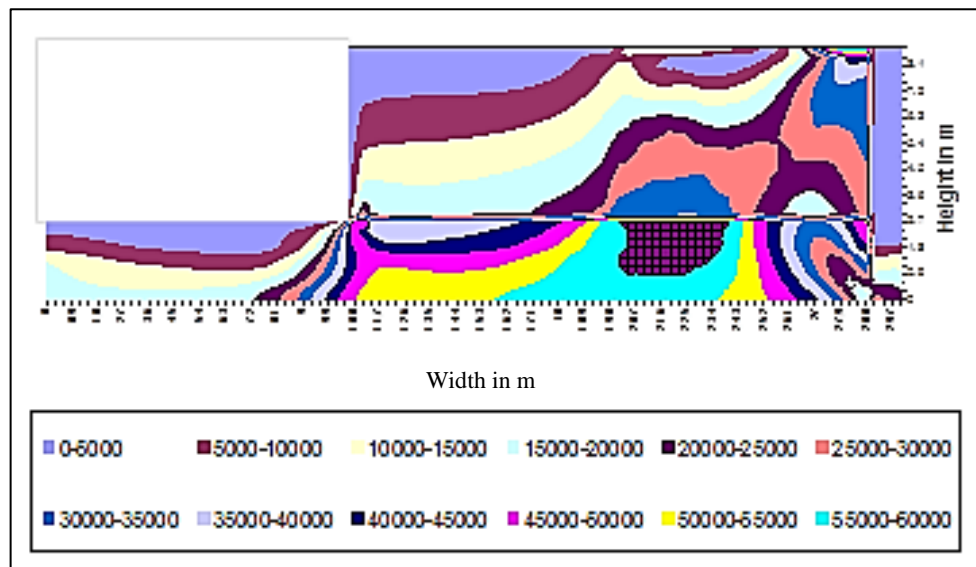


**Fig.5.57** Maximum Shear stresses predicted in reinforced soil retaining wall for Linear analysis under self weight for  $E_s/E_r=0.001$ ,  $k_s/E_s=10+E03$  obtained using RWSW-INT

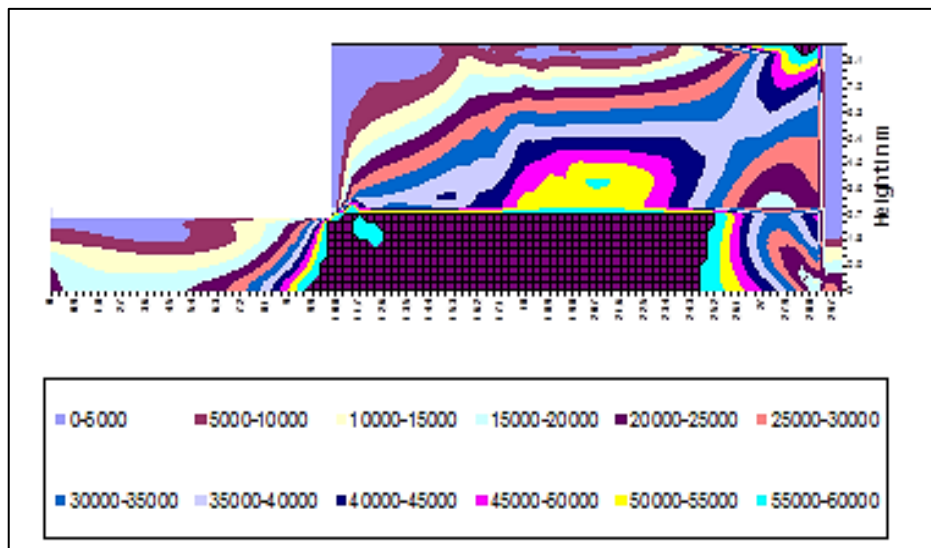


**Fig.5.58** Maximum Shear stresses predicted in reinforced soil retaining wall for Linear analysis under self weight for  $E_s/E_r=0.001$ ,  $k_s/E_s=10+E04$  obtained using RWSW-INT



### 5.4.8.5 Major Principal Stresses in Soil for Different Cases

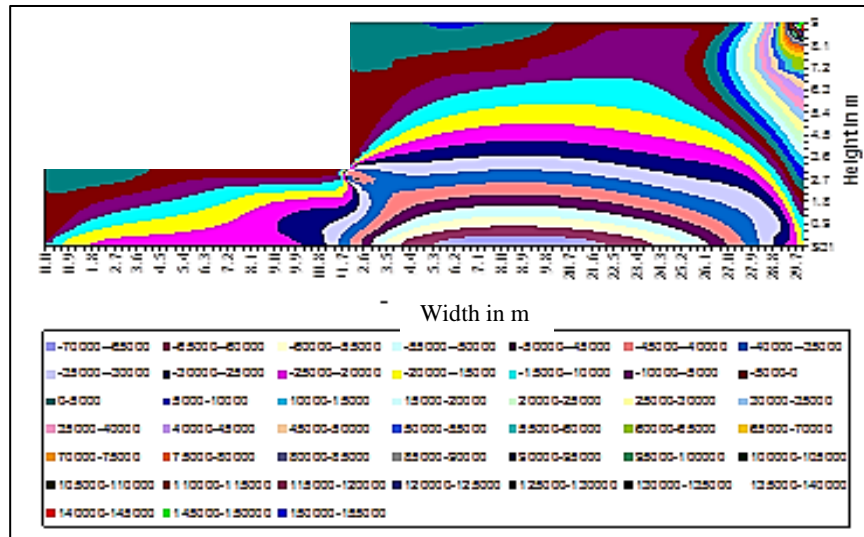


Fig 5.59. Major Principal Stresses (kPa) predicted in unreinforced soil retaining wall for Linear analysis,  $E_s=21\text{MPa}$  obtained using RWSW-LIN

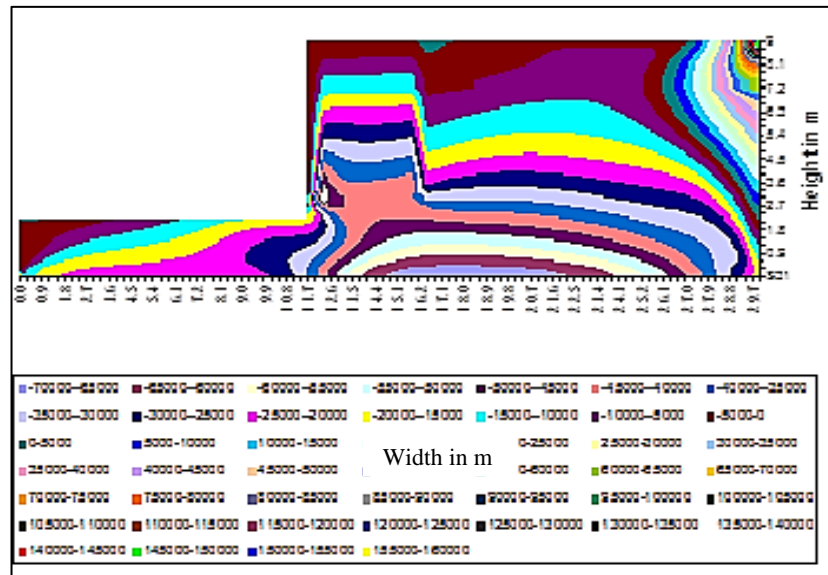


Fig 5.60. Major Principal Stresses (kPa) predicted in reinforced soil retaining wall for Linear analysis under self weight for,  $E_s/E_r=0.001, 100\%$  Coupling obtained using RWSW-LIN

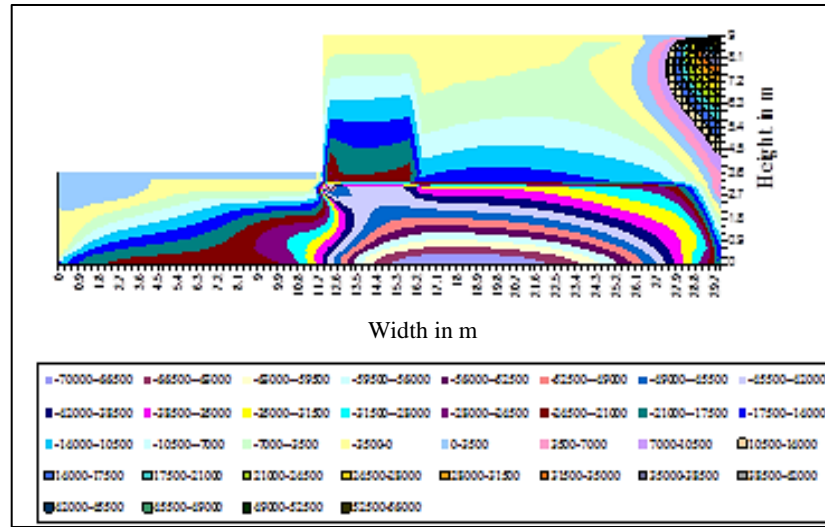


Fig. 5.61 Major Principal Stresses (kPa) predicted in reinforced soil retaining wall for Linear analysis under self weight,  $E_s/E_r=0.001$ ,  $k_s/E_s=10+E02$  obtained using RWSW-INT

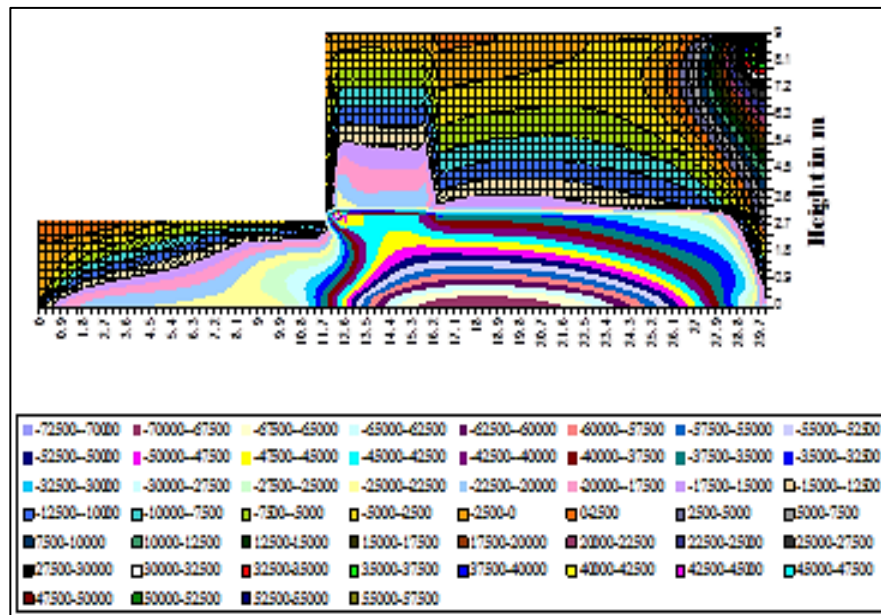
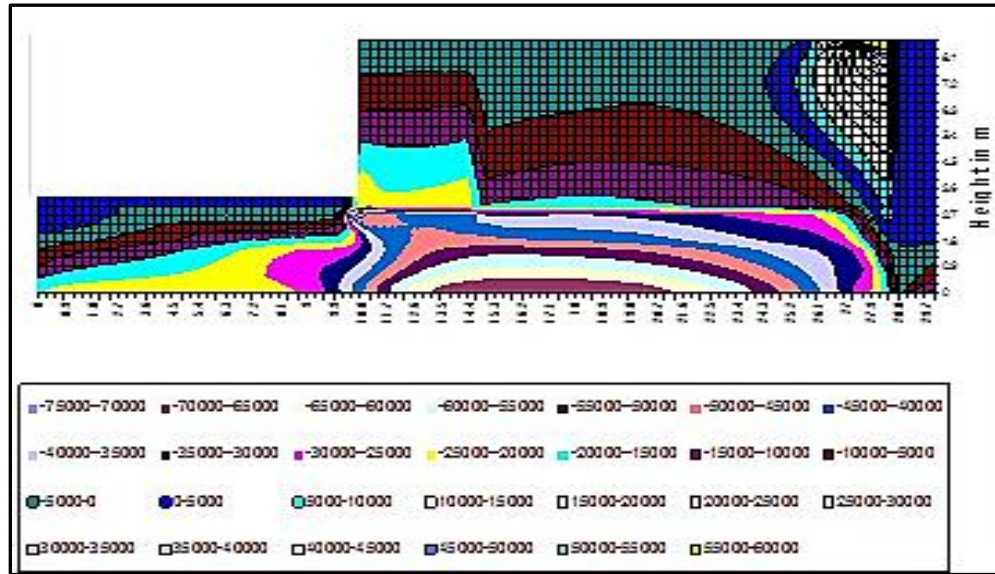
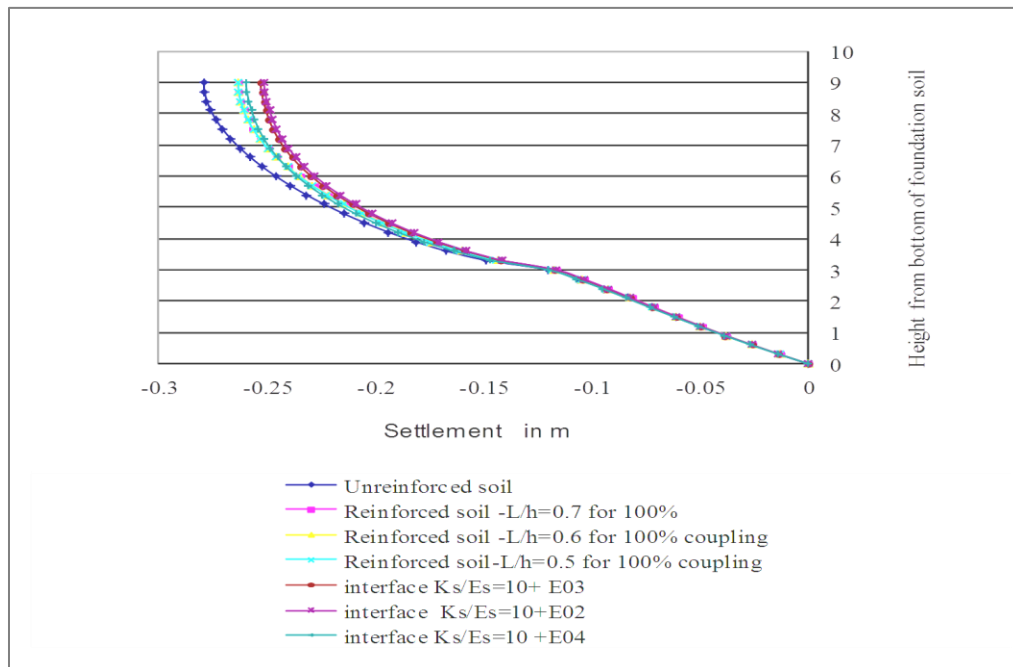


Fig. 5.62 Major Principal Stresses (kPa) predicted in reinforced soil retaining wall for Linear analysis under self weight,  $E_s/E_r=0.001$ ,  $k_s/E_s=10+E03$  obtained using RWSW-INT



**Fig. 5.63 Major Principal Stresses (kPa) predicted in reinforced soil retaining wall for Linear analysis under self weight,  $E_s/E_r=0.001$ ,  $k_s/E_s=10+E04$  obtained using RWSW-INT**



**Fig. 5.64 Horizontal Displacements predicted in reinforced soil retaining wall for Linear analysis under self weight,  $E_s/E_r=0.001$  obtained using RWSW-LIN and RWSW-INT**

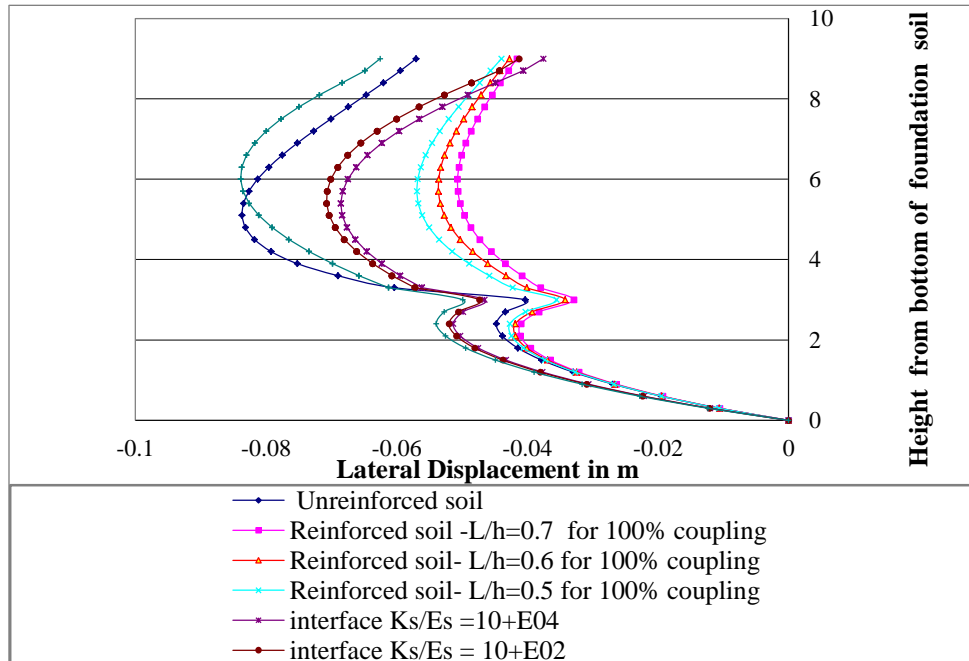


**Fig. 5.65 Vertical settlements of unreinforced and reinforced soil retaining wall for Linear analysis under self weight,  $E_s/E_r=0.001$  obtained using RSW-LIN and RSW-INT**

## 5.5 VARIOUS TABLES RELATED TO STUDIES ON RETAINING WALL

**Table 5.1 Input for the programs RWPT-LIN,RWSW-LIN and RWSW-INT**

<b>Material</b>	<b>Poisson's Ratio</b>	<b>Young's Modulus</b>	<b>Density</b>	<b>No of Elements</b>
Geostrip	0.2	12GPa	78 kN/m <sup>3</sup>	1080
				Bar elements
Soil	0.3	12MPa	19 kN/ m <sup>3</sup>	3080 Rectangular elements

**Table 5.2 Predicted Lateral Displacements(m) and Settlements (m) under Point loads for unreinforced and reinforced soil vertical cut at x=12.00m at all levels of y using RWPT-LIN**

Unreinforced Soil					Reinforced Soil	
1	2	3	4	5	6	7
Node No	X Co-ordinate	Y Co-ordinate	Lateral Displacements	Settlements	Lateral Displacement	Settlements
3071	12	9	-0.0015	-0.00476	-0.00036	-0.00114
2970	12	8.7	-0.00203	-0.00487	-0.00049	-0.00117
2869	12	8.4	-0.00239	-0.00491	-0.00057	-0.00118
2768	12	8.1	-0.00269	-0.00494	-0.00065	-0.00119
2667	12	7.8	-0.00292	-0.00497	-0.0007	-0.00119
2566	12	7.5	-0.00308	-0.00499	-0.00074	-0.0012
2465	12	7.2	-0.00317	-0.00498	-0.00076	-0.0012
2364	12	6.9	-0.0032	-0.00494	-0.00077	-0.00119
2263	12	6.6	-0.00318	-0.00487	-0.00076	-0.00117
2162	12	6.3	-0.00311	-0.00475	-0.00075	-0.00114
2061	12	6	-0.00302	-0.0046	-0.00072	-0.0011
1960	12	5.7	-0.00289	-0.00441	-0.00069	-0.00106
1859	12	5.4	-0.00274	-0.00419	-0.00066	-0.00101
1758	12	5.1	-0.00257	-0.00393	-0.00062	-0.00094
1657	12	4.8	-0.00238	-0.00363	-0.00057	-0.00087
1556	12	4.5	-0.00217	-0.0033	-0.00052	-0.00079
1455	12	4.2	-0.00193	-0.00291	-0.00046	-0.0007
1354	12	3.9	-0.00165	-0.00245	-0.00039	-0.00059
1253	12	3.6	-0.00128	-0.00191	-0.00031	-0.00046
1152	12	3.3	-0.00054	-0.00132	-0.00013	-0.00032
1051	12	3	-0.00087	-0.00139	-0.00021	-0.00033
950	12	2.7	-0.00092	-0.00129	-0.00022	-0.00031
849	12	2.4	-0.00092	-0.00116	-0.00022	-0.00028
748	12	2.1	-0.00088	-0.00101	-0.00021	-0.00024
647	12	1.8	-0.00082	-0.00086	-0.0002	-0.00021
546	12	1.5	-0.00074	-0.00072	-0.00018	-0.00017
445	12	1.2	-0.00064	-0.00057	-0.00015	-0.00014
344	12	0.9	-0.00052	-0.00042	-0.00012	-0.0001

**Table 5.3 Predicted Horizontal, Vertical and Shear Strains for Unreinforced and reinforced soil under Point Loads at y=9.00m using RWPT-LIN**

Unreinforced Soil				Reinforced Soil				
Node No	x	y	Horizontal Strains	Vertical Strains	Shear Strains	Horizontal Strains	Vertical Strains	Shear Strains
3071	12	9	-0.000925	0.0002132	-0.000867	-0.00022	5.12E-05	-0.000208
3072	12.3	9	-0.000394	4.78E-05	-0.000481	-9.46E-05	1.15E-05	-0.000115
3073	12.6	9	4.58E-05	-1.67E-05	0.0001163	1.10E-05	-4.01E-06	2.79E-05
3074	12.9	9	0.0001142	-4.92E-05	0.0001807	2.74E-05	-1.18E-05	4.34E-05
3075	13.2	9	0.0001665	-7.04E-05	0.0002006	4.00E-05	-1.69E-05	4.82E-05
3076	13.5	9	0.0001682	-5.49E-05	0.0002018	4.04E-05	-1.32E-05	4.84E-05
3077	13.8	9	8.87E-05	-8.66E-05	7.52E-05	2.13E-05	-2.08E-05	1.80E-05
3078	14.1	9	-0.000413	0.0003253	-0.000311	-9.90E-05	7.81E-05	-7.47E-05
3079	14.4	9	-0.001354	-0.004471	-0.008566	-0.00032	-0.001073	-0.002056
3080	14.7	9	-0.000157	-0.005794	0.0025733	-3.77E-05	-0.001391	0.0006176
3081	15	9	0.0004535	-0.000903	0.0032869	0.000109	-0.000217	0.0007888
3082	15.3	9	-0.000324	-3.01E-05	0.0014879	-7.79E-05	-7.23E-06	0.0003571
3083	15.6	9	0.0001188	-0.00013	0.0005239	2.85E-05	-3.12E-05	0.0001257
3084	15.9	9	0.0003158	-0.000166	0.0003073	7.58E-05	-3.99E-05	7.37E-05
3085	16.2	9	0.0004053	-0.000187	0.0001992	9.73E-05	-4.48E-05	4.78E-05
3086	16.5	9	0.0004322	-0.000187	0.0001526	0.000104	-4.49E-05	3.66E-05
3087	16.8	9	0.0004154	-0.000172	0.0001285	9.97E-05	-4.13E-05	3.08E-05
3088	17.1	9	0.0003442	-0.000123	0.0001171	8.26E-05	-2.96E-05	2.81E-05
3089	17.4	9	0.0001974	-0.000126	-9.00E-06	4.74E-05	-3.03E-05	-2.16E-06
3090	17.7	9	-0.000362	0.00031	-0.00039	-8.69E-05	7.44E-05	-9.35E-05
3091	18	9	-0.001352	-0.004467	-0.008638	-0.00032	-0.001072	-0.002073
3092	18.3	9	-0.000195	-0.005774	0.002508	-4.67E-05	-0.001386	0.0006019
3093	18.6	9	0.0003859	-0.000871	0.003227	9.26E-05	-0.000209	0.0007745
3094	18.9	9	-0.000414	9.83E-06	0.0014319	-9.93E-05	2.36E-06	0.0003437
3095	19.2	9	1.54E-05	-8.55E-05	0.00047	3.69E-06	-2.05E-05	0.0001128
3096	19.5	9	0.0002067	-0.000121	0.0002532	4.96E-05	-2.90E-05	6.08E-05
3097	19.8	9	0.0003001	-0.000145	0.0001427	7.20E-05	-3.49E-05	3.42E-05
3098	20.1	9	0.0003436	-0.000156	9.04E-05	8.25E-05	-3.75E-05	2.17E-05
3099	20.4	9	0.0003627	-0.00016	5.94E-05	8.71E-05	-3.85E-05	1.43E-05

**Table 5.4 Comparison of Predicted Horizontal Stresses (kPa) between Unreinforced, Reinforced(100% coupling) soil, reinforced also considering Different interfaces using RWSW-**

Node No	x-co-ord	y co-ord	Unreinforced	Reinforced		Reinforced soil with Interfaces		
				Soil	Node No	ks/Es	ks/Es	ks/Es
				100% coupling		10+E02	10+E03	10+E04
2271	12	9	-128.12	-50.29	6909	-55.26	-56.19	-57.94
2272	12.3	9	237.42	-34.78	6910	-832.14	-836.36	-842.40
2273	12.6	9	291.72	-33.80	6911	-987.35	-981.19	-986.49
2274	12.9	9	578.37	59.34	6912	-990.78	-974.91	-976.36
2275	13.2	9	1034.19	220.69	6913	-930.13	-904.14	-899.90
2276	13.5	9	1623.14	433.06	6914	-855.61	-821.70	-811.02
2277	13.8	9	2306.92	680.36	6915	-784.72	-744.54	-726.69
2278	14.1	9	3051.00	950.10	6916	-718.00	-673.35	-647.17
2279	14.4	9	3826.87	1233.37	6917	-651.00	-604.43	-567.82
2280	14.7	9	4612.42	1524.17	6918	-580.01	-536.54	-485.96
2281	15	9	5391.24	1818.68	6919	-506.01	-476.60	-407.28
2282	15.3	9	6151.73	2114.57	6920	-440.39	-448.27	-357.80
2283	15.6	9	6886.02	2410.49	6921	-411.44	-505.27	-414.97
2284	15.9	9	7589.12	2705.76	6922	-526.88	-762.58	-749.85
2285	16.2	9	8258.14	3000.28	6923	-1081.05	-1377.97	-1495.17
2286	16.5	9	8891.63	3294.83	6924	-640.91	-1129.96	-1317.31
2287	16.8	9	9489.12	3592.04	6925	-1596.21	-2030.64	-2253.27
2288	17.1	9	10050.78	3898.79	6926	-2157.75	-2399.35	-2819.80
2289	17.4	9	10577.10	4229.66	6927	-2245.92	-2322.77	-2911.31
2290	17.7	9	11068.76	4556.99	6928	-1938.48	-2155.60	-2889.34
2291	18	9	11526.46	4719.03	6929	-1657.00	-2099.51	-2797.59
2292	18.3	9	11950.85	5832.35	6930	-1660.97	-1987.49	-2618.34
2293	18.6	9	12342.45	6089.89	6931	-2024.89	-2186.47	-2666.33
2294	18.9	9	12701.61	6349.99	6932	-2416.55	-2485.90	-2850.56
2295	19.2	9	13028.50	6609.08	6933	-2545.31	-2569.28	-2867.79
2296	19.5	9	13323.06	6853.34	6934	-2504.13	-2528.75	-2729.45
2297	19.8	9	13585.01	7079.07	6935	-2946.53	-2976.70	-3074.38



Table 5.5 Predicted Vertical Stresses (kPa) in Unreinforced, Reinforced(100% coupling) soil, reinforced also considering Different interfaces using RWSW-LIN									
Node No	x-co-ord	y co-ord	Unreinforce	Reinforce	Node No	Reinforced soil with different Interfaces			
			Soil	Soil		ks/Es	ks/Es	ks/Es	
				100% cou		10+E02	10+E03	10+E04	
2271	12	9	-824.93	-669.32	6909.00	-1285.23	-1282.89	-1282.05	
2272	12.3	9	-1315.21	-1291.23	6910.00	-2801.19	-2799.41	-2798.22	
2273	12.6	9	-1361.39	-1289.60	6911.00	-2800.98	-2800.04	-2799.05	
2274	12.9	9	-1409.56	-1302.59	6912.00	-2835.66	-2836.40	-2836.19	
2275	13.2	9	-1455.54	-1314.74	6913.00	-2850.94	-2851.60	-2851.66	
2276	13.5	9	-1492.43	-1324.05	6914.00	-2854.84	-2855.34	-2855.41	
2277	13.8	9	-1518.87	-1330.58	6915.00	-2853.73	-2854.06	-2853.96	
2278	14.1	9	-1535.65	-1334.90	6916.00	-2851.07	-2851.45	-2851.00	
2279	14.4	9	-1544.40	-1337.61	6917.00	-2848.55	-2849.46	-2848.45	
2280	14.7	9	-1546.85	-1339.20	6918.00	-2847.28	-2849.69	-2848.00	
2281	15	9	-1544.59	-1340.03	6919.00	-2848.34	-2854.62	-2853.00	
2282	15.3	9	-1538.96	-1340.35	6920.00	-2856.69	-2869.19	-2871.24	
2283	15.6	9	-1531.01	-1340.30	6921.00	-2865.45	-2897.81	-2928.90	
2284	15.9	9	-1521.57	-1339.92	6922.00	-3008.83	-2978.14	-3001.91	
2285	16.2	9	-1511.22	-1339.06	6923.00	-3211.04	-3094.61	-3069.50	
2286	16.5	9	-1500.39	-1337.22	6924.00	-2679.18	-2686.98	-2658.12	
2287	16.8	9	-1489.36	-1333.03	6925.00	-2655.55	-2657.61	-2639.00	
2288	17.1	9	-1478.32	-1322.93	6926.00	-2627.47	-2664.26	-2648.22	
2289	17.4	9	-1467.36	-1301.77	6927.00	-2768.77	-2876.45	-2865.79	
2290	17.7	9	-1456.55	-1354.82	6928.00	-2904.25	-2864.26	-2827.23	
2291	18	9	-1445.89	-1567.33	6929.00	-2953.13	-2865.26	-2790.20	
2292	18.3	9	-1435.36	-1315.18	6930.00	-2956.60	-2961.97	-2994.39	
2293	18.6	9	-1424.95	-1338.01	6931.00	-2797.54	-2811.58	-2872.74	
2294	18.9	9	-1414.58	-1340.26	6932.00	-2666.85	-2681.77	-2687.69	
2295	19.2	9	-1404.22	-1338.83	6933.00	-2856.80	-2874.45	-2871.36	
2296	19.5	9	-1393.79	-1336.74	6934.00	-2968.21	-2969.27	-2997.43	
2297	19.8	9	-1383.23	-1334.38	6935.00	-2765.14	-2772.14	-2787.30	

<b>Table 5.6 Predicted shear stresses (kPa) using RSW-LIN in Unreinforced soil</b>								
Reinforced(100% coupling) soil, reinforced also considering Different interfaces								
Node	x-co-ord	y co-ord	Unreinforced	Reinforced		Reinforced soil with Interfaces		
			Soil	Soil	Node	ks/Es	ks/Es	ks/Es
				100% coupling		10+E02	10+E03	10+E04
2271	12	9	-107.98	-57.38	6909	-67.37	-68.64	-70.71
2272	12.3	9	-212.30	-135.27	6910	-206.22	-207.21	-211.78
2273	12.6	9	-104.96	-90.20	6911	-75.63	-68.56	-69.27
2274	12.9	9	16.00	-37.35	6912	20.46	30.73	32.77
2275	13.2	9	117.09	5.11	6913	61.13	71.96	75.68
2276	13.5	9	194.41	36.63	6914	75.03	86.12	91.22
2277	13.8	9	250.15	59.53	6915	81.35	92.66	99.32
2278	14.1	9	287.98	76.19	6916	89.42	100.80	109.66
2279	14.4	9	311.59	88.54	6917	102.71	113.26	125.53
2280	14.7	9	324.29	98.04	6918	121.08	128.20	145.80
2281	15	9	328.89	105.76	6919	141.09	138.44	163.45
2282	15.3	9	327.63	112.44	6920	153.33	127.29	158.82
2283	15.6	9	322.27	118.63	6921	140.15	61.99	78.81
2284	15.9	9	314.11	124.80	6922	22.07	-125.93	-180.82
2285	16.2	9	304.12	131.54	6923	-389.03	-501.07	-634.74
2286	16.5	9	292.97	139.95	6924	-772.48	-731.46	-818.84
2287	16.8	9	281.13	152.70	6925	-714.59	-666.27	-707.32
2288	17.1	9	268.88	176.39	6926	-492.98	-417.75	-495.06
2289	17.4	9	256.40	225.33	6927	-109.14	-38.21	-146.88
2290	17.7	9	243.78	280.81	6928	112.30	-56.62	-148.14
2291	18	9	231.04	212.80	6929	31.62	-144.26	-172.42
2292	18.3	9	218.17	132.95	6930	-185.95	-106.90	31.33
2293	18.6	9	205.10	139.38	6931	-457.77	-368.76	-272.61
2322	27.3	9	-614.91	-378.52	6960	1411.22	1411.00	1410.24
2323	27.6	9	-621.60	-387.73	6961	1988.80	1988.53	1987.66
2324	27.9	9	-613.02	-387.95	6962	2775.99	2775.64	2774.65
2325	28.2	9	-585.23	-376.70	6963	3829.30	3828.85	3827.73
2326	28.5	9	-533.63	-351.08	6964	5204.27	5203.67	5202.37
2327	28.8	9	-452.92	-307.67	6965	7300.82	7299.98	7298.45
2328	29.1	9	-337.68	-242.58	6966	10791.04	10789.87	10788.10
2329	29.4	9	-187.01	-152.17	6967	17851.72	17850.04	17848.24
2330	29.7	9	-43.99	-63.58	6968	44789.50	44787.45	44788.53
2331	30	9	27.19	2.99	6969	53961.82	53959.23	53960.63

**Table 5.7 Horizontal, Vertical and Shear Strains Predicted in Unreinforced and Reinforced soil Retaining wall under self weight for different Young's modulus of Soil using RSW-LIN**

UNREINFORCED SOIL RETAINING WALL								
Horizontal Strains			Vertical strains			Shear Strains		
2.1 MPa	21MPa	210MPa	2.1 MPa	21MPa	210MPa	2.1 MPa	21MPa	210MPa
-0.0612 to 0.0545	-0.00612 to 0.00545	-0.000612 to 0.000545	-0.0845 to 0.001176	-0.0084 to 0.001176	-0.00084 to 0.0000118	-0.151 to 0.0651	-0.0151 to 0.00651	-0.00151 to 0.00065
REINFORCED SOIL RETAINING WALL								
Horizontal Strains			Vertical strains			Shear Strains		
2.1 MPa	21 MPa	210 MPa	2.1 MPa	21 MPa	210 MPa	2.1MPa	21 MPa	210 MPa
-0.05819 to 0.0547	-0.00787 to 0.000259	-0.000591 to 0.00546	-0.07854 to 0.00267	-0.00787 to 0.000259	-0.0008 to .000021	-0.1173 to 0.0652	-0.01187 to 0.006524	-0.001287 to 0.000652

**Table 5.8 Predicted Horizontal displacements (m) and Vertical Settlements (m) for Unreinforced and Reinforced soil Retaining wall under self weight for different Young's modulus of Soil**

Es=2.1 MPa			
Lateral/Horizontal Displacements		Vertical Settlements	
Unreinforced Soil	Reinforced Soil	Unreinforced Soil	Reinforced Soil
0.0837 to 0.0244	-0.0645 to 0.0270	-0.289 to 0.0041	-0.2869 to -0.0041
Es=21 MPa			
Lateral/Horizontal		Vertical Settlements	
Unreinforced Soil	Reinforced Soil	Unreinforced Soil	Reinforced Soil
0.0084 to 0.0024	-0.0065 to 0.0027	-0.029 to -0.004	-0.0287 to -0.0004
Es=210 MPa			
Lateral/Horizontal		Vertical Settlements	
Unreinforced Soil	Reinforced Soil	Unreinforced Soil	Reinforced Soil
-0.0008 to 0.002	-0.0006 to 0.0002	-0.0029 to -0.0001	-0.0029 to -0.0001

<b>Table 5.9 Predicted Lateral and Vertical displacements (m) for Unreinforced and Reinforced Soil under dead load using RWSW-LIN</b>						
Node No	x co-ord	y co-ord	Unreinforced Soil		Reinforced Soil	
			x-disp	y disp	x-disp	y disp
3071	12	9	-0.0057	-0.0279	-0.0043	-0.0264
3072	12.3	9	-0.0057	-0.0282	-0.0043	-0.0265
3073	12.6	9	-0.0057	-0.0284	-0.0043	-0.0267
3074	12.9	9	-0.0057	-0.0285	-0.0043	-0.0268
3075	13.2	9	-0.0057	-0.0287	-0.0043	-0.0269
3076	13.5	9	-0.0056	-0.0288	-0.0043	-0.027
3077	13.8	9	-0.0056	-0.0288	-0.0043	-0.0272
3078	14.1	9	-0.0055	-0.0289	-0.0043	-0.0273
3079	14.4	9	-0.0055	-0.0289	-0.0043	-0.0274
3080	14.7	9	-0.0054	-0.029	-0.0043	-0.0276
3081	15	9	-0.0053	-0.029	-0.0043	-0.0277
3082	15.3	9	-0.0053	-0.029	-0.0043	-0.0279
3083	15.6	9	-0.0052	-0.029	-0.0043	-0.0281
3084	15.9	9	-0.0051	-0.029	-0.0043	-0.0282
3085	16.2	9	-0.005	-0.029	-0.0043	-0.0284
3086	16.5	9	-0.0049	-0.0289	-0.0042	-0.0285
3087	16.8	9	-0.0048	-0.0289	-0.0042	-0.0286
3088	17.1	9	-0.0048	-0.0289	-0.0042	-0.0286
3089	17.4	9	-0.0047	-0.0289	-0.0042	-0.0287
3090	17.7	9	-0.0046	-0.0288	-0.0042	-0.0287
3091	18	9	-0.0045	-0.0288	-0.0042	-0.0287
3092	18.3	9	-0.0045	-0.0287	-0.0042	-0.0287
3093	18.6	9	-0.0044	-0.0287	-0.0041	-0.0287
3094	18.9	9	-0.0044	-0.0286	-0.0041	-0.0286
3095	19.2	9	-0.0043	-0.0285	-0.0041	-0.0286
3096	19.5	9	-0.0043	-0.0285	-0.0041	-0.0285
3097	19.8	9	-0.0043	-0.0284	-0.0041	-0.0285
3098	20.1	9	-0.0042	-0.0283	-0.0041	-0.0284
3099	20.4	9	-0.0042	-0.0282	-0.0042	-0.0283
3100	20.7	9	-0.0042	-0.0281	-0.0042	-0.0281

## **5.6 SUMMARY OF STUDIES ON LINEAR ANALYSIS OF REINFORCED SOIL RETAINING WALL UNDER POINT LOADS**

The developed software RWPT-LIN can predict stresses, strains and settlements at all the nodes for the cases studied. The results of the numerical analysis is as below;

For the case considered, with two point loads of 57kN (IRC Class A load) spaced at 3.60m as shown in Fig. 5.1a, it is found that the lateral displacements and settlements decrease in case of a reinforced backfill when compared to displacements in unreinforced backfill by 25% and 24% respectively. Table 5.2 depicts the lateral displacements and settlements for the unreinforced and reinforced soil retaining wall. The horizontal displacements in unreinforced soil retaining wall are more than reinforced soil retaining wall. They vary by 2% to 33%. Beyond the length of 8.40m, they are equal at many locations and are found to be less at few locations as presented in Table 5.2.

The horizontal stresses are found to reduce from 40% to 75% in varying percentages in reinforced soil retaining wall when compared with unreinforced soil retaining wall.

The vertical stresses are found to reduce from 1% to 20% in varying percentages in reinforced soil retaining wall when compared with unreinforced soil retaining wall up to a length of 9.6m from the facing of the retaining wall. Beyond 9.6m the vertical stresses are found to increase from 1% to 20% in varying percentages in reinforced soil retaining wall when compared with the unreinforced wall. Though the range of vertical stresses remain nearly the same for the unreinforced and reinforced soil retaining wall, it is observed that the stress contours vary in their distribution at different locations.

The shear stresses are found to reduce from 10% to 90% in varying percentages in reinforced soil retaining wall when compared with unreinforced soil retaining wall.

At few locations, the stresses in reinforced soil retaining wall are more than those in unreinforced soil retaining wall.

The horizontal strains are found to reduce from 75% to 76% in varying percentages in reinforced soil retaining wall when compared with unreinforced soil retaining wall. (Table 5.3). The vertical strains are found to reduce by 76% in reinforced soil retaining wall when compared with unreinforced soil retaining wall (Table 5.3). The shear strains are found to reduce from 75% to 76% in varying percentages in reinforced soil retaining wall when compared with unreinforced soil retaining wall. (Refer Table 5.3) Table 5.3 depicts the horizontal, vertical and shear strains for the unreinforced and in reinforced soil retaining wall.

## **5.7 SUMMARY OF STUDIES ON LINEAR ANALYSIS OF REINFORCED SOIL RETAINING WALL UNDER DEAD LOADS**

The results of the developed software RWSW-LIN and RWSW-INT under self weight of a 6.0m high retaining wall for the linear analysis can be summarized as below.

Table 5.4 shows that the horizontal stresses in reinforced soil retaining wall reduce from 50% to 90% of those found in unreinforced soil retaining wall. Table 5.4 also shows the horizontal stresses in reinforced soil with the introduction of interface elements show the development of compressive stresses while the unreinforced and reinforced soil with 100% coupling show tensile horizontal stresses.

Table 5.5 shows that that the vertical stresses in reinforced soil retaining wall with 100% coupling are the least when compared with the unreinforced soil wall and reinforced wall with interface elements. Table 5.5 also shows the vertical stresses in reinforced soil with the introduction of interface elements show the increase of compressive stresses.

Table 5.6 shows that that the shear stresses in reinforced soil retaining wall with 100% coupling are the least when compared with the unreinforced soil wall and reinforced wall with interface elements up to a length of 3.9m from the facing of the retaining wall. The shear stress are found to be maximum for the unreinforced soil retaining wall. Table 5.6 also shows the shear stresses in reinforced soil with the introduction of interface elements show a reversal of line of action of the stresses beyond 3.9m (at the end of reinforcement).

From Table 5.7, it can be observed that for the reinforced soil retaining wall, the horizontal strains are found to reduce by 86% and 98% for soil with  $E_s=21\text{MPa}$  and

$E_s=210\text{MPa}$  (Young's Modulus) which is incidentally 10% and 100% more than soil of  $E_s=2.1\text{MPa}$ .

From Table 5.7, it can be observed that for the reinforced soil retaining wall the vertical strains are found to reduce by 89% and 98% for soil with  $E_s=21\text{MPa}$  and  $E_s=210\text{MPa}$  (Young's Modulus) which is incidentally 10% and 100% more than soil of  $E_s=2.1\text{MPa}$ .

From Table 5.7, it can be observed that for the reinforced soil retaining wall, the shear strains are found to reduce by 89% and 98% for soil with  $E_s=21\text{MPa}$  and  $E_s=210\text{MPa}$  (young's modulus) which is incidentally 10% and 100% more than soil of  $E_s=2.1\text{MPa}$ .

From Table 5.8, it can be observed that for the unreinforced and reinforced soil retaining wall the horizontal displacements and vertical settlements are found to reduce by 10% and 100% for soil with  $E_s=21\text{MPa}$  and  $E_s=210\text{MPa}$  (Young's Modulus) which is incidentally 10% and 100% more than Young's Modulus of soil with  $E_s=2.1\text{MPa}$ . But the results are different for reinforced soil retaining wall. Table 5.9 depicts the lateral displacements and vertical settlements for unreinforced and reinforced soil retaining wall under self weight at  $y=9.00\text{m}$ .



## CHAPTER 6

### STUDIES ON MECHANICALLY STABILIZED EARTH WALL (MSE WALL)

#### 6.1 GENERAL

Mechanically stabilized earth wall or MSE wall is the soil structure constructed by reinforcing it using different reinforcing elements. It can be used to construct dykes, abutments, seawalls and retaining walls. MSE in its current form evolved since 1960s. The term MSE was formed to differentiate it from, patent of the Reinforced Earth Company, the "Reinforced Earth". The MSE walls serve as good substitute to conventional reinforced retaining walls due to their ability to retain earth fills upto greater heights. The long term behavior of MSE wall is more important than its short term behavior. The French engineer, Vidal was the first one to propose the basic theory of MSE walls. While the backfill develops the lateral pressure that should be supported, the backfill-reinforcement interaction can resist such lateral pressure.

As per its structural behavior, the reinforced soil is divided into active and passive zones (Schlosser and Long, 1974). Schlosser and Long conducted full-scale tests at Incarville, France) which is a MSE wall, 10 m high. The strain gauges were attached to the steel reinforcements during the construction of the wall. The distribution of tensile stresses along the reinforcement was found to be nonlinear. A parabolic curve was used to locate the maximum tension in each layer which also divides the soil mass into two zones active and passive.

The first MSE wall in America was built in 1972 in California, (Chang et al. 1977). The authors showed that stress distribution was similar to that of the Incarville wall. The stresses in the soil near the wall face at the top were in accordance to Rankine's earth pressure theory, while in the midsection, they followed Jaky's earth pressure at rest theory.

Shivashankar (1991) conducted full-scale tests on a MSE system, 5.85 m high built inside Asian Institute of Technology, Bangkok. It was built in sections consisting of three different backfill soils as weathered clay, clayey sand and lateritic soil using steel grids. They also numerically analysed the pullout tests. Pullout tests were conducted to investigate the interaction between steel grid and backfill soils.

In the present part of the research, parametric studies have been conducted by introducing different facings to evaluate the performance of the chosen MSE (AIT) wall. A program was developed for the analyses of the MSE (AIT) wall considering nonlinearity of soil to obtain displacements, stresses and strains. The nonlinear model of the soil and FEM model have been validated with the experimental results of Shivashankar (1991). The parametric studies are done for the following cases:

- MSE (AIT) wall without facing ( Refer Fig. 6.1)
- MSE (AIT) wall with steel wire facing (Refer Fig. 6.2)
- MSE (AIT) wall with Reinforced Concrete facing( RC facing)

For the RC facing, the Poisson's ratio considered is 0.15 and unit weight is  $24 \text{ kN/m}^3$

## **6.2 DETAILS OF THE EXPERIMENTAL PROGRAMME CHOSEN FOR NUMERICAL STUDY**

### **6.2.1 Case Study**

The MSE wall considered for the study is 5.85m high about 14.64m long at the top and is divided into three sections along its length (Shivashankar, 1991). This welded wire wall was constructed at the northern part of the campus of the Asian Institute of Technology (AIT), Bangkok, Thailand. The researcher validated his experimental observations with the results of Reinforced Earth Analysis (REA) software adopting Duncan Chang's constitutive model.

They used standard reinforcement of the Hilfiker welded wire wall with a vertical wire mesh facing. They used reinforcing mats each of 2.44m width. The

reinforcement used consisted of longitudinal and transverse bars of 6.07mm x 5.36mm diameter respectively with grid openings of 0.15m x 0.225m. The horizontal and vertical spacing of reinforcement layers used were 0.15m and 0.46m respectively.

The total length of the reinforcing mats, including the bent-up portion, which would eventually become a part of the facing was 5.72m. The backfill soil was considered to have an internal frictional angle of  $30^{\circ}$  and cohesion intercept of 10kPa with a total unit weight of  $19.25\text{kN/m}^3$ . The foundation subsoil was assumed to be uniform, corresponding to soft clay having an undrained shear strength of 29.3kPa.

The external stability was established and checks for bearing capacity failures were done. The conventional Bishop's Slope stability analysis was carried out to identify the potential failure surfaces. They assumed that the soil strength was fully mobilized along the potential failure surface. They estimated the base pressures beneath the MSE wall using the Meyerhof's distribution and compared with the ultimate bearing capacity calculated from Terzaghi's bearing capacity equation.

They monitored the lateral and vertical movements regularly at every stage of construction. They retrieved this data and plotted them immediately which helped them to keep a constant check on the ground movements.

### **6.3 CONSTRUCTION OF MSE WALL AND ANALYSIS (Using Program REA) (Shivashankar, 1991)**

The construction of the wall involved the placement of the reinforcement in such a way that the bentup portion of the reinforcement formed the facing. Backing mats and 6.25mm screens were provided along the vertical face of the wall, behind the bent-up portion of the reinforcement to prevent the erosion of the soil. To prevent the erosion of the soil, pea size gravel was extended upto 0.2m behind the wall face. They broke the weathered clay crust along the edges of the welded wire wall/ embankment system along with the centre both along the longitudinal and transverse directions for a width of 0.3m to a depth of 2m below the general ground level. It was then filled with the same excavated material and compacted with the hand compactor before placing the first layer of reinforcement. The main objective was to prevent the embankment to act

as rigid raft foundation. After placing the first layer of reinforcement, backing mats were placed against the face of the wall on the inside and then the screen was clipped with hog rings.

Three different locally available backfill soils have been used corresponding to each section. Weathered Bangkok clay was obtained from the top 2m thickness of the weathered clay crust. Clayey sand backfill is brownish in colour with 45% passing U.S. standard sieve No 200. The height of the embankment system was raised equally at all the three equal sections. The fill between the reinforcing mats was compacted in three equal lifts of 0.15m to a total thickness of 0.45m corresponding to the vertical spacing between the reinforcing grids. Currently MSE wall with weathered clay only has been considered.

The foundation boundary lines at the bottom were chosen at a depth of 9.15m below the general ground surface. The top 1.83m of the subsoil was taken as the weathered Bangkok clay and the 7.32m of the subsoil beneath it was taken as the compromise of the soft Bangkok clay. A width of 15.24m was taken in front of the toe and a width of 9.15m was taken at the rear behind the heel. Refer Fig. 6.4. The lateral displacements of the subsoil observed at the rear were very small. The subsurface settlements recorded at a depth of 8.00m were found to be negligible. Duncan's characterization were employed to represent the different soils.

The welded wire wall was first transformed to a strip reinforced wall to suit the format in REA program (Shivashankar, 1991). The values of friction coefficients for the different layers were higher near the top of the wall and decreased with the increase in the overburden pressures. The effects of compaction induced stresses and the circular cross section of the longitudinal wires of the grid were also incorporated by taking the average overburden pressure as 1.15 times the actual normal stresses acting on the reinforcements.

The program REA allows for the construction sequence to be adopted in the analysis. The construction sequence as followed in the actual wall construction at the site was

also adopted in the analysis. There were sixteen solution increments. The settlements were found to be sensitive to the values of bulk moduli of the subsoils. The settlements at the end of construction as obtained from the finite element analysis program REA agreed with the observed values immediately after construction.

Typical values of the properties of the weathered clay, soft clay and Lateritic residual soils used for the study have been presented in Table 6.1. The various components of the welded wire MSE(AIT) wall that comprise of the main reinforcement and the facing units are shown in Figs. 6.1 and 6.2. The construction of the wall involved the placement of the reinforcement in such a way that the bent-up portion of the reinforcement formed the facing. The reinforcement used was 16 feet 6 inches (5.1 m) long.

The welded wire wall/embankment system was extensively instrumented both in the subsoil and within the embankment itself. This system enabled the researchers to monitor the behaviour of the wall both during construction and in the post construction phase. Nine surface settlement plates (S1 to S9) were placed beneath the MSE wall at 0.45m depth below the general ground surface. Settlements were measured by precise levelling with reference to a bench mark. Currently, observations of 3 gauges installed horizontally at 15.30 m, 18.00m and 20.70m have been considered.

## **6.4 FEM ANALYSIS AND RESULTS**

### **6.4.1 FEM Model**

This part of the research considers 100% coupling between the soil and reinforcement. The total number of nodes, soil elements and bar elements and interface elements are 4001, 3976, 204 and 408 respectively. The soil element was considered as rectangular of size 0.30m x 0.30m up to a depth of 8.10m. Beyond 8.10m up to the top of the MSE wall, the size of the soil element considered was 0.45m. The reinforcement was considered to be truss element and the element sizes were considered as 0.3m wide up to 8.10m and 0.45m up to the top of the wall. The reinforcement considered is 5.10m

long placed horizontally with a vertical spacing of 0.45m. Thus a total of 14 layers of reinforcements are being used. The side boundaries are rollers whereas the base is hinged. Only static stresses due to gravity have been considered in this analysis. This parametric study has been carried out by including steel wire facing and excluding the facing. The characteristics of the reinforcement are given in Table 6.2. The properties of the soil considered are as per Table 6.1. Section 6.4.5 shows the Figures plotted in MSE (AIT) wall studies.

Figures 6.1 and 6.2 show the MSE (AIT) wall with and without the steel wire facing. Figure 6.3 shows the AIT Wall with foundation details. Fig. 6.4 shows the FEA Model of MSE (AIT) wall representing mesh co-ordinates (Shivashankar, 1991). Figure 6.5 shows the plan of the MSE (AIT) wall with three sections consisting of different soils used in the study.

In the present part of research, parametric studies have been conducted by introducing different facings to evaluate the performance of the chosen MSE wall. A programme was developed for the analyses of the MSE wall considering nonlinearity of soil to obtain displacements, stresses and strains. The experimental results of Shivashankar (1991) have been validated with nonlinear model of the soil and the FEM modelling carried out in this research.

#### **6.4.2 Results and Discussions**

The settlements obtained from the experimental studies (from literature, Shivashankar, 1991) and the numerical analysis have been plotted in Figs. 6.6 to 6.8 at depths of 0.45m, 3.0m and 6.0m along reinforcement length, between 15m and 20.1m (reinforcement length). Figure 6.9 shows the settlements predicted across the width of the MSE (AIT) wall at 3.00m and 6.00m below the ground level obtained using the developed program by adopting Non-linear Analysis with and without facing. The settlements obtained at 0.45m, 3.00m and 6.00m using REA and experimental studies have been plotted in Fig. 6.10 for the MSE (AIT) wall without the facing. The settlements predicted at all levels using developed program have been

plotted in Fig. 6.11 for the MSE wall without the wire facing. Figure. 6.12 shows the settlements predicted using developed software MSE-PRO at different levels for the MSE (AIT) wall with RC facing.

Figure 6.13 shows the reference X-Y axes for the MSE (AIT) wall. Figures 6.14 to 6.21 depict the lateral displacements for the linear and nonlinear analysis obtained using the developed programme at different locations along the MSE (AIT) wall. Figures 6.22 and 6.25 depict the shear and vertical stresses in MSE Wall with and without wire Facing obtained using MSE-PRO. Section 6.4.7 presents the tables related to MSE wall.

Section 6.4.3 presents the various figures plotted in MSE (AIT) wall studies. Section 6.4.4 presents the various graphs plotted in MSE (AIT) wall studies. Section 6.4.5 presents the various figures plotted in MSE (AIT) wall studies.

### 6.4.3 Figures Plotted from MSE (AIT) Wall Studies

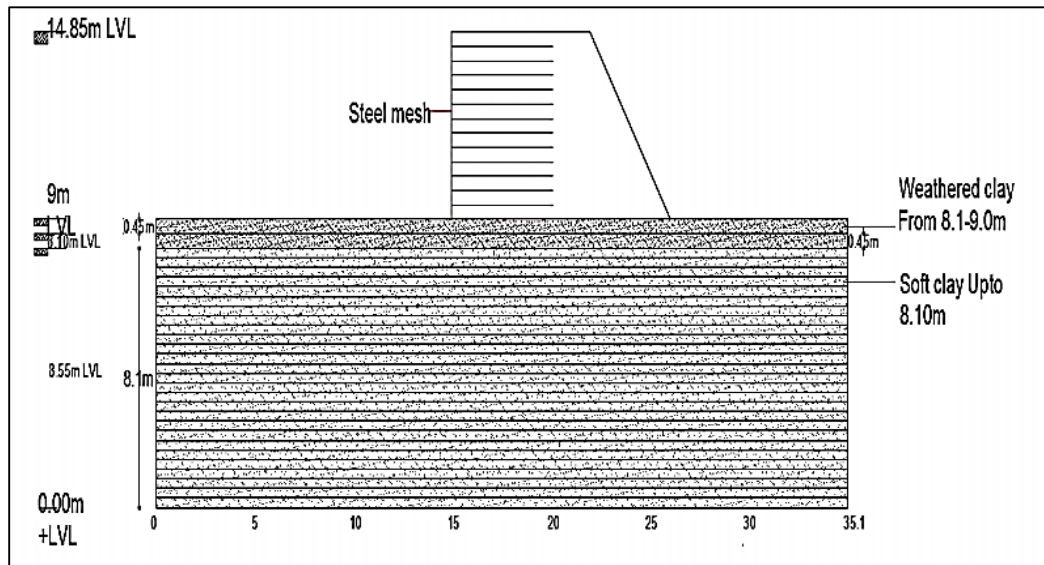


**Fig. 6.1 MSE (AIT) Wall with steel wire facing, Shivashankar (1991) used in Experimental and Numerical studies (MSE-PRO)**

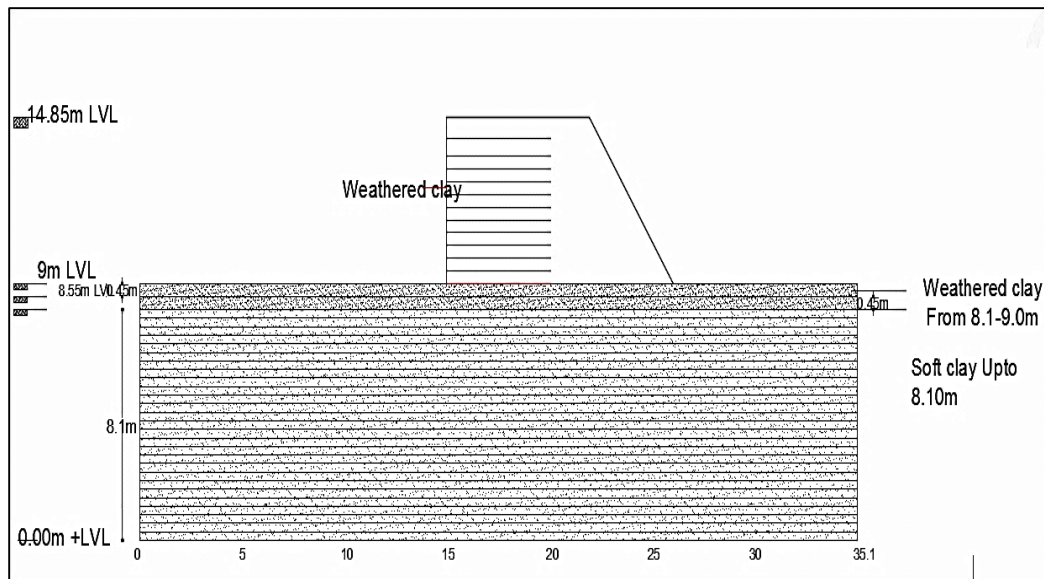


**Fig. 6.2 MSE (AIT) Wall without steel wire facing, Shivashankar (1991) used in Numerical studies (MSE-PRO)**



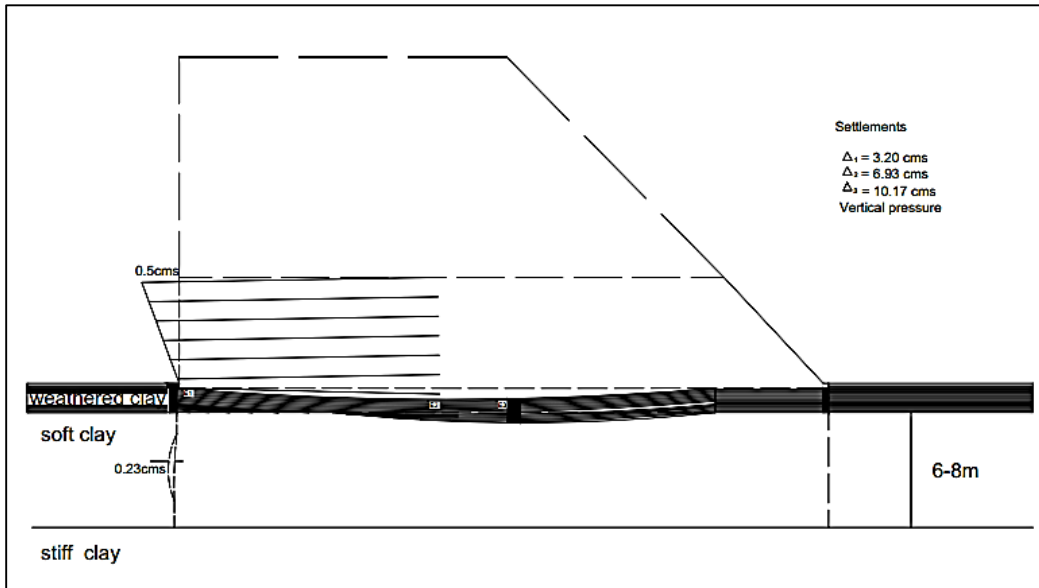


**Fig. 6.3 MSE (AIT) Wall, Shivashankar (1991) used in Experimental studies**

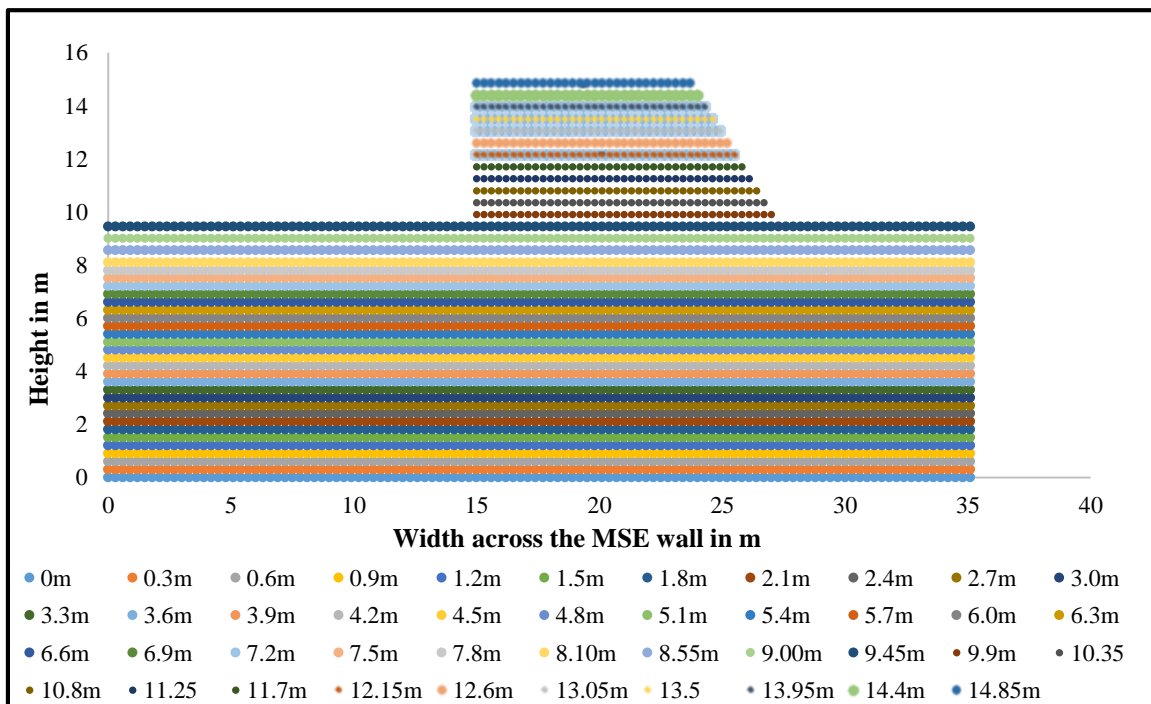


**Fig. 6.4 FEA Model of MSE (AIT) Wall representing mesh co-ordinates, Shivashankar (1991) used in Numerical studies (MSE-PRO)**

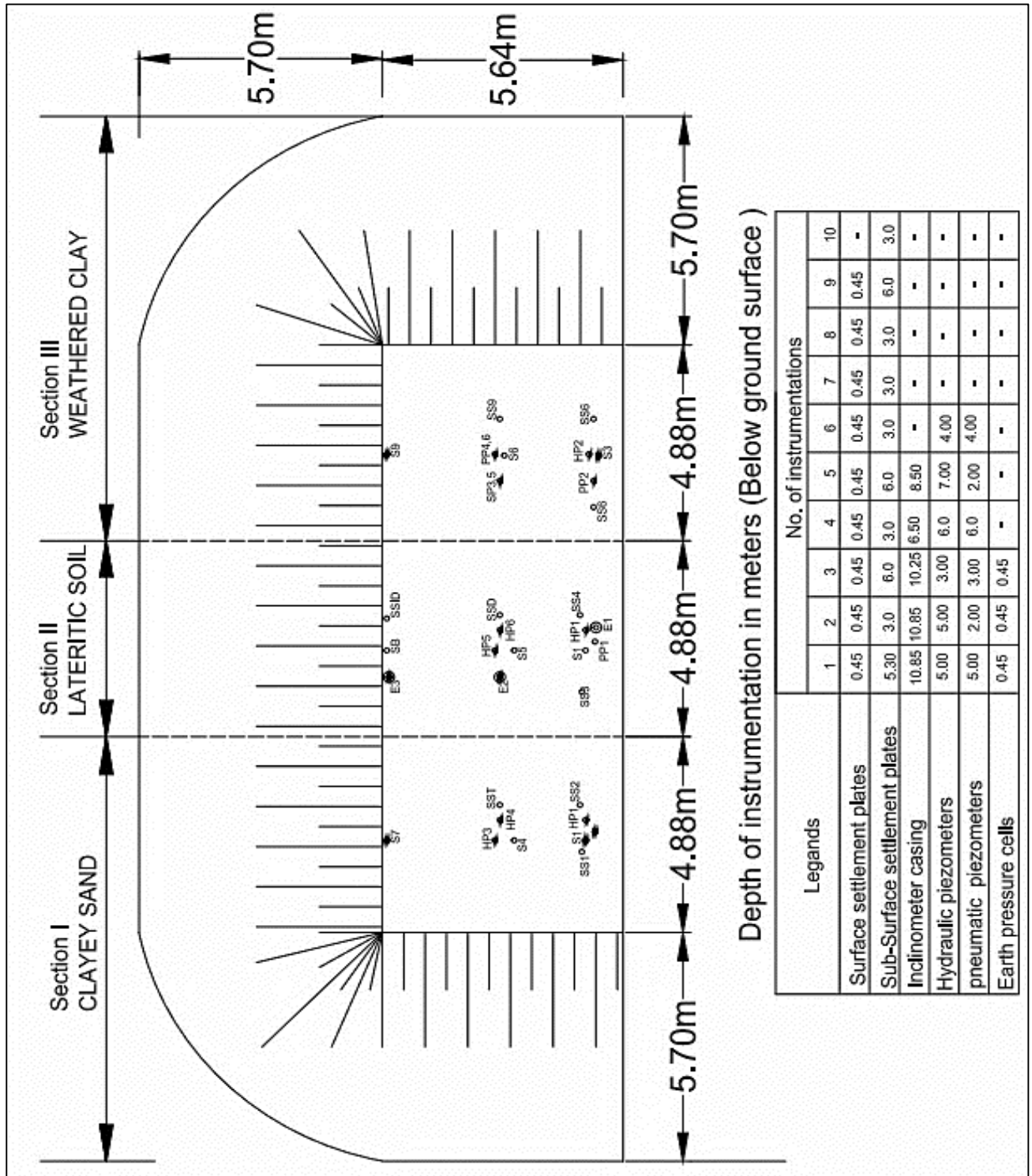


**Fig. 6.5. Plan of MSE (AIT) Wall showing three sections of soil along with strain gauges fitted, Shivashankar (1991)**

#### 6.4.4 Graphs Plotted from MSE (AIT) Wall Studies

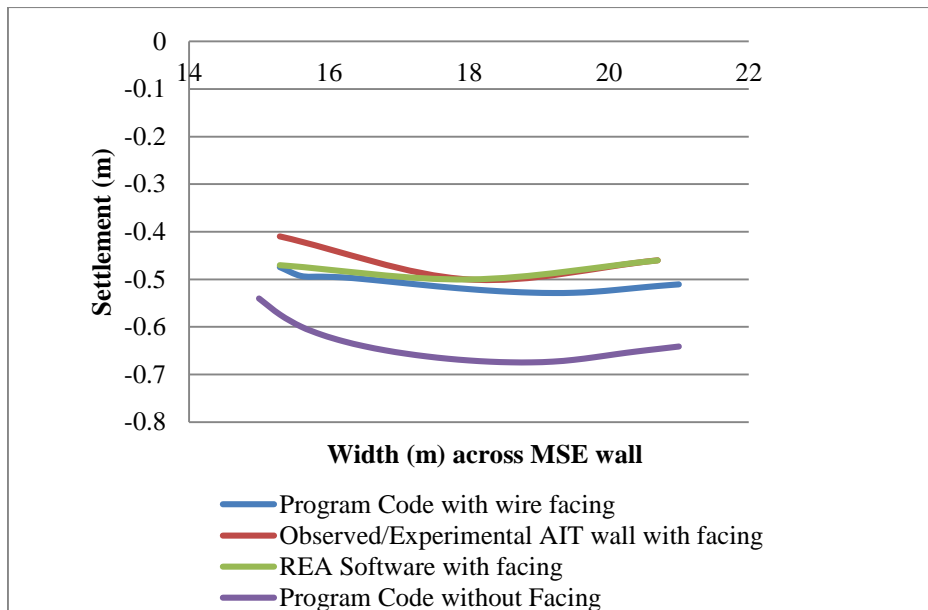


**Fig. 6.6 Settlements at 0.45m below Ground Surface obtained from different studies with strain gauges between 15.0m to 20.10m**

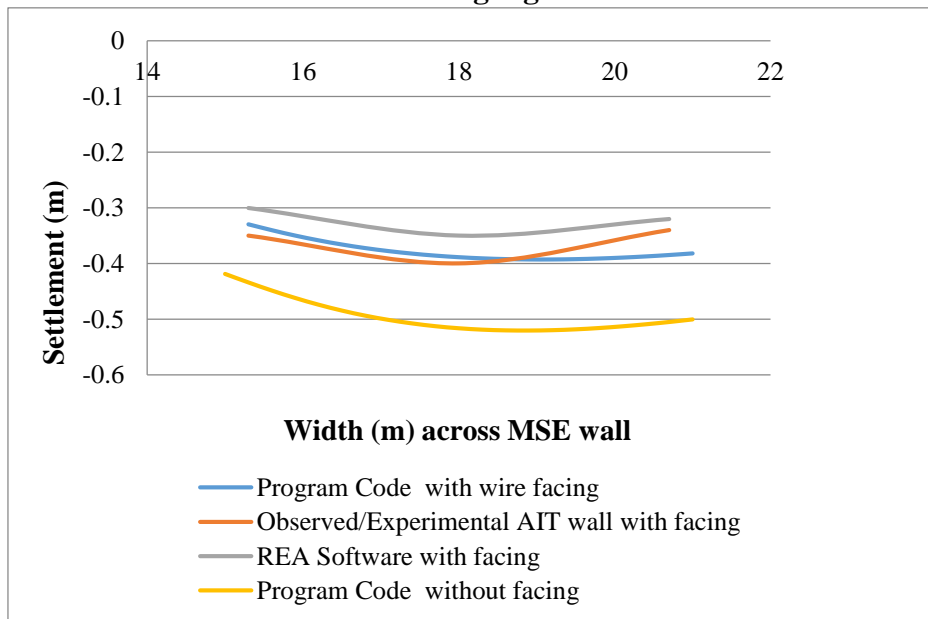


**Fig. 6.7 Settlements at 3.00m below Ground Surface obtained from different studies with strain gauges between 15.0m to 20.10m**

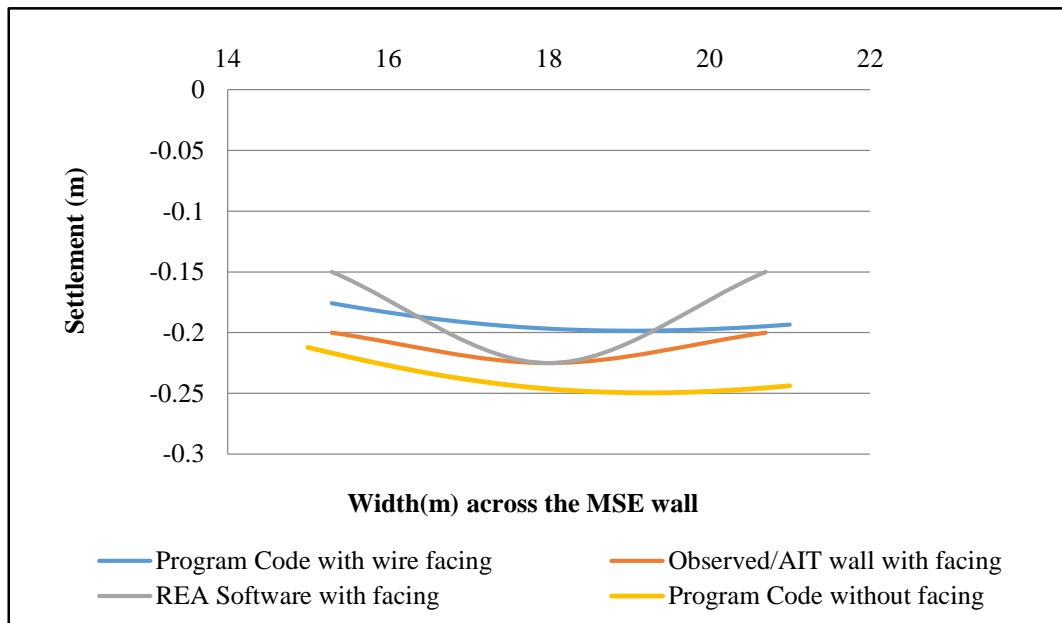


**Fig. 6.8 Settlements at 6.00m below Ground Surface obtained using different studies (15.0m to 20.10m) with and without facing**

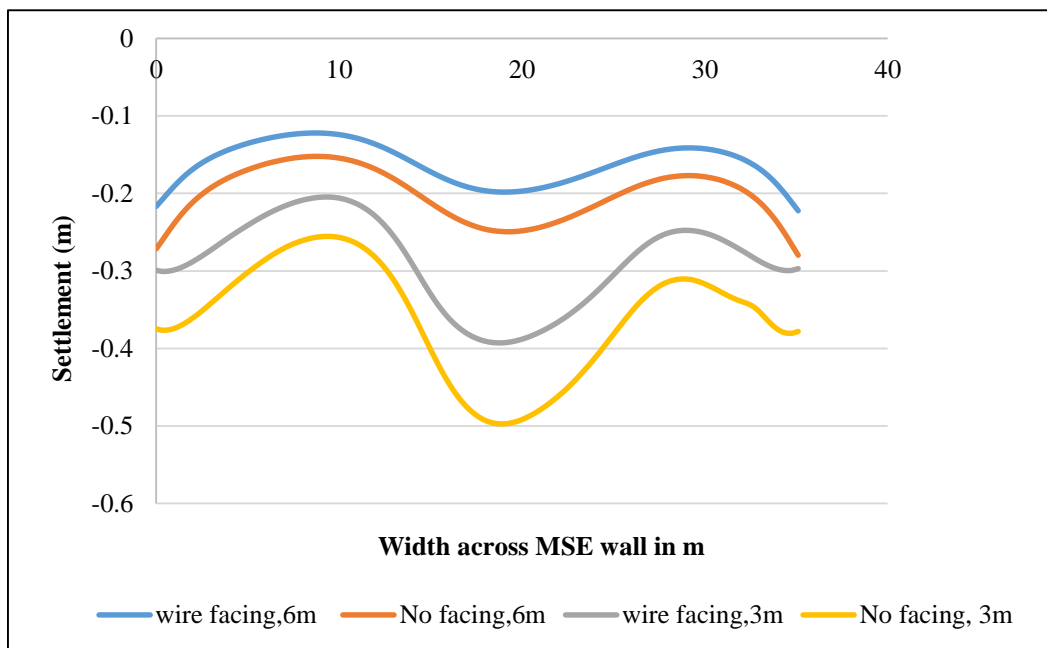


**Fig. 6.9 Settlements at 3.00m and 6.00m from Ground Surface obtained from MSE-PRO by adopting non-linear analysis with and without facing**

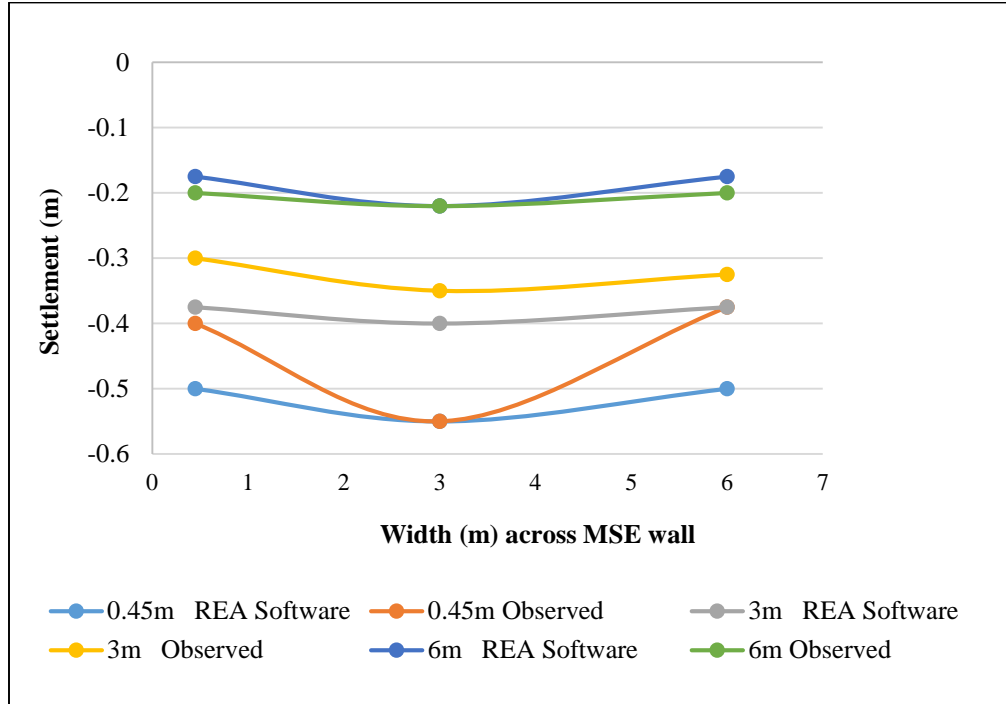


**Fig. 6.10 Settlements at 0.45m, 3.00m and 6.00m depths from Ground Surface plotted using REA software and Experimental studies depths, Shivashankar (1991)**

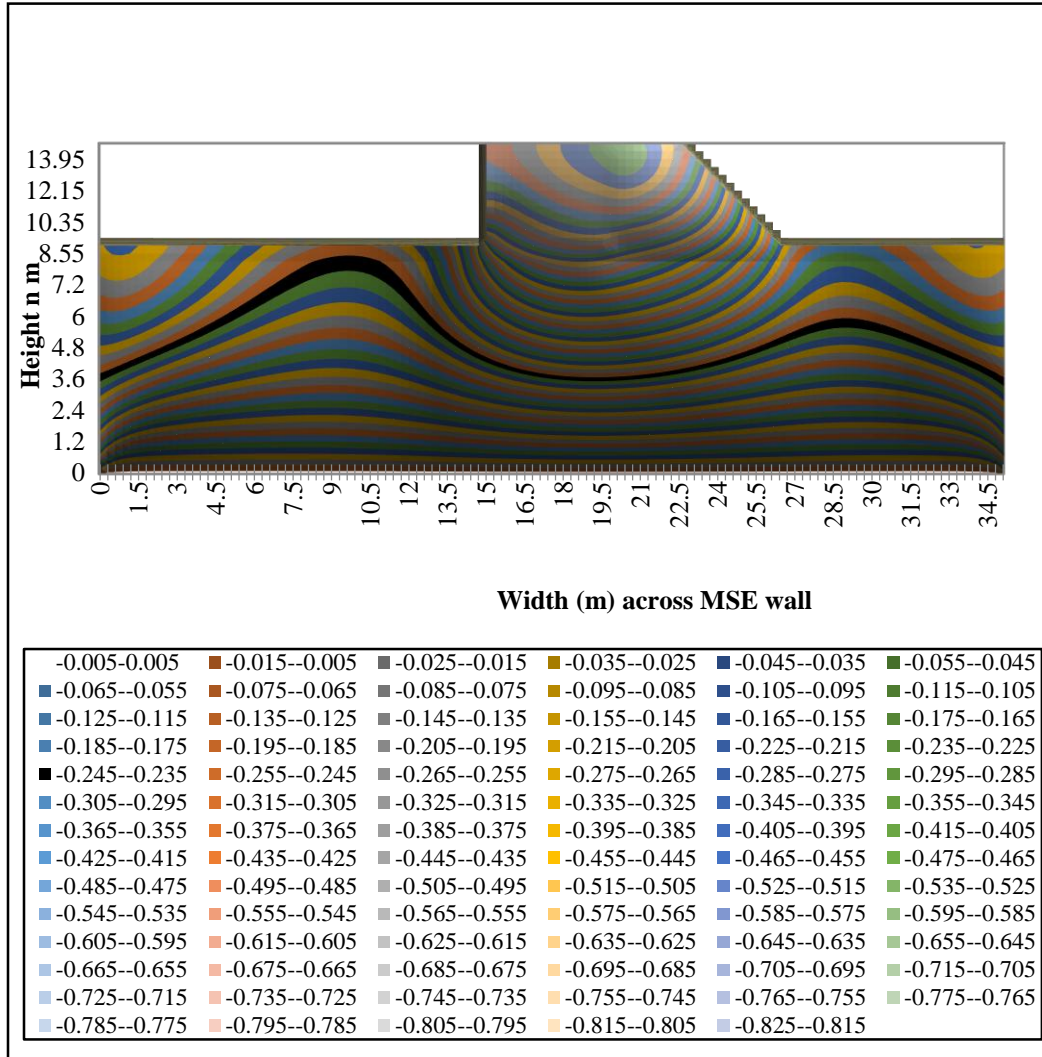


**Fig. 6.11 Settlements (m) predicted using developed software using MSE-PRO at different levels for the MSE wall without facing**

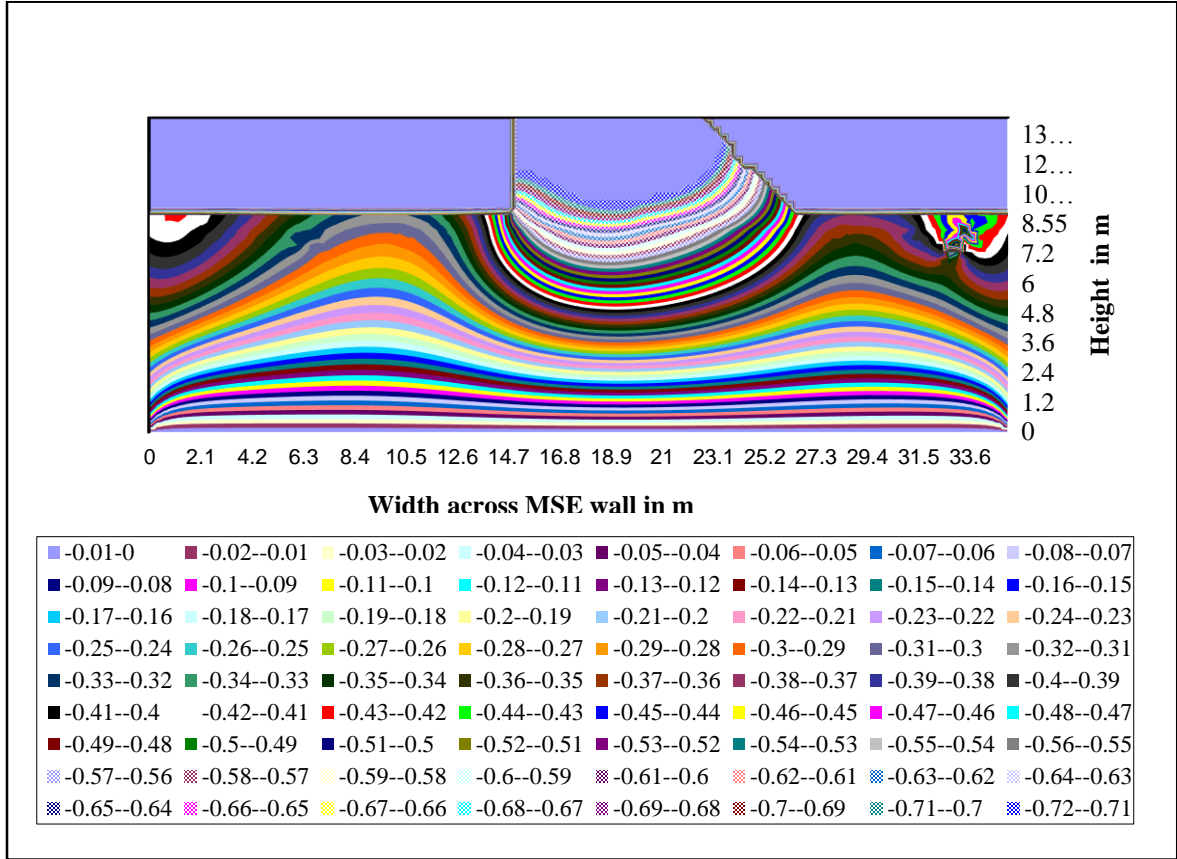


**Fig. 6.12 Settlements (m) predicted using developed software using MSE-PRO at different levels for the MSE (AIT) wall with RC facing**

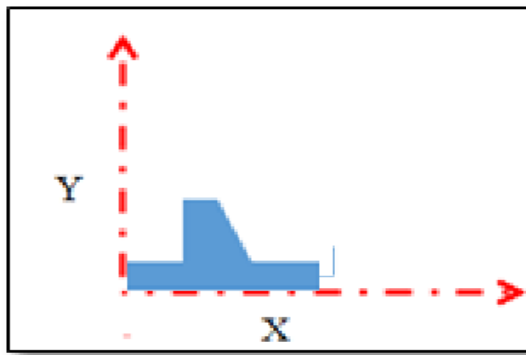


**Fig. 6.13 Reference X-Y axes for the AIT wall**

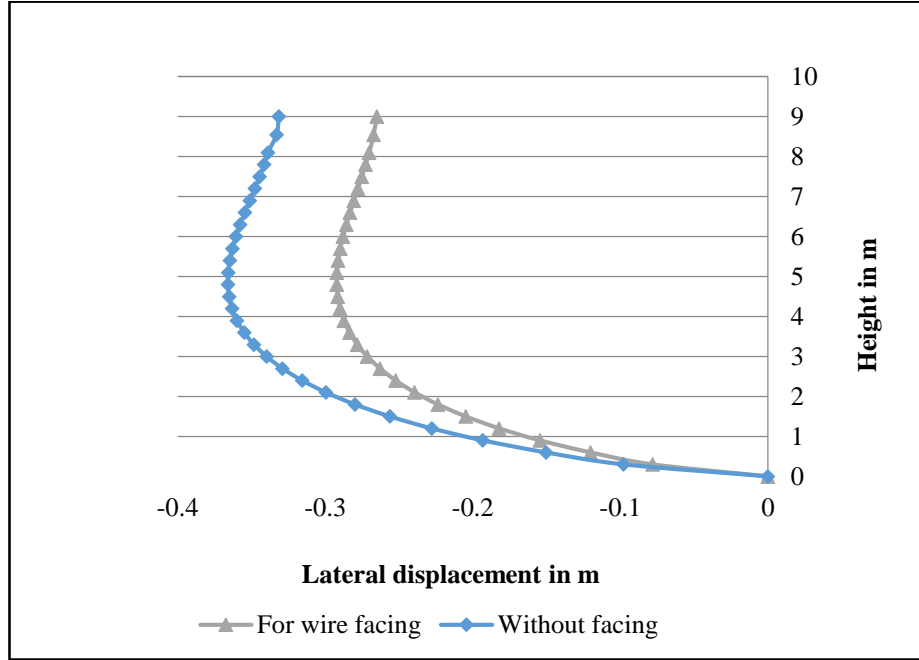


**Fig. 6.14** Lateral displacements predicted using MSE-PRO by adopting non-linear analysis at  $x= 0\text{m}$  (foundation soil)

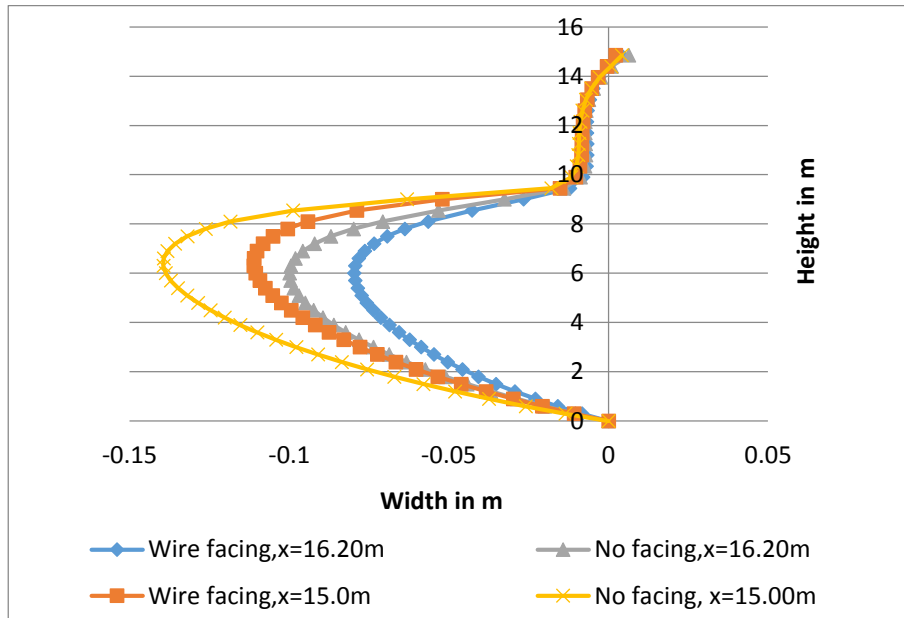


**Fig. 6.15** Lateral displacements predicted using MSE-PRO by adopting non-linear analysis at  $x=15.0\text{m}$  and  $x=16.20\text{m}$



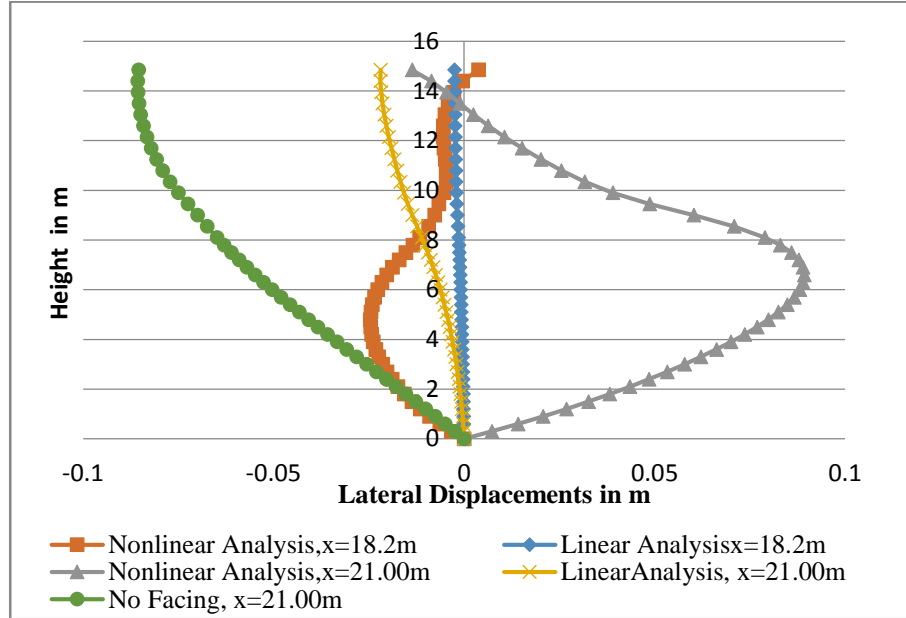


**Fig. 6.16 Lateral displacements predicted using MSE-PRO adopting linear and non-linear analysis at x=18.20m and x=21.00m**

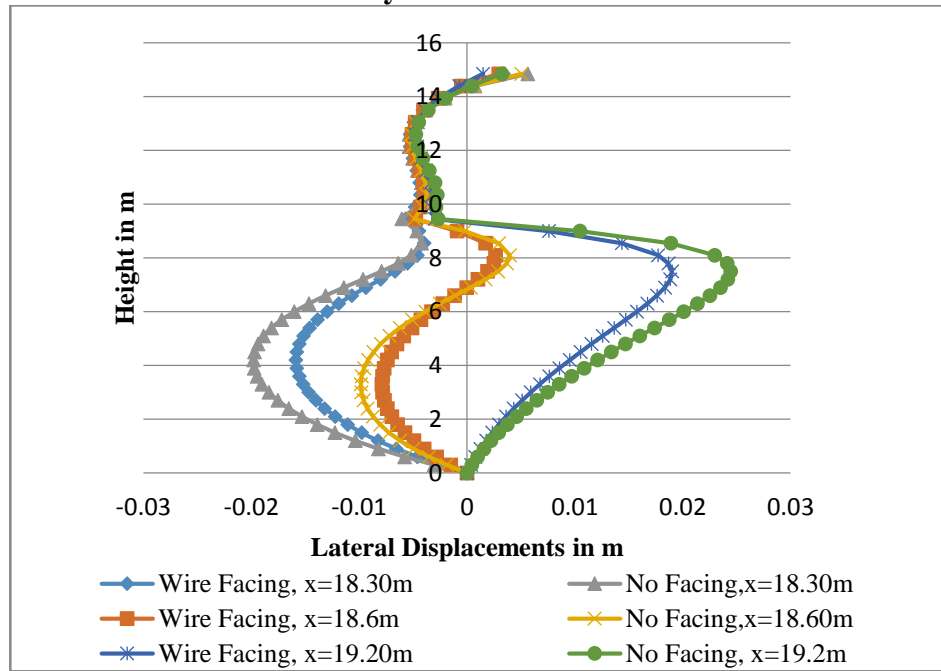


**Fig. 6.17 Lateral displacements predicted using MSE-PRO adopting non-linear analysis with and without wire facing at x=18.30m, x=18.60m and x=19.20m**

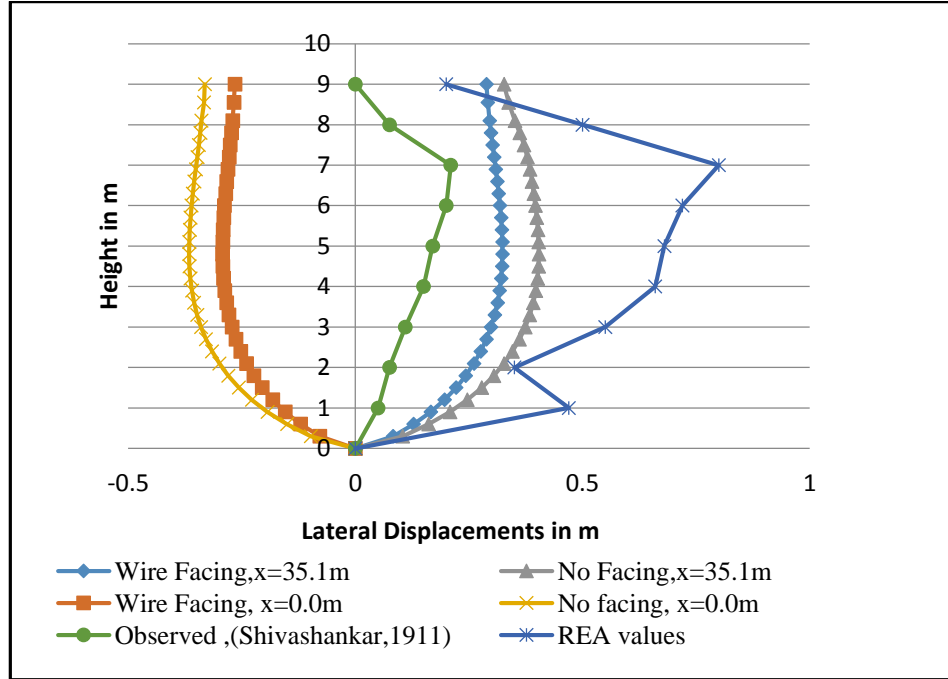


**Fig. 6.18 Lateral Displacements observed in experiments and predicted using MSE-PRO by adopting non-linear analysis at x=0.0m and x=35.1m**

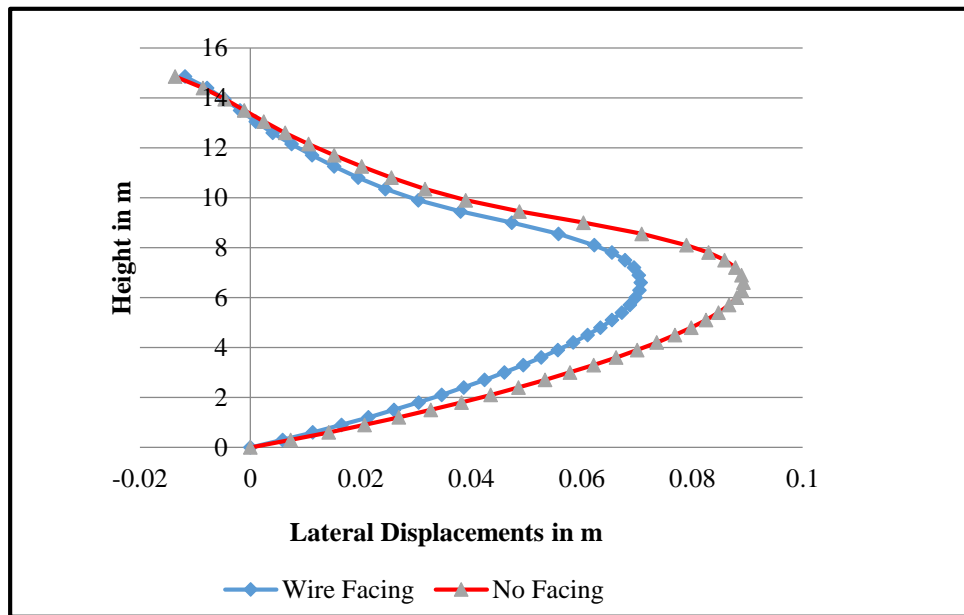


**Fig. 6.19 Lateral Displacements predicted at x=21.00m using MSE-PRO by adopting non-linear analysis**

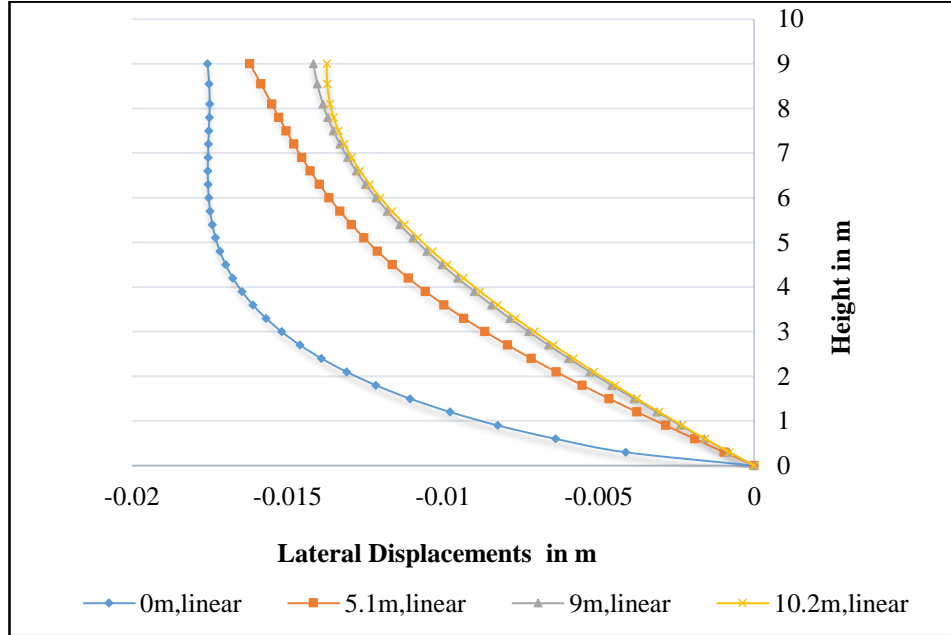


**Fig. 6.20 Lateral Displacements predicted using MSE-PRO by adopting linear analysis at x=0.0m, x=5.1m, x=9.0m, x=10.2m**

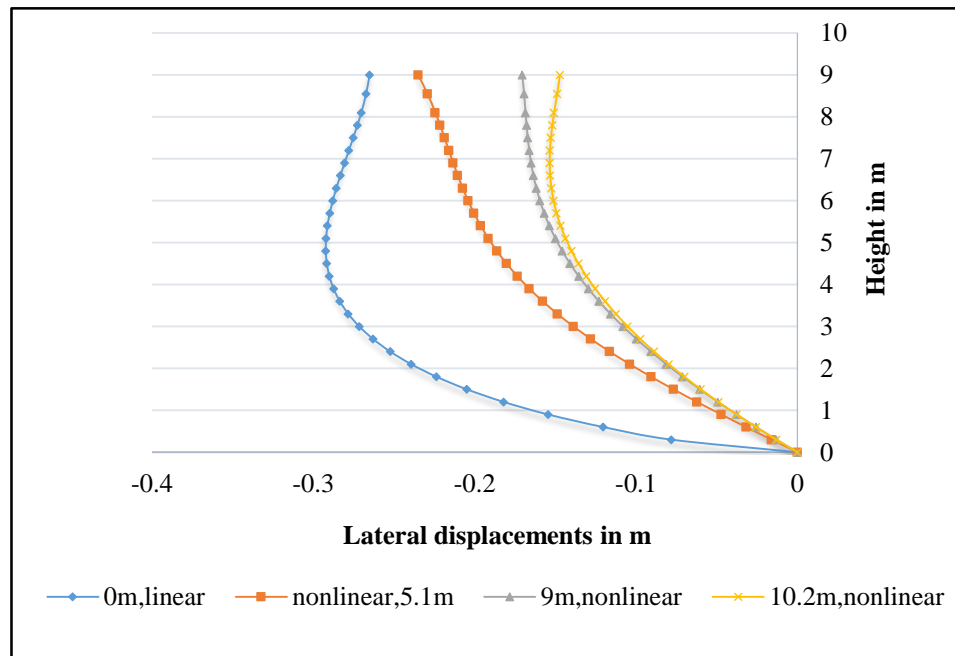


**Fig. 6.21 Lateral Displacements predicted using MSE-PRO by adopting for non-linear analysis at x=0.0m, x=5.1m, x=9.0m, x=10.2m**

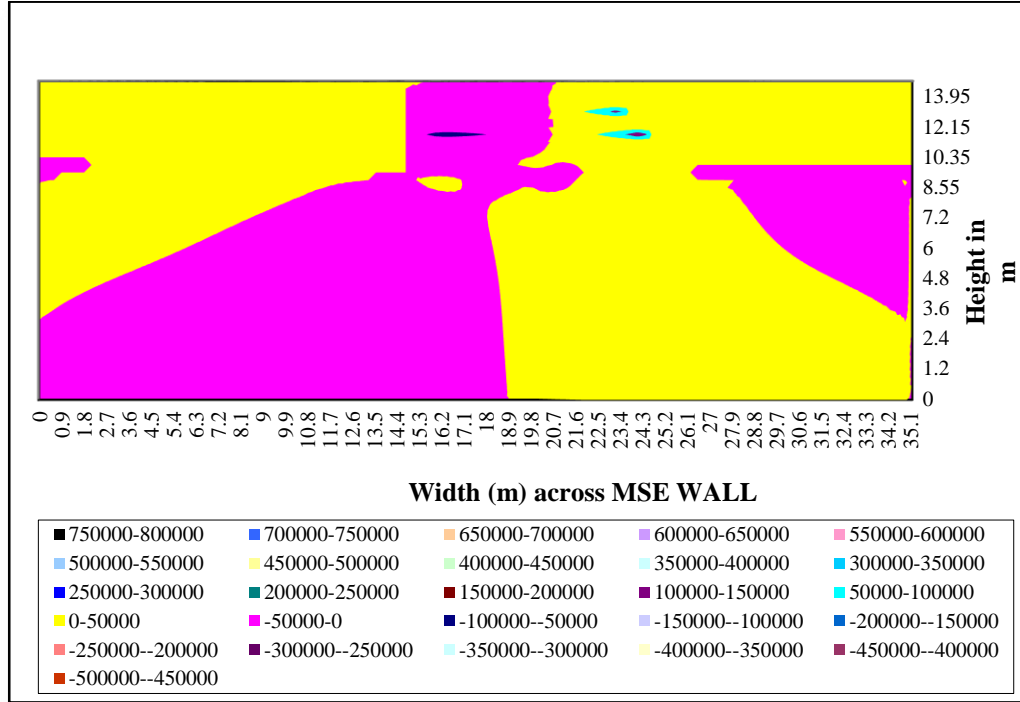


**Fig. 6.22 Shear Stresses (kPa) predicted in MSE Wall at all levels without facing obtained using MSE-PRO by adopting non-linear analysis**

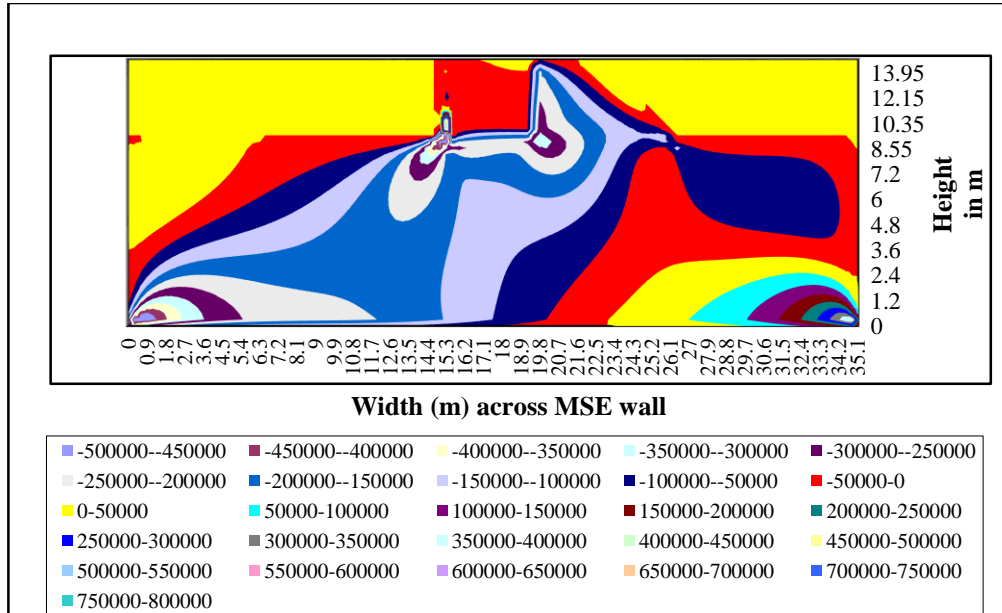


**Fig. 6.23 Shear Stresses (kPa) predicted in MSE Wall at all levels with RC facing obtained using MSE-PRO by adopting non-linear analysis**

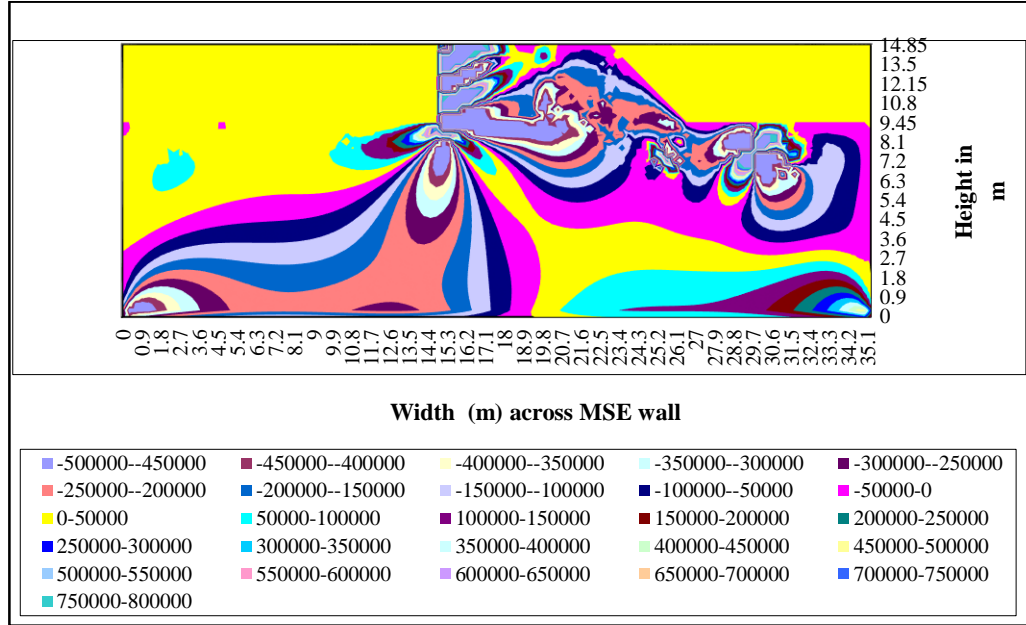


**Fig. 6.24 Shear Stresses (kPa) predicted in MSE Wall at all levels with wire facing obtained using MSE-PRO by adopting non-linear analysis**

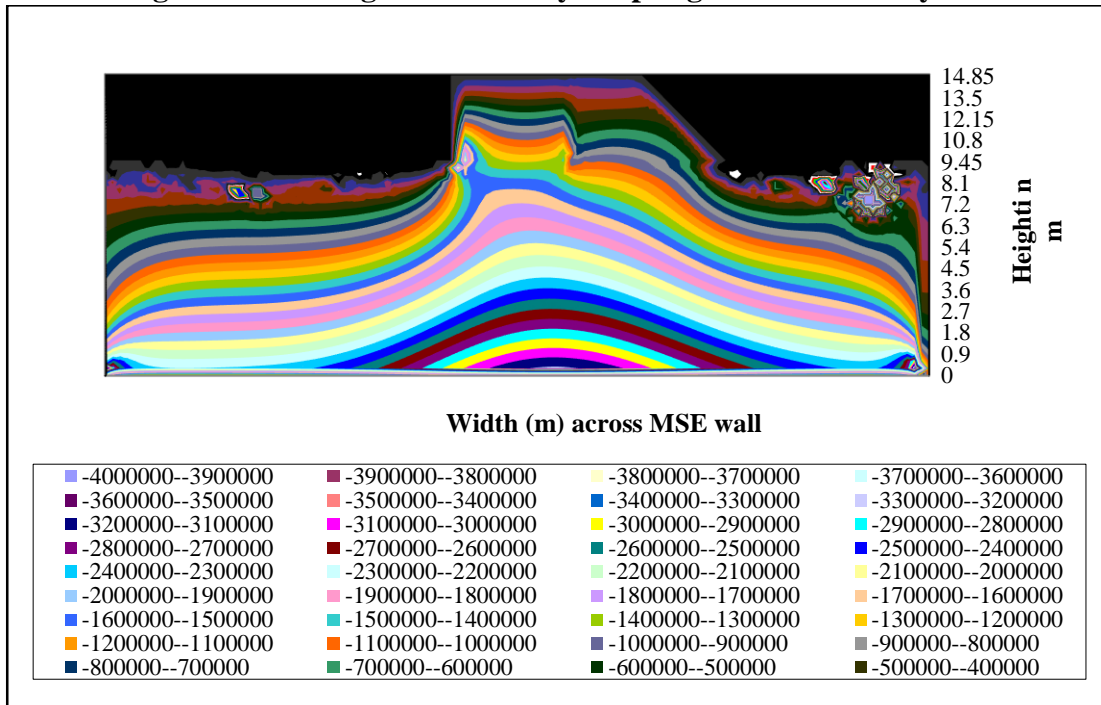


**Fig. 6.25 Vertical Stresses (kPa) predicted in MSE Wall at all levels with wire facing obtained using MSE-PRO by adopting non-linear analysis**

#### 6.4.5 Tables used in and obtained from MSE (AIT) Wall Studies

**Table 6.1. Soil Parameters obtained from experimental studies (Shivashankar,1991) used in the FEM Analysis (Numerical Analysis)**

Parameter	Symbol	Soft clay subsoil	Weathered clay subsoil	Lateritic soil Backfill
Unit weight (kN/m <sup>3</sup> )	$\gamma$	15.0	16	20
Cohesion( kN/m <sup>2</sup> )	c	4.9	11	50.8
Angle of internal friction	$\Phi$	13.5 <sup>0</sup>	20 <sup>0</sup>	38.5 <sup>0</sup>
Young's Modulus ( kN/m <sup>2</sup> )	E	316901	2476479	10985920

**Table 6.2 Properties of Geostrips used for studies on MSE Wall**

Elastic modulus of the strip (GPa)	210
Constitutive model	Nonlinear, Drucker Prager
Width (m)	0.00678
Thickness (m)	0.00573

**Table 6.3 Maximum and minimum Settlements obtained from Experimental observations and predicted using developed software for MSE Wall**

<b>Case</b>	<b>Maximum settlement (m)</b>	<b>Minimum Settlement (m)</b>
Numerical Analysis with wire facing (Nonlinear Analysis)	0.64	0.013
Numerical Analysis without facing (Nonlinear Analysis)	0.825	0.0075
Numerical Analysis without facing ( Linear Analysis)	0.034	0.00073
Numerical Analysis with RC facing ( Non-Linear Analysis)	0.67	----
Observed values from AIT wall test with wire facing	0.74	----
REA Program with facing	0.72	----

**Table 6.4 Settlements obtained from Experimental observations and predicted using developed software MSE-PRO at depths of 0.45m, 3.00m and 6.00m for MSE Wall**

<b>Case</b>	<b>Settlement at 0.45m</b>	<b>Settlement at 3m</b>	<b>Settlement at 6m</b>
Numerical Analysis with facing	0.51m	0.39m	0.195m
Numerical Analysis without facing	0.671m	0.51m	0.25m
Observed values from AIT wall test with facing	0.50m	0.4m	0.225m

Table 6.5 Displacements for different facings and no facing(m)										
Node No	X-Co-ordinate	Y-Co-ordinate	Linear Analysis				Non-Linear Analysis			
			Wire Facing		Wire Facing		RC Facing		No Facing	
			Lateral Disp	Settlements	Lateral Disp	Settlements	Lateral Disp	settlements	Lateral Disp	Settlements
3931	15	14.85	0.004091	-0.08043	-0.05438	-0.52011	-0.08043	-0.523	-0.08043	-0.76307
3932	15.3	14.85	0.004091	-0.08068	-0.05489	-0.52434	-0.08068	-0.52299	-0.08068	-0.76553
3933	15.6	14.85	0.004601	-0.08097	-0.05671	-0.54178	-0.08097	-0.52401	-0.08097	-0.76836
3934	15.9	14.85	0.004858	-0.08131	-0.05818	-0.55514	-0.08131	-0.52619	-0.08131	-0.77163
3935	16.2	14.85	0.004902	-0.08168	-0.05952	-0.56775	-0.08168	-0.52876	-0.08168	-0.7753
3936	16.5	14.85	0.004833	-0.08209	-0.06071	-0.57896	-0.08209	-0.53153	-0.08209	-0.77927
3937	16.8	14.85	0.004714	-0.08252	-0.06176	-0.58873	-0.08252	-0.53433	-0.08252	-0.78341
3938	17.1	14.85	0.004577	-0.08295	-0.06268	-0.59738	-0.08295	-0.53705	-0.08295	-0.78758
3939	17.4	14.85	0.004437	-0.08338	-0.0635	-0.60506	-0.08338	-0.53959	-0.08338	-0.79171
3940	17.7	14.85	0.004301	-0.0838	-0.06422	-0.61188	-0.0838	-0.54187	-0.0838	-0.79572
3941	18	14.85	0.004171	-0.08419	-0.06487	-0.61798	-0.08419	-0.54384	-0.08419	-0.79954
3942	18.3	14.85	0.004046	-0.08456	-0.06546	-0.62347	-0.08456	-0.5455	-0.08456	-0.80313
3943	18.6	14.85	0.003919	-0.08491	-0.06599	-0.62844	-0.08491	-0.54689	-0.08491	-0.8065
3944	18.9	14.85	0.003781	-0.08524	-0.06648	-0.63296	-0.08524	-0.54829	-0.08524	-0.80968
3945	19.2	14.85	0.003615	-0.08555	-0.06691	-0.63702	-0.08555	-0.55052	-0.08555	-0.81263
3946	19.5	14.85	0.003395	-0.08581	-0.06727	-0.64043	-0.08581	-0.56248	-0.08581	-0.81514
3947	19.8	14.85	0.003082	-0.08593	-0.06743	-0.64216	-0.08593	-0.58741	-0.08593	-0.81627
3948	20.1	14.85	0.002814	-0.08594	-0.06751	-0.64306	-0.08594	-0.6097	-0.08594	-0.81645
3949	20.4	14.85	0.00247	-0.08591	-0.06762	-0.64408	-0.08591	-0.62733	-0.08591	-0.81621
3950	20.7	14.85	0.002092	-0.08575	-0.06763	-0.64418	-0.08575	-0.64136	-0.08575	-0.8147
3951	21	14.85	0.001716	-0.08543	-0.06752	-0.6431	-0.08543	-0.65229	-0.08543	-0.8117
3952	21.3	14.85	0.00137	-0.08495	-0.06729	-0.64082	-0.08495	-0.66031	-0.08495	-0.80717
3953	21.6	14.85	0.001077	-0.08432	-0.06693	-0.63741	-0.08432	-0.66601	-0.08432	-0.8012
3954	21.9	14.85	0.000862	-0.08356	-0.06648	-0.63307	-0.08356	-0.66884	-0.08356	-0.79402
3955	22.2	14.85	0.000748	-0.08271	-0.06597	-0.62814	-0.08271	-0.6694	-0.08271	-0.78601
3956	22.5	14.85	0.000788	-0.08196	-0.06556	-0.62413	-0.08196	-0.66912	-0.08196	-0.77889

Note: All the dimensions are in m except node numbers



Table 6.6 Horizontal Stresses (kPa) predicted for MSE wall for Linear and Non-linear Analysis					
Node No	x-co-ordinate	y-co-ordinate	Wire Facing	No Facing	Wire Facing
			Linear Analysis	Linear Analysis	Non-Linear Analysis
3931	15	14.85	-218	-368.3	14297.28
3932	15.3	14.85	-86.29	-4159.81	201921.52
3933	15.6	14.85	390.1	-4363.6	-87066.66
3934	15.9	14.85	891.55	-4753.25	116989.32
3935	16.2	14.85	1395.1	-5337.41	-27733.21
3936	16.5	14.85	1888.68	-6052.93	56122.47
3937	16.8	14.85	2364.54	-6811.99	20976.25
3938	17.1	14.85	2819.1	-7545.41	29012.03
3939	17.4	14.85	3254.08	-8219.26	-436757.43
3940	17.7	14.85	3679.16	-8841.6	-101580.38
3941	18	14.85	4116.98	-9468.16	-60578.89
3942	18.3	14.85	4612.3	-10211.68	149889.75
3943	18.6	14.85	5248.28	-11251.71	551233.95
3944	18.9	14.85	6136.29	-12835.77	708876.65
3945	19.2	14.85	5834.2	-15132.84	-411244.69
3946	19.5	14.85	3813.73	-17099.34	-78028.5
3947	19.8	14.85	7806.87	-14569.99	420678.54
3948	20.1	14.85	5668.69	-31206.42	-130758.94
3949	20.4	14.85	3785.07	-33039.97	3919.66
3950	20.7	14.85	2259.4	-32890.39	-59508.43
3951	21	14.85	1054.2	-31516.46	107108.08
3952	21.3	14.85	172.66	-28831.81	14029.5
3953	21.6	14.85	-373.96	-24737.86	108429.76
3954	21.9	14.85	-575.51	-19283.29	34271.71
3955	22.2	14.85	-834.26	-16141.78	384935.42
3956	22.5	14.85	-869.02	-12078.35	253678.69
3931	15	14.85	-280.51	-472.55	-39510.97
3932	15.3	14.85	-111.18	-5342.89	-19432.88
3933	15.6	14.85	501.32	-5604.64	-10844.88
3934	15.9	14.85	1146.06	-6105.31	-1377.99

Table 6.7 Vertical Stresses (kPa) for MSE Wall for Linear and Non-Linear analysis with and without facing obtained using developed software MSE-PRO					
Node No	x-co-ordinate	y-co-ordinate	Wire Facing	No Facing	Wire Facing
	(m)	(m)	Linear Analysis	Linear Analysis	Non-Linear Analysis
3931	15	14.85	-545.99	-2469.18	-187103.06
3932	15.3	14.85	-936.77	-7764.48	-46562.55
3933	15.6	14.85	-802.33	-7895.17	-293474.08
3934	15.9	14.85	-639.14	-7996.2	-57742.13
3935	16.2	14.85	-468.53	-8112.39	-157916.64
3936	16.5	14.85	-296.19	-8275.54	-143180.77
3937	16.8	14.85	-125.09	-8476.79	-247682.17
3938	17.1	14.85	44.07	-8699.03	-282366.03
3939	17.4	14.85	213.43	-8932	-671495.74
3940	17.7	14.85	389.78	-9180.47	-438882.72
3941	18	14.85	588.42	-9469.28	-309602.1
3942	18.3	14.85	841.2	-9846.93	13650.46
3943	18.6	14.85	1212.94	-10382.31	389774.15
3944	18.9	14.85	1774.96	-11151.72	528113.21
3945	19.2	14.85	163.42	-12015.07	-401019.48
3946	19.5	14.85	-2046.67	-11148.65	-331135.09
3947	19.8	14.85	2543.28	-5315.96	-99187.67
3948	20.1	14.85	1824.47	-16177.58	-437354.17
3949	20.4	14.85	1072.26	-16806.55	-186582.91
3950	20.7	14.85	483.67	-16842.71	-224176.39
3951	21	14.85	20.05	-16506.25	-93043.35
3952	21.3	14.85	-314.3	-15688.75	-144340.99
3953	21.6	14.85	-518.24	-14384.24	-62521.75
3954	21.9	14.85	-602.77	-12763.97	-88840.18
3955	22.2	14.85	-1238.86	-16668.54	234928.53
3956	22.5	14.85	-1199.59	-14031.9	99729.02
3931	15	14.85	-702.01	-3171.04	-510871.7
3932	15.3	14.85	-1204.37	-9972.8	-465235.75
3933	15.6	14.85	-1031.62	-10140.67	-413674.12
3934	15.9	14.85	-821.8	-10270.54	-347940

Table 6.8 Shear Stresses (kPa)for Linear and Nonlinear Analysis for MSE Wall with and without facing obtained using developed software MSE-PRO					
Node No	x-co-ordinate	y-co-ordinate	Wire Facing	No Facing	Wire Facing
			Linear Analysis	Linear Analysis	Non-Linear Analysis
3931	15	14.85	41.37	83.63	-23616.07
3932	15.3	14.85	154.43	131.71	-8092.4
3933	15.6	14.85	193.54	41.1	-18179.64
3934	15.9	14.85	208.59	-187.36	-12884.06
3935	16.2	14.85	212.43	-392.15	-43248.28
3936	16.5	14.85	210.24	-521.06	-34289.87
3937	16.8	14.85	205.46	-572.83	-51150.84
3938	17.1	14.85	201.45	-568.46	-22083.42
3939	17.4	14.85	202.55	-537.51	-32801.07
3940	17.7	14.85	215.43	-513.88	-21847.39
3941	18	14.85	251.18	-537.98	17661.1
3942	18.3	14.85	328.93	-662.2	18967.29
3943	18.6	14.85	482.64	-956.08	3888.64
3944	18.9	14.85	765.48	-1503.8	-47363.85
3945	19.2	14.85	936.85	-2352.05	-88498.02
3946	19.5	14.85	205.76	-3110.21	-150019.13
3947	19.8	14.85	-1523.99	-3105.74	-71581.65
3948	20.1	14.85	-1155.2	-2489.42	11945.99
3949	20.4	14.85	-968.11	-1621.58	-11204.28
3950	20.7	14.85	-794.71	-614.52	-42630.54
3951	21	14.85	-624.27	370.8	-38528.64
3952	21.3	14.85	-438.86	1400.52	-42337.26
3953	21.6	14.85	-222.64	2555.7	-40784.45
3954	21.9	14.85	37.52	3855.05	-33091.27
3955	22.2	14.85	259.21	4448.18	-40832.06
3956	22.5	14.85	286.59	3297.73	-37421.1

#### **6.4.6 Summary of Results of studies carried out on MSE (AIT) Wall**

Figure 6.14 shows lateral displacements predicted at  $x = 0.0\text{m}$  (foundation soil) using MSE-PRO by adopting Non-linear Analysis. Figure 6.15 shows the lateral displacements predicted at  $x=15.0\text{m}$  and  $x=16.20\text{m}$  using MSE-PRO by adopting non-linear analysis.

Figure 6.16 shows lateral displacements predicted at  $x=18.20\text{m}$  and  $x=21.00\text{m}$  using MSE-PRO adopting linear and non-linear analysis. Figure 6.17 shows lateral displacements predicted using MSE-PRO at  $x=18.30\text{m}$ ,  $x=18.60\text{m}$  and  $x=19.20\text{m}$  using MSE-PRO adopting Non-linear Analysis with and without wire facing. It can be observed that till the end of reinforcement, the wall moves to the left. Beyond the length of reinforcement, the wall moves to the right. For the MSE (AIT) wall, up to 66.7% of the length of the reinforcement the wall moves to the left. Figure 6.18 shows the lateral displacements predicted at  $x=0.0\text{m}$  and  $x=35.1\text{m}$  (extreme ends of the MSE wall) using MSE-PRO by adopting non-linear analysis.

Figure 6.19 shows lateral displacements predicted at  $x=21.00\text{m}$  using MSE-PRO by adopting non-linear analysis. Figure 6.20 shows the lateral displacements predicted at  $x=0.00\text{m}$ ,  $x=5.1\text{m}$ ,  $x=9.0\text{m}$ ,  $x=10.2\text{m}$  using MSE-PRO by adopting for linear analysis obtained from MSE-PRO. Figure 6.21 shows the lateral displacements predicted at  $x=0.00\text{m}$ ,  $x=5.1\text{m}$ ,  $x=9.0\text{m}$ ,  $x=10.2\text{m}$  using MSE-PRO by adopting for non-linear analysis  $x=18.90\text{m}$ .

Figure 6.22 shows shear stresses predicted in MSE wall at all levels without any facing obtained using MSE-PRO by adopting nonlinear analysis. Figure 6.23 shows the shear stresses predicted in MSE wall at all levels with RC facing obtained using MSE-PRO by adopting nonlinear analysis. Figure 6.24 shows the shear stresses predicted in MSE Wall at all levels with wire facing obtained using MSE-PRO by adopting nonlinear analysis. Figure 6.25 shows the vertical stresses predicted in MSE wall at all levels with wire facing obtained using MSE-PRO by adopting nonlinear analysis. Section 6.4.7 presents the tables used in MSE (AIT) wall studies.

Table 6.3 shows the maximum and minimum settlements obtained from experimental observations and predicted using developed software. Table 6.4 shows the settlements obtained from Experimental observations and predicted using developed software at 0.45m, 3.00m and 6.00m.

Table 6.5 shows the lateral displacements and vertical settlements predicted using the developed software MSE-PRO. The results show that the linear analysis for the AIT wall with the wire facing predict the least lateral displacements and vertical settlements. While the maximum displacements and settlements are obtained for the nonlinear analysis of the MSE wall without the wall facing.

Table 6.6 shows the horizontal stresses predicted using the developed software MSE-PRO for the MSE Wall for linear and non-linear analyses with and without facing. Table 6.7 shows the vertical stresses predicted using the developed software MSE-PRO for the MSE Wall for linear and non-linear analyses with and without facing. Table 6.8 shows the shear stresses predicted using the developed software MSE-PRO for the MSE Wall for linear and non-linear analyses with and without facing.

#### **6.4.7 Conclusions of Studies on MSE Wall**

- 1) The MSE full scale wall test results, the settlements predicted using REA software and the results from the developed software MSE-PRO show that the facing does influence the settlements.
- 2) The developed software shows that the wire facing reduces the maximum settlement of soil by 26% when compared with that without facing predicted using MSE-PRO.
- 3) The experimental observations show that the wire facing reduces the maximum settlement of soil by 13% when compared with that without facing predicted using MSE-PRO.
- 4) The settlements predicted using REA software show that the wire facing reduces the maximum settlement of soil by 16% when compared with that without facing predicted using MSE-PRO.

- 5) The difference in the settlements predicted by developed software MSE-PRO and REA can be attributed to the difference in modelling and difference in the constitutive models adopted.
- 6) The experimental results of the MSE wall, show the maximum settlements probably because FEM models are stiff and the steel grid reinforcement used is modelled as equivalent strips.

## **CHAPTER 7**

### **STUDIES ON REINFORCED FOUNDATION SOIL**

#### **7.1 GENERAL**

Scarcity of land with good bearing capacity is one of the major problems the world faces now. The construction of structures on weak ground often requires the soil to be improved in order to ensure the safety and the stability of the structures. Ground improvement in granular soils can be achieved by different methods such as vibro-flotation, compaction piles, compaction with explosives, reinforced soil, grouting etc. The method of ground improvement technique adopted depends on the soil to be treated and availability of material required for improving the soil and also on the cost effectiveness.

Many researches have been conducted to investigate the behavior of reinforced soil foundations (RSF). These works have indicated that the reinforced soil shows significant increase in bearing capacity and there is a reduction of the settlement of soil foundations. Research has shown that the reinforced soil foundations are cost-effective solution to increase the ultimate bearing capacity and/or reduce the settlement of shallow footings when compared to the conventional methods, such as replacing natural soils or by increasing footing dimensions.

In this part of the research, an effort has been made to study the improvement in load bearing capacity and settlement behaviour of square and circular footings on a reinforced granular bed overlying weak soil. The test results have also been used to compute the modulus of subgrade reaction of reinforced soil foundation. The following parameters have been studied.

- 1) Effect of type of footing
- 2) Effect of type of geosynthetics

- 3) Effect of number of reinforcement layers
- 4) Effect of length of reinforcement
- 5) Effect of varying the depth of top geosynthetic layer

## **7.2 EXPERIMENTAL STUDY**

Ever since and after Binquet and Lee (1975a) conducted an experimental study to evaluate the bearing capacity of metal strips on reinforced sandy soil, numerous experimental and numerical studies on the bearing capacity of footings on reinforced sandy soil have been carried out.

### **7.2.1 Experimental Programme**

The experimental programme involves a series of load tests on a model footing resting on unreinforced and reinforced granular beds overlying weak soil. In this study, experiments are conducted mainly in four different cases. They are:

Case (1): Unreinforced and Reinforced soil foundation, overlying loose granular bed only under square footing.

Case (2): Unreinforced and Reinforced soil foundation, overlying dense granular bed under both the circular and square footings.

Case (3): Unreinforced and Reinforced soil foundation, overlying weak soil under both the circular and square footings.

Case (4): Unreinforced and Reinforced soil foundation overlying weak soil for different  $u/B$  ratios under both the circular and square footings.

Details of the materials used, test setup, experimental programme and test procedures are presented in Table 7.1.

### **7.2.2 Properties of materials used**

Sand and the weak silty soil used in the experiments were tested in the laboratory



for various parameters. The properties of soil and sand used are presented in Table 7.2. The reinforcements used are Geogrids and Geotextiles. The properties of geogrids and geotextiles are given in Tables 7.3 and 7.4. The geogrid is a weak geogrid of tensile strength 7.6kN/m for the purpose of laboratory scale model tests.

Laboratory scale plate load tests are carried out on

- 1) Model square footing made of steel
- 2) Model circular footing made of steel.

The dimensions of the model footing are 0.10m x 0.10m x 0.020m thick square footing and 0.10m dia x 0.02m thick circular footing. The model footing is kept on the surface during all the tests. The test tank is made of Ferrocement having internal dimensions of 0.9 m x 0.9 m in plan and 0.8m deep. The test tank has been designed in such a way that both the length and width are nine times that of the footing dimensions so that there will not be any effect on the boundaries while conducting the tests.

The reinforcements used are:

- a) Single layer (Geogrid / Geotextile, 4B x 4B and 8B x 8B)
- b) Double layer (Geogrid / Geotextile, 4B x 4B and 8B x 8B)
- c) Three layers (Geogrid / Geotextile, 4B x 4B and 8B x 8B)
- d) Four layers (Geogrid / Geotextile, 4B x 4B and 8B x 8B)

### **7.2.3 Test Procedure**

The load is applied using a hand operated jack of 50kN capacity. The load is measured using a proving ring and deformation is measured using two dial gauges placed diametrically opposite to each other. Preparation of underlying soil in all the tests involved compaction using a rammer. The granular foundation bed was prepared using a plate vibrator. Figure 7.1 shows the sectional elevation of the test setup for granular foundation bed for both the reinforced and unreinforced cases. Figure 7.2 depicts the sectional elevation of the test setup for weak silty soil as foundation bed. Refer Fig 7.3 for the geometric parameters for a reinforced soil foundation.

The line diagrams of the experimental setup and loading arrangement are as shown in the Figs 7.4a and 7.4b. Figures 7.5a and 7.5b show the photographs of the loading setup. Figures 7.6a and 7.6b show the plan of different sizes of geosynthetics used. In the literature, it is reported that the optimum depth of placement of the first reinforcement layer is  $0.2B$  to  $0.5B$  ( $B$  is the width of the footing) (Sharma et al., 2009). The depth of reinforcement from the base of footing was adopted as  $0.5B$ . The tests were also conducted for various depths of top layer reinforcement as  $0.2B$ ,  $0.4B$ ,  $0.6B$ ,  $0.8B$ ,  $B$ .

#### **7.2.4 Test Details**

At first, the tank is filled with loose sand in the required amount and required height ( $0.80\text{m}$ ) based on its predetermined density. It is compacted suitably to achieve the required density and load is applied. The model footing is kept on the surface during all the tests. An extra steel plate of  $20\text{mm}$  thickness and having the same length and width of footing sizes is placed at the top of the footing so that there will not be any bending effect while loading. The load is measured using a proving ring and deformation using two dial gauges placed diametrically opposite to each other. The load is applied using a hand operated jack of  $50\text{kN}$  capacity. The corresponding settlement is measured using the two dial gauges and their average value is obtained at regular intervals till failure. The sand is removed and refilled. It is reinforced with 1, 2, 3 and 4 layers of Geogrid and the above test is repeated maintaining the predetermined density. The above test is repeated similarly for dense sand for both the reinforced and unreinforced cases.

In case of tests on the weak silty soil, it is filled in the tank upto the required level with compaction done in layers by using circular steel hammer having weight of  $148\text{N}$ , to achieve predetermined density. Then sand is filled up to the bottom level of the reinforcement and compacted by using plate vibrator. The reinforcement is placed with its centre exactly beneath the jack and load applied at regular intervals and the corresponding settlement is recorded. Load is applied

at regular intervals and the corresponding settlement is measured using the two dial gauges

In this study, the depth of the first layer of reinforcement is adopted as  $0.5B$  (where  $B$  is the width of footing) and for the remaining reinforcements 2, 3, 4..... $N$  at different layers, each depth ( $d$ ) of the reinforcement layer from the base of a footing can be calculated by using equation (7.1) given as

$$d = u + (N-1) \times h \quad (7.1)$$

Width or layer of each reinforcement layer ( $b$ ) = 800mm (0.8m)/ 400mm (0.4m),

$b/B = 8$  &  $4$ ,  $h/B = 5$ ,  $u/B = 5$ ,  $d/D = 0, 0.625, 0.125, 0.187, \& 0.25$

' $d$ ' is the depth of reinforcement layer from the base of the footing,  $u$  is the depth of the first layer of reinforcement from the base of the footing,  $N$  is the number of reinforcement layers provided, and  $h$  is the distance between reinforcement layers.

Refer Fig. 7.3

In the case of studies on different  $u/B$  ratios, experimental procedure adopted is similar as in previous cases. The only difference in this case is that only one layer of reinforcement is used at different  $u/B$  ratio of 0.2, 0.4, 0.6, 0.8, and 1.0. Experiments are conducted for two different kinds of reinforcement for two different lengths under two different types of footings circular and rectangular. Load is applied at regular intervals and the corresponding settlement is measured using the two dial gauges and their average value is obtained at regular intervals till failure for all the different cases.

## **7.2.5 Results of Experimental Studies**

### **7.2.5.1 Improvement in Bearing Capacity**

The various figures related to experimental and numerical studies are presented in Section 7.2.6. The results obtained from the experiments conducted on granular bed underlain by weak silty soil for both the unreinforced and reinforced cases have been presented in section 7.2.7. The tables related to Reinforced soil foundation are

presented in Section 7.4.10. Figure 7.7 depicts the settlement/width ratio versus stress plotted for reinforced soil (geogrid of size 0.40m x 0.40m, 4B x 4B) and unreinforced soil under circular footing. Settlement/width ratio of footing vs stress curves are plotted as shown in the Figs. 7.7 to 7.13 for geogrids and geotextiles of two different sizes under square and circular footings with weak silty soil as foundation bed. Figure 7.7 shows that the stiffness of the soil increases with the increase in the number of reinforcement layers.

The results of experiments conducted on loose and dense sand using geogrids of size 0.4m x 0.4m (4B x 4B) under square footing have been plotted in Fig. 7.14. It is clearly observed that the addition of reinforcement improves the bearing capacity of the soil. The load carrying capacity of footing is also significantly improved.

It is observed that the maximum improvement is when four layers of geogrids are used. It is also observed that the dense sand foundation bed shows a significantly more load carrying capacity (nearly twice) when compared with the loose sand bed. Reinforced soil (with 4 layers of geogrids) shows a remarkable increase in the load carrying capacity (nearly two times as for Unreinforced sand bed). Bearing capacity ratio (BCR) is defined as the ratio of bearing capacity of reinforced soil to that of unreinforced soil. Figure 7.16 depicts the plot of bearing capacity ratio vs  $u/B$  (top layer / width) ratio for the reinforced granular bed underlain by weak silty soil. Figure 7.17 shows the plot of BCR vs number of reinforcement layers.

The BCR for geogrids and geotextiles under square and circular footing for different  $u/B$  ratios have been presented in Table 7.5. Table 7.6 illustrates the BCR obtained for geogrids and geotextiles under square and circular footing for varying number of reinforcement layers. The settlements under square and circular footing for geotextiles of sizes 0.40m x 0.40m (4Bx4B) and 0.80m x 0.80m (8Bx8B) and for unreinforced silty soil also have been presented in Table 7.7.

### **7.2.5.2 Effect of Reinforcement on u/B ratio and BCR values**

It is observed from Fig. 7.15 that the reinforced granular bed underlain by weak silty soil for all the lengths and both the types of reinforcements show that the maximum BCR is achieved for depth of top layer of reinforcement/width (u/B) ratio of footing of 0.40. Figure 7.16 shows that BCR is maximum for 4 layers of reinforcement for both the geogrids and geotextiles under circular footing. Theoretically, it is well established that square footings perform better than circular footings. But model plate load tests show that circular footings give higher Bearing capacity, probably due to the boundary effects.

- Improvement in load carrying capacity was observed to be considerable in reinforced soil in comparison with the unreinforced soil for varying number of reinforcements.
- Improvement in load carrying capacity was observed to be considerable in reinforced soil over the unreinforced soil for all types of reinforcement.
- Load carrying capacity of soil below circular footing for 4 layers of geogrid is the maximum for dense sand as foundation bed.
- Geogrid /geotextile beyond the effective length (4.0~6.0B) provides negligible reinforcement benefit as reported in literature and also proved by our experiments.
- The least settlement is observed for Reinforced dense sand with 4 layers of reinforcement and the maximum settlement is observed for loose sand.

### 7.2.6 Figures Plotted in Reinforced Soil Foundation

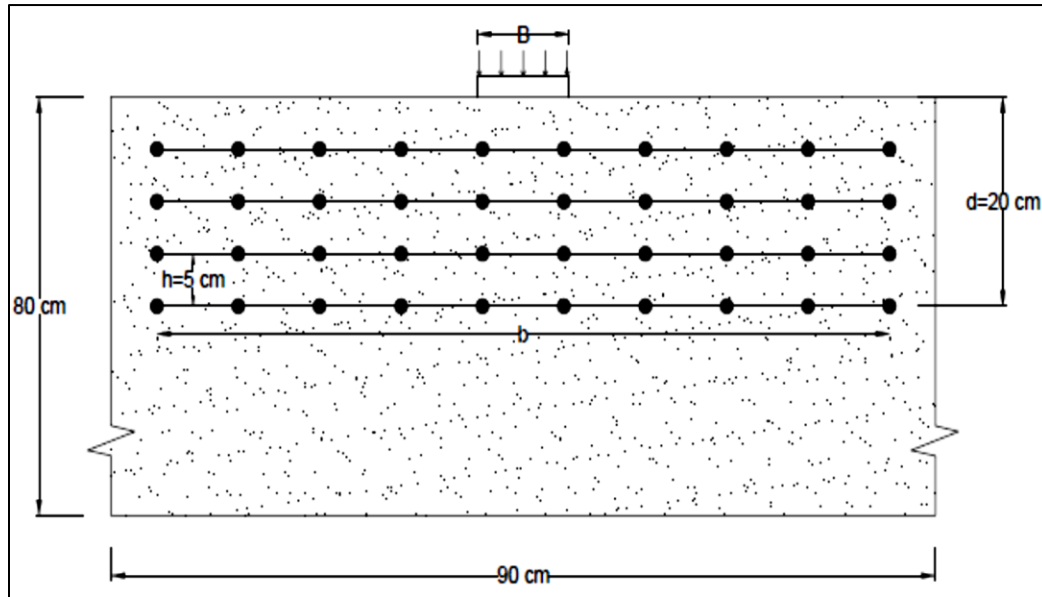


Fig. 7.1 Sectional Elevation of geogrids placed on weak foundation bed

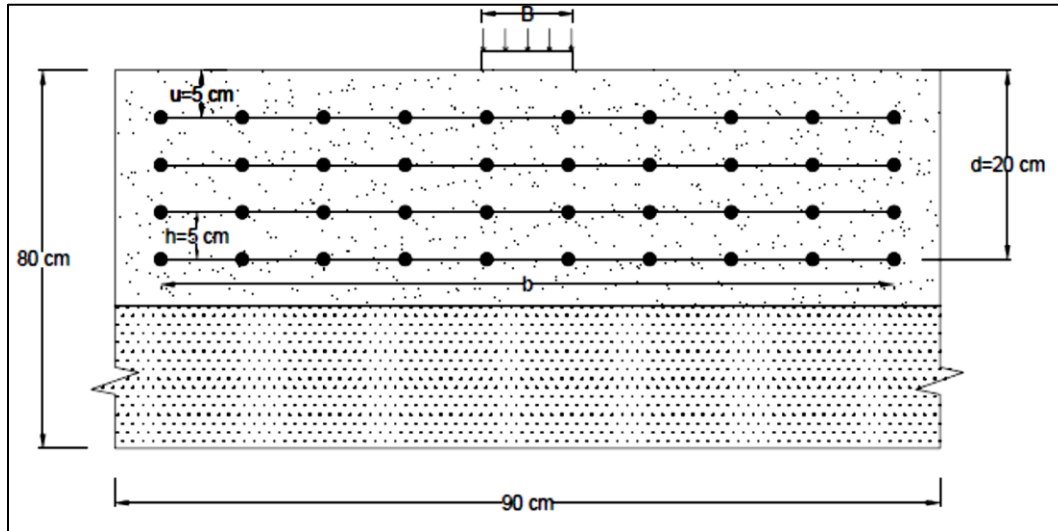
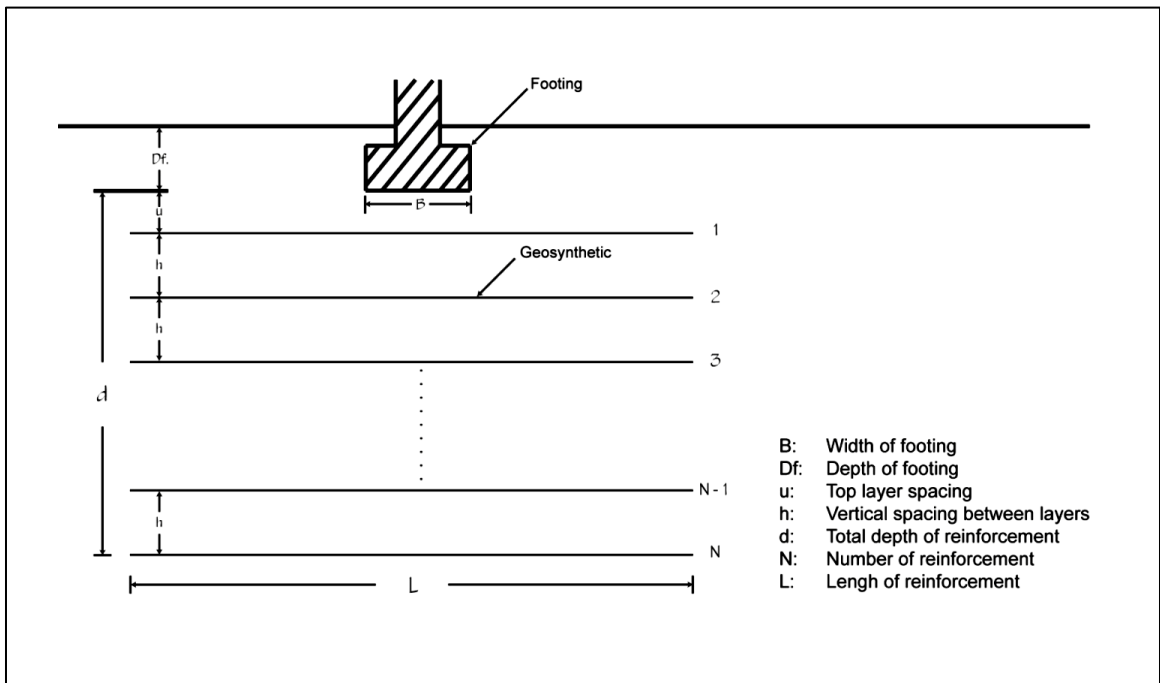
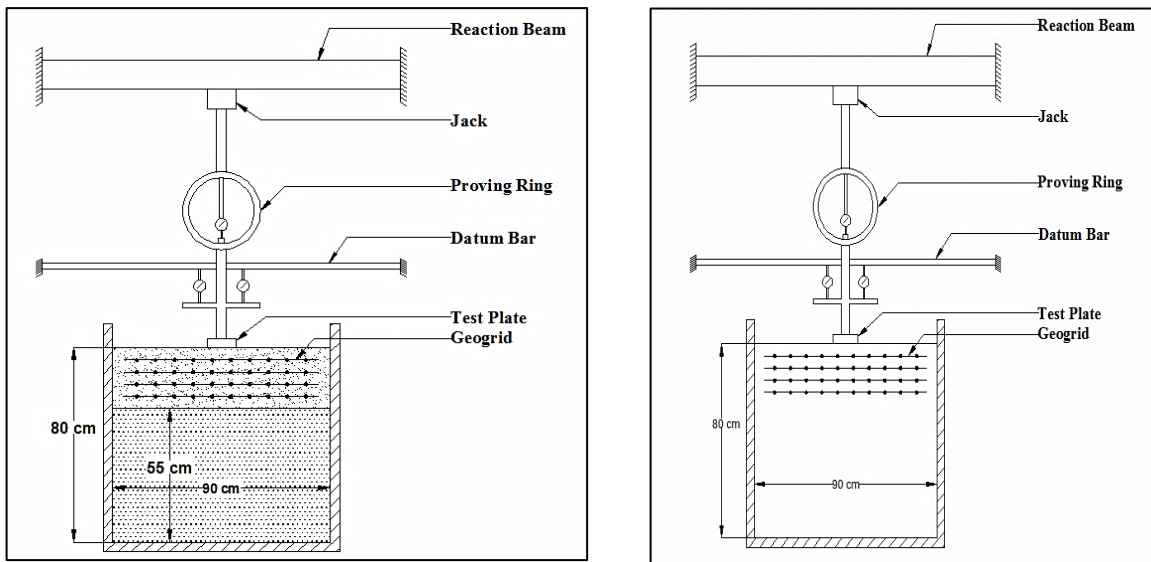


Fig. 7.2 Sectional Elevation of geogrids placed on weak foundation bed



**Fig. 7.3 Geometric parameters for reinforced soil foundation (Gu-Jie, 2011)**



**Fig. 7.4 Loading arrangement along with the test set-up for a) weak silty soil b) sandy soil**

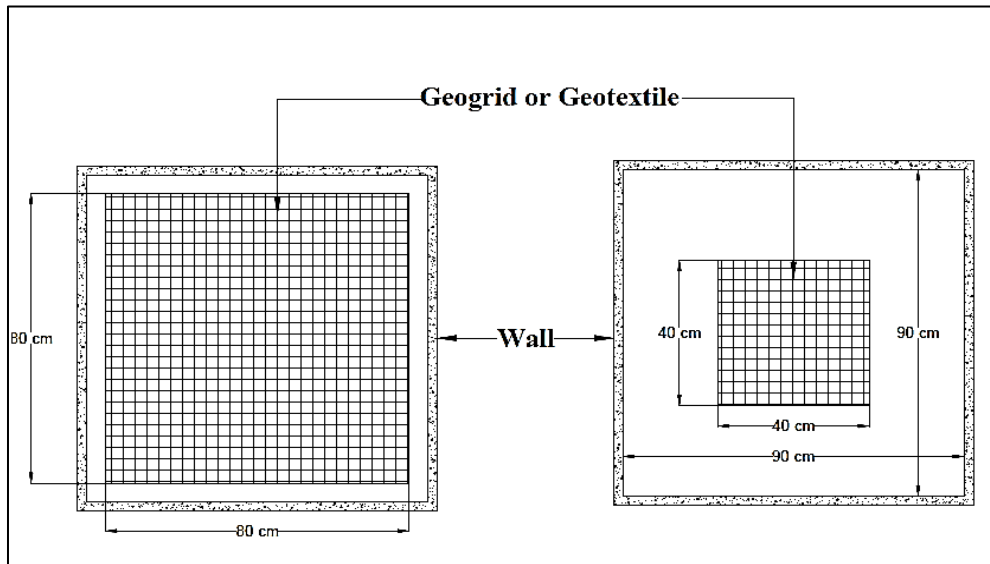


a



b

**Fig. 7.5 a,b Photographs of the Test Setup**



a

b

**Fig. 7.6 Plan of two sizes of Geosynthetics**  
 a) (0.80m x 0.80m, 8B x 8B) and b) (0.40m x 0.40m, 4B x 4B)



### 7.2.7 Graphs Plotted in Reinforced Soil Foundation

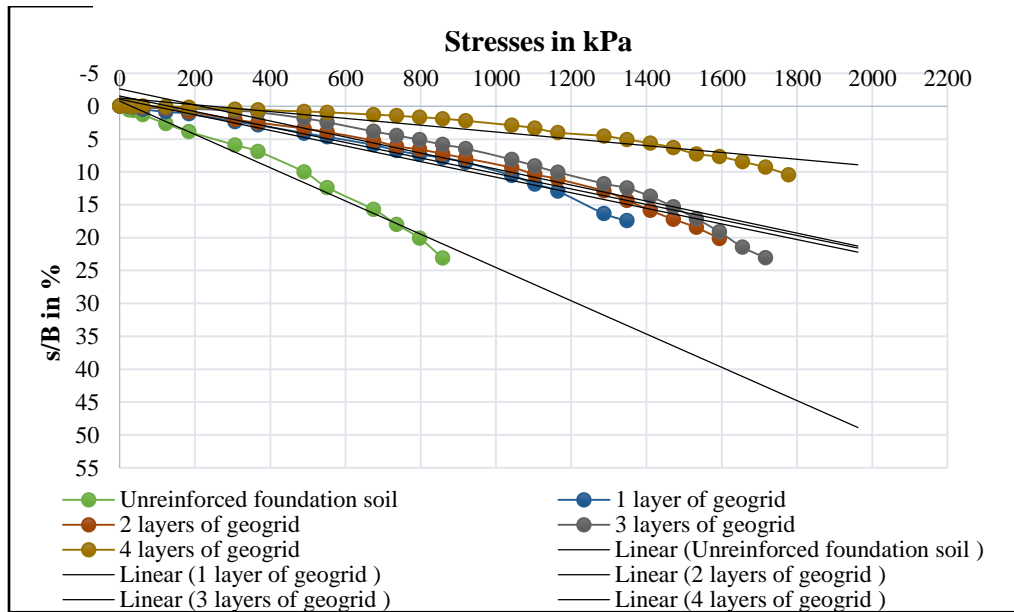


**Fig. 7.7 Settlement/width ratio of footing vs. stresses for unreinforced and reinforced granular bed overlain by weak silty soil under circular footing (Geogrid of size 0.40m x 0.40m, 4B x 4B)**

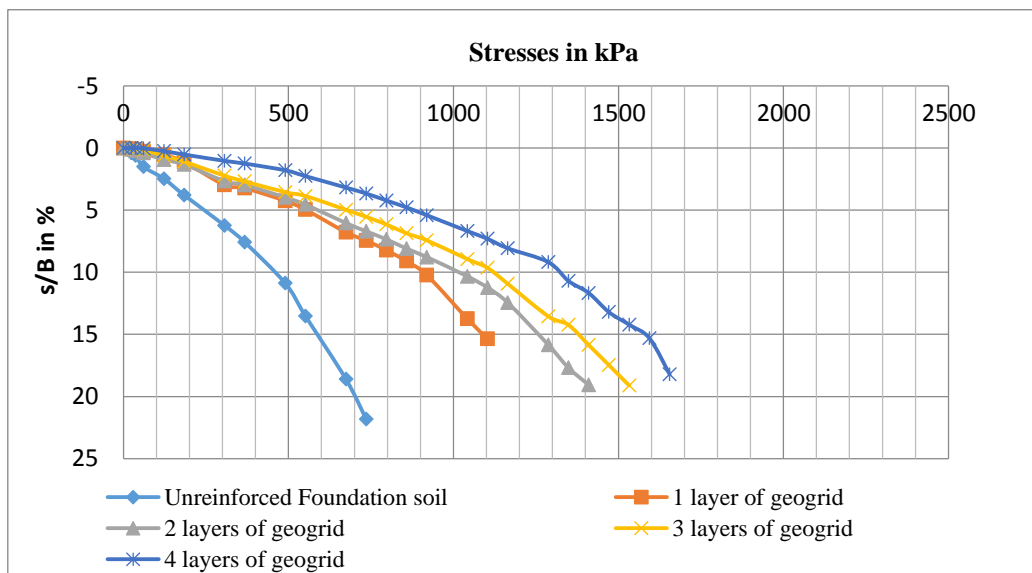


**Fig. 7.8 Settlement/width ratio of footing vs. stresses for unreinforced and reinforced granular bed overlain by weak silty soil under square footing (Size of Geogrid 0.4m x 0.4m, 4B x 4B)**

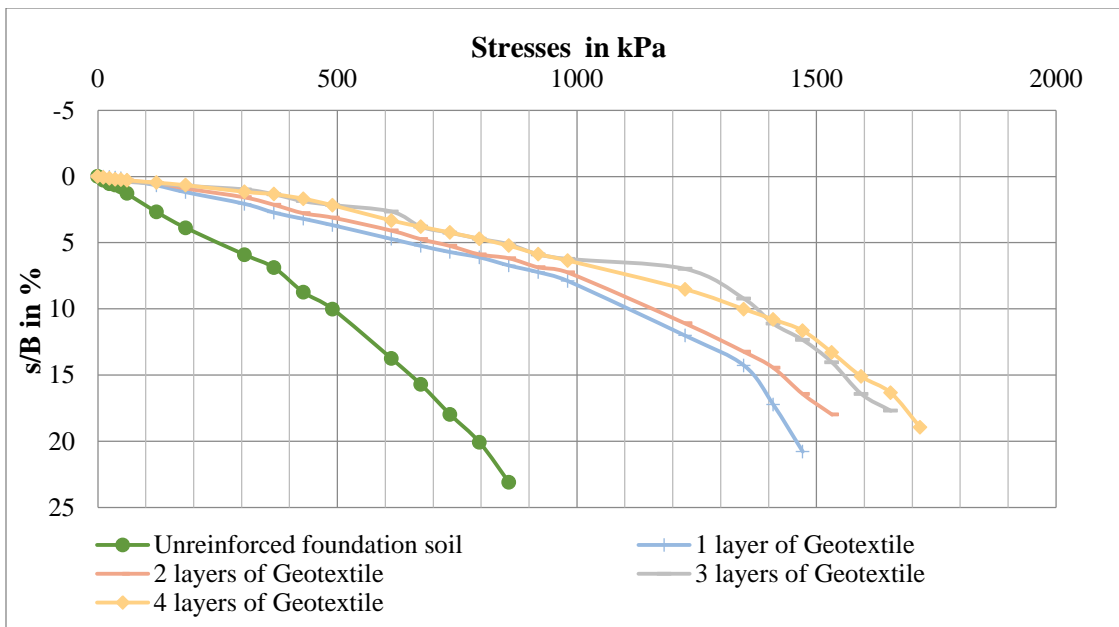


**Fig. 7.9 Settlement/width of footing ratio vs. stresses for unreinforced and reinforced granular bed overlain by weak silty soil under circular footing (Geotextile 0.4m x 0.4m, 4B x 4B)**

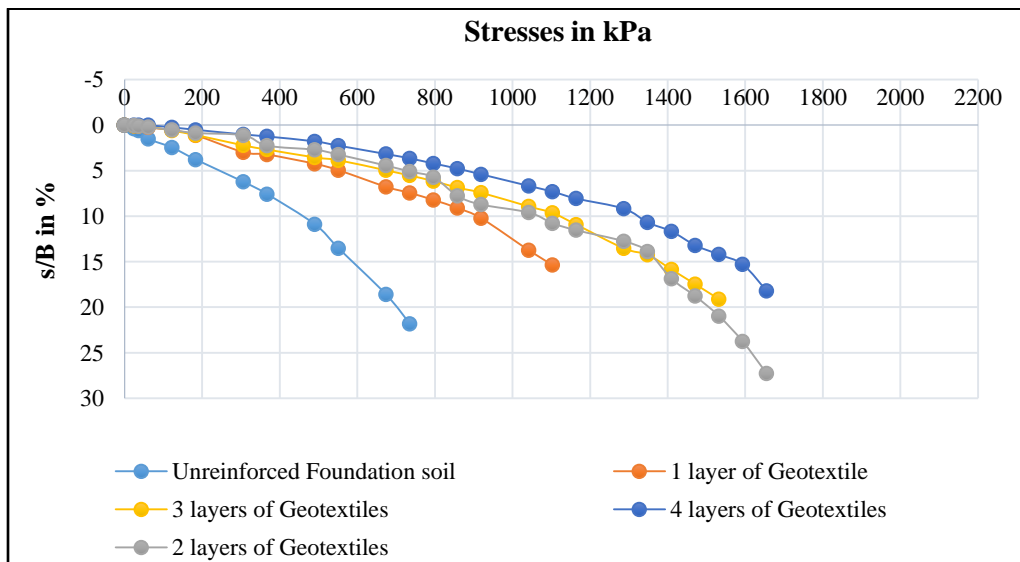


**Fig. 7.10 Settlement/width ratio of footing vs. stresses for unreinforced and reinforced granular bed overlain by weak silty soil under circular footing (Geotextiles of size 0.8m x 0.8m, 8B x 8B)**

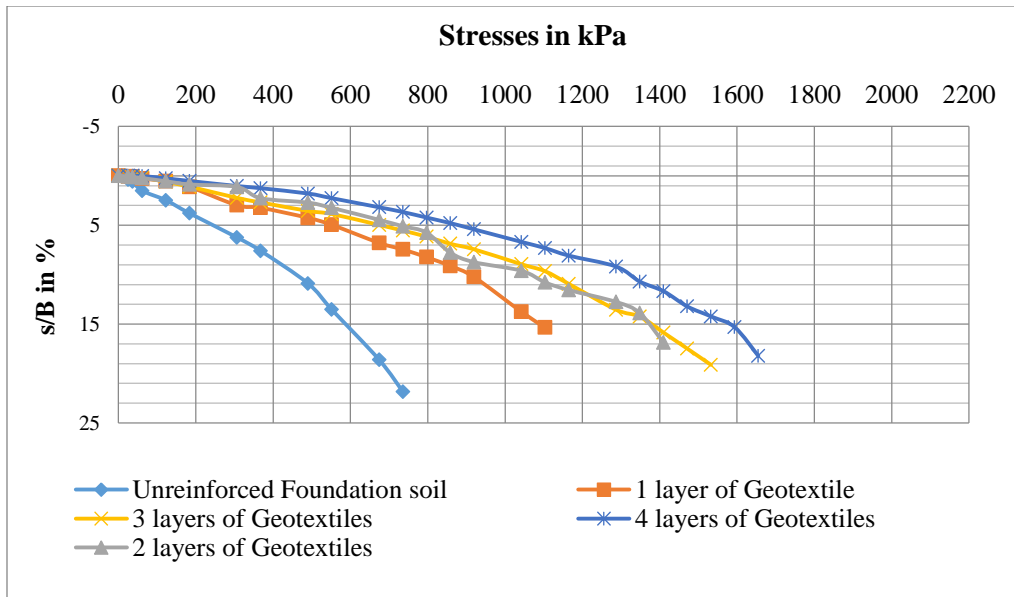


**Fig. 7.11 Settlement/width ratio of footing vs. stresses for unreinforced and reinforced granular bed overlain by weak silty soil under square footing (Geotextiles of size 0.8m x 0.8m, 8B x 8B)**

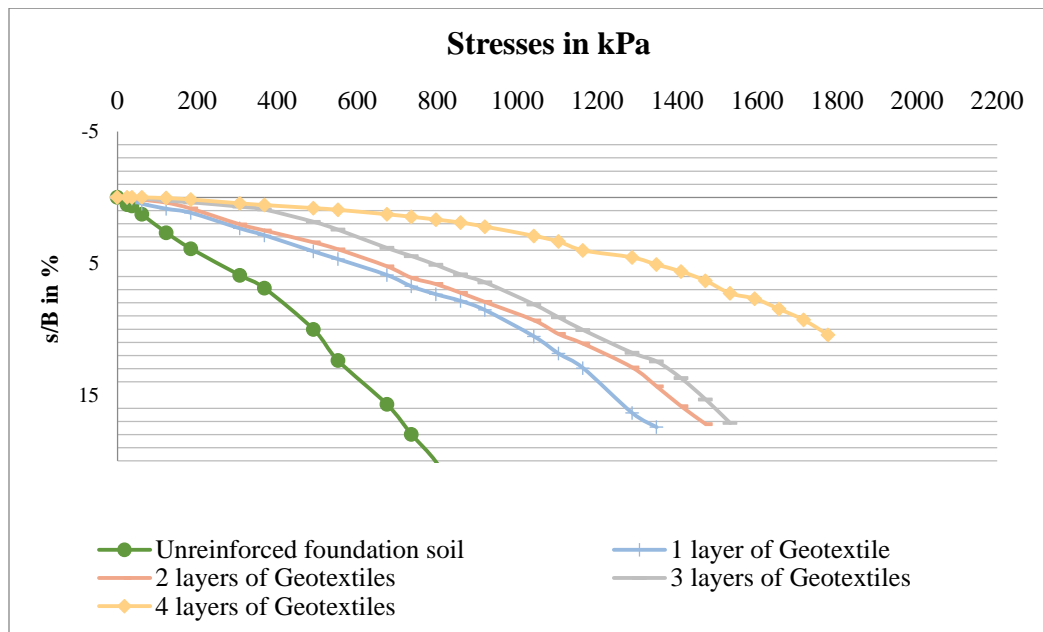


**Fig. 7.12 Settlement/width ratio of footing vs. stresses for unreinforced and reinforced granular bed overlain by weak silty soil under square footing (Size of Geotextile 0.4m x 0.4m, 4B x 4B)**

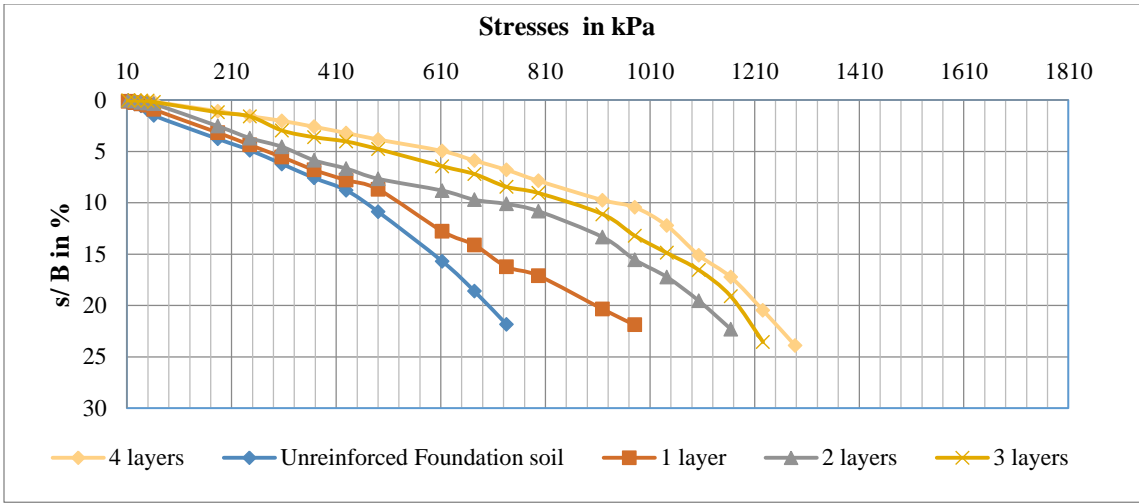


**Fig. 7.13 Settlement/width ratio of footing vs. stresses for unreinforced and reinforced granular bed overlain by weak silty soil under square footing (Size of Geotextile 0.8m x 0.8m, 8B x 8B)**

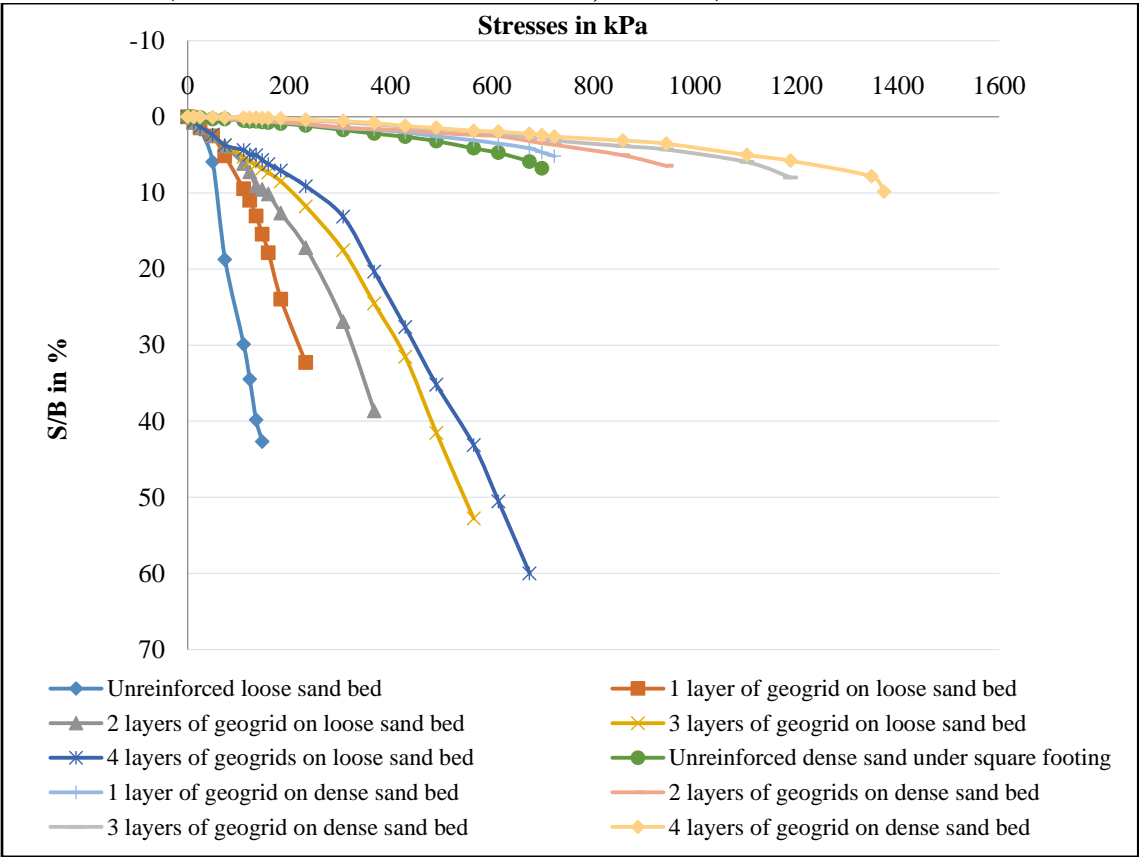


**Fig. 7.14 Settlement/width ratio of footing vs. stresses for Loose and Dense Sand for Geogrids (0.4m x 0.4m, 4B x 4B) under square footing**

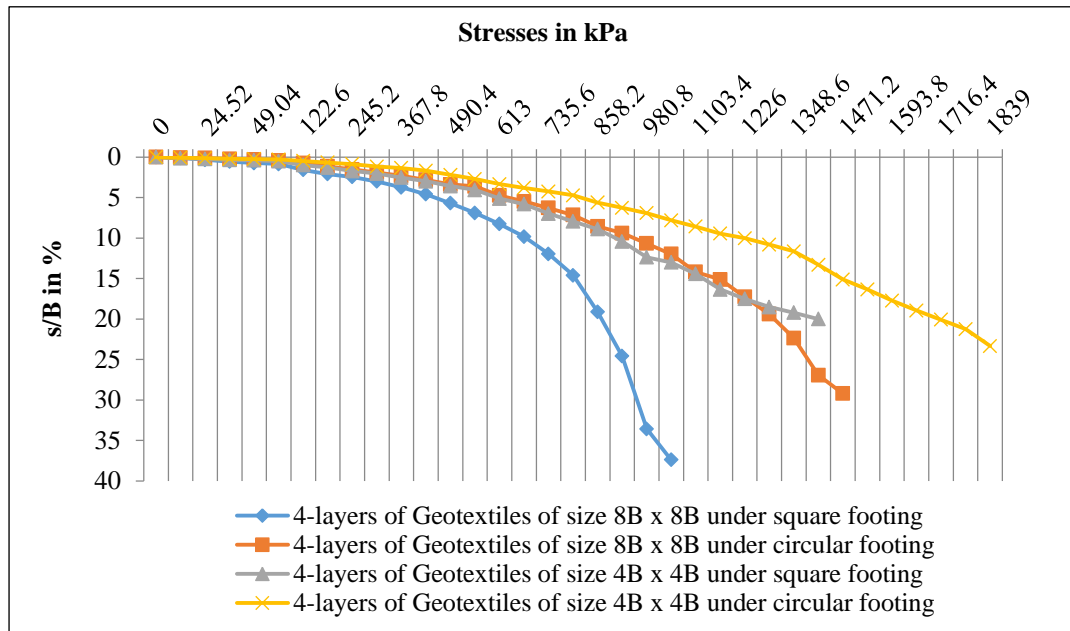


**Fig. 7.15 Settlement/width of footing ratio vs. stresses for unreinforced and reinforced granular bed overlain by weak silty soil under square and circular footing (Geotextiles 4B x 4B and 8B x 8B)**

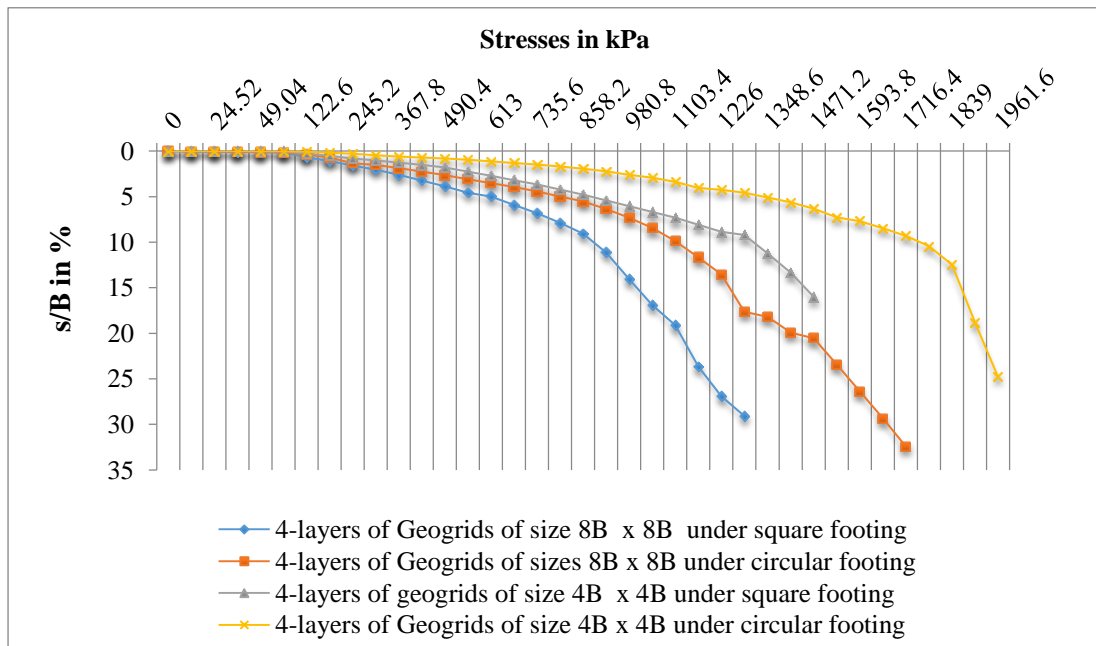


**Fig. 7.16 Settlement/width of footing ratio vs. stresses for unreinforced and reinforced granular bed overlain by weak silty soil under square and circular footing (Geogrids 4B x 4B and 8B x 8B)**

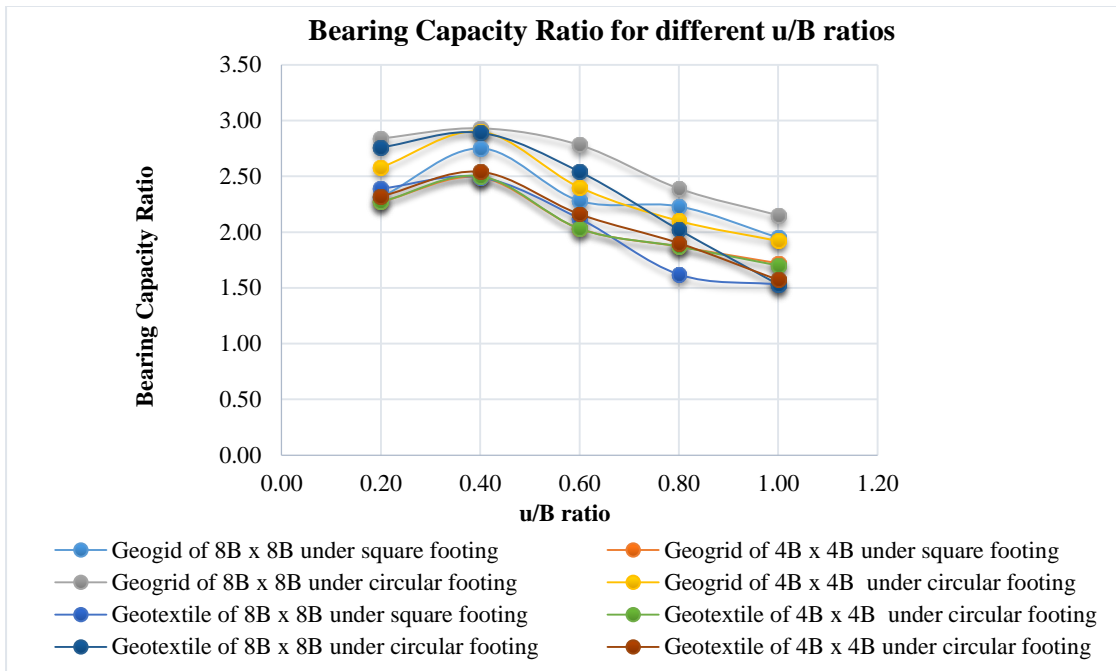


**Fig. 7.17 Bearing Capacity Ratio for different u/B ratios for reinforced granular bed overlain by weak silty soil under square and circular footing (Geogrids and Geotextiles 4B x 4B and 8B x 8B)**

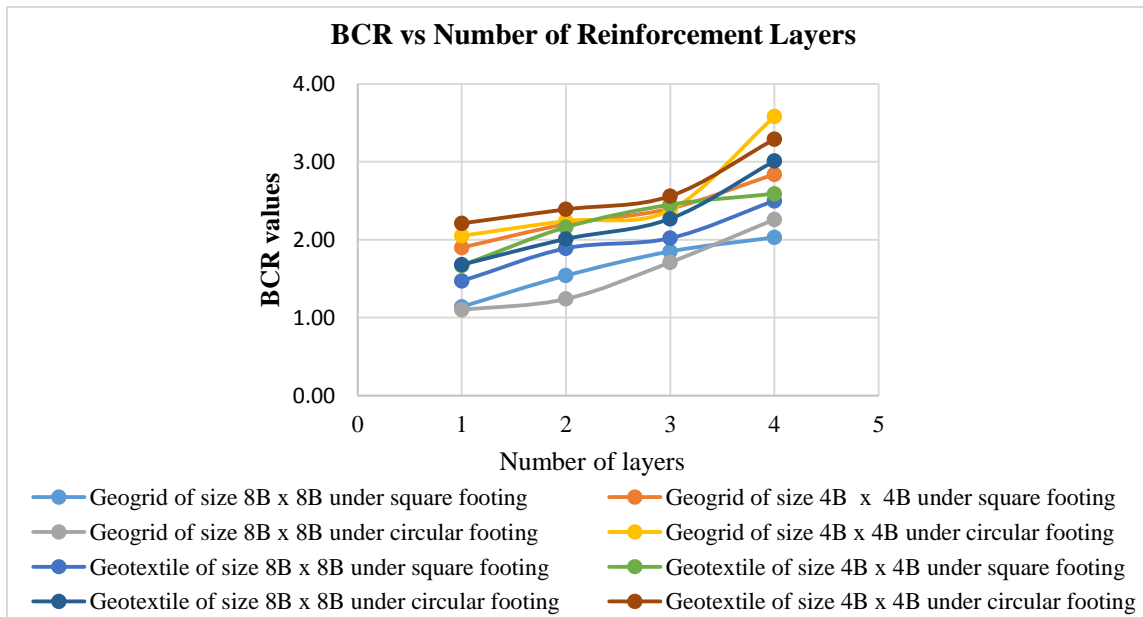


**Fig. 7.18 BCR vs Number of Reinforcement Layers for reinforced granular bed overlain by weak silty soil under square and circular footing (Geogrids and Geotextiles 4B x 4B and 8B x 8)**

## **7.3 STUDIES ON EFFECT OF REINFORCED SOIL FOUNDATION ON MODULUS OF SUBGRADE REACTION**

### **7.3.1 General**

The bearing capacity and modulus of subgrade reaction are the indicators of the strength-deformation properties of soil. The coefficient of subgrade reaction “ $k_s$ ” is an important and useful parameter used to perform the structural analysis of footings. As such  $k_s$  is not an intrinsic soil property. It is just a response of the soil to a given load over a given area and depends not only on the deformation characteristics of the soil but also on the size of contact area between the plate and subgrade. One of the most popular models used in the determination of the modulus of subgrade reaction is the Winkler (1867) model. In this model, a linear force-deflection relationship is presumed and the subgrade soil is assumed to behave like infinite number of linear elastic springs and the stiffness of the spring is named as the modulus of subgrade reaction. In its basic form, Winkler’s Hypothesis assumes that the soil medium is a system of identical, independent, loosely spaced, discrete and linearly elastic springs. The ratio between contact pressure and settlement produced by the load application at an arbitrary point, on the contact surface, is given by the coefficient of subgrade reaction,  $k_s$  (or spring stiffness). This modulus depends on some parameters such as soil type, size, shape, depth and type of foundation.

Another approach is the elastic continuum idealization, where generally the soil is assumed to be a linearly elastic half space and isotropic for the sake of simplicity. This approach provides much more information on the variation of stress and deformation within the soil mass compared to the Winkler model. It has an important advantage in the simplicity of inputting the parameters, the Young’s modulus and Poisson’s ratio. Both the approaches, Winkler and Elastic Continuum idealization, require appropriate values for the input parameters, subgrade reaction coefficient and Young’s modulus (and Poisson’s ratio). A direct method to estimate both  $E$  and  $k_s$  is Plate Load test (PLT) and is conducted with circular plates or rectangular/square plates. Plate Load tests can be conducted full scale at site, or laboratory scale tests in

laboratories. In this study, laboratory scale plate load tests are conducted as discussed in section 7.2.

### 7.3.2. Determination of modulus of subgrade reaction of soil “ $k_s$ ”

A major problem in soil mechanics is to estimate the numerical value of “ $k_s$ ”. The plate-load test provides a direct measure of compressibility and occasionally of the bearing capacity of soils which are not easily sampled. The modulus of subgrade reaction can be determined by using the plate-load tests.

One of the early findings was that of Terzaghi (1955). He proposed different formulae of  $k_s$  for a (1 × 1) ft rigid slab placed on a soil medium. “ $k_{sf}$ ” for full-sized footings could be obtained from plate-load tests using the following equations:

- 1) For square footing on cohesionless soil with dimensions =  $B \times B$ . (Equation 7.2)

$$k_{sf} = k_{sp} \left[ \frac{B + 0.305}{2B} \right]^2 \quad (7.2)$$

- 2) For rectangular footing on cohesionless soil with dimensions =  $B \times L$ .

(Equation 7.3)

$$k_{sfr} = \frac{k_{sf} \left( 1 + \frac{B}{L} \right)}{1.50} \quad (7.3)$$

- 3) For long foundation [strip footing] with a width  $B$

$k_{sp}$  = plate-load test value of modulus of subgrade reaction  $\text{kN/m}^3$ , using square plate (1 × 1) ft or circular plate with diameter = 0.305 m;

$k_{sf}$  = desired value of modulus of subgrade reaction for square footings  $B \times B$ ,  $\text{kN/m}^3$ ;

$k_{sfr}$  = desired value of modulus of subgrade reaction for rectangular full-sized footings  $B \times L$ ,  $\text{kN/m}^3$ ;  $B$  = footing width, dimension of rectangular or strip.

Table 7.8. illustrates different formulae proposed to calculate the modulus of subgrade reaction of soil. Egyptian Code method discussed in Chapter 3, (Section 3.3.3) used in the present study is used for the computation of modulus of subgrade reaction of reinforced soil.



### **7.3.3 Results and Discussions**

The results of the experimental studies carried out on reinforced granular bed underlain by weak silty soil are used to compute the modulus of subgrade reaction of reinforced soil. The experimental results have been used to plot semilog graphs to obtain ultimate bearing capacity using Egyptian Code method. The various semilog graphs used to compute the modulus of subgrade reaction of reinforced soil have been plotted in section 7.3.4. Figures 7.19 to 7.21 show the plot of semi log graphs of settlement vs stress for geosynthetics of two sizes 0.40m x 0.40m (4B x 4B) and 0.80 x 0.80m (8B x 8B) under square and circular footings (To find  $k_s$ ). Figures 7.21 to 7.25 show the variation of  $k_s$  for Geogrid / Geotextile of two sizes 0.40m x 0.40m (4B x 4B) and 0.80 x 0.80m (8B x 8B) under both the square and circular footings. Section 7.4.10 presents the various tables used and tabulated from obtained results in this study.

#### **7.3.3.1 Determination of ultimate bearing capacity using model test**

The ultimate bearing capacity of the reinforced granular bed underlain by weak silty soil can be obtained from the relationships between the stresses and the settlement recorded at the surface and at different depths for all the cases by tangent-tangent method according to the Egyptian code method. Figures 7.22 and 7.23 illustrate the method of finding the ultimate bearing capacity using semilog graphs.

#### **7.3.3.2 Determination of subgrade reaction “ $k_s$ ” using experimental results**

The allowable bearing capacity ( $q_a$ ) is obtained from ultimate bearing capacity ( $q_u$ ) by dividing it by factor of safety (F.S. = 3.0), after which the corresponding settlement ( $s$ ) is determined. Thus,  $k_s$  is calculated by dividing the allowable bearing capacity ( $q_a$ ) by the corresponding settlement ( $s$ ). Table 7.9 illustrates the modulus of subgrade reaction of reinforced granular bed underlain by weak silty soil reinforced with geotextiles under square and circular footing for two sizes of reinforcement.

The different values of subgrade reaction ( $k_s$ ) for both the model circular and square footing under Geotextile for both the sizes have been plotted against the number of layers. Figures 7.24 to 7.26 illustrate the variation of modulus of subgrade reaction for both the circular and square footing under geotextiles for varying number of reinforcement layers. It is observed from the graphs that the modulus of subgrade reaction increases for both the footings for both the sizes of Geotextiles with the increase in the number of reinforcement layers. It is maximum for four layers for all the cases.

Under circular footing, 4 layers of Geotextile of both the sizes 0.4m x 0.4m (4B x 4B) and 0.8m x 0.8m (8B x 8B) give better results for the modulus of subgrade reaction. The modulus of subgrade reaction has been enhanced due to the introduction of reinforcement. The modulus of subgrade reaction is more under circular footing for both the cases.

**7.3.4 Graphs Plotted in Reinforced Soil Foundation to obtain Modulus of subgrade reaction of soil (ks)**

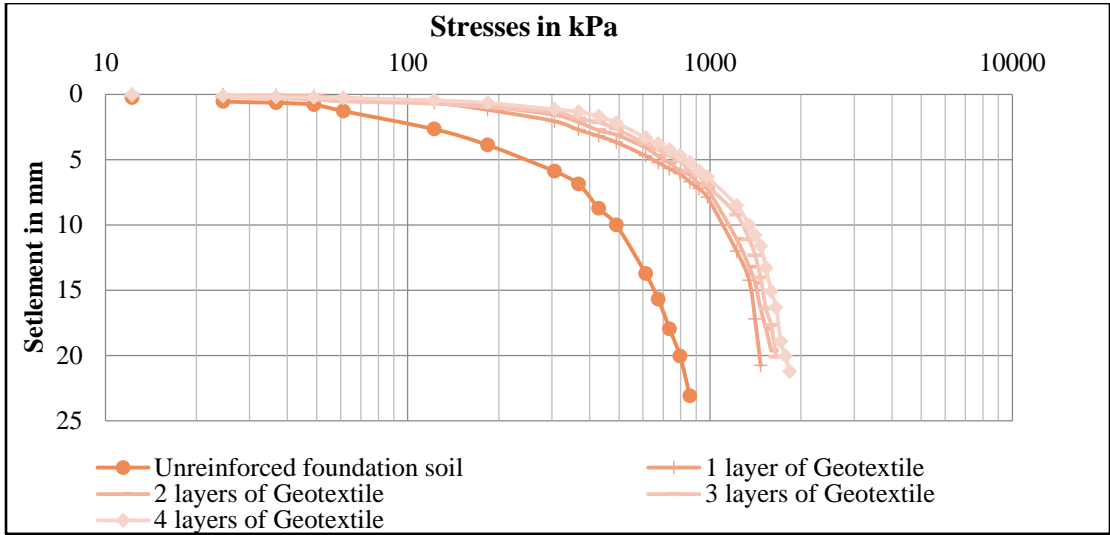


**Fig. 7.19 Semi-log graph of Settlement vs. stresses for unreinforced and reinforced granular bed overlain by weak silty soil under circular footing (Geotextile 0.40 x 0.40, 4B x 4B) (To find ks)**

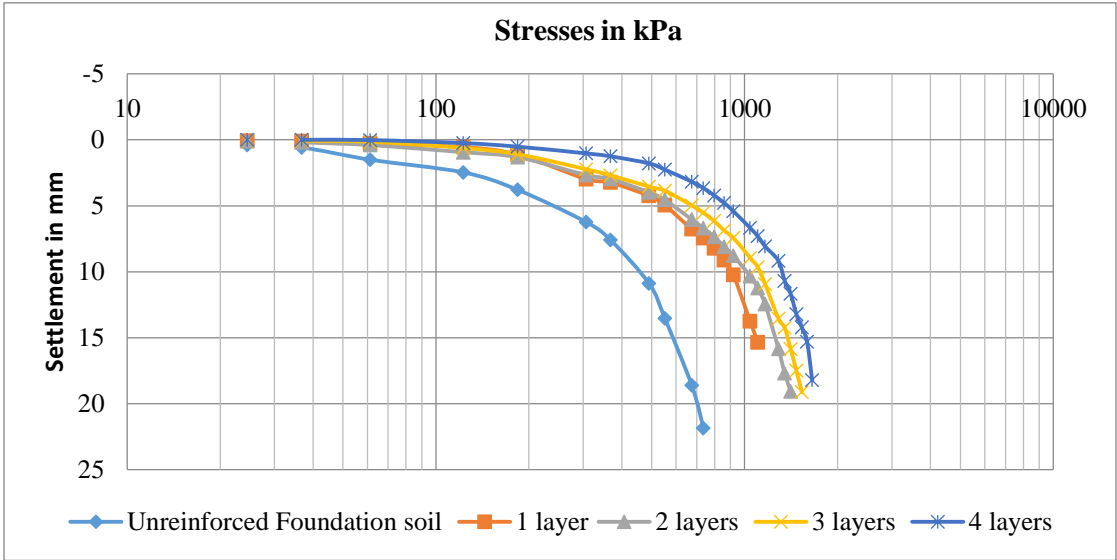


**Fig. 7.20 Semi-log graph of Settlement vs. stresses for unreinforced and reinforced granular bed overlain by weak silty soil under square footing (Geogrid 0.40 x 0.40m, 4B x 4B) (To find ks)**

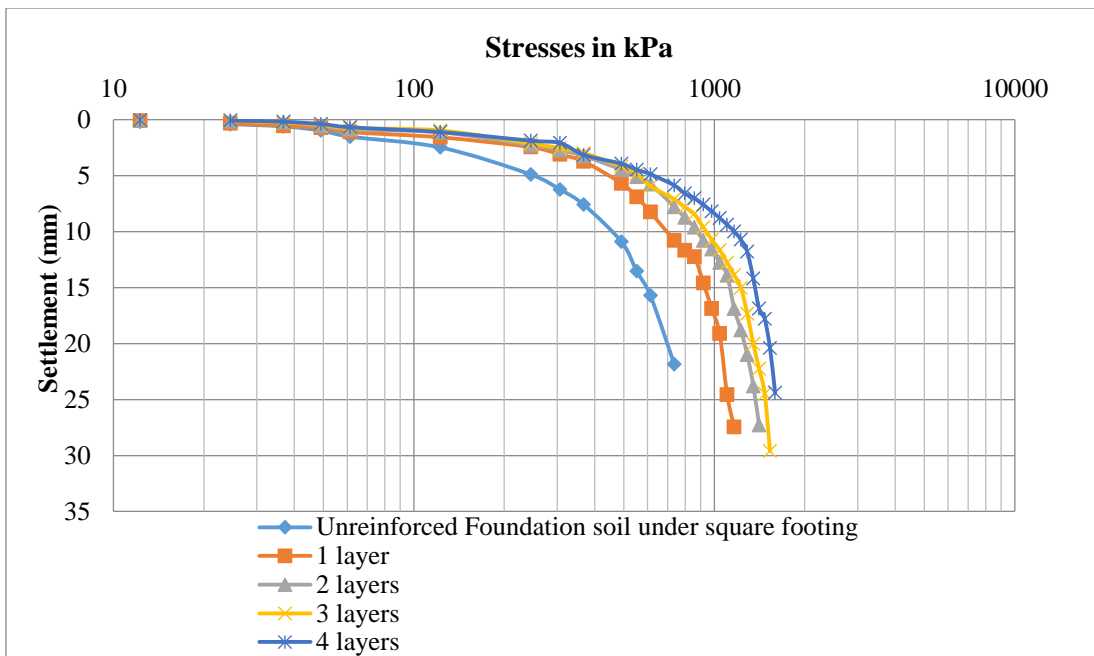


**Fig. 7.21** Semi-log graph of Settlement vs. stresses for unreinforced and reinforced granular bed overlain by weak silty soil under square footing (Geotextile 0.40mx0.40m, 4B x 4B) (To find ks)

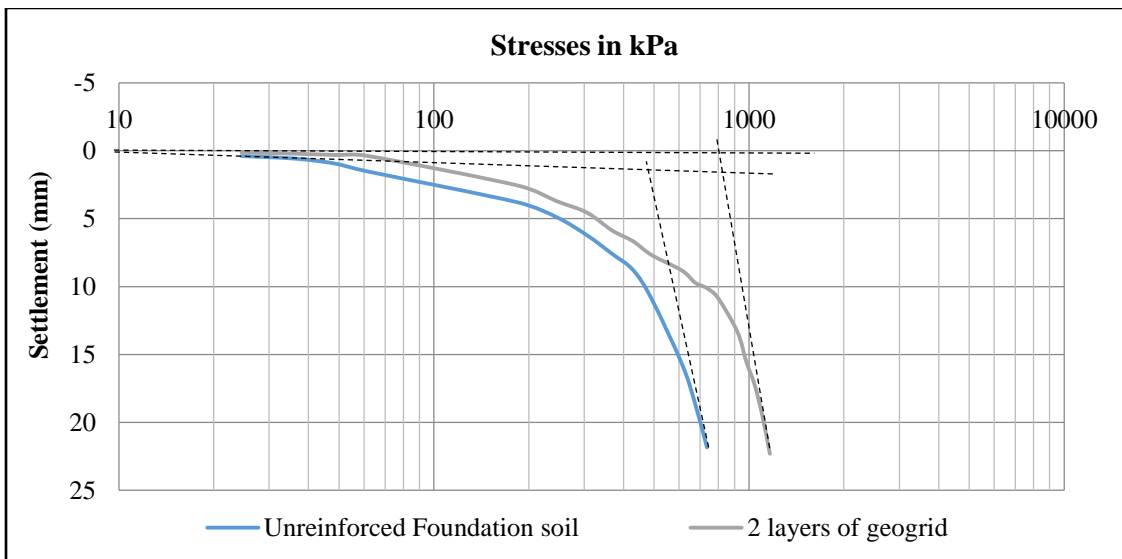


**Fig. 7.22** Semi-log graph of Settlement vs. stresses for unreinforced and reinforced granular bed overlain by weak silty soil under square footing (Geogrid 0.8m x0.8m, 8B x 8B) (To find ks)

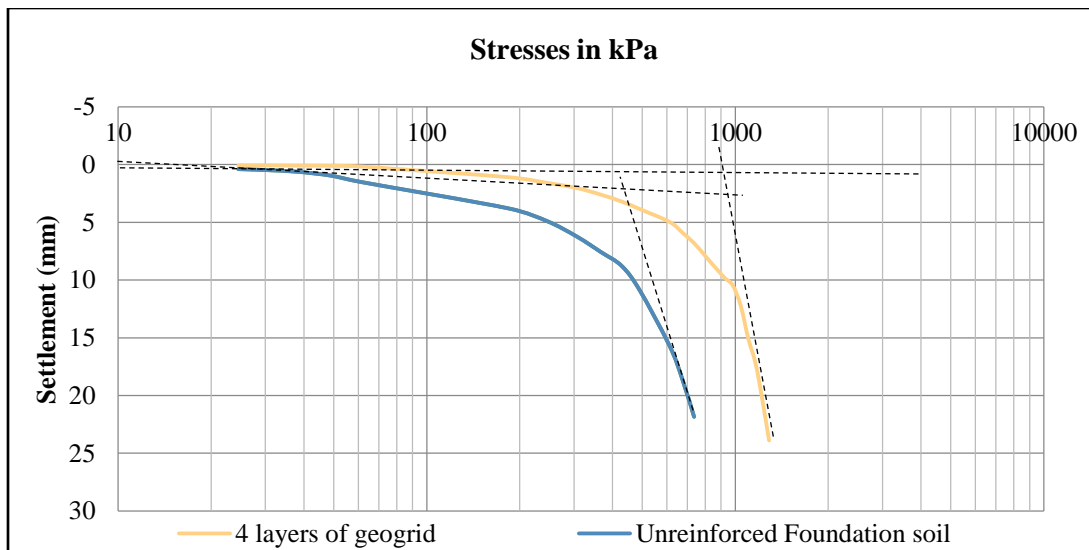


**Fig.7.23 Semi-log graph of Settlement vs. stress for unreinforced and reinforced granular bed overlain by weak silty soil under square footing (Geogrid 0.80 x 0.80m, 8B x 8B) (To find ks)**

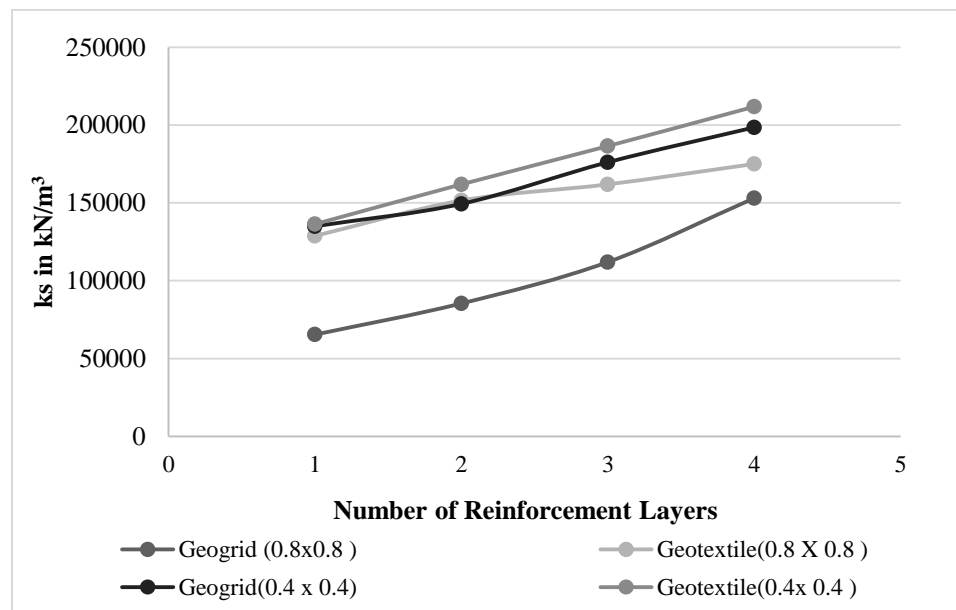


**Fig. 7.24 Variation of ks for unreinforced and reinforced granular bed overlain by weak silty soil under circular footing (Geogrid / Geotextile 4B x 4B and 8B x 8B)**

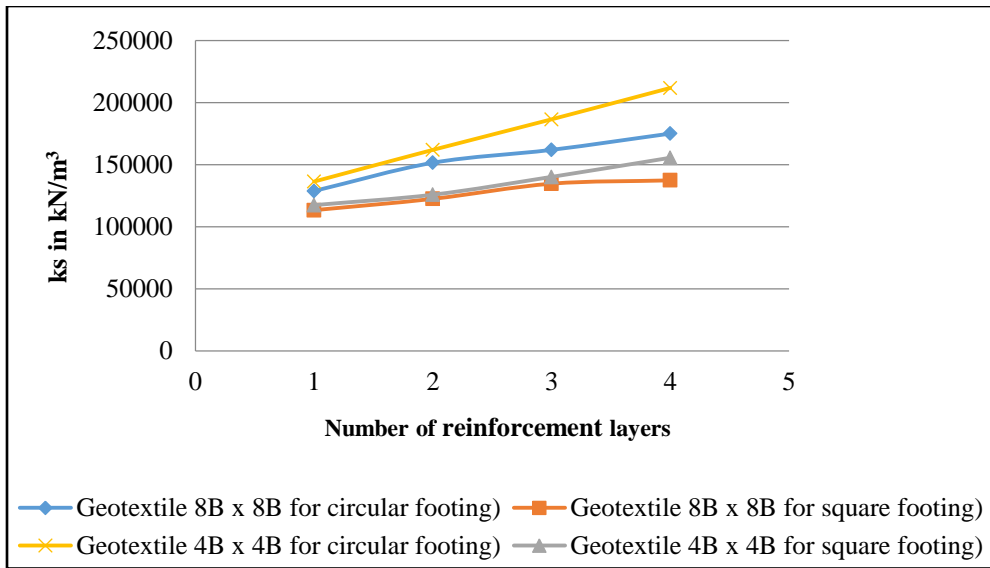


**Fig. 7.25 Variation of  $k_s$  for unreinforced and reinforced granular bed overlain by weak silty soil under square and circular footing (Geotextile 4B x 4B and 8B x 8B)**

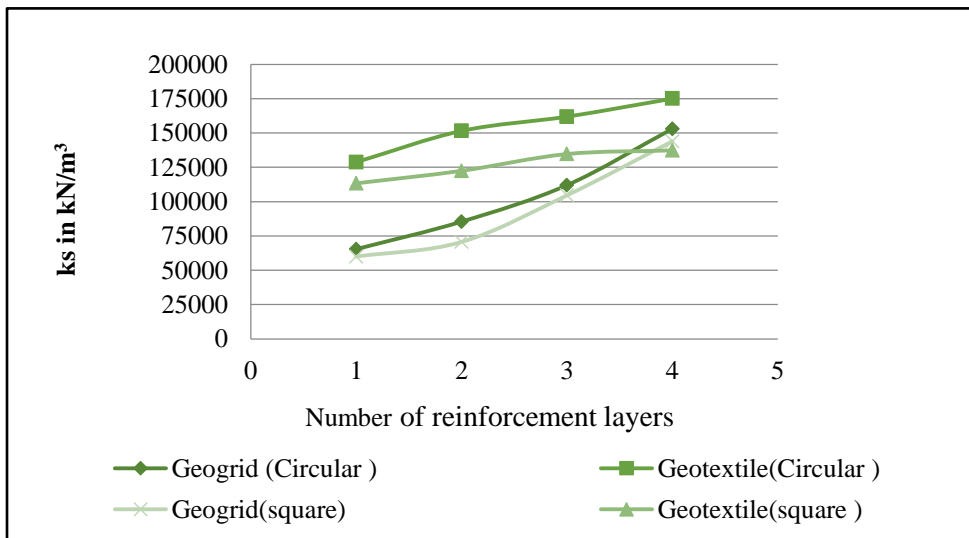


**Fig. 7.26 Variation of  $k_s$  for unreinforced and reinforced granular bed overlain by weak silty soil Geogrid/Geotextile under circular and square footing for a size of (0.80m x 0.80m, 8B x 8B)**

## **7.4 COMPARITIVE STUDIES ON LOAD SETTLEMENT CHARACTERISTICS OF SQUARE FOOTING RESTING ON GEOSYNTHETIC REINFORCED LOOSE SAND**

In this part of the study, a numerical model has been built to investigate the performance of a square footing resting on Geosynthetic reinforced sand by developing a programme code to validate the experimental results. The effects of different parameters of the reinforcing layers on the bearing capacity of the sandy soil have been investigated. Nonlinear Drucker-Prager model is used as a constitutive material model to simulate the soil behavior. Numerical model of dimensions 0.90m x 0.90m x 0.80m and 0.10m x 0.10m x 0.020m are used to simulate the soil and the square footing for experimental model simulation.

Improvement in bearing capacity due to reinforcing layers obtained by numerical model is compared with experimental results. The comparison showed a good convergence between results which leads to successful model validation. Comparative studies have been carried out between the results of experimental and numerical simulations on square footing resting on sand and clay with and without geosynthetic reinforcement. The main objective of this part of the study is to predict the behaviour of geosynthetic layers in improving the bearing capacity of the square footings.

### **7.4.1 Details of Various Studies Carried out on Foundation Soil**

Experimental and Numerical studies have been carried out on reinforced granular bed (loose sand) in a tank. The studies have been carried out for varying number of reinforcement layers to investigate the effect on settlements and loads at failure. The nonlinear analysis of reinforced soil foundation has been done using Drucker-Prager constitutive model.

### **7.4.2 Numerical Studies (By Developing Software RSF-PRO)**

Numerical studies have been carried out for the reinforced foundation soil by applying FEM techniques and coding in FORTRAN. Both the linear and nonlinear

analyses have been carried out. The results of the code are plotted in MS-Excel and compared with Experimental results in section 7.4.8.

### **7.4.3. FEM Model**

Figure 7.27 shows the typical mesh where the soil is modelled as rectangular element with four nodes and reinforcement is modelled as bar element with two nodes. The total number of nodes, soil elements, bar elements are 323, 288, 40 (for 4 layers) respectively. The reinforcement layout length is 0.40m. Table 7.9 (Section 7.4.10) gives the details of the mesh used in the developed programme RSF-PRO.

### **7.4.4 Geosynthetic Reinforcement Modelling**

In this part of the study, geotextiles are used. Poisson's ratio of the reinforcement used = 0.42, and the cross-section area of the reinforcement = 0.00056 m x 0.40m. Table 7.4 gives the properties of the geotextiles used.

### **7.4.5 Soil Modelling**

The soil used in this study is loose sand, modulus of elasticity=  $3 \times 10^3$  kPa, Poisson's ratio=0.3, density =  $1368 \text{ kg/m}^3$  and friction angle= $31^\circ$ . A 3D finite element model was used to simulate the sand using Drucker-Prager as material model. Table 7.11 shows the material properties used in the developed software.

### **7.4.6 Modelling of Square Footing**

The square footing was modelled as a steel footing of dimensions 0.1m x 0.1m x 0.020 m, Modulus of elasticity=  $2.1 \times 10^{11}$  GPa and Poisson's ratio = 0.3. The outer four sides of the model were restricted to move in a direction normal to its plan and free to move in the other directions. The bottom of the model was restricted to move in all directions.



#### **7.4.7 Results of Numerical and Experimental Studies for varying number of reinforcement layers**

The results obtained from the model plate load tests (stress vs. settlements) and the developed software RSF-PRO for unreinforced and reinforced foundation soil bed under square footing are plotted as shown in the Figs. 7.28 to 7.31. The reinforcement used is in varying number of layers (1 to 4) of Geotextiles of size 0.4m x 0.4m (4B x 4B). It may be observed that the maximum load at failure occurs when four layers of Geotextiles are used (1042 kPa). It shows a remarkable increase in the load carrying capacity (nearly two times) that of unreinforced foundation bed. The settlement is also found to decrease. The results obtained from different methods of studies have been presented in Table 7.12 (section 7.4.10)

#### **7.4.8 Conclusions drawn from this study**

1. The settlement and the load at failure for the varying number of reinforcement layers was found to be in reasonably good agreement with the developed program RSF-PRO (specially for single layer and 4 layers) where the Nonlinear analysis is being carried out using Drucker Prager models.
2. The developed software is working well for linear analysis and non-linear analysis using the Drucker Prager model.
3. The settlement obtained from the linear analysis using developed code RSF-PRO are least in comparison with those obtained from the experimental studies and nonlinear analysis using developed program.
4. The current studies have been carried out for 100% coupling between soil and reinforcement as studies have proved that interface element between reinforcement and soil are irrelevant for vertical loading.
5. The developed program can also be used to plot the stresses and strains in the reinforced soil for different loadings and extended to studies in Retaining walls.

### 7.4.9 Graphs Plotted in Numerical Studies carried out on Reinforced Soil Foundation

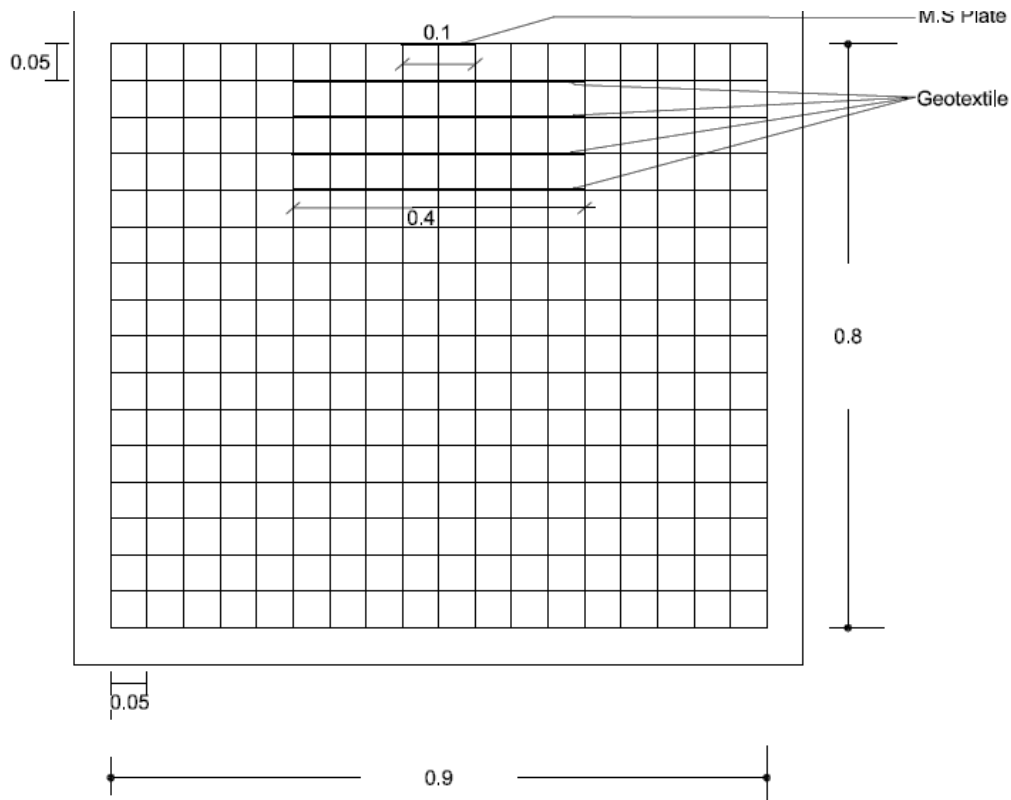


**Fig.7.27 Typical mesh of the model Plate Load test**

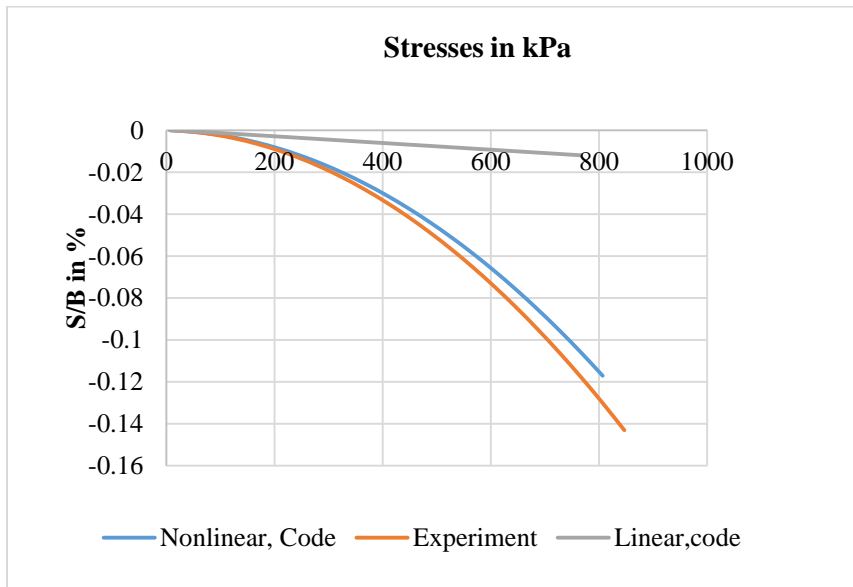


**Fig. 7.28 Settlement/width of footing vs. Stress Graphs for reinforced granular bed underlain by loose sandy soil (1 layer of Geotextile 4B x 4B)**

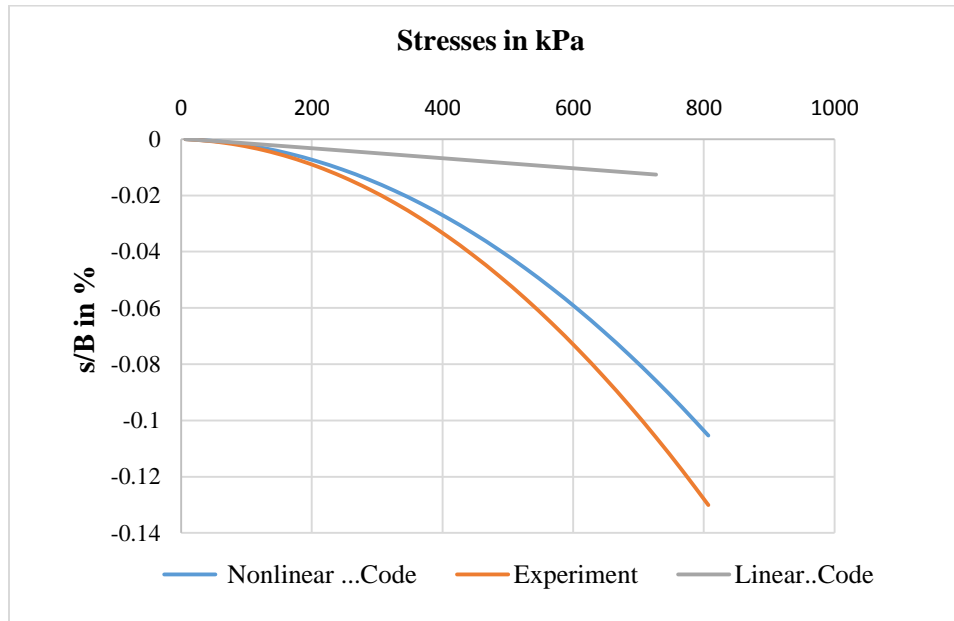


**Fig. 7.29 Settlement/width of footing vs. Stress Graphs for reinforced granular bed underlain by loose sandy soil (2 layers of Geotextiles 4B x 4B)**

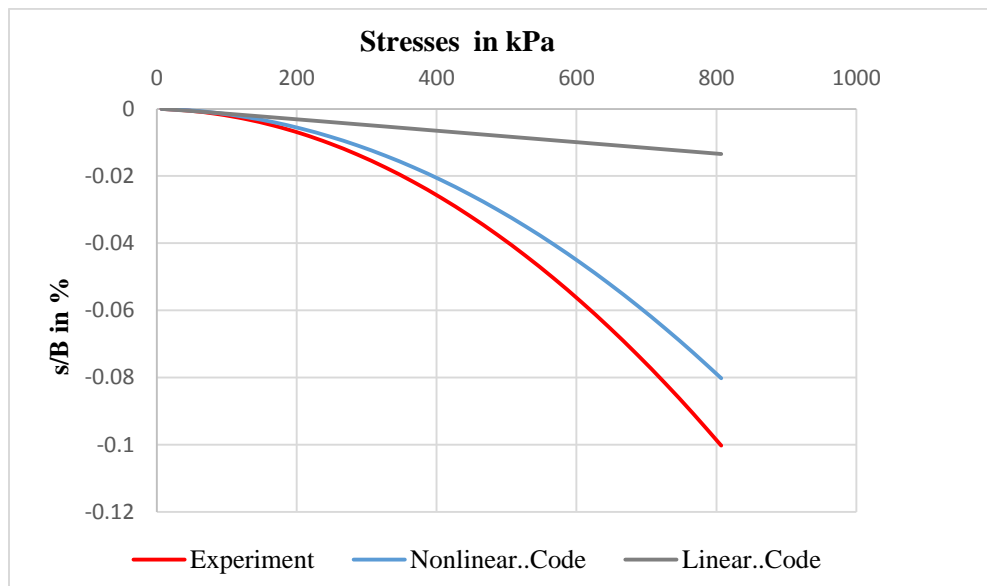


**Fig. 7.30 Settlement /width ratio vs. Stress Graphs for reinforced granular bed underlain by loose sand (3 layers of Geotextiles, 4B x 4B)**

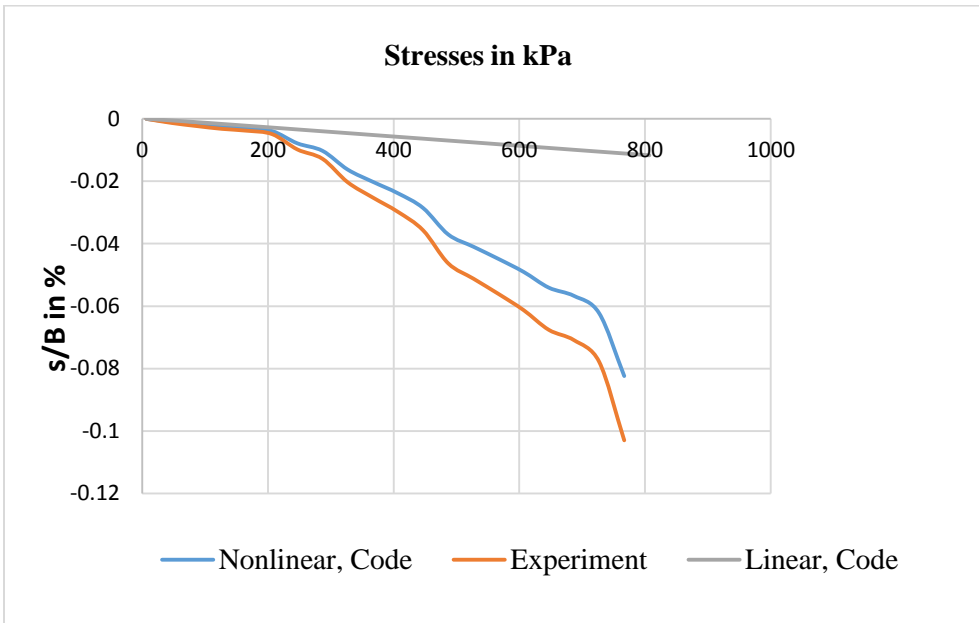


**Fig. 7.31 Settlement /width vs. stresses for reinforced granular bed underlain by loose sand (4 layers of Geotextiles, 4B x 4B)**

### 7.4.10 Tables Used in studies on Reinforced Soil Foundation

Series	Type of soil	Number of layers of reinforcement	Reinforcement type	Type of test	Type of footing
I	Loose Sand	-----	-----	UnReinforced	Square
II	Loose Sand	1,2,3,4	Geogrid	Reinforced	Square
III	Dense Sand	-----	-----	UnReinforced	Square
IV	Dense Sand	1,2,3,4	Geogrid	Reinforced	Square
V a	Unreinforced granular bed on weak soil	-----	-----	UnReinforced	a) Square
Vb					b) Circular
VI	Reinforced granular bed on weak soil	1,2,3,4	Geogrid	Reinforced	Square
VII			Geotextile		Square
VIII			Geogrid		Circular
IX			Geotextile		Circular
X a,b	Reinforced granular bed on weak soil	u/B=0.2,0.4,0.6,0.8,1.00	Geogrid	Reinforced	a) Square
XI a,b	Reinforced granular bed on weak soil	u/B=0.2,0.4,0.6,0.8,1.00	Geotextile		a) Square

SL.NO	PROPERTIES	Soil	Sand
1	Specific Gravity, (Gs)	2.40	2.73
2	Max. Density, ( $\gamma_{dmax}$ ) (kg/m <sup>3</sup> )	1635	1810
3	Density for Loose Sand, ( $\gamma_{dmin}$ ) ( kg/m <sup>3</sup> )	-----	1386
4	Liquid Limit (LL), (%)	37.6	NA
5	Plastic Limit (PL), (%)	18.0	NA
6	Optimum Moisture Content (OMC), (%)	21.0	NA
7	Undrained Cohesion (c), (kN/m <sup>2</sup> )	42.0	NA
8	USCS Classification	CL	SP
9	Coefficient of Uniformity (Cu)	NA	1.72
10	Coefficient of Curvature (Cc)	NA	0.94
11	Angle of Internal Friction for Loose sand ( $\Phi$ in degree)	NA	31
12	Angle of Internal Friction for dense sand ( $\Phi$ in degree)	NA	36

Table 7.3 Properties of Geogrids used

PROPERTIES	VALUES
Rib Thickness(mm)	0.75
Aperture size(MD/XD) (mm)	25/33
Junction Thickness (mm)	2.8
Tensile strength at 5% strain(kN/m)	8.46(MD) , 13.42(XD)
Aperture Shape	Rectangular
Colour	Black
Type of Polymer used	Polyethyelene

Table 7.4 Properties of Geotextiles used

PROPERTIES	VALUES
Mass per unit area (gm/m <sup>2</sup> )	206
Breaking strength-Warp (5 x 20 cm)	257.7 kg
Breaking strength-Weft (5 x 20 cm)	181.9
Thickness (mm)	0.58
Extension at break (weft)	30.20%
Extension at break (warp)	36.90%
Style (quality no)	P.D. 381
Type of Polymer used	Polypropylene
Young's modulus	0.9GPa
Density	1000
Poisson's ratio	0.42

<b>Reinforcement at different u/B ratio</b>	<b>BCR for case of Geogrid with Square footing</b>		<b>BCR for case of Geogrid with Circular footing</b>		<b>BCR for case of Geotextile with Square footing</b>		<b>BCR for case of Geotextile with Circular footing</b>	
	<b>Size of Geogrid in m</b>		<b>Size of Geogrid in m</b>		<b>Size of Geotextile in m</b>		<b>Size of Geotextile in m</b>	
	<b>0.80 x 0.80</b>	<b>0.40 x 0.40</b>	<b>0.80 x 0.80</b>	<b>0.40 x 0.40</b>	<b>0.80 x 0.80</b>	<b>0.40 x 0.40</b>	<b>0.80 x 0.80</b>	<b>0.40 x 0.40</b>
	0.2	2.31	2.27	2.84	2.58	2.39	2.27	2.76
0.4	2.75	2.49	2.93	2.9	2.49	2.5	2.89	2.54
0.6	2.28	2.03	2.78	2.4	2.12	2.03	2.54	2.16
0.8	2.23	1.87	2.39	2.1	1.62	1.87	2.02	1.9

<b>No of layers</b>	<b>BCR with Geogrid under Square footing</b>		<b>BCR with Geogrid under Circular footing</b>		<b>BCR with Geotextile under Square footing</b>		<b>BCR with Geotextile under Circular footing</b>	
	<b>Size of Geogrid in m</b>		<b>Size of Geogrid in m</b>		<b>Size of Geotextile in m</b>		<b>Size of Geotextile in m</b>	
	<b>0.80 x 0.80</b>	<b>0.40 x 0.40</b>	<b>0.80 x 0.80</b>	<b>0.40 x 0.40</b>	<b>0.80 x 0.80</b>	<b>0.40 x 0.40</b>	<b>0.80 x 0.80</b>	<b>0.40 x 0.40</b>
	1-layer	1.14	1.9	1.1	2.05	1.47	1.67	1.68
2-layers	1.54	2.2	1.24	2.24	1.89	2.16	2.01	2.39
3-layers	1.85	2.4	1.71	2.38	2.02	2.45	2.27	2.56
4-layers	2.03	2.84	2.26	3.58	2.5	2.59	3.01	3.29



**Table 7.7 Settlements under square and circular footings for unreinforced and reinforced granular bed underlain by w and 0.80x0.80m (8B x 8B) and Unreinforced soil**

SL.No	Load in kN/m2	Settlements of Geotextile (0.80 x 0.80)with square footing (in mm)					Settlements of Geotextile 0.40 x0.40 with square footing (in mm)				
		unreinforced	1-layer	2-layer	3-layers	4-layers	unreinforced	1-layer	2-layers	3-layers	4-layers
1	0	0	0	0	0	0	0	0	0	0	0
2	12.26	0.17	0.09	0.05	0.075	0.025	0.17	0.3	0.08	0.02	0.13
3	24.52	0.39	0.33	0.12	0.1	0.074	0.39	0.4	0.097	0.07	0.23
4	36.78	0.59	0.54	0.22	0.25	0.18	0.59	0.57	0.14	0.12	0.32
5	49.04	0.96	0.73	0.55	0.45	0.38	0.96	0.7	0.22	0.18	0.38
6	61.3	1.51	1.1	0.87	0.74	0.67	1.51	0.92	0.68	0.3	0.49
7	122.6	2.47	1.57	1.12	0.95	1.1	2.47	1.13	1.16	0.65	0.98
8	245.2	4.89	2.44	2.26	2.12	1.87	3.79	1.67	1.72	1.33	1.28
9	306.5	6.23	3.1	2.71	2.53	2.06	6.23	2.95	2.62	2.25	2.03
10	367.8	7.59	3.73	3.24	2.97	3.14	7.59	3.59	3.08	3.06	2.52
11	490.4	10.89	5.68	4.45	4.18	3.92	8.79	4.22	3.69	3.37	2.98
12	551.7	13.53	6.89	5.1	4.84	4.46	10.89	5.55	4.16	3.81	3.57
13	613	15.71	8.25	5.7	5.93	4.86	15.71	6.95	5.53	5.15	4.63
14	735.6	21.84	10.78	7.77	7.1	5.86	18.61	7.63	6.17	5.64	5.12
15	796.9		11.67	8.73	7.81	6.58	21.84	9.46	6.87	6.1	5.61
16	858.2		12.23	9.6	8.42	7.01		10.21	7.61	6.52	6.13
17	919.5		14.59	10.78	9.62	7.59		10.72	8.24	7.1	6.76
18	980.8		16.87	1.55	10.72	8.19		12.01	8.91	7.64	7.09
19	1042.1		19.11	12.76	11.63	8.77		12.88	9.69	8.23	7.78
20	1103.4		24.58	13.89	12.78	9.37		17.01	13.07	10.89	10.3
21	1164.7		27.46	16.87	13.87	9.97		22.77	17.05	12.97	11.64
22	1226			18.79	15.02	10.71		25.22	19.58	14.55	12.37
23	1287.3			20.98	17.33	11.79			21.48	16.34	14.42
24	1348.6			23.78	20.01	14.2			24.55	18.49	16.33
25	1409.9			27.27	22.25	16.87				21.66	18.23
26	1471.2				24.48	17.78				24.02	20.78
27	1532.5				29.6	20.39					23.78

No.	Researcher	Formula
1	Winkler (1867)	$k_1 = \frac{Q}{\delta}$
2	Biot (1937)	$k_1 = \frac{0.95 E_1}{B(1-\nu_1^2)} \left[ \frac{B^4 E_1}{(1-\nu_1^2) EI} \right]$
3	Terzaghi (1955)	$k_s = k_{ap} \left[ \frac{B+E_1}{2B} \right]$
4	Vesic(1961)	$k_s = \frac{0.65 E_1}{B(1-\nu_1^2)} \sqrt{\frac{E_1 B^4}{EI}}$
5	Meyerhof and Baker (1965)	$k_s = \frac{E_1}{B(1-\nu_1^2)}$
6	Selvadurai (1984)	$k_s = \frac{0.65 E_1}{0.85 (1-E_1 \nu_1^2)}$
7	Bowles(1998)	$k_s = \frac{B(1-\nu_1^2) M_{1,1F}}{B(1-\nu_1^2) M_{1,1F}}$

**Table 7.9 Modulus of Subgrade for Reinforced soil under two model footings obtained using plate load test for granular bed underlain by silty soil**

Footing	No of layers	Geotextile							
		Size	Allowable	Settlement	Modulus	Size	Allowable	Settlement	Modulus
		0.8 X 0.8	qa (kN/m <sup>2</sup> )	S(m)	ks (kN/m <sup>3</sup> )	0.4 X 0.4	qa (kN/m <sup>2</sup> )	S(m)	ks(kN/m <sup>3</sup> )
Circular	1	850	283.33	0.0022	128787.879	900	300.00	0.0022	136363.64
	2	1000	333.33	0.0022	151515.152	1020	340.00	0.0021	161904.76
	3	1020	340.00	0.0021	161904.762	1035	345.00	0.00185	186486.49
	4	1050	350.00	0.002	175000	1150	383.33	0.00181	211786.37
Square	1	850	283.33	0.0025	113333.333	810	270.00	0.0023	117391.30
	2	900	300.00	0.00245	122448.98	1000	333.33	0.00265	125786.16
	3	1010	336.67	0.0025	134666.667	1030	343.33	0.00245	140136.05
	4	1030	343.33	0.0025	137333.333	1050	350.00	0.00225	155555.56

**Table 7.10 Details of Mesh used in developed programme RSF-PRO**

Sl.No	Mesh Details	Number
1	Number of Soil Elements	288
2	Number of Reinforcement Elements	
	1 layer	10
	2 layers	20
	3 layers	30
	4 layers	40
3	Number of joints	323

**Table 7.11. Material Properties used in the Code RSF-PRO**

Material	Angle of friction (degree)	Young's modulus	Density	Cohesion	Poisson's ratio
Sand	31	3 MPa	13680N/m <sup>3</sup>	0	0.3
Geotextiles	--	0.9 GPa	1000 N/m <sup>3</sup>	---	0.42

<b>Table 7.12 Settlements corresponding to varying number of reinforcement layers at failure for different studies carried out</b>						
<b>No of Layers</b>	<b>Linear...Code</b>		<b>NonLinear...code</b>		<b>Experimental studies</b>	
	Stress kPa	Settlement m	Stress kPa	Settlement m	Stress kPa	Settlement m
1 layer	806.9	0.153	806	0.117	846.9	0.143
2 Layers	806.9	0.1401	806	0.105	806	0.130
3 Layers	806.9	0.1261	806	0.080	806.9	0.100
4 Layers	806.9	0.1108	766.9	0.02761	800	0.0108

## CHAPTER 8

### REINFORCED SOIL-STRUCTURE-INTERACTION ANALYSIS OF THREE DIMENSIONAL FRAMES

#### 8.1 Introduction to SSI and RSSI

Many problems in structural engineering involve interaction between the soil and the structure. This interaction plays a major role in the response of a structure and may alter the magnitude of stresses, displacements and other responses of a structure compared to the non-interactive analysis, where the structure is assumed to have fixed supports and do not undergo any relative motions. The analysis that treats structure-foundation-soil as a single system is called as Soil Structure Interaction (SSI) analysis. In SSI analyses the displacements and stress resultants are found to deviate considerably from non-interactive analysis there by rendering the non-interactive analysis as nonrealistic and it is necessary to consider SSI in the analysis and design of structures.

A limited number of studies have been conducted on soil–structure interaction effect considering three dimensional space frames. SSI studies that take into account the yielding of structures and soil non–linearity are scarce, especially investigating the effects of non-linearity of SSI system on overall behaviour in terms of displacements and stresses.

The SSI studies conducted by King et al. (1974, 1977, and 1983) and Roy and Dutta (2001) were the few researchers who made use of the finite element method to consider super structure – raft / combined footing soil as a single compatible unit.

The SSI studies conducted by Viladkar (1991) and Noorzai (1994) clearly indicated that a two-dimensional plane frame SSI analysis might substantially overestimate or underestimate the actual interaction effect in a space frame.

The interactive behaviour of the 3D frame-Isolated footing-soil system was studied by Swamy et al. (2011). Swamy et al. (2013) conducted linear and Non-linear SSI analyses of structure resting on raft foundation to find the maximum settlement as well as differential settlements in soil increase in non-linear analysis when compared to linear analysis. They observed that maximum vertical stresses decrease in non-linear analysis when compared to linear analysis. However the stress resultants, in members of the frame were found to vary (either decrease or increase) depending on location in non-linear analysis when compared to linear analysis. Axial forces in columns vary within 20% in non-linear and 10% in linear analysis with respect to non-interactive analyses. Shear forces in beams vary by 6% in linear analysis and vary up to 14% in non-linear SSI analysis with respect to non-interactive analysis. Shear forces in columns in linear SSI analysis vary from 15% to 22% with respect to non-interactive analysis where as in non-linear SSI analysis they vary from 40% to 70% with respect to non-interactive analysis. SSI studies have been carried out for structures supported on unreinforced soil. But Reinforced soil-structure interaction (RSSI) dealing with structures supported on reinforced soil is yet to be explored. The analysis that treats structure-foundation-reinforced soil as a single system is coined as Reinforced Soil Structure Interaction (RSSI) analysis in this work. To start with following research gaps are observed:

- Though experimental and numerical studies have been conducted on reinforced soil, they were on mostly on isolated footings and reduced scaled models.
- Parametric study on settlement of foundations resting on reinforced soil using numerical methods.
- Study of stress resultants in members of the frame resting on reinforced soil.
- Study of stresses in the reinforced soil.

- Comparative study of unreinforced soil structure interaction analysis and reinforced soil structure interaction analysis.
- Study of interaction effects on RC frame resting on Reinforced soil

In the present study, the response of a structure supported on soil reinforced with geosynthetics is considered and its effect is studied. Numerical studies have been carried out by using finite element analyses to study the SSI effects of a 3D frame resting on reinforced and unreinforced soil by developing programmes SSI-LIN and SSI-NLIN. The responses investigated are displacements, stresses in soil and member end actions in the structural members.

Though the structural field and geotechnical field have advanced computational tools offering sophisticated non-linear modelling in their respective fields, they fail together, to model an SSI problem to the same degree of sophistication. It is therefore a real challenge to achieve the same amount of sophistication in modelling both the soil and the structure in a single soil-structure interaction analysis. In this respect, existing advanced discipline-oriented computational tools are inadequate, on their own, for modelling a reinforced soil-structure- interaction problem that involves considerable nonlinearity in both the structure and the soil. As the formulation consists of a variety of elements with varied degrees of freedom and with different material properties, the analysis has been carried out using a specially developed Computer program. The analysis is done by using skyline technique (explained in Chapter 4) and applicability of the present improved physical and material modelling has been demonstrated by conducting the following interactive analysis:

#### 1. Linear SSI analysis of space frame-Footing -soil system

- i) Verification of the proposed physical modelling by comparing the linear SSI analysis with a standard published data.
- ii) Conducting linear SSI analysis taking elastic properties of the soil. A comparison of the linear SSI analysis has been with Non-interactive analysis.

## 2. Linear RSSI analysis of space frame-footing -soil system

Conducting RSSI analysis for elastic behaviour of soil by developing a programme RSSI-LIN. A comparison of the linear RSSI analysis has been made with linear SSI analysis done in 1(ii). In the elastic behaviour, the modulus of elasticity of soil is considered to be constant throughout the soil medium.

## 3. Non-Linear SSI analysis of space frame-footing -soil system

Conducting SSI interactive analysis taking nonlinear properties of the soil and validating the results with a standard published data using developed programme SSI-NLIN. Here the constitutive model developed by Yin (2000) is used. The Hypoelastic parameters were obtained from the experimental work done by Krishnamoorthy and Rao (2001). Validation of the SSI analysis has been made with work done by Swamy et al. (2011).

## 4. Non-Linear RSSI analysis of space frame-footing -soil system by self developed programme RSSI-NLIN

The linear RSSI analysis has been further extended for studying the effect of non-linearity and compared with SSI analysis involving non-linearity of soil. Further RSSI and SSI interactive behaviour has also been compared with the non-interactive analysis. The methodology to conduct above studies is to develop software which can handle non-interactive analysis, SSI analysis and RSSI analysis.

After conducting non-interactive analysis, the behaviour of the same structure on unreinforced and reinforced soil foundation considering structure interaction effects is studied. The soil is reinforced with geosynthetics and the response is studied. Responses such as displacements and member end actions in structural members are compared between the fixed base structure, structure resting on unreinforced soil and reinforced soil. The analysis is done for both the linear and nonlinear behaviour of soil. Nonlinear analysis is carried out by adopting Hypoelastic model for soil.



## 8.2 Linear SSI analysis of space frame-Footing -soil system

### 8.2.1 Problem Definition:

For the purpose of the validation of the new formulation physical model and the program, an attempt has been made to compare the results of the interactive analysis with those obtained earlier by Swamy et al., (2011). The proposed physical model has been used for the interactive analysis of a four storey, five bay by three bay, space frame-isolated footings-soil system. Figure 8.1 shows the isometric view of the space frame-isolated foundation-soil system. The layout details of the frame are shown in Fig. 8.2. The geometrical and material properties of the frames, its components and the isolated foundation are presented in Table 8.1. The load considered for analysis is 31kN/m on beams, which is a service load on the structure. As the soil is semi infinite, the size of the soil mass considered is 153 x 20 x 95m as shown in Fig. 8.1

### 8.2.2 Discretisation

Finite element formulation in the SSI analysis of the frame-isolated footings -soil system is as shown in Fig. 8.3(a, b, c). The soil is modelled with 43 x 10 x 27 layers in the longitudinal, vertical and transverse directions respectively resulting in 11,610 brick elements. Each footing of size 2 x 2m is modelled by four plate elements of size 1m x 1m. The number of plate elements used is 96. The number of beam elements in the longitudinal direction (X-direction) is 80, 72 in transverse (Z-direction) and 96 in the vertical (Y-direction). The graphs are plotted in terms of dimensionless Parameters X/L and Z/B where L and B are dimensions of the frame in X and Z directions as shown in Fig.8.3 (a).

The various components of the system with respective degrees of freedom are shown in Fig. 8.4 and are modelled as follows:

1. Columns and beams are modelled as one-dimensional beam elements with six degrees of freedom per node (three translational and three rotational degrees of freedom) as shown in Fig 8.4(a)
2. Soil mass is modelled as eight-noded brick element with three translational degrees of freedom per node as shown in Fig 8.4 (b).
3. Individual footing is modelled using plate elements with five degrees of freedom per node i.e., three translational degrees of freedom and two rotational degrees of freedom as shown in Fig. 8.4(c).

In the linear SSI analysis finite element model of the soil and footing system consists of:

1.  $43 * 10 * 27$  layers of soil elements in the longitudinal, vertical and transverse directions
2.  $44 * 11 * 28$  nodes in soil
3.  $6 * 4 * 5$  nodes in 3D-frame
4.  $(44 * 11 * 28 * \text{DOFNS} + 6 * 4 * 5 * \text{DOFNF})$  degrees of freedom in the system, where
  - DOFNS is Degree of Freedom per Node in Soil
  - DOFNF is Degree of Freedom per Node in the Frame

Taking DOFNS as 3 and DOFNF as 6, soil-footing-frame system results in 41286 degrees of freedom.

### 8.2.3 Validity of the proposed physical model

Figure 8.5 shows the settlements of the isolated footings obtained from the proposed analysis and their comparison with Swamy et al. (2011). Glance at the figure suggests that there is a very good agreement between the values of settlement. This justifies the finite element mesh extent considered.

### 8.3 Linear RSSI analysis of space frame-footing -soil system

To conduct linear RSSI analysis, the frame-footing-reinforced soil model used is as shown in the Figs. 8.6 and 8.7. The geometrical and material properties of the frames, its

components and the isolated foundation are presented in Table 8.2. Under each column footing four layers of geogrid are laid at D/B ratios of 0.25, 0.5, 0.75 and 1 as shown in Fig. 8.6. The size of isolated footing is 2m x 2m and the sizes of geogrid are 4m x 4m. The geometric details of geo-grid are shown in Fig. 8.8. Properties of geogrid are given in Table No 7.3.

Geogrid consists of apertures of size 25 x 34 mm as shown in Fig. 8.8.b. For a 1 x 1 m size geogrid the number of apertures are 30 x 40 in mutually perpendicular directions for as shown in Fig. 8.8.a.

If 4m x 4m geogrids were modelled with grid of bar elements, then it would require 19840 (i.e.,  $40 * 31 * 4 * 4$ ) number of bar elements and 20992 (i.e.,  $41 * 32 * 4 * 4$ ) nodes. In the linear SSI analysis, the soil and footing system consists of:

1. Keeping the thickness of hexahedron elements which represent soil as .025 m, to maintain aspect ratio nodes in soil is  $10978564772$  (i.e.,  $155*95*20 / (0.029*0.037*0.025)$ )
2.  $120$  (i.e.,  $6 * 4 * 5$ ) nodes in 3D-frame

This results in the reinforced soil-footing-frame system having  $32935695036$  (i.e.,  $10978564772 * \text{DOFNS} + 120 * \text{DOFNF}$ ) degrees of freedom. DOFNS and DOFNF can be taken as 3 and 6 respectively as in the linear SSI analyses.

Since modelling a single geogrid of given dimensions (4m x 4m) with apertures requires large memory requiring long time to analyse, macro elements of size 1 x 1m are developed and used in the RSSI analysis. The geo-grid of 1m x 1m with aperture size of 33mm x 25mm (shown in figure 8.8.a) is modelled using 2 dimensional rectangular element having 4 nodes with 2 degrees of freedom per node as shown in figure 8.8(c).

Figure 8.9(a) shows the arrangement of footings underlain by geogrid and Fig 8.9(b) shows Finite element modelling of geogrid. Each isolated footing of size 2 x 2 x 0.2 m is modelled with 4 four plate elements of size 1 x 1 x 0.2 m. Each geogrid of size 4 x 4m is modelled with 16 macro elements of size 1 x 1m. The stiffness matrix of macro element is evaluated from basic principles adopting the numerical method. The geogrid of size 1 x 1

m with given aperture sizes as shown in the Fig. 8.10, is modelled with 1240 (i.e., 40 \* 31) bar elements of width 4mm and thickness 3.3mm. The geogrid is allowed to have displacement in the direction where unit load is applied keeping all the other degrees of freedom restricted. Force required to cause unit displacement is found out and stiffness matrix is obtained. Diagonal stiffness co-efficient for a co-ordinate is defined as force applied to cause unit displacement in the direction of co-ordinate and the induced reactions along other constraints give the off diagonal stiffness coefficients of stiffness matrix.

For example to find the first column of stiffness matrix, restraints are applied at all coordinates except coordinate 1 along which unit force is applied as shown in Fig. 8.10. The displacements along co-ordinate 1 and reactions induced at the other co-ordinates are found out. The force required to produce unit displacement along first co-ordinate and induced forces are evaluated which are nothing but stiffness coefficients. The stiffness matrix obtained is as shown below

$$[K] = \begin{pmatrix} 83.39 & 25.017 & -60.753 & 2.082 & -17.423 & -25.018 & -5.214 & -2.082 \\ 25.017 & 88.66 & -2.083 & -5.411 & -25.017 & -17.826 & 2.082 & -65.423 \\ -60.753 & -2.083 & 83.39 & -25.017 & -5.214 & 2.082 & -17.423 & 25.018 \\ 2.082 & -5.411 & -25.017 & 88.66 & -2.082 & -65.423 & 25.017 & -17.826 \\ -17.423 & -25.018 & -5.214 & -2.052 & 83.39 & 25.017 & -60.753 & 2.082 \\ -25.017 & -17.826 & 2.082 & -65.423 & 25.017 & 88.66 & -2.083 & -5.411 \\ -5.214 & 2.082 & -17.423 & 25.019 & -60.753 & -2.083 & 83.39 & -25.017 \\ -2.082 & -65.423 & 25.017 & -17.826 & 2.082 & -5.411 & -25.017 & 88.66 \end{pmatrix}$$

## **8.4 Results of Linear SSI and RSSI analyses and discussions**

The location of a point in soil is expressed in terms of dimensionless parameters  $X/L$  and  $Z/B$ . The terms  $L$  and  $B$  are length and breadth of building along  $X$  and  $Y$  directions as shown in Fig.8.3 (a). All the output parameters or responses related to semi infinite media are plotted both in two dimensional and three dimensional graphs during the course of study. Due to constraint in the volume of the thesis, only critical cases are presented in three dimensional graphs to indicate spatial variation.

### **8.4.1 Displacements in linear analyses**

#### **8.4.1.1 Displacements in Linear SSI analysis**

Figure 8.11(a) shows the vertical deformation at foundation level in the longitudinal direction of the soil mass. Maximum vertical displacement of -156.63 mm in  $X$ -direction occur at  $X/L = \pm 0.267$  and  $Z/B = \pm 0.04$ . Figure 8.11(b) shows the displacement contours at foundation level. Figure 8.11(c) shows the displacements along longitudinal section.

Figure 8.12 shows horizontal displacements in longitudinal and transverse directions. In Fig 8.12(a) and (b) longitudinal displacements, at foundation levels are shown. Similarly in the Figs 8.12(c) and (d) transverse displacements at foundation levels are shown. Maximum horizontal displacement of 9.69 mm along  $X$ -direction occur at  $X/L = \pm 0.82$  and  $Z/B = \pm 0.167$ . Maximum horizontal displacement of 12.98 mm along  $Z$ -direction occur at  $X/L = \pm 1.03$  and  $Z/B = \pm 0.04$

#### **8.4.1.2 Displacements in Linear RSSI analysis**

Figure 8.13(a) shows the vertical deformation at foundation level along the longitudinal direction of the soil mass. Maximum vertical displacement of -150.8 mm along  $X$ -direction occurs at  $X/L = \pm 0.267$  and  $Z/B = \pm 0.16$ .

Figure 8.13(b) shows the displacement contours at foundation level. Figure 8.13(c) shows displacements along longitudinal section taken at centre. Maximum horizontal displacement of 5.62 mm along the X-direction occurs at  $X/L = \pm 0.82$  and  $Z/B = \pm 0.167$ . Maximum horizontal displacement of 7.03 mm along the Z-direction occurs at  $X/L = \pm 1.03$  and  $Z/B = \pm 0.04$ .

Figure 8.14 shows horizontal displacements along the longitudinal and transverse directions in the linear RSSI analysis. In Fig. 8.14(a) and (b) longitudinal displacements at foundation levels are shown. Similarly in the Figs. 8.14(c) and (d) transverse displacements at foundation levels are shown. The maximum horizontal displacement of 6.52 mm along X-direction occur at  $X/L = \pm 0.82$  and  $Z/B = \pm 0.167$ . Maximum horizontal displacement of 7.03 mm along Z-direction occurs at  $X/L = \pm 1.03$  and  $Z/B = \pm 0.04$ .

## **8.4.2 Stresses in soil**

### **8.4.2.1 Stresses in soil in Linear SSI analysis**

Vertical stress contours at foundation level in the linear SSI are shown in Figure 8.15(a). Figure 8.15(b) shows stress distribution at section A-A. Figure 8.15(c) shows variation of stresses at foundation level along longitudinal sections taken across breadth for different values of  $Z/B$ . The maximum stresses of  $0.041 \text{ N/mm}^2$  occur at  $X/L = \pm 0.33$  and  $Z/B = \pm 0.55$ .

Figure 8.16(a) shows contours and Fig. 8.16 (b) shows longitudinal stresses at foundation level along longitudinal sections taken across breadth for different values of  $Z/B$ . The maximum horizontal longitudinal stresses of  $0.02018 \text{ N/mm}^2$  occur at  $X/L = \pm 0.4$ ,  $Z/B = \pm 0.2167$ . Figure 8.16(c) shows contours and Fig. 8.16 (d) shows transverse stresses at foundation level along longitudinal sections taken across the breadth for different values of  $Z/B$ . The maximum horizontal transverse stresses of  $0.02281644 \text{ N/mm}^2$  occur at  $X/L = \pm 0.13$ , and  $Z/B = \pm 0.33$ .

#### **8.4.2.2 Stresses in soil in Linear RSSI analysis**

Vertical stress contours at foundation level in linear RSSI analysis are shown in Fig. 8.17(a). Figure 8.17(b) shows stress distribution at section A-A. Figure 8.17(c) shows variation of vertical stress at section taken along X-direction located at different positions along Z-direction. The maximum stresses of  $0.04379 \text{ N/mm}^2$  occur at  $X/L = \pm 0.33$  and  $Z/B = \pm 0.55$

Figure 8.18(a) shows stress contour and Fig. 8.18 (b) shows longitudinal stresses at foundation level along longitudinal sections taken across the breadth for different values of Z/B. The maximum horizontal longitudinal stresses of  $0.01849099 \text{ N/mm}^2$  occur at  $X/L = \pm 0.33$  and  $Z/B = \pm 0.2167$ .

Figure 8.18(c) shows stress contour and Fig. 8.18(d) shows transverse stresses at foundation level along with the longitudinal sections taken across breadth for different values of Z/B. The maximum horizontal transverse stresses of  $0.018659375 \text{ N/mm}^2$  occur at  $X/L = \pm 0.33$  and  $Z/B = \pm 0.33$ .

#### **8.4.3 Stress resultants in members of 3-Dimensional frame**

The frame shown in Fig. 8.2 is analysed for three cases viz., Linear Non-interactive (NI) analysis, Linear SSI analysis and Linear RSSI analysis. As one of the main objectives is to study the effect of reinforcement in soil on structural behaviour the stress resultants in each member is compared in these three analyses. Tables 8.3 to 8.7 give values of axial and shear forces in the members of the frame. Tables 8.8 to 8.10 give bending moments in all the members. In all the tables, members are classified based on whether they are a part of external or internal frames. As the frame-foundation-soil model has two axes of symmetry, only the members of quarter frame are considered. In Fig. 8.2 the quarter

frame is enclosed by the grid lines 1, 2, A, B and C. The frames along grid lines 1 and A are referred to as external frames. The frames along grids 2, B and C are referred to as interior frames.

#### **8.4.3.1 Axial and shear forces in beams.**

The axial and shear forces in X-beams in external and internal frames are given in Tables 8.3 and 8.4. The structure of the tables is as follows:

Column 1	Gives whether the frame is external or internal
Column 2	Gives the floor
Column 3	Gives the member number
Column 4,5,6	Give X,Y and Z co-ordinates of nodes of members
Columns 7,8	Give axial force and shear force (kN) along Y direction of beams in local co-ordinates for NI analysis
Columns 9,10	Give axial force and shear force (kN) along Y direction of beams in local co-ordinates for SSI analysis
Columns 11,12	Give axial force and shear force (kN) along Y direction of beams in local co-ordinates for RSSI analysis
Columns 13,14	Give ratio of axial force, shear force along Y direction of beams in SSI analysis to NI analysis
Columns 15,16	Give ratio of axial force, shear force along Y direction of beams in RSSI analysis to NI analysis
Columns 17,18	Give ratio of axial force, shear force along Y direction of beams in RSSI analysis to SSI analysis

#### **i) Axial and Shear forces along X-beams**

From column 7 of Tables 8.3 and 8.4, it can be observed that in NI analysis, axial forces in members are greater in external storeys when compared to internal storeys. The shear



force (column 8) is maximum at the support next to end support of end span followed by shear force in interior spans and end support.

From columns 9 and 13 of Tables 8.3 and 8.4 it can be viewed that in linear SSI analysis, axial forces in x-beams are -0.73 to 10.01 times axial forces along X-beams in NI analysis. Axial forces are increased by many folds with respect to NI analysis especially in top storeys. The shear forces in linear SSI analysis -0.04 to 2.18 times NI analysis. The shear force is maximum at end support followed by shear forces on internal side of support next to end support and shear forces at interior spans.

The trends of axial forces from RSSI analysis along X-beams are 2.37 to 8.28 times the axial forces in X-beams in NI analysis. Shear forces in X-beams in linear RSSI analysis are 0.15 to 1.92 times the shear forces along X-beams in NI analysis. Axial forces and shear forces are found to have lesser differential values between two ends of a member as observed from columns 11, 12, 15 and 16 of Tables 8.3 and 8.4. Axial forces along X-beams from linear RSSI analysis are found to exceed axial forces along X-beams in linear SSI analysis only in the ground floor where as in higher floors, these values are found to decrease. Shear forces along X-beams in linear RSSI analysis are lesser in external spans when compared to shear forces along X-beams from linear SSI analysis.

**ii. Axial and Shear forces along Z-beams** Table 8.5 gives the axial and shear forces along Z-beams. The general trends in NI, linear SSI and linear RSSI analysis follow the foot steps of trends in X-beams. Axial forces along Z-beams in linear SSI are -3.29 to 6.19 times the axial forces along Z-beams in NI analysis. Shear forces along Z-beams in linear SSI are 0.01 to 2.07 times the shear forces along Z-beams in NI analysis.

Axial forces along Z-beams in linear RSSI vary from -1.87 to 7.12 times the axial forces in Z-beams in NI analysis. Shear forces along Z-beams in linear RSSI vary from 0.19 to 1.9 times the shear forces along Z-beams in NI analysis. Over all both axial forces and shear forces were found to reduce in linear RSSI analysis when compared to linear SSI analysis.

### 8.4.3.2 Axial and Shear forces in Columns

The values of the axial forces in the column members at various storey levels corresponding to NI, linear SSI and linear RSSI analysis have been presented in Tables 8.6 and 8.7. Forces in columns along grid line 1 and grid line 2 are given in Tables 8.6 and 8.7 respectively. The structure of the tables are as mentioned as below

Column 1	Gives whether the frame is external or internal
Column 2	Gives the floor
Column 3	Gives the member number
Column 4,5, 6	Give X,Y Z co-ordinates of nodes of members
Columns 7,8, 9	Give axial force(kN), shear force (kN) along Y and Z direction of beams in local co-ordinates for NI analysis
Columns 10,11,12	Give axial force(kN), shear force (kN) along Y and Z direction of beams in local co-ordinates for SSI analysis
Columns 13,14,15	Give axial force(kN), shear force (kN)along Y and Z direction of beams in local co-ordinates for RSSI analysis
Columns 16,17,18	Give ratio of axial force, shear force along Y and Z direction of beams in SSI analysis to NI analysis
Columns 19, 20,21	Give ratio of axial force, shear force along Y and Z direction of beams in RSSI analysis to NI analysis
Columns 22,23,24	Give ratio of axial force, shear force along Y and Z direction of beams in RSSI analysis to SSI analysis

Comparing columns 7 of Tables 8.6 and 8.7 it can be observed that columns in external frame along grid line 1 carry 41.37% total loads when compared to columns in internal frame along line 2 which carry 58.63% of the total load. It is evident from this table that axial forces in NI analysis can be put under three categories based on their values. Corner columns carry 10.03%, peripheral columns carry 42.84% and internal columns carry 47.12% of total load.

On the contrary in linear SSI analysis, external columns in external frame along grid line 1 carry 45% total loads when compared to columns in internal frame along line 2 which carry 55% of total load. Corner columns carry 12.32%, peripheral columns carry 28.79 %

and internal columns carry 52.27% of total load. When linear RSSI is done at a glance, it is evident from this table that axial forces have reduced marginally by about 2 percent when compared to linear SSI analysis.

Shear forces in columns in NI analysis are negligible. 1.2% to 8.3% of axial forces carried by columns. However in linear SSI analysis, shear forces in column are 6% to 30% of axial forces. Introduction of reinforcement in soil reduces the shear forces in linear SSI analysis. Shear forces in RRSI analysis are 3.6% to 24 % of axial forces.

### 8.4.3.3 Bending moments along beams

Table 8.8 gives the values of bending moments in X-beams in NI, linear SSI and linear RSSI analysis. Table 8.9 gives the comparative values of bending moments along Z-beams in NI, linear SSI and RSSI analysis.

Column 1	Gives whether the frame is external or internal
Column 2	Gives the floor
Column 3	Gives the member number
Column 4,5, 6	Give X,Y Z co-ordinates of nodes of members
Columns 7,8, 9	Give bending moments (kNm) in beams about local z-axis in NI, SSI and RSSI analysis respectively
Columns 10,11,12	Give ratio of bending moments SSI to NI, RSSI to NI and RSSI to SSI

#### i. Bending moments (BM) in X-beams

Bending moments along X-beams in linear SSI analysis vary from -2.23 to 6.28 times bending moments in NI analysis. Corresponding to these limits the ratio of bending moments in RSSI analysis to linear SSI analysis vary from 0.77 to 0.88. Bending

moments along X-beams in RSSI analysis vary from -0.87 to 1.23 times bending moments in NI analysis.

## **ii. Bending moments in Z-beams**

Bending moments along Z-beams in linear SSI analysis vary from -2.03 to 5.88 times the bending moments in NI analysis. Corresponding to these limits the ratio of bending moments in RSSI analysis to linear SSI analysis vary from 0.66 to 1.47. Bending moments along X-beams in RSSI analysis vary from -1.71 to 4.73 times the bending moments in NI analysis.

### **8.4.3.4 Bending moments in columns**

The values of the axial forces in the column members at various storey levels corresponding NI, linear SSI and RSSI analysis have been presented in the Table 8.10. The structure of the table is as follows

Column 1	Gives whether the frame is external or internal
Column 2	Gives the floor
Column 3	Gives the member number
Column 4,5,6	Give X,Y Z co-ordinates of nodes of members
Columns 7, 8	Give BM (kNm) in columns about local Y and Z axes in NI analysis
Columns 9,10	Give BM (kNm)in columns about local Y and Z axes in SSI analysis
Columns 11,12	Give BM (kNm) in columns about local Y and Z axes in RSSI analysis
Columns 13,14	Give ratio BM in columns about local Y and Z in SSI to NI analysis
Columns 15,16	Give ratio BM in columns about local Y and Z in RSSI to NI analysis
Columns 17,18	Give ratio BM in columns about local Y and Z in RSSI to SSI analysis

From table 8.10 it can be observed that bending moments will increase in interactive analyses when compared to NI analysis due to the fact that the non-interactive analysis ignores the effect of differential settlements. Bending moments in columns of external frames are more than the bending moment in columns of interior frames. It was found that for the values of  $M_y$  and  $M_z$  of magnitude greater than 25kNm in NI analysis the moments vary from 3.71 to 4.47 and 4.3 to 5.1 times in linear SSI with respect to NI analysis. For the values of  $M_y$  and  $M_z$  of magnitude greater than 25kNm in NI analysis the moments vary from 3.26 to 4.06 and 3.68 to 4.41 in linear RSSI with respect to NI analysis. However provision of reinforcement reduces BM in columns up to 46%.

#### **8.4.4. Discussions on linear SSI and RSSI analyses**

##### **8.4.4.1 Discussion on displacements in soil**

Figure 8.19.a and 8.19.b show lateral displacements at foundation level along X and Z directions are reduced by 42% and 45.8% respectively in Linear RSSI analysis with respect to linear SSI analysis. Figure 8.20 shows the vertical displacements in linear SSI and RSSI analyses at foundation level along longitudinal line at  $Z/B=0.0$ . it can be observed that the vertical displacements are reduced merely by 3.72 %. In RSSI analysis when compared to linear SSI.

##### **8.4.4.2 Discussion on stresses in soil**

The contact pressure on isolated footings follows the same trend as that of vertical displacement. In the longitudinal direction, the contact pressure at various points has increased. However, this increase has been compensated by a corresponding reduction in the contact pressure at various other points along longitudinal sections. This is logical as the total soil reaction offered must be equal to the total applied load on the structure-foundation system. The contact pressure distribution obtained on the basis of both the analysis follows almost similar trend. However the maximum stresses in linear RSSI

analysis seem to merge to a common value. The maximum vertical stress in linear RSSI analysis is 6% more than linear SSI analysis. But the horizontal stresses are reduced by 8.4% and 18.7% in longitudinal and transverse directions respectively.

Section 8.4.5 presents the Figures and Graphs related to Linear SSI and RSSI Analyses.  
Section 8.4.6 presents the Figures and Graphs related to Linear SSI and RSSI Analyses.

### 8.4.5 Figures and Graphs plotted in Linear SSI and RSSI Analysis

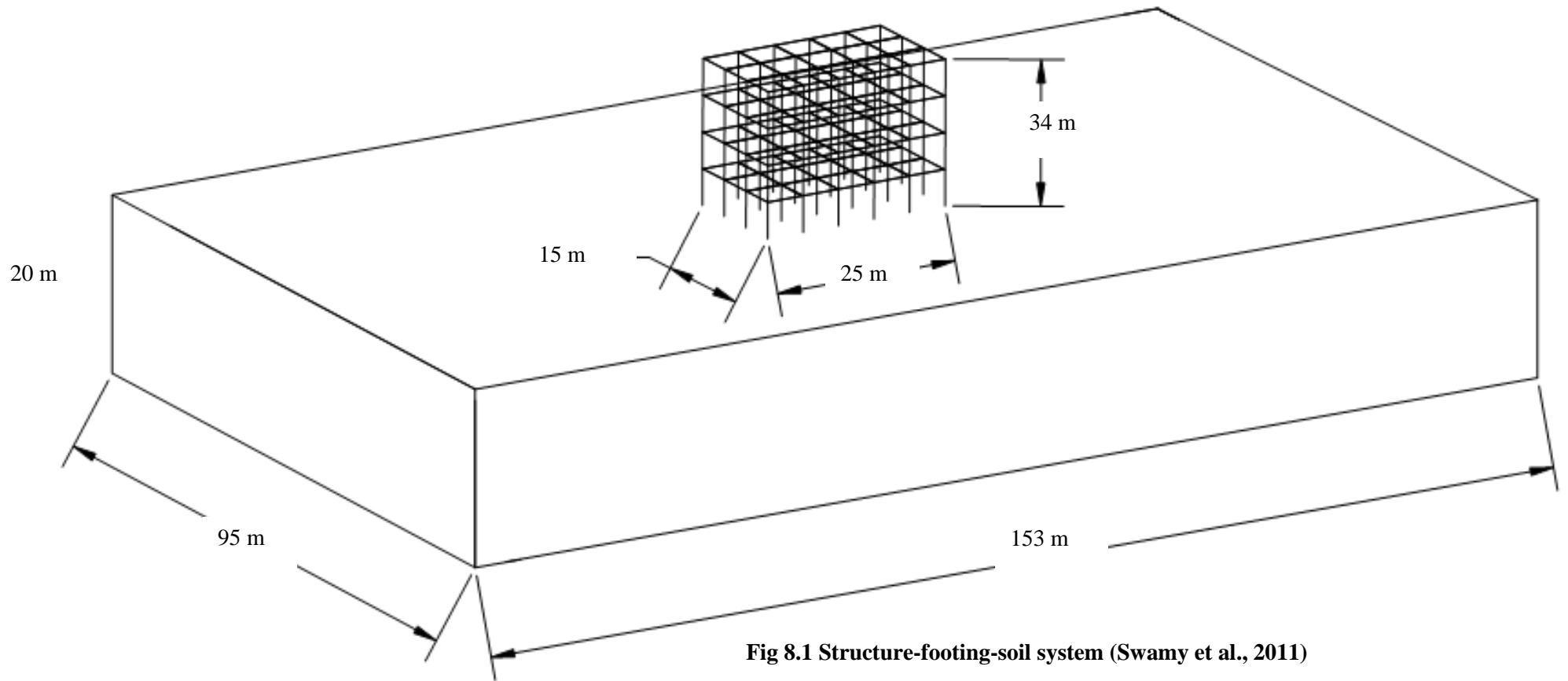
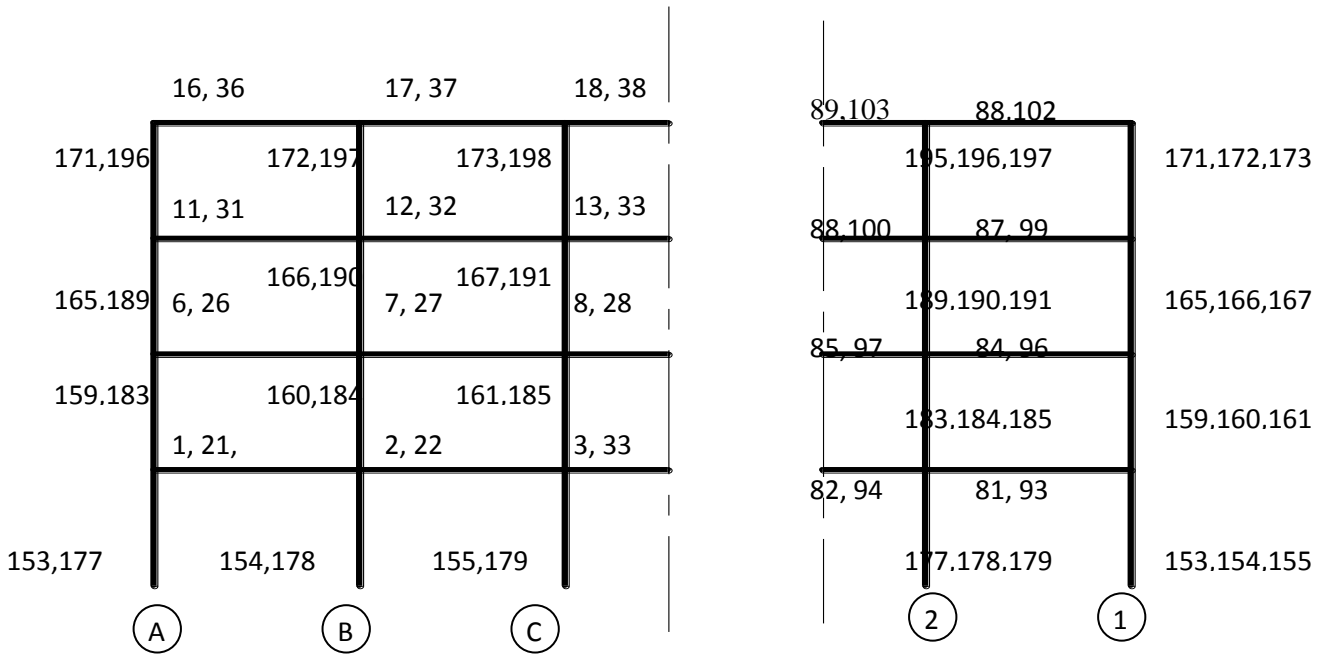
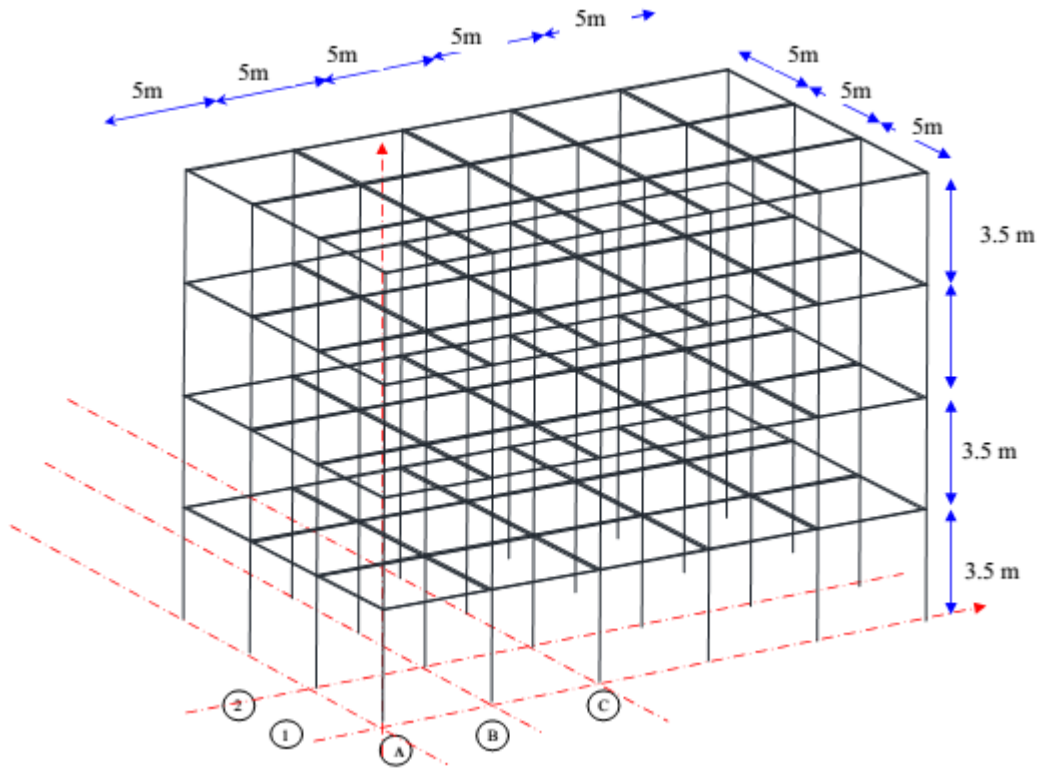


Fig 8.1 Structure-footing-soil system (Swamy et al., 2011)



**Fig 8.2: Details of quarter frame (Swamy et. al. (2011))**



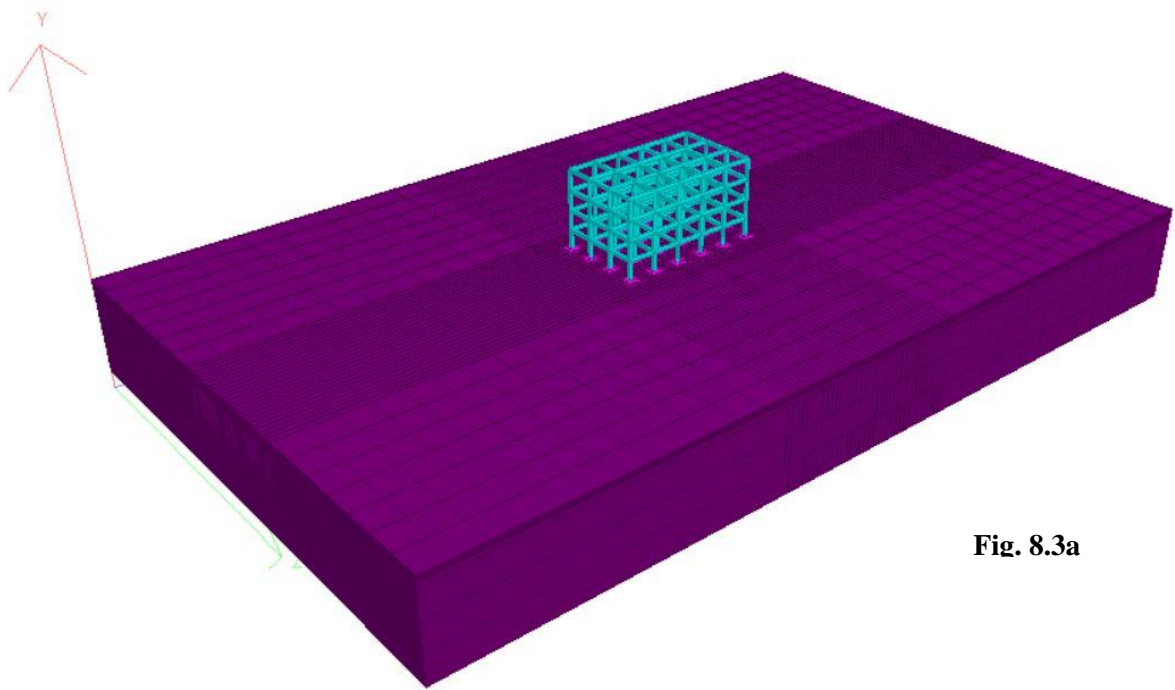


Fig. 8.3a

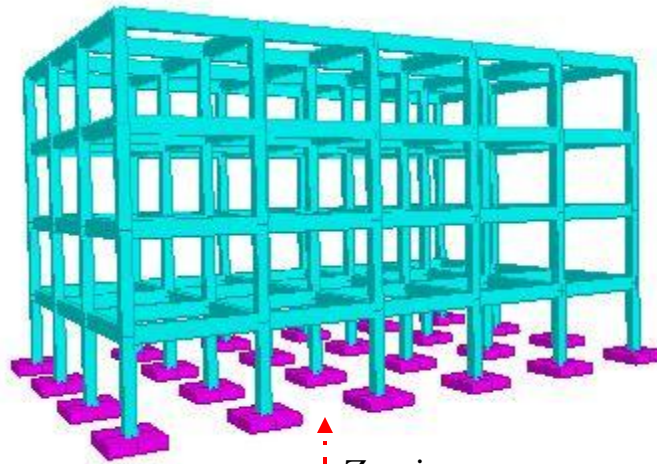


Fig. 8.3b

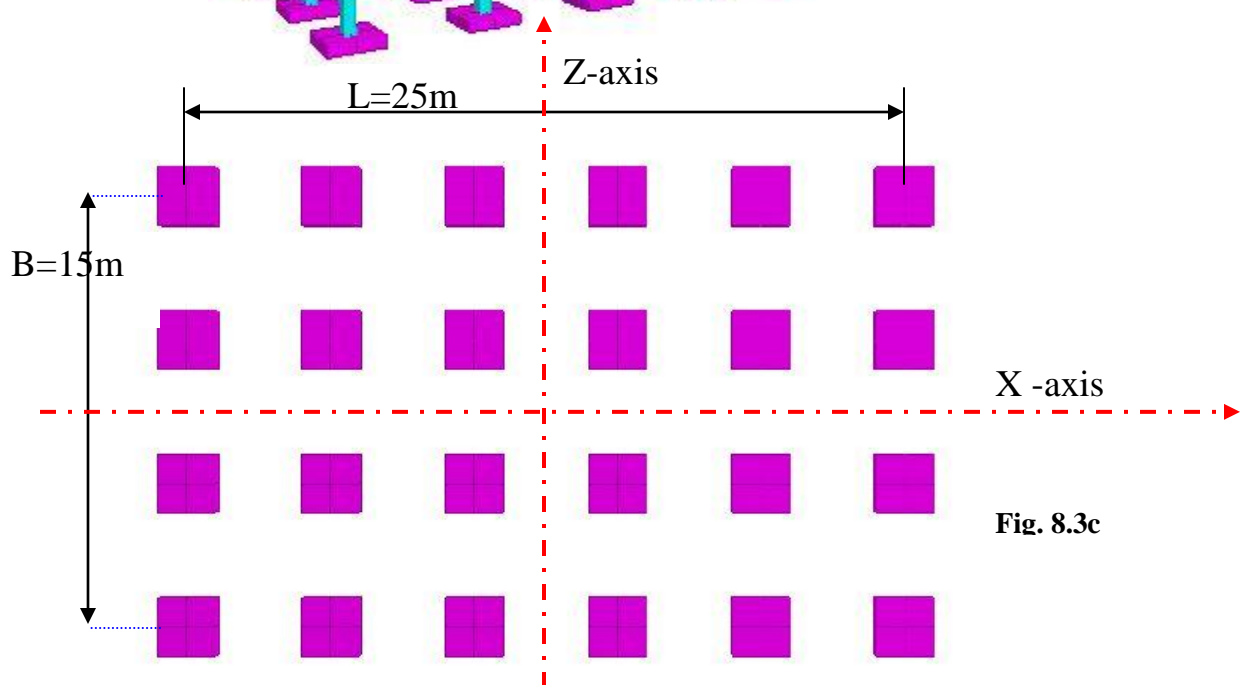
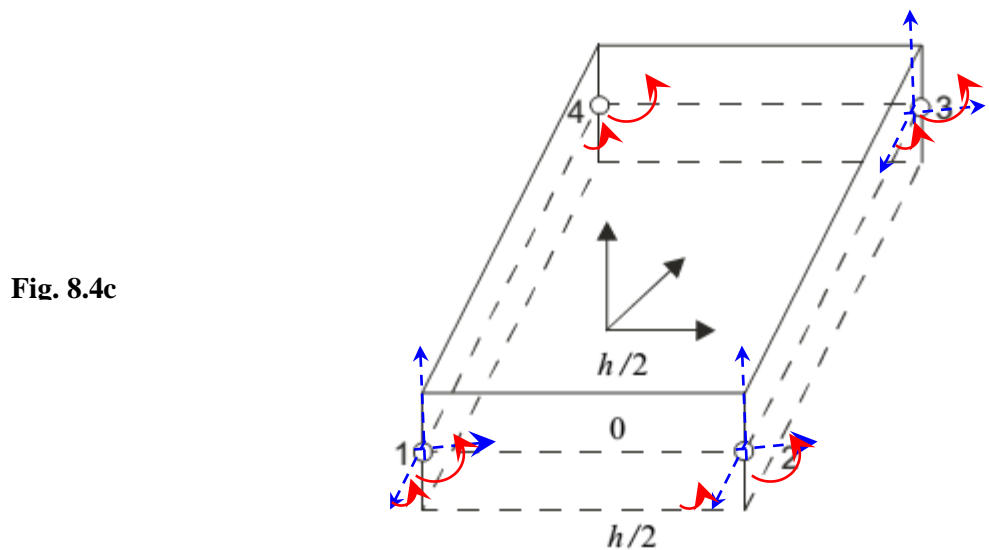
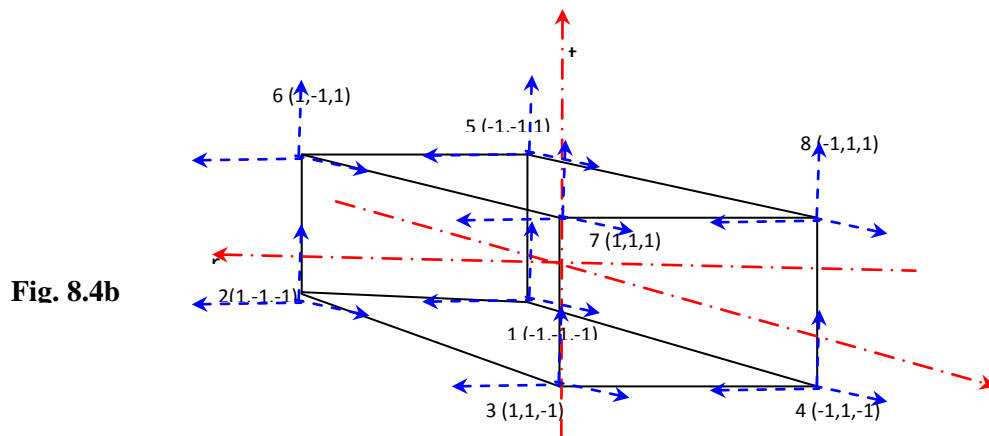
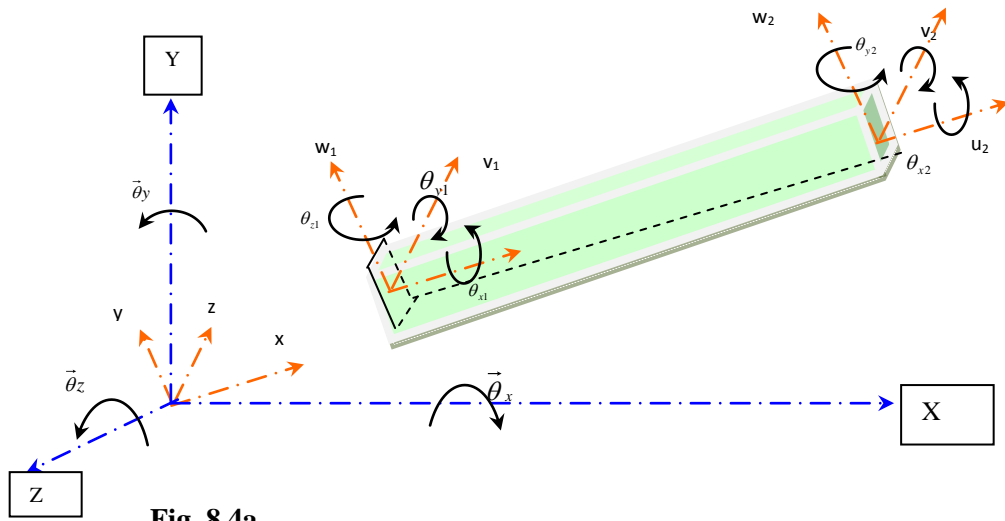
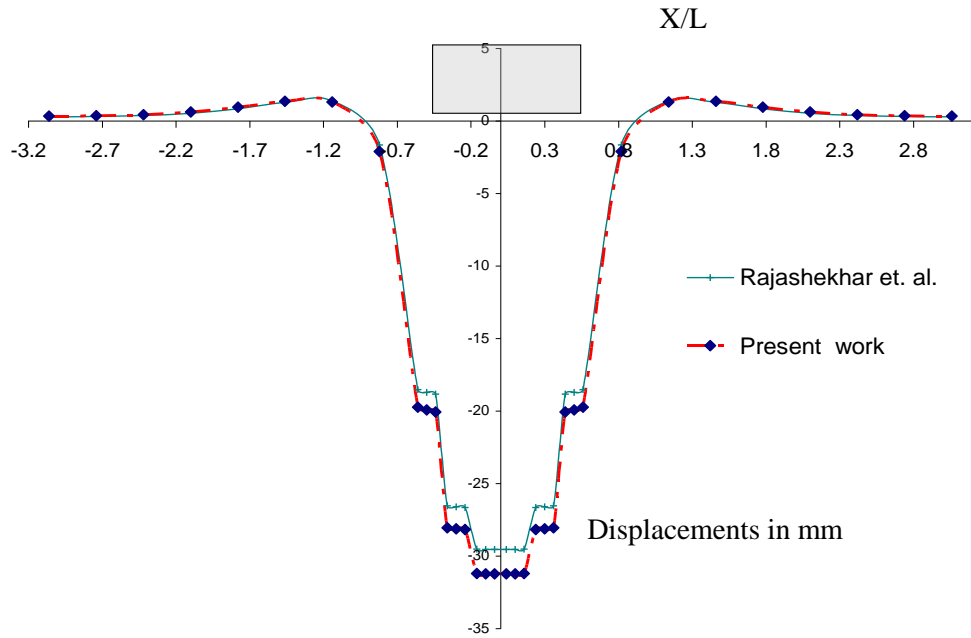


Fig. 8.3c

Fig. 8.3(a) Frame-isolated footing-soil system. (b) Structure foundation system. (c) Reference axis and arrangement of isolated footings



**Fig. 8.4** Details of element types (a) Euler-Bernoulli beam element used for beams and columns (b) Brick element for soil (c) Plate element used for footing



**Fig. 8.5 Comparative settlements in mm at the centre in the present work and the referred work (Swamy et. al.(2011))**

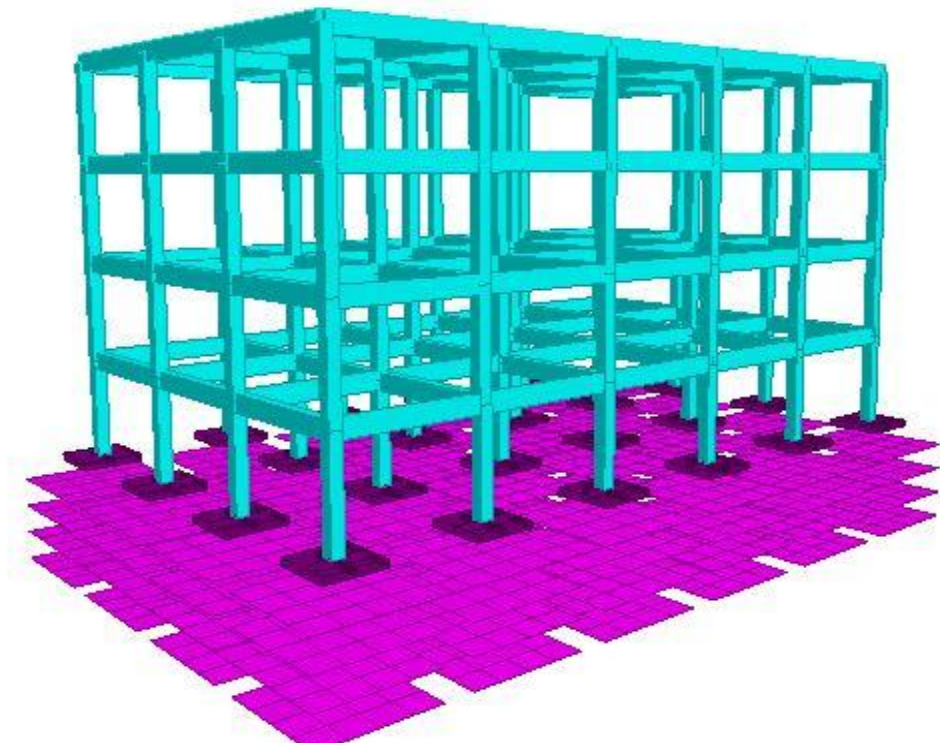


**Fig. 8.6: Frame-footing-reinforcement module**

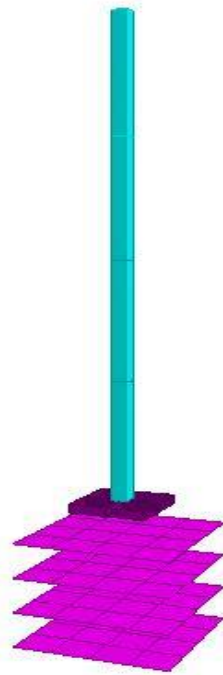


**Fig. 8.7a**

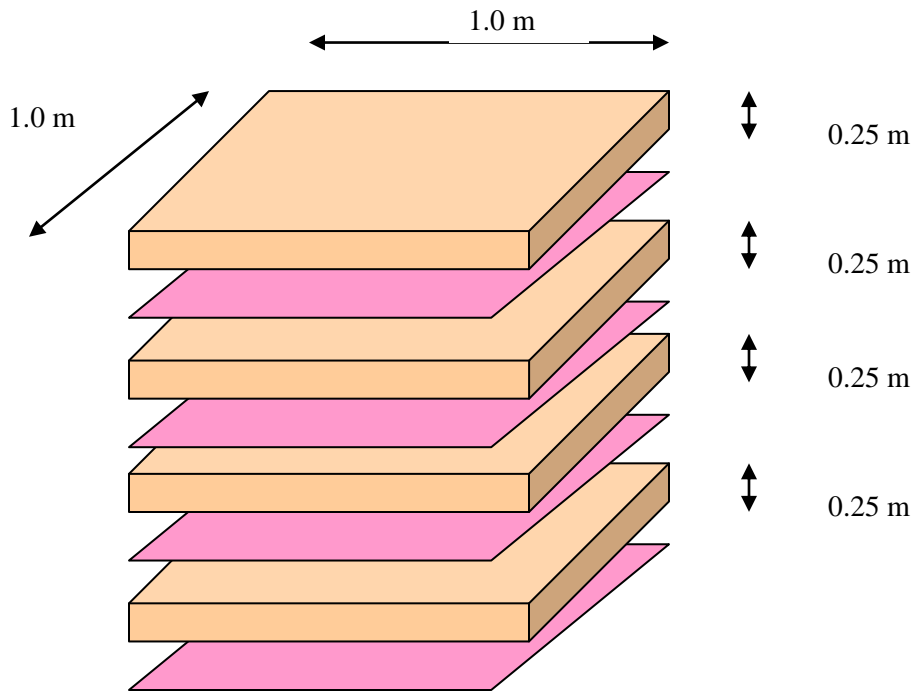


**Fig. 8.7b**

**Fig. 8.7** Arrangement of geogrid (a) Modelling of column-foundation- Geogrid (b) soil-geogrid arrangement represented as macroelement in RSSI analysis

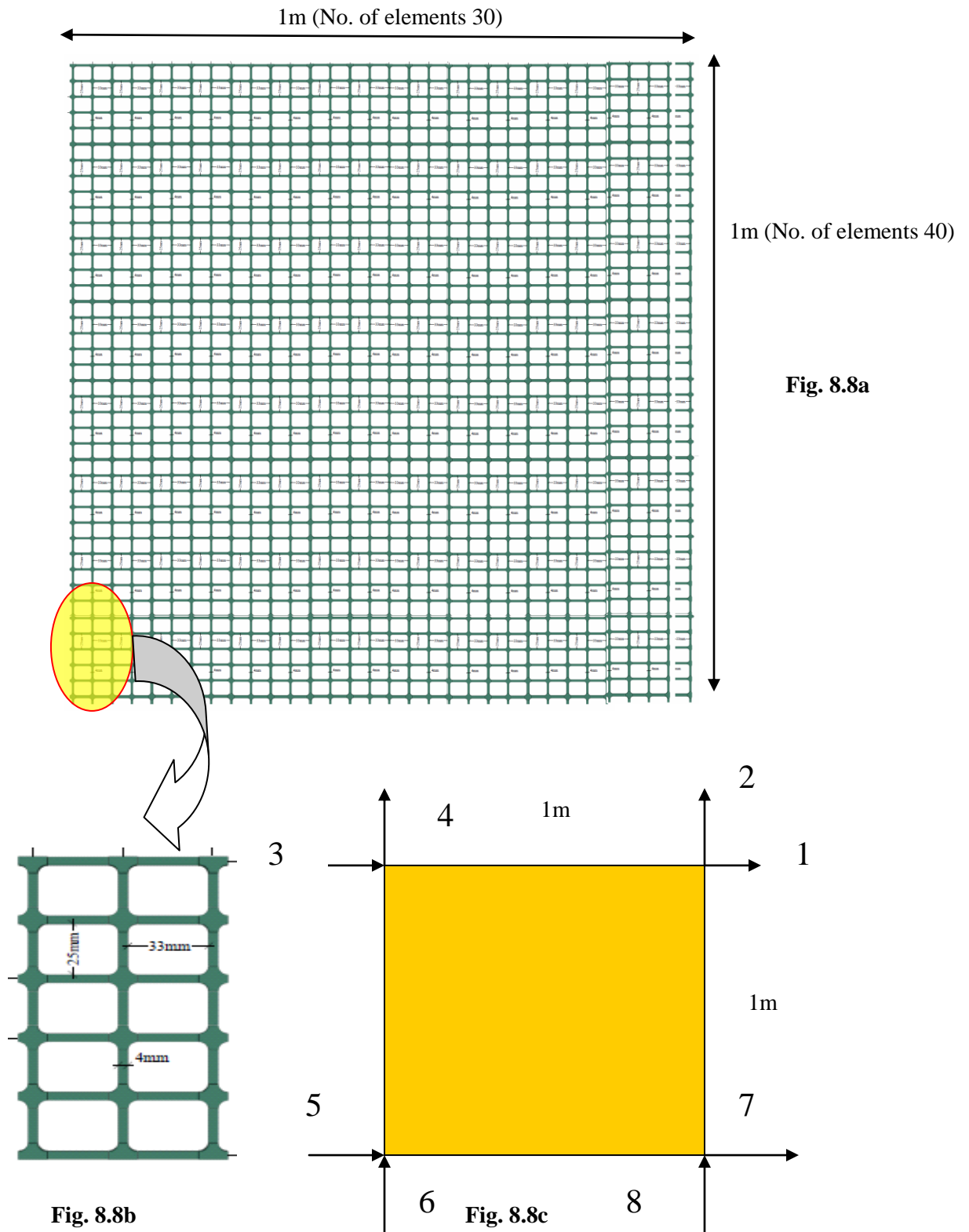


**Fig. 8.8: Details of Geogrid and Macro element (a) Geogrid of size 1m x 1m with apertures (b) Geometrical details of geogrid (c) Geogrid represented as macro element of size 1m x 1m**



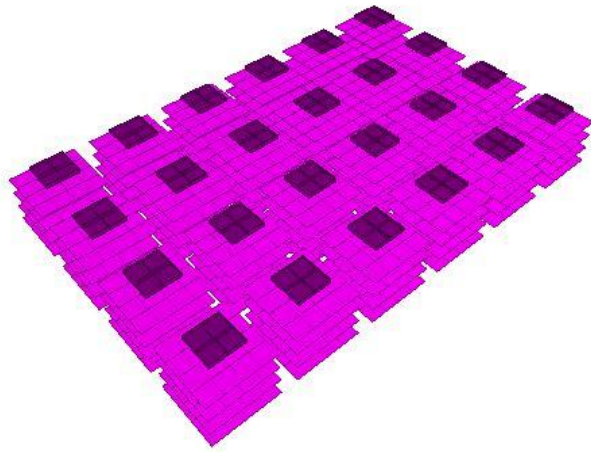


Fig. 8.9a

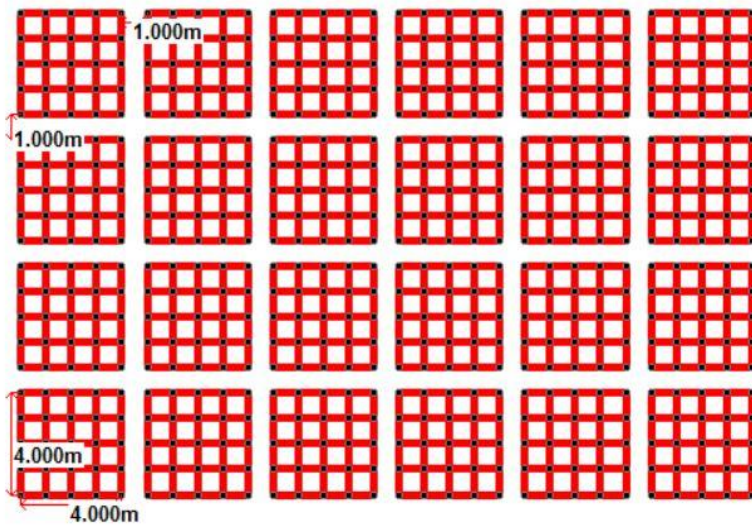


Fig. 8.9b

Fig. 8.9 (a) Footing and geogrid arrangements (b) FEM modelling geogrid

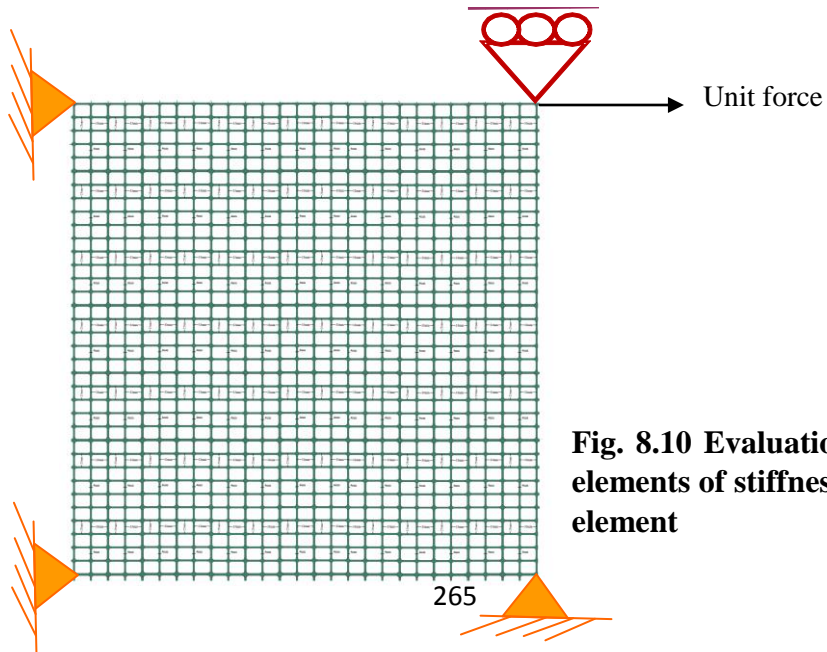


Fig. 8.10 Evaluation of first column elements of stiffness matrix of macro-element

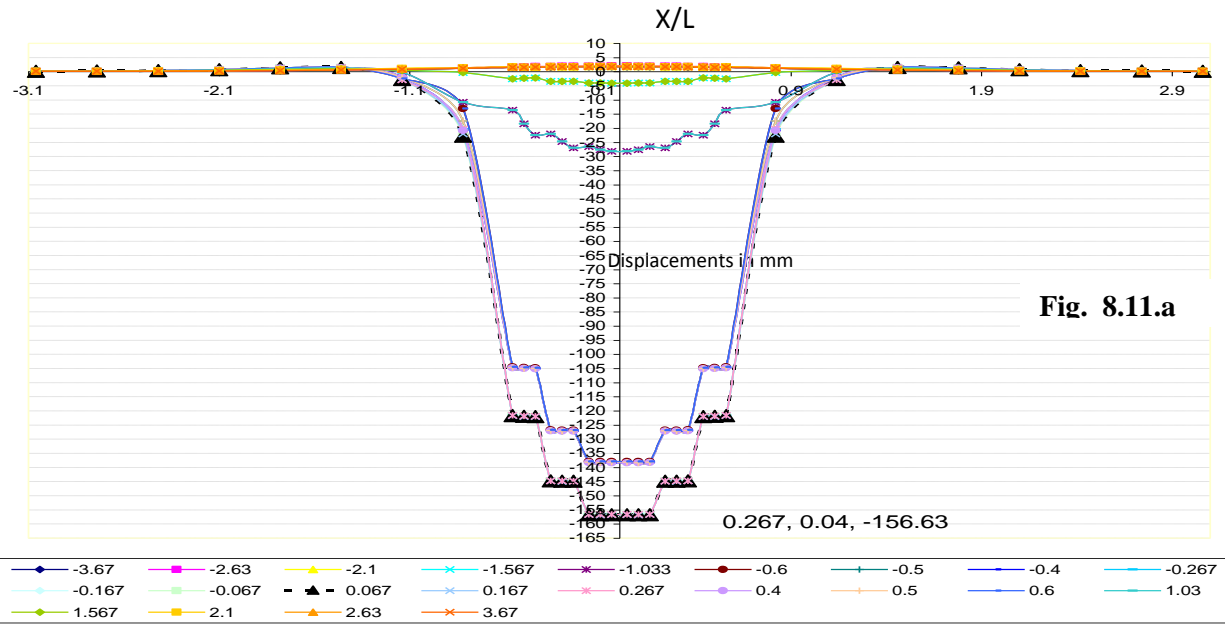


Fig. 8.11.a

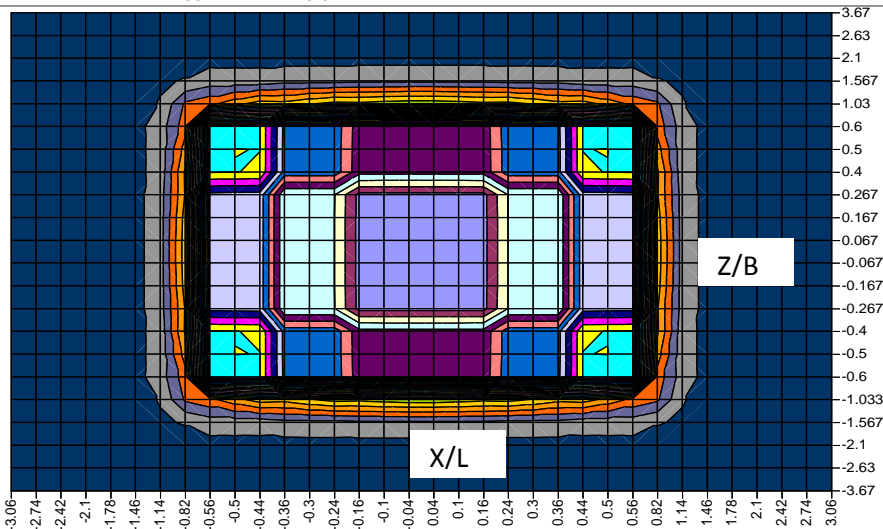


Fig. 8.11.b

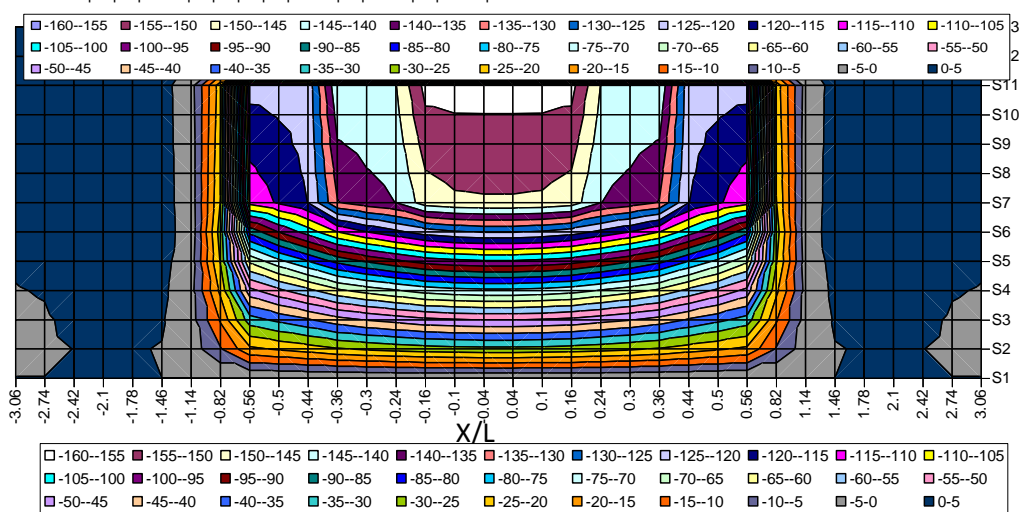


Fig. 8.11.c

Fig. 8.11: Vertical settlements in mm in Linear SSI analysis (a) Vertical settlements at foundation level (b) Contours of vertical settlements at footing level (c) Vertical settlements along longitudinal section

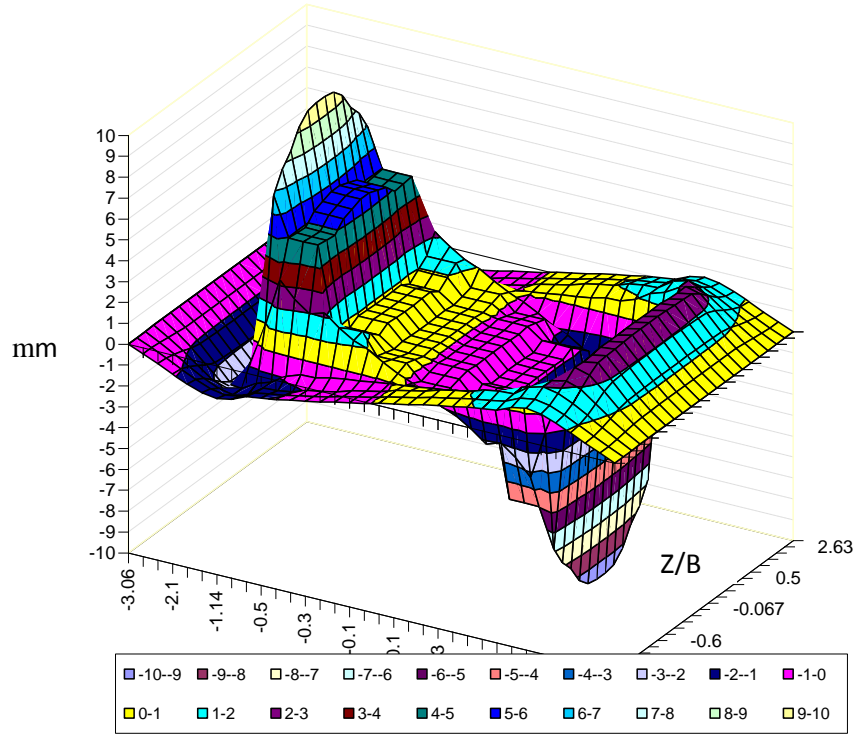


Fig. 8.12.a

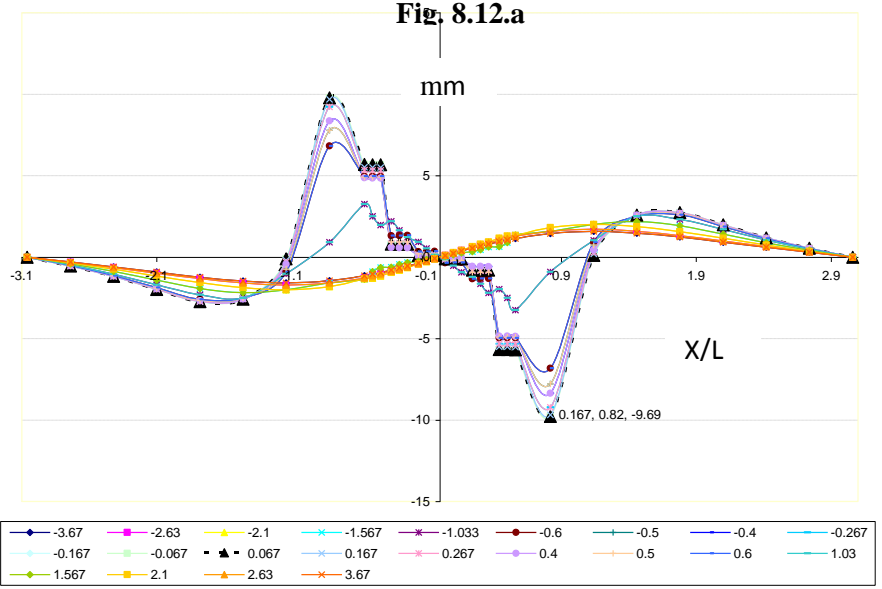


Fig.8.12.b

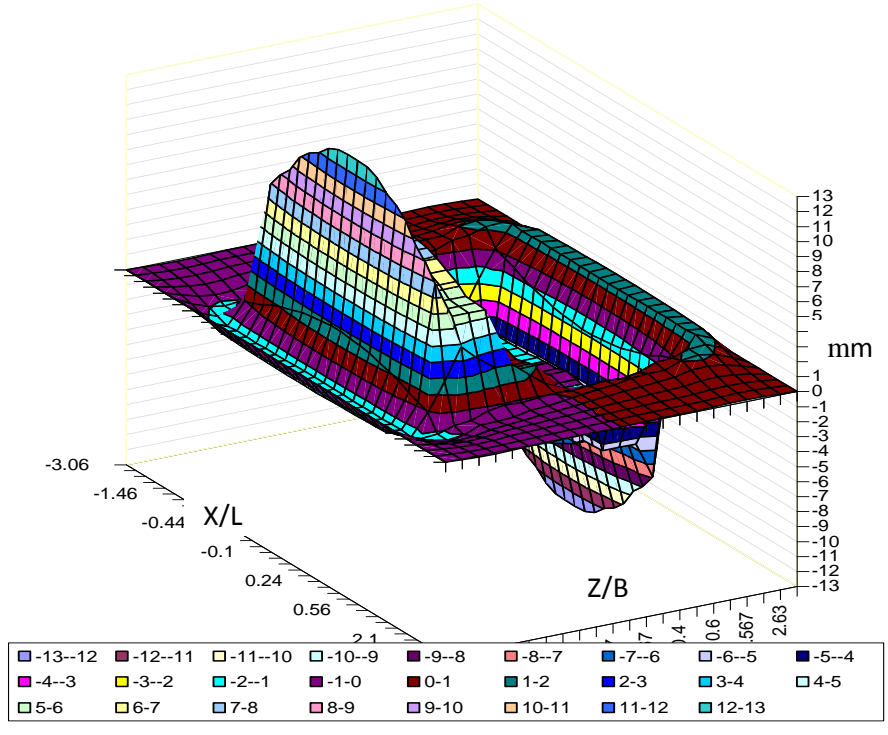


Fig. 8.12.c

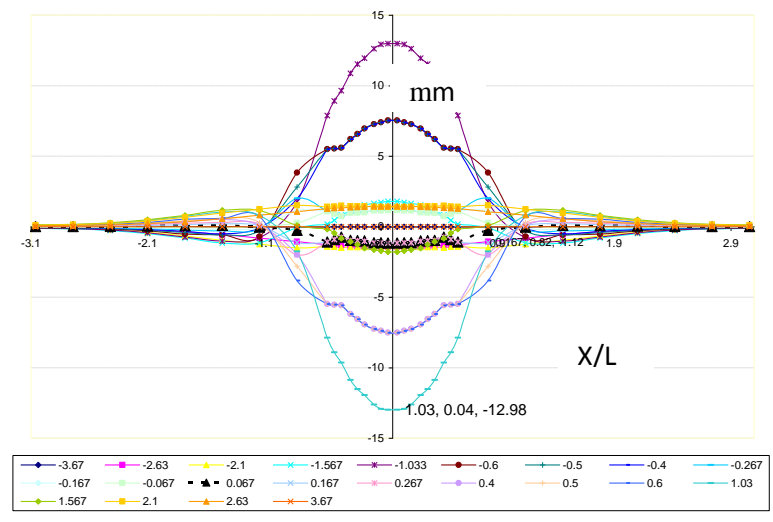
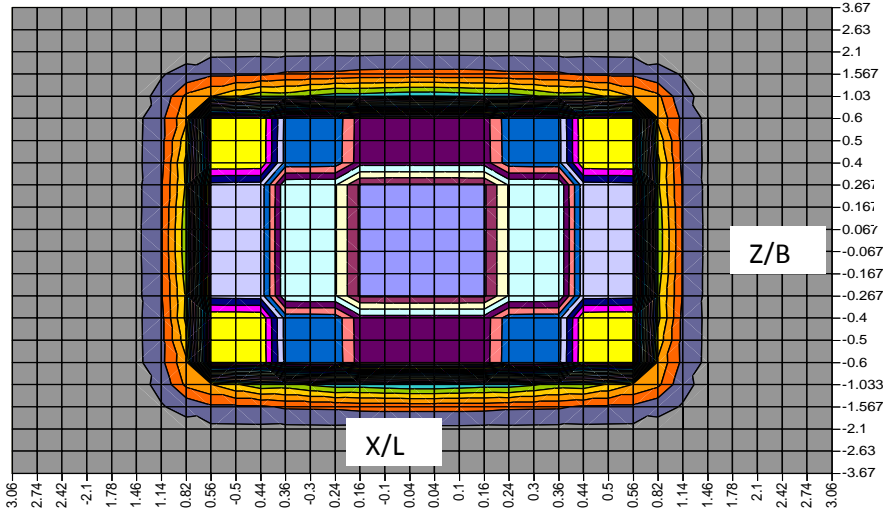
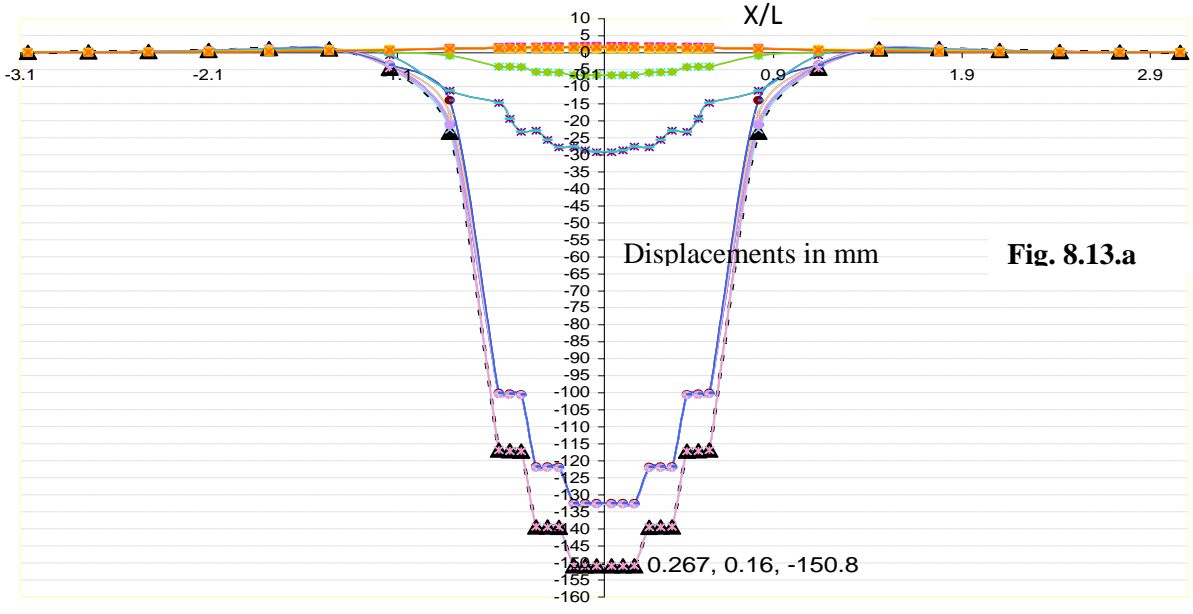


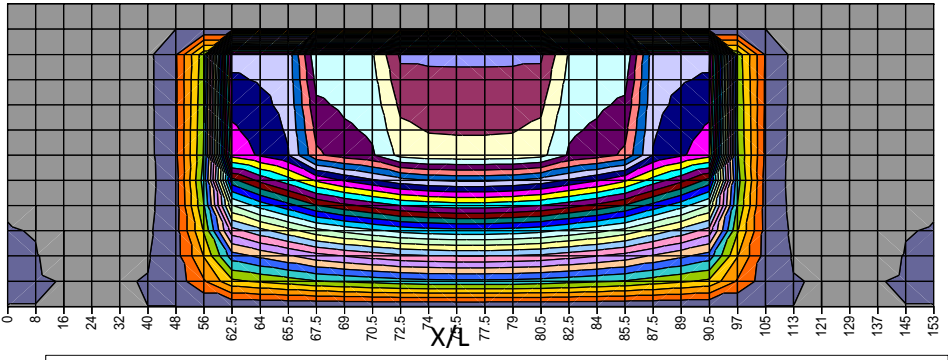
Fig. 8.12.d

Fig. 8.12 Horizontal displacements in mm in linear SSI analysis: (a) and (b) longitudinal displacements at foundation level (c) and (d) Transverse displacements at foundation level





-155--150	-150--145	-145--140	-140--135	-135--130	-130--125	-125--120	-120--115	-115--110	-110--105	-105--100
-100--95	-95--90	-90--85	-85--80	-80--75	-75--70	-70--65	-65--60	-60--55	-55--50	-50--45
-45--40	-40--35	-35--30	-30--25	-25--20	-20--15	-15--10	-10--5	-5-0	0-5	



-155--150	-150--145	-145--140	-140--135	-135--130	-130--125	-125--120	-120--115	-115--110	-110--105	-105--100
-100--95	-95--90	-90--85	-85--80	-80--75	-75--70	-70--65	-65--60	-60--55	-55--50	-50--45
-45--40	-40--35	-35--30	-30--25	-25--20	-20--15	-15--10	-10--5	-5-0	0-5	

**Fig. 8.13: Vertical settlements in mm in Linear RSSI analysis (a) Vertical settlements at foundation level (b) Contours of vertical settlements at footing level. (c) Vertical settlements along longitudinal section at centre.**

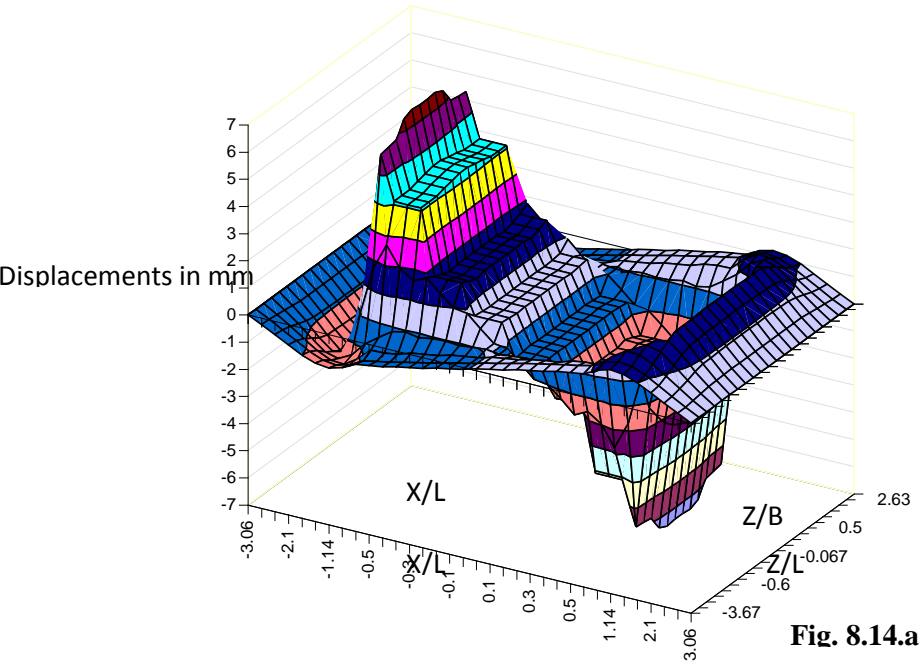


Fig. 8.14.a

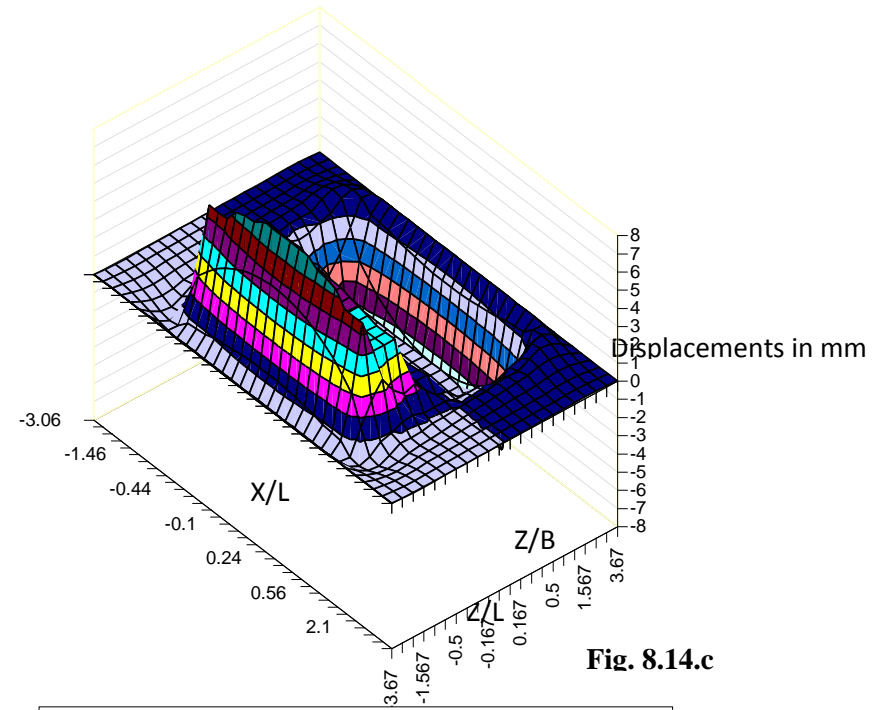


Fig. 8.14.c

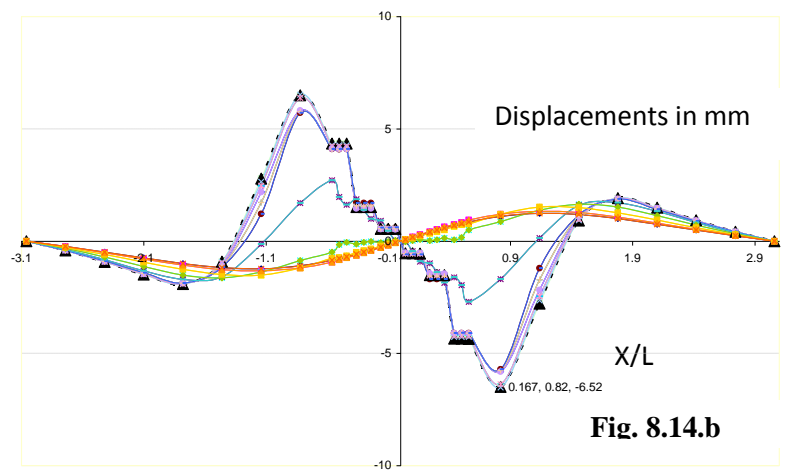
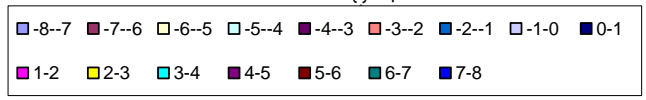


Fig. 8.14.b

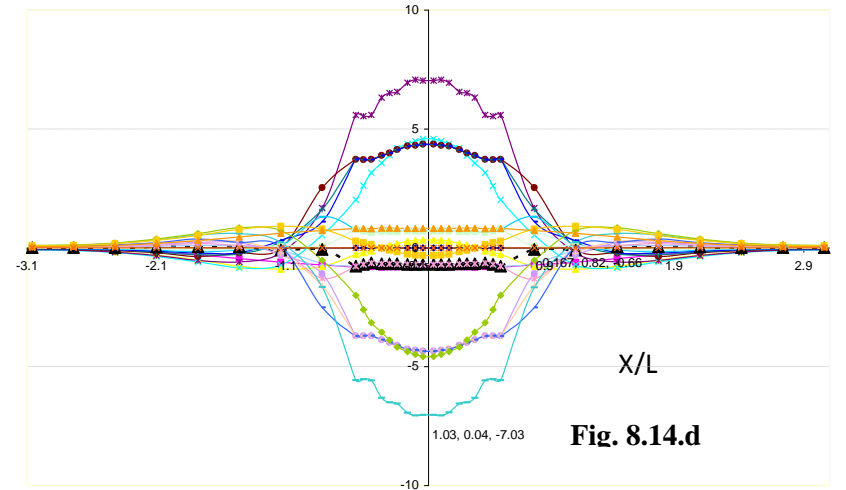
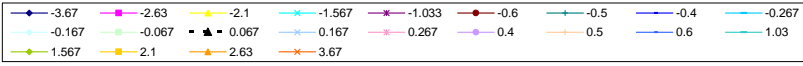


Fig. 8.14.d

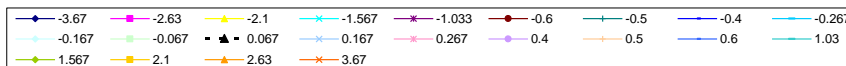


Fig. 8.14 Horizontal displacements in mm in linear RSSI analysis (a) and (b) longitudinal displacements at foundation level (c) and (d) transverse displacements at foundation level

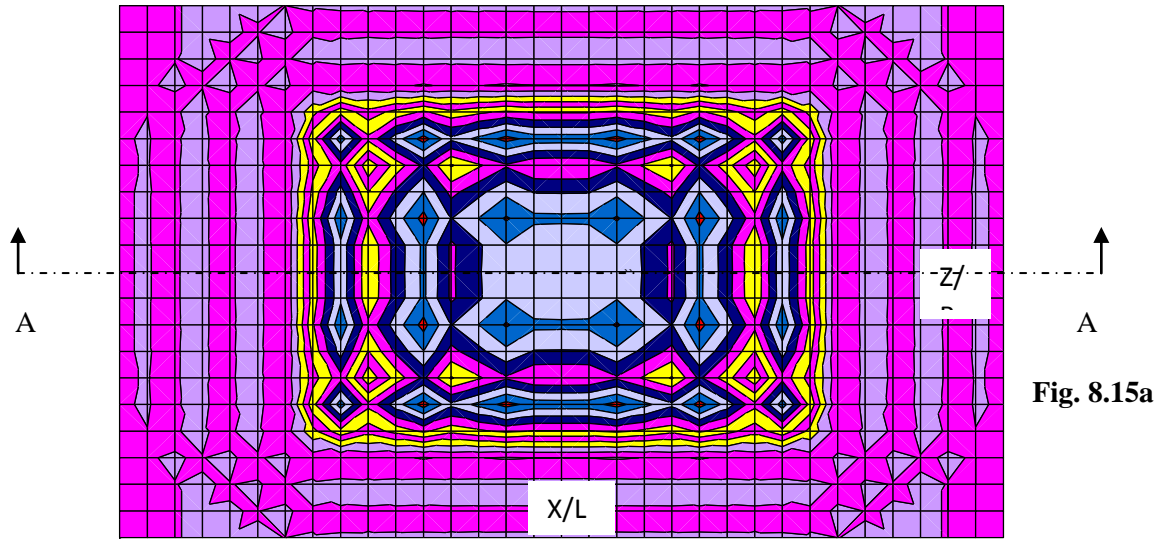


Fig. 8.15a

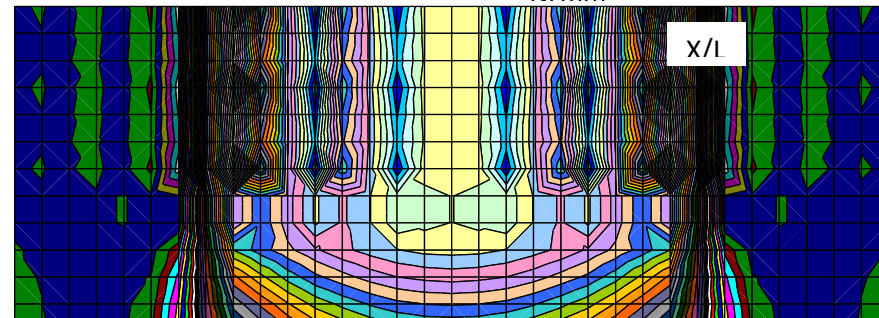
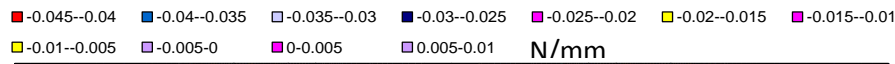


Fig. 8.15b

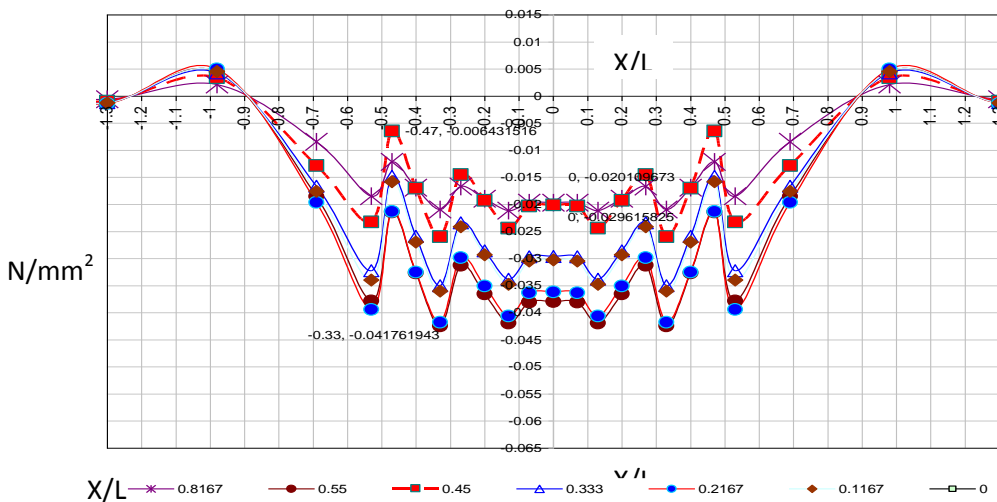
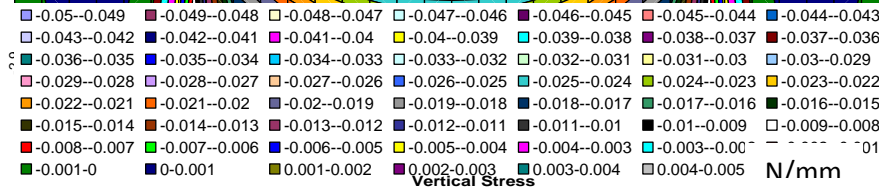


Fig. 8.15c

Fig. 8.15: Vertical stresses in  $N/mm^2$  linear SSI analysis (a) Contours of vertical stresses; footing level (b) Vertical stresses along longitudinal section at centre (c) Vertical stresses foundation level along longitudinal sections for different values of  $Z/L$

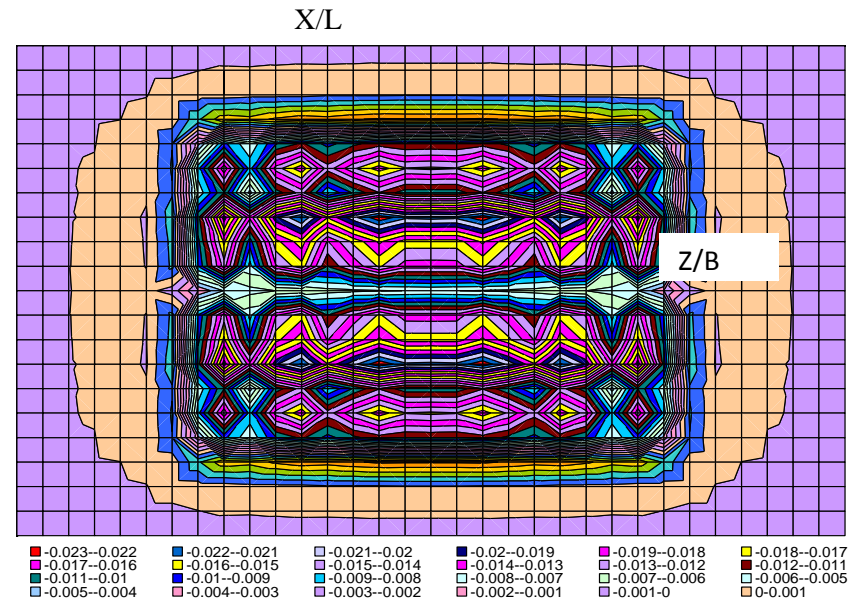
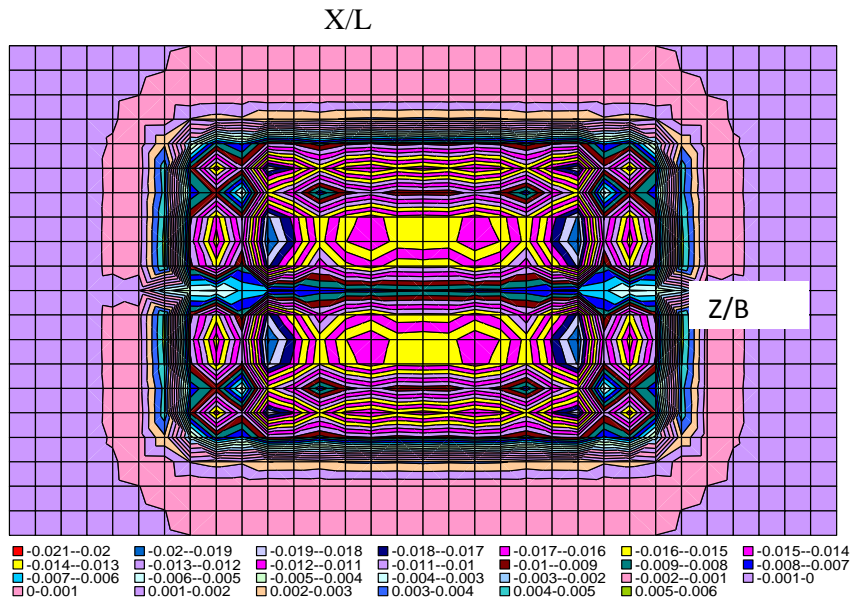


Fig. 8.16 a

Fig. 8.16 c

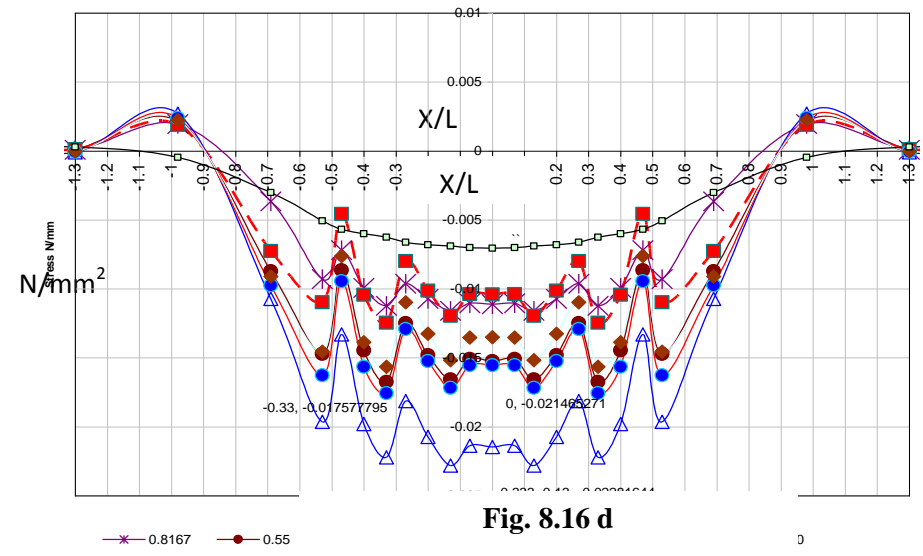
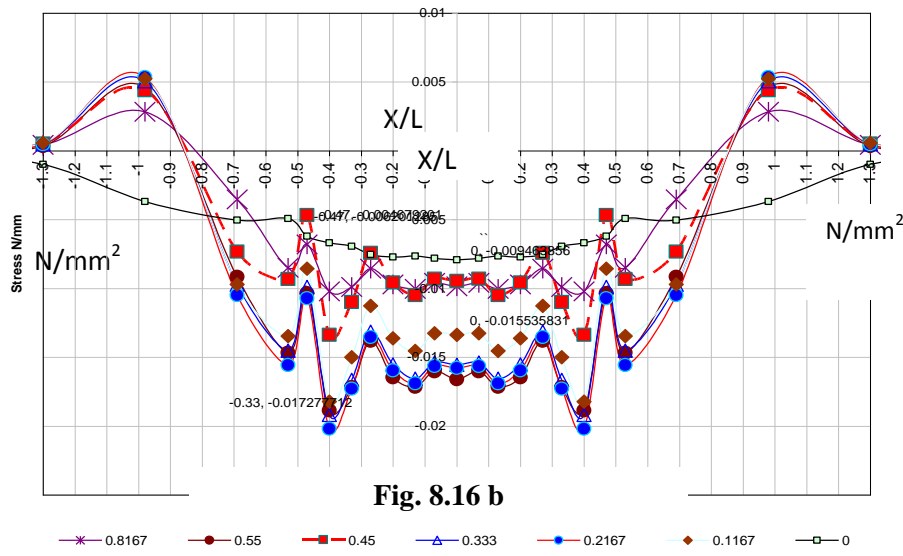


Fig. 8.16 b

Fig. 8.16 d

Fig. 8.16 Horizontal stresses in  $N/mm^2$  in linear SSI analysis (a) and (b) longitudinal stresses at foundation level (c) and (d) Transverse stresses at foundation level



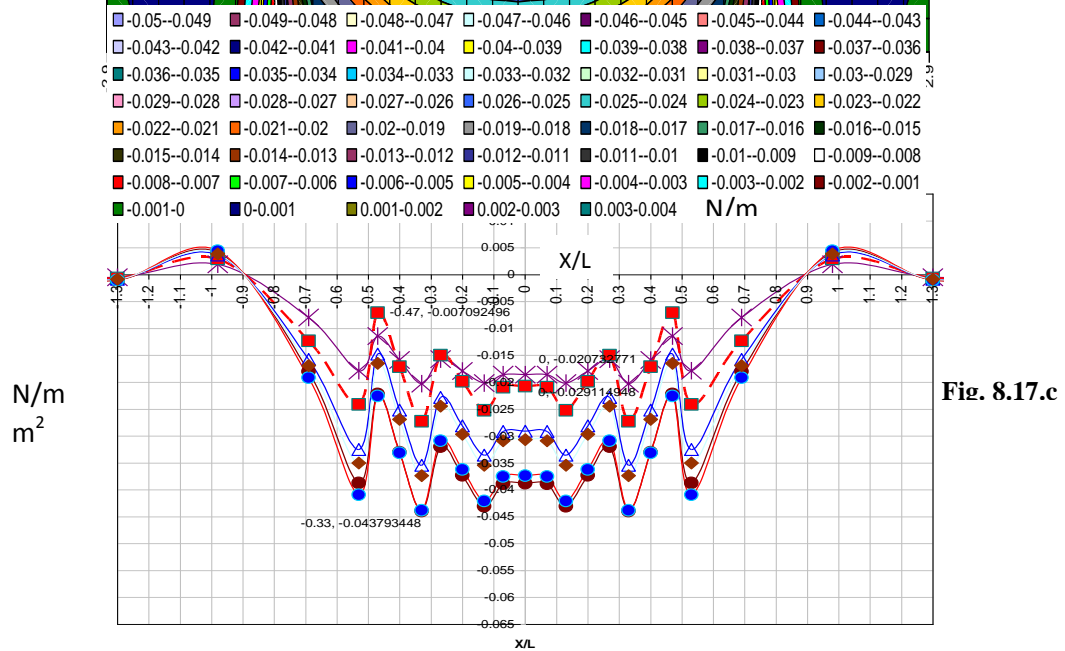
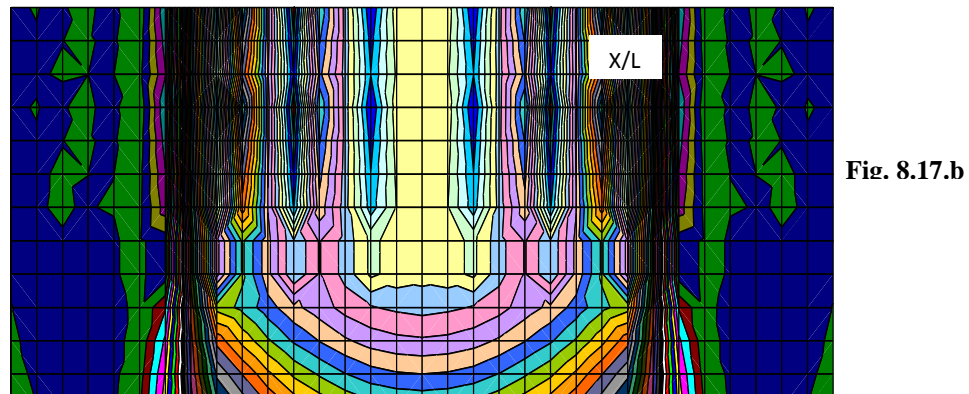
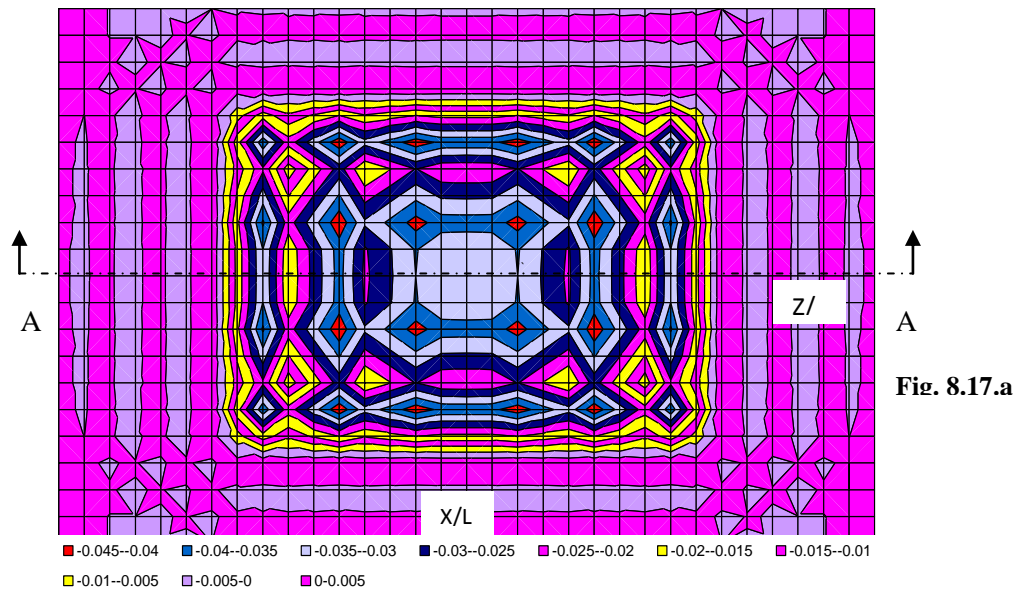


Fig. 8.17: Vertical stresses in  $N/mm^2$  in linear RSSI analysis (a) Contours of vertical stresses at footing level (b) Vertical stresses along longitudinal section at centre (c) Vertical stresses at foundation level along longitudinal sections for different values

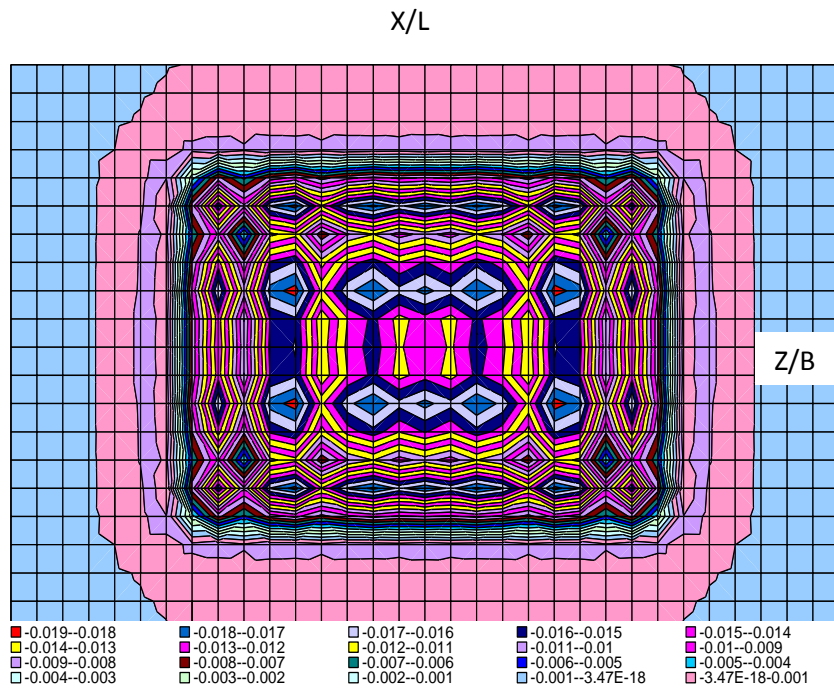


Fig. 8.18.a

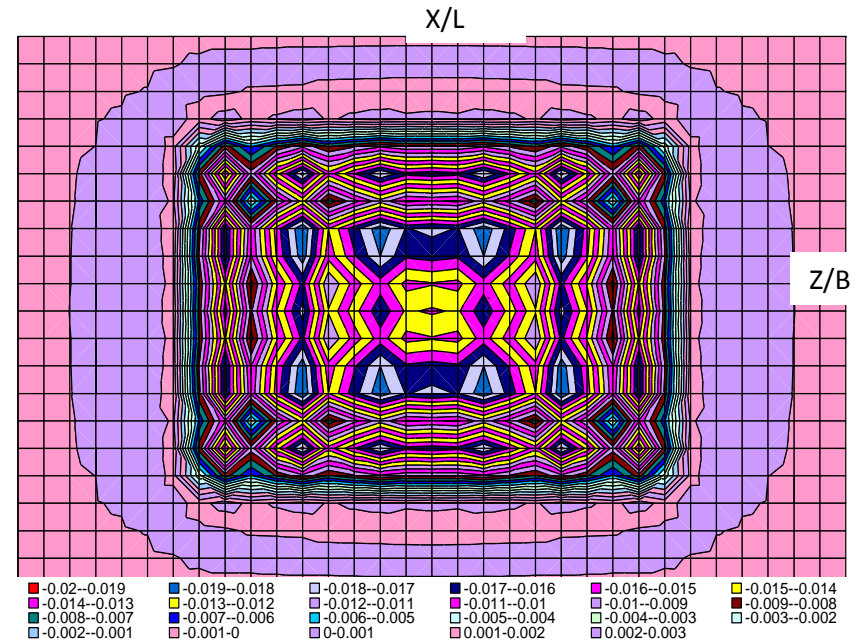


Fig. 8.18.c

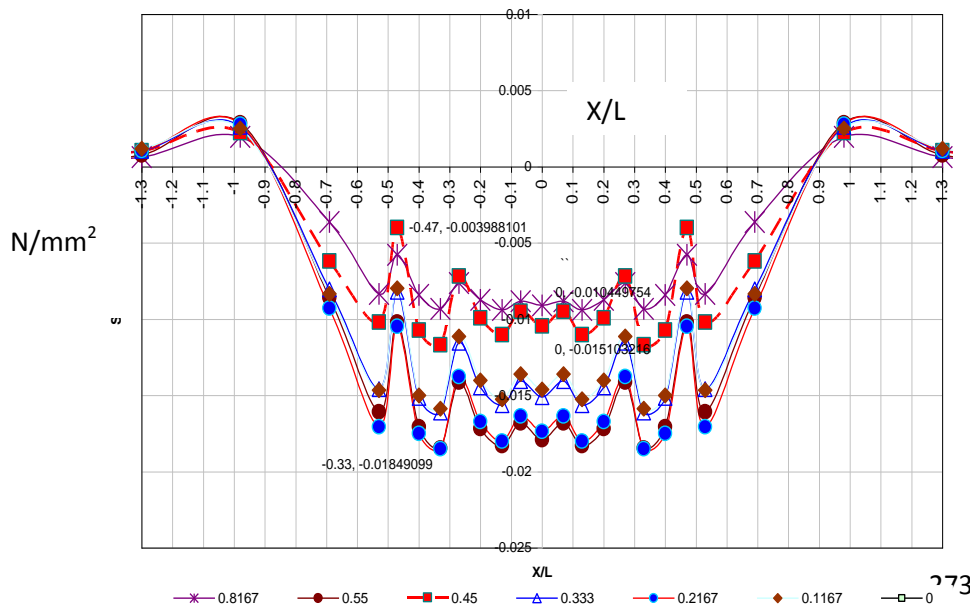


Fig. 8.18.b

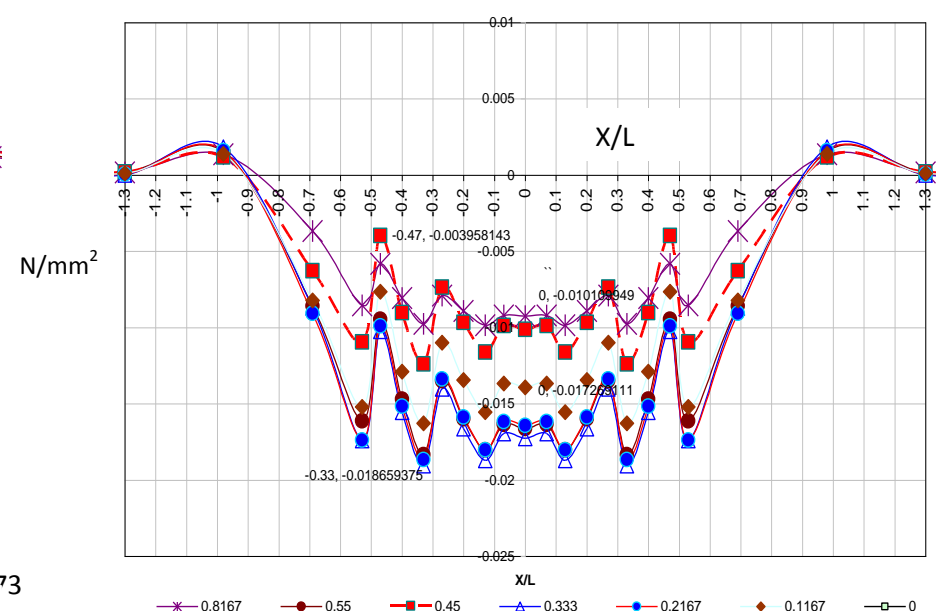


Fig. 8.18.d

Fig. 8.18 Horizontal stresses in linear RSSI analysis (a) and (b) longitudinal stresses at foundation level (c) and (d) transverse stresses at foundation level

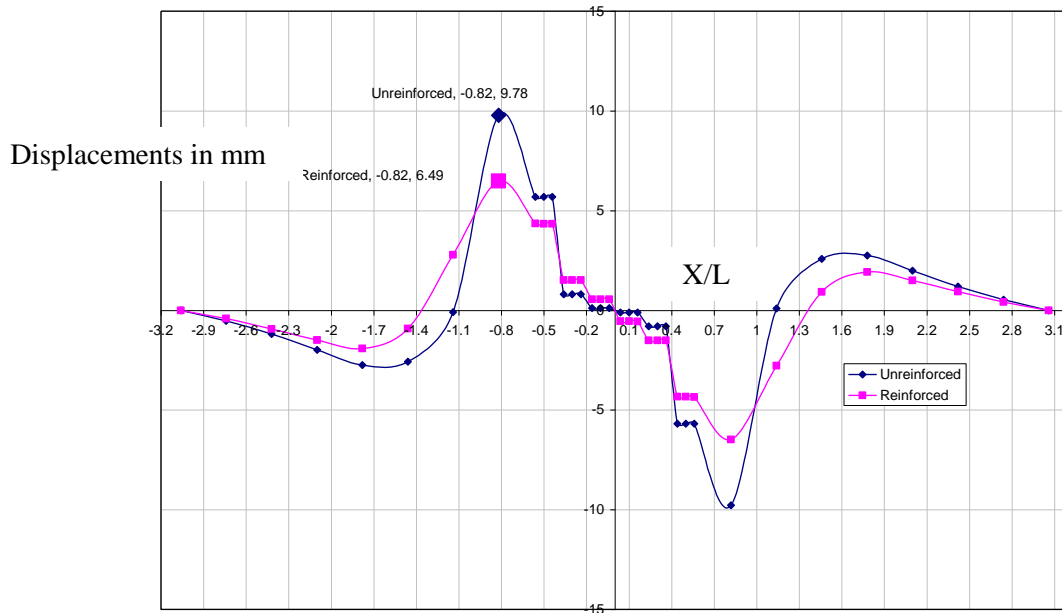


Fig. 8.19.a

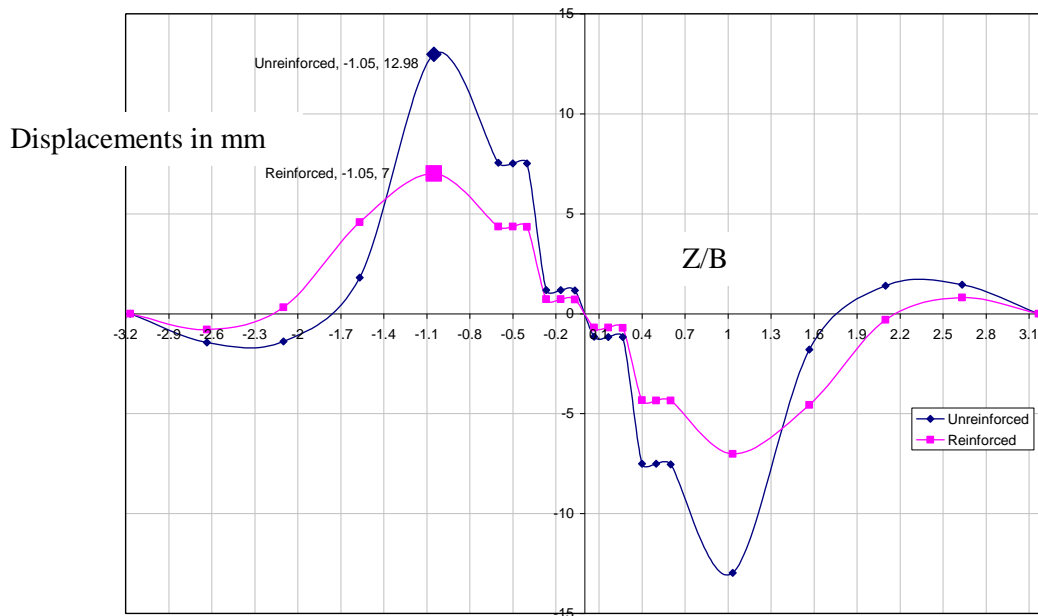
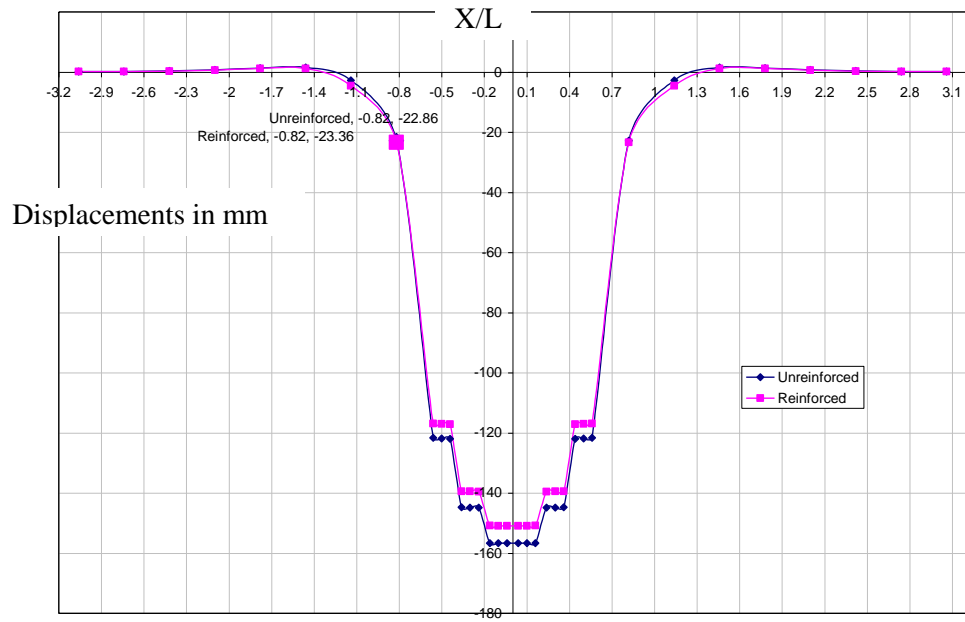


Fig. 8.19.b

Fig. 8.19 Horizontal displacements in mm in linear RSSI analysis (a) longitudinal displacements at foundation level (b) transverse displacements at foundation level



**Fig. 8.20 Vertical settlements in mm in linear SSI and RSSI analyses at foundation level along longitudinal line at  $Z/B=0.0$**



#### 8.4.6 Tables Related To Linear Analysis in SSI and RSSI

**Table 8.1: Details of the Validation of SSI Problem**

(Swamy et al., 2011)

Sl	Structure	Component	Details
1	Frame	No of storeys	5
		No of bays	5x3
		Storey height	3.5m
		Bay width	5m
		Beam size	0.3m x 0.6m
		Column size	0.4m x 0.4m
		Footing size	3.0m x3.0m x0.4m
2	Soil mass		153.0m x 95.0m x 0.0m
3	Elastic modulus of soil		$1.33 \times 10^7 \text{ N/m}^2$
4	Poisson's ratio of soil		0.45
5	Bulk modulus of concrete		$6.1 \times 10^6 \text{ N/m}^2$
6	Elastic modulus of concrete		$1.4 \times 10^{10} \text{ N/m}^2$

**Table 8.2: Details of the SSI analysis Problem in the present work**

Sl	Structure	Component	Details
1	Frame	No of storeys	5
		No of bays	5x3
		Storey height	3.5m
		Bay width	5m
		Beam size	0.3 x 0.6m
		Column size	0.4m x 0.4m
		Footing size	2.0m x 2.0m x 0.4m
2	Soil Mass		153.0m x 95.0m x20.0m
3	Elastic modulus of soil		$0.3 \times 10^7 \text{ N/m}^2$
4	Poisson's ratio of soil		0.45
5	Bulk modulus of concrete		$6.1 \times 10^6 \text{ N/m}^2$
6	Elastic modulus of concrete		$1.4 \times 10^{10} \text{ N/m}^2$

Table 8.3. Axial and Shear forces (kN) in beams (X-direction) of external frames in Linear SSI and RSSI analysis

Direction of Frame	Floor	Mem ber No.	(X,Y,Z) coordinates of beam nodes			NI Analysis		SSI Analysis		RSSI Analysis		Ratio of SSI/NI		Ratio of RSSI/NI		Ratio of RSSI/SSI	
			X	Y	Z	Axial	Shear	Axial	Shear	Axial	Shear	Axial	Shear	Axial	Shear	Axial	Shear
(1)	(2)	(3)	(4)	(5)	(6)	(7)	(8)	(9)	(10)	(11)	(12)	(13)	(14)	(15)	(16)	(17)	(18)
External frame in X-direction	Ground floor	1	64	23.5	40	-6.71	72.47	1.12	154.8	-17.7	134.1	-0.17	2.14	2.64	1.85	-15.80	0.87
		1	69	23.5	40	6.71	82.53	-1.12	0.25	17.7	20.89	-0.17	0.00	2.64	0.25	-15.80	83.56
		2	69	23.5	40	-6.54	77.92	-24.9	102	-39.3	94.81	3.80	1.31	6.01	1.22	1.58	0.93
		2	74	23.5	40	6.54	77.08	24.87	53.05	39.28	60.19	3.80	0.69	6.01	0.78	1.58	1.13
		3	74	23.5	40	-6.38	77.5	-33.8	77.5	-45.3	77.5	5.29	1.00	7.10	1.00	1.34	1.00
	First floor	6	64	27	40	-0.02	74.96	-2.73	152.6	0.79	137.7	136.50	2.04	-39.50	1.84	-0.29	0.90
		6	69	27	40	0.02	80.04	2.73	2.42	-0.79	17.33	136.50	0.03	-39.50	0.22	-0.29	7.16
		7	69	27	40	-1.28	77.2	-1.24	106.7	0.76	97.82	0.97	1.38	-0.59	1.27	-0.61	0.92
		7	74	27	40	1.28	77.8	1.24	48.34	-0.76	57.18	0.97	0.62	-0.59	0.73	-0.61	1.18
	Second floor	8	74	27	40	-1.12	77.5	-1.36	77.5	0.43	77.5	1.21	1.00	-0.38	1.00	-0.32	1.00
		11	64	30.5	40	-4.27	76.48	-11.1	154.5	-10.1	139.2	2.60	2.02	2.37	1.82	0.91	0.90
		11	69	30.5	40	4.27	78.52	11.11	0.49	10.12	15.85	2.60	0.01	2.37	0.20	0.91	32.35
		12	69	30.5	40	-3.34	76.65	-14.2	106.5	-12.1	97.89	4.25	1.39	3.61	1.28	0.85	0.92
	Third floor	12	74	30.5	40	3.34	78.35	14.2	48.47	12.07	57.11	4.25	0.62	3.61	0.73	0.85	1.18
		13	74	30.5	40	-3.22	77.5	-15.3	77.5	-12.8	77.5	4.75	1.00	3.96	1.00	0.83	1.00
		16	64	34	40	18.74	71.58	82.62	119.6	69.92	110.4	4.41	1.67	3.73	1.54	0.85	0.92
		16	69	34	40	-18.7	83.42	-82.6	35.41	-69.9	44.56	4.41	0.42	3.73	0.53	0.85	1.26
	Third floor	17	69	34	40	18.53	77.44	153.8	93.51	125.2	88.26	8.30	1.21	6.76	1.14	0.81	0.94
17		74	34	40	-18.5	77.56	-154	61.49	-125	66.74	8.30	0.79	6.76	0.86	0.81	1.09	
		18	74	34	40	18.22	77.5	176.3	77.5	141.6	77.5	9.68	1.00	7.77	1.00	0.80	1.00

Note: Section 8.4.3.1 gives details about Table 8.3

In columns 13 to 18 negative sign indicates the reduction in the values and positive sign indicates an increase in the values

Direction of Frame	Floor	Mem ber No.	(X,Y,Z)			NI Analysis		SSI Analysis		RSSI Analysis		Ratio of SSI/NI		Ratio of RSSI/NI		Ratio of RSSI/SSI	
			X	Y	Z	Axial	Shear	Axial	Shear	Axial	Shear	Axial	Shear	Axial	Shear	Axial	Shear
(1)	(2)	(3)	(4)	(5)	(6)	(7)	(8)	(9)	(10)	(11)	(12)	(13)	(14)	(15)	(16)	(17)	(18)
Internal frame in X-direction	Ground floor	21	64	23.5	45	-6.71	72.47	4.89	157.99	-15.93	139.27	-0.73	2.18	2.37	1.92	-3.26	0.88
		21	69	23.5	45	6.71	82.53	-4.89	-2.99	15.93	15.73	-0.73	-0.04	2.37	0.19	-3.26	-5.26
		22	69	23.5	45	-6.54	77.92	-23.54	103.39	-38.89	96.79	3.60	1.33	5.95	1.24	1.65	0.94
		22	74	23.5	45	6.54	77.08	23.54	51.61	38.89	58.21	3.60	0.67	5.95	0.76	1.65	1.13
		23	74	23.5	45	-6.38	77.5	-33.78	77.5	-45.44	77.5	5.29	1.00	7.12	1.00	1.35	1.00
	First floor	26	64	27	45	-0.02	74.96	-3.47	154.91	0.51	142.09	173.50	2.07	-25.50	1.90	-0.15	0.92
		26	69	27	45	0.02	80.04	3.47	0.09	-0.51	12.91	173.50	0.00	-25.50	0.16	-0.15	143.44
		27	69	27	45	-1.28	77.2	-1.43	108.75	0.83	100.05	1.12	1.41	-0.65	1.30	-0.58	0.92
		27	74	27	45	1.28	77.8	1.43	46.25	-0.83	54.95	1.12	0.59	-0.65	0.71	-0.58	1.19
		28	74	27	45	-1.12	77.5	-1.4	77.5	0.54	77.5	1.25	1.00	-0.48	1.00	-0.39	1.00
	Second floor	31	64	30.5	45	-4.27	76.48	-11.19	156.88	-10.42	143.53	2.62	2.05	2.44	1.88	0.93	0.91
		31	69	30.5	45	4.27	78.52	11.19	-1.88	10.42	11.47	2.62	-0.02	2.44	0.15	0.93	-6.10
		32	69	30.5	45	-3.34	76.65	-14.46	108.5	-12.56	100.07	4.33	1.42	3.76	1.31	0.87	0.92
		32	74	30.5	45	3.34	78.35	14.46	46.5	12.56	54.93	4.33	0.59	3.76	0.70	0.87	1.18
		33	74	30.5	45	-3.22	77.5	-15.66	77.5	-13.32	77.5	4.86	1.00	4.14	1.00	0.85	1.00
	Third floor	36	64	34	45	18.74	71.58	84.56	120.93	73.43	113.06	4.51	1.69	3.92	1.58	0.87	0.93
		36	69	34	45	-18.74	83.42	-84.56	34.07	-73.43	41.94	4.51	0.41	3.92	0.50	0.87	1.23
		37	69	34	45	18.53	77.44	158.58	94.8	132.96	89.53	8.56	1.22	7.18	1.16	0.84	0.94
		37	74	34	45	-18.53	77.56	-158.6	60.2	-133	65.47	8.56	0.78	7.18	0.84	0.84	1.09
		38	74	34	45	18.22	77.5	182.41	77.5	150.84	77.5	10.01	1.00	8.28	1.00	0.83	1.00

Note : Section 8.4.3.1 gives details about Tables 8.4 and 8.5

In columns 13 to 18 Negative sign indicates the reduction in the values and positive sign indicates an increase in the values

Table 8.5. Axial and Shear forces(kN) in beams (Z-direction) of Internal frames in Linear SSI and RSSI analysis

Direction of Frame	Floor	Member No.	(X,Y,Z) coordinates of			NI Analysis		RSSI Analysis		SSI Analysis		Ratio of SSI/NI		Ratio of RSSI/NI		Ratio of RSSI/SSI	
			X	Y	Z	Axial	Shear	Axial	Shear	Axial	Shear	Axial	Shear	Axial	Shear	Axial	Shear
(1)	(2)	(3)	(4)	(5)	(6)	(7)	(8)	(9)	(10)	(11)	(12)	(13)	(14)	(15)	(16)	(17)	(18)
External frame in Z-direction	Ground floor	81	64	23.5	40	-6.88	72.52	10.58	145.5	-12.9	128.5	-1.54	2.01	1.87	1.77	-1.22	0.88
		81	64	23.5	45	6.88	82.48	-10.6	9.53	12.86	26.51	-1.54	0.12	1.87	0.32	-1.22	2.78
		82	64	23.5	45	-6.94	77.5	-0.95	77.5	-25.6	77.5	0.14	1.00	3.68	1.00	26.89	1.00
	First floor	84	64	27	40	0.17	74.93	-3.03	140.2	1.21	130.3	-17.82	1.87	7.12	1.74	-0.40	0.93
		84	64	27	45	-0.17	80.07	3.03	14.83	-1.21	24.72	-17.82	0.19	7.12	0.31	-0.40	1.67
		85	64	27	45	-1.16	77.5	-1.09	77.5	2	77.5	0.94	1.00	-1.72	1.00	-1.83	1.00
	Second floor	87	64	30.5	40	-4.57	76.45	-11.8	142.6	-11.1	132.1	2.58	1.86	2.43	1.73	0.94	0.93
		87	64	30.5	45	4.57	78.55	11.81	12.43	11.1	22.94	2.58	0.16	2.43	0.29	0.94	1.85
		88	64	30.5	45	-3.94	77.5	-14.7	77.5	-13.3	77.5	3.74	1.00	3.37	1.00	0.90	1.00
	Third floor	90	64	34	40	18.94	71.71	71.2	115.5	62.99	108.6	3.76	1.61	3.33	1.51	0.88	0.94
90		64	34	45	-18.9	83.29	-71.2	39.47	-63	46.4	3.76	0.47	3.33	0.56	0.88	1.18	
91		64	34	45	19.18	77.5	111.1	77.5	96.58	77.5	5.79	1.00	5.04	1.00	0.87	1.00	
Internal frame in Z-direction	Ground floor	93	69	23.5	40	-6.88	72.52	17.47	150.3	-11.4	134.3	-2.54	2.07	1.65	1.85	-0.65	0.89
		93	69	23.5	45	6.88	82.48	-17.5	4.68	11.38	20.74	-2.54	0.06	1.65	0.25	-0.65	4.43
		94	69	23.5	45	-6.94	77.5	5.74	77.5	-25.3	77.5	-0.83	1.00	3.65	1.00	-4.41	1.00
	First floor	96	69	27	40	0.17	74.93	-4.27	143	1	135.4	-25.12	1.91	5.88	1.81	-0.23	0.95
		96	69	27	45	-0.17	80.07	4.27	12.01	-1	19.61	-25.12	0.15	5.88	0.24	-0.23	1.63
		97	69	27	45	-1.16	77.5	-1.9	77.5	2.16	77.5	1.64	1.00	-1.86	1.00	-1.14	1.00
	Second floor	99	69	30.5	40	-4.57	76.45	-12	145.6	-11.6	137.2	2.62	1.90	2.54	1.79	0.97	0.94
		99	69	30.5	45	4.57	78.55	11.98	9.45	11.61	17.83	2.62	0.12	2.54	0.23	0.97	1.89
		100	69	30.5	45	-3.94	77.5	-15.1	77.5	-14	77.5	3.84	1.00	3.56	1.00	0.93	1.00
	Third floor	102	69	34	40	18.94	71.71	73.49	117.5	66.95	112	3.88	1.64	3.53	1.56	0.91	0.95
102		69	34	45	-18.9	83.29	-73.5	37.51	-67	43.03	3.88	0.45	3.53	0.52	0.91	1.15	
103		69	34	45	19.18	77.5	115.1	77.5	103.6	77.5	6.00	1.00	5.40	1.00	0.90	1.00	
Internal frame in Z-direction	Ground floor	105	74	23.5	40	-6.88	72.52	22.62	154.4	-10.6	137.9	-3.29	2.13	1.53	1.90	-0.47	0.89
		105	74	23.5	45	6.88	82.48	-22.6	0.59	10.55	17.15	-3.29	0.01	1.53	0.21	-0.47	29.07
		106	74	23.5	45	-6.94	77.5	11.38	77.5	-25.1	77.5	-1.64	1.00	3.61	1.00	-2.20	1.00
	First floor	108	74	27	40	0.17	74.93	-5.18	145.4	0.84	138.6	-30.47	1.94	4.94	1.85	-0.16	0.95
		108	74	27	45	-0.17	80.07	5.18	9.57	-0.84	16.39	-30.47	0.12	4.94	0.20	-0.16	1.71
		109	74	27	45	-1.16	77.5	-2.59	77.5	2.17	77.5	2.23	1.00	-1.87	1.00	-0.84	1.00
	Second floor	111	74	30.5	40	-4.57	76.45	-12.2	148.1	-12	140.4	2.66	1.94	2.62	1.84	0.98	0.95
		111	74	30.5	45	4.57	78.55	12.16	6.89	11.96	14.57	2.66	0.09	2.62	0.19	0.98	2.11
		112	74	30.5	45	-3.94	77.5	-15.5	77.5	-14.6	77.5	3.92	1.00	3.70	1.00	0.94	1.00
	Third floor	114	74	34	40	18.94	71.71	75.49	119.2	69.53	114.1	3.99	1.66	3.67	1.59	0.92	0.96
114		74	34	45	-18.9	83.29	-75.5	35.82	-69.5	40.86	3.99	0.43	3.67	0.49	0.92	1.14	
115		74	34	45	19.18	77.5	118.7	77.5	108.1	77.5	6.19	1.00	5.64	1.00	0.91	1.00	

Table 8.6 Axial and Shear forces (kN) in columns (forces) of external frames in Linear SSI and RSSI analysis

Direction of Frame	Floor	Member	(X,Y,Z) coordinates			NI Analysis			SSI Analysis			RSSI Analysis			Ratio of SSI/NI			Ratio of RSSI/NI			Ratio of RSSI/SSI		
			X	Y	Z	Axial	Shear-X	Shear-Y	Axial	Shear-X	Shear-Y	Axial	Shear-X	Shear-Y	Axial	Shear-X	Shear-Y	Axial	Shear-X	Shear-Y	Axial	Shear-X	Shear-Y
(1)	(2)	(3)	(4)	(5)	(6)	(7)	(8)	(9)	(10)	(11)	(12)	(13)	(14)	(15)	(16)	(17)	(18)	(19)	(20)	(21)	(22)	(23)	(24)
External columns	Ground floor	153	64	20	40	591.09	7.74	-7.66	1125.2	69.86	-66.92	1020.8	42.85	-40.21	1.90	9.03	8.74	1.73	5.54	5.25	0.91	0.61	0.60
		153	64	24	40	-591.09	-7.74	7.66	1125.2	-69.86	66.92	1020.8	-42.85	40.21	-1.90	9.03	8.74	-1.73	5.54	5.25	0.91	0.61	0.60
		154	69	20	40	929.32	-0.36	-7.66	1003.6	43.58	-74.72	996.2	31.7	-44.99	1.08	-121.1	9.75	1.07	-88.06	5.87	0.99	0.73	0.60
		154	69	24	40	-929.32	0.36	7.66	1003.6	-43.58	74.72	-996.2	-31.7	44.99	-1.08	-121.1	9.75	1.07	-88.06	5.87	-0.99	0.73	0.60
		155	74	20	40	916.39	0.12	-7.66	1088.5	12.35	-80.78	1082.25	9.27	-47.88	1.19	102.9	10.55	1.18	77.25	6.25	0.99	0.75	0.59
		155	74	24	40	-916.39	-0.12	7.66	1088.5	-12.35	80.78	1082.25	-9.27	47.88	-1.19	102.9	10.55	-1.18	77.25	6.25	0.99	0.75	0.59
	First floor	159	64	24	40	446.1	14.45	-14.5	824.94	68.75	-56.35	758.2	60.55	-53.07	1.85	4.8	3.88	1.70	4.19	3.65	0.92	0.88	0.94
		159	64	27	40	-446.1	-14.45	14.54	-824.9	-68.75	56.35	-758.2	-60.55	53.07	1.85	4.8	3.88	1.70	4.19	3.65	0.92	0.88	0.94
		160	69	24	40	696.34	-0.53	-14.5	751.06	69.59	-57.25	746.25	53.29	-56.36	1.08	-131.3	3.94	1.07	-100.55	3.88	0.99	0.77	0.98
		160	69	27	40	-696.34	0.53	14.54	-751.1	-69.59	57.25	-746.25	-53.29	56.36	1.08	-131.3	3.94	1.07	-100.55	3.88	0.99	0.77	0.98
		161	74	24	40	689.3	-0.03	-14.5	803.52	21.27	-58.16	806.71	15.3	-58.42	1.17	-709.0	4.00	1.17	-510.00	4.02	1.00	0.72	1.00
		161	74	27	40	-689.3	0.03	14.54	-803.5	-21.27	58.16	-806.71	-15.3	58.42	1.17	-709.0	4.00	1.17	-510.00	4.02	1.00	0.72	1.00
	Second floor	165	64	27	40	296.22	14.47	-14.4	532.19	71.48	-59.37	490.25	59.77	-51.86	1.80	4.9	4.13	1.66	4.13	3.61	0.92	0.84	0.87
		165	64	31	40	-296.22	-14.47	14.36	-532.2	-71.48	59.37	-490.25	-59.77	51.86	1.80	4.9	4.13	1.66	4.13	3.61	0.92	0.84	0.87
		166	69	27	40	464.18	0.73	-14.4	498.99	68.09	-61.52	495.7	53.32	-55.36	1.07	93.3	4.28	1.07	73.04	3.86	0.99	0.78	0.90
		166	69	31	40	-464.18	-0.73	14.36	-499	-68.09	61.52	-495.7	-53.32	55.36	1.07	93.3	4.28	1.07	73.04	3.86	0.99	0.78	0.90
		167	74	27	40	459.07	-0.19	-14.4	532.25	21.4	-63.34	533.42	15.63	-57.58	1.16	-112.6	4.41	1.16	-82.26	4.01	1.00	0.73	0.91
		167	74	31	40	-459.07	0.19	14.36	-532.3	-21.4	63.34	-533.42	-15.63	57.58	1.16	-112.6	4.41	1.16	-82.26	4.01	1.00	0.73	0.91
	Third floor	171	64	31	40	143.29	18.74	-18.9	235.12	82.59	-71.18	219.04	69.88	-62.96	1.64	4.4	3.76	1.53	3.73	3.32	0.93	0.85	0.88
		171	64	34	40	-143.29	-18.74	18.94	-235.1	-82.59	71.18	-219.04	-69.88	62.96	1.64	4.4	3.76	1.53	3.73	3.32	0.93	0.85	0.88
		172	69	31	40	232.56	-0.2	-18.9	246.42	71.18	-73.5	244.79	55.27	-66.97	1.06	-355.9	3.88	1.05	-276.35	3.54	0.99	0.78	0.91
172		69	34	40	-232.56	0.2	18.94	-246.4	-71.18	73.5	-244.79	-55.27	66.97	1.06	-355.9	3.88	1.05	-276.35	3.54	0.99	0.78	0.91	
173		74	31	40	226.77	-0.31	-18.9	258.17	22.51	-75.5	258.38	16.31	-69.55	1.14	-72.6	3.99	1.14	-52.61	3.67	1.00	0.72	0.92	

Note: See Section 8.4.3.2 for more details about Table 8.6

In columns 16 to 24 negative sign indicates the reduction in the values and positive sign indicates an increase in the values

Table 8.7. Axial and Shear forces (kN) in columns of internal frames in Linear SSI and RSSI analysis

Direction of Frame	Floor	Member No.	(X,Y,Z) coordinates of beam			NI Analysis			SSI Analysis			RSSI Analysis			Ratio of SSI/NI			Ratio of RSSI/NI			Ratio of RSSI/SSI		
			X	Y	Z	Axial	Shear-X	Shear-Y	Axial	Shear-X	Shear-Y	Axial	Shear-X	Shear-Y	Axial	Shear-X	Shear-Y	Axial	Shear-X	Shear-Y	Axial	Shear-X	Shear-Y
(1)	(2)	(3)	(4)	(5)	(6)	(7)	(8)	(9)	(10)	(11)	(12)	(13)	(14)	(15)	(16)	(17)	(18)	(19)	(20)	(21)	(22)	(23)	(24)
Internal columns	Ground floor	177	64	20	45	929.89	7.74	0.51	976.97	74.82	-27.33	968.52	47.63	-19.49	1.05	9.67	-53.59	1.04	6.15	-38.2	0.99	0.64	0.71
		177	64	24	45	-929.89	-7.74	-0.51	-977	-74.82	27.33	-968.52	-47.63	19.49	1.05	9.67	-53.59	1.04	6.15	-38.2	0.99	0.64	0.71
		178	69	20	45	1268.12	-0.36	0.51	818.38	44.41	-29.16	879.69	34.79	-21.43	0.65	-123.4	-57.18	0.69	-96.64	-42.0	1.07	0.78	0.73
		178	69	24	45	1268.12	0.36	-0.51	-818.4	-44.41	29.16	-879.69	-34.79	21.43	-0.65	-123.4	-57.18	-0.69	-96.64	-42.0	1.07	0.78	0.73
		179	74	20	45	1255.19	0.12	0.51	877.44	12.44	-31.24	942.53	10.3	-22.78	0.70	103.7	-61.25	0.75	85.83	-44.7	1.07	0.83	0.73
		179	74	24	45	1255.19	-0.12	-0.51	-877.4	-12.44	31.24	-942.53	-10.3	22.78	-0.70	103.7	-61.25	-0.75	85.83	-44.7	1.07	0.83	0.73
	First floor	183	64	24	45	697.44	14.45	0.45	731.95	69.92	-38.88	725.24	63.56	-32.19	1.05	4.8	-86.40	1.04	4.40	-71.5	0.99	0.91	0.83
		183	64	27	45	-697.44	-14.45	-0.45	-732	-69.92	38.88	-725.24	-63.56	32.19	1.05	4.8	-86.40	1.04	4.40	-71.5	0.99	0.91	0.83
		184	69	24	45	947.68	-0.53	0.45	635.79	72.81	-40.88	668.93	57.75	-35.36	0.67	-137.4	-90.84	0.71	-108.96	-78.6	1.05	0.79	0.86
		184	69	27	45	-947.68	0.53	-0.45	-635.8	-72.81	40.88	-668.93	-57.75	35.36	0.67	-137.4	-90.84	0.71	-108.96	-78.6	1.05	0.79	0.86
		185	74	24	45	940.63	-0.03	0.45	670.24	22.67	-42.47	712.17	16.84	-37.3	0.71	-755.7	-94.38	0.76	-561.33	-82.9	1.06	0.74	0.88
		185	74	27	45	-940.63	0.03	-0.45	-670.2	-22.67	42.47	-712.17	-16.84	37.3	0.71	-755.7	-94.38	0.76	-561.33	-82.9	1.06	0.74	0.88
	Second floor	189	64	27	45	464.91	14.47	-0.87	484.71	73.39	-36.94	480.93	63.05	-31.4	1.04	5.1	42.46	1.03	4.36	36.1	0.99	0.86	0.85
		189	64	31	45	-464.91	-14.47	0.87	-484.7	-73.39	36.94	-480.93	-63.05	31.4	1.04	5.1	42.46	1.03	4.36	36.1	0.99	0.86	0.85
		190	69	27	45	632.87	0.73	-0.87	437.44	70.77	-38.51	458.86	57.43	-34.19	0.69	96.9	44.26	0.73	78.67	39.3	1.05	0.81	0.89
		190	69	31	45	-632.87	-0.73	0.87	-437.4	-70.77	38.51	-458.86	-57.43	34.19	0.69	96.9	44.26	0.73	78.67	39.3	1.05	0.81	0.89
	Third floor	191	74	27	45	627.76	-0.19	-0.87	459.42	22.65	-39.87	485.83	17.13	-35.97	0.73	-119.2	45.83	0.77	-90.16	41.3	1.06	0.76	0.90
		191	74	31	45	-627.76	0.19	0.87	-459.4	-22.65	39.87	-485.83	-17.13	35.97	0.73	-119.2	45.83	0.77	-90.16	41.3	1.06	0.76	0.90
		195	64	31	45	232.38	18.74	-0.24	237.9	84.58	-39.86	236.96	73.47	-33.56	1.02	4.5	166.08	1.02	3.92	139.8	1.00	0.87	0.84
		195	64	34	45	-232.38	-18.74	0.24	-237.9	-84.58	39.86	-236.96	-73.47	33.56	1.02	4.5	166.08	1.02	3.92	139.8	1.00	0.87	0.84
		196	69	31	45	321.65	-0.2	-0.24	243.87	74.04	-41.64	251.99	59.58	-36.61	0.76	-370.2	173.50	0.78	-297.90	152.5	1.03	0.80	0.88
		196	69	34	45	-321.65	0.2	0.24	-243.9	-74.04	41.64	-251.99	-59.58	36.61	0.76	-370.2	173.50	0.78	-297.90	152.5	1.03	0.80	0.88
	197	74	31	45	315.86	-0.31	-0.24	251.02	23.84	-43.18	261.33	17.89	-38.56	0.79	-76.9	179.92	0.83	-57.71	160.7	1.04	0.75	0.89	
	197	74	34	45	-315.86	0.31	0.24	-251	-23.84	43.18	-261.33	-17.89	38.56	0.79	-76.9	179.92	0.83	-57.71	160.7	1.04	0.75	0.89	

Note See Section 8.4.3.2 for more details about Table 8.7

In columns 16 to 24 Negative sign indicates the reduction in the values and positive sign indicates an increase in the values

Table 8.8. Bending moment (kNm) about z-axis in X-beams in linear SSI and RSSI analysis

Direction of Frame	Floor	Member No.	(X,Y,Z) coordinates of beam nodes			NI Analysis	SSI Analysis	RSSI Analysis	Ratio of SSI/NI	Ratio of RSSI/NI	Ratio of RSSI/SSI
			X	Y	Z	Mz1	Mz2	Mz3			
(1)	(2)	(3)	(4)	(5)	(6)	(7)	(8)	(9)	(10)	(11)	(12)
External frame in X-direction	Ground floor	1	64	23.5	40	43.33	261.94	202.25	6.05	4.67	0.77
		1	69	23.5	40	-68.5	124.29	80.82	-1.81	-1.18	0.65
		2	69	23.5	40	66.28	97.74	86.05	1.47	1.30	0.88
		2	74	23.5	40	-64.16	24.52	0.51	-0.38	-0.01	0.02
		3	74	23.5	40	64.43	41.02	47.43	0.64	0.74	1.16
	First floor	6	64	27	40	50.51	249.03	210.67	4.93	4.17	0.85
		6	69	27	40	-63.21	126.39	90.19	-2.00	-1.43	0.71
		7	69	27	40	63.65	112.54	95.23	1.77	1.50	0.85
		7	74	27	40	-65.14	33.24	6.39	-0.51	-0.10	0.19
	Second floor	8	74	27	40	64.72	41.37	47.69	0.64	0.74	1.15
		11	64	30.5	40	54.91	256.83	216.24	4.68	3.94	0.84
		11	69	30.5	40	-60.01	128.2	92.01	-2.14	-1.53	0.72
		12	69	30.5	40	61.68	111.59	95.02	1.81	1.54	0.85
		12	74	30.5	40	-65.93	33.54	6.93	-0.51	-0.11	0.21
	Third floor	13	74	30.5	40	64.9	41.56	47.75	0.64	0.74	1.15
		16	64	34	40	35.93	156.01	132.1	4.34	3.68	0.85
		16	69	34	40	-65.52	54.43	32.59	-0.83	-0.50	0.60
		17	69	34	40	64.69	74.33	67.28	1.15	1.04	0.91
17		74	34	40	-65.02	5.73	-13.49	-0.09	0.21	-2.35	
18		74	34	40	64.56	35.32	43.24	0.55	0.67	1.22	
Internal frame in X-direction	Ground floor	21	64	23.5	45	43.33	272.06	216.39	6.28	4.99	0.80
		21	69	23.5	45	-68.5	130.38	92.47	-1.90	-1.35	0.71
		22	69	23.5	45	66.28	100.14	89.25	1.51	1.35	0.89
		22	74	23.5	45	-64.16	29.31	7.2	-0.46	-0.11	0.25
		23	74	23.5	45	64.43	39.35	45.73	0.61	0.71	1.16
	First floor	26	64	27	45	50.51	255.14	222.08	5.05	4.40	0.87
		26	69	27	45	-63.21	131.9	100.87	-2.09	-1.60	0.76
		27	69	27	45	63.65	117.03	99.38	1.84	1.56	0.85
		27	74	27	45	-65.14	39.22	13.37	-0.60	-0.21	0.34
		28	74	27	45	64.72	39.99	46.04	0.62	0.71	1.15
	Second floor	31	64	30.5	45	54.91	263.3	227.72	4.80	4.15	0.86
		31	69	30.5	45	-60.01	133.61	102.43	-2.23	-1.71	0.77
		32	69	30.5	45	61.68	115.72	99.05	1.88	1.61	0.86
		32	74	30.5	45	-65.93	39.27	13.78	-0.60	-0.21	0.35
		33	74	30.5	45	64.9	40.24	46.16	0.62	0.71	1.15
	Third floor	36	64	34	45	35.93	159.76	138.86	4.45	3.86	0.87
		36	69	34	45	-65.52	57.39	38.97	-0.88	-0.59	0.68
		37	69	34	45	64.69	76.59	68.75	1.18	1.06	0.90
37		74	34	45	-65.02	9.89	-8.61	-0.15	0.13	-0.87	
37		74	34	45	64.56	33.62	41.24	0.52	0.64	1.23	
38		74	34	45							

**Note: See Section 8.4.3.3 for more details about Table 8.8**  
**In columns 10 to 12 negative sign indicates the reduction in the values and positive sign indicates an increase in the values**

Table 8.9 Bending moment in Z-beams (kNm)in linear SSI and RSSI analysis

Direction of Frame	Floor	Member No.	(X,Y,Z) coordinates of beam nodes			NI Analysis	SSI Analysis	RSSI Analysis	Ratio of SSI/NI	Ratio of RSSI/NI	Ratio of RSSI/SSI
			X	Y	Z						
(1)	(2)	(3)	(4)	(5)	(6)	(7)	(8)	(9)	(10)	(11)	(12)
External frame in Z-direction	Ground floor	81	64	23.5	40	43.37	229.61	181.2	5.29	4.18	0.79
		81	64	23.5	45	-68.28	110.27	73.75	-1.61	-1.08	0.67
		82	64	23.5	45	65.82	19.65	27.86	0.30	0.42	1.42
	First floor	84	64	27	40	50.5	207.43	184.45	4.11	3.65	0.89
		84	64	27	45	-63.37	105.91	79.42	-1.67	-1.25	0.75
		85	64	27	45	64.23	25.06	30.88	0.39	0.48	1.23
	Second floor	87	64	30.5	40	55.04	216.86	191.05	3.94	3.47	0.88
		87	64	30.5	45	-60.29	108.46	81.76	-1.80	-1.36	0.75
		88	64	30.5	45	63.09	24.09	30.34	0.38	0.48	1.26
Third floor	90	64	34	40	36.29	134.56	119.04	3.71	3.28	0.88	
	90	64	34	45	-65.27	55.6	36.47	-0.85	-0.56	0.66	
	91	64	34	45	65.14	16.26	23.97	0.25	0.37	1.47	
Internal frame in Z-direction	Ground floor	93	69	23.5	40	43.37	243.57	196	5.62	4.52	0.80
		93	69	23.5	45	-68.28	120.5	87.77	-1.76	-1.29	0.73
		94	69	23.5	45	65.82	17.08	24.04	0.26	0.37	1.41
	First floor	96	69	27	40	50.5	213.97	196.75	4.24	3.90	0.92
		96	69	27	45	-63.37	113.5	92.71	-1.79	-1.46	0.82
		97	69	27	45	64.23	23.43	27.84	0.36	0.43	1.19
	Second floor	99	69	30.5	40	55.04	224.19	203.55	4.07	3.70	0.91
		99	69	30.5	45	-60.29	116.04	94.8	-1.92	-1.57	0.82
		100	69	30.5	45	63.09	22.32	27.34	0.35	0.43	1.22
Third floor	102	69	34	40	36.29	138.96	126.61	3.83	3.49	0.91	
	102	69	34	45	-65.27	61.02	45.76	-0.93	-0.70	0.75	
	103	69	34	45	65.14	14.08	20.22	0.22	0.31	1.44	
Internal frame in Z-direction	Ground floor	105	74	23.5	40	43.37	255.05	205.19	5.88	4.73	0.80
		105	74	23.5	45	-68.28	129.48	96.57	-1.90	-1.41	0.75
		106	74	23.5	45	65.82	15.19	21.75	0.23	0.33	1.43
	First floor	108	74	27	40	50.5	219.66	204.49	4.35	4.05	0.93
		108	74	27	45	-63.37	119.99	101.06	-1.89	-1.59	0.84
		109	74	27	45	64.23	21.98	25.91	0.34	0.40	1.18
	Second floor	111	74	30.5	40	55.04	230.48	211.54	4.19	3.84	0.92
		111	74	30.5	45	-60.29	122.55	103.12	-2.03	-1.71	0.84
		112	74	30.5	45	63.09	20.8	25.41	0.33	0.40	1.22
Third floor	114	74	34	40	36.29	142.74	131.46	3.93	3.62	0.92	
	114	74	34	45	-65.27	65.67	51.73	-1.01	-0.79	0.79	
	115	74	34	45	65.14	12.2	17.81	0.19	0.27	1.46	

Note: See Section 8.4.3.3 for more details about Table 8.9

In columns 10 to 12 Negative sign indicates the reduction in the values and positive sign indicates an increase in the values



## 8.5 Non-Linear SSI and RSSI analyses of space frame-footing -soil system

### Definition of the problem

The objective of the present study is to estimate the realistic displacements and force quantities in the structural members, accounting for their three dimensional behavior and nonlinear constitutive relations of unreinforced and reinforced soil. A program has been developed in the present work to compare soil-structure interaction analyses of a three dimensional frame resting on isolated footings for nonlinear constitutive relations of unreinforced and reinforced soil.

The finite element model for non-linear SSI nonlinear analysis is similar to the model used in linear SSI analysis as shown in Fig. 8.1 and 8.2 except for nonlinear material property of soil. In non-linear analysis the soil is modelled as hypoeleastic material. Hypoelasticity constitutes a generalized incremental law in which behaviour can be simulated from increment to increment rather than entire load or stress at a time. In hypoelasticity, the increment of stress is expressed as a function of stress and increment of strain.

The model consists of three stress dependent modulus functions, which are as follows,

- Bulk modulus  $K$
- Shear modulus  $G$
- The coupling modulus  $J$  that relates effective mean stress  $p'$  to shear strain  $\epsilon_s$  as well as shear stress  $q$  to volumetric strain  $\epsilon_v$ .

Hypo-elastic model developed by Yin, J.H., (2000) is used in the present work. The equations for the constitutive relationship proposed by Yin, J.H.(2000) are given in Chapter 5.

The Hypoelastic parameters were obtained from the experimental work done by Krishnamoorthy and Rao (1995). The model properties are mentioned in Tables 8.10 and 8.11. To conduct nonlinear RSSI analysis, the frame-footing-reinforced soil model adopted is as shown in the Fig. 8.6 which is same as the model in linear RSSI model. Under each column footing, four layers of geogrid are laid at D/B ratios of 0.25, 0.5, 0.75 and 1 as shown in Fig. 8.7. The size of isolated footing is 2m x 2m and the sizes of geogrid are 4m x 4m. The geometric details of geo-grid are shown in Fig. 8.8.

### **8.5.1 Results of Nonlinear SSI and RSSI analyses and discussions**

All the output parameters or responses related to semi infinite media are plotted both in two dimensional and three dimensional graphs during the course of study. Due to constraints in volume of thesis, only critical cases are presented in three dimensional graphs to indicate spatial variation.

#### **8.5.1.1 Deformation and settlements in nonlinear SSI analysis**

Figure 8.21(a) shows the vertical deformation at foundation level in the longitudinal direction of the soil mass. Maximum vertical displacement of -185.3 mm in X-direction occur at  $X/L = \pm 0.16$  and  $Z/B = \pm 0.267$ . Figure 8.21(b) shows displacement contours at foundation level. Figure 8.21(c) shows displacements along longitudinal section. Figure 8.22 shows horizontal displacements along longitudinal and transverse directions. In Fig. 8.22(a) and (b) longitudinal displacements at foundation levels are shown. Similarly the Figs. 8.22(c) and (d) transverse displacements at foundation levels are shown. Maximum horizontal displacement of 11.32 mm in X-direction occur at  $X/L = \pm 0.82$  and  $Z/B = \pm 0.167$ . Maximum horizontal displacement of 12.925 mm along Z-direction occur at  $X/L = \pm 0.04$  and  $Z/B = \pm 1.03$

### **8.5.1.2 Deformation and settlements in Nonlinear RSSI analysis**

Figure 8.23(a) shows the vertical deformation at foundation level in the longitudinal direction of the soil mass. Maximum vertical displacement of -173.8 mm in X-direction occur at  $X/L = \pm 0.16$  and  $Z/B = \pm 0.267$ . Figure 8.23(b) shows displacement contour at foundation level. Figure 8.24(c) shows displacements along longitudinal section. Maximum horizontal displacement of 9.72 mm in X-direction occur at  $X/L = \pm 0.04$  and  $Z/B = \pm 0.103$ . Maximum horizontal displacement of 10.98mm along Z-direction occur at  $Z/B = \pm 1.03$  and  $X/L = \pm 0.04$ .

### **8.5.1.3 Discussion on Displacements in Non-Linear Analyses**

Maximum lateral displacements along X and Z directions are reduced by 14% and 15% in non-linear RSSI analysis when compared to Nonlinear SSI analysis. But the vertical displacements are reduced merely by 6.2%.

## **8.5.2 Stresses in soil**

### **8.5.2.1 Stresses in soil in Nonlinear SSI analysis**

Vertical stress contours at foundation level are shown in Fig. 8.25(a). Figure 8.25(c) shows variation of vertical stresses at sections taken along X-direction located across different positions in Z-direction. The maximum stresses of  $0.056 \text{ N/mm}^2$  occur at  $X/L = \pm 0.33$  and  $Z/B = \pm 0.2167$ .

Figure 8.26(a) shows contour and figure 8.26 (b) shows longitudinal stresses at foundation level along longitudinal sections taken across breadth for different values of  $Z/B$ . The maximum horizontal longitudinal stresses of  $0.0101 \text{ N/mm}^2$  occur at  $X/L = \pm 0.2$  and  $Z/B = \pm 0.2167$ .

Figure 8.26(c) shows stress contours and Fig. 8.26 (d) shows transverse stresses at foundation level along longitudinal sections taken across breadth for different values of Z/B. The maximum horizontal transverse stresses of  $0.006655 \text{ N/mm}^2$  occur at  $X/L = \pm 0.07$ , and  $Z/B = \pm 0.33$ .

### **8.5.2.2 Stresses in soil in Non-Linear RSSI analysis**

Vertical stress contours are shown in Fig. 8.27(a). Figure 8.27(b) shows stress distribution at section X-X. Figure 8.27(c) shows variation of vertical stress at section taken along X-direction located across and taken at different positions in Z-direction. The maximum stresses of  $0.0561 \text{ N/mm}^2$  occur at  $X/L = \pm 0.33$  and  $Z/B = \pm 0.2167$

Figure 8.28(a) shows horizontal stress contour and Fig. 8.28(b) shows longitudinal stresses at foundation level along with the longitudinal sections taken across breadth for different values of Z/B. The maximum horizontal longitudinal stresses of  $0.00444784 \text{ N/mm}^2$  occur at  $X/L = \pm 0.2$ , and  $Z/B = \pm 0.2167$ .

Figure 8.28(c) shows shear stress contours and Fig. 8.28 (d) shows transverse stresses at foundation level along longitudinal sections taken across breadth for different values of Z/B. The maximum horizontal transverse stresses of  $0.004317 \text{ N/mm}^2$  occur at  $X/L = \pm 0.13$  and  $Z/B = \pm 0.33$ .

### **8.5.2.3 Discussion on stresses in Non-Linear Analyses**

In non-linear SSI analysis, the vertical contact pressure of the footings follows the same trend as that of vertical displacement. The vertical pressure at various points are not affected much in non-linear RSSI analysis compared to non-linear SSI. However there is

reduction in longitudinal stresses by 56% and transverse stresses by 35% in non-linear RSSI analysis compared to non-linear SSI. There is also a change in the pressure bulb below foundation level. In the horizontal direction, there is a reduction in longitudinal stress at various points in non-linear RSSI analysis when compared to the non-linear SSI analysis which is exactly reverse of the trend in linear analyses. Similarly same trend is observed in transverse direction.

### **8.5.3 Stress resultants in members of 3-Dimensional frame in Nonlinear SSI and RSSI analyses**

The frame shown in Fig. 8.2 is analysed for three cases viz., Linear Non-interactive (NI) analysis, nonlinear SSI analysis and nonlinear RSSI analysis. As one of the main objectives is to study the effect of reinforcement in soil on structural behaviour, the stress resultants in each member is compared in these three analyses. Tables 8.12 to 8.16 give the comparative values of axial forces and shear forces in the members of the frame. Tables 8.17 to 8.19 give bending moments in the members.

#### **8.5.3.1 Axial and shear forces in beams.**

The axial and shear forces in X-beams in external and internal frames from nonlinear analysis are given in tables 8.12 and 8.13. The structure of the tables is as follows:

Column 1	Gives whether the frame is external or internal
Column 2	Gives the floor
Column 3	Gives the member number
Column 4,5,6	Give X,Y Z co-ordinates of nodes of members
Columns 7,8	Give axial force(kN) and shear force(kN) along Y direction of beams in local co-ordinates for NI analysis

Columns 9, 10	Give axial force (kN) and shear force (kN) along Y direction of beams in local co-ordinates for SSI analysis
Columns 11,12	Give axial force(kN) and shear force (kN)along Y direction of beams in local co-ordinates for RSSI analysis
Columns 13,14	Give ratio of axial force, shear force along Y direction of beams in SSI analysis to NI analysis
Columns 15,16	Give ratio of axial force, shear force along Y direction of beams in RSSI analysis to NI analysis
Columns 17,18	Give ratio of axial force, shear force along Y direction of beams in RSSI analysis to SSI analysis

#### **i. Axial and Shear forces in X-beams**

From column 7 of Tables 8.12 and 8.13, it can be observed that from NI analysis axial forces in members are greater in extreme storeys with respect to internal storeys. The shear force (column 8) is maximum at the support next to end support of end span followed by shear force in interior spans and end support.

From columns 9 and 13 of Tables 8.12 and 8.13, it can be viewed that in SSI analysis axial forces are increased (-3.11 to 3.41) by many folds with respect to NI analysis especially in top storeys. The shear forces in SSI analysis vary by 0.72 to 1.32 times NI analysis. The shear forces are maximum at end support followed by shear forces on internal side of support next to end support and shear forces at interior spans.

The variation of axial forces 0.32 to 3.03 and shear forces in RSSI analysis (0.71 to 1.28) are same as SSI analysis but are found to have lesser differential values between two ends of a member as observed from columns 11, 12, 15 and 16 of tables 8.12 and 8.13. From column 17 it can be observed that reinforcement reduces the axial forces in X-beams. From column 18 it can be observed that Shear Force in beams is unaffected with the provision of reinforcement.

## ii. Axial and Shear forces in Z-beams

Table 8.14 gives the axial and shear forces in Z-beams. The general trends in NI, SSI and RSSI analysis follow the foot steps of trends in X-beams. From columns 9 and 13 of Table 8.14 it can be viewed that in SSI analysis, axial forces are increased (-2.10 to 3.18) by many folds with respect to NI analysis especially in top storeys. The shear forces in SSI analysis are 0.64 to 1.41 times those in NI analysis. The shear forces are maximum at end support followed by shear forces on internal side of support next to end support and shear forces at interior spans.

Though the axial forces vary from -0.64 to 1.01 and shear forces vary from 0.95 to 1.03 in RSSI analysis when compared to SSI analysis lesser differential values exist between two ends of a member as observed from columns 11, 12, 15 and 16 of Table 8.15. From column 18, it can be observed that reinforcement does not have much effect on axial forces of Z-beams. Shear force is changing from -6% to 11% depending on the location of beams.

### 8.5.3.2 Axial and Shear forces in Columns

The values of the axial forces in the column members at various storey levels corresponding to NI, SSI and RSSI analysis have been presented in the Tables 8.15 and 8.16. Forces in columns along grid line 1 and grid line 2 are given in Table 8.15 and 8.16 respectively. The structure of the tables is as follows

Column 1	Gives whether the frame is external or internal
Column 2	Gives the floor
Column 3	Gives the member number
Column 4,5,6	Give X,Y Z co-ordinates (in meters) of nodes of members
Columns 7,8,9	Give axial force, shear force (kN) along Y and Z direction of beams in local co-ordinates for NI analysis

Columns 10,11,12	Give axial force, shear force (kN) along Y and Z direction of beams in local co-ordinates for SSI analysis
Columns 13,14,15	Give axial force, shear force (kN) along Y and Z direction of beams in local co-ordinates for RSSI analysis
Columns 16,17,18	Give ratio of axial force, shear force along Y and Z direction of beams in SSI analysis to NI analysis
Columns 19, 20,21	Give ratio of axial force, shear force along Y and Z direction of beams in RSSI analysis to NI analysis
Columns 22,23, 24	Give ratio of axial force, shear force along Y and Z direction of beams in RSSI analysis to SSI analysis

In NI analysis, from columns 7 of tables 8.15 and 8.16, it can be observed that columns in external frame along grid line 1 carry 41.37 % total loads when compared to columns along line 2 which carry 58.63 % of total load. As done in previous chapter axial forces are put under three categories based on their values. Corner columns carry 10%, peripheral columns carry 42.84 % and internal columns carry 47.12% of total load.

In nonlinear SSI analysis external columns in external frame along grid line 1 carry 45.43 % total loads when compared to columns along line 2 which carry 55.56 % of total load. Corner columns carry 12.32 %, peripheral columns carry 38.4% and internal columns carry 49.27 % of total load. Axial forces in RSSI have reduced marginally by about 2 percent when compared to SSI analysis. Shear forces in columns in NI analysis are negligible (1.2% to 8.3%) of axial forces carried by columns. However in non-linear SSI analysis shear forces in column are 4.24% to 15.5% of axial forces. Introduction of reinforcement in soil reduces the shear forces in SSI analysis. Shear forces in non-linear RSSI analysis are 3.1% to 15.2 % of axial forces.

### **8.5.3.3 Bending moments in beams**

Table 8.17 gives the comparative values of bending moments in X-beams in NI, SSI and RSSI analysis. Table 8.18 gives the comparative values of bending moments in Z-beams in NI, SSI and RSSI analysis.



Column 1	Gives whether the frame is external or internal
Column 2	Gives the floor
Column 3	Gives the member number
Column 4,5,6	Give X,Y Z co-ordinates of nodes of members
Columns 7,8,9	Give bending moments in beams (kNm) about local z-axis in NI, SSI and RSSI analysis respectively
Columns 10,11,12	Give ratio of bending moments –SSI to NI, RSSI to NI and RSSI to SSI

#### **i. Bending moments in X-beams**

Bending moments in X-beams from nonlinear SSI analysis are varying from 0.1 to 2.77 times bending moments in NI analysis. Corresponding to these limits the ratios of bending moments in RSSI analysis to SSI analysis vary from 1.32 to 0.87. Bending moments in X-beams in RSSI analysis vary from 0.13 to 2.41 times bending moments in NI analysis.

Effect of SSI is reduced in nonlinear analysis when compared to linear analysis. Reinforcement in soil improves in normalising values of bending moments of X-beams.

#### **ii. Bending moments in Z-beams**

Bending moments in Z-beams from SSI analysis are varying from -0.05 to 2.78 times bending moments in NI analysis. Corresponding to these limits the ratio bending moments in RSSI analysis to SSI analysis vary from 2.27 to 0.85. Bending moments in X-beams in RSSI analysis vary from 0.04 to 2.38 times bending moments in NI analysis.

#### **8.5.3.4 Bending moments in columns**

The values of the axial forces in the column members at various storey levels corresponding to NI, SSI and RSSI analysis have been presented in the Table 8.19. The explanatory notes for table contents is as follows

Column 1	Gives whether the frame is external or internal
Column 2	Gives the floor
Column 3	Gives the member number
Column 4,5,6	Give X,Y Z co-ordinates of nodes of members
Columns 7, 8	Give BM in columns about local Y and Z axes in NI analysis
Columns 9,10	Give BM in columns about local Y and Z axes in SSI analysis
Columns 11,12	Give BM in columns about local Y and Z axes in RSSI analysis
Columns 13,14	Give ratio BM in columns about local Y and Z in SSI to NI analysis
Columns 15,16	Give ratio BM in columns about local Y and Z in RSSI to NI analysis
Columns 17,18	Give ratio BM in columns about local Y and Z in RSSI to SSI analysis

As the bending moments in NI analysis are of lesser magnitude interaction effects are discussed for members where  $M_y$  and  $M_z$  of magnitude greater than 25kNm in NI analysis. The same moments have increased from 1.58 to 2.13 and from 1.7 to 2.1 in non-linear SSI analysis with respect to NI analysis. Where as  $M_y$  and  $M_z$  in nonlinear analysis RSSI varied from 1.64 to 2.07 and 1.7 to 2.06 respectively. However provision of geogrid reinforcement reduces BM in columns up to 46% with respect to nonlinear SSI analysis where as in some cases the same enhanced by 10%.

Section 8.5.4 presents the Graphs plotted in Non-Linear SSI and RSSI analyses.

Section 8.5.5 presents Tables related to nonlinear analysis of SSI and RSSI analyses.

### 8.5.4 Graphs plotted in Non-Linear SSI and RSSI Analyses

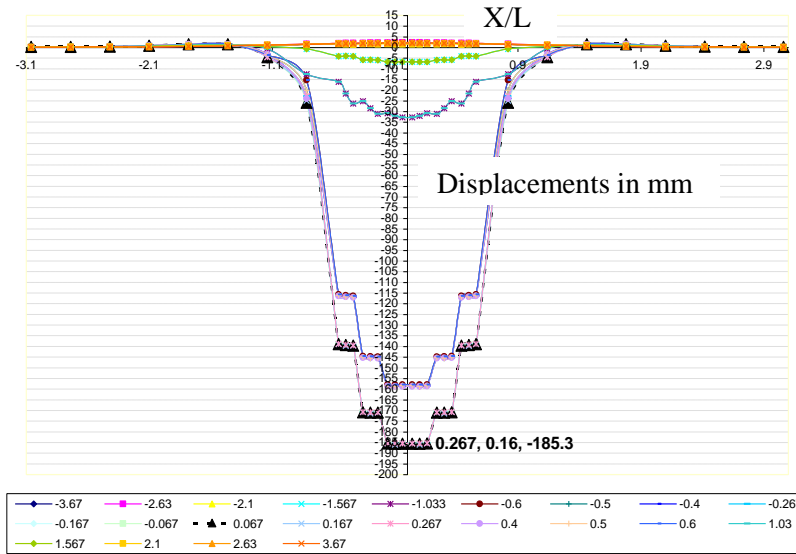


Fig. 8.21a

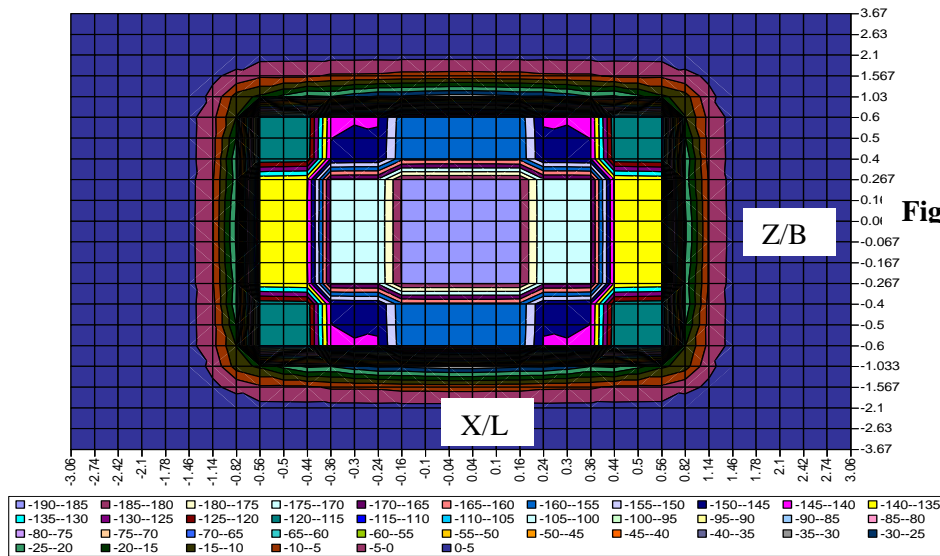


Fig. 8.21b

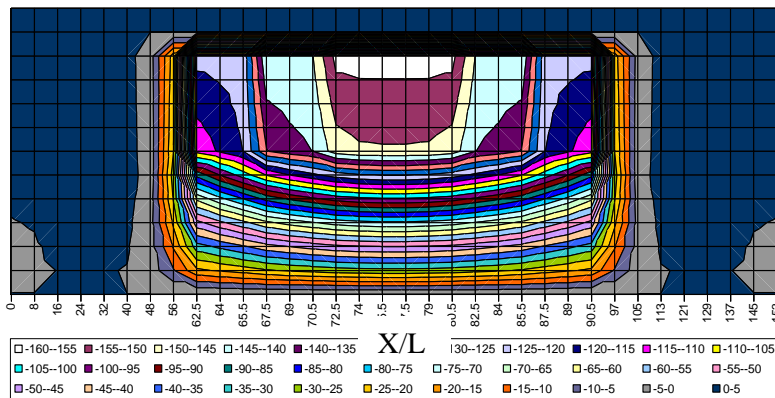


Fig. 8.21c

Fig. 8.21: Vertical settlements in mm in non-linear SSI analysis (a) Vertical settlements at foundation level (b) Contours of vertical settlements footing level (c) Vertical settlements along longitudinal section at centre.

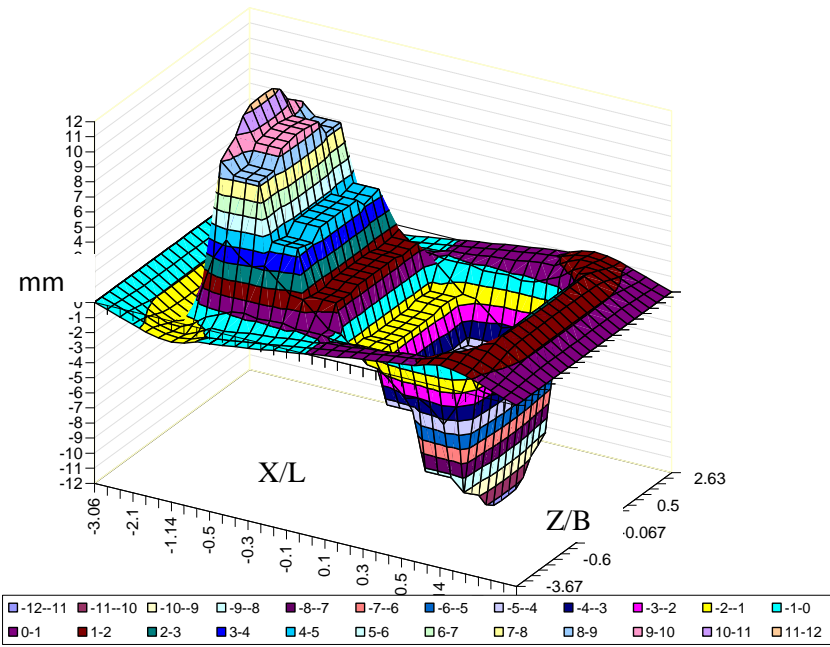


Fig. 8.22a

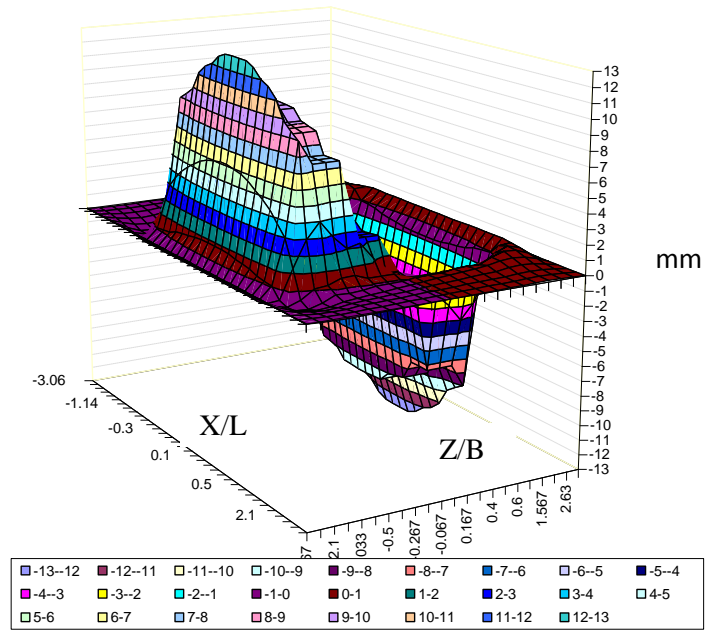


Fig. 8.22c

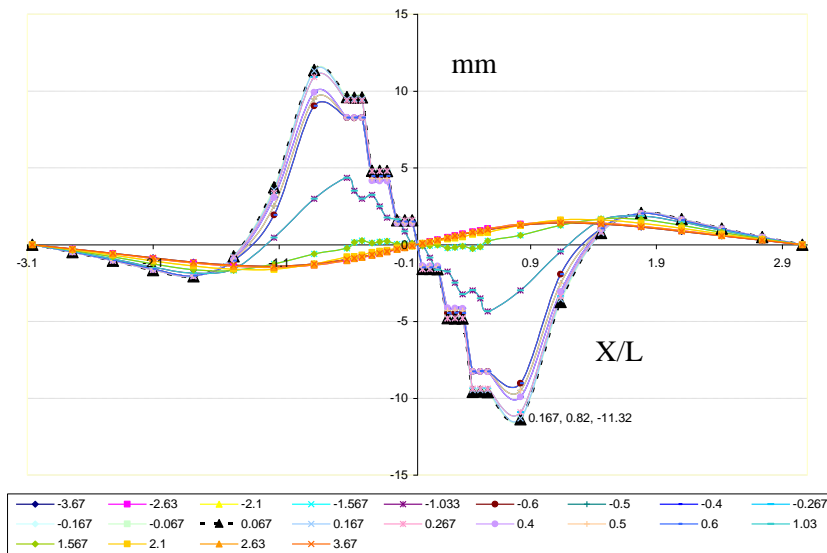


Fig. 8.22b

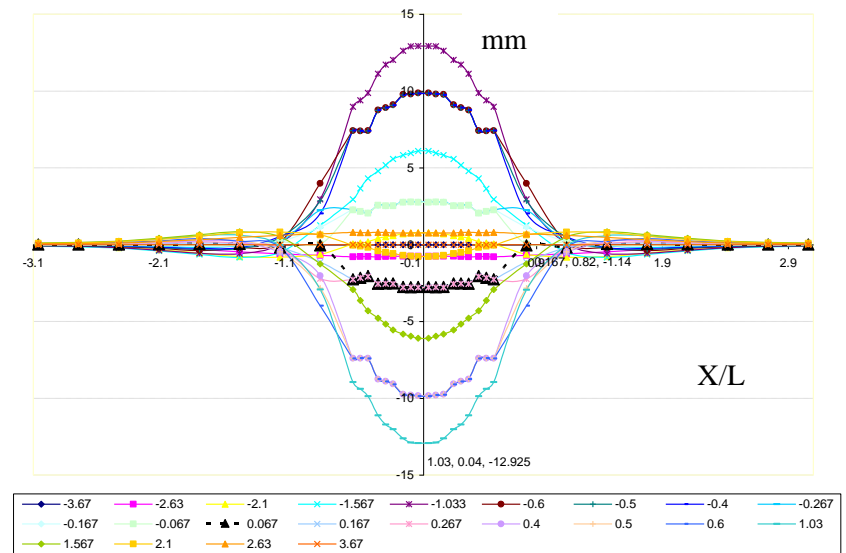
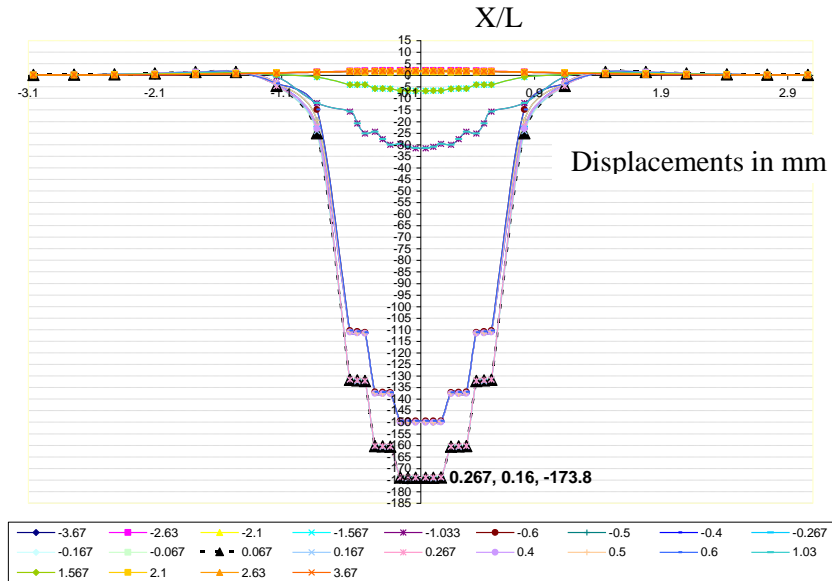
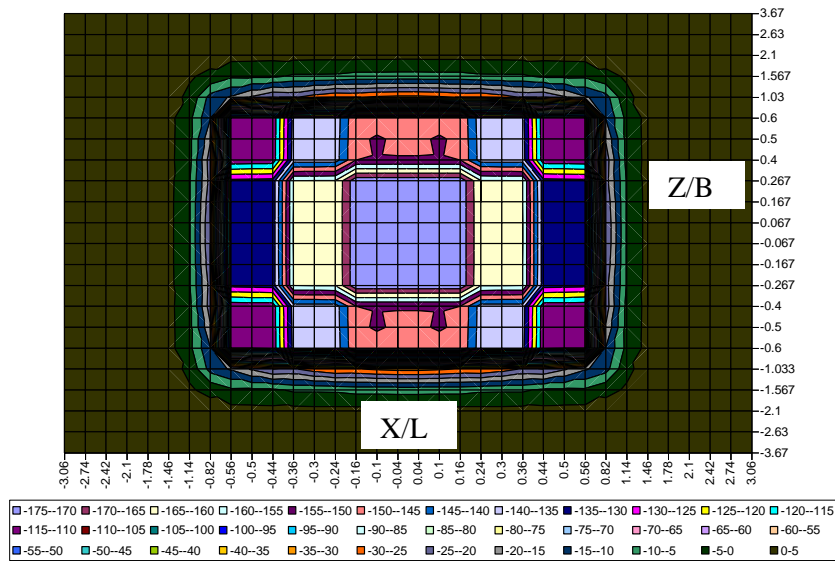


Fig. 8.22d

Fig. 8.22: Horizontal displacements in mm in non-linear SSI analysis (a) and (b) Longitudinal displacements at foundation level (c) and (d) Transverse displacements at foundation level



**Fig. 8.23a**



**Fig. 8.23b**

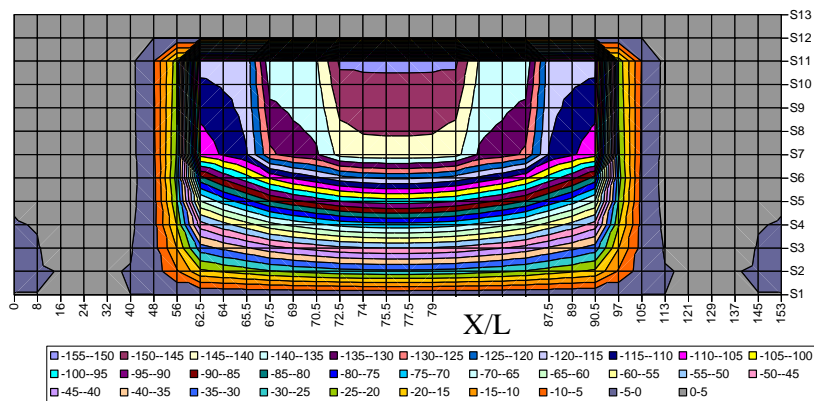


**Fig. 8.23c**

**Fig. 8.23: Vertical settlements in mm in Non-Linear RSSI analysis (a) Vertical settlements at foundation level along longitudinal directions. (b) Contours of vertical settlements at footing level. (c) Vertical settlements along longitudinal section at centre.**

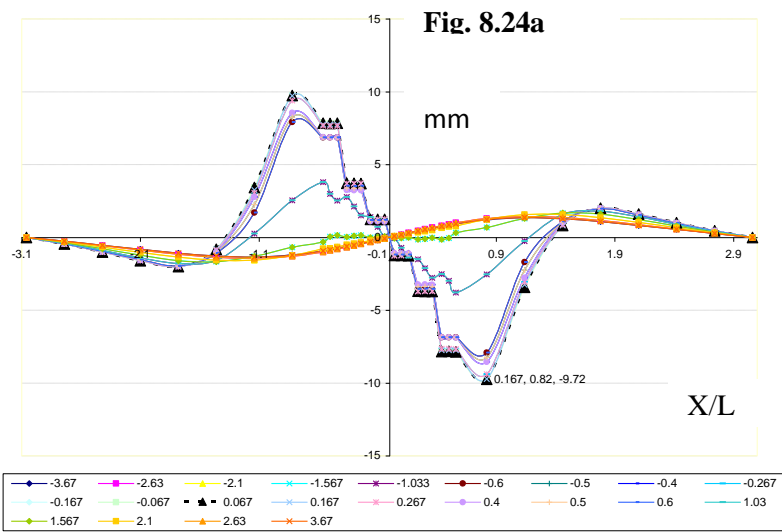
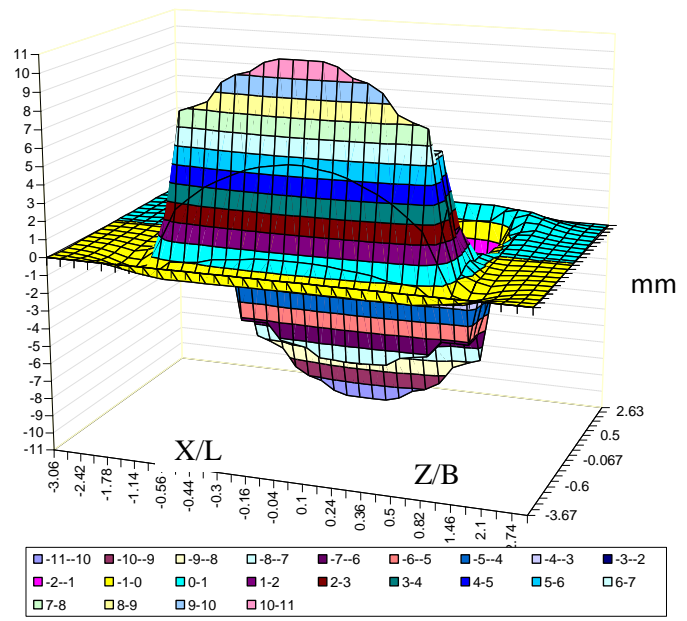
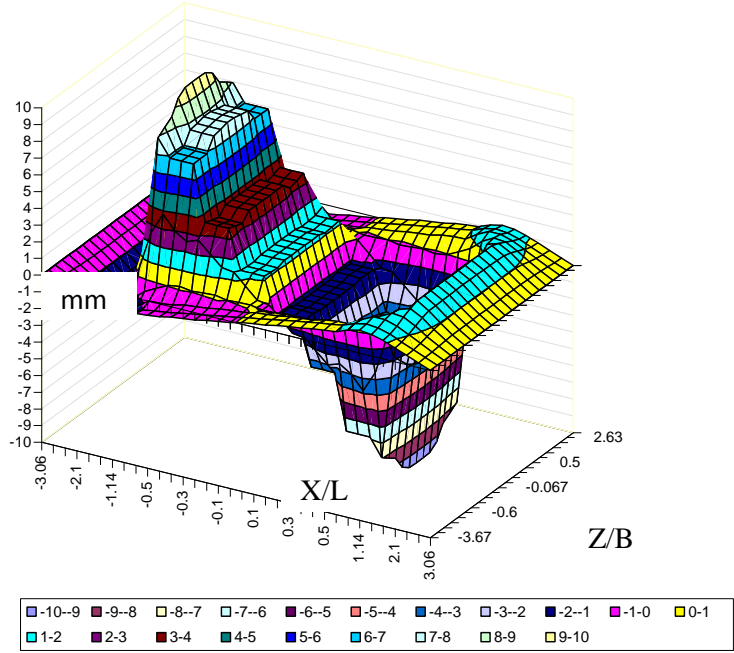


**Fig. 8.24b**

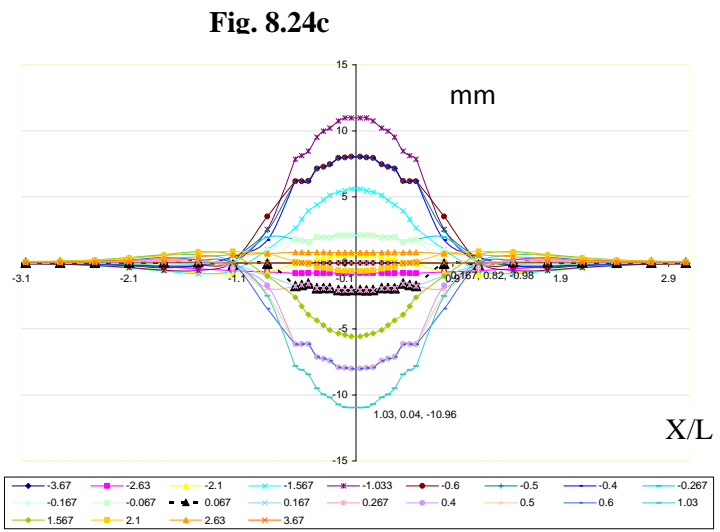


**Fig. 8.24d**

**Fig. 8.24** Horizontal displacements in mm in Non-linear RSSI analysis (a) and (b) longitudinal displacements at foundation level (c) and (d) transverse displacements at foundation level

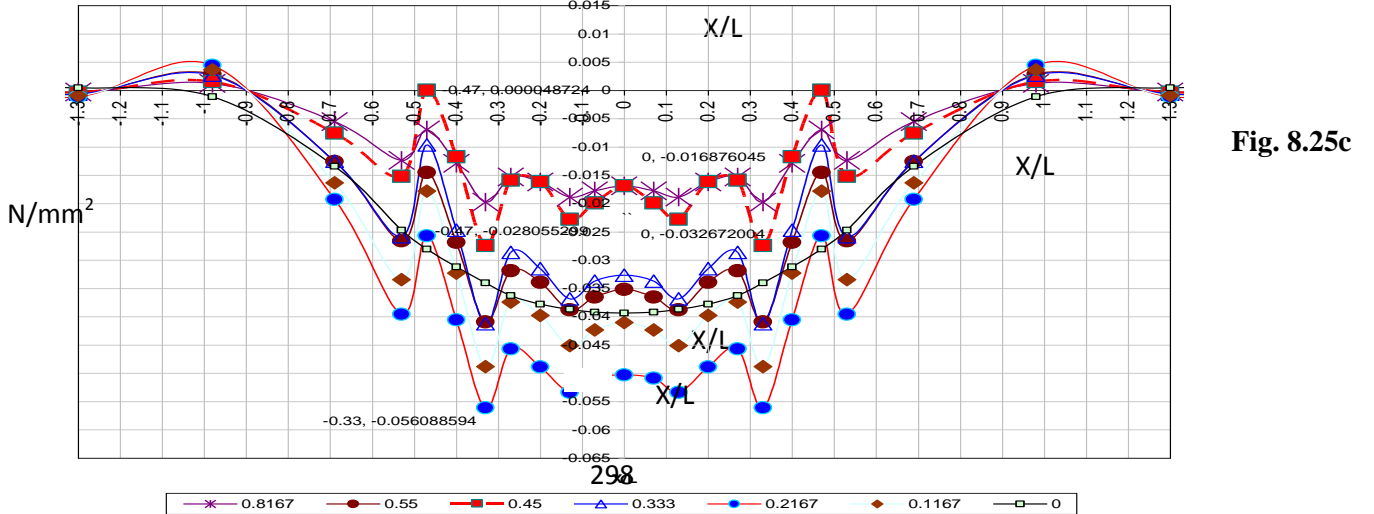
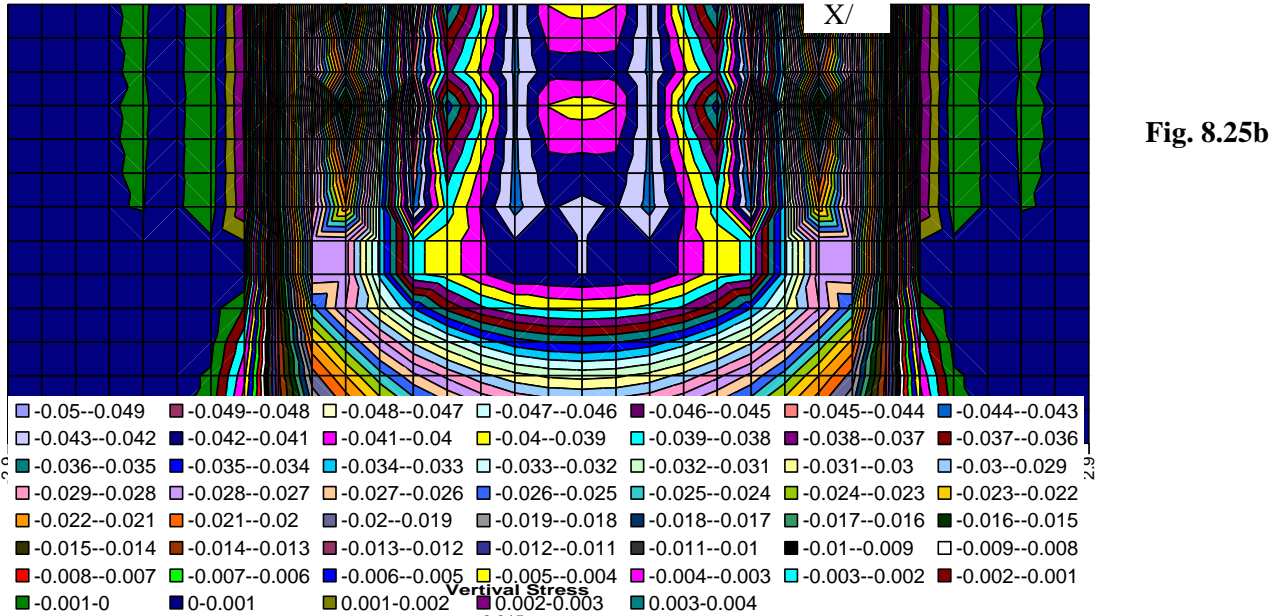
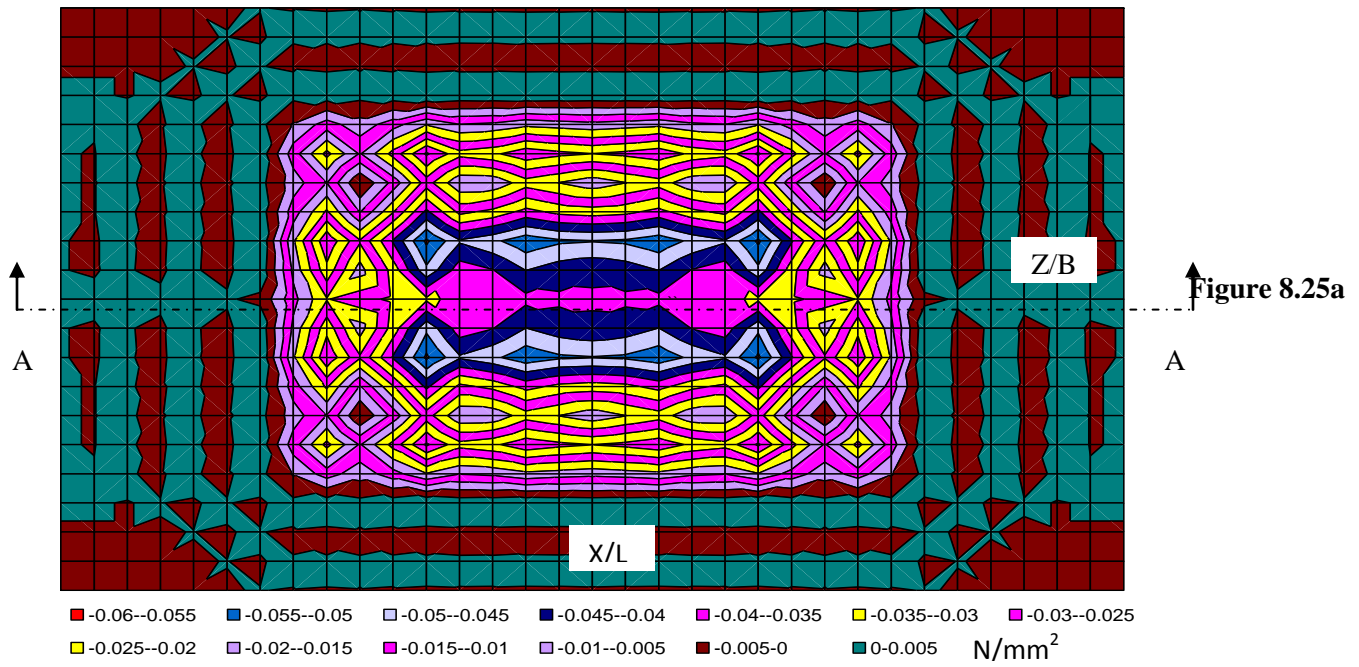


Fig. 8.25: Vertical stresses in Non-linear SSI analysis (a) Contours of vertical stresses at footing level (b) Vertical stresses along longitudinal section at centre (c) Vertical stresses at foundation level along longitudinal sections for different values of  $Z/L$



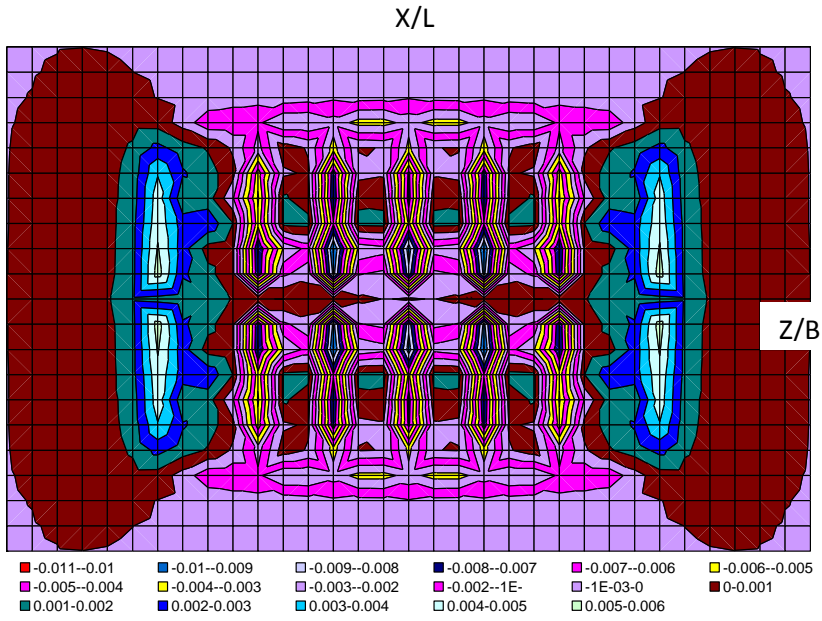


Fig. 8.26 a

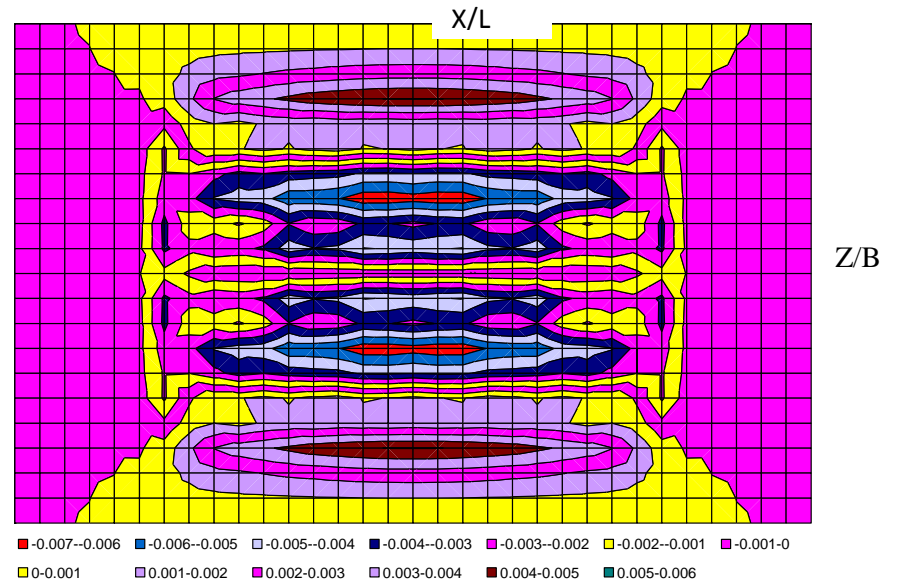


Fig. 8.26 c

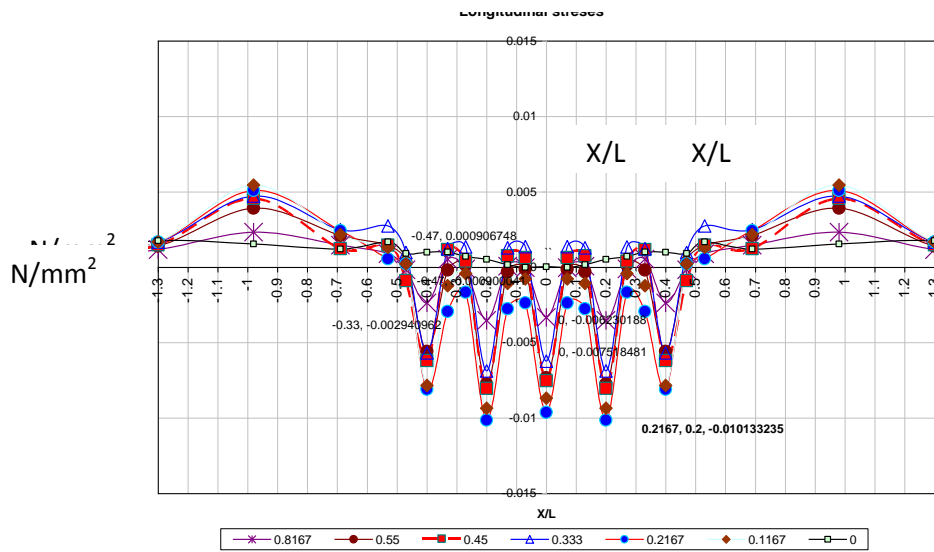


Fig. 8.26 b

299

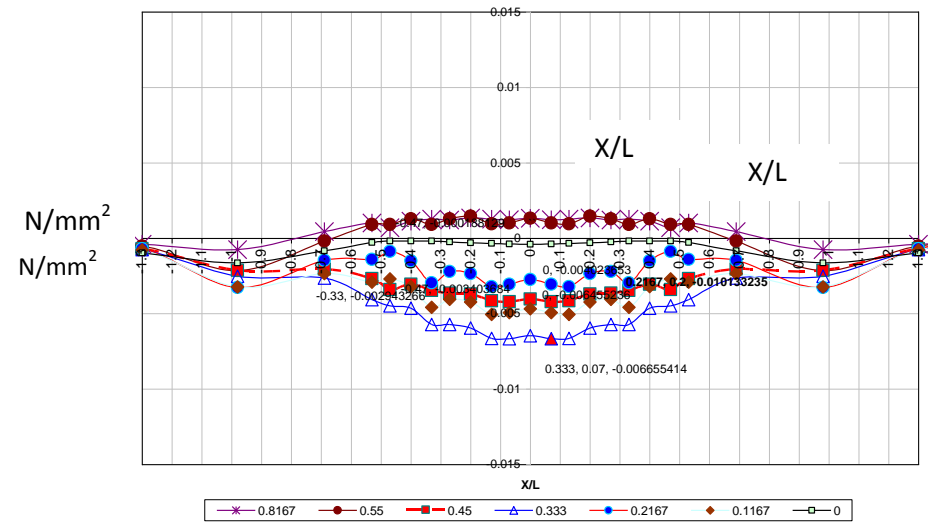


Fig. 8.26 d

Fig. 8.26 Horizontal stresses  $N/mm^2$  in Non-linear SSI analysis (a) and (b) longitudinal stresses at foundation level (c) and (d) Transverse stresses at foundation



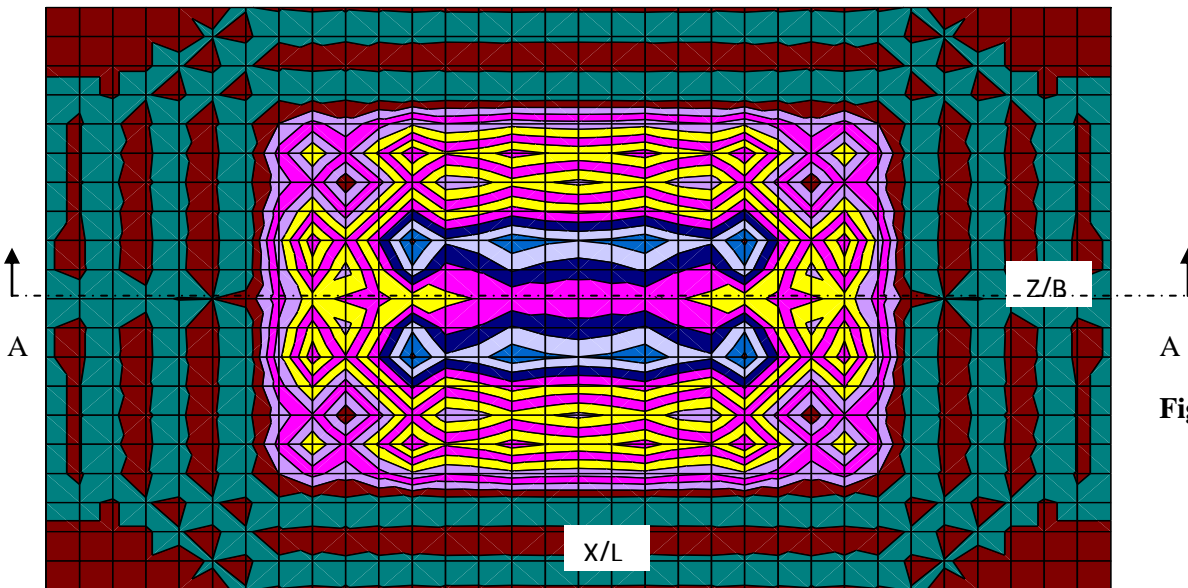


Fig. 8.27a

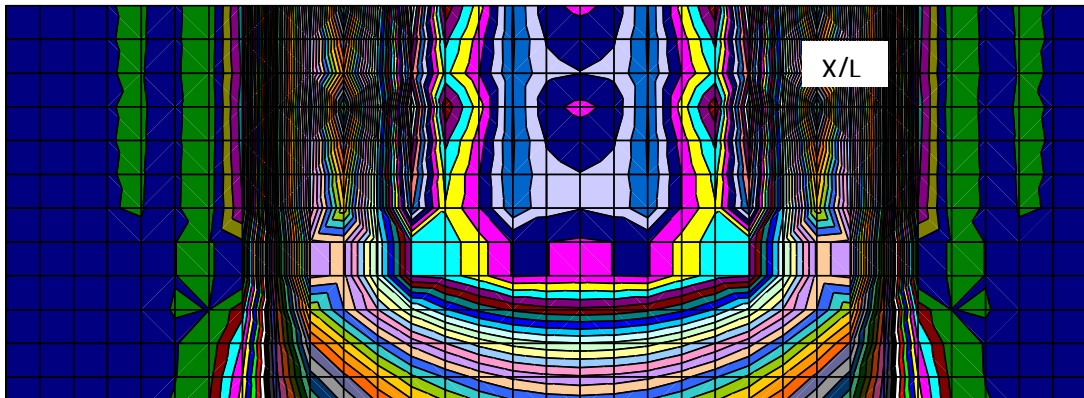
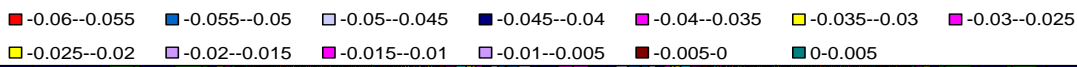


Fig. 8.27 b

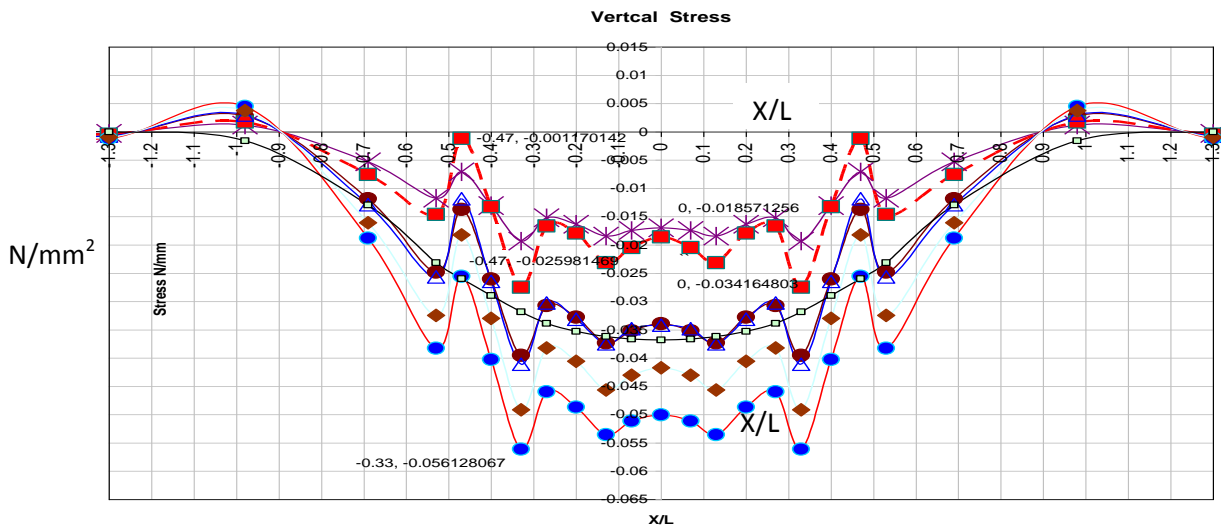
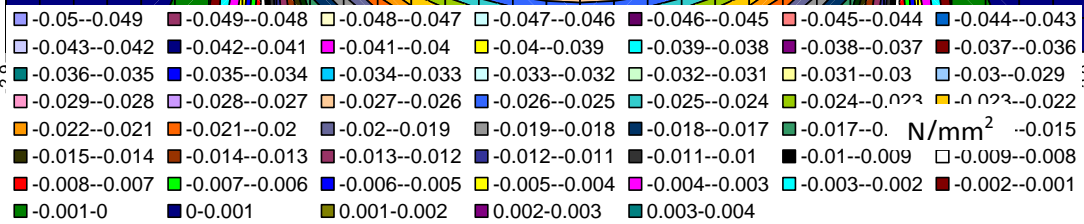


Fig. 8.27c

Fig. 8.27: Vertical stresses in Non-linear RSSI analysis (a) Contours of vertical stresses at footing level (b) Vertical stresses along longitudinal section at centre (c) Vertical stresses at foundation level along longitudinal sections for different values of Z/L

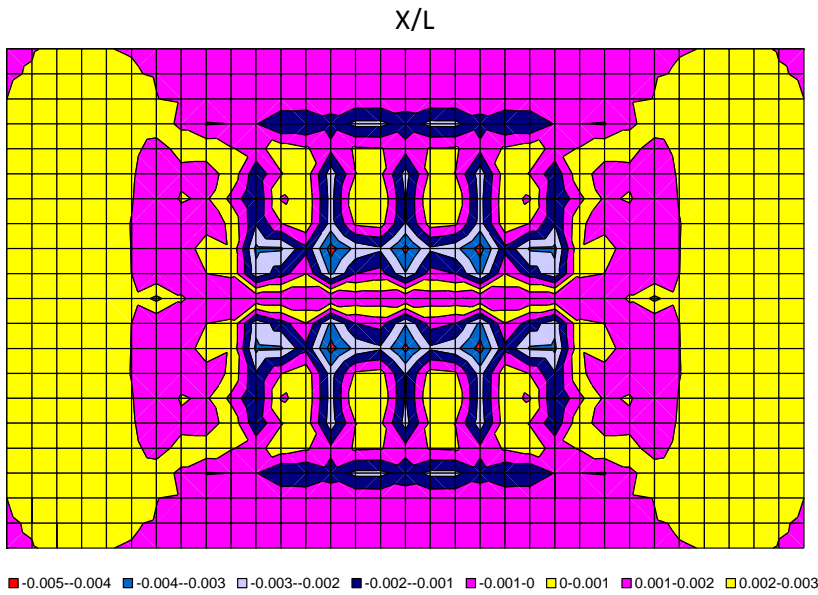


Fig. 8.28.a

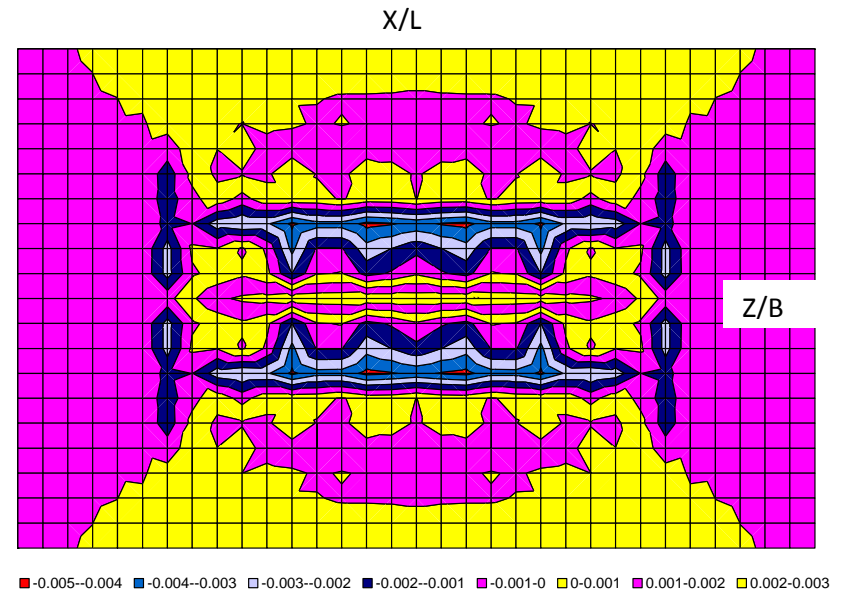


Fig. 8.28.c

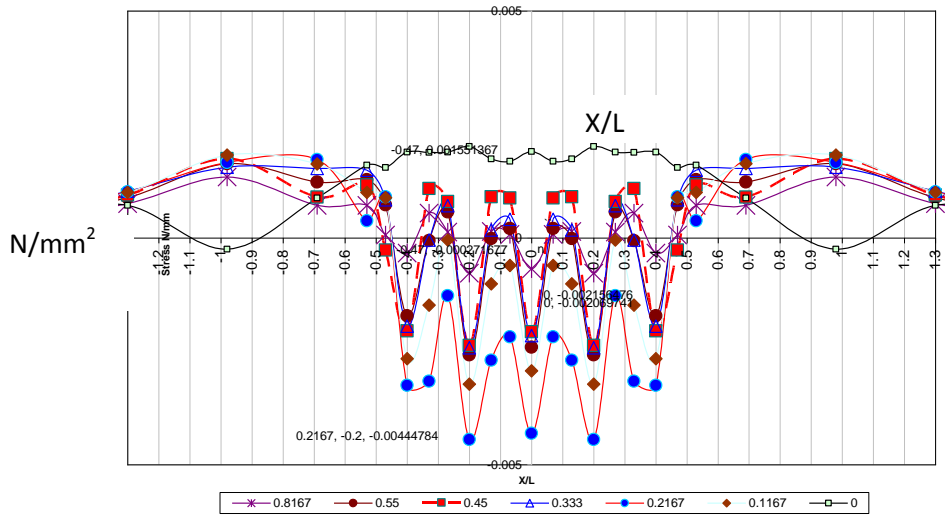


Fig. 8.28.b

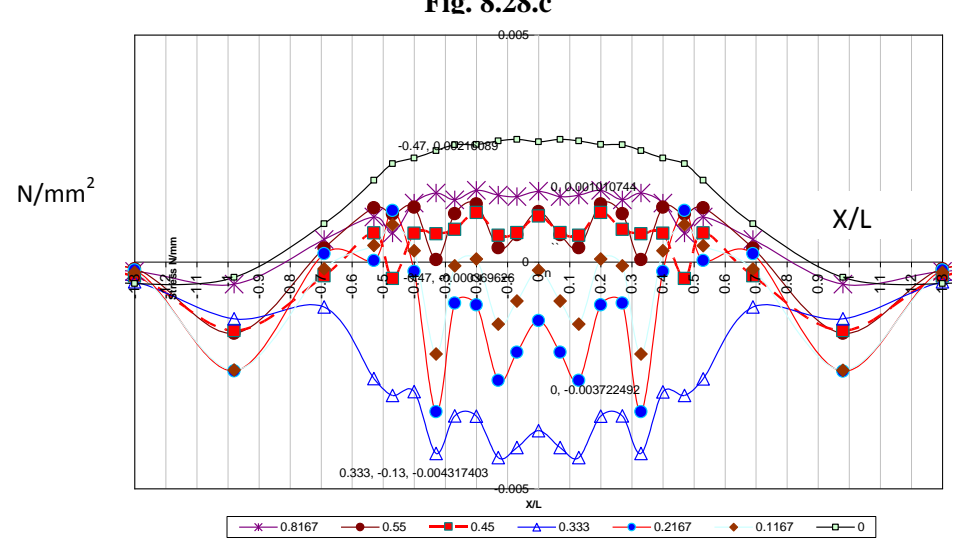


Fig. 8.28.d

Fig. 8.28 Horizontal stresses in Non-linear RSSI analysis (a) and (b) longitudinal stresses at foundation level (c) and (d) Transverse stresses at foundation level

### 8.5.5 Tables related to nonlinear analysis of SSI and RSSI

**Table 8.10: Properties of soil used in Non-linear SSI and RSSI analysis (After Krishnamoorthy and Rao, 1995)**

Properties	Soil 2
Liquid limit	54
Plastic limit	40
Plasticity Index	14
Shrinkage limit	20
Water content	28
Specific gravity	2.65
Wet density(kN/m <sup>3</sup> )	18.18

**Table 8.11: Hypoelastic model Parameters used in Non-linear SSI and RSSI analysis (After Krishnamoorthy and Rao, 1995)**

Model parameters		Soil 2
K modulus	$\lambda/V_i$	0.020
	$\kappa/V_i$	0.003
	$P'_{cons}$	21000 Pa
J modulus	A	100
	N	100
G modulus	E	0.001
	F	0.56

Table 8.12. Stress resultants, Axial forces (kN) in X-Beams of external frames in non-linear SSI and RSSI analysis

Direction of Frame	Floor	Member	(X,Y,Z) coordinates of			NI Analysis		SSI Analysis		RSSI Analysis		Ratio of SSI/NI		Ratio of RSSI/NI		Ratio of RSSI/SSI	
			X	Y	Z	Axial	Shear	Axial	Shear	Axial	Shear	Axial	Shear	Axial	Shear	Axial	Shear
(1)	(2)	(3)	(4)	(5)	(6)	(7)	(8)	(9)	(10)	(11)	(12)	(13)	(14)	(15)	(16)	(17)	(18)
External frame in X-direction	Ground floor	1	64	23.5	40	-6.71	72.47	5.51	95.79	-3.55	91.36	-0.82	1.32	0.53	1.26	-0.64	0.95
		1	69	23.5	40	6.71	82.53	-5.51	59.21	3.55	63.64	-0.82	0.72	0.53	0.77	-0.64	1.07
		2	69	23.5	40	-6.54	77.92	12.15	82.36	-2.92	80.89	-1.86	1.06	0.45	1.04	-0.24	0.98
		2	74	23.5	40	6.54	77.08	-12.15	72.64	2.92	74.11	-1.86	0.94	0.45	0.96	-0.24	1.02
		3	74	23.5	40	-6.38	77.5	14.95	77.5	-2.03	77.5	-2.34	1.00	0.32	1.00	-0.14	1.00
	First floor	6	64	27	40	-0.02	74.96	-1.86	92.41	-0.59	91.45	93.00	1.23	29.50	1.22	0.32	0.99
		6	69	27	40	0.02	80.04	1.86	62.59	0.59	63.55	93.00	0.78	29.50	0.79	0.32	1.02
		7	69	27	40	-1.28	77.2	-3.23	80.53	-1.86	80.08	2.52	1.04	1.45	1.04	0.58	0.99
		7	74	27	40	1.28	77.8	3.23	74.47	1.86	74.92	2.52	0.96	1.45	0.96	0.58	1.01
	Second floor	8	74	27	40	-1.12	77.5	-3.49	77.5	-2.02	77.5	3.12	1.00	1.80	1.00	0.58	1.00
		11	64	30.5	40	-4.27	76.48	-5.84	94.19	-5.83	93.07	1.37	1.23	1.37	1.22	1.00	0.99
		11	69	30.5	40	4.27	78.52	5.84	60.81	5.83	61.93	1.37	0.77	1.37	0.79	1.00	1.02
		12	69	30.5	40	-3.34	76.65	-5.7	80.16	-5.58	79.73	1.71	1.05	1.67	1.04	0.98	0.99
	Third floor	12	74	30.5	40	3.34	78.35	5.7	74.84	5.58	75.27	1.71	0.96	1.67	0.96	0.98	1.01
		13	74	30.5	40	-3.22	77.5	-5.65	77.5	-5.5	77.5	1.75	1.00	1.71	1.00	0.97	1.00
		16	64	34	40	18.74	71.58	33.05	82.81	32.14	82.13	1.76	1.16	1.72	1.15	0.97	0.99
		16	69	34	40	-18.74	83.42	-33.05	72.19	-32.14	72.87	1.76	0.87	1.72	0.87	0.97	1.01
		17	69	34	40	18.53	77.44	46.92	78.64	44.98	78.4	2.53	1.02	2.43	1.01	0.96	1.00
17		74	34	40	-18.53	77.56	-46.92	76.36	-44.98	76.6	2.53	0.98	2.43	0.99	0.96	1.00	
18	74	34	40	18.22	77.5	49.81	77.5	47.53	77.5	2.73	1.00	2.61	1.00	0.95	1.00		

Note: Section 8.5.3.1 gives details about Table 8.12

In columns 13 to 18, negative sign indicates the reduction in the values and positive sign indicates an increase in the values

Table 8.13 Stress resultants (Axial forces in kN) in X-Beams of internal frames in Non-linear SSI and RSSI analysis																	
Direction of Frame	Floor	Mem ber No.	(X,Y,Z) coordinates of beam nodes			NI Analysis		SSI Analysis		RSSI Analysis		Ratio of SSI/NI		Ratio of RSSI/NI		Ratio of RSSI/SSI	
			X	Y	Z	Axial	Shear	Axial	Shear	Axial	Shear	Axial	Shear	Axial	Shear	Axial	Shear
(1)	(2)	(3)	(4)	(5)	(6)	(7)	(8)	(9)	(10)	(11)	(12)	(13)	(14)	(15)	(16)	(17)	(18)
Internal frame in X-direction	Ground floor	21	64	23.5	45	-6.71	72.47	8.85	101.7	-3.83	96.42	-1.32	1.40	0.57	1.33	-0.43	0.95
		21	69	23.5	45	6.71	82.53	-8.85	53.28	3.83	58.58	-1.32	0.65	0.57	0.71	-0.43	1.10
		22	69	23.5	45	-6.54	77.92	16.6	83.11	-4.06	81.27	-2.54	1.07	0.62	1.04	-0.24	0.98
		22	74	23.5	45	6.54	77.08	-16.6	71.89	4.06	73.73	-2.54	0.93	0.62	0.96	-0.24	1.03
		23	74	23.5	45	-6.38	77.5	19.84	77.5	-3.31	77.5	-3.11	1.00	0.52	1.00	-0.17	1.00
	First floor	26	64	27	45	-0.02	74.96	-2.28	96.75	-0.47	96.19	#####	1.29	23.50	1.28	0.21	0.99
		26	69	27	45	0.02	80.04	2.28	58.25	0.47	58.81	#####	0.73	23.50	0.73	0.21	1.01
		27	69	27	45	-1.28	77.2	-3.5	81.16	-1.58	80.65	2.73	1.05	1.23	1.04	0.45	0.99
		27	74	27	45	1.28	77.8	3.5	73.84	1.58	74.35	2.73	0.95	1.23	0.96	0.45	1.01
		28	74	27	45	-1.12	77.5	-3.82	77.5	-1.8	77.5	3.41	1.00	1.61	1.00	0.47	1.00
	Second floor	31	64	30.5	45	-4.27	76.48	-6.15	98.5	-6.21	97.7	1.44	1.29	1.45	1.28	1.01	0.99
		31	69	30.5	45	4.27	78.52	6.15	56.5	6.21	57.3	1.44	0.72	1.45	0.73	1.01	1.01
		32	69	30.5	45	-3.34	76.65	-6.14	80.8	-6.06	80.34	1.84	1.05	1.81	1.05	0.99	0.99
		32	74	30.5	45	3.34	78.35	6.14	74.2	6.06	74.66	1.84	0.95	1.81	0.95	0.99	1.01
		33	74	30.5	45	-3.22	77.5	-6.08	77.5	-5.98	77.5	1.89	1.00	1.86	1.00	0.98	1.00
	Third floor	36	64	34	45	18.74	71.58	36.41	85.54	35.75	85.07	1.94	1.20	1.91	1.19	0.98	0.99
		36	69	34	45	-18.7	83.42	-36.4	69.46	-35.8	69.93	1.94	0.83	1.91	0.84	0.98	1.01
		37	69	34	45	18.53	77.44	53.46	78.78	51.95	78.49	2.89	1.02	2.80	1.01	0.97	1.00
37		74	34	45	-18.5	77.56	-53.5	76.22	-52	76.51	2.89	0.98	2.80	0.99	0.97	1.00	
38		74	34	45	18.22	77.5	56.96	77.5	55.12	77.5	3.13	1.00	3.03	1.00	0.97	1.00	

**Note: Section 8.5.3.1 gives details about Table 8.13**

**In columns 13 to 18, negative sign indicates the reduction in the values and positive sign indicates an increase in the values**

Table 8.14 Stress resultants (Axial forces in kN) in beams in Z-direction in Non-linear SSI and RSSI analysis (discussion in section 8.5.3.1)

Direction of Frame	Floor	Member No.	(X,Y,Z) coordinates of beam nodes			NI Analysis		RSSI Analysis		SSI Analysis		Ratio of SSI/NI		Ratio of RSSI/NI		Ratio of RSSI/SSI	
			X	Y	Z	Axial	Shear	Axial	Shear	Axial	Shear	Axial	Shear	Axial	Shear	Axial	Shear
(1)	(2)	(3)	(4)	(5)	(6)	(7)	(8)	(9)	(10)	(11)	(12)	(13)	(14)	(15)	(16)	(18)	(19)
External frame in Z-direction	Ground floor	81	64	23.5	40	-6.88	72.52	4.25	93.52	-5.51	89.4	-0.62	1.29	0.80	1.23	-1.30	0.96
		81	64	23.5	45	6.88	82.48	-4.25	61.48	5.51	65.6	-0.62	0.75	0.80	0.80	-1.30	1.07
		82	64	23.5	45	-6.94	77.5	6.78	77.5	-6.85	77.5	-0.98	1.00	0.99	1.00	-1.01	1.00
	First floor	84	64	27	40	0.17	74.93	-1.78	91.16	-0.12	90.37	-10.47	1.22	-0.71	1.21	0.07	0.99
		84	64	27	45	-0.17	80.07	1.78	63.84	0.12	64.63	-10.47	0.80	-0.71	0.81	0.07	1.01
		85	64	27	45	-1.16	77.5	-2.84	77.5	-1.08	77.5	2.45	1.00	0.93	1.00	0.38	1.00
	Second floor	87	64	30.5	40	-4.57	76.45	-6.33	93.17	-6.38	92.11	1.39	1.22	1.40	1.20	1.01	0.99
		87	64	30.5	45	4.57	78.55	6.33	61.83	6.38	62.89	1.39	0.79	1.40	0.80	1.01	1.02
		88	64	30.5	45	-3.94	77.5	-6.6	77.5	-6.55	77.5	1.68	1.00	1.66	1.00	0.99	1.00
	Third floor	90	64	34	40	18.94	71.71	32.17	82.79	31.37	82.1	1.70	1.15	1.66	1.14	0.98	0.99
		90	64	34	45	-18.94	83.29	-32.17	72.21	-31.37	72.9	1.70	0.87	1.66	0.88	0.98	1.01
		91	64	34	45	19.18	77.5	42.46	77.5	41.02	77.5	2.21	1.00	2.14	1.00	0.97	1.00
Internal frame in Z-direction	Ground floor	93	69	23.5	40	-6.88	72.52	8.52	99.87	-5.85	94.73	-1.24	1.38	0.85	1.31	-0.69	0.95
		93	69	23.5	45	6.88	82.48	-8.52	55.13	5.85	60.27	-1.24	0.67	0.85	0.73	-0.69	1.09
		94	69	23.5	45	-6.94	77.5	11.9	77.5	-7.99	77.5	-1.71	1.00	1.15	1.00	-0.67	1.00
	First floor	96	69	27	40	0.17	74.93	-2.43	95.74	0.04	95.4	-14.29	1.28	0.24	1.27	-0.02	1.00
		96	69	27	45	-0.17	80.07	2.43	59.26	-0.04	59.6	-14.29	0.74	0.24	0.74	-0.02	1.01
		97	69	27	45	-1.16	77.5	-3.3	77.5	-0.69	77.5	2.84	1.00	0.59	1.00	0.21	1.00
	Second floor	99	69	30.5	40	-4.57	76.45	-6.73	97.81	-6.9	97.07	1.47	1.28	1.51	1.27	1.03	0.99
		99	69	30.5	45	4.57	78.55	6.73	57.19	6.9	57.93	1.47	0.73	1.51	0.74	1.03	1.01
		100	69	30.5	45	-3.94	77.5	-7.22	77.5	-7.28	77.5	1.83	1.00	1.85	1.00	1.01	1.00
	Third floor	102	69	34	40	18.94	71.71	35.75	85.84	35.21	85.37	1.89	1.20	1.86	1.19	0.98	0.99
		102	69	34	45	-18.94	83.29	-35.75	69.16	-35.21	69.63	1.89	0.83	1.86	0.84	0.98	1.01
		103	69	34	45	19.18	77.5	48.77	77.5	47.78	77.5	2.54	1.00	2.49	1.00	0.98	1.00
Internal frame in Z-direction	Ground floor	105	74	23.5	40	-6.88	72.52	10.65	102.3	-5.69	96.56	-1.55	1.41	0.83	1.33	-0.53	0.94
		105	74	23.5	45	6.88	82.48	-10.65	52.75	5.69	58.44	-1.55	0.64	0.83	0.71	-0.53	1.11
		106	74	23.5	45	-6.94	77.5	14.55	77.5	-8.03	77.5	-2.10	1.00	1.16	1.00	-0.55	1.00
	First floor	108	74	27	40	0.17	74.93	-2.83	97.38	-0.02	97.12	-16.65	1.30	-0.12	1.30	0.01	1.00
		108	74	27	45	-0.17	80.07	2.83	57.62	0.02	57.88	-16.65	0.72	-0.12	0.72	0.01	1.00
		109	74	27	45	-1.16	77.5	-3.69	77.5	-0.73	77.5	3.18	1.00	0.63	1.00	0.20	1.00
	Second floor	111	74	30.5	40	-4.57	76.45	-6.92	99.55	-7.13	98.86	1.51	1.30	1.56	1.29	1.03	0.99
		111	74	30.5	45	4.57	78.55	6.92	55.45	7.13	56.14	1.51	0.71	1.56	0.71	1.03	1.01
		112	74	30.5	45	-3.94	77.5	-7.52	77.5	-7.61	77.5	1.91	1.00	1.93	1.00	1.01	1.00
	Third floor	114	74	34	40	18.94	71.71	37.15	87	36.64	86.56	1.96	1.21	1.93	1.21	0.99	0.99
		114	74	34	45	-18.94	83.29	-37.15	68	-36.64	68.44	1.96	0.82	1.93	0.82	0.99	1.01
		115	74	34	45	19.18	77.5	51.21	77.5	50.29	77.5	2.67	1.00	2.62	1.00	0.98	1.00

Table 8.15 Stress resultants (Axial and shear forces in kN) in columns of external frames in Nonlinear SSI and RSSI analysis (discussion in section 8.3.2.2)

Directi on of Frame	Floor	Mem ber	(X,Y,Z) coordinates			NI Analysis			SSI Analysis			RSSI Analysis			Ratio of SSI/NI			Ratio of RSSI/NI			Ratio of RSSI/SSI		
			X	Y	Z	Axial	Shear- X	Shear - Y	Axial	Shear- X	Shear - Y	Axial	Shear- X	Shear - Y	Axia l	Shea r-X	Shea r-Y	Axia l	Shear-X	Shea r-Y	Axia l	Shea r-X	Shea r-Y
(1)	(2)	(3)	(4)	(5)	(6)	(7)	(8)	(9)	(10)	(11)	(12)	(13)	(14)	(15)	(16)	(18)	(19)	(20)	(21)	(23)	(24)	(25)	(26)
External columns	Ground floor	153	64	20	40	591.09	7.74	-7.66	725.8	30.81	-28.27	711.99	22.14	-19.34	1.23	3.98	3.69	1.20	2.86	2.52	0.98	0.72	0.68
		153	64	24	40	-591.09	-7.74	7.66	-725.8	-30.81	28.27	-711.99	-22.1	19.34	1.23	3.98	3.69	1.20	2.86	2.52	0.98	0.72	0.68
		154	69	20	40	929.32	-0.36	-7.66	955.8	19.22	-35.15	953.66	12.44	-22.52	1.03	-5.3	4.59	1.03	-34.56	2.94	1.00	0.65	0.64
		154	69	24	40	-929.32	0.36	7.66	-955.8	-19.22	35.15	-953.66	-12.4	22.52	1.03	-5.3	4.59	1.03	-34.56	2.94	1.00	0.65	0.64
		155	74	20	40	916.39	0.12	-7.66	994.5	5.46	-38.07	990	3.34	-23.81	1.09	45.5	4.97	1.08	27.83	3.11	1.00	0.61	0.63
		155	74	24	40	-916.39	-0.12	7.66	-994.5	-5.46	38.07	-990	-3.34	23.81	1.09	45.5	4.97	1.08	27.83	3.11	1.00	0.61	0.63
	First floor	159	64	24	40	446.1	14.45	-14.5	536.5	25.32	-24.04	531.23	25.68	-24.84	1.20	1.8	1.65	1.19	1.78	1.71	0.99	1.01	1.03
		159	64	27	40	-446.1	-14.45	14.54	-536.5	-25.32	24.04	-531.23	-25.7	24.84	1.20	1.8	1.65	1.19	1.78	1.71	0.99	1.01	1.03
		160	69	24	40	696.34	-0.53	-14.5	714.3	12.62	-26.61	714.4	11.8	-28.37	1.03	-23.8	1.83	1.03	-22.26	1.95	1.00	0.94	1.07
		160	69	27	40	-696.34	0.53	14.54	-714.3	-12.62	26.61	-714.4	-11.8	28.37	1.03	-23.8	1.83	1.03	-22.26	1.95	1.00	0.94	1.07
		161	74	24	40	689.3	-0.03	-14.5	742.1	2.66	-27.41	741.83	2.44	-29.5	1.08	-88.7	1.89	1.08	-81.33	2.03	1.00	0.92	1.08
		161	74	27	40	-689.3	0.03	14.54	-742.1	-2.66	27.41	-741.83	-2.44	29.5	1.08	-88.7	1.89	1.08	-81.33	2.03	1.00	0.92	1.08
	Second floor	165	64	27	40	296.22	14.47	-14.4	353	27.18	-25.82	349.41	26.28	-24.96	1.19	1.9	1.80	1.18	1.82	1.74	0.99	0.97	0.97
		165	64	31	40	-296.22	-14.47	14.36	-353	-27.18	25.82	-349.41	-26.3	24.96	1.19	1.9	1.80	1.18	1.82	1.74	0.99	0.97	0.97
		166	69	27	40	464.18	0.73	-14.4	475.5	13.98	-29.04	475.37	13.06	-28.33	1.02	19.2	2.02	1.02	17.89	1.97	1.00	0.93	0.98
		166	69	31	40	-464.18	-0.73	14.36	-475.5	-13.98	29.04	-475.37	-13.1	28.33	1.02	19.2	2.02	1.02	17.89	1.97	1.00	0.93	0.98
		167	74	27	40	459.07	-0.19	-14.4	492.8	2.92	-30.24	492.28	2.61	-29.52	1.07	-15.4	2.11	1.07	-13.74	2.06	1.00	0.89	0.98
		167	74	31	40	-459.07	0.19	14.36	-492.8	-2.92	30.24	-492.28	-2.61	29.52	1.07	-15.4	2.11	1.07	-13.74	2.06	1.00	0.89	0.98
	Third floor	171	64	31	40	143.29	18.74	-18.9	165.6	33.02	-32.14	164.23	32.11	-31.34	1.16	1.8	1.70	1.15	1.71	1.65	0.99	0.97	0.98
		171	64	34	40	-143.29	-18.74	18.94	-165.6	-33.02	32.14	-164.23	-32.1	31.34	1.16	1.8	1.70	1.15	1.71	1.65	0.99	0.97	0.98
		172	69	31	40	232.56	-0.2	-18.9	236.7	13.84	-35.78	236.64	12.8	-35.23	1.02	-69.2	1.89	1.02	-64.00	1.86	1.00	0.92	0.98
172		69	34	40	-232.56	0.2	18.94	-236.7	-13.84	35.78	-236.64	-12.8	35.23	1.02	-69.2	1.89	1.02	-64.00	1.86	1.00	0.92	0.98	
173		74	31	40	226.77	-0.31	-18.9	240.9	2.87	-37.16	240.66	2.54	-36.65	1.06	-9.3	1.96	1.06	-8.19	1.94	1.00	0.89	0.99	
173		74	34	40	-226.77	0.31	18.94	-240.9	-2.87	37.16	-240.66	-2.54	36.65	1.06	-9.26	1.96	1.06	-8.19	1.94	1.00	0.89	0.99	

Table 8.16, Stress resultants (Axial and shear forces in kN) in columns of internal frames in nonlinear SSI and RSSI analysis (discussion in section 8.3.2.2)

Directi on of Frame	Floor	Me m ber No.	(X,Y,Z)			NI Analysis			SSI Analysis			RSSI Analysis			Ratio of SSI/NI			Ratio of RSSI/NI			Ratio of RSSI/SSI		
			X	Y	Z	Axial	Shear- X	Shear Y	Axial	Shear- X	Shear - Y	Axial	Shear- X	Shear - Y	Axial	Shear- X	Shear - Y	Axial	Shear-X	Shear -Y	Axial	Shear- X	Shear -Y
(1)	(2)	(3)	(4)	(5)	(6)	(7)	(8)	(9)	(10)	(11)	(12)	(13)	(14)	(15)	(16)	(18)	(19)	(20)	(21)	(23)	(24)	(25)	(26)
Internal columns	Ground floor	177	64	20	45	929.89	7.74	0.51	951.9	36.87	-11.44	951.41	25.26	-7.16	1.02	4.76	-22.43	1.02	3.26	-14.0	1.00	0.69	0.63
		177	64	24	45	929.89	-7.74	-0.51	951.9	-36.87	11.44	951.44	-25.3	7.16	1.02	4.76	-22.43	1.02	3.26	-14.0	1.00	0.69	0.63
		178	69	20	45	1268.12	-0.36	0.51	1112	23.66	-15.05	1122.78	15.04	-9.32	0.88	-65.7	-29.51	0.89	-41.78	-18.3	1.01	0.64	0.62
		178	69	24	45	1268.12	0.36	-0.51	1112	-23.66	15.05	1122.78	-15	9.32	0.88	-65.7	-29.51	0.89	-41.78	-18.3	1.01	0.64	0.62
		179	74	20	45	1255.19	0.12	0.51	1150	6.49	-16.52	1160.15	3.8	-10.13	0.92	54.1	-32.39	0.92	31.67	-19.9	1.01	0.59	0.61
		179	74	24	45	1255.19	-0.12	-0.51	1150	-6.49	16.52	1160.15	-3.8	10.13	0.92	54.1	-32.39	0.92	31.67	-19.9	1.01	0.59	0.61
	First floor	183	64	24	45	697.44	14.45	0.45	711.2	28	-8.93	711.89	29.1	-8.5	1.02	1.9	-19.84	1.02	2.01	-18.9	1.00	1.04	0.95
		183	64	27	45	-697.44	-14.45	-0.45	-711.2	-28	8.93	-711.89	-29.1	8.5	1.02	1.9	-19.84	1.02	2.01	-18.9	1.00	1.04	0.95
		184	69	24	45	947.68	-0.53	0.45	843.1	15.88	-11.66	845.17	15.28	-11.47	0.89	-30.0	-25.91	0.89	-28.83	-25.5	1.00	0.96	0.98
		184	69	27	45	-947.68	0.53	-0.45	-843.1	-15.88	11.66	-845.17	-15.3	11.47	0.89	-30.0	-25.91	0.89	-28.83	-25.5	1.00	0.96	0.98
		185	74	24	45	940.63	-0.03	0.45	870.3	3.24	-12.61	872.98	3.04	-12.46	0.93	-108.0	-28.02	0.93	-101.33	-27.7	1.00	0.94	0.99
		185	74	27	45	-940.63	0.03	-0.45	-870.3	-3.24	12.61	-872.98	-3.04	12.46	0.93	-108.0	-28.02	0.93	-101.33	-27.7	1.00	0.94	0.99
	Second floor	189	64	27	45	464.91	14.47	-0.87	473.1	30.28	-9.99	473.56	29.57	-9.46	1.02	2.1	11.48	1.02	2.04	10.9	1.00	0.98	0.95
		189	64	31	45	-464.91	-14.47	0.87	-473.1	-30.28	9.99	-473.56	-29.6	9.46	1.02	2.1	11.48	1.02	2.04	10.9	1.00	0.98	0.95
		190	69	27	45	632.87	0.73	-0.87	566.9	17.09	-12.54	568.62	16.38	-12.21	0.90	23.4	14.41	0.90	22.44	14.0	1.00	0.96	0.97
		190	69	31	45	-632.87	-0.73	0.87	-566.9	-17.09	12.54	-568.62	-16.4	12.21	0.90	23.4	14.41	0.90	22.44	14.0	1.00	0.96	0.97
		191	74	27	45	627.76	-0.19	-0.87	583.9	3.57	-13.47	585.75	3.26	-13.17	0.93	-18.8	15.48	0.93	-17.16	15.1	1.00	0.91	0.98
		191	74	31	45	-627.76	0.19	0.87	-583.9	-3.57	13.47	-585.75	-3.26	13.17	0.93	-18.8	15.48	0.93	-17.16	15.1	1.00	0.91	0.98
	Third floor	195	64	31	45	232.38	18.74	-0.24	235.3	36.44	-10.26	235.47	35.79	-9.63	1.01	1.9	42.75	1.01	1.91	40.1	1.00	0.98	0.94
		195	64	34	45	-232.38	-18.74	0.24	-235.3	-36.44	10.26	-235.47	-35.8	9.63	1.01	1.9	42.75	1.01	1.91	40.1	1.00	0.98	0.94
		196	69	31	45	321.65	-0.2	-0.24	294.9	17.09	-13.03	295.55	16.24	-12.58	0.92	-85.5	54.29	0.92	-81.20	52.4	1.00	0.95	0.97
196		69	34	45	-321.65	0.2	0.24	-294.9	-17.09	13.03	-295.55	-16.2	12.58	0.92	-85.5	54.29	0.92	-81.20	52.4	1.00	0.95	0.97	
197		74	31	45	315.86	-0.31	-0.24	299.2	3.51	-14.07	299.95	3.18	-13.66	0.95	-11.3	58.63	0.95	-10.26	56.9	1.00	0.91	0.97	
197		74	34	45	-315.86	0.31	0.24	-299.2	-3.51	14.07	-299.95	-3.18	13.66	0.95	-11.3	58.63	0.95	-10.26	56.9	1.00	0.91	0.97	



Direction of Frame	Floor	Member No.	(X,Y,Z) coordinates of beam nodes			NI Analysis	SSI Analysis	RSSI Analysis	Ratio of SSI/NI	Ratio of RSSI/NI	Ratio of RSSI/SSI
			X	Y	Z						
(1)	(2)	(3)	(4)	(5)	(6)	(7)	(8)	(9)	(10)	(11)	(12)
External frame in X-direction	Ground floor	1	64	23.5	40	43.33	104.45	91.78	2.41	2.12	0.88
		1	69	23.5	40	-68.5	-13	-22.49	0.19	0.33	1.73
		2	69	23.5	40	66.28	71.87	68.24	1.08	1.03	0.95
		2	74	23.5	40	-64.16	-47.59	-51.3	0.74	0.80	1.08
		3	74	23.5	40	64.43	62.33	62.12	0.97	0.96	1.00
	First floor	6	64	27	40	50.51	94.05	91.78	1.86	1.82	0.98
		6	69	27	40	-63.21	-19.51	-22.02	0.31	0.35	1.13
		7	69	27	40	63.65	66.47	65.66	1.04	1.03	0.99
		7	74	27	40	-65.14	-51.32	-52.77	0.79	0.81	1.03
		8	74	27	40	64.72	61.37	61.74	0.95	0.95	1.01
	Second floor	11	64	30.5	40	54.91	99.86	96.93	1.82	1.77	0.97
		11	69	30.5	40	-60.01	-16.4	-19.08	0.27	0.32	1.16
		12	69	30.5	40	61.68	64.94	64.24	1.05	1.04	0.99
		12	74	30.5	40	-65.93	-51.66	-53.09	0.78	0.81	1.03
		13	74	30.5	40	64.9	61.49	61.82	0.95	0.95	1.01
	Third floor	16	64	34	40	35.93	62.81	61.1	1.75	1.70	0.97
		16	69	34	40	-65.52	-36.24	-37.95	0.55	0.58	1.05
		17	69	34	40	64.69	60.87	60.71	0.94	0.94	1.00
17		74	34	40	-65.02	-55.16	-56.2	0.85	0.86	1.02	
18		74	34	40	64.56	60.46	60.89	0.94	0.94	1.01	
Internal frame in X-direction	Ground floor	21	64	23.5	45	43.33	120.07	104.54	2.77	2.41	0.87
		21	69	23.5	45	-68.5	1.04	-9.92	-0.02	0.14	-9.54
		22	69	23.5	45	66.28	72.28	67.51	1.09	1.02	0.93
		22	74	23.5	45	-64.16	-44.23	-48.67	0.69	0.76	1.10
		23	74	23.5	45	64.43	61.87	61.49	0.96	0.95	0.99
	First floor	26	64	27	45	50.51	104.8	103.6	2.07	2.05	0.99
		26	69	27	45	-63.21	-8.55	-10.13	0.14	0.16	1.18
		27	69	27	45	63.65	66.68	65.6	1.05	1.03	0.98
		27	74	27	45	-65.14	-48.41	-49.88	0.74	0.77	1.03
		28	74	27	45	64.72	60.68	61.04	0.94	0.94	1.01
	Second floor	31	64	30.5	45	54.91	110.72	108.58	2.02	1.98	0.98
		31	69	30.5	45	-60.01	-5.74	-7.59	0.10	0.13	1.32
		32	69	30.5	45	61.68	65.23	64.36	1.06	1.04	0.99
		32	74	30.5	45	-65.93	-48.72	-50.15	0.74	0.76	1.03
		33	74	30.5	45	64.9	60.78	61.11	0.94	0.94	1.01
	Third floor	36	64	34	45	35.93	69.27	68.04	1.93	1.89	0.98
		36	69	34	45	-65.52	-29.05	-30.17	0.44	0.46	1.04
		37	69	34	45	64.69	59.59	59.17	0.92	0.91	0.99
37		74	34	45	-65.02	-53.19	-54.23	0.82	0.83	1.02	
38		74	34	45	64.56	59.64	60.07	0.92	0.93	1.01	

Table 8.18 Stress resultants(bending moment about z-axis) in Z-beams in Non-linear SSI and RSSI analysis

Direction of Frame	Floor	Member No.	(X,Y,Z) coordinates of beam nodes			NI Analysis	SSI Analysis	RSSI Analysis	Ratio of SSI/NI	Ratio of RSSI/NI	Ratio of RSSI/SSI
			X	Y	Z						
(1)	(2)	(3)	(4)	(5)	(6)	(7)	(8)	(9)	(10)	(11)	(12)
External frame in Z-direction	Ground floor	81	64	23.5	40	43.37	97.64	85.45	2.25	1.97	0.88
		81	64	23.5	45	-68.28	-17.56	-25.94	0.26	0.38	1.48
		82	64	23.5	45	65.82	55.65	55.76	0.85	0.85	1.00
	First floor	84	64	27	40	50.5	89.41	87.8	1.77	1.74	0.98
		84	64	27	45	-63.37	-21.1	-23.45	0.33	0.37	1.11
		85	64	27	45	64.23	54.29	54.85	0.85	0.85	1.01
	Second floor	87	64	30.5	40	55.04	95.98	93.35	1.74	1.70	0.97
		87	64	30.5	45	-60.29	-17.62	-20.29	0.29	0.34	1.15
		88	64	30.5	45	63.09	53.23	53.87	0.84	0.85	1.01
	Third floor	90	64	34	40	36.29	61.13	59.6	1.68	1.64	0.97
		90	64	34	45	-65.27	-34.7	-36.61	0.53	0.56	1.06
		91	64	34	45	65.14	52.77	53.54	0.81	0.82	1.01
Internal frame in Z-direction	Ground floor	93	69	23.5	40	43.37	114.3	98.56	2.64	2.27	0.86
		93	69	23.5	45	-68.28	-2.45	-12.4	0.04	0.18	5.06
		94	69	23.5	45	65.82	52.59	52.3	0.80	0.79	0.99
	First floor	96	69	27	40	50.5	100.35	99.98	1.99	1.98	1.00
		96	69	27	45	-63.37	-9.14	-10.48	0.14	0.17	1.15
		97	69	27	45	64.23	51.51	51.81	0.80	0.81	1.01
	Second floor	99	69	30.5	40	55.04	107.35	105.48	1.95	1.92	0.98
		99	69	30.5	45	-60.29	-5.79	-7.62	0.10	0.13	1.32
		100	69	30.5	45	63.09	50.5	50.95	0.80	0.81	1.01
	Third floor	102	69	34	40	36.29	67.98	66.94	1.87	1.84	0.98
		102	69	34	45	-65.27	-26.28	-27.6	0.40	0.42	1.05
		103	69	34	45	65.14	49.38	49.9	0.76	0.77	1.01
Internal frame in Z-direction	Ground floor	105	74	23.5	40	43.37	120.67	103.14	2.78	2.38	0.85
		105	74	23.5	45	-68.28	3.09	-7.82	-0.05	0.11	-2.53
		106	74	23.5	45	65.82	51.59	51.2	0.78	0.78	0.99
	First floor	108	74	27	40	50.5	104.23	104.14	2.06	2.06	1.00
		108	74	27	45	-63.37	-4.85	-6.02	0.08	0.09	1.24
		109	74	27	45	64.23	50.51	50.77	0.79	0.79	1.01
	Second floor	111	74	30.5	40	55.04	111.62	109.85	2.03	2.00	0.98
		111	74	30.5	45	-60.29	-1.35	-3.07	0.02	0.05	2.27
		112	74	30.5	45	63.09	49.47	49.9	0.78	0.79	1.01
	Third floor	114	74	34	40	36.29	70.58	69.61	1.94	1.92	0.99
		114	74	34	45	-65.27	-23.08	-24.3	0.35	0.37	1.05
		115	74	34	45	65.14	48.08	48.57	0.74	0.75	1.01

Table 9.18 Stress resultants (moments in kN-m about x and z axes) in columns in non-linear SSI and RSSI analysis

Discussion 8.5.3.4

Direction of Frame	Floor	Member No.	Coordinates of beam nodes			Non-interactive Analysis		SSI Analysis		NSSI Analysis		Ratio of SSI/NI		Ratio of RSSI/NI		Ratio of RSSI/SSI	
			X	Y	Z	My	Mz	My	Mz	My	Mz	My	Mz	My	Mz	My	Mz
(1)	(2)	(3)	(4)	(5)	(6)	(7)	(8)	(9)	(10)	(11)	(12)	(13)	(14)	(15)	(16)	(18)	(19)
External columns	Ground floor	153	64	20	40	9.0	9.2	41.8	45.9	25.4	30.1	4.62	5.0	2.81	3.28	0.61	0.66
		153	64	24	40	17.8	17.9	57.2	61.9	42.3	47.4	3.22	3.5	2.38	2.65	0.74	0.77
		154	69	20	40	9.0	-0.3	53.1	29.8	29.7	18.0	5.88	-93.0	3.28	-56.28	0.56	0.60
		154	69	24	40	17.8	-0.9	70.0	37.5	49.2	25.5	3.94	-40.8	2.77	-27.74	0.70	0.68
		155	74	20	40	9.0	0.2	58.0	8.8	31.5	5.1	6.42	51.5	3.49	29.71	0.54	0.58
		155	74	24	40	17.8	0.3	75.3	10.3	51.8	6.7	4.24	39.7	2.92	25.58	0.69	0.64
	First floor	159	64	24	40	25.6	25.4	40.5	42.6	43.2	44.4	1.58	1.7	1.69	1.75	1.07	1.04
		159	64	27	40	25.3	25.1	43.7	46.1	43.8	45.5	1.73	1.8	1.73	1.81	1.00	0.99
		160	69	24	40	25.6	-1.3	44.3	21.4	49.4	20.3	1.73	-16.4	1.93	-15.58	1.11	0.95
		160	69	27	40	25.3	-0.6	48.8	22.8	49.9	21.1	1.93	-40.0	1.98	-36.95	1.02	0.92
		161	74	24	40	25.6	0.0	45.4	4.4	51.3	4.2	1.77	220.0	2.00	208.5	1.13	0.95
		161	74	27	40	25.3	-0.1	50.5	4.9	52.0	4.4	2.00	-35.1	2.06	-31.29	1.03	0.89
	Second floor	165	64	27	40	25.2	25.4	45.7	48.0	44.1	46.3	1.81	1.9	1.75	1.83	0.96	0.96
		165	64	31	40	25.1	25.3	44.6	47.1	43.3	45.7	1.78	1.9	1.73	1.81	0.97	0.97
		166	69	27	40	25.2	1.0	51.5	24.2	50.1	22.6	2.04	23.9	1.98	22.37	0.97	0.93
		166	69	31	40	25.1	1.6	50.1	24.8	49.1	23.1	2.00	16.0	1.96	14.92	0.98	0.93
		167	74	27	40	25.2	-0.3	53.7	5.1	52.2	4.6	2.13	-17.7	2.07	-15.83	0.97	0.89
		167	74	31	40	25.1	-0.4	52.2	5.1	51.2	4.5	2.08	-13.0	2.04	-11.64	0.98	0.89
	Third floor	171	64	31	40	30.0	29.7	51.4	52.7	50.1	51.3	1.71	1.8	1.67	1.73	0.97	0.97
		171	64	34	40	36.3	35.9	61.2	62.8	59.6	61.1	1.69	1.7	1.64	1.70	0.97	0.97
		172	69	31	40	30.0	0.1	57.2	23.8	56.4	22.0	1.91	198.3	1.88	183.67	0.99	0.93
172		69	34	40	36.3	-0.8	68.0	24.7	66.9	22.8	1.87	-29.7	1.84	-27.43	0.98	0.92	
173		74	31	40	30.0	-0.6	59.5	4.8	58.7	4.2	1.98	-7.4	1.96	-6.55	0.99	0.88	
173		74	34	40	36.3	-0.5	70.6	5.3	69.6	4.7	1.94	-11.5	1.92	-10.20	0.99	0.88	
Internal columns	Ground floor	177	64	20	45	-0.6	9.2	17.2	55.8	9.8	34.3	-30.21	6.1	-17.26	3.74	0.57	0.62
		177	64	24	45	-1.2	17.9	22.8	73.3	15.2	54.1	-18.57	4.1	-12.37	3.02	0.67	0.74
		178	69	20	45	-0.6	-0.3	22.7	36.6	12.7	21.5	-39.77	-114.3	-22.25	-67.13	0.56	0.59
		178	69	24	45	-1.2	-0.9	30.0	46.2	20.0	31.2	-24.40	-50.3	-16.22	-33.87	0.66	0.67
		179	74	20	45	-0.6	0.2	24.9	10.4	13.8	5.7	-43.72	61.4	-24.14	33.35	0.55	0.54
		179	74	24	45	-1.2	0.3	32.9	12.3	21.7	7.6	-26.75	47.2	-17.63	29.27	0.66	0.62
	First floor	183	64	24	45	-1.2	25.4	15.3	46.8	14.6	50.4	-12.51	1.8	-11.98	1.98	0.96	1.08
		183	64	27	45	-0.4	25.1	16.0	51.2	15.1	51.4	-43.2	2.0	-40.8	2.05	0.94	1.00
		184	69	24	45	-1.2	-1.3	20.1	27.1	19.9	26.4	-16.49	-20.8	-16.34	-20.32	0.99	0.98
		184	69	27	45	-0.4	-0.6	20.7	28.5	20.2	27.0	-55.9	-50.0	-54.6	-47.4	0.98	0.95
		185	74	24	45	-1.2	0.0	21.8	5.4	21.7	5.2	-17.85	268.0	-17.78	260.0	1.00	0.97
		185	74	27	45	-0.4	-0.1	22.4	6.0	21.9	5.4	-60.4	-42.8	-59.2	-38.86	0.98	0.91
	Second floor	189	64	27	45	1.2	25.4	17.2	53.6	16.3	52.2	14.11	2.1	13.35	2.06	0.95	0.97
		189	64	31	45	1.8	25.3	17.8	52.4	16.8	51.3	9.72	2.1	9.19	2.03	0.95	0.98
		190	69	27	45	1.2	1.0	21.7	29.6	21.1	28.4	17.76	29.3	17.32	28.15	0.98	0.96
		190	69	31	45	1.8	1.6	22.2	30.2	21.6	28.9	12.14	19.5	11.80	18.66	0.97	0.96
		191	74	27	45	1.2	-0.3	23.3	6.3	22.8	5.7	19.09	-21.6	18.70	-19.72	0.98	0.91
		191	74	31	45	1.8	-0.4	23.9	6.2	23.3	5.7	13.03	-15.9	12.73	-14.59	0.98	0.91
	Third floor	195	64	31	45	1.0	29.7	17.8	58.3	16.8	57.2	18.39	2.0	17.28	1.93	0.94	0.98
		195	64	34	45	-0.1	35.9	18.1	69.3	16.9	68.0	-139.1	1.9	-130.3	1.89	0.94	0.98
		196	69	31	45	1.0	0.1	22.5	29.3	21.7	27.8	23.20	244.0	22.41	232.00	0.97	0.95
196		69	34	45	-0.1	-0.8	23.1	30.5	22.3	29.0	-177.6	-36.8	-171.5	-34.93	0.97	0.95	
197		74	31	45	1.0	-0.6	24.3	5.8	23.5	5.3	25.01	-9.1	24.27	-8.25	0.97	0.90	

## 8.6 Summary

1. Maximum lateral displacements along X and Z directions are reduced by 42% and 45.8% in Linear RSSI analysis when compared to linear SSI analysis. But the vertical displacements are reduced merely by 3.72%. Maximum lateral displacements along X and Z directions are reduced by 14% and 15% in nonlinear RSSI analysis when compared to Nonlinear SSI analysis. But the vertical displacements are reduced merely by 6.2%. As a result of this, the axial forces in beams have increased in ground floor and have reduced in higher floors.
2. The contact pressure on isolated footings follows the same trend as that of vertical displacement. In the longitudinal direction, the contact pressure at various points has increased. However, this increase has been compensated by a corresponding reduction in the contact pressure at various other points along longitudinal sections. This is logical as the total soil reaction offered must be equal to the total applied load on the structure-foundation system. The contact pressure distribution obtained from linear SSI and RSSI analyses follows almost the same trend. However the maximum stresses in linear RSSI analysis seem to reach a common value. The maximum vertical stresses in linear RSSI analysis are 6% more than linear SSI analysis. But the horizontal stresses are reduced by 8.4% and 18.7% in longitudinal and transverse directions respectively. This seems to indicate that aspect ratio building affects lateral components of contact stresses between foundation and soil.
3. In non-linear SSI, the vertical contact pressure of the footings follows the same trend as that of vertical displacement. The vertical pressure at various points is not affected much in non-linear RSSI analysis compared to non-linear SSI. However there is reduction in longitudinal stresses (by 56%) and transverse stresses (by 35%) in non-

linear RSSI analysis compared to non-linear SSI. There is also a change in the pressure bulb below the foundation level. In the horizontal direction, there is a reduction in longitudinal stress at various points in non-linear RSSI analysis when compared to the non-linear SSI analysis. Similarly same trend is observed in transverse direction.

4. Axial forces in X-beams in linear RSSI analysis are found to exceed the axial forces in X-beams in linear SSI analysis only in ground floor where as in higher floors, these values have been found to decrease. Shear forces along X-beams in linear RSSI analysis are lesser in external spans when compared to Shear forces along X-beams in linear SSI analysis.
5. In linear SSI analysis shear forces in columns are 6% to 30% of axial forces. Shear forces in linear RSSI analysis are 3.6% to 24 % of axial forces. Introduction of geogrid reinforcement in soil reduces the shear forces in linear RSSI analysis. However in non-linear SSI analysis, shear forces in columns are 4.24% to 15.5% of axial forces. Introduction of reinforcement in soil reduces the shear forces in SSI analysis. Shear forces in non-linear RSSI analysis are 3.1% to 7.52 % of axial forces.
6. It was found that for the values of  $M_y$  and  $M_z$  of magnitude greater than 25kNm in NI analysis the moments vary from 3.71 to 4.47 and 4.3 to 5.1 times in linear SSI with respect to NI analysis. For the values of  $M_y$  and  $M_z$  of magnitude greater than 25kNm in NI analysis the moments vary from 3.26 to 4.06 and 3.68 to 4.41 in linear RSSI with respect to NI analysis. However provision of reinforcement reduces BM in columns up to 46%.

7. As the bending moments in NI analysis are of lesser magnitude interaction effects are discussed for members where  $M_y$  and  $M_z$  of magnitude greater than 25kNm in NI analysis. The same moments have increased from 1.58 to 2.13 and from 1.7 to 2.1 in non-linear SSI analysis with respect to NI analysis. Where as  $M_y$  and  $M_z$  in nonlinear analysis RSSI varied from 1.64 to 2.07 and 1.7 to 2.06 respectively. However provision of geogrid reinforcement reduces BM in columns up to 46% with respect to nonlinear SSI analysis where as in some cases the same enhanced by 10%.

It has been an established by now that any change in the differential settlement, contact pressure and foundation stiffness results in significant changes in the moments and forces in the superstructure. It can be observed that in RSSI analysis, horizontal displacements and horizontal stresses have reduced compared to SSI analysis as a consequence of which shear forces have reduced in columns. The changes in bending moments in RSSI analysis with respect SSI analysis are again indicating that reinforcement has a considerable influence in sharing the bending moments

## **CHAPTER 9**

### **CONCLUSIONS**

#### **9.1 GENERAL**

In this research work, attempts have been made to study the behaviour of Reinforced soil structures mainly numerically by suitable developed software and by conducting some experimental studies on reinforced soil foundation. The advantages of reinforcing the soil behind the retaining wall, below the foundations and in an MSE wall have been studied. As the interaction between soil and structure is important and plays a major role in the performance of structures, an attempt has also been made to study the SSI and RSSI for 3D space frame structures.

The major conclusions drawn from the present studies may be grouped into five parts as:

- Conclusions on studies on reinforced soil retaining Walls
- Conclusions on studies carried out on MSE wall
- Conclusions on reinforced soil foundation
- Conclusions on SSI and RSSI
- General Conclusions

#### **9.2 CONCLUSIONS ON STUDIES ON RETAINING WALLS**

##### **9.2.1 Linear Analysis of Reinforced Soil Retaining Wall under Point Loads**

The results of the linear analysis of reinforced soil retaining wall under point loads show that the lateral displacements and settlements decrease in case of a reinforced backfill when compared to displacements in unreinforced backfill by 25% and 24% respectively.

The horizontal, vertical and shear stresses are found to reduce from 40% to 75% , 1% to 20%, 10% to 90% in varying percentages in a reinforced soil retaining wall when compared with unreinforced soil retaining wall.

The vertical stresses are found to reduce in varying percentages in Reinforced soil retaining wall when compared with unreinforced soil retaining wall up to a length nearly twice the reinforcement length (2L) from the facing of the retaining wall. Beyond the length of 2L, vertical stresses are found to increase in varying percentages in reinforced soil retaining wall when compared with those in unreinforced wall. Though the range of vertical stresses remain nearly the same for the unreinforced and reinforced soil retaining wall, it is observed that the stress contours vary in their distribution.

The horizontal, vertical and shear strains are found to reduce from 75% to 76% in varying percentages in reinforced soil retaining wall when compared with unreinforced soil retaining wall

The horizontal displacements in unreinforced soil retaining wall are more than reinforced soil retaining wall. They are more by 2% to 33%. Beyond twice the length of reinforcement (8.40m), they are equal at many locations and are found to be less at few locations.

### **9.2.2 Linear analysis of reinforced soil retaining wall under dead loads**

The results of the linear analysis from the developed software under self weight can be summarized as below. It can be observed that for the unreinforced soil retaining wall the horizontal displacements and vertical settlements are found to reduce by 10% and 100% for soil with  $E_s=21\text{MPa}$  and  $E_s=210\text{MPa}$  (Young's modulus) which is incidentally 10% and 100% more than Young's modulus of soil with  $E_s=2.1\text{MPa}$ . But the results are different for Reinforced soil retaining wall.



It can be observed that for the unreinforced soil retaining wall the horizontal, vertical and shear strains are found to reduce by 10% and 100% for soil with  $E_s=21\text{MPa}$  and  $E_s=210\text{MPa}$  (Young's modulus) which is incidentally 10% and 100% more than soil of  $E_s=2.1\text{MPa}$ . But the results are different for Reinforced soil retaining wall

The horizontal, vertical and shear strains in reinforced soil are 95%, 92% and 77% that of unreinforced soil retaining wall for  $E_s=2.1\text{MPa}$  (Table 5.7). The horizontal strains are 95% that of unreinforced soil retaining wall for soils with  $E_s=21\text{MPa}$  and  $E_s=210\text{MPa}$ . The vertical strains are 93% and 95% that of unreinforced soil retaining wall for soils with  $E_s=21\text{MPa}$  and  $210\text{MPa}$  respectively. It is observed the shear strains are 78% and 85% that of unreinforced soil retaining wall for soils with  $E_s=21\text{MPa}$  and  $E_s=210\text{MPa}$ .

The results predicted from the developed software show that that the horizontal stresses in reinforced soil retaining wall reduce from 50% to 90% of those found in unreinforced soil retaining wall for different stiffnesses of soil. It is observed that the horizontal stresses in reinforced soil with the introduction of interface elements show the development of compressive stresses while the unreinforced and reinforced soil with 100% coupling show tensile horizontal stresses. In case of reinforced soil with 100% coupling, the tensile stresses have reduced in comparison with the unreinforced soil.

It is observed that the vertical and shear stresses in reinforced soil retaining wall with 100% coupling are the least when compared with the unreinforced soil wall and reinforced wall with interface elements. The vertical stresses in reinforced soil with the introduction of interface elements show the increase of compressive stresses. The shear stress are found to be maximum for the unreinforced soil retaining wall. It is also observed that the shear stresses in reinforced soil with the introduction of interface elements show a reversal of line of action beyond 3.9m (at the end of reinforcement).

The horizontal displacements and vertical settlements are maximum for unreinforced soil. They are least for the reinforced soil with 100% coupling and the length of the reinforcement is 4.2m (0.7 times the height of wall h).

### **9.3 CONCLUSIONS ON STUDIES CARRIED OUT ON MSE WALL**

- 1) The MSE wall test results, the settlements predicted in an earlier study using REA software and the results obtained from the developed software show that the wall facing does influence the settlements.
- 2) The developed software shows that the wire facing reduces the maximum settlement of soil by 26%
- 3) The experimental observations show that the wire facing reduces the maximum settlement of soil by 13% when compared with the settlements predicted using developed software.
- 4) The settlements predicted in an earlier study (Shivashankar,1991) using REA software show that the wire facing reduces the maximum settlement of soil by 16% in comparison with the settlements predicted using MSE-PRO for the MSE wall without facing.
- 5) The difference in the settlements predicted by developed software and REA can be attributed to the difference in modelling and difference in the constitutive models adopted.
- 6) The experimental results of the MSE wall, show the maximum settlements probably because FEM models are stiff.
- 7) The settlements and displacements obtained from non-linear analysis of the MSE Wall with the steel wire facing are found to be in reasonably good agreement with those of experimental studies.
- 8) The settlements and displacements obtained from non-linear analysis of the MSE Wall with the steel wire facing are found to be in reasonably good agreement with those of experimental studies.
- 9) The linear analysis give results which do not match the field values may be in the form of displacements, stresses or strains. Hence nonlinear analysis is more reliable in predicting the performance of structures.

## **9.4 CONCLUSIONS ON STUDIES CARRIED OUT ON REINFORCED FOUNDATION SOIL**

### **9.4.1 Results of experimental studies on reinforced soil foundation**

In this research, an effort has been made to study the improvement in load carrying capacity and the settlement behaviour of square and circular footings on a reinforced granular bed overlying weak soil using both the geogrids and geotextiles. The test results have also been used to compute the modulus of subgrade reaction of reinforced soil foundation.

### **9.4.2 Effect of Reinforcement on u/b ratio and BCR values**

- Improvement in load carrying capacity was observed to be considerable in reinforced soil over the unreinforced soil for all layers of reinforcement.
- Improvement in load carrying capacity was observed to be considerable in reinforced soil over the unreinforced soil for all types of reinforcement.
- Load carrying capacity of soil below circular footing for 4 layers of geogrids is the maximum for dense sand when used as foundation bed.
- Geosynthetics beyond the effective length (4.0~6.0B) provides negligible benefits as proved by our experiments.
- The least settlement is observed for reinforced dense sand with 4 layers of reinforcement.
- The maximum settlement is observed for unreinforced and reinforced loose sand.

### **9.4.3 Conclusions on determination of modulus of subgrade reaction of reinforced soil foundation “ $k_s$ ”**

- The modulus of subgrade reaction has been enhanced due to the introduction of reinforcement.
- It is observed that the modulus of subgrade reaction is maximum for geogrid of size 0.40m x 0.40m, 4B x 4B under circular footing for four layers.

- It is least for geogrid of size 0.80m x 0.80m, 8B x 8B under circular footing.
- Under circular footing, 4 layers of Geotextiles of both the sizes 0.4mx0.4m, 4B x 4B and 0.8m x 0.8m, 8B x 8B give better results for the modulus of subgrade reaction.

#### **9.4.4 Conclusions on numerical and experimental studies carried out on reinforced soil foundation**

Experimental and numerical studies have been carried out on a two layered reinforced soil foundation (loose sandy soil) in a tank. The studies have been carried out for varying number of reinforcement layers to investigate the effect on settlement and load at failure. The linear and nonlinear analysis of reinforced foundation soil has been done using Drucker-Prager constitutive model.

Following were the conclusions drawn from the study:

- 1) The settlement and the load at failure for the varying number of reinforcement layers was found to be in reasonably good agreement for the developed program and the standard software ANSYS (specially for single layer and 4 layers) where the Nonlinear analysis is being carried out using Drucker Prager models.
- 2) The developed software is working well for linear analysis and non-linear analysis using the Drucker Prager model.
- 3) The settlement obtained from the linear analysis using developed code are least in comparison with those obtained from the experimental studies, nonlinear analysis using developed program.
- 4) The current studies have been carried out for 100% coupling between soil and reinforcement as studies have proved that interface element between reinforcement and soil are irrelevant for vertical loading( Swamy et al.,2011)

The developed program can also be used to plot the stresses and strains in the reinforced soil foundation for different loadings.

## **9.5 CONCLUSIONS ON STUDIES CARRIED OUT ON SSI and RSSI**

In the present study, the response of a structure supported on soil reinforced with geosynthetics is used and its effect is studied. As available in literature, numerical studies have been carried out by using finite element analyses to study the SSI effects of a 3D frame resting on reinforced and unreinforced soil. The responses investigated are displacements, stresses in soil and member end actions in the structural members.

### **9.5.1 Linear Interactive Analysis of Space Frame-Footing -Soil System**

Lateral displacements along X and Z directions are reduced by 42% and 45.8% in RSSI analysis in comparison with SSI analysis. But the vertical displacements are reduced by only 3.72 %.

It can be observed that columns in external frame along grid line 1 carry 42% total loads when compared to columns along line 2 (Fig. 8.2) which carry 58% of total load. Corner columns carry 10%, peripheral columns carry 16% and internal columns carry 22% of total load. In the SSI analysis, external columns in external frame along grid line 1 carry 45% total loads when compared to columns along line 2 which carry 55% of total load. Corner columns carry 12%, peripheral columns carry 16% and internal columns carry 20% of total load. When RSSI is observed at a glance, it is evident that axial forces have reduced marginally by about 2 percent when compared to SSI analysis.

Shear forces in columns in NI analysis are negligible (1.2% to 8.3%) of axial forces carried by columns. However in SSI analysis, shear forces in columns are 6% to 30% of axial forces. Introduction of reinforcement in soil reduces the shear forces in SSI analysis. Shear forces in RSSI analysis are 3.6% to 24 % of the corresponding axial forces.

Bending moments along X and Z beams are found to be least in NI analysis. They are found to be maximum in SSI analysis. They are found to be around 70 to 80% of those values found in SSI analysis.

The contact pressure below the footing follows the same trend as that of vertical displacement. In the longitudinal direction, the contact pressure at various points has increased. However, this increase has been compensated by a corresponding reduction in the contact pressure at various points along longitudinal sections. This is logical as the total soil reaction offered must be equal to the total applied load on the structure-foundation system. The contact pressure distribution obtained on the basis of both the analysis follows almost the same trend, however the maximum stresses in RSSI analysis seem to reach a common value.

In NI analysis, axial forces in members are more in **extreme** storeys with respect to internal storeys. The shear force is maximum at the support next to end support of end span followed by shear force in interior spans and end support.

In SSI analysis, axial forces are increased by many folds with respect to NI analysis especially in top storeys. The shear forces are maximum at end support followed by shear forces on internal side of support next to end support and shear forces at interior spans. The trends of axial forces and shear forces in RSSI analysis are same as SSI analysis but are found to have lesser differential values between two ends of a member.

### **9.5.2 Non-Linear Interactive Analysis of Space Frame-Footing -Soil System**

Lateral displacements along X and Z directions are reduced by 14% and 15% in RSSI analysis with respect to nonlinear SSI analysis. But the vertical displacements are reduced by only 6.2%.

In non-linear SSI analysis, the vertical contact pressure of the footings follows the same trend as that of vertical displacement. The vertical pressure at various points are not affected much in non-linear RSSI analysis compared to non-linear SSI. However there is reduction in longitudinal stresses by 56% and transverse stresses by 35% in

non-linear RSSI analysis compared to non-linear SSI. There is also a change in the pressure bulb below foundation level. In the horizontal direction, there is a reduction in longitudinal stress at various points in non-linear RSSI analysis when compared to the non-linear SSI analysis which is exactly reverse of the trend in linear analyses. Similarly same trend is observed in transverse direction.

In nonlinear SSI analysis external columns in external frame along grid line 1 carry 45.43 % total loads when compared to columns along line 2 which carry 55.56 % of total load. Corner columns carry 12.32 %, peripheral columns carry 38.4% and internal columns carry 49.27 % of total load. Axial forces in RSSI have reduced marginally by about 2 percent when compared to SSI analysis. Shear forces in columns in NI analysis are negligible (1.2% to 8.3%) of axial forces carried by columns. However in non-linear SSI analysis shear forces in column are 4.24% to 15.5% of axial forces. Introduction of reinforcement in soil reduces the shear forces in SSI analysis. Shear forces in non-linear RSSI analysis are 3.1% to 15.2 % of axial forces.

Bending moments in X-beams in nonlinear SSI analysis are varying from 0.1 to 2.77 times bending moments in NI analysis. Corresponding to these limits the ratios of bending moments in RSSI analysis to SSI analysis vary from 1.32 to 0.87. Bending moments in X-beams in RSSI analysis vary from 0.13 to 2.41 times bending moments in NI analysis. Bending moments in Z-beams from SSI analysis are varying from -0.05 to 2.78 times bending moments in NI analysis. Corresponding to these limits the ratio bending moments in RSSI analysis to SSI analysis vary from 2.27 to 0.85. Bending moments in X-beams in RSSI analysis vary from 0.04 to 2.38 times bending moments in NI analysis

## **9.6 GENERAL CONCLUSIONS**

- 1) The performance of all reinforced soil structures in comparison with the unreinforced soil structures improves under different loading conditions with

respect to horizontal and vertical displacements and for all types of stresses and strains.

- 2) The inclusion of reinforcement in a retaining wall reduces the maximum shear stresses in the backfill with an increase in the vertical stresses and horizontal stresses at few locations.
- 3) The reinforcement is found to influence the redistribution of stresses and is found to reduce displacements, in particular the horizontal displacements.
- 4) The wall facing in an MSE wall influences its performance with respect to its displacement.
- 5) The reinforced soil foundation performs very well in comparison with unreinforced soil foundation. However the improvement in Bearing capacity, bearing capacity ratio (BCR) and modulus of subgrade reaction of soil depends upon the size, the type and number of reinforcement layers. The BCR is maximum for the top layer spacing / width of footing ratio of 0.4. The effective length of reinforcement is 4 to 6 times the width of footing in Reinforced soil foundation. The geogrid and geotextile of lesser size (0.4m x 0.4m) shows better results than that of bigger size (0.8 x 0.8m). This may be due to the fact that the presence of geosynthetics beyond the stress isobars may not be effective.
- 6) Nonlinear analysis of reinforced soil structures provides results which agree reasonably well with the experimental results and published data when compared with the linear analysis. Non-linear analysis for all types of structures predicts displacements which are close to the field values.
- 7) The Goodman's interface element used along with the Drucker Prager constitutive model is found to reverse the direction of horizontal stresses obtained in the unreinforced soil when compared with those obtained in reinforced soil as observed in the reinforced soil retaining wall.
- 8) The interface elements are found to enhance the vertical compressive stresses obtained in the unreinforced soil when compared with those of reinforced soil. The interface elements are found to reverse the direction of shear stresses obtained in the unreinforced soil when compared with those of reinforced soil as observed in the reinforced soil retaining wall



- 9) It can be observed that in linear RSSI analysis, horizontal displacements and horizontal stresses have reduced compared to linear SSI analysis as a consequence of which shear forces have reduced in columns. At the same time, axial forces in beams have increased in ground floor and have reduced in higher floors.
- 10) It has been well established by now that any change in the differential settlement, contact pressure and foundation stiffness results in significant changes in the moments and forces in the superstructure. However the changes in bending moments in linear RSSI analysis with respect linear SSI analysis are again indicating that reinforcement has a considerable influence in sharing the bending moments.
- 11) In non-linear SSI, the vertical contact pressure of the footings follows the same trend as that of vertical displacement. The vertical pressure at various points are not affected much in non-linear RSSI analysis compared to non-linear SSI. However there is reduction in longitudinal and transverse stresses in non-linear RSSI analysis compared to non-linear SSI. There is change in the pressure bulb below foundation level.
- 12) In the horizontal direction, there is a decrease in longitudinal stress at various points in non-linear RSSI analysis when compared to the non-linear SSI analysis which is exactly reverse of the trend in linear analyses. Similarly, the same trend is observed in transverse direction.
- 13) It can be observed from Non-linear analysis that the reinforcement reduces axial forces of X-beams. But Shear Forces in beams is unaffected with the provision of reinforcement.
- 14) It can be observed from Non-linear analysis, that reinforcement does not have much effect on axial forces of Z-beams. Shear force reduces by -6% to 11% depending on the location of beams
- 15) Effect of SSI is reduced in nonlinear analysis. When compared to linear analysis reinforcement in soil improves in normalising values of bending moments of X-beams.
- 16) As per Non-linear analysis, provision of reinforcement reduces Bending moment in columns by 7% to 17%.

- 17) The developed software works well for all unreinforced and reinforced soil structures for different cases of study and linear and nonlinear constitutive relations.
- 18) The developed software works well for SSI and RSSI.

## 9.7 SCOPE OF FUTURE WORK

- 1) The studies can be extended further by using a different interface element.
- 2) Model scale experiments can be carried out on RSSI studies.
- 3) RSSI studies can be conducted for dynamic analysis too.

## APPENDIX

c Program on Retaining Wall

```

IMPLICIT REAL*8(A-H,O-Z)
DIMENSION X(4200),Y(4200),NCODE(6000,8)
DIMENSION NP(6000,8)
DIMENSION MAT(4000,2),ND(8)
DIMENSION SSK(7066400),Elstif(8,8),p(6000),eldisp(8)
DIMENSION STRESS(6000,2,2,3),stressn(6000,4,3)
DIMENSION strain(6000,2,2,3),strainn(6000,4,3)
DIMENSION Xdisp(8000),ydisp(8000)
DIMENSION snode(6000,3),stnode(6000,3)
INTEGER CHT(8000),NDS(8000),ETYPE,nndro,nndco
integer NEL(5),NDE(5),DOFN(5),ndofe(5),nelro(5),nelco(5)
dimension ppr(5),eeE(5),barstress(400) ,ym(10000)

OPEN(UNIT=8,FILE='twall13.in')
OPEN(UNIT=10,FILE='telement13.dat')

OPEN(UNIT=22,FILE='tdisp13.dat')
OPEN(UNIT=15,FILE='tstress13.dat')
C read NEL-nor of elements,NDE-nodes per element, DOFN-degree of freedom
C per node,PR-poissons ratio,E-youngs modulus
  Read(8,*)etype,GDOFN,TNEL,nndro,nndco,h
  Write(*,*)'types of elements,global dofn,total nor of elements'
  Write(*,*)'number of nodes in a row, nor of nodes in column'
  Write(*,*)'height of wall'
  Write(*,*)etype,gdofn,TNEL,nndro,nndco,h
  DO 51 i=1,etype
  READ(8,*)NEL(i),NDE(i),DOFN(i),Ppr(i),eeE(i),nelro(i),nelco(i)
  Write(*,*)'NEL,NDE,DOFN,PR,E,nor of ele in row and in column'
  Write(*,*)'NEL(i),NDE(i),DOFN(i),pPR(i),eeE(i),nelro(i),nelco(i)
c NDOFE-nor of dergrees of freedom per element
  NDOFE(i)=NDE(i)*DOFN(i)
  Write(*,*)'element type',I,' number of dof per element',ndofe(i)
51  CONTINUE

c loop 6 generates number of global node point(element,element nodewise).loop
c variable k gives maximum nodal number.NP() gives global node number.
  write(*,*)'hai raaaaaaaaaaam'

  do 6 i=1,etype
  write(*,*)'I,nel(i),nelro(i)'
  write(*,*)'I,nel(i),nelro(i)
  inelro=1
  tnelro=1
  DO 6 inel=1,NEL(I)
  If(i.eq.1) then
61  NP(inel,1)=(inelro-1)*nndro+tnelro
  NP(inel,2)=(inelro-1)*nndro+tnelro+1
  NP(inel,3)=inelro*nndro+tnelro+1
  NP(inel,4)=inelro*nndro+tnelro
  Write(15,*)'inel=',inel,(NP(Inel,J),j=1,4)
c here if statement will change perticular num of elements as ym=0.00000005
  if ((inelro.gt.11).and.(tnelro.le.41)) then
  ym(inel)=0.00000005

```

```

else
ym(inel)=eee(i)
endif
tnelro=tnelro+1

if (tnelro.gt.nelro(i)) then
inelro=inelro+1
tnelro=1
endif
tnel=inel
endif

if(i.eq.2) then
tnel=nel(i-1)+inel
62  NP(tnel,1)=(inelro)*nndro+tnelro
   NP(tnel,2)=(inelro)*nndro+tnelro+1
write(15,*)'inel=',inel,(NP(tnel,J),j=1,2)
write(*,*)i,inel,tnel,inelro,tnelro,nelro(i)
write(*,*)i,inel,tnel,inelro,tnelro,nelro(i)

c*****
   if ((inelro.gt.11).and.(tnelro.le.41)) then
   ym(tnel)=0.00000005
   else
   ym(tnel)=eee(i)
   write(19,*)i,ym(tnel)
   endif

c*****
   tnelro=tnelro+1
   if (tnelro.gt.nelro(i)) then
   inelro=inelro+1
   tnelro=1
   endif
   tnel=tnel+inel
   endif

6   continue
c   Write(*,*)k='
c   Read(*,*)k
   If(ttnel.ne.tnel) then
   Write(*,*)'discrepancy in number of members fed'
   Endif

c loop 5 reads cartisian co-ord of each node local or global coordinates

   write(*,*)'hoizontal grid and vertical grid'
   read(*,*)dx,dy
   write(*,*)'node number  ,x-cord  ,y coord'
   k=nndro*nndco
   write(*,*)'nndro,nndco'
   do 515 ik=1,k
   x(ik)=0.0
   y(ik)=0.0
515  continue
   write(15,*)'inndco,inndro,ik,X(ik),Y(ik)'

```

```

        ddy=0.0
    do 55 inndco=1,nndco
        ddx=0.0
        do 5 inndro=1,nndro
c         if(inndro.lt.21)dx=0.3
c         if(inndco.gt.4)dy=0.25
c         if(inndro.lt.32)dx=0.3
c         if(inndco.gt.4)dy=0.25
c         if((inndco.gt.5).and.(inndro.lt.32))dx=0.3
c         if((inndco.gt.4).and.(inndro.lt.32))dy=0.25
c         if((inndro.gt.5).and.(inndco.lt.32))dx=0.3
c         if((inndco.gt.4).and.(inndro.lt.32))dy=0.25
c         if((inndco.gt.5).and.(inndro.lt.32))dx=0.3
c         if(inndco.gt.4)dy=0.25
c         if(inndco.gt.5)dx=0.3

```

```

c*****
*****

```

```

c here 3-if statements will change the grid as 0.3x0.3m upto depth of 3m and length of 9m
        if(inndco.gt.8)dy=0.3
        if(inndro.lt.30)dx=0.3
c         if(inndro.gt.30)dx=1
        ik=(inndco-1)*nndro+inndro
        x(ik)=ddx
        y(ik)=ddy
        write(15,*)inndco,inndro,ik,X(ik),Y(ik)
        ddx=x(ik)+dx
    5    continue
    55   ddy=y(ik)+dy

```

C global node number NP(element,no deof element)

c

```

*****
*****

```

```

***** C   DO 16 INEL=1,NEL
C 16 write(*,*)(NP(INEL,J),J=1,NDE)
c loop 21 initializes values of MAT(K,DOFN) to 1 where K is the max global node number
        DO 21 I=1,K
        DO 21 J=1, GDOFN
    21   MAT(I,J)=1
        DO 26 I=1,K
    26   write(*,*)(MAT(I,J),J=1,GDOFN)
c read NVFIX-the number of nodes which are suppressed,NNN-their global node
c number and MAT (NNN,J) is made zero for j=1,3
c WRITE(*,*)'GIVE THE NUMBER OF NODES WHERE SUPPRESSED'
c read(8,*)NFIX
c DO 31 I=1,NFIX
c WRITE(*,*)'GIVE THE NODE and dof to be suppressed'
c 31   read(8,*)NNN,mat(nnn,1),mat(nnn,2)
        do 31 i=1,nndro
            j=i*nndro
            if(j.le.k) then
                mat(j,1)=0.0
                mat(j,2)=0.0
            endif

```

```

      mat(i,2)=0.0
c      mat(i,1)=0.0

31  continue
      DO 36 I=1,K
36  write(*,*)(mat(I,J),J=1,GDOFN)

```

C Loop 38 and 39 gives MAT(nodewise,degree of freedom perNodewise)=globaldegree  
c of freedom for each active node. the loopvariable KOUNT gives max value of  
c global degree of freedom. Loop 46 writes the same.

```

      KOUNT=0
      write(*,*)'i j KOUNT'
      DO 38 I=1,K
      DO 39 J=1, GDOFN
      IF(MAT(I,J).NE.0) THEN
      KOUNT=KOUNT+1
      MAT(I,J)=KOUNT
      ENDIF
      write(*,*)i ,j,KOUNT
39  continue
38  continue
      HNODE=K

```

C NCODE gives global degree of freedom number for every element and local degree  
c-of freedom ie.,basically relates local dof of each element with global dof

```

c      write(*,*)'hoizontal grid and vertical grid'
c      read(*,*)dx,dy
c      k=nndro*nndco
      Write(22,*)'DOF (SYSTEM) NODE-WISE'
      write(22,*)'*****'
      write(22,*)'node no (MAT(I,J),J=1,GDOFN) X(i) Y(i)'
      DO 46 I=1,K

```

```

46  write(22,*)i,(MAT(I,J),J=1,GDOFN),X(i),Y(i)
      itnel=0

```

c\*\*\*\*\*

```

      write(22,*)'DOF (SYSTEM)ELEMENT-WISE'
      DO 666 I=1, ETYPE
      DO 66 INEL=1,NEL(I)
      if(i.ne.1) then
      itnel=nel(i-1)+inel
      else
      itnel=inel
      endif
      DO 66 J=1,NDE(I)
      DO 66 KK=1, dofN (I)
      LL=(J-1)*DOFN(I)+KK

```

C gobal dof (element,local dof)=MAT(global node number,dof of each node)

C gobal dof (1 TO NEL,1 TO 24)=MAT(1 TO MAX global node number, 1 to DOFN)

```

c      write(*,*)itnel,np(itnel,j)
      NCODE(itnel,LL)=MAT(NP(itnel,J),kK)
      write(22,*)'NCODE(,itnel,"ll,)',ncode(ITNEL,ll)
66  continue

```

```

itnell=nel(ii)

666 continue
C*****end of loop 666*****
    NEQ=KOUNT
    Write(*,*)'HIGHEST DOF-NNO of EQUATIONS',NEQ
    pause
    DO 50 I=1,NEQ
    NDS(I)=0

50    CHT (I)=0

c loop 100 is executed for every element.ND(local dof of an element)=global dof
c*****beginning of loop 100*****
    DO 100 J=1, ETYPE
    write(*,*)'*****'
    DO 100 INEL = 1, NEL(j)
    write(*,*)'etype=',j, 'nel(type)=' ,nel(J), 'inel=',inel
    if(j.gt.1) then
    iii=nel(j-1)+inel
    else
    iii=inel
    endif
    write(*,*)'nor of element= ',III
    DO 120 I=1,NDOFE(j)
120    ND(I)=NCODE(III,I)
        ndofpe=ndofe(j)
        CALL COLUMH(CHT, ND,NDOFPE,NEQ)
c hoow to pass ndofe verify in subroutine
c SUBROUTINE COLUMH (CHT, ND, NED,NEQ)
100 CONTINUE

c*****end of loop 100*****
    write (*,*)' COLUMN HEIGHTS'
    write(*,*) (CHT (I), I=1, NEQ)
    NEQ1=NEQ+1
    pause
c to find diagonal address of global stiffness matrix
    CALL CADNUM (CHT, NDS, NEQ, NEQ1, NSKY)
    write(*,*)'NSKY',NSKY
c stop
    DO 110 I=1,NSKY
110    SSK (I)=0.0
        write(*,*)' DIAGONAL ADDRESSES'
        write(77,*) (NDS (I), I=1, NEQ)
        pause
        write(*,*)' ASSEMBLED MATRIX IN SKYLINE FORM'
C*****Combination of trial 1.f and sub 2.d.f ***** STARTING OF LOOP200

c*****
    DO 200 j=1, ETYPE
    DO 200 INEL=1, NEL(J)
    write(*,*)j=',j',' ','inel=',inel
    if(J.GT.1) then
    iii=nel (J-1)+inel
    else
    iii=inel

```

```

endif
write(15,*)'nor of element= ', III
DO 220 I=1, NDOFE(j)
220 ND(I)=NCODE(III,I)
Write(*,*)'j mew iii nd'
e=ym(iii)
emew=ppr(j)
Write(*,*)j,mew,iii,(nd(i),i=1,ndofe(j))
call bstif(j,elstif,x,y,e,emew,np,III)
do 1122 ii=1, NDOFE(j)
do 1122 jj=1, ndofe(j)
WRITE(15,*)'In main----elstif(",jj,)=',ii,jj,elstif(ii,jj)
c elstif(ii,jj)=jj
c write(15,*)'elstif=',ii,jj,elstif(ii,jj)
c write(18,*)iii,ym(iii)
1122 continue
NED=NDOFE(J)
write(77,*)NDOFE(J)
CALL PASSEM (SSK,ELSTIF,NDS,ND,NED,NEQ1,NSKY)
C SUBROUTINE PASSEM(SE,EK,NDS,ND,NED,NEQ1,NSKY)
c CALL PASSEM(GLOBAL STIFFNESS MATRIX(NSKY),ELEMENT STIFFNESS MATRIX)
C NDS-DIAGONAL ADDRESS,GLOBAL DOF OF EACH LOCAL
DOF,NEQ1=NEQ+1,
C NOR OF ELEMENTS IN SSK
200 CONTINUE

```

C\*\*\*\*\*END OF LOOP 200\*\*\*\*\*

```

2234 format(1x,i2,1x,12(f5.1,1x))
Write(*,*)'SSK'
DO 12345 I =1, NSKY
12345 write (*,*)I, SSK(I)
Do 250 I=1,NEQ
250 P(I) = 0.0
WRITE(*,*)'NEQ',NEQ
c DO 251 JI =1223,1229
c Kount=mat(ji,2)
c if(kount.eq.2344)p(2344)=-57000
c if(kount.eq.2356)p(2356)=-57000
c write(14,*)ji,kount,p(kount)
c 251 CONTINUE
p(mat(3080,2))=-57000
p(mat(3092,2))=-57000
Write(*,*)k=',k
c*****self
weight*****
c do 252 ji=68,1273
c kount=mat(ji,2)
c if(kount.eq.68)p(kount)=-27000
c if((kount.ge.70).and.(kount.le.126))p(kount)=-54000
c if(kount.eq.128)p(kount)=-117000
c if((kount.ge.130).and.(kount.le.198))p(kount)=-180000
c if(kount.eq.200)p(kount)=-24300
c if((kount.ge.202).and.(kount.le.258))p(kount)=-48600
c if(kount.eq.260)p(kount)=-105300
c if((kount.ge.262).and.(kount.le.330))p(kount)=-162000

```



c if(kount.eq.332)p(kount)=-21600  
c if((kount.ge.334).and.(kount.le.390))p(kount)=-43200  
c if(kount.eq.392)p(kount)=-93600  
c if((kount.ge.394).and.(kount.le.462))p(kount)=-144000  
  
c if((kount.ge.484).and.(kount.le.522))p(kount)=-37800  
c if(kount.eq.524)p(kount)=-81900  
c if((kount.ge.526).and.(kount.le.594))p(kount)=-126000  
  
c if((kount.ge.616).and.(kount.le.654))p(kount)=-32400  
c if(kount.eq.656)p(kount)=-70200  
c if((kount.ge.658).and.(kount.le.726))p(kount)=-108000  
  
c if((kount.ge.748).and.(kount.le.786))p(kount)=-27000  
c if(kount.eq.788)p(kount)=-58500  
c if((kount.ge.790).and.(kount.le.858))p(kount)=-90000  
  
c if((kount.ge.880).and.(kount.le.918))p(kount)=-21600  
c if(kount.eq.920)p(kount)=-46800  
c if((kount.ge.922).and.(kount.le.990))p(kount)=-72000  
  
c if((kount.ge.1012).and.(kount.le.1050))p(kount)=-16200  
c if(kount.eq.1052)p(kount)=-35100  
c if((kount.ge.1054).and.(kount.le.1122))p(kount)=-54000  
  
c if((kount.ge.1144).and.(kount.le.1182))p(kount)=-14580  
c if(kount.eq.1184)p(kount)=-31590.0  
c if((kount.ge.1186).and.(kount.le.1254))p(kount)=-48600  
  
c if((kount.ge.1276).and.(kount.le.1314))p(kount)=-12960  
c if(kount.eq.1316)p(kount)=-28080.0  
c if((kount.ge.1318).and.(kount.le.1386))p(kount)=-43200  
  
c if((kount.ge.1408).and.(kount.le.1446))p(kount)=-11340  
c if(kount.eq.1448)p(kount)=-24570.0  
c if((kount.ge.1450).and.(kount.le.1518))p(kount)=-37800  
  
c if((kount.ge.1540).and.(kount.le.1578))p(kount)=-9720  
c if(kount.eq.1580)p(kount)=-21060.0  
c if((kount.ge.1582).and.(kount.le.1650))p(kount)=-32400  
  
c if((kount.ge.1672).and.(kount.le.1710))p(kount)=-8100  
c if(kount.eq.1712)p(kount)=-17550.0  
c if((kount.ge.1714).and.(kount.le.1782))p(kount)=-27000  
  
c if((kount.ge.1804).and.(kount.le.1842))p(kount)=-6480  
c if(kount.eq.1844)p(kount)=-14040.0  
c if((kount.ge.1846).and.(kount.le.1914))p(kount)=-21600  
  
c if((kount.ge.1936).and.(kount.le.1974))p(kount)=-4860  
c if(kount.eq.1976)p(kount)=-10530.0  
c if((kount.ge.1978).and.(kount.le.2046))p(kount)=-16200  
  
c if((kount.ge.2068).and.(kount.le.2106))p(kount)=-3240  
c if(kount.eq.2108)p(kount)=-7020.0  
c if((kount.ge.2110).and.(kount.le.2178))p(kount)=-10800

```

c
c      if((kount.ge.2200).and.(kount.le.2238))p(kount)=-1620
c      if(kount.eq.2240)p(kount)=-3510.0
c      if((kount.ge.2242).and.(kount.le.2310))p(kount)=-5400
c      write(20,*)ji,kount,p(kount)
c 252  continue
c*****self weight*****
c      do 1145 ii=1,neq
c 1145  write(22,*)(p(ii),';ii=1,neq)
        write(*,*)'verify load vector'

        write(*,*)' DIAOGAONAL ASEM STIFF MAT',neq

c      write(22,*)'SSK(NDS(I)) p(i)'
c      do 10034 I=1,NEQ
c10034  write(22,*)SSK(NDS(I)),p(i)

c      DO 5234 i=1,neq
c5234  write(*,*)I,p(i),neq,neql,nsky
        inde=0
ccccccccccccccccccccccccccccccccccccccccccccccccccccccccpre processing ends
        call PASOLV(SSK,P,NDS,Neq,NEQ1,NSKY,inde)
ccccccccccccccccccccccccccccccccccccccccccccccccccccccccpost processing starts
        write(*,*)'dlp inde',inde
        write(*,*)'inde',inde
        if (inde.eq.1)stop
        write(*,*) 'gdof disp'
c      DO 1234 i=1, neq
c1234  write(22,*)'dlp',i,p(i)
        Write(*,*)j,ym,mew,iii,ndopfe'
        do 11112 j=1,Etype
        Do 11112 INEL=1, NEL(J)
        if(J.GT.1) then
        iii=nel(J-1)+inel
        else
        iii=inel
        endif
        ndopfe=ndofe(j)
        do 11113 i=1,ndopfe
        eldisp(i)=0.0
        if(ncode(iii,i).ne.0.0) then
        eldisp(i)=p(ncode(iii,i))
        endif
c      write(22,*)'element ', at displacement ',i', = ', eldisp(i)
11113  continue
        e=ym(iii)
        Emew=ppr(j)
c      Write(*,*)j,mew,iii,ndopfe
        write(51,*)'iii ixx iyy (stress(iii,ixx,iyy,kkk) kkk=1,3)'
        write(52,*)'iii ixx iyy (strain(iii,ixx,iyy,kkk) kkk=1,3)'
        call ELESTRESS(j,iii,nodopfe,eldisp,stress,x,y,e,emew,np,
1  barstress,strain)
        do 11231 ixx=1,2
        do 11231 iyy=1,2
        if(j.eq.1)then
        write(51,*)'iii,ixx,iyy,(stress(iii,ixx,iyy,kkk),kkk=1,3)
        write(52,*)'iii,ixx,iyy,(strain(iii,ixx,iyy,kkk),kkk=1,3)

```

```

endif
11231 continue
c*****new loop starts
ixx=0
do 1228 ix=1,2
do 1228 iy=1,2
ixx=ixx+1
c nodeii=NP(III,ixx)
do 1229 i=1,3
stressn(iii,ixx,i)=stress(iii,ix,iy,i)
strainn(iii,ixx,i)=strain(iii,ix,iy,i)
1229 continue
1228 continue
write(65,*)'III,NP(III,ixx),eldisp(i1),eldisp(i2)'
do 1999 ixx=1,4
nodei=Np(III,ixx)
i1=(ixx-1)*2+1
i2=(ixx-1)*2+2
write(65,*)III,NP(III,ixx),eldisp(i1),eldisp(i2)
do 1999 jj=1,3
snode(nodei,jj)=snode(nodei,jj)+stressn(iii,ixx,jj)
stnode(nodei,jj)=stnode(nodei,jj)+strainn(iii,ixx,jj)
1999 continue
11112 continue
c*****ends
Write(*,*)k=',k
Write(22,*)'iiii,x(III),y(III),xdisp(III),ydisp(III)'
do 999 iii=1,k
xdisp(iiii)=0.0
ydisp(iiii)=0.0
999 continue
Write(*,*) 'bol baba',k
do 9999 iii=1,k
xdisp(iiii)=p(mat(iiii,1))
ydisp(iiii)=p(mat(iiii,2))
if (iiii.eq.100)pause
9999 write (22,*)iiii,x(III),y(III),xdisp(III),ydisp(III)
c*****new loop starts
c this loop 2000 will caculate the avg values of stresses strains at each node points
write(99,*)'nodei,X(nodei),Y(nodei),Xdisp(nodei),Y disp(nodei),(snode(nodei,jj),jj=1,3),(stnode(nod
ei,jj),jj=1,3)'
do 2000 inndco=1,nndco
do 2000 inndro=1,nndro
nodei=(inndco-1)*nndro+iinndro
c write(21,*)nodei,(snode(nodei,jj),jj=1,3),(stnode(nodei,jj),jj=1,3)
if((inndco.eq.1).and((inndro.gt.1).and((inndro.lt.nndro))))then
c if(nodei.eq.1)then
c write(*,*)'loop no191'
c pause
c endif
do 191 jj=1,3
snode(nodei,jj)=snode(nodei,jj)/2
stnode(nodei,jj)=stnode(nodei,jj)/2
191 continue
endif
if((inndco.eq.nndco).and((inndro.gt.1).and((inndro.lt.nndro))))then
c if(nodei.eq.1)then

```

```

c      write(*,*)'loop no192'
c      pause
c      endif
      do 192 jj=1,3
      snode(nodei,jj)=snode(nodei,jj)/2
      stnode(nodei,jj)=stnode(nodei,jj)/2
192    continue
      endif
      if((inndro.eq.1).and.((inndco.gt.1).and.(inndco.lt.nndco)))then
c      if(nodei.eq.1)then
c      write(*,*)'loop no193'
c      pause
c      endif
      do 193 jj=1,3
      snode(nodei,jj)=snode(nodei,jj)/2
      stnode(nodei,jj)=stnode(nodei,jj)/2
193    continue
      endif
      if((inndro.eq.nndro).and.((inndco.gt.1).and.(inndco.lt.nndco)))then
c      if(nodei.eq.1)then
c      write(*,*)'loop no194'
c      pause
c      endif
      do 194 jj=1,3
      snode(nodei,jj)=snode(nodei,jj)/2
      stnode(nodei,jj)=stnode(nodei,jj)/2
194    continue
      endif
      if(((inndro.gt.1).and.(inndro.lt.nndro)).and.((inndco.gt.1).and.(inndco.lt.nndco))) then
c      if(nodei.eq.1)then
c      write(*,*)'loop no195'
c      pause
c      endif
      do 195 jj=1,3
      snode(nodei,jj)=snode(nodei,jj)/4
      stnode(nodei,jj)=stnode(nodei,jj)/4
195    continue
      endif
2000   continue
      k=nndro*nndco
      do 625 nodei=1,k
      write(99,*)nodei,X(nodei),Y(nodei),Xdisp(nodei),Ydisp(nodei),
1      (snode(nodei,jj),jj=1,3),(stnode(nodei,jj),jj=1,3)
      write(98,*)nodei,(snode(nodei,jj),jj=1,3)
      write(97,*)nodei,(stnode(nodei,jj),jj=1,3)
      625 write(96,*)nodei,X(nodei),Y(nodei),Xdisp(nodei),Ydisp(nodei)
c*****
***c
c $ stresses & strains before taking average $
c      write(88,*)'ik,X(ik),Y(ik),Xdisp(ik),ydisp(ik),(snode(ik,jj),jj=1,3),(stnode(ik,jj),jj=1,3)'
c      do 4 inndco=1,nndco
c      do 4 inndro=1,nndro
c      ik=(inndco-1)*nndro+inndro
c      write(88,*)ik,' ',X(ik),Y(ik),' ',Xdisp(ik),' ',ydisp(ik),
c 1      (snode(ik,jj),jj=1,3),(stnode(ik,jj),jj=1,3)
c4    continue
      close(8)

```

```

        close(10)
        CLOSE(15)
        CLOSE(22)
        Stop
        END
c*****
***c
c    CALL COLUMH(CHT,ND,NDOFE(etype),NEQ)
        SUBROUTINE COLUMH(CHT,ND,NED,NEQ)
c    ND(local dof of an element)=global dof, NED =24

        INTEGER CHT(NEQ),ND(NED)
c    write(15,*)'subroutine COLUMH STARTS

        LS=100000
c    write(15,*)'ND(K) VALUES'
c    WRITE(15,*)ND(K),K=1,NED)
c    write(15,*)'loop 30 results'
        DO 30 K=1, NED

            IF(ND(K))30,30,10
10         IF(ND(K)-LS)20,30,30
20         LS=ND(K)

30         CONTINUE

c    write(15,*)'loop 40 results'
        DO 40 K=1,NED
            II=ND(K)
            IF(II.EQ.0) GOTO 40
            ME=II-LS
            IF (ME.GT. CHT(II))CHT(II)=ME
c    write(15,*)'K,II,ME,CHT(II)'
c    write(15,*)K,II,ME,CHT(II)
40         CONTINUE
            RETURN
        END
c*****C
c    CALL CADNUM(CHT,NDS,NEQ,NEQ1,NSKY)
        SUBROUTINE CADNUM(CHT,NDS,NEQ,NEQ1,NSKY)
        INTEGER CHT (NEQ), NDS(NEQ1)
c    WRITE(15,*)'SUBROUTINE CADNUM STARTS'
        DO 10 I=1, NEQ+1
10         NDS(I)=0
            NDS(1)=1
            NDS(2)=2
            DO 20 I=2,NEQ
20         NDS(I+1)=NDS(I)+CHT(I)+1
c    write(15,*)'CHT (NEQ)'
c    write(15,*)CHT (NEQ)
            NSKY=NDS(NEQ)+CHT(NEQ)
            RETURN
        END
c*****C
c    call bstif(elstif,x,e,pr,np,III)
c    call bstif(j,elstif,x,y,ym,emew,np,III)

```

```

subroutine bstif(ietype,ek,xL,yL,e,pr,np,III)
IMPLICIT double precision(A-H,O-Z)
dimension ek(8,8),c(3,3),xL(4),yL(4),r(4),s(4),ekk(8,8)
dimension xjaci(2,2),sfdg(2,4),sf(4),b(3,8),xjac(2,2)
dimension db(3,8),gp(2),wg(2),sfd(2,4),np(6000,8)
DIMENSION XYZ(4,2),COF(2,2),ANS(2,2)
integer ietype
data wg/1.D0,1.D0/
data gp/-0.5773502691896,0.5773502691896/
data r/-1.D0,1.D0,1.D0,-1.D0/
data s/-1.D0,-1.D0,1.D0,1.D0/

c      pr=0
c      e=2000
c      t=20
c      xL(1)=0
c      xL(2)=40
c      xL(3)=40
c      xL(4)=0
c      yL(1)=0
c      yL(2)=0
c      yL(3)=30
c      yL(4)=30
C      INTIALIZE STIFFNESS AND STABLITY MATRIX

      write(10,*)'starting of subroutine bstif'
      write(10,*)'*****'
      write(10,*)'ietype=',ietype,'element number=',iii
      write(*,*)'pr=',pr,'e=',e
      do 20 i= 1,8
      do 20 j= 1,8
20      ek(i,j)=0.0
      If(ietype.eq.1)then
      do 21 i=1,3
      do 21 j=1,3
C      INTIALIZE STIFFNESS AND STABILITY MATRIX
21      c(i,j)=0.0
      EE=E/(1+PR)/(1-2*PR)
      Write(10,*)'ee',ee
      C(1,1)=(1.0-PR)*EE
      C(1,2)=pr*EE
      C(1,3)=0.0
      C(2,1)=pr*EE
      C(2,2)=(1.0-PR)*EE
      C(3,3)=(1.0-2.0*PR)/2.0*EE
      Write(10,*)'constitute matrix'

C      compute the ss-matrix
C      ENTER THE LOOP FOR INTEGRATION
      Do 51 i=1,4
51      write (10,211)r(i),s(i)
211  format(f4.1,2x,f4.1,2x,f8.6,2x,f8.6)

      do 170 ix=1,2
      do 170 iy=1,2
C      CALUCALATE SHAPE FUNCTIONS AND THEIR DERVATIVES
      Write(10,*)'Gauss points',GP(IX),GP(IY)

```

```

do 50 i=1,4
aa=(1.0+r(i)*gp(ix))
bb = (1.0+s(i)*gp(iy))
sf(i)=0.25*aa*bb
sfd(1,i)=0.25*bb*r(i)
sfd(2,i)=0.25*aa*s(i)
50  continue

Write(10,*)'sfd mat'
do 1871 i=1,4
1871 write(10,*) (sfd(j,i),j=1,2)

WRITE(10,*)'NP(III,I)  XL  YL'
DO 10011 I=1,4

XYZ(I, 1)=XL(NP(III,I))
XYZ(I,2)=YL(NP(III,I))
10011 WRITE(10,*)NP(III,I),XYZ(I,1),XYZ(I,2)

DO 22211 I=1,2
DO 22211 J=1,2
XJAC(I,J)=0.0
DO 22211 K=1,4
22211 XJAC(I,J)=XJAC(I,J)+SFD(I,K)*XYZ(K,J)

WRITE(10,*)' JAC MAT'
DO 1223 J=1,3
WRITE(10,*)(XJAC(J,I),I=1,3)

1223  CONTINUE

cof(1,1)=xjac(2,2)
cof(1,2)=-xjac(2,1)
cof(2,1)=-xjac(1,2)
cof(2,2)=xjac(1,1)

dj=xjac(1,1)*xjac(2,2)-xjac(1,2)*xjac(2,1)

write(10,*)'dj', dj
do 2001 i=1,2
do 2001 j=1,2
2001  XJACI(i,j)=cof(j,i)/dj

WRITE(10,*)' INVERSE JAC MAT'
DO 1103 J=1,2
WRITE(10,*)(XJACI(J,I),I=1,2)
1103  CONTINUE

c*****To prove that|J|*|J|Inverse is unity*****
do 1001 i=1,2
do 1001 j=1,2
ans(i,j)=0.0
do 1001 k=1,2
1001  ans(i,j)=ans(i,j)+xjaci(i,k)*xjac(k,j)
Write(10,*)'unit mat'

```

```

do 1002 i=1,2
1002 write(10,*)(ans(i,j),j=1,2)

c*****c

do 80 i =1,2
do 80 j = 1,4

80 sfdg(i,j) =0.0

do 90 i =1,2
do 90 j = 1,4
do 90 k=1,2

90 sfdg(i,j)=sfdg(i,j)+xjaci(i,k)*sfd(k,j)
write(10,*)'sfdg mat'
do 1872 i=1,4
1872 write(10,*)(sfdg(j,i),j=1,2)

do 100 i =1,3
do 100 j =1,8

100 b(i,j)=0.0

do 110 i =1,4
k1 = 2*(i-1)+1
k2 = k1+1
k3 = k2+1
b(1,k1) = sfdg(1,i)
b(2,k2) = sfdg(2,i)
b(3,k1) = sfdg(2,i)
b(3,k2) = sfdg(1,i)

110 continue

write (10,*)' constitute matrix'
do 1091 i =1,3
1091 write(10,*)( c(i,j),j=1,3)
Write(10,*)'B MATRIX'
do 116 i = 1,3

116 write(10,*)(b(i,j),j=1,8)

do 120 i = 1,3
do 120 j = 1,8
db(i,j) = 0.0
do 120 k = 1,3

120 db(i,j) = db(i,j)+c(i,k)*b(k,j)

do 122 i = 1,8
do 122 j = 1,8
ekk (i,j) =0.0
do 122 k = 1,3

122 ekk(i,j)=ekk(i,j)+b(k,i)*db(k,j)*dj*1.0
do 175 i=1,8

```



```

do 175 j = 1,8

175  ek(i,j)=ek(i,j)+ekk(i,j)
    Write(10,*)'element stiffness matrix'
do 2117 i =1,8
2117  write(10,*)(ekk(i,j),j=1,8)
170  continue

write(10,*)'final element stiffness matrix'
do 1117 i =1,8
1117  write(10,*)(ek(i,j),j=1,8)
    else
    ek(1,1)=.025*e/1
    ek(1,3)=-ek(1,1)
    ek(3,1)=-ek(1,1)
    ek(3,3)=ek(1,1)
    write(18,*)'iii,e'
    endif
    return
    end
c*****
*****C
SUBROUTINE ELESTRESS(ietype,III,ndopfe,eldisp,stress,xl,yl,e,
1 pr,np,barstress,strain)
IMPLICIT real*8(A-H, O-Z)
dimension c(3,3),xl(4),yl(4),r(4),s(4),STRESS(6000,2,2,3)
dimension xjaci(2,2),sfdg(2,4),sf(4),b(3,8),xjac(2,2)
dimension db(3,8),gp(2),wg(2),sfd(2,4),np(6000,8)
DIMENSION strain(6000,2,2,3)
DIMENSION XYZ(4,2), COF(2,2),ans(2,2),ELDISP(8),barstress(400)
Integer ietype
data wg/1.D0,1.D0/
data gp/-0.5773502691896,0.5773502691896/
data r/-1.D0,1.D0,1.D0,-1.D0/
data s/-1.D0,-1.D0,1.D0,1.D0/

c pr=0.25
c e=2000
c eldisp(1)=0.2
c eldisp(2)=0.3
c eldisp(3)=0.5
c eldisp(4)=0.6
c eldisp(5)=0.4
c eldisp(6)=0.3
c eldisp(7)=0.2
c eldisp(8)=0.7

C INITIALIZE STIFFNESS AND STABILITY MATRIX

if(ietype.eq.1)then
do 21 i= 1,3
do 21 j = 1,3
C INITIALIZE STIFFNESS AND STABILITY MATRIX
21 c(i,j) = 0.0
EE=E/(1+PR)/(1-2*PR)
C(1,1)=(1.0-PR)*EE
C(1,2)=pr*EE

```

```

C(1,3)=0.0
C(2,1)=pr*EE
C(2,2)=(1.0-PR)*EE
C(3,3)=(1.0-2.0*PR)/2.0*EE
C    COMPUTE THE SS - MATRIX

C    ENTER THE LOOP FOR INTEGRATION
211  format(f4.1,2x,f4.1,2x,f8.6,2x,f8.6)

do 170 ix =1,2
do 170 iy =1,2
C    CALUCALATE SHAPE FUNCTIONS AND THEIR DERVATIVES
do 50 i=1,4
aa = (1.0+r(i)*gp(ix))
bb = (1.0 + s(i)*gp(iy))
sf(i) = 0.25*aa*bb
sfd(1,i) = 0.25*bb*r(i)
sfd(2,i) = 0.25*aa*s(i)
50  continue

DO 10011 I=1,4
XYZ(I,1)=XL(NP(III,I))
XYZ(I,2)=YL(NP(III,I))
10011 continue

DO 22211 I=1,2
DO 22211 J=1,2
XJAC(I,J)=0.0
DO 22211 K=1,4
22211  XJAC(I,J)=XJAC(I,J)+SFD(I,K)*XYZ(K,J)

cof(1,1)=xjac(2,2)
cof(1,2)=-xjac(2,1)
cof(2,1)=-xjac(1,2)
cof(2,2)=xjac(1,1)

dj=xjac(1,1)*xjac(2,2)-xjac(1,2)*xjac(2,1)

do 2001 i=1,2
do 2001 j=1,2
2001  XJACI(i,j)=cof(j,i)/dj

c*****To Prove that |J|*|J|Inverse is unity*****
do 1001 i=1,2
do 1001 j=1,2
ans(i,j)=0.0
do 1001 k=1,2
1001  ans(i,j)=ans(i,j)+xjaci(i,k)*xjac(k,j)

c*****
do 80 i = 1,2
do 80 j = 1, 4
80  sfdg(i,j)=0.0

do 90 i = 1,2

```

```

do 90 j = 1,4
do 90 k = 1,2
90  sfdg(i,j) = sfdg(i,j)+xjaci(i,k)*sfd(k,j)

do 100 i =1,3
do 100 j =1,8
100  b(i,j)=0.0

do 110 i =1,4
k1 = 2*(i-1)+1
k2 = k1 +1
k3 = k2+1
b(1,k1) = sfdg(1,i)
b(2,k2) = sfdg(2,i)
b(3,k1) = sfdg(2,i)
b(3,k2) = sfdg(1,i)

110  continue
c*****c
c  write (12,*)' constitute matrix'
c  do 1091 i =1,3
c1091 write(12,*)( c(i,j),j=1,3)
write(12,*)'B matrix'
do 116 i=1,3
116  write(12,*)(b(i,j),j=1,8)

do 120 i =1,3
do 120 j = 1,8
db(i,j) = 0.0
do 120 k = 1,3
120  db(i,j) = db(i,j)+c(i,k)*b(k,j)
do 122 i = 1,3
stress(iii,ix,iy,i)=0.0
do 122 k = 1,8
122  stress(iii,IX,IY,I)=STRESS(III,IX,IY,I)+db(I,K)*ELDISP(K)
c*****c new loop
starts
do 123 i=1,3
strain(iii,ix,iy,i)=0.0
do 123 k=1,8
123  strain(iii,IX,IY,I)=STRAIN(III,IX,IY,I)+b(i,k)*ELDISP(K)

c*****c ends
170 CONTINUE
else
write(15,*)'element,height from base, barstress,barstrain'
l=xl(np(iii,1))-xl(np(iii,2))
barstress(iii)=(eldisp(3)-eldisp(1))*e/l
barstrain=barstress(iii)/e
write(15,*)iii,yl(np(iii,1)),barstress(iii),barstrain
ENDIF
return
end

c*****c

```

SUBROUTINE PASSEM (SK,EK,NDS,ND,NED,NEQ1,NSKY)

```

c      CALL PASSEM (SSK,ELSTIF,NDS,ND,NED,NEQ1,NSKY)

c      CALL PASSEM(GLOBAL STIFFNES MATRIX(NSKY),ELEMENT STIFFNESS MATRIX,
C      NDS-DIAGONAL ADDRESS,ND-GLOBAL DOF OF EACH LOCAL
DOF,NED-NOR OF DOF PER ELEMENT
C      NEQ1=NEQ+1,NOR OF ELEMENTS IS SSK)
      IMPLICIT REAL*8(A-H,O-Z)
c      double precision SK(nsky),EK(ned,ned)
      INTEGER NDS (NEQ1),ND (NED)
      Double precision ek(8,8),sk(44256)

      WRITE(15,*)'NED=',NED

c      DO 69 I=1,NED
c 69   WRITE(15,*)'In Passem-----elstif)=',(ek(I,J),J=1,NED)
c      WRITE(15,*)'I=NED J=NED II=ND(I) JJ=ND(J) MI=NDS(JJ) IJ=JJ-II KK=MI+IJ EK(I,J)
SK(KK)'

      DO 70 I=1,NED
C DO FOR ALL DEREES OF FREEDOM OF ELEMENT - NED IN MAIN PROGRAM IS NDOFE
      II=ND(I)
      IF(II)70,70,30
30   CONTINUE
      DO 60 J=1, NED
      JJ=ND(J)
C CORRESPONDING GLOBAL DOF OF J
      IF(JJ)60,60,40
40   CONTINUE
      MI=NDS(JJ)
c      CORRESPONDING DIAGONAL ADDRESS OF GLOBAL DOF
      IJ=JJ-II
      IF(IJ)60,50,50
50   KK=MI+IJ
      SK(KK)=SK(KK)+EK(I,J)
c      WRITE(15,16)I,J,II,JJ,MI,IJ,KK,EK(I,J),SK(KK)
C 16   format(4i6,3i1 1,2f10.1)
60   CONTINUE
70   CONTINUE
      RETURN
      END
c*****c
c   call PASOLV(SSK,P,NDS,Neq,NEQ1,NSKY,inde)
      SUBROUTINE PASOLV(SK,P,NDS,NN,NEQ1,NSKY,inde)
      Implicit double precision(a-h,o-z)
      DIMENSION SK(NSKY),P(NN),NDS(NEQ1)
c      WRITE(15,*)' N KN KL KU KH K KLT KI ND K'
      DO 140 N=1,NN
      KN=ndS(N)
      KL=KN+1
      KU=ndS(N+1)-1
      KH=KU-KL
      IF(KH) 110,90,50
50   K=N-KH
      IC=0
      KLT=KU
      DO 80 J=1,KH

```

```

        IC=IC+1
        KLT=KLT-1
        KI=ndS(K)
        nd=ndS(K+1)-KI-1
        IF(nd)80,80,60
60      KK=MIN0(IC,nd)
        C=0.0
        DO 70 L=1,KK
70      C=C+SK(KI+L)*SK(KLT+L)
        SK(KLT)=SK(KLT)-C
80      K=K+1
90      K=N
        B=0.0
        DO 100 KK=KL,KU
        K=K-1
        KI=ndS(K)
        C=SK(KK)/SK(KI)
        B=B+C*SK(KK)
100     SK(KK)=C
        SK(KN)=SK(KN)-B
        IF(SK(KN))120,120,140
c      WRITE(15,223)N,KN,KL,KU,KH,K,KLT,KI,ND,K,SK(KN)
223    FORMAT(10I4,e20.12,' ',e20.12)
110    if(sk(kn) .gt. -0.0000000001) goto 140
        Write(15,*)'N,KN,SK(KN)'
120    WRITE(*,222)N,KN,SK(KN)
        inde=1
        return
        STOP

140    CONTINUE

C      RETURN
C      REDUCE RIGHT HandSIDELOADVECTOR
150    DO 180 N=1,NN
        KL=ndS(N)+1
        KU=ndS(N+1)-1
        IF(KU-KL)180,160,160
160    K=N
        C=0.0
        DO 170 KK=KL,KU
        K=K-1
170    C=C+SK(KK)*P(K)
        P(N)=P(N)-C
180    CONTINUE
C      BACK SUBSTITUTION
        DO 200 N=1,NN
        K=ndS(N)
200    P(N)=P(N)/SK(K)
        IF(NN.EQ.1)RETURN

        N=NN
        DO 230 L=2,NN
        KL=ndS(N)+1
        KU=ndS(N+1)-1
        IF(KU-KL)230, 210, 210
210    K=N

```

```
DO 220 KK=KL,KU
  K=K-1
220 P(K)=P(K)-SK(KK)*P(N)
230 N=N-1
  RETURN
222 FORMAT(//20X,'STOP-STIFFNESS MATRIX NOT POSITIVE DEFINITE'
1 , 'NONPOSITIVE PIVOT FOR EQUATION',I4, //110X, 'PIVOT=',E20.12)
  END
```

## REFERENCES

- Abu-Farsakh M., Chen Q., Sharma R (2013). "An experimental evaluation of the behavior of footings on geosynthetic-reinforced sand." *Soil Found.* 2013; 53(2):335–348.
- Adams, M. T. and Collin, J. G. (1997). "Large model spread footing load tests on geosynthetic reinforced soil foundations." *Journal of Geotechnical and Geoenvironmental Engineering*, ASCE, Vol. 123, No.1, 66-72.
- Agrawal, R. and Hora, M.S. (2012). "Nonlinear interaction behaviour of plane frame-layered soil system subjected to seismic loading". *Int. J. Struct. Eng. Mech.*, 11(6), 2012, 711-734.
- Akinmusuru, J. O. and Akinbolade, J.A. (1981). "Stability of loaded footing on reinforced soil." *Journal of Geotechnical Engineering*, ASCE, Vol. 107, No.6, 819-827.
- Bassett, R.H. and Last, N.C. (1978). "Reinforcing earth below footing and embankments." *Symposium on Earth Reinforcement*, ASCE, Pittsburgh. 202-231.
- Bauer, G.E. and Halim, A. O. A. E. (1989). "The deformation and stress responses and stability analysis of reinforced soil structures". *Computer and Physical Modelling in Geotechnical Engineering*, Balkema, Rotterdam, 13 - 24.
- Bergado, D. T., Chai, J. C. and Miura, N. (1995). "FE analysis of grid reinforced embankment system on soft Bangkok clay". *Computers and Geotechnics*, Vol. 17, 447 - 471.
- Bennis, M. and DeBuhan, P. (2003). "A multiphase constitutive model of reinforced soils accounting for soil-inclusion interaction behaviour Mathematical and Computer Modelling, 37, 469–475.
- Binquet, J., Lee, K.L. (1975a)." Bearing capacity tests on reinforced earth slabs.". *J. Geotech.Eng.Div.101 (GT12)*, 1241–1255.
- Binquet, J., Lee, K.L. (1975b)."Bearing capacity analysis on reinforced earth slabs.". *J. Geotech. Eng. Div.101 (GT12)*, 1257–1276.
- Biot, M. A. (1937), "Bending of Infinite Beams on an Elastic Foundation." *Journal of Applied Mechanics Trans AmSoc. Mech. Eng.*, Vol. 59, 1937, A1-A7. (After Wael N. Abd Elsamee, 2013. "An Experimental Study on the Effect of Foundation Depth, Size and Shape on Subgrade Reaction of Cohesionless Soil", *Engineering*, 2013, 5, 785-795)
- Bhattacharya, K. Dutta, S.C. and Roy, R.(2006). " Seismic design aids for buildings incorporating soil-flexibility effect." *J. Asian Archit. Build.*, 5(2), 341-348.
- Bonaparte, R. and Schmertmann, G.R. (1987). "Reinforcement Extensibility in Reinforced Soil Wall Design." *The Application of Polymeric Reinforcement in Soil Retaining Structures*, 409–457.

Brocklehurst, C.J. (1993). "Finite Element Studies of Reinforced and Unreinforced two-layer soil systems." *PhD Thesis*, Wolfson College, Oxford University

Cai, Y.X. , Gould P.L, Desai C.S. (2005). "Nonlinear analysis of 3D seismic interaction of soil–pile–structure." *Systems and application Engineering Structures* 22 191–199

Chang, J.C., Hannon, J.B. and Forsyth, R.A (1977). " Pullout resistance and interaction of earthwork reinforcement and soil." *Transportation Research Record* 640. National Research Council, Washington, DC, pp 1–7

Chang, D.T.-T., Wey, W. T. and Chen, T.C. (1993). "Study on Geotextiles Behaviors of Tensile Strength and Pull-out Capacity under Confined Condition." *Geosynthetics'93*, pp 607-618.

Chen, W.F. and Mizuno, E. (1990). "Non-linear analysis in Soil Mechanics- Theory and implementation". Elsevier Science Publisher B.V., U.S.A.

Chen, Q.M. (2007). "An Experimental Study on Characteristics and Behavior of Reinforced Soil Foundation." PhD dissertation, Louisiana State University, Baton Rouge, L.A.

Chew, S. H. and Schmertmann, G. R. (1990). "Reinforced soil deformations by finite element method". *Performance of Reinforced Soil Structures, British Geotechnical Society*, 35 - 40.

Christopher, B.R., Gill, S.A., Juran, I., Mitchell, J.K. (1990). *Reinforced Soil Structures, Vol. 1, Design and Construction Guidelines*, FHWA-RD-89-043

Coon, M.D. and Evans, R.J. (1971). "Recoverable Deformation of Cohesionless Soils." *J. of Soil. Mech.Found.div. ASCE*, 93 97(2), 375-391.

Das, B.M., Shin, E.C. and Omar, M.T. (1994). "The bearing capacity of surface strip foundations on geogrid reinforced sand and clay – a comparative study." *Geotechnical and Geological Engineering*, Vol. 12, No. 1, 1-14.

Dan M. Ghiocel, and Roger G. Ghanem (2002)." Stochastic Finite-Element Analysis of Seismic Soil–Structure Interaction. " *Journal of Engineering Mechanics*, Vol. 128, No. 1, January 1, 2002. ©ASCE, ISSN 0733-9399/2002/1-66

Desai, C.S., Phan, H.V. and Perumpral, J.V. "Mechanics of three-dimensional soil-structure interaction." *J. Eng. Mech.,ASCE*, 108(5), 1982, 731-747.

Desai, C. S. and Abel, L. F. (1987)." Introduction to the finite element method for engineering analysis." CBS publishers, New Delhi, India.

Desai, C.S, El-Hoseiny K.E. (2005). "Prediction of field behavior of reinforced soil wall using advanced constitutive model." *Journal of Geotech Geoenviron Eng* 131(6):729–739.



- Ding, D. and Hargrove, S. (2006). "Nonlinear Stress-Strain Relationship of Soil Reinforced with Flexible Geofibers." *Journal Geotech. Geoenviron. Eng.*, 132(6), 791–794.
- Drucker, D.C. and Prager, W. (1952). "Soil Mechanics and Plastic Analysis or limit Design." *Appl.Meth.* 10(2), 157-165.
- Duncan, J.M. and Seed, R.B. (1986). "Compaction-induced Earth Pressures under Ko Conditions." *ASCE Journal of Geotechnical Engineering*, Vol. 112, No. GT1, 1-22
- Duncan, J. M. and Chang, C.Y. (1970). "Nonlinear analysis of stress and strain in soil." *ASCE Journal of Soil Mechanics and Foundations Division*, Vol. 96, 1629 - 1653.
- Duncan, J.M. and Chang, C.Y. (1972). "Nonlinear analysis of stress and strain in soils." *J. Soil Mech. Found. Eng. Div. ASCE*, 96(5), 1972, 1629-1653.
- Elsamny, M. K., Elsedek, M. B. and Elsamee, W. N. Abd (2010), "Effect of 'Es' for Cohesionless Soil." *Civil Engineering Researches Magazine of Al-Azhar University*. Vol. 32, No. 3,938. (After Wael N. Abd Elsamee, 2013. "An Experimental Study on the Effect of Foundation Depth, Size and Shape on Subgrade Reaction of Cohesionless Soil", *Engineering*,5, 785-795)
- Egyptian Code,( 2001),"Soil Mechanics and Foundation," Organization, Cairo.
- Filz, G.M. and Duncan, J. M. (1997), "Vertical shear loads on nonmoving walls I: Theory.", *ASCE Journal of Geotechnical and Geoenvironmental Engineering Division*, Vol. 123, No. 9, September, 1997, 856 - 862.
- Fragaszy, J.R., and Lawton, E. (1984). "Bearing Capacity of Reinforced Sand Subgrades." *ASCE Journal of Geotechnical Engineering*, Vol. 110, No.10, 1984, 1500-1507.
- Fukuda, H. & Chou, T. W. (1982). "A probabilistic theory of the strength of short-fibre composites with variable fibre length and orientation." *J. Muter. Sci.*, 17, 1003-1011.
- Gabr, M.A., Dodson, R., and Collin, J.G. (1998). "A study of stress distribution in geogrid-reinforced sand." In: *Proceedings of Geosynthetics in Foundation Reinforcement and Erosion Control Systems.* ASCE Geotechnical Special Publication no. 76, Reston, Va., pp 62–76.
- Ghaboussi, J., Wilson, E. L. and Isenberg, J. (1973). "Finite element for rock joints and interfaces." *ASCE Journal of Soil Mechanics and Foundations Division*, Vol. 99, No. SM10, pp 833 - 848.
- Goldscheider, M. (1984) "True triaxial tests on dense sands". In: G. Gudehus, F.Darve, I. Vardoulakis; editors. *Constitutive relations for soils*. Balkema, Rotterdam.
- Goodman, R. E., Taylor, R. L., and Brekke, T. L.(1968). "A model for the mechanics of jointed rock." *ASCE Journal of Soil Mechanics and Foundations Division*, 99(SM3),637-659.

Gurung, N. (2000). "A Theoretical Model for Anchored Geosynthetics in Pull-Out Tests", *Geosynthetics International*, Vol. 7, No. 3, pp. 269-284.

Gu, Jie. (2011). "Computational modelling of geogrid reinforced soil foundation and geogrid reinforced base in flexible pavement" (2011). *LSU Doctoral Dissertations*. 1920. [http://digitalcommons.lsu.edu/gradschool\\_dissertations/1920](http://digitalcommons.lsu.edu/gradschool_dissertations/1920)

Hirai, T., Konami, T., Yokata, Y., Utani Y., Ogata, K. (2003). Case histories of earth reinforcement technique in Japan. In: Proceedings of the International Symposium on Earth Reinforcement, IS-Kyushu 2003, A.A. Balkema, Fukuoka, Kyushu, Japan, pp. 1009–1020.

Huang, E.E. (1992). "Report on Three Unsuccessful Reinforced Walls", Recent Case Histories of Permanent Geosynthetic-Reinforced Soil Retaining Walls, Tatsuoka, and Leshchinsky, D., Eds., Balkema 1994, Proceedings of the symposium Tokyo, Japan, pp. 219-222.

Hausmann, M.R. (1976). "Strength of Reinforced Soil." *Australian Road Research Board Proceedings*, (8), Session 13, 1-8.

Hermann, L.R.(1978), "Finite element analysis of contact problems", *Journal of Engineering Mechanics*, ASCE, 104(5): 1043-1059,1978

Hokmabadi A.S., Fatahi B., Samali B. (2013) "Seismic Response of Superstructure on Soft Soil Considering Soil-Pile-Structure Interaction." Proceedings of the 18th International Conference on Soil Mechanics and Geotechnical Engineering, Paris

Hora, M.(2006). Nonlinear interaction analysis of infilled building frame-soil system, *J. Struct. Eng.*, 33(4), 309-318.

Huang, C. C. and Tatsuoka, F. (1990). "Bearing capacity reinforced horizontal sandy ground." *Geotextiles and Geomembranes*, Vol. 9, 51-82.

Iancu, B. T. and Ionut, O. T. (2009). "Numerical Analyses of Plate Loading Test Numerical Analyses of Plate Loading Test." *Buletinul Institutului Politehnic Din IASI Publicat de Universitatea Tehnică, Gheorghe Asachi.* Tomul LV (LIX), Fasc. 1, Sectia Construct II. Arhitectură (Iancu- Bogdan Teodoru and Ionut-Ovidiu Toma),57-65. (After Wael, N. Abd Elsamee (2013). "An Experimental Study on the Effect of Foundation Depth, Size and Shape on Subgrade Reaction of Cohesionless Soil." *Engineering*, 5, 785-795.)

Ingold, T.S. (1982). "Mechanics and concept. Reinforced earth." Chapter 2 London. Thomas Telford, 4-32.

"IRC 006: Standard Specifications and Code of Practice for Road Bridges, Section II – Loads and Stresses (Fourth Revision)"

Jayasree, P. K. and Beena, K.S. (2008). "Performance of Gabion Faced Reinforced Earth Retaining Walls." PhD. Thesis submitted to Cochin University of Science and Technology

Jayamohan, J. and Shivashankar, R. (2012), "Some Studies on Prestressed Reinforced Granular Beds Overlying Weak Soil." *ISRN Civil Engineering*, vol. 2012, Article ID 436327, 13 pages, 2012.

Juran, I., and Schlosser, F. (1978). "Theoretical Analysis of Failure in Reinforced Earth Structures." *Proceedings, ASCE Symposium on Earth Reinforcement*, Pittsburgh, pp528-555.

Jianchao, Li. and Victor N. Kaliakin. (1993). "Numerical study of interface elements: Applications to reinforced soil structures". *Civil engineering report*, University of Delaware, Newark, DE.

Jiang, Yan. Jie Han, Robert L. P.E., Parsons, P.E., Hongyi Cai. (2015), "Field Instrumentation and Evaluation of Modular-Block MSE Walls with Secondary Geogrid Layers ", Report No. KS-15-09, FINAL REPORT, December 2015, The University of Kansas

Jones, C. J. F. P. *Earth Reinforcement and Soil Structures*. Butterworths, London, England (1988).

Kalpna Maheshwari, Desai, A. K. and Solanki, C. H. (2011). "Application and Modelling of fiber reinforced soil." *Proceedings of Indian Geotechnical Conference*, Kochi (paper No H-362)

Karim, Md. Rezaul and Saiful, Alam Siddiquee Md. (2009)." Improvement of bearing capacity of strip footing on sand by using metal strip reinforcement." *Journal of Civil Engineering (IEB)*, 37 (2) pp165-177.

Karpurapu, R. and Bathurst, J. (1992), "Numerical Investigation of Controlled Yielding of Soil-Retaining Wall Structures." *Geotextiles and Geomembranes*, Vol. 11, pp 115 – 131

Khing, K.H., Das, B.M., Puri, V.K., Cook, E.E., and Yen, S.C. (1993). "The bearing capacity of a strip foundation on geogrid-reinforced sand." *Geotextiles and Geomembranes*, 12(4), pp 351-361.

King, G.J.W. and Chandrashekharan, V.S., (1974a),"An Assesment of the effects of interaction between a structure and its foundation", *Proc. Conf. on Settlement of Structures, British Geotechnical Soc.* Cambridge, pp 368-383

King, G.J.W. (1977)," An Introduction to Superstructure/Raft/ Soil Interaction", *Proc. Int.Symp. on Soil Structure Interaction*, Roorkee, India, Vol. I, pp. 453-466.

King, G.J.W. and Yao, Z.E. (1983),"Simplified Interactive Analysis of Long Framed Building on raft Foundation", *Jnl. Structural Engineer*, Vol.61, B(3)pp.62-67.

Kishan, D., Dindorkar, N., Srivastava, R. Ankesh Shrivastava.(2016), *Analysis & Design Of 44 Meter M.S.E. (Mechanically Stabilized Earth) Wall By Using Plaxis 8.2*,

Kolay, P K., Kumar, S. and Tiwari, D. (2013). "Improvement of Bearing Capacity of Shallow Foundation on Geogrid Reinforced Silty Clay and Sand", Hindawi Publishing Corporation Journal of Construction Engineering (Volume 2013, Article ID 293809, 10 pages)

Kondner, R. L. (1963), "Hyperbolic stress - strain response: Cohesive soils." *Journal of Soil Mechanics and Foundations Division*, Vol. 89. No. SM 1. 115-143.

Krishnamoorthy, (1995) "Studies on Hypoeleasticity", PhD Thesis, Dept of Applied Mechanics, KREC, Suratkal

Krishnamoorthy C. S. (1995) "Finite Element Analysis: Theory and Programming". Tata McGraw-Hill Education, 1995 - 710 pages.

Krishnamoorthy and Rao, N.B.S. (2001). "Prediction of stress strain behaviour of soil using hypoeleasticity constitutive model." *Indian Geotechnical journal*, 31(3), 2001.

Kumar A.,Saran S. (2003). "Bearing Capacity of rectangular footing on reinforced soil." *Geotechnical and Geological Engineering* 21, pp 201-224.

Kumar, A., Walia, B.J.S.H., and Saran, S. (2005), "Pressure-settlement characteristics of rectangular footings on reinforced sand", *Geotechnical and Geological Engineering* 23: pp 469-481 Springer 2005

Kumar, A., Singh, D.P. and Bajaj, V. (2008). "Strengthening of soil by randomly distributed fiber inclusions." *Journal of Indian Highways*, Vol. 36, No. 8, 21-26

Kutanis, M. and Elmas, M. (2001). "Non-linear seismic soil structure interaction analysis based on the substructure method in the time domain." *Turk. J. Eng. Environ. Sci.*, 25, 617- 626.

Ling, Hoe I. and Liu, Huabei (2009). "Deformation analysis of reinforced soil retaining walls - simplistic versus sophisticated finite element analyses." *Acta Geotechnica*, 203-213.

Mandal, J. N. and Sah, H. S., (1992). "Bearing capacity tests on geogrid-reinforced clay." *Geotextiles and Geomembranes*, Vol. 11, No. 3, 327-333.

Matsuzawa, H. and Hazarika, H. (1996). "Wall displacement modes dependent active earth pressure analyses using smeared shear band method with two bands." *Computers and Geotechnics*, Vol. 19, 193 - 219.

McGown, A., Andrawes, K.Z. and Al-Hasani, M.M., (1978), "Effect of Inclusion Properties on the Behaviour of Sand." *Geotechnique*, Vol. 28, No. 3, 327-346.

Mehrad Kamalzare and Reza Ziaie-Moayed, (2011). " Influence of geosynthetic reinforcement on the shear strength characteristics of two-layer sub-grade." *Acta Geotechnica Slovenica*. Vol 1, 39-49

Michalowski, R. L. (2004). "Limit loads on reinforced foundation soils." *ASCE Journal of Geotechnical and Geoenvironmental Engineering.*, Vol. 130, No.4, 381-390.

Mirmoradi, S. and Ehrlich, M. (2017). Effects of facing, reinforcement stiffness, toe resistance, and height on reinforced walls. *Geotextiles and Geomembranes*, 45(1), pp.67-76.

Mofiz Syed Abdul , Mohd. Raihan Taha and Dipok Chandra Sharker.(2004). "Mechanical Stress-Strain Characteristics and Model Behaviour Of Geosynthetic Reinforced Soil Composites." 17<sup>th</sup> ASCE Engineering Mechanics Conference June 13-16, 2004, University of Delaware, Newark, DE, 1-8

Mofiz, S.A. and Rahman, M.M., Alim, M.A. (2004). "Stress-Strain Behaviour and Model Prediction of Reinforced Residual Soil." Southeast Asian Geotechnical Society Conference. 22 to 26 November (2004). Bangkok. Thailand

Mofiz, S. A. and Rahman, M. M. (2010). "Evaluation of failure load-deformation characteristics of geo-reinforced soil using simplified approach." *11th IAEG Congress*, 5-10 September, Auckland, New Zealand, pp 4383-4392.

Munoz, H. Tatsuoka, F., Hirakawa, D., Nishikiori, H., Soma, R., Tateyama, M. and Waranabe, K. (2012). "Dynamic stability of geosynthetic-reinforced soil integral bridge." *Geosynthetics International*, 19(1), pp 11-38.

Naylor, D. J. and Richard H. (1978), "Slipping strip analysis of reinforced earth." *International Journal for Numerical and Analytical Methods in Geomechanics*, 2, 343-366.

Noorzaei, J., Viladkar, M.N. and Godbole, P.N.(1994). "Nonlinear soil-structure interaction in plane frames." *Eng.Comput.*, 11, 303-316

Noorzaei, J. (1996). "Concepts and application of three dimensional infinite elements to soil-structure-interaction problems" *Int. J. Eng.*, 9(3), 1996, 131-142.

Omar, M.T., Das, B.M., Puri,V.K., & Yen, S.C.,(1993). "Ultimate bearing capacity of shallow foundations on sand with geogrid.", *Canadian Geotechnical Journal*, 30, 545-549.

M.T. Omar, B.M. Das, S.C. Yen, V.K. Puri, E.E. Cook. (1993a) Ultimate bearing capacity of rectangular foundations on geogrid-reinforced sand, *Geotechnical Testing Journal*, ASTM, 16 (2) (1993), pp. 246-252

Ogisako, E. Ochiai, H., Hayashi, S. and Sakai, A. (1988). "FEM analysis of polymer grid reinforced - soil retaining walls and its application to the design method." *International Geotechnical Symposium on Theory and Practice of Earth Reinforcement*, Fukuoka, Japan, October (1988), 559 - 564.

Osman, Emad Abd El-Moniem Mohamed (1990). "Experimental, theoretical and finite element analysis of a reinforced earth retaining wall including compaction and

construction procedures.” PhD thesis. A Thesis Submitted for the degree of Doctor of Philosophy, University of Glasgow, Department of Civil Engineering, October, 1990  
<http://theses.gla.ac.uk/2820/>

Parkin, A., Trollope, D. H. and Lawson, J. D. (1966). "Rockfill Structures subject to Water Flow." *ASCE Journal of the Soil Mechanics and Foundation Division*, Vol. 92, No.SM6, pp 135-151.

Ping-Sien Lin, Li-Wen Yang, C Hsein Juang. (1998). “Subgrade reaction and load-settlement characteristics of gravelly cobble deposits by plate-load tests.” *Canadian Geotechnical Journal*, 1998, Vol. 35, No. 5. Pp 801-810  
<https://doi.org/10.1139/t98-044>

Prakash, M. Y., Ghugal, Y. M. , Wankhade R. L.(2016),”Study on Soil-Structure Interaction: A Review.” *International Journal of Engineering Research* ISSN:2319-6890, Volume No.5 Issue: Special 3, pp: 737-741 27-28

Ramaswamy, S. D. and Puroshothama, P. (1992). “Model footings of geogrid reinforced clay.” *Proceedings of the Indian Geotechnical Conference on Geotechnique Today*, Vol. 1,pp 183-186.

Roy, R. and Dutta, S.C. (2001). “Differential settlement among isolated footings of building frames: the problem, its estimation and possible measures.” *Int. J. Appl. Mech. Eng.*, 6(1), pp 165-186.

Sharma, R., Chen, Q., Abu-Farsakh, M., S. Yoon. (2009), “Analytical modelling of reinforced soil foundation.”, *Geotextiles and Geomembranes*, 27 (1) pp 63-72.

Rajagopal and Hari. (1996). “Effect of stiffness of reinforcing tendon on the behavior of anchored earth wall supporting soft backfill.” *Proceedings of the Eastern Asia Society for Transportation Studies*.” Vol. 5, pp 829 – 844.

Rajagopal, Karpurapu and Richard J. Bathurst (1994) “Behaviour of geosynthetic reinforced soil retaining walls using the finite element method”, *Computers and Geotechnics*, Volume 17, Issue 3, pp 279-424

Rajasankar, J., Iyer N. R., Yerraya Swamy B.,Gopalakrishnan N., Chellapandi P., “SSI analysis of a massive concrete structure based on a novel convolution/deconvolution technique”, *Sādhanā* Vol. 32, Part 3, June 2007, pp. 215–234.

Rajashekhar Swamy, H.M., Krishnamoorthy, Prabakhara, D.L., and Bhavikatti, S.S. (2011a), “Relevance of interface elements in soil structure interaction analysis of three dimensional multiscale structure on raft foundation”, *Electronic Journal of Geotechnical Engineering*, 2011, Vol 16B, pp 199-218.

Rajashekhar Swamy, H.M., Krishnamoorthy, Prabakhara, D.L., and Bhavikatti, S.S.(2011b), “Evaluation of the influence of interface elements for structure-isolated footing-soil interaction analysis”, *Interaction and Multiscale Mechanics*, Vol. 4, No.1, March,pp. 65-83

Rajashekhar Swamy, H.M., (2012). “ Non-linear Dynamic analysis of Soil Structure Interaction of Three Dimensional Structure for Varied Soil conditions”, Thesis Submitted to Manipal Institute of Technology, Manipal

Rezaul Karim Md. and Saiful Alam Siddiquee. Md. (2009). “Improvement of bearing capacity of strip footing on sand by using metal strip reinforcement.” *Journal of Civil Engineering (IEB)*, 37 (2) pp 165-177.

Rowe, R.K. and Ho, S.K. (1993). "A review of the behaviour of reinforced soil walls.", *International Symposium on Soil Reinforcement*, Kyushu, November, pp 47-76.

Rowe, R.K. and Ho, S.K. (1996). "Some insights into reinforced wall behaviour based on finite element analysis.", *Proceedings of the International Symposium on Earth Reinforcement*, Fukuoka, pp 485-490.

Roy, R., and Dutta, S.C. (2001), “Differential settlement among isolated footings of building frames: the problem, its estimation and possible measures.” *Int J Appl Mech Eng*; 6(1) pp165–86.

Sayed, Abdul Mofiz, Mohd. Raihan Taha and Dipok Chandra Sharker (2004), “Mechanical Stress- Strain Characteristics and model Behavior of Geosynthetic Reinforced Soil Composites”, *17th ASCE Engineering Mechanics Conference*, June 13-16, 2004.

Schlosser, F. (1982),”Reinforced Earth- Mechanism, Behaviour and Design methods”, *Symposium on Soil and Rock Improvement Techniques Including Geotextiles Reinforced Earth and Modern Piling Methods*”, Bangkok, pp. F-1-1 pp. F-1-26

Schlosser, F. and Long, N.T. (1972). “Comport de la Terre Armee dans les Ouvrages de Soutenement” *Proceedings of the 5th European Conference on Soil Mechanics and Foundation Engineering*, Vol. 1, pp. 299-306, Madrid.

Schlosser, F. and Long, N. (1974). Recent Results in French Research on Reinforced Earth , *Journal of the Construction Division, ASCE*, 100 (CO3), pp. 223-237

Schlosser, F. and Delage. (1987). “Reinforced Soil retaining structures and polymeric materials. The Application of Polymeric Reinforcement in Soil Retaining Structures.” *Proc. NATO Advanced Research Workshop on Applications for Polymeric Reinforcement in Soil Retaining Structures*, Kingston, Kluwer Academic Publishers, The Netherlands, 3-65.

Shen, C. K., Romstad, K. M. and Herrmann, L. R. (1976). “Integrated study of reinforced earth - II Behaviour and design.” *ASCE Journal of Geotechnical Engineering Division*, Vol. 102, No. GT 6, June 1976, pp 577 - 590.

Shin, E. C., Das, B. M., Puri, V. K., Yen, S. C. and Cook, E. E. (1993). “Bearing capacity of strip foundation on geogrid-reinforced clay.” *Geotechnical Testing Journal, ASTM*, Vol. 16, No. 4, pp 534-541.

Shivashankar, R. (1991). "Behaviour of a Mechanically Stabilised Earth (MSE) Embankment with poor quality Backfills on soft clay deposits including a study of pullout Resistance". Phd. Thesis , Asian Institute of Technology, Bangkok

Shouling, He. and Jiang, Li. (2009). "Modelling nonlinear elastic behaviour of reinforced soil using artificial neural networks.", *Applied Soft Computing*. 9(3), pp 954-961

Suleyman, Kocak and Yalcin, Mengi (2000). "A simple soil structure interaction model." *Applied Mathematical Modelling*, 24 pp 607-635

Syed Mohd., Ahmad and Basudhar, P. K. (2008). "Behaviour of Reinforced Soil Retaining Wall under Static Loading Using Finite Element Method." *The 12th International Conference of International Association for Computer Methods and Advances in Geomechanics. (IACMAG)* 1-6 October, Goa, India

Tatsuoka, F., Tateyama, M. and Murata, O. (1989). "Earth Retaining Wall with a Short Geotextile and a Rigid Facing." *Proceedings of the Twelfth International Conference on Soil Mechanics and Foundation Engineering*, Balkema, 1992, Vol. 2, Rio de Janeiro, Brazil, pp 1311-1314.

Tatsuoka, F. (1992). "Roles of facing rigidity in soil reinforcing." Keynote Lecture, Proc. Earth Reinforcement Practice, IS- Kyushu '92, Ochiai et al. eds., 2, 831-870.

Terzaghi, K. (1955). "Evaluation of Coefficients of subgrade Reaction." *Geotechnique*, 5 (4), pp 297 -326.

Teodoru, I.B., (2009). Beams on Elastic Foundation. The Simplified Continuum Approach. Bulletin of the Poly-technic Institute of Jassy, Constructions, Architecture Section, Vol. 55, pp.37-45

Truesdell, C. (1955a) "The simplest rate theory of pure elasticity," *Comm Pure Appl Math*: 8. pp 123-132.

Truesdell, C. (1955b). "Hypoelasticity", *Journal of rational Mechanics and analysis*, Vol.4, No 1, 83-133

Vidal, H. (1969). "The Principle of Reinforced Earth." *Highway Research Record*, No. 282, 1 - 16.

Viladkar, M.N., Godbole, P.N., Noorzaeei, J. (1991). "Soil-structure interaction in plane frames using coupled finite infinite elements.", *Computers and Structures*; 39(5):pp 535-46.

Viladkar, M.N., Ranjan, G. and Sharma, R.P. (1993). "Soil structure interaction in the time domain." *J. of Comput. Struct.*, 46(3), 1993, pp 429-442.

Viladkar, M.N., Godbole, P.N., Noorzaeei, J. (1994). Interactive analysis of a space frame-raft-soil system considering soil nonlinearity *Comput. Struct.*, 51, (1994), pp 343-356.



Vesic, A. B. (1961). "Beams on Elastic Subgrade and Winkler's Hypothesis," *Proceedings of the 5th International Conference on Soil Mechanics and Foundation Engineering*, Paris, 1961, pp 845-850.

Wael, N. Abd. Elsamee. (2013). "An Experimental Study on the Effect of Foundation Depth, Size and Shape on Subgrade Reaction of Cohesionless Soil." *Engineering*, 2013, 5, pp 785-795.

Wayne, M.H., Han, J., Akins, K., October 1998. The design of geosynthetic reinforced foundations. In: *Proceedings of ASCE's 1998 Annual Convention & Exposition*, ASCE Geotechnical Special Publication, 76, pp. 1-18.

Winkler, E. (1987). "Die Lehre von Elastizitat and Festigkeit." (on Elasticity and Fixity)," Prague, 1987, 182 (After Wael N. Abd Elsamee, 2013. "An Experimental Study on the Effect of Foundation Depth, Size and Shape on Subgrade Reaction of Cohesionless Soil", *Engineering*, 5, pp 785-795

Y.X. Cai a, P.L. Gould b, C.S. Desai c Nonlinear analysis of 3D seismic interaction of soil–pile–structure, systems and application *Engineering Structures* 22 pp 191–199  
Yang, Z.Z., (1972), "Strength and Deformation Characteristics of Reinforced Sand", Ph.D. Thesis, University of California, Los Angeles, California, USA.

Yetimoglu, T., Wu, J. T. H. and Saglamer, A., 1994. "Bearing capacity of rectangular footings on geogrid-reinforced sand." *Journal of Geotechnical Engineering*, ASCE, Vol. 120, No.12, pp. 2083-2099.

Yin, J.H., (2000), "Generalization of three-moduli incremental non-linear constitutive models for soils", *The Geotechnical Engineering Journal, The South east Asian Geotechnical Society*, Vol.30, No. 3, December

Yoshihisa Miyata and Richard J. Bathurst (2007), "Development of the K-stiffness method for geosynthetic reinforced soil walls constructed with c-  $\Phi$  soils" *Canadian Geotechnical Journal*, 44(12): pp 1391-1416.

SI No	JOURNAL / CONFERENCE PUBLICATIONS	Details
1	” <i>Effect of relative stiffness of soil and reinforcements on pressure-settlement characteristics in a reinforced earth retaining wall</i> ” , International Civil Eng Symposium at VIT, Vellore (Presented)	14 <sup>th</sup> -16 <sup>th</sup> March,2014
2	“ <i>Comparitive studies of Reinforced and Unreinforced Foundation soil</i> ”, International Conference on Emerging trends in Engineering, NMAM, Nitte (Presented)	May 2014
3	“ <i>Effect of interface on pressure-settlement characteristics of reinforced earth retaining wall</i> , International Conference of the International Association for Computer Methods and Advances in Geomechanics (14th ICIACMAG), Kyoto University, Japan (Published)	September 2014
4	“ <i>Load Settlement Characteristics of Reinforced and Unreinforced Foundation Soil</i> ”, International Journal of Engineering Research & Technology (IJERT) ISSN: 2278-0181	Vol. 3 Issue 5, May, 2014
5.	“ <i>Studies on modulus of subgrade reaction of reinforced foundation soil using model Plate Load test</i> ”, International Conference on Civil, Mechanical and Environmental Engineering Technologies, SVS College of Engg , Coimbatore	26 <sup>th</sup> -27 <sup>th</sup> February 2016
6	<i>Studies on modulus of subgrade reaction of reinforced foundation soil using model Plate Load test</i> , In Journal of Chemical and Pharmaceutical Sciences (Published)	2016, August Special Issue 2
7	<i>Effect of Facing on the Settlement of Mechanically Stabilised Earth (MSE) Embankment</i> , 10 <sup>th</sup> International Symposium on Lowland Technology at Mangalore, India (organized by NIT-K and ILMR, Japan)(Presented) September 15-17(Presented)	September 15-17, 2016
8	<i>Comparitive Studies on Load Settlement Characteristics of Square Footing resting on Geosynthetic Reinforced Sand</i> , International Conference on	27th & 28th February

	<i>GEOTECHNIQUES FOR INFRASTRUCTURE PROJECTS,</i> Thiruvananthapuram	2017
9	<i>Effect of Reinforced Soil Structure Interaction on Foundation Settlement Characteristics of a Three Dimensional Structure,</i> 1 st International Conference on the Energy, Materials and Information Technology, Jharkhand University, Ranchi.	23 <sup>rd</sup> and 24 <sup>th</sup> December 2017

# CURRICULUM VITAE

**Mrs. Nayana N. Patil** B E., M Tech., (Ph.D)

E-mail: [nayanateju14@gmail.com](mailto:nayanateju14@gmail.com), [swamyraja2005@gmail.com](mailto:swamyraja2005@gmail.com), [swamyraja2001@yahoo.co.in](mailto:swamyraja2001@yahoo.co.in)

---

## HIGHER EDUCATION

1. **B.E. at B.V.B. College of Engg & Technology, Hubli, 1988**
2. **M.Tech. in Geotechnical Engineering at Basaveshwara Engg College, Bagalkot, 2006**  
*Thesis Topic: Parametric studies of reinforced earth retaining wall*  
*Advisor: Dr. Basavaraj Katageri*
3. **Pursuing Ph.D. in Civil Engineering, NITK, Suratakal (registered in the year 2008)**  
*Dissertation Topic: "Non-linear analysis and behavior of reinforced soil structures"*  
*Advisors: Dr. R. Shivashankar Prof, NITK, Surathkal.*

## MILE STONES IN EDUCATION

1. Secured III rank in B.E.(Civil), Karnataka University , Dharwad in May 1988.
2. Obtained 16th rank to the state in PUC II year, 197th rank in CET for PCM and 454 rank in PCB cycle.
3. Obtained 2nd rank in 7th standard in Belgaum District.

## RESEARCH INTERESTS

Reinforced soil, Soil-structure interaction, Foundation engineering, Alternate, Construction materials, Prestressed concrete, Concrete technology

## PROFESSIONAL EXPERIENCE IN THE ACADEMIC ENVIRONMENT

### 1) July 2014 till date

*Assistant Professor Department of Civil Engineering, Faculty of Engineering and Technology , MS Ramaiah University of Applied Sciences, Bangalore*

**Duties:** Teaching undergraduate and Post-graduate courses, Supervisor of graduate student project works, Supervisor for M.Tech Dissertations, Head Proctor of FET

**2) June 2011 till June 2014 ; August 2007 to June 2010**

*Associate Professor Department of Civil engineering, Sahyadri college of Engg. and Management, Mangalore-575007.*

**Duties:** Teaching undergraduate and Post-graduate courses, Student Welfare Officer, Deputy Dean of Examinations, Faculty advisor for students association, NBA Co-ordinator, Internal tests Co-ordinator, Survey Camp Officer, Supervisor of graduate student project works.

**3) July 2010 to May 2011**

*Assistant Professor ( V pay,) Department of Civil Engineering, Srinivas School of Engineering, Mukka, Mangalore*

**Duties:** Teaching undergraduate courses , Lab incharge for BMT Laboratory

**4) September 2001 to July 2007**

*Lecturer , Department of Civil Engineering, Bellary Engineering college, Bellary-583104*

Duties: Teaching undergraduate courses, Staff coordinator for ladies, Incharge for ladies hostel, Editor of college magazine "Bhoomika", Faculty advisor for students association.

**5) 3 yrs in Polytechnic Colleges at Bellary and Dharwad (Part-time)**

**EXPERIENCE IN THE INDUSTRIAL ENVIRONMENT**

1. 6 yrs as Consultant Heading Techno consultancy and Engineering Services
2. 8 yrs as Director of Computer Centre First Computers @ Bellary
3. Panel Valuer for LIC-HFL of India, Bellary

**TEACHING**

**I) Subjects Handled for Under Graduates**

GeoTechnical Engg-I, GeoTechnical Engg-II ,Prestressed Concrete Structures, Hydraulics and Hydraulic Machinery, Fluid Mechanics, Fluid Mechanics Laboratory, Basic Material Testing Laboratory, Elements of Civil Engg & Engg Mechanics, CCP Theory, CCP Lab, Surveying-I, Environmental Studies, Materials of Construction

## **II) Subjects handled For Post Graduation (MTech. (Structures), (CADS), (CSD), (CEM), (TRN)**

Computer Aided Analysis and Design of Foundations and Earth Retaining structures, Design Concept of Substructures, Theory of Elasticity and Plasticity, Advanced Concrete Technology and Pre-cast structures, Forensics, Rehabilitation and Structural Health Monitoring, Bridge Engineering

### **STUDENT PROJECTS GUIDED**

Guided 25 project works for UG and 21 M.Tech Dissertations

### **RESEARCH**

#### **I) International Conferences**

1. *“A case of Interaction between frame & masonry for face lifting & increasing its functional utility of a structure”*, International conference on “ Rehabilitation, Renovation and Repairs of structures, January 9-11,1994, Andhra University, Vishakapatnam
2. *“Parametric Studies of reinforced earth wall subjected to surcharge loading”*, 2nd International Conference on“PROBLEMATIC SOILS”, 04-05 December 2006, Selangor, MALAYSIA.
3. *“Effect of relative stiffness of soil and reinforcements on pressure-settlement characteristics in a reinforced earth retaining wall”* , International Civil Engg Symposium at VIT, Vellore, 14-16 March,2014
4. *“Comparitive studies of Reinforced and Unreinforced Foundation soil”*,International Conference on Emerging trends in Engineering ,NMAM, Nitte , May 2014
- 5 *“ Effect of interface on pressure-settlement characteristics of reinforced earth retaining wall , International Conference of the International Association for Computer Methods and Advances in Geomechanics (14th ICIACMAG), Kyoto University, Japan September 2014 (Scopus Indexed)*
6. *“Rate Of Strength Development In Normal Strength And High Strength Geopolymer Concrete With Micronized Bio Mass Silica”*, International Conference on Sustainable Civil Infrastructure 2014, Department of Civil Engineering, Indian Institute of Technology Hyderabad

7. “*Studies on modulus of subgrade reaction of reinforced foundation soil using model Plate Load test*”, International Conference on Civil, Mechanical and Environmental Engineering Technologies, SVS College of Engg , 26<sup>th</sup> -27<sup>th</sup> February 2016, Coimbatore
8. “ *Effect of Facing on the Settlement of Mechanically Stabilised Earth (MSE) Embankment*”, 10<sup>th</sup> International Symposium on Lowland Technology at Mangalore, India (organized by NIT-K and ILMR, Japan)(Presented) September 15-17, 2016
9. “ *Comparitive Studies on Load Settlement Characteristics of Square Footing resting on Geosynthetic Reinforced Sand*”, International Conference on *Geotechniques For Infrastructure Projects*, Thiruvananthapuram 27th & 28th February 2017
10. *Effect of Reinforced Soil Structure Interaction on Foundation Settlement Characteristics of a Three Dimensional Structure*, 1 st International Conference on the Energy, Materials and Information Technology, Jharkhand University, Ranchi.
11. "*Studies on prestressed and reinforced concrete flyovers*", First International Conference on Innovations in Thermal, Manufacturing, Structural and Environmental Engineering (ICITMSEE'18) Kongunadu College of Engineering and Technology, Trichy.
12. " *Parametric studies of piled raft foundation resting on cohesive soil*", First International Conference on Innovations in Thermal, Manufacturing, Structural and Environmental Engineering (ICITMSEE'18) Kongunadu College of Engineering and Technology, Trichy.

## **II) National Conferences**

1. “*The Challenges Faced by Regulating and Controlling Authorities of Technical Education in the New Millennium*”, III State level convention of ISTE, 2000 at Vijayanagar Engineering College, 2000 December.
2. “*Water-Too much or too little –The major cause of natural disasters*”, State level ISTE Convention, 15th- 17th December 2005, Bapuji Institute of Engg & Te”chnology, Davanagere.
3. “*Problems associated with Disaster Management*”, State level ISTE Convention, 15th- 17th December 2005, Bapuji Institute of Engg & Technology, Davanagere.
4. “*Finite Element Analysis Of Reinforced Earth*”, “*RADECON*”, 20th & 21st Nov 2006, KBN College of Engineering, Gulbarga.

5. “*Modern Construction Methods*”, “*RADECON*”, 20th & 21st Nov 2006, KBN College of Engineering, Gulbarga.
6. “*Values and Ethics in Technical Education*”, ISTE National Convention, 14th- 16th 2006, Bannari Amman Institute of Technology, Sathyamangalam

### **III) International Journals**

- 1) “*Load Settlement Characteristics of Reinforced and Unreinforced Foundation Soil*”, International Journal of Engineering Research & Technology (IJERT), ISSN: 2278-0181, Vol. 3 Issue 5, May - 2014
- 2) *Studies on modulus of subgrade reaction of reinforced foundation soil using model Plate Load test*, In Journal of Chemical and Pharmaceutical Sciences, 2016, August, Special Issue 2 (**Scopus Indexed**)
- 3) *Experimental And Analytical Studies of 3D Frame Structure With Buckling Restrained Bracing (BRB)*, International Journal of Civil Engineering and Technology (IJCIET) Volume 7, Issue 5, September-October 2016, pp. 78–86, © IAEME Publication (**Scopus Indexed**)

### **MEMBERSHIP OF PROFESSIONAL BODIES/ ORGANIZATIONS/ ASSOCIATIONS/ SOCIETIES.**

Life Member of Indian Society for Technical Education.

### **SHORT TERM COURSES/ WORKSHOPS**

1. “*STTP on Structural Steel Design*”, MIT, Manipal at Jan 5-10, 2010
2. “*Geo information Technologies and their role in Environmental Management & Eco sustainable development*” Lions Seva Mandir, M'lore , April 3, 2009
3. “*Applications of Reinforced Earth in Civil Engg* “, NMAM,Nitte, June 02 to June 06 2008
4. “*Development of applications of bamboo in construction and energy sectors*”, Sahyadri College of Engg & Management , November 9 2011
5. “*Computational Mechanics*”, Sahyadri College of Engg & Management, May 2013
6. “*Ground Improvement and Use of Geosynthetics*” NIT-K,Surathkal , 5<sup>th</sup> and 6<sup>th</sup> September,2013
7. “*Research process, Technical Paper writing and patenting*”, M S Engineering College, Bangalore, 22<sup>nd</sup> to 24<sup>th</sup> January 2014